LA-8835-C
Conference

MASTER

Intermediate-Energy Nuclear Chemistry Workshop

Held at the Los Alamos National Laboratory

Los Alamos, New Mexico

June 23—27, 1980

University of California

LOS ALAMOS SCIENTIFIC LABORATORY
Post Office Box 1663 Los Alamos, New Mexico 87545

This work was supported by the US Department of Energy, Office of High Energy and Nuclear Physics, Division of Nuclear Physics.

LA-8835-C
Conference

UC-34c
Issued: May 1981

Intermediate-Energy Nuclear Chemistry Workshop

Held at the Los Alamos National Laboratory

Los Alamos, New Mexico

June 23—27, 1980

Prepared by

G. W. Butler
G. C. Giesler
L.-C. Liu
B. J. Dropesky
J. D. Knight
F. Lucero
C. J. Orth

Workshop Organizing Committee

P. J. Karol (Carnegie-Mellon University) Chairman
B. J. Dropesky (Los Alamos National Laboratory) Co-Chairman
D. J. Vieira (Los Alamos National Laboratory) Administrative Assistant
M. M. Sternheim (University of Massachusetts)
E. P. Steinberg (Argonne National Laboratory)
R. A. Naumann (Princeton University)
R. G. Korteling (Simon Fraser University)
A. L. Turkevich (University of Chicago/Los Alamos National Laboratory)
N. Imanishi (Kyoto University/Los Alamos National Laboratory)
T. Nishi (Kyoto University) Japanese Contact
H. S. Pruys (SIN) European Contact
L.-C. Liu (Los Alamos National Laboratory)
C. J. Orth (Los Alamos National Laboratory)
J. D. Knight (Los Alamos National Laboratory)
G. W. Butler (Los Alamos National Laboratory)

INTERMEDIATE-ENERGY NUCLEAR CHEMISTRY WORKSHOP

ABSTRACT

This report contains the proceedings of the LAMPF Intermediate-Energy Nuclear Chemisty Workshop held in Los Alamos, New Mexico, June 23-27, 1980. The first two days of the Workshop were devoted to invited review talks highlighting current experimental and theoretical research activities in intermediate-energy nuclear chemistry and physics. Working panels representing major topic areas carried out in-depth appraisals of present research and formulated recommendations for future research directions. The major topic areas were Pion-Nucleus Reactions, Nucleon-Nucleus Reactions and Nuclei Far from Stability, Mesonic Atoms, Exotic Interactions, New Theoretical Approaches, and New Experimental Techniques and New Nuclear Chemistry Facilities.

CONTENTS

WELCOMING REMARKS

by

G. A. Cowan
Associate Director for Chemistry, Earth, and Life Sciences
Los Alamos Scientific Laboratory

It is a particular pleasure to welcome this group to Los Alamos on behalf of the Director, Donald Kerr, who is in France today. It is a happy task, because I feel closer to this work than to most of the subjects in which my office is involved. I see many old familiar faces here. I remember it was in 1968 when we were planning a Nuclear Chemistry program at Intermediate Energy at LAMPF and tried to identify the topics that would be lively when a beam was achieved. I think many of you who are present today were at that meeting. You will surely agree that, in the intervening years, the research program in intermediate energy and nuclear chemistry has more than met our expectations. In looking over the program for this week, I was particularly impressed by its breadth and its emphasis on theory, which I think was missing twelve years ago. I am most pleased to see this growth, because I think it is a measure of the strength and viability of the program in general.

A word about Los Alamos: The Laboratory consists of about 6800 employees. It is important to remember that it is a mission oriented laboratory, in which research is considered as supportive. However, despite its supportive role, it would be a mistake to consider research a secondary activity. Actually, it is our most important activity because the research base is an absolute prerequisite for the effective pursuit of our applied programs. Something else on the personnel distribution chart you should notice, is that 34% of the people in the laboratory are physicists, 34% are in several branches of engineering, and 14% are chemists. This is a physics and engineering laboratory to a large extent. But don't let that discourage you if you are a chemist; these numbers don't tell the whole story.

Regarding funding: In 1950 Los Alamos, as you know, was entirely a nuclear weapons oriented laboratory, all of its money came from defense programs. That

had changed rather sharply by 1960 and is continuing to change. In fact, this past year the Weapons Program became less than 50% of the laboratory's funded effort; most of the new programs are in the energy field. To give you a further breakdown of staff composition, the chemistry degree is the second largest disciplinary degree at Los Alamos.

Once again, welcome. If anything has been missed in the excellent planning of the meeting, please call it to our attention.

WELCOMING REMARKS

by

D. C. Hoffman
CNC-Division Leader
Los Alamos Scientific Laboratory

It is a real pleasure to welcome you on behalf of the Chemistry and Nuclear Chemistry Division. As an old nuclear chemist myself, it is a particular pleasure to be among so many people who claim Nuclear Chemistry as their profession, and to have a workshop devoted to Nuclear Chemistry. I have been anticipating this workshop ever since I heard about its formation. I am looking forward to the interaction among the participants and the new avant-garde ideas and original research that will come out of it. I think it is a real opportunity for us to host this meeting, and it is a particular pleasure for me, and it's overwhelming to see so many of you here. I just came from the Nuclear Chemistry Gordon Conference, and there are more nuclear chemists here than there were there. And, as George (Cowan) said, if there is anything we can do to make your stay more pleasant or anything you would like to see while you are here that may not be on the agenda, please contact one of us and we'll see what we can do.

Since many of you are familiar with the Division and many of you have visited our nuclear chemistry section at LAMPF, this may be redundant, but you have not had the opportunity to learn much about the rest of the Chemistry and Nuclear Chemistry Division. So, perhaps it might be worthwhile to take just a couple of minutes to tell you something about the Division as a whole. Then you will know a little more about the resources that stand behind us, so to speak, and the technical expertise that we do have and the opportunities that there may be for cross-disciplinary, chemistry-type collaborations. The Chemistry and Nuclear Chemistry Division has around 155 peopie, which includes 95 professional scientists, 75 with Ph.D.s, so we have a fair share of the Ph.D.s in chemistry in the Lab in our Division. I might also mention that we have had 45 Visiting Staff Members and Consultants during last year. This is rather a large number. We maintain fairly close ties with a lot of universities in this country and with

research installations around the world. I think 26 nuclear chemistry research visitors to LAMPF is a low figure; by now it is no doubt much higher.

We have three groups, CNC-2, CNC-4, and CNC-11. CNC-11 is the largest group and has more than 90 people. It is the Nuclear and Radiochemistry group with which most of you are most familiar. We have two other groups, CNC-2 which is the Physical Chemistry-Chemical Physics group which has a strong research program in experimental and theoretical chemical dynamics, ion-molecule kinetics, and laser chemistry and analysis. CNC-4 has strong inorganic, synthetic, and structural analysis capabilities and expertise in actinide chemistry, and I think that the expertise of both these groups could be useful in the context of Nuclear Chemistry research at LAMPF. Nick Matwiyoff is the Alternate Division Leader. The Physical Chemistry-Chemical Physics Group is under John Sullivan. Bob Penneman is Group Leader of the Inorganic Chemistry group, and James Sattizahn of the Nuclear and Radiochemistry group.

I thought I would also tell you what the major responsibilities and research projects in the Division are. We have a strong weapons component; about 50% of the Division's funds come from weapons sources, about 27% is for radiochemical diagnostics and interpretation of underground nuclear tests, and the rest is supporting research. Some of our other activities are shown in Fig. 1. I have broken these down by percentages, so you will get some feel for what the major activities are. The percentages are about the same in money or people. We are getting into a fairly large program in nuclear waste management and in fundamental geochemical research, with an emphasis on nuclide migration and nuclide immobilization. These things fit together rather well and have grown rather naturally out of our expertise in analyzing debris from underground nuclear tests for all the various nuclides present. In other words, we became geochemists probably before we knew it, and now we are emphasizing these areas. The chemistry and structure of novel heavy element compounds and emphasis on structure in bonding and catalysts we are getting into is because of the organo-metallic expertise, particularly in CNC-4. We have a state-of-the-art crossed molecular beam machine in CNC-2 and have both theoretical and experimental chemical dynamics efforts. We have recently started an inter-divisional project called USAP (Ultra Sensitive Analysis Project) which will make use of laser-based analytical methods and laser-induced chemistry to push detection limits to very low levels. It will also concentrate on mass spectrometric analyses, perhaps using laser-ionization to measure only a few hundred atoms. The ICONS program, which you may be familiar with, is

the program to separate the stable isotopes of carbon, oxygen, nitrogen, and perhaps, in the near future, sulfur. One of most important aspects of that is the National Institutes of Health programs which emphasize research aspects of these isotopes in biomedical, biochemical, agricultural, and environmental research. The medical radioisotopes research program you are probably familiar with emphasizes the production of these isotopes at the LAMPF beam stop. It utilizes a number of our capabilities inasmuch as the isotopes are produced there, brought to the hot cell at TA-48, which is the site of CNC-11, and chemically and sometimes isotopically separated there. New methods for processing and isolating isotopes for radiochemical generators for use in nuclear medicine and new methods for labeling pharmaceuticals are being developed under that program.

Then, of course, we have the Nuclear Chemistry program at LAMPF, which you are primarily concerned with this week. We have some other research in fission studies of the actinides and heavy elements which are carried on here, at LAMPF, at the Van de Graaff, and at other accelerators both here in the U.S. and at GSI and some other installations in Europe, and some activities in lunar studies and cosmo-chemistry. I think that gives you just a brief survey of some of our activities and if you want to know in detail about any of these things, please ask and we will see that your requests are taken care of.

Figure 2 lists some of the facilities that we have within CNC Division, many of which you may not be familiar with. Probably you are familiar with our extensive facilities for the measurement and handling of radioactivity. You may not be as familiar with our mass spectrometry capabilities, because they have been expanded greatly over the last couple of years. We now have in the Division 10 mass spectrometers, and several of these are state-of-the-art machines. We can now analyze for as few as 10^6 atoms of plutonium and uranium, and we have an automated mass spectrometer for carbon and nitrogen isotope measurements. We also have a 2-stage gas mass spectrometer which allows us to measure methane-2l (used in atmospheric tracer studies) down to concentrations of 10^{-12} relative to normal methane. We have instrumentation for chemical structural analysis, NMR, and various types of vibrational Raman spectrometry and so on. We have a hydrothermal laboratory for research in geochemistry, microscopy (conventional and scanning electron), and some of the more usual analytical chemistry type of analysis facilities. I think that gives you at least an idea of some of the things that the Division is involved in, some of the capabilities and some of the research programs, and the more programmatic and applied programs that we are

concerned with. Again, I would like to welcome you on behalf of the Division, and assure you we will do everything possible to make your stay pleasant.

MARCH 1980

CNC DIVISION
CURRENT MAJOR RESPONSIBILITIES
AND
RESEARCH PROJECTS

- Radiochemical Diagnostics: WPO; 27%
- Atmospheric Science: DOE, ASEV, NASA; 5%
- Sorption, Migration, and Immobilization of Radionuclides: DOE; 11%
- Fundamental Geochemical Research: DOE, DGE, BES; 4%
- Chemistry and Structure of Novel Heavy Element Compounds: ISR and DOE, BES; 4%
- Synthesis, Structure, and Bonding in Catalysts: ISR and DOE, BES; 4%
- Molecular Beam and Theoretical Chemical Dynamics: WSR; 5%
- Laser Based Analytical Methods and Laser-Induced Chemistry: ISR and WSR; 5%
- ICONS: DOE, ASEV and NIH; 12%
- Medical Radioisotopes Research Program: DOE, ASEV; 8%
- Nuclear Chemistry at LAMPF: DOE, ASER; 5%
- Fission Studies; Actinides and Heavy Elements; Lunar Studies and Cosmochemistry: Other; 10%

Fig. 1

CNC DIVISION FACILITIES March 1980

MEASUREMENT AND HANDLING OF RADIOACTIVITY

Automatic Beta and Gamma Counting Systems
Alpha, Beta, and Gamma-ray Spectrometers
Computer Control and Data Collection and Data Reduction
Hot Cells for High Level Gamma- and Beta-Active Materials
Facilities for Alpha-Emitting Materials

MASS SPECTROMETRY

Two Surface Thermal Ionization, Pulse-counting Instruments
Three Surface Thermal Ionization With Ion Detection By Faraday Cage
One "Precision-Ratio" Gas-Source
One Gas-Source Two-Stage for "Heavy Methanes"
Two Magnetic Deflection Isotope Separators
Quadrupole Gas Chromatograph
Time-of-Flight

INSTRUMENTATION FOR CHEMICAL STRUCTURE ANALYSIS

Varian XL-100-Fourier Transform Nuclear Magnetic Resonance (NMR) Spectrometer for ^{13}C and Other Nuclei
EM-390 Fluorine NMR; EM-360 Proton NMR
Superconducting Magnet for High Field NMR of Solids
Perkin Elmer L80 Infrared (IR) Spectrometer
Nicolet FT-IR Spectrometer
(Cryo-Matrix Equipment)
Cary-81 Laser-Raman Spectrometer
Precession and Powder Diffraction (X-Ray)
Picker FACS-1 X-Ray Diffractometer
VAX-11/780 Digital Equipment Corporation Computer

HYDROTHERMAL LABORATORY - Circulation Loops, Rocking Vessels, Permeability Systems

MICROSCOPY: Scanning-Electron-Microscope (with nondispersive X-Ray Analyser); OPTICAL: Microautoradiography

INSTRUMENTS FOR ELEMENTAL ANALYSIS

Atomic Absorption Spectrometer (In Fume Hood)
Plasma Emission Spectrometer
X-Ray Fluorescence Spectrometer (Automatic Read-Out and Data Analysis)

Fig. 2

INTRODUCTION TO THE WORKSHOP

by

P. J. Karol
Carnegie-Mellon University

I am to give a brief introduction addressing the purpose of the Workshop. I had fun going back into the literature to get some ideas. As it turns out, the first cyclotron went on line just about 50 years ago, so perhaps this is an anniversary of the birth of intermediate energy nuclear science, although the definition of what is meant by intermediate energy seems to change every decade.

What I really want to talk about is the Workshop itself. There are two phases to the Workshop. Basically, you can describe the first half as concerning "Where are we now?" the second half being "Where are we going?" or "Where should we be going?". One of the purposes of the Workshop is to review contributions, both experimental and theoretical, of the international nuclear science community to our understanding of the properties and structure of nuclei, and also the complex interactions that occur at intermediate energy. An additional purpose of the meeting is really to inspire young scientists. I would like to welcome the graduate students that are present and encourage their active participation in the Workshop. I would like to encourage my distinguished and established colleagues to communicate with the students.

While looking selectively through literature of exactly fifty years ago, I found two interesting items. One was a brief Letter discussing the Raman Effect in nitrogen, where the alternating even-odd intensities was used as proof, fifty years ago, that the electron, (which everyone knew had to be inside the nucleus to balance the charge appropriately), had no spin. There was considerable discussion in the Letter since neutrons had not been discovered yet, as to the status of the structure of the nucleus. If you look back exactly fifty years ago, this was one of two pieces of conclusive evidence that showed: Yes, there are electrons inside the nucleus, and the reason they have not been behaving properly is that, for some as-yet unknown reason, they lose their spin when they are inside the nucleus. A second piece of interesting material that showed up in literature

fifty years ago was a review on the origin of cosmic rays. It was stated in this review that there now existed clear and convincing evidence that nucleosynthesis took place, not in depths of stars, but actually in depths of interstellar space. I use these two examples to t y to "alert" the students. Invariably you will hear statements caged in extreme confidence; but sometimes the level of confidence is inversely proportional to....

The remaining major purpose of this Workshop is to prepare a report that is to delineate and emphasize the discussion from the first two days--reviews of recent nuclear chemistry contributions--and also to make very strong recommendations as to what the future directions will be. I hesitate to bring this up, but to encourage dropping inhibitions I'll use it anyway. I enjoy looking around for metaphors and what I am about to say will temporarily sound extremely irrelevant. Recently, (in a moment of temporary insanity), I signed up for disco lessons. I find there is a strong parallelism between modern dancing and nuclear science. The correlation I find is the following: recognizing that modern dances have evolved very rapidly over the past fifty years, disco seems to represent, in a sense, the current status of interaction between nuclear chemists and physicists, and between theorists and experimentalists. By this I mean that, if you have ever discoed or have seen disco dancing, there is an enormous variety of extraordinary steps by the two partners involved, but they rarely touch each other.* The implication of the metaphor that I am using is that for fifty years we have had chemists and physicists in nuclear science, experimentalists and theorists, and that there is now a profusion of activity developing, but limited contact between "partners." Perhaps, then, one of the objectives of the Workshop will be to bring these groups together and allow them to "touch."

I hope you find these sessions, especially the first two days which I know will be informative, both provocative and stimulating and that you will all very actively participate in the second half of the session.

---

* NOTE ADDED IN PROOF, This point has been contested by a representative of the European nuclear chemistry community.

PION NUCLEUS INTERACTIONS

by

H. K. Walter

Laboratorium für Hochenergiephysik der ETH-Zürich, c/o SIN,

CH-5234 Villigen, Switzerland

I. INTRODUCTION

The period when the meson factories at LAMPF, TRIUMF, and SIN came into operation is called the industrial revolution of pion and muon physics. Before this revolution, people had already recognized the following advantages of using pions for the study of nuclear reactions compared to other hadronic probes like protons and α particles. i) Since the pion comes in three charge states, one should be able to correct for Coulomb effects. ii) We have to deal with only one strong wave, at least near the (3,3) resonance, which is a p-wave with J,T = 3/2, 3/2. iii) Near that resonance we have a strong selectivity of the probe to protons and neutrons since the elementary pion-nucleon cross sections behave like $\pi^+p \to \pi^+p$: $\pi^+n \to \pi^0p$: $\pi^+n \to \pi^+n$ = 9:2:1. iv) This high isospin selectivity, it was hoped, would give information about the neutron distribution both in ground and excited states; the nuclear density seen by a π^- is $\rho_{\pi^-} = 3/2\ \rho_n + 1/2\ \rho_p$. v) It was not clear whether one should consider the unique feature of pions, to be created and absorbed, as an advantage or as a disadvantage which complicates the calculations. With the advent of microscopic theories one realized the usefulness of this reaction channel for the study of the formation and propagation of Δ's in nuclei. vi) Finally, charge exchange and double charge exchange provide the opportunity to study higher order processes in rather pure form. Before the revolution, it was known that total cross sections scaled like $A^{2/3}$, i.e., are essentially black disc cross sections. Very beautiful elastic scattering data were available and for years were analyzed successfully in terms of first order static (i.e. fixed scatters) theories. Also, there were isolated data for components of the inelastic channel, for example, knockout reactions induced by π^+ and π^- to specific bound states.

Missing were the gross features of the other parts of the total cross section: the reaction, the absorption, and the quasi-elastic cross sections. The lack of systematic data led to widespread optimism concerning the understanding of the reaction mechanism, which is necessary to obtain nuclear structure information. The purpose of this talk will be to show that we are just beginning to understand the reaction mechanism and that we should be very cautious to extract nuclear structure information with the help of models which do not include, in a microscopic way, the effects of Coulomb distortion, Pauli-principle, and Fermi motion, to list only the most important. These models should take into account π absorption and Δ formation and propagation, since these effects are not only interesting but also dominant.

II. ELASTIC SCATTERING

Figure 1 shows elastic cross sections at resonance measured by Zeidman et al.[1] They are essentially diffractive over 6 orders of magnitude. Because of the blackness of the nucleus, reaction mechanisms are hidden in small deviations from diffraction. The curves shown in Fig. 1 are first order momentum space optical potential calculations, which later were improved[2] to include local energy variations and binding effects. Although a reduction of the radius of the matter distribution was necessary to obtain a good fit to the data, the reason for this reduction is not understood. Most of the differences for π^+ and π^- scattering seen in Fig. 1 are due to Coulomb effects; only $\sim$ 25% of the shift of the minimum in ^{208}Pb is due to the 44 extra neutrons, and again only a small fraction of this shift could eventually be attributed to different radial distributions of protons and neutrons. The danger in extracting radius information with the help of simple first order models might be seen from calculations by Lenz and Thies.[3] In an attempt to unify all the pion-nucleus interactions by the use of the Δ isobar-hole picture, they try to introduce the smallest possible amount of phenomenology through the addition of a spreading potential to the Δ-h Hamiltonian. Figure 2 shows π^--^{12}C elastic scattering at 162 MeV and the comparison with static and nonstatic calculations. In order to bring the minimum of the static calculation in agreement with experiment, a reduction of the nuclear radius by 5-10% would be necessary. The nonstatic description reproduced the position of the first minimum correctly, and the remaining discrepancy could be traced back to the influence of the Δ-nucleus spin-orbit interaction. Not only the influence of

quasi-free knockout and true pion absorption on elastic scattering could be demonstrated but even a rather quantitative determination of the Δ-nucleus single-particle potential was possible.

The most promising procedure to obtain nuclear radius information seems to be to look for isotopic variations, e.g., shifts of the minima between two isotopes with π^+ and π^-. One can hope that the lack of knowledge will somehow cancel out. Two nuclei are chosen, one with N = Z as reference, the other with an excess of neutrons, like $^{40,48}Ca$, $^{12,13}C$, $^{16,18}O$. In the N = Z nucleus the Coulomb effects can be studied, which are hopefully the only reason of breaking the π^+-π^- invariance. An upper limit has been given for $^{16,18}O$ $\Delta\langle r_n^2\rangle^{1/2} \leq 0.15$ fm by Ingram.[4] For the same quantity, a value of (0.21 ± 0.03) fm has been quoted by Johnson et al.[5] from low energy scattering. Here the large s-wave isovector part of the πN interaction and the relatively small sensitivity to details of the optical potential were exploited to deduce the quoted small error.

In Table 1 are listed experimental values for $^{40,48}Ca$, including determinations from total cross section differences[6] and π^- atoms.[7] Also in these cases, objections have been raised concerning the influence of phase space difference for outgoing nucleons from π^- absorption for the former[15] and the theoretical justification of the ρ^2 and $\Delta\rho^2$ terms in the optical potential for the latter.[16]

TABLE I

Radius difference for neutron distributions in ^{48}Ca versus ^{40}Ca obtained by various authors.

Method	$\Delta\langle r_n^2\rangle^{1/2}$ [fm]	References
600 MeV pp	0.20 ± 0.06	8)
1 GeV pp	0.16 ± 0.03	9)
800 MeV $\vec{p}\vec{p}$	0.13 ± 0.04	10)
1.3 GeV αα	0.22 ± 0.07	11)
$\Delta\sigma_{tot}(\pi^+, \pi^-)$	0.14 ± 0.05	6)
π-atoms	0.24 ± 0.07	7)
Coulomb energy	0.06	12)
HFD	0.18	13)
HFD	0.27	14)

Some confidence perhaps can be gained from the agreement of the values from widely different methods. The proposal by Moniz[17] to use the data together with Hartree-Fock calculations to study the isospin dependence of the optical potential appears to be somewhat precarious considering the scatter of the latter as seen in Table 1.

III. INELASTIC, CHARGE EXCHANGE, AND DOUBLE CHARGE EXCHANGE REACTIONS

New interesting results are expected from quasi-elastic scattering,[18] single[19] and double charge exchange,[20] and in particular, from a combined interpretation. Preliminary zero degree single charge exchange data for $^{40-48}Ca$[19] are shown in Fig. 3. It is seen that the isobaric analog state (IAS) is strongly excited as N-Z becomes larger. According to a semiclassical model by Johnson and Bethe,[19a] analog state charge exchange is proportional to $(\Delta\rho)^2/N\text{-}Z$, and analog state double charge exchange is proportional to the square of this expression, where $\Delta\rho$ is the valence neutron density. Figure 4 shows double charge exchange (DCE) data for ^{12}C and $^{40-48}Ca$ at 290 MeV.[20] The ratio for π^--induced and π^+-induced DCE drops by more than a factor of 10 in going from ^{40}Ca to ^{48}Ca. Although, large isotope effects are seen (also for quasi-elastic backward scattering from $^{16,18}O$, see below) any quantitative interpretation must wait for a more sophisticated and, preferably, combined theoretical treatment.

A similar high sensitivity to the pion charge is expected for inelastic scattering to bound single particle states. With the high resolution of the two pion spectrometers, EPICS at LAMPF and SUSI at SIN, these studies are beginning to yield rather detailed nuclear structure information. Figure 5 shows one of the most famous examples, $\pi^\pm$ scattering at 162 MeV from ^{13}C.[21] The state at 9.5 MeV is excited by π^- 9 times stronger than by π^+, a value consistent with a pure neutron excitation. On the other hand, a group of states at 16 MeV is excited more strongly by π^+. Simple shell model weak coupling considerations gave qualitative agreement with the observations,[21] although more refined calculations[22] must be done in order to understand the relatively weak discrimination for states otherwise known as single neutron states. The same method of high resolution inelastic scattering with π^+ and π^- has been applied also to T = 0 targets. Figure 6 shows $\pi^\pm$ scattering at 162 MeV from ^{12}C;[23] the interesting structure appearing at ~ 19.5 MeV, where two states with different isospin mix, give the bipolar shape in the difference spectrum. Recently a three-level, isospin mixing has been observed for 4^- states in ^{16}O.[24] It is likely that by comparing π^+ with

π^- inelastic scattering to isospin mixed states in self-conjugate nuclei, a determination of the charge dependence in the short-range part of the nuclear force will be possible.

IV. QUASI-FREE SCATTERING AND ABSORPTION

I tried to show that nuclear structure information can be obtained only by comparison of the data with rather refined microscopic calculations. These calculations should also be able to reproduce the other large contributions to the total cross section, the reaction cross section and, moreover, the contributions from quasi-free and absorptive reactions. Only recently the gross features, i.e. the mass and energy dependence of these cross sections, could be determined.[25-30] Navon et al.[25-27] measured inclusive pion scattering at 6 energies between 85 and 315 MeV for 6 targets between Li and Bi. In a second experiment, the cross section,

$$\sigma_{tr}(\Omega) = \sigma_{abs} + \sigma_{CEX} + \int_{\Omega}^{4\pi} \frac{d\sigma_{sc}}{d\Omega}\, d\Omega \quad ,$$

for removal of charged pions out of the solid angle Ω was determined, where $d\sigma_{sc}/d\Omega$ is the inclusive differential scattering cross section (measured in the first experiment), which includes elastic scattering, inelastic scattering to bound states, quasi-elastic scattering and the small double charge exchange scattering cross sections. By extrapolating $\sigma_{tr}(\Omega) - \int_{\Omega}^{4\pi} (d\sigma_{sc}/d\Omega)d\Omega$ to $\Omega = 0$ the sum of absorption and single charge exchange cross sections was obtained, and after (in most cases) a small correction for the latter, the cross section for true pion absorption was obtained. By comparison with data for total cross sections[31] and data and calculations for elastic cross sections a decomposition of the total cross section was made and the energy and mass dependence parametrized through power laws. The data have been extended to lower energy at TRIUMF.[32]

Nakai et al.[28] used a different technique to determine the absorption cross sections for 5 elements from Al to Au and at energies between 23 and 280 MeV. Gamma-ray spectra and γ-γ coincidences were measured with NaI(Tl) detectors with and without the requirement of an additional coincidence with a scattered pion. From the data the γ-ray multiplicity and the absorption cross section were deduced. Figure 7 shows the angular distribution for π^+ inclusive scattering at resonance.[27] At forward angles elastic scattering predominates, as indicated by the dashed lines, resulting from calculations with the program PIRK.[33] At backward angles

the cross section is almost totally inelastic and the shape of the angular distribution follows the shape of the free pion-nucleon scattering. This similarity suggests that the scattering to backward angles can be described as a quasi-free process. This hypothesis is supported by the shape of the energy spectrum measured for pions scattered to backward angles.[4] The normalization factor N_{eff} needed to bring the sum of the free π^+p and π^-p (equal to π^+n) cross sections in agreement with the data is a measure of the effective number of nucleons which participate in the process. N_{eff}, shown in Fig. 8, has almost the same shape for all targets. The minimum at resonance reflects the behavior of the mean free path of the pion in the nucleus, being smallest here because of strong absorption. As outlined above, the inclusive angle-integrated inelastic cross section was also obtained and can be divided by $N_{eff} \cdot \sigma(\pi N)$. This ratio is shown in Fig. 9, and is seen to be fairly constant at higher energies, independent of energy and A, with a value of 0.6 - 0.8. It reflects the effects of Pauli blocking, which reduces the quasi-elastic forward scattering. The effect has been directly observed in emulsion studies[34] and recently in quasi-elastic scattering with the *SUSI* spectrometer,[4] and has been interpreted in terms of a reduced width of the intermediate Δ in the presence of other nucleons.[3] At 60 MeV, Gismatullin et al.[34] found an enhancement in the forward direction and a corresponding enhancement of low energy protons, in line with our observation that in heavier targets at lower energy the quasi-elastic cross section in the forward direction is enhanced compared to the free π-nucleon cross section. Related to this observation are the experiments on quasi-elastic single charge exchange done by Bowles et al.[35] N_{eff} very near to this in Fig. 8 have been found, which together with the shape of the π^0 spectrum favors the quasi-elastic nature of this process. For ^{16}O at 50 MeV incident energy at forward angles, an enhancement is also found, which together with the observation of low energy components in the forward π^0 energy spectrum (Fig. 10) suggests multistep processes or the excitation of particle-unstable collective resonances. Such giant resonance excitation for forward scattered pions at energies of 163 and 241 MeV has been observed by Arvieux et al.,[36] and a suggestion is to look at them at lower energy and for heavy targets. On the other hand multistep processes are difficult to isolate at forward angles. They have been observed at 60° for ^{16}O (Ref.4), as seen for 240 MeV in Fig. 11 taken from Ref. 37. Data from quasi-elastic scattering of pions are compared with those from electron scattering[38], a calculation for single scattering from Ref. 39, and with data from inclusive double charge exchange at 50°. The isotropic angular distribution

of the latter and the low energy of the outgoing pions support the expected picture of multiple quasi-free scattering in the DCE reaction. An arbitary factor of 15 was necessary to bring the cross section for DCE scattering to the same scale as that for quasi-elastic scattering in the low energy part of Fig. 11, whereas a factor of 26 is expected from (3,3) dominance and double scattering. The angle integrated cross section of (5.8 ± 0.9) mb multiplied by 15 can be compared to 285 mb total inelastic cross section to obtain a 30% contribution of multiple scattering at 240 MeV.

Figure 12 shows the absorption cross sections as measured by the two groups mentioned above[27,28] and as calculated by Stricker et al.[40] Although there is general agreement on the order of magnitude of this cross section, there are marked differences between the two experiments. Whereas the KEK data[28] exhibit a rather flat energy dependence and peaking at ~100 MeV, the SIN cross sections,[27] at least for light targets, show a pronounced peaking near 160 MeV. In fact, as seen from Fig. 13 for ^{12}C (Ref. 27), the absorption cross section shows the strongest energy dependence of all the particle cross sections. Large differences for π^+ and π^- absorption are seen in both experiments and ascribed to Coulomb effects, which is supported by the calculation of Stricker et al.,[40] who use an optical potential derived from pionic atom data. These calculations predict insufficient absorption for energies above the resonance. A comparison of the absorption cross section for ^{12}C with other theoretical predictions is presented in Fig. 14. Lenz and Moniz[41] derive a spreading potential for the Δ in the nuclear medium from comparison with total and elastic cross sections in light nuclei, which in turn is used to predict pion absorption via the $\Delta N \rightarrow NN$ process. A partial wave decomposition shows that for peripheral waves inelastic scattering dominates, whereas the absorption width decreases with increasing ℓ. Ginocchio and Johnson[42] studied the pion and Δ optical potentials with special emphasis on properly accounting for pion and nucleon distortions through Monte Carlo intranuclear cascade calculations. Hüfner and Thies[43] compute inclusive inelastic pion nucleus reactions using a transport model, and apparently overestimate absorption at the high energies. Common to all these approaches is the strong interrelation between quasi-free scattering and absorption,[44] the latter taking strength away from the former (mainly from multiple scattering), thereby guaranteeing the convergence of the multiple scattering expansion. This strong interconnection can be seen from Table 2, which contains data for $^{16,18}O$.[45]

TABLE II

E_π	Target	Projectile	N_{eff}	σ_{abs} [mb]
165 MeV	^{16}O	π^+	1.52	216
		π^-	1.51	206
	^{18}O	π^+	1.28	267
		π^-	1.84	227
315 MeV	^{16}O	π^+	5.11	98
	^{18}O	π^+	5.27	89

For π^-, quasi-free scattering (proportional to N_{eff}) at resonance is stronger for ^{18}O than for ^{16}O, as expected from the two extra neutrons, whereas absorption is about equal. For π^+, although π^+ scattering takes place primarily with protons, which have essentially the same distribution in $^{16,18}O$, scattering is reduced (about 15%) in ^{18}O because absorption is increased (about 25%). Absorption here is thought to proceed via $\pi^+pn \rightarrow \Delta^{++}n \rightarrow pp$ and therefore depends on the neutron density and takes flux away from the quasi-elastic channel, $\Delta^{++} \rightarrow \pi^+p$. The various cross sections have been parametrized in Ref. 27 by power laws, from which one can see that absorption and elastic scattering, being connected with the small partial waves, take an increasing fraction of the total cross section with increasing mass, whereas (peripheral) quasi-free scattering loses importance in heavy targets.

V. KNOCKOUT AND SPALLATION REACTIONS

Having elucidated the gross features of the partial cross sections, one can ask what the main contributions to the partial reaction cross sections are. It is believed that quasi-free scattering proceeds mainly through one-nucleon knock-out and absorption mainly through the quasi-deuteron process. To verify this hypothesis (π,πN) and (π, 2N) reactions have to be measured. Although systematic

studies are lacking, there are indirect indications for the dominance of these processes from activation measurements (only knockout to bound final states can be observed)[46-48], from on-line γ-spectroscopy,[49,50] from single arm proton spectroscopy,[51-54] and from γ-particle coincidence measurements.[55-60] Apart from emulsion studies[61,62,34] only a few π^--particle coincidence experiments are available.[63,64,53] The quantity most discussed in the knockout reaction is the ratio for knockout of protons or neutrons by π^+ and π^-. In activation experiments, where angle integrated cross sections to bound final states are measured and where also charge exchange contributes to the one nucleon removal, ratios less than 3 (the value expected from the impulse approximation) are measured for neutron removal with π^- and π^+.[47] Of the many explanations for this phenomenon the most successful seems to be the model of Sternheim and Silbar,[65] who invoke nucleon charge exchange to account for the deviations. Since the nucleon charge exchange cross sections drop like $T^{-1.9}$ and since the free ratio is dependent on the scattering angle in the c.m. system, quite different suppression can be obtained in coincidence experiments, where, for example, forward protons are measured in coincidence with backward pions.[63] In fact, too much charge exchange is predicted,[65] while experimentally the ratio corresponds to the free ratio for the excitation of ^{11}B bound states from forward knockout in ^{12}C.[63] Preliminary results from (π, πN) coincidence measurements done at SIN with plastic counters are shown in Fig. 15. The proton (not yet corrected for deuteron contamination) angular distribution, with the pion detector fixed at 90 and 120°, is shown for π^+ and π^- at 245 MeV on ^{12}C, where we have multiplied the π^- scale by 5.8, corresponding to the free π^+:π^- ratio at this angle. In Fig. 16 this ratio is plotted for other π angles and compared with the free ratios. This agreement and the peaking at the quasi-free angle again shows the dominance of the one-nucleon knockout process. In the SIN experiment the energy and mass dependence of this reaction, as well as the (π,2N) reaction, is being studied.

From a comparison of the results of Ref. 46 with those of Ref. 27, one concludes that for ^{12}C at resonance more than 50% (150 mb) of the inelastic cross section is exhausted by one-nucleon knockout. The same holds true for 60-MeV emulsion studies.[62] For heavier nuclei, where knockout accounts for only ~ 12%,[47] the knockout ratio from activation measurements is not changed drastically,[47] although the predictions of the nucleon charge exchange model,[65] which are very sensitive to the assumption of analog dominance in heavy nuclei, do not agree very well with experiment. Instead, the results of intranuclear cascade calcu-

lations,[66,42] underestimating mainly (π^-,p) or (π^+,n) cross sections in low mass nuclei, are in better agreement with experiments in heavy nuclei. However, in heavy nuclei, where the contribution of absorption gets more important,[27] just this absorption is underestimated by the intranuclear cascade calculations,[47] manifesting itself in an underestimation of the yields of residual masses far from the target mass. These spallation reactions are characterized by the removal of a large number of nucleons. The mean number $\langle\Delta A\rangle$ of nucleons removed by pions from Au increases linearly with energy,[47]

$$\langle\Delta A\rangle \approx 7 + 0.015 \cdot T_\pi \text{ [MeV]} \quad ,$$

which is the same energy dependence as for proton induced reactions in the Ni region,[67]

$$\langle\Delta A\rangle \approx 2 + 0.015 \cdot T_p \text{ [MeV]} \quad .$$

For stopped pions and medium mass to heavy nuclei this quantity increases linearly with the target mass[68]

$$\langle\Delta A\rangle \approx 5.5 + 0.0072 \cdot A \quad .$$

For the different residual elements the distributions over the isotopes are very well fitted by Gaussians,[68] the widths of which for stopped pions are again linearly increasing with Z, like

$$\text{FWHM}(n) \approx Z/10 \quad .$$

From a study of the Ni isotopes with stopped π^- the asymmetry between removal of neutrons and protons has been determined by particle spectroscopy to vary linearly with target isospin:

$$\langle N\rangle - \langle Z\rangle \approx 1.2\ T$$

as can be seen from Figs. 17 and 18. This result is twice that obtained from proton-induced reactions between 80 and 200 MeV.[67]

Since these yields mainly are determined by the evaporative phase of the reaction, they are determined by the amount of energy deposited in the nucleus. For pion-induced reactions, the main energy transfer comes from π absorption, where half the pion rest mass energy is transferred to the nucleus, the other half being transferred as kinetic energy to one nucleon.[69] In proton-induced reactions at ~ 100 MeV the protons similarly lose about half of the energy, thus leaving the nucleus excited to 50 MeV.[70] From this consideration, it follows that comparisons between p-, π^+-, and π^--induced spallation reactions should be done at comparable total energy (including the pion rest mass), and that proton (neutron) multiplicities measured by particle spectroscopy should be increased (decreased) by one unit, respectively, for π^-- compared to π^+- and p-induced reactions. Element yields should peak at one neutron less (more) for $\pi^+(\pi^-)$ ("memory effect") compared to p-induced reactions. All differences should vanish with increasing bombarding energy. The experiments are in fair agreement with this picture (see Figs. 17, 18 and e.g. Refs. 67, 68, 71-75). Small deviations[72] can be explained by Coulomb effects for the incoming pion and/or binding effects for outgoing nucleons. The large isotope effect for high energy protons (factor of 2 between ^{58}Ni and ^{64}Ni) seen in Figs. 17 and 18 can only partly be explained by binding energy effects as calculated with the exciton model (factor ~ 1.4).[76]

VI. CONCLUSION

We now have better data on not only elastic and total cross sections, but also on inelastic excitations of bound and unbound states and on partial reaction cross sections, quasi-free absorption, single and double charge exchange. The variation of target mass and the beam energy turns out to be a very powerful tool. Great progress has been made during the past few years to develop microscopic theories of pion-nucleus interactions, the improvement being the unification of elastic, quasi-elastic, and absorption cross sections. We still probably have not reached the position where our understanding of the pion-nucleus problem is sufficient to extract neutron radii. The next step will be to do $(\pi,\pi N)$ coincidence experiments in order to single out single and multiple scattering and the eventual contribution of giant resonance excitations in quasi-free scattering. On the other hand, (π, two particles) coincidence experiments should be done as a function of energy and target mass to separate the quasi-deuteron mechanism from the large effects of final state interactions. Last but not least, systematic

single charge exchange data are needed to obtain smaller errors for the absorption cross sections measured by Ashery et al.[27] and by Nakai et al.[28]

NOTES ADDED IN PROOF

Absorption cross sections for ^{12}C between 90 and 140 MeV were recently measured by Sober et al.[77] by a calorimetric technique. The resulting values are larger than those of Ref. 26, 27 by a factor of ~1.8.

Quasi-elastic scattering for ^{12}C and $^{40-48}Ca$ at 180 and 290 MeV at 60° and 120° has been measured by Burleson et al.[78] Strong deviations from quasi-free single scattering are seen at 60°. A very simplified model, not including absorption, leads to N_{eff} larger than those of Ref. 27 and a larger multiple scattering contribution of 50%.

REFERENCES

1. B. Zeidman et al., Phys. Rev. Lett. 40, 1316 (1978).
2. C. Olmer et al., Phys. Rev. C 21, 254 (1980).
3. F. Lenz and M. Thies, preprint MIT CPT #832, 1980.
4. C. H. Q. Ingram, Proc. of the 2nd Conference on Meson-Nuclear Physics, E. V. Hungerford, ed., Houston 1979, p. 455 and to be published.
5. R. R. Johnson et al., Phys. Rev. Lett. 43, 844 (1979).
6. M. J. Jakobson et al., Phys. Rev. Lett. 38, 1201 (1977).
7. R. J. Powers et al., Nucl. Phys. A336, 475 (1980).
8. I. Brissaud and X. Campi, Phys. Lett. 86B, 141 (1979).
9. S. Shlomo and R. Schaefier, Phys. Lett. 83B, 5 (1979).
10. L. Ray Phys. Rev. C 19, 1855 (1979).
11. G. Alkhazov et al., Nucl. Phys. A280, 365 (1977).
12. J. A. Nolen and J. P. Schiffer, Ann. Rev. Nucl. Sci. 19, 475 (1969).
13. H. S. Köhler, Nucl. Phys. A258, 301 (1976).
14. J. W. Negele, Phys. Rev. C 1, 523 (1970).
15. R. S. Bhalerao et al., Phys. Rev. C 21, 1903 (1980).

16. L. S. Kisslinger and A. N. Saharia, preprint 1980.

17. E. J. Moniz, Proc. of the 2nd Conference on Meson-Nuclear Physics, E. V. Hungerford, ed., Houston 1979, p. 288.

18. G. S. Blanpied et al., Proc. of the 2nd Conference on Meson-Nuclear Physics, E. V. Hungerford, ed., Houston 1979, p. 281.

19. D. Bowman, LAMPF, private communication 1980.

19a. M. B. Johnson and H. Bethe, Comments in Nuclear and Particle Physics 8, 75 (1978).

20. J. Davis et al., Phys. Rev. C 20, 1946 (1979).

21. D. Dehnhard et al., Phys. Rev. Lett. 43, 1091 (1979).

22. T. S. H. Lee and D. Kurath, Phys. Rev. C 21, 293 (1980).

23. C. L. Morris et al., Phys. Lett. 86B, 31 (1979).

24. W. J. Braithwaite et al., LAMPF Progress Report 1980, p. 105.

25. I. Navon et al., Phys. Rev. Lett. 42, 1465 (1979).

26. I. Navon et al., Phys. Rev. C, in press.

27. D. Ashery et al., Phys. Rev. C, to be published.

28. K. Nakai, Phys. Rev. Lett. 44, 1446 (1980).

29. K. Aniol et al., Bull. Am. Phys. Soc. 25,4, 505 (1980).

30. S. J. Sanders et al., Bull. Am. Phys. Soc. 25,4, 560 (1980) and private communication.

31. A. S. Carroll et al., Phys. Rev. C 14, 635 (1976).

32. D. Ashery, Tel Aviv, private communication 1980.

33 R. A. Eisenstein and G. A. Miller, Comp. Phys. Comm. 8, 130 (1974).

34. Y. R. Gismatullin et al., Sov. J. Nucl. Phys. 11, 159 (1970); 19, 22 (1974); 21, 488 (1975).

35. T. J. Bowles et al., Phys. Rev. Lett. 40, 97 (1978) and to be published in Phys. Rev. C.

36. J. Arvieux et al., Phys. Rev. Lett. 42, 753 (1979) and Phys. Lett. 90B, 371 (1980).

37. R. E. Mischke et al., Phys. Rev. Lett. 44, 1197 (1980).

38. J. Mougey et al., Phys. Rev. Lett. 41, 1645 (1978).

39. M. Thies, Y. Horikawa, and F. Lenz, private communication 1979.

40. K. Stricker et al., Phys. Rev. C 19, 929 (1979).

41. F. Lenz and E. J. Moniz, to be published in Comments in Nuclear and Particle Physics.

42. J. N. Ginocchio and M. B. Johnson, Phys. Rev. C 21, 1056 (1980).

43. J. Hüfner and M. Thies, Phys. Rev. C 20, 273 (1979).

44. D. Koltun, Proc. of the 2nd Conference on Meson-Nuclear Physics, E. V. Hungerford, ed., Houston 1979, p.87.

45. I. Navon et al., to be published in Phys. Rev. Lett.

46. B. J. Dropesky et al., Phys. Rev. C 20, 1844 (1979).

47. S. B. Kaufmann et al., Phys. Rev. C 21, 262 and 2293 (1979); and E. P. Steinberg et al., Proc. Int. Conf. on Nuclear Reaction Mechanisms, Verenna 1979, p. 329.

48. L. B. Church and A. A. Caretto, Phys. Rev. C 21, 246 (1980).

49. H. S. Plendl et al., Proc. Int. Conf. on Reaction Mechanisms, Varenna 1979, p. 345.

50. J. E. Bolger et al., Phys. Rev. Lett. 37, 1206 (1976).

51. H. E. Jackson et al., Phys. Rev. C 16, 730 (1977).

52. H. E. Jackson et al., Phys. Rev. Lett. 39, 1601 (1977).

53. T. C. Sharma et al., Nucl. Phys. A333, 461 (1980).

54. R. D. McKeown et al., Phys. Rev. Lett. 44, 1033 (1980).

55. R. Legrain et al., Phys. Lett. 74B, 207 (1978).

56. R. Legrain et al., Proc. of the 2nd Conference on Meson-Nuclear Physics, E. V. Hungerford ed., Houston 1979, p. 180.

57. R. E. Adams et al., Proc. of the 2nd Conference on Meson-Nuclear Physics, E. V. Hungerford ed., Houston 1979, p. 178.

58. V. G. Lind et al., Proc. of the 2nd Conference on Meson-Nuclear Physics, E. V. Hungerford ed., Houston 1979, p. 284.

59. Y. Cassagnou, Proc. Conf. on Clustering Aspects of Nuclear Structure and Nuclear Reaction, Winnipeg 1978, p. 434.

60. J. Julien et al., to be published in Phys. Rev. C.

61. Y. A. Berdnikov et al., Sov. J. Nucl. Phys. 25,5, 499 (1977); 25,6, 610 (1977).

62. Y. R. Gismatullin and I. A. Lantsev. Sov. J. Nucl. Phys. 29,5, 588 (1979).

63. R. J. Ellis et al., Proc. of the 2nd Conference on Meson-Nuclear Physics, E. V. Hungerford ed., Houston 1979, p. 274: and J. Arvieux et al., Sin Newsletter No. 12, 1979. p. 19.

64. L. W. Swenson et al., Phys. Rev. Lett. 40, 10 (1978).

65. M. M. Sternheim and R. R. Silbar, Phys. Rev. C 21, 1974 (1980); see also R. R. Silbar et al., Phys. Rev. C 18, 2785 (1978); C 15, 371 (1977).

66. J. N. Ginocchio, Phys. Rev. C 17, 195 (1978).

67. M. Sadler et al., Phys. Rev. Lett. 38, 950 (1977).

68. H. S. Pruys et al., Nucl. Phys. A316, 365 (1979).

69. M. P. Locher and F. Myhrer, Helv. Phys. Acta 49, 123 (1976).

70. H. D. Holmgren et al., Contributed paper to 9th Int. Conf. on Few Body Problems, Eugene, OR. Aug. 1980, and A. A. Cowley et al , Contributed paper to Int. Conf. on Nuclear Physics, Berkeley, CA, August 1980.

71. J. R. Wu et al., Phys. Rev. C 19, 698 (1979).

72. C. J. Orth et al., Phys. Rev. C 21, 2524 (1980).

73. C. J. Orth et al., Phys. Rev. C 18, 1426 (1978).

74. P. E. Haustein and T. J. Ruth, Phys. Rev. C 18, 2241 (1978).

75. L. B. Church and A. A. Caretto, Phys. Rev. C 21, 246 (1980).

76. T. Kozlowski and Z. Zglinski, SIN, private communication 1980.

77. D. I. Sober et al., Phys. Rev. C 21, 1495 (1980).

78. G. R. Burleson et al., Phys. Rev. C 21, 1452 (1980).

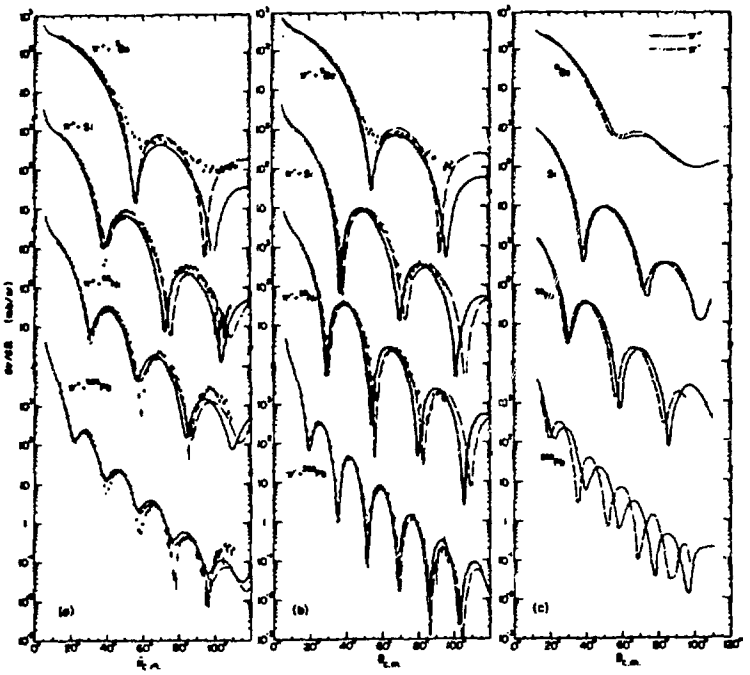

Fig. 1.

Angular distributions for elastic scattering of 162 MeV (a) π^+ and (b) π^- by ^{9}Be, Si, ^{58}Ni, and ^{208}Pb from Ref. 1. The curves result from optical potential calculations. c) Comparision of π^+ and π^- scattering with smooth curves representing the data.

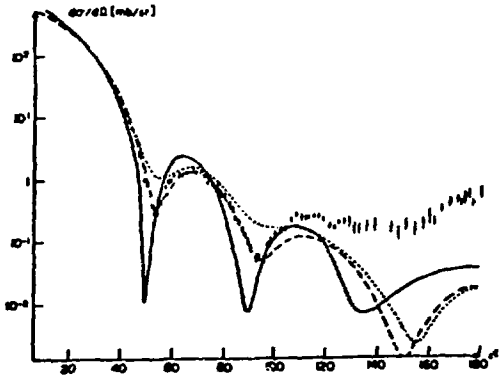

Fig. 2.

$\pi^- - ^{12}$C scattering at 162 MeV taken from Ref. 3. Data are compared with static (solid line) and nonstatic calculations. Short dashed: central spreading potential only. Long dashed: Δ-nucleus spin-orbit interaction included.

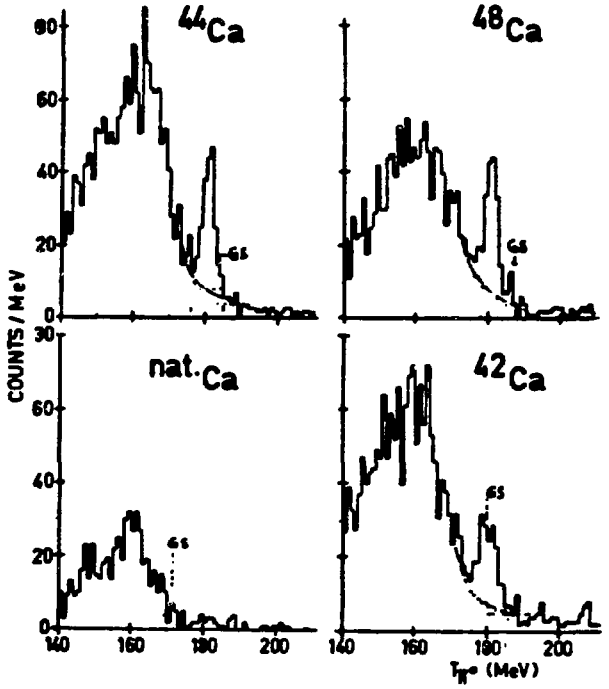

Fig. 3.

Preliminary energy spectra of π^0 at 0° from the charge exchange (π^+,π^0) reaction on the Ca isotopes at 180 MeV.[19] The excitation of the isobaric analog state is seen to increase with target isospin. The data are not normalized yet.

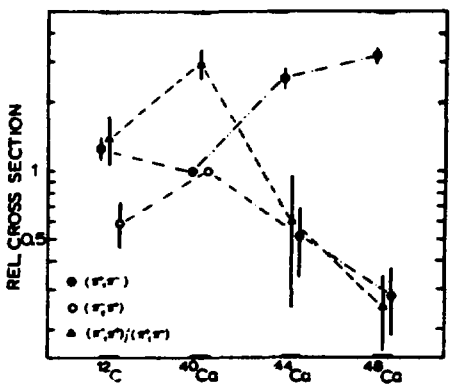

Fig. 4.

Double charge exchange cross sections at 60° for π^+ and π^- and their ratio at 290 MeV, integrated over outgoing π energy from 175 to 255 MeV and normalized to ^{40}Ca. For ^{40}Ca the cross sections are (4.3 ± 0.4) and (12.7 ± 1.6) μb/sr MeV for π^+ and π^-, respectively. Data are taken from Ref. 20.

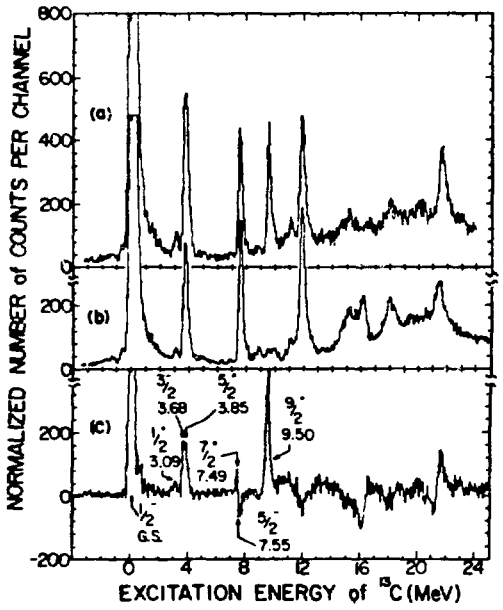

Fig. 5.

Normalized yield spectra (a) Y_{π^-} and (b) Y_{π^+} for $^{13}C(\pi^{\pm},\pi^{\pm\prime})^{13}C^*$ at 162 MeV summed over angles from 62° to 86° and (c) $Y_{\pi^-} - Y_{\pi^+}$ from Ref. 21.

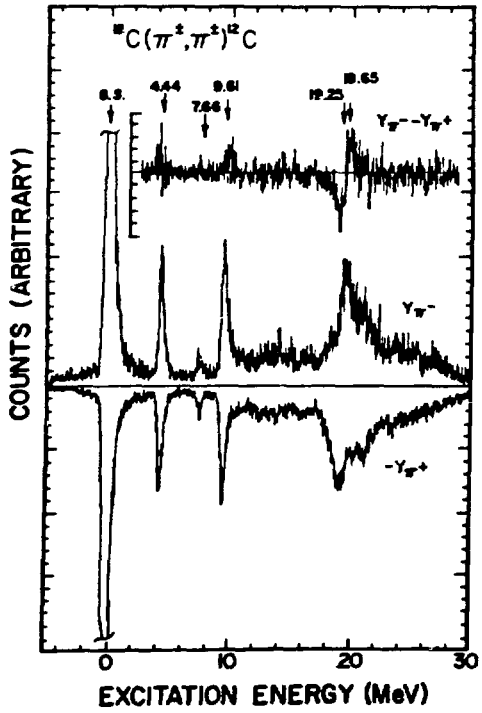

Fig. 6.

Normalized yield spectra Y_{π^-} and $-Y_{\pi^+}$ for $^{12}C(\pi^{\pm},\pi^{\pm\prime})^{12}C^*$ at 162 MeV and 70° and (insert on top) $Y_{\pi^-} - Y_{\pi^+}$ from Ref. 23.

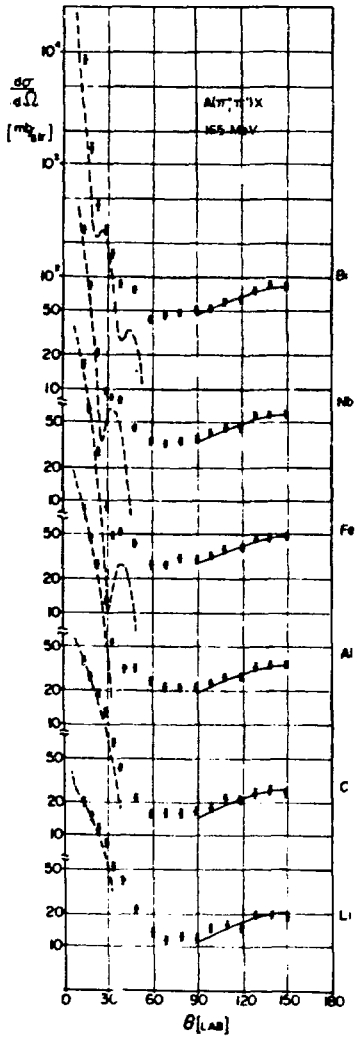

Fig. 7.

Differential scattering cross section of 165 MeV π^+ on 6 nuclei from Li and Bi. Dashed lines at forward angles are the result of elastic scattering calculations. Solid lines are the free (π^+,p) + (π^+,n) cross section normalized to the date. From Ref. 27.

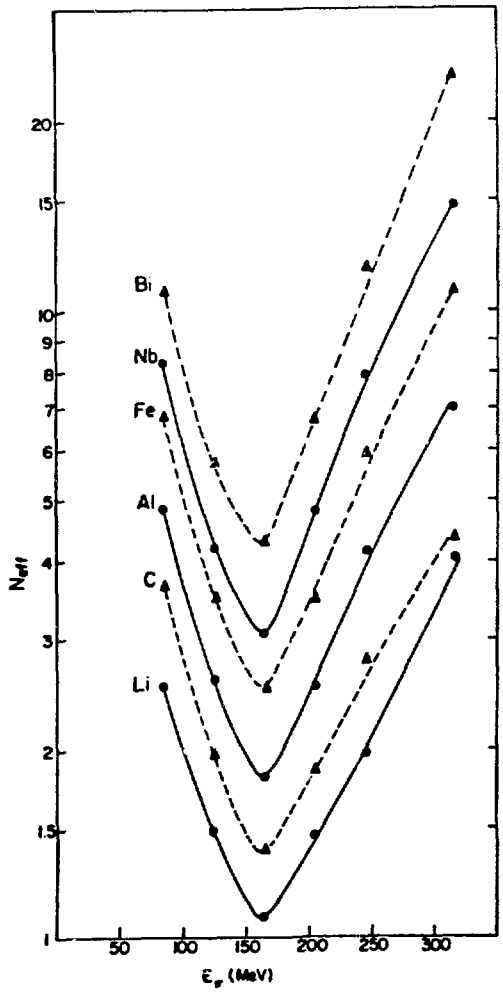

Fig. 8.

N_{eff} from π^+ quasi-free scattering as a function of the bombarding energy. Lines are drawn to guide the eye. From Ref. 27.

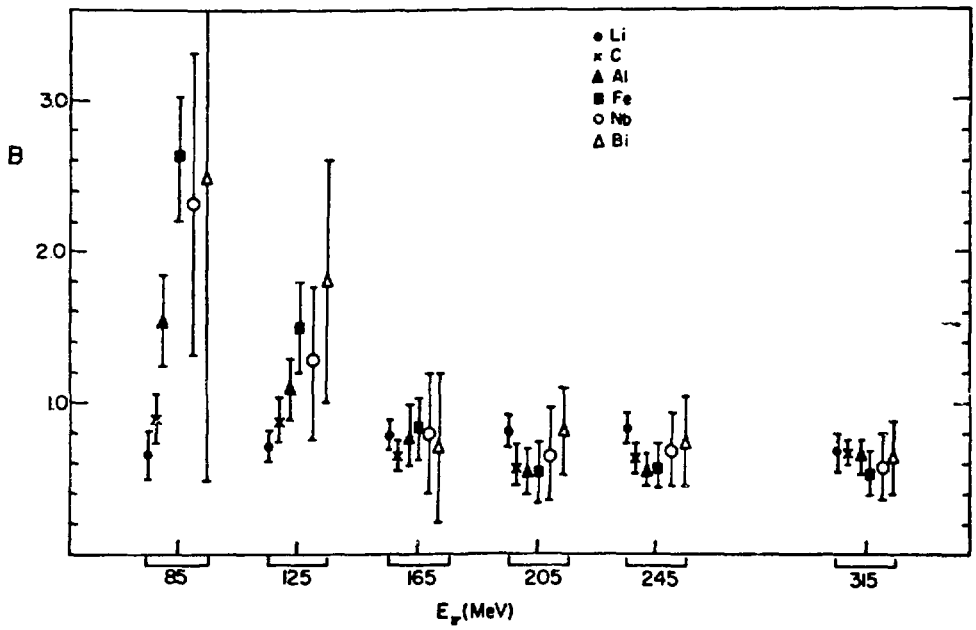

Fig. 9.

Values of $B(A,E) = \sigma_{inel}/N_{eff} \cdot \sigma(\pi N)$ for 6 targets from Li to Bi at 6 energies between 85 and 315 MeV (from Ref. 27).

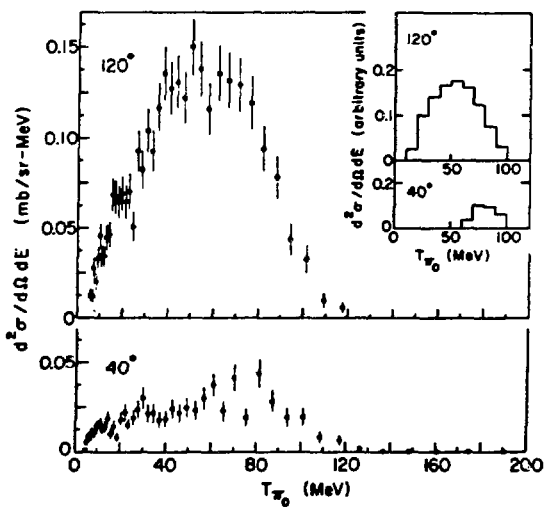

Fig. 10.

Energy spectra of π° emitted in backward (120°) and forward (40°) direction for inclusive single charge exchange on ^{16}O at 100 MeV incident energy (from Ref. 35).

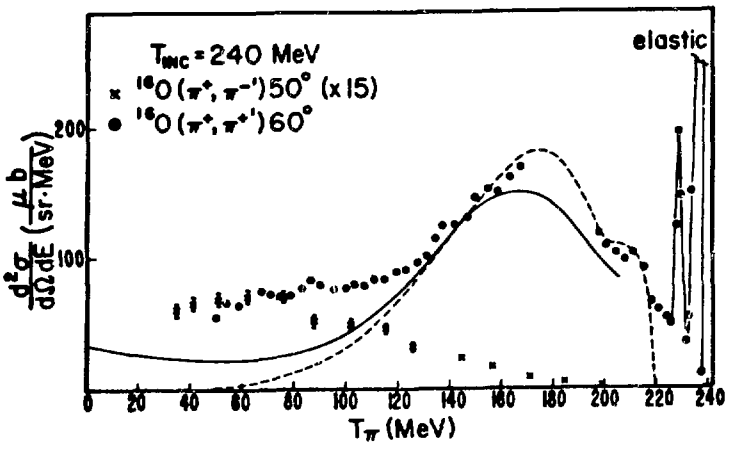

Fig. 11.

Spectra of quasi-elastically scattered pions from ^{16}O at 60° [4] and of double charge exchange from ^{16}O at 50° (multiplied by 15),[37] both at 240 MeV incident energy. Also, shown are (arbitrarily normalized) $^{12}C(e,e')$ data at 60° and 360 MeV (solid curve)[38] and a single scattering calculation (dashed curve).[39]

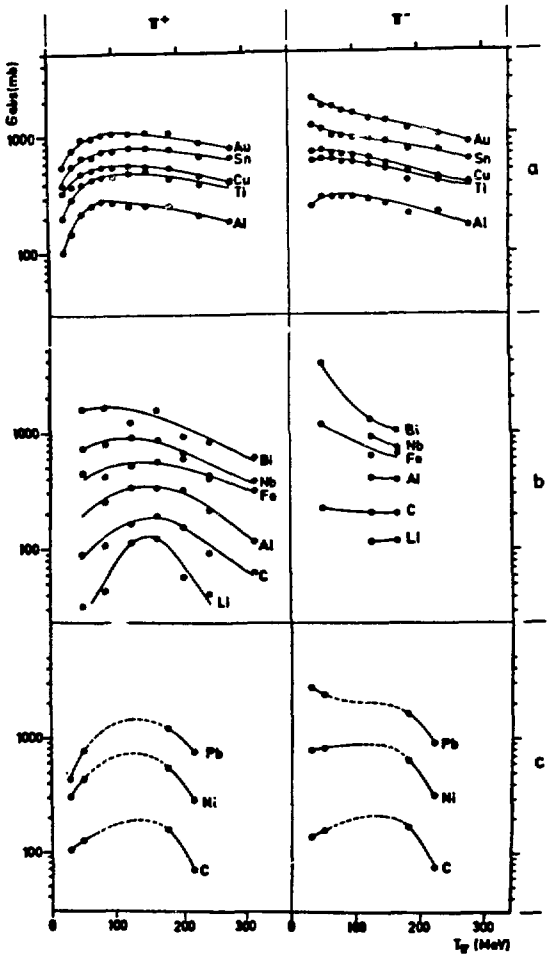

Fig. 12.

Absorption cross sections for several elements between Li and Bi as a function of energy for π^+ (left) and π^- (right)

a) from Ref. 28.

b) from Ref. 27 (open points at 50 MeV from Ref. 32.

c) calculations from Ref. 40. Curves are drawn to guide the eye. Error discussions can be found in the corresponding references.

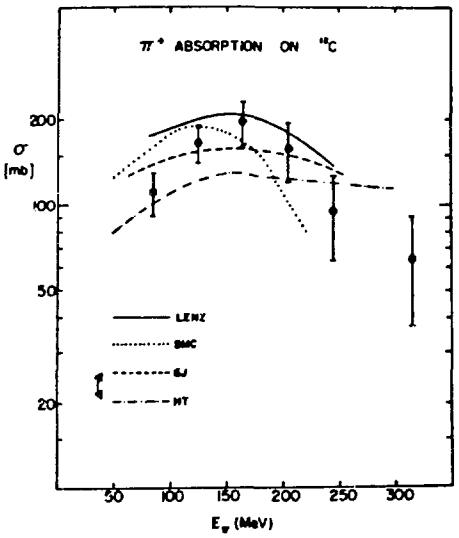

Fig. 13.

Decomposition of the total π^+-^{12}C cross section. Lines are drawn to guide the eye. From Ref. 27.

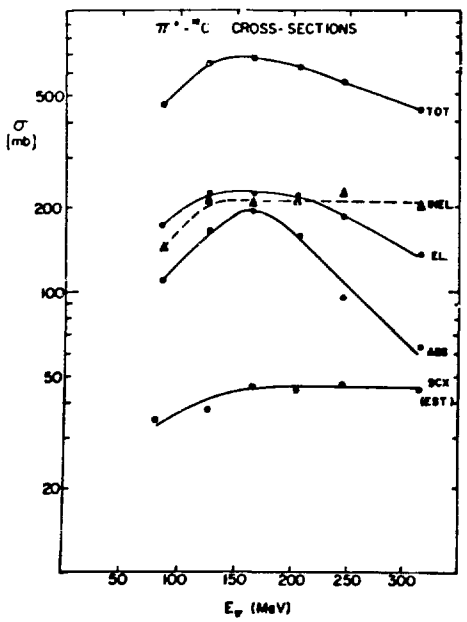

Fig. 14.

True absorption cross section of π^+ on ^{12}C [27] and comparison with calculations from Ref. 41 (solid), Ref. 40 (dotted), Ref. 43 (dashed), and Ref. 42 (dash-dotted).

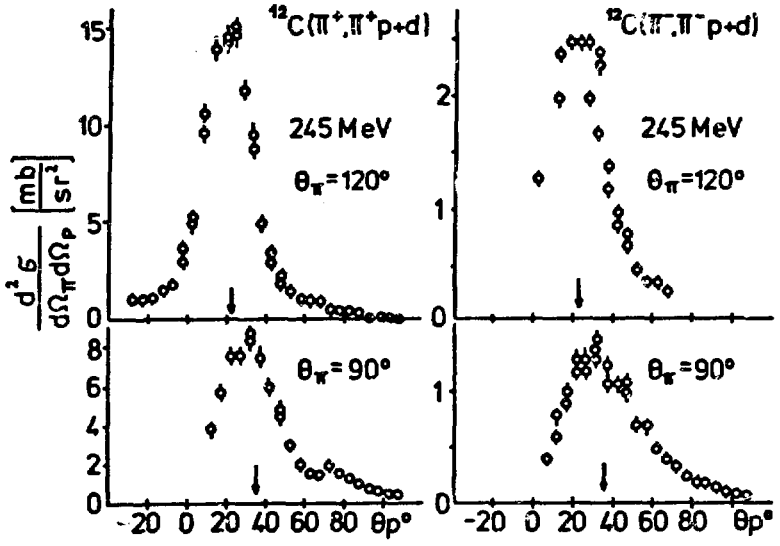

Fig. 15.

Preliminary angular distributions for (π^+,π^+p) and (π^-,π^-p) reactions (not yet corrected for the deuteron contamination) at 120° and 90° pion angle and 245 MeV beam energy. The scale for π^- scattering is 5.8 times that for π^+ scattering corresponding to the free ratio. The arrows mark the angle for the quasi-free kinematics.

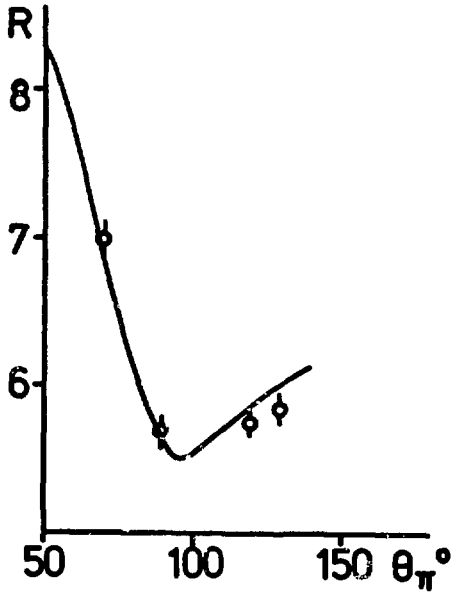

Fig. 16.

Preliminary ratios for knockout of protons (not yet corrected for deuterons) by π^+ and π^- as a function of the pion angle. The line is the corresponding curve for free pion-proton scattering.

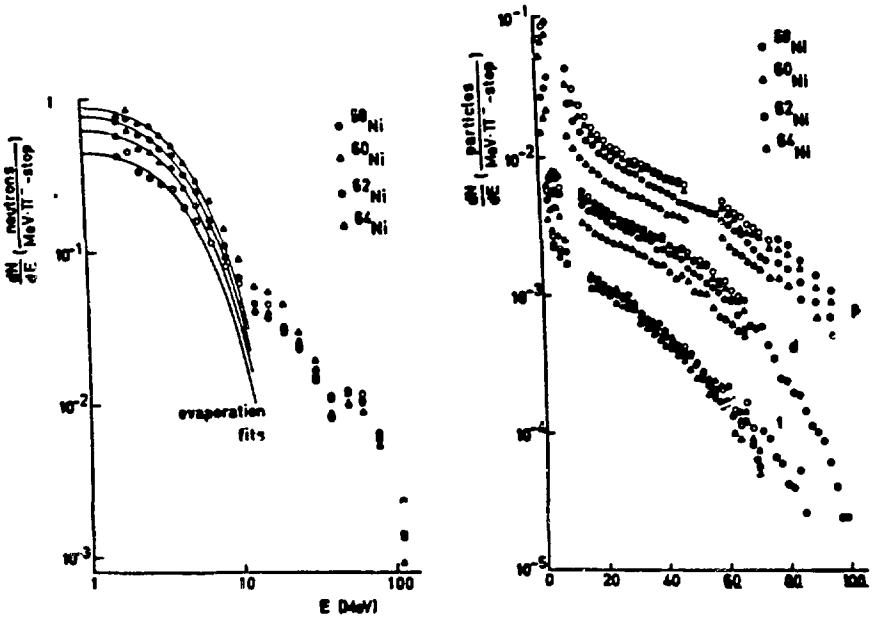

Fig. 17.

Neutron (left) and charged particle (right) spectra from π^- absorption at rest in the Ni isotopes.

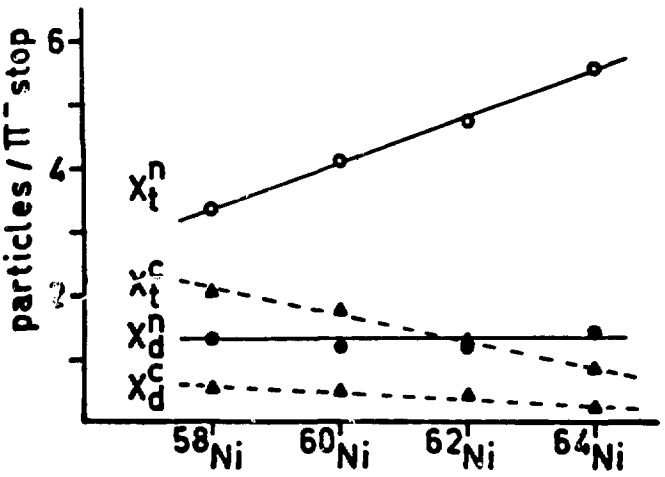

Fig. 18.

Multiplicities of neutrons and charged particles from π^- absorption at rest in the Ni isotopes. Total multiplicities are given as well as those for the direct component, defined for neutrons as total minus fitted evaporation yield, and for charged particles as the yield above 20 MeV.

FORMATION AND PROPERTIES OF MESONIC ATOMS

by

H. Daniel
Physics Department, Technical University of Munich
Garching, Federal Republic of Germany

I. INTRODUCTION

A mesonic particle traveling in matter may react or decay, or it may slow down to about zero energy and then become captured by electromagnetic forces to form a mesonic atom (Coulomb capture). No mesonic band structure matters, although it must exist in crystals, due to the large mass of mesonic particles (μ^-, π^-, K^-, $\bar{p}$, etc.) compared to the electron mass. Also, there is no filling of bands possible as there is never more than one mesonic particle present in the interaction volume.

In order to characterize the mechanisms of energy loss, the quantity

$$W_B = \frac{M}{2}(\alpha c)^2 = \frac{M}{m}\ 13.6\ \text{eV}, \tag{1}$$

where M and m are the mesonic particle and electron rest masses, respectively, α the fine structure constant and c the velocity of light, is a useful number. For mesonic particle energies $W >> W_B$ nothing peculiar happens. At smaller energies, say below 1 MeV for muons, the Barkas effect[1] shows up:

$$S_+(W) > S_-(W), \tag{2}$$

where $S_+(W)$ and $S_-(W)$ are the stopping powers for positively and negatively charged particles of the same kind at energy W. It is due to higher order terms in the Born approximation generally used to calculate the stopping power S(W). Z_1^3 and Z_1^4 terms show up where Z_1 is the charge number of the projectile.

Mesonic particles yield, by direct comparison of S_+ (W) and S_- (W), the Z_1^3 term immediately. The first counter experiment was recently performed by the Munich group.[2] More results are now available.[3] As an example, Table I shows results on Al. They are compared with semiempirical or theoretical results from other groups.[4-6]

TABLE I

Barkas effect in Al. Values of the Z_1^3 term (in per cent of Z_1^2 term)

energy[a] (keV)	v/c	Munich group[b]	Andersen[c]	Ritchie[d]	Jackson[e]
812 (80)	0.213	1.4 ± 0.7	1.4	0.8	0.5
510 (50)	0.098	1.9 ± 0.9	2.5	1.6	0.9
350 (40)	0.081	6.0 ± 1.3	4	2.7	1.5
217 (20)	0.064	7 ± 2	7	5	2.6
108 (10)	0.045	19 ± 5	16	12	6
69 (8)	0.036	23 ± 12	27	20	9

a. in parentheses, fwhm of distribution

b. experimental values (Ref. 2,3)

c. semi-empirical formula based on positive atomic ion data (Ref. 4)

d. theory with adapted parameter (Ref. 5)

e. theory (Ref. 6)

At very low energies, $W \gtrsim W_B$, the energy loss is mostly treated being due to collisions with the electrons forming a Fermi gas. The main feature at kinetic energies $W_{Kin} \gtrsim 0$ is an energy loss proportional to the particle velocity,

$$-\frac{dW}{ds} \propto v. \tag{3}$$

Experimental values[3] are only available for μ^- (cf. Section V.1). No experiment was performed, however, at energies where capture is expected to take place on the basis of the semiclassical theory (cf. Section III.3). This is at energies of the order of 100 eV, depending, of course, on the atomic number Z of the capturing element.

The capture process can either be treated quantum mechanically or semiclassically (cf. Section III).

In matter not containing hydrogen a mesonic particle captured into an individual atom will stay in this atom until it decays or reacts with the nucleus. First, it usually cascades down to lower levels by Auger transitions and later by radiative transitions, emitting mesonic x-rays. The investigation of this cascade is usually done with muons because they yield the maximum information on the electromagnetic cascade. Investigation of a hadronic cascade, on the other hand, yields valuable information about the interaction of the hadron with the nucleus. Usually the hadron interacts before it reaches the 1s level.

In hydrogen-containing matter an effect not discussed before in this paper may occur. It has been established for muons in gaseous hydrogen only. Mesonic hydrogen is electrically neutral. Hence, it can penetrate into other atoms. It then experiences an attractive polarization potential yielding a closer approach to the nucleus of the penetrated atom, which is assumed to have $Z > 1$. The atomic levels of the two systems cross (actually it is a pseudocrossing), and the mesonic particle may be transferred to the heavier atom. A satisfactory theoretical description in agreement with experiment has been given by Holzwarth and Pfeiffer[7] for the case of F.

Mesonic atoms, while existing, are very useful in many fields of physics. Useful information is also obtained from mesonic atoms while disappearing (cf. Section II).

II. SHORT SURVEY OF NEW RESULTS ON MESONIC ATOMS WHILE EXISTING OR BEING ANNIHILATED

1. Muonic atoms

For a variety of "applications" the nucleus is just an accumulation of charge. This is the case in experiments on vacuum polarization. Table II summarizes recent results from the crystal diffraction spectrometer at SIN.[8] The average of the last column for the relative differences of experimental and theoretical wavelengths λ_{ex} and λ_{th}, respectively, is

$$\frac{\lambda_{ex} - \lambda_{th}}{\lambda_{th}} = (4 \pm 8) \times 10^{-6} \quad .$$

TABLE II

Experimental and theoretical wave lengths λ_{ex} and λ_{th}, respectively (ref. 8)

		Experiment λ_{ex}(pm)	Theory (QED) λ_{th}(pm)	$\frac{\lambda_{ex}-\lambda_{th}}{\lambda_{th}}$ (ppm)
^{24}Mg:	$3d_{5/2}$-$2p_{3/2}$	22.05511(19)	22.05500(12)	5(10)
	$3d_{3/2}$-$2p_{1/2}$	21.98616(34)	21.98639(12)	-10(17)
^{28}Si:	$3d_{5/2}$-$2p_{3/2}$	16.18242(23	16.18235(9)	4(15)
	$3d_{3/2}$-$2p_{1/2}$	16.11426(39)	16.11406(9)	12(25)
^{31}P:	$3d_{5/2}$-$2p_{3/2}$	14.08663(38)	14.08669(8)	-4(28)
	$3d_{3/2}$-$2p_{1/2}$	14.02180(130)	14.01863(8)	230(90)

So experiment and theory agree nicely, at least at lower Z. The largest uncertainty, by the way,comes from imperfect knowledge of the status of the electronic shell while the muonic transition takes place.

So-called "model-independent" radial charge distribution differences ΔR_K have been measured by Fricke et al.[9] See Fig. 1.

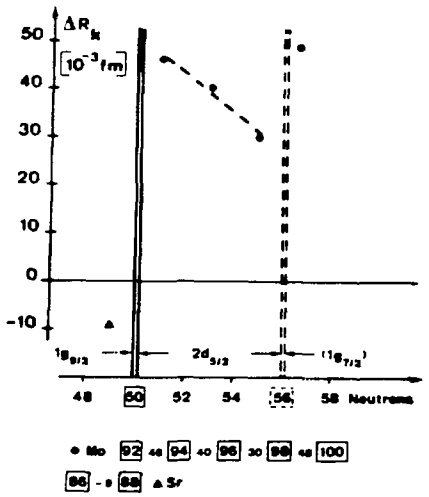

Figure 1.

Nuclear charge distribution differences ΔR_K vs number of neutrons (ref. 9)

The theoretically and experimentally difficult question of nuclear polarization in muonic atoms has recently been attacked by Yamazaki et al.[10] By establishing correlations between nuclear polarization corrections in different muonic states compatible with the experiments, they found discrepancies between these correlations and theoretical values. They concluded that something must be basically wrong with the calculations, maybe the neglect of transverse interaction.

2. Pionic atoms

The final results from pionic atoms are parameters of the optical potential used to describe the π-nucleus interaction. No reliable conclusion on π- nucleon scattering lengths can be drawn, however. A new approach on the old problem of differences between neutron and proton distributions was done by Batty et al.[11] He treated, for the first time, neutron and proton distributions separately in the absorptive part of the potential also and found the neutron and proton rms radii difference in the case of ^{44}Ca

$$r_{rms}^{(n)} - r_{rms}^{(p)} = -0.05 \pm 0.05 \text{ fm.}$$

Resonances in pionic atoms were recently determined by Leon et al.[12] Table III summarizes some results. The resonances are important to further explore the π-nucleus potential.

TABLE III

Attenuation of π-mesic x-rays (ref. 12)

	Nucl.	Exp.(%)	Theory (%)
$1 - \frac{5 \to 4}{6 \to 5}$	^{111}Cd	21.8 ± 3.7	15.7 ± 4.1
$1 - \frac{4 \to 3}{6 \to 5}$	^{111}Cd	9.2 ± 5.9	11.5 ± 3.2
$1 - \frac{5 \to 4}{6 \to 5}$	^{112}Cd	50.5 ± 2.9	44.8 ± 2.8
$1 - \frac{4 \to 3}{6 \to 5}$	^{112}Cd	28.5 ± 3.7	15.7 ± 4.1

3. Kaonic and antiprotonic atoms

Kaonic atom data reveal an optical potential. Two parameters are sufficient. Antiprotonic atoms show deeply lying narrow states. Not much more information from these data, except, of course, the particle masses, as in other mesonic atoms, has been obtained from kaonic and antiprotonic atoms.

III. THEORY OF SLOWING DOWN AND COULOMB CAPTURE

1. Slowing down

At small energies details of the electronic structure are important for the slowing down process. Usually the electrons are treated as *Fermi gas*. *In* condensed matter serious difficulties arise as to how to take the higher electron density and smaller atomic dimensions, both compared to the gaseous state, into account. Recently calculations were performed by W. Wilhelm for muons in the KeV region and below.[13] He integrated numerically the energy loss, applying various models of electron charge distribution in the atom. *Figure 2 shows an* example.

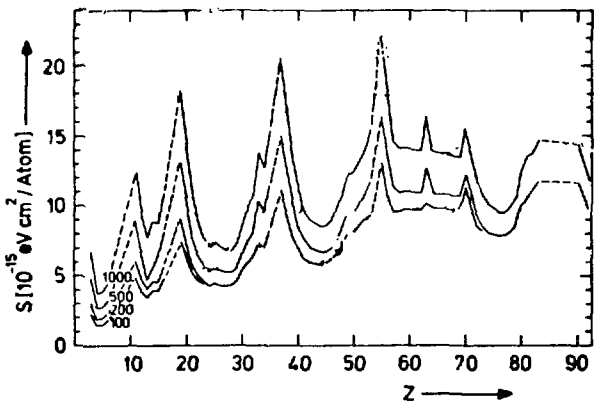

Figure 2.

Calculated stopping power for muons vs atomic number. Electrons treated as Fermi-gas of free atom density filling a volume given by the macroscopically determined atomic volume. Parameter: incoming muon energy in eV (ref. 13).

The energy loss at very low energies was recently calculated in closed form by the present author.[14] Figure 3 shows the energy loss for gaseous Ar and a hypothetical Ar with the density of condensed matter.

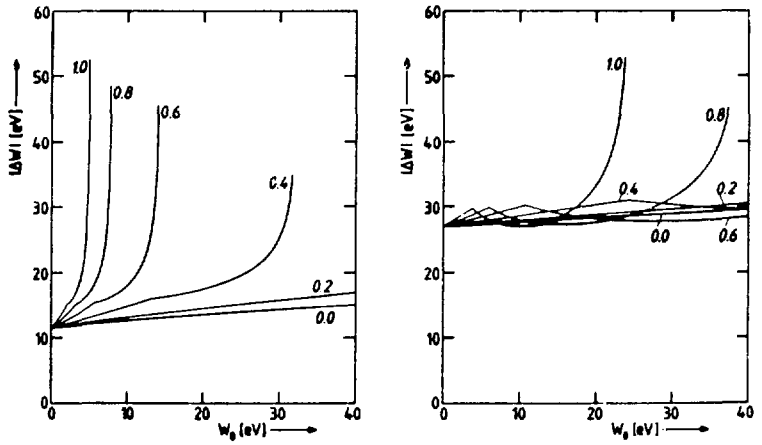

Figure 3.

Energy loss of μ^- during one full orbit through an Ar atom vs incoming muon energy. Parameter: impact parameter in units of atomic radius. Left: free atom. Right: hypothetical condensed Ar with condensed-matter density (ref. 14).

In any theory on slowing down and Coulomb capture, it is essential to use correct transport theory:

a. particles captured already at higher energies are no longer available as low-energy particles;

b. even without this trivial effect there is an important relation between slowing down and spectral flux density of the mesonic particles.

Spectral flux density n(W) here means, as usual, the number of particles with energies between W and W + dW which enter a sphere of radius r per unit time, divided by πr^2. As can easily be shown[15], the following equation holds:

$$n(W)\, S(W) = n(W_0)\, S(W_0) = \text{const} \qquad (4)$$

where W_0 is the energy of the incoming beam.

2. Coulomb capture treated quantum mechanically

About half of all papers on Coulomb capture which have appeared at any time treat the problem quantum mechanically, and about half treat it semiclassically. In the quantum mechanical treatment the mesonic particle "suddenly" jumps

from a continuum state (traveling wave) into a bound state. This jump is accompanied by the emission of either an Auger electron or an x-ray. The treatment is difficult because there are large Coulomb effects on both incoming mesonic particle and outgoing electron. Hence almost all computations are for free atoms where one knows at least the initial electron states fairly well.

Older quantum mechanical treatments do not agree with experiment. In particular the Coulomb capture is calculated to take place already at high energies. Also, transport theory is often not properly taken into account.

Newer results by Korenman and Rogovaya[16] with transport theory built in, show a nonstatistical population of levels with given principal quantum number n and a large variety of n levels populated primarily.

3. Coulomb capture treated semiclassically

Semiclassical treatment here means that the mesonic particle follows a classical trajectory while the electrons are treated quantum mechanically. The mesonic particle is mostly assumed to orbit in the potential of a Thomas-Fermi atom. As in Section III.1, serious difficulties arise if one wants to treat condensed matter.

An important simplification results from treating the energy loss, which actually is due to individual collisions with a limited number of electrons, as arising from a continuously effective frictional force.

Older calculations yielded for the per-atom Coulomb capture ratio between elements Z_1 and Z_2 a rather strong Z dependence, for example[17]

$$A(Z_1, Z_2) = \left(\frac{Z_1}{Z_2}\right)^{7/6} , \tag{5}$$

in disagreement with experiment. The gross features, not taking individual atomic data into account, are fairly well represented by[18]

$$A(Z_1,Z_2) = \frac{Z_1 \ln 0.57\, Z_1}{Z_2 \ln 0.57\, Z_2} . \tag{6}$$

There are two new approaches taking "chemistry" to some extent into account. Schneuwly et al.[19] count basically the number k of "loosely bound" electrons per atom, setting one binding energy limit per period of the Periodic Chart, and postulate that the capture is directly proportional to k (with no other Z dependence). Chemical bonding is taken into account by distributing fractions of

the "common" electrons to individual atoms according to the ionicity. For results see Section VI.3. In a paper by the present author[20] the formula eq. (6) is refined by taking the electron density change due to the condensed state into account. This yields

$$A(Z_1, Z_2) = \frac{Z_1 \ell n(0.57Z_1)\ R(Z_2)}{Z_2 \ell n(0.57Z_2)\ R(Z_1)} \tag{7}$$

where $R(Z_1)$ and $R(Z_2)$ are the atomic radii of atoms Z_1 and Z_2, respectively, for the respective valence states. A further result of these calculations is a basically flat ("white") spectral flux density.[14,18] The initial distribution, also calculated in closed form,[14] is not statistical, as shown in Fig. 4.

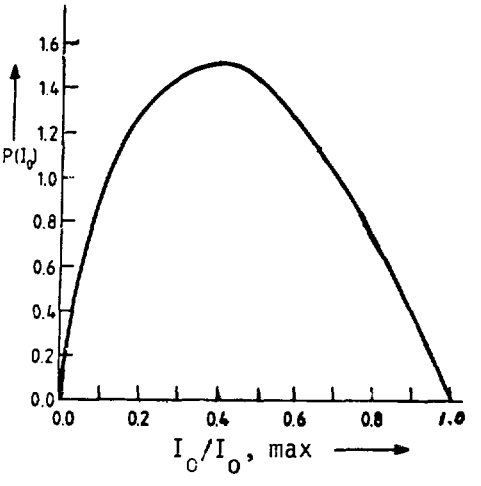

Figure 4.

Initial distribution of angular momentum of captured muons, calculated semiclassically, vs incoming particle angular momentum l_0, measured in units of maximum incoming particle angular momentum $l_{0,max}$ (ref. 14).

IV. THE CASCADE

The first steps in the cascade, Auger transitions between very high-lying states, are hard to treat adequately in a quantum mechanical theory. However, results were obtained with semiclassical theories, either by numerical integration or in closed form.

More work has been devoted to the later steps of the cascade where radiative transitions can compete with Auger transitions, at least in the case of levels with low angular momentum quantum number ℓ. Several cascade codes are in use. In the Hüfner code[21] only electric dipole transitions are taken into account, penetration is not. In the Akylas code[22] E1, E2, and E3 transitions are taken into account, as well as penetration. Computation with this code is more time consuming than with Hüfner's code. The results are considered more reliable though the differences with those from the Hüfner code are not large.[3]

As the highest radiative transitions observed[23] are from $n_{init} = 20$, quantum mechanical cascade computations nowadays usually start at this value, some also lower. Various assumptions are made concerning the population of the ℓ substates at n_{init}:

$$P(\ell) \propto 2\ell + 1 \quad \text{(statistical)} \tag{8}$$

$$P(\ell) \propto (2\ell + 1) \exp(\alpha\ell) \quad \text{(modified statistical)} \tag{9}$$

$$P(\ell) \propto 1 + a\ell \quad \text{(linear)} \tag{10}$$

$$P(\ell) \propto 1 + a\ell + b\ell^2 \quad \text{(quadratic)} \tag{11}$$

Another parameter which turned out to be important is the K refilling rate, which may very well deviate from the value tabulated for electronic atoms due to a depletion of the L shell.

Comparison with experiment is usually done with the χ^2 value taken as the criterion for the quality of the fit. This comparison is sometimes difficult due to an insufficient knowledge of the electronic structure. Nevertheless, in many cases excellent agreement is obtained, despite the many numbers to fit and the small number of parameters available. The type of initial distribution needed differs strongly for different Z value. In the case of Fe, for example, an almost "horizontal" distribution is adequate,[23] whereas in Mg and Al almost statistical distributions[3] are found.

V. EXPERIMENTAL RESULTS ON n(W)

1. Direct measurement

No direct measurement of n(W) in the capture region of the semiclassical treatment is available yet (cf. Section I). There are, however, very recent results in the region immediately above it which, by the way, is the capture region of

some quantum mechanical treatments. Figure 5 shows the set-up used by the Munich group[3] for their experimental determination of n(W) in the case of μ^- of very low energies. Figure 6 shows a typical spectrum in a two-dimensional plot. Figure 7 shows n(W). It is important that there are muons well below 1 KeV. Hence older quantum mechanical treatments, predicting capture at energies well above 1 KeV, cannot be correct (cf. ref. 24 for a survey).

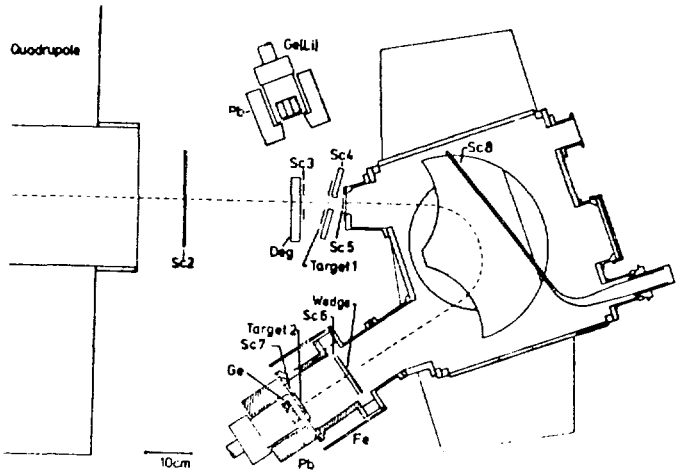

Figure 5.

Set-up for very slow muons. Sc2, Sc3, Sc4, Sc5, Sc6, Sc7, Sc8 scintillation counters (Sc6: 3 mg/cm^2). Ge(Li) and Ge germanium detectors. Deg degrader. Events (Sc2, $\overline{Sc3}$, $\overline{Sc4}$, Sc5, Sc6, $\overline{Sc7}$, $\overline{Sc8}$, Ge)are registered for the spectral flux density experiment. The μ time of flight between Sc6 and target 2 (for example, 40 μg/cm^2 Cu on Si) is measured for each event individually. Deflecting magnet and wedge transform a thin beam of large energy spread into a broad beam of small energy spread. The degrader thickness is such that the maximum of the μ stopping distribution is on the downstream surface of Sc6 (ref. 3).

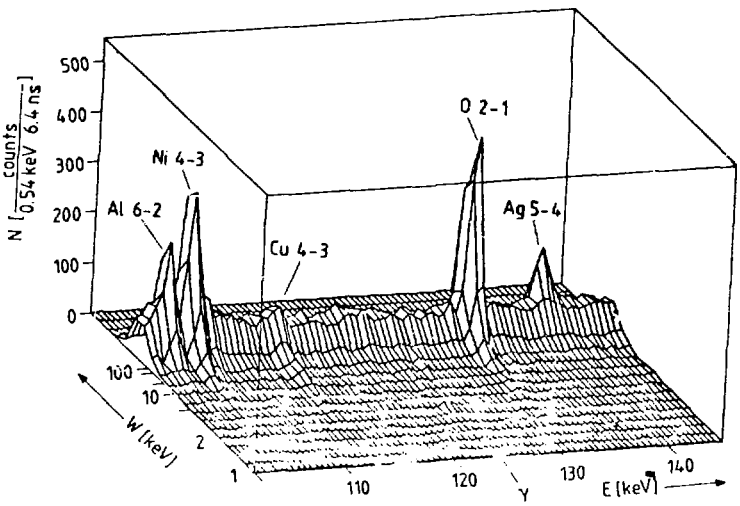

Figure 6.

Two-dimensional spectrum. Target 2 consisted of 60 μg/cm^2 Cu on Si. A Ag foil (0.16 mg/cm^2) covered the downstream surface of Sc6 in this run. It is that material whose spectral μ flux density n(W) was measured, and gave also a zero marker for the time-of-flight electronics. N is the numbers of counts per energy channel (0.54 keV) and time-of-flight channel (6.4 ns). E is the x-ray energy, W the muon energy as measured by the time of flight. Accumulation time 14 hours (ref. 3).

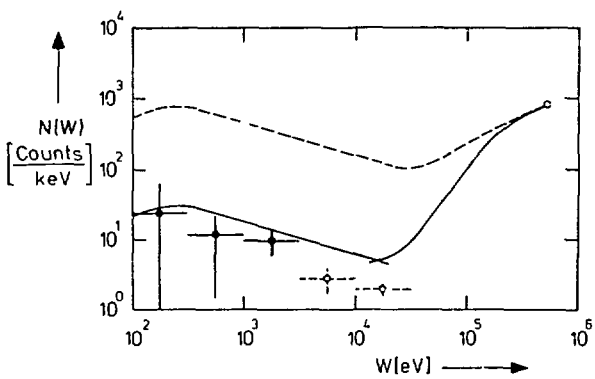

Figure 7.

Spectral flux density n(W) versus muon energy W. Open circle: Normalization point. At this energy "ordinary" energy loss calculations are still reliable and the multiple scattering is negligible under run conditions. Dashed line: Calculation of n(W) performed by our group neglecting multiple scattering. Solid curve: Calculation of n(W) taking multiple scattering into account; right part: Gaussian

approximation; left part: validity of Lambert's law assumed. 40 $\mu g/cm^2$ Cu on Si. Accumulation time 16 hours. The two high energy points are somewhat too low because the Cu layer was not thick enough to reliably stop all muons (ref. 3).

2. Indirect evidence

Indirect evidence on n(W) is again only available for μ^-. Naumann and Daniel[25] extracted striking evidence from x-ray data that the shape of n(W) is about the same in all solid alkali halides investigated so far. If this would not be the case one would not expect the same intensity patterns of the x-ray cascade in a given element, regardless of what the other ion is, and not capture integrals

$$I_{capt} = \int_0^\infty n(w)\, \sigma_{capt}(W)\, dW, \tag{12}$$

where $\sigma_{capt}(W)$ denotes the capture cross section at energy W, which can be characterized by a dependence on Z_1 of the capturing element only (and not an additional dependence on Z_2).

The situation is obviously completely different in the case of gases. The Munich group[3] found recently that A(Ne,Kr) varies, depending on whether there is much Ar present (ternary mixture), or there is no Ar present (binary mixture). The ratio of the A(Ne,Kr) values was found to be

$$\frac{A(Ne,Kr)_{\text{much Ar}}}{A(Ne,Kr)_{\text{no Ar}}} = 1.14 \pm 0.05. \tag{13}$$

As $\sigma_{capt}(W)$ in dilute gases, which was applied, cannot depend on the presence of a third component, there must be a change in n(W) induced by the presence of much Ar. This is the first time that such an effect was observed.

VI. EXPERIMENTAL RESULTS ON COULOMB CAPTURE

1. General remarks

One may ask whether radiative Coulomb capture, that is, capture accompanied by the emission of quantum radiation, occurs to a substantial amount or not. Experimental evidence is against radiative capture. An upper limit of $8 \cdot 10^{-4}$ for free muon energies between 0 and 1 KeV was set[3] in the case of a

radiative transition to the 1s level of Al (90% confidence). Similar results, though less precise, were obtained for other transitions and other elements.[3] The same experiment delivers also strong evidence against the large mesonic molecule model.

2. Dependence of $A(Z_1,Z_2)$ on concentration

In many cases a dependence of $A(Z_1,Z_2)$ on concentration was searched for in the case of condensed state targets but never was found. Figure 8 shows the result by Bergmann et al.[26] in the case of a Nb-V alloy (solid solution). Similar results were obtained at Los Alamos.

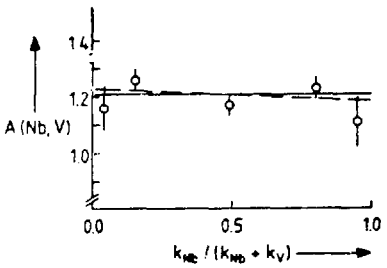

Figure 8.

Per-atom capture ratio for muons in a Nb-V alloy (solid solution) vs Nb concentration (atom percent). Solid line: weighted average. Dashed line: fitted straight line. The solid line is the better fit (smaller χ^2, due to one parameter less) (ref. 26).

Preliminary data of the Munich group[3] indicate a concentration dependence in the case of Ar-Kr mixtures. This is in line with the effect observed when adding Ar to a Ne-Kr mixture (cf. Section V.2)

3. Dependence of $A(Z_1,Z_2)$ on the Z values

Extensive work was performed both by the Los Alamos group and the Munich group on capture ratios from solid and gaseous targets. The capture ratios $A(Z_1,Z_2)$, with Z_2 fixed to O, F, S, and CL, show a periodic behavior with the position of Z_1 within the period of the Periodic Chart, as anticipated by Zinov et al.[27] Figure 9 shows recent results from the Munich group[3] compared to Schneuly's[19] and Daniel's[20] predicted values.

4. Dependence of $A(Z_1,Z_2)$ on valence state and ionicity

Although different $A(Z_1,Z_2)$ values were reported for different valence states of elements in the same kind of compound, for example oxides, the situation does not appear quite clear. Table IV summarizes recent values.[3] Although all ratios of ratios listed in this table point in the same direction, no single result is statistically significant. The average value is neither. The table shows the urgent need for more precise data.

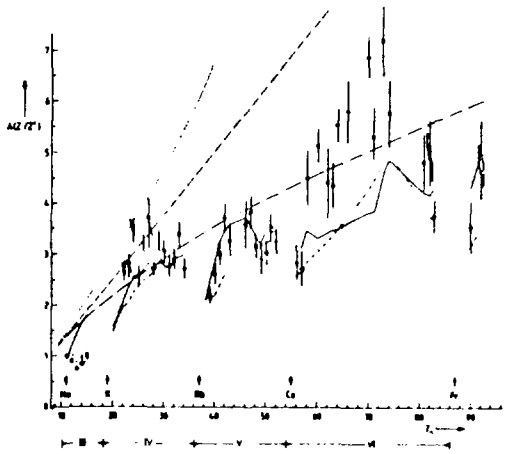

Figure 9.

Experimental values per atom μ capture ratios of oxides vs atomic number of oxidized element. Periods of the Periodic Chart are indicated. Dotted line: eq. (5). Dashed line: Z law. Dot-dashed line (long dashes): eq. (6). Dot-dashed line (short dashes): according to ref. 19 Full line: eq. (7). (ref. 3).

TABLE IV

Ratios of Coulomb Capture Ratios of Oxides of the Same Element with Different Valency (ref. 3)

Oxides	Ratio	Average
TiO/TiO_2	0.98 ± 0.08	0.96 ± 0.04
V_2O_4/V_2O_5	0.94 ± 0.09	
Cr_2O_3/CrO_3	0.98 ± 0.09	
Co_3O_4/Co_2O_3	0.91 ± 0.13	
PbO/PbO_2	0.97 ± 0.16	
UO_2/U_3O_8	0.93 ± 0.18	

The nature of the chemical bonding may very well affect $A(Z_1,Z_2)$. In the absence of a profound theory one may go back to statistical correlation theory. When doing so[28] a rather strong correlation between $A(Z_1,Z_2)$ and the ionicity of the bonding shows up,[3] particularly after elimination of common dependences on Z_1 and $R(Z_1)$.

VII. EXPERIMENTAL RESULTS ON HYDROGEN CONTAINING TARGETS

1. Transfer in gases

The transfer of negative muons in gaseous targets with a low concentration of heavier elements was established a long time ago. No agreement, however, was obtained on the transfer rate from H to Ar, the most investigated mixture. Table V lists a recent high pressure result[29] and previous values obtained at low pressure,[30-32] all reduced to an Ar density (atoms per unit volume) corresponding to that of liquid hydrogen. One may conclude that there is a density effect which, however, has not yet been explained.

TABLE V

Reduced Transfer Rates; ρ Hydrogen Pressure, λ_{trans} Reduced Transfer Rate (ref. 29)

	ρ[atm]	λ_{trans} [$10^{11}s^{-1}$]
Basiladze et al.[30]	45	1.20 ± 0.19
Alberigi Quaranta et al.[31]	26	3.5 ± 0.6
Placci et al[32]	10	1.46 ± 0.14
Daniel et al[29]	600	9.8 ± 1.5

The transfer in dilute gases is expected to occur from thermalized muonic hydrogen. A large enhancement of np → 1s transitions, n > 2, compared to condensed targets is observed.

The transfer of negative hadrons is more difficult to observe than that of muons, as hadrons may be annihilated in high lying states or during a collision. It seems to me that no striking evidence for hadron transfer was found. A high pressure experiment performed some time ago at CERN[33] did not give a clear answer. However, an upper limit on the transfer could be obtained.

2. Results on condensed targets containing hydrogen

As in the case of hydrogen-containing dilute gas targets hydrogen-containing condensed targets show an intensity pattern with increased np → 1s intensities of the heavier elements (n > 2). So it is tempting to ascribe this to a transfer of mesonic particles from hydrogen to the heavier elements. However, no striking evidence for such a transfer can be found, and in my opinion all observed facts may also be explained without transfer. I do not want to say,

on the other hand, that transfer can be ruled out. The problem has just not been solved.

Although most of the experimental information comes from muonic atoms, a hydrogen effect was also seen in pionic x-ray spectra.[34]

An isotope effect, the first one ever observed with muonic x-rays, was seen in the comparison between normal and deuterated compounds of light elements.[35] The deuterated compounds show smaller intensities in $np \rightarrow 1s$ transitions, $n > 2$, compared to the normal compounds.

VIII. EXPERIMENTAL RESULTS ON CASCADES AND INTENSITY PATTERNS FROM HYDROGEN-FREE TARGETS

The experimental information on cascades and the whole intensity pattern is rarer than that on capture ratios. The reason is apparently that much more work is needed to measure and evaluate all the observed lines, and to fit the pattern with a cascade program. The general conclusion to be drawn is that both the Hüfner[21] and the Akylas[22] codes are valuable tools to work with, and in particular, to draw conclusions from the observed x-ray pattern on the population at some intermediate level with n_{init} around 20.

The statistical correlation theory mentioned in Section IV.4 may also be used to search for correlations among x-ray intensities and between intensities and capture ratios or atomic or molecular quantities such as radii and ionicity. This has been successfully done in the case of muonic x-rays and binary compounds.[3,28] It is interesting that not only the x-ray intensities in element Z_1 vary periodically with Z_1 and show correlations, but also the intensities in Z_2, Z_2 fixed for all targets considered, show these periodicities with Z_1 and correlations with quantities of or from element Z_1. Of course, these effects are less pronounced.

Periodic variations with Z for single element targets were observed for kaonic x-ray intensities already a long time ago.[36] Very recently the variation of pionic intensities with Z was measured and found to show similar periodicities as the muonic intensities.[37]

IX. APPLICATIONS

For non-destructive chemical analysis muons seem to be best suited due to their spectra with pronounced narrow lines above low background. All elements

except hydrogen are easily identified. In bulk analysis, averaging over the whole sample volume is easily accomplished as long as the samples are not too large and too thick. This averaging causes serious difficulties in conventional analysis of inhomogenous specimens.

Bulk analysis of tissue-equivalent material of known composition was performed by Reidy et al.[38] at Los Alamos. Table VI summarizes some of his results. "Modified Z law" here means expectations based on the Z law (capture fraction proportional to Z) with the exception that the hydrogen atom's share is added to the element at which the H atom is bonded. Other laws, such as eq. (6), would yield comparable results for the low Z main components. Hutson et al.[39] again at Los Alamos, performed a thorough study of muscle and bone, mostly in the deep frozen state, and showed that the muonic x-ray technique can be used for the elemental analysis of such organic material. Differences between the spectra from healthy and diseased animals were already earlier measured at CERN.[40,41]

TABLE VI

Elemental analysis of tissue equivalent plastic and tissue equivalent liquid. Column 1: element. Column 2: composition normalized to 100% for the heavier elements. Column 3: expected μ capture yield according to modified Z law. Column 4: experimental μ capture yield (ref. 38)

	Atomic %	Modified Z-law	Measured
		Shonka plastic	
C	89.61 ± 0.31	87.99 ± 0.30	87.78 ± 0.29
N	3.50 ± 0.06	3.76 ± 0.06	3.67 ± 0.13
O	5.81 ± 0.37	6.65 ± 0.42	6.48 ± 0.25
F	0.72 ± 0.18	0.85 ± 0.21	0.93 ± 0.20
Ca	0.36 ± 0.09	0.94 ± 0.24	0.46 ± 0.15
		TE liquid	
C	17.56 ± 0.18	14.70 ± 0.15	14.12 ± 0.55
N	4.29 ± 0.04	5.00 ± 0.05	3.94 ± 0.22
O	78.15 ± 0.80	80.30 ± 0.80	81.94 ± 0.59
S	0.16 ± 0.03		
K	0.16 ± 0.03		

Recently the Munich group[3] at SIN started a systematic investigation of the application of muonic x-ray analysis to archeometry. Firing conditions were found to have no effect on either x-ray patterns within a given element or the per atom capture ratios from pottery except for oxygen (via the amount of adsorbed water) and, maybe, magnesium.

Besides for bulk analysis, muonic x-ray techniques are also very useful for scanning analysis. By correctly adjusting energy and energy spread of the incoming beam narrow layers at the surface or also deeply inside the specimen can be selected and analyzed. Up to now Islamic pottery from the 14th century A.D. was investigated with this technique, and a very clear separation of glaze and base material was achieved.[3]

When more precisely locating the point where the mesonic particle came to rest, visualization, even in three dimensions,[42] is possible. One way of doing so is to follow the trajectory of the incoming particle (for example μ^-, μ^+ or π^+) and also observe the trajectory of the outgoing decay electron. In a pilot experiment[43] with π^+ measuring only the e^+, two-dimensional images were obtained, at a resolution of about 1 cm. Very recently Matthäy et al.[44] obtained one- and two-dimensional pictures by recording negatrons and positrons from in-target conversion of quantum radiation emitted at radiative capture of π^- or at e^+ annihilation. In contrast to the former experiment[43] where all events falling in the very large acceptance angle of a proportional chamber set-up were registered, in the latter experiment[44] collimators were used (either slits, for the one-dimensional pictures, or holes, for the two-dimensional pictures).

Mesonic radiotherapy is done with negative pions, making use of the high-LET low-range radiation of heavy particles emerging from nuclear capture of the pions reacting with the nucleus while being in an atomic orbit. This technique whose importance is generally accepted, may turn out to be a very powerful tool in fighting cancer.

REFERENCES

1. W. H. Barkas, N. J. Dyer, and H. H. Heckman, Phys. Rev. Lett. 11, 26 (1963).

2. R. Bergmann, H. Daniel, T. von Egidy, P. Ehrhart, G. Fottner, H. Hagn, F. J. Hartmann, E. Köhler, and W. Wilhelm, SIN - Newsletter No. 12, 63 (1979).

3. Munich group, unpublished (1980).

4. H. H. Andersen, J. F. Bak, H, Knudsen, and B. R. Nielsen, Phys. Rev. A 16 1929 (1977).

5. R. H. Ritchie and W. Brandt, Phys. Rev. A 17, 2102 (1978).

6. J. D. Jackson and R. L. McCarthy, Phys. Rev. B 6, 4131 (1972).

7. G. Holzwarth and H. J. Pfeiffer, Z. Physik A 272, 311 (1975).

8. B. Aas, thesis, ETH, Zürich, (unpublished).

9. Mainz-Fribourg group, G. Fricke, et al., SIN Jahresbericht 1979, C 37 (1979).

10. Y. Yamazaki, H. D. Wohlfahrt, E. B. Shera, and M. V. Hoehn, Phys. Rev. Lett. 42, 1470 (1979).

11. C. J. Batty, S. F. Biagi, E. Friedman, S. D. Hoath, J. D. Davies, G. J. Pyle, T. A. Squier, D. M. Asbury, and M. Leon, Phys. Lett. 81 B, 165 (1979).

12. M. Leon, J. N. Bradbury, P. A. M. Gram, R. L. Hutson, M. E. Schillaci, C. K. Hargrove, and J. J. Reidy, Nucl. Phys. A 322, 397 (1979).

13. W. Wilhelm, unpublished (1980).

14. H. Daniel, unpublished (1980).

15. H. Daniel, Nucl Instr. Meth. 147, 297 (1977).

16. G. Ya. Korenman and S. I. Rogovaya, J. Phys. B 13, 641 (1980).

17. P. Vogel, P. K. Haff, V. Akylas, and A. Winther, Nucl. Phys. A 254, 445 (1975).

18. H. Daniel, Phys. Rev. Lett. 35, 1649 (1975).

19. H. Schneuwly, V. I. Pokrovsky, and L. I. Ponomarev, Nucl. Phys. A 312 419 (1978).

20. H. Daniel, Z. Physik A 291, 29 (1979).

21. Program CASCADE by J. Hufner; J. Hufner, Z. Physik 195, 365 (1966).

22. V. R. Akylas, thesis, Cal Inst. Techn., Pasadena, CA, 1978 (unpublished).

23. F. J. Hartmann, T. von Egidy, R. Bergmann, M. Kleber, H. - J. Pfeiffer, K. Springer, and H. Daniel, Phys. Rev. Lett. 37, 331 (1976).

24. H. Daniel, Radiation Effects 28, 189 (1976).

25. R. A. Naumann and H. Daniel, Z. Physik A 291, 33 (1979).

26. R. Bergmann, H. Daniel, T. von Egidy, F. J. Hartmann, J. J. Reidy, and W. Wilhelm, Phys. Rev. A 20, 633 (1979).

27. V. G. Zinov, A. D. Konin, and A. I. Mukhin, Yad. Fiz. 2, 859 (1965); transl. p. 613.

28. H. Daniel, W. Denk, F. J. Hartmann, W. Wilhelm, and T. von Egidy, Phys. Rev. Lett. 41, 853 (1978).

29. H. Daniel, H. - J. Pfeiffer, P. Stoeckel, T. von Egidy, and H. P. Povel, to appear in Nucl. Phys. A.

30. S. G. Basiladze, P. F. Ermolov, and K. O. Oganesyan, Sov. Phys. JETP 22, 725 (1966).

31. A. Alberigi Quaranta, A. Bertin, G. Matone, F. Palmonari, A. Placci, P. Dalpiaz, G. Torelli, and E. Zavattini, Nuovo Cim. 47B, 92 (1967).

32. A. Placci, E. Zavattini, A. Bertin, and A. Vitale, Nuovo Cim 64A, 1053 (1969).

33. H. Daniel, H. - J. Pfeiffer, and K. Springer, Z. Physik A 275, 369 (1975).

34. H. Daniel, R. L. Hutson, M. Leon, M. E. Schillaci, and R. Seki, Phys. Lett. 75A, 282 (1980).

35. L. F. Mausner, J. D. Knight, C. J. Orth, M. E. Schillaci, and R. A. Naumann, Phys. Rev. Lett. 38, 953 (1977).

36. C. E. Wiegand and G. L. Godfrey, Phys. Rev. A 9, 2282 (1974).

37. R. M. Pearce, G. A. Beer, M. S. Dixit, S, K. Kim, J. A. Macdonald, G. R. Mason, A. Olin, C. Sabev, W. C. Sperry, and C. Wiegand, Can. J. Phys. 57, 2084 (1979).

38. J. J. Reidy, R. L. Hutson, H. Daniel, and K. Springer, Anal. Chem. 50, 40 (1978).

39. R. L. Hutson, J. J. Reidy, K. Springer, H. Daniel, and H. B. Knowles, Radiology 120, 193 (1976).

40. H. Daniel, H. - J. Pfeiffer, and K. Springer, Biomed. Techn. 18, 222 (1973).

41. H. Daniel, H. - J. Pfeiffer, and K. Springer, Phys. Med. Biol. 20, 1035 (1975).

42. H. Daniel, Nucl. Med. 8, 311 (1969).

43. H. Daniel, J. Reidy, R. Hutson, J. Bradbury, and J. Helland, Rad. Res. 68, 171 (1976).

44. H. Matthäy, G. Büche, U. Klein, W. Kluge, D. Münchmeyer, A. Moline, D. Schmidt F. Stabl, and H. P. Walther, Rad. Environm. Biophys. 16, 231 (1979).

THEORIES OF THE PION NUCLEUS INTERACTION

by

W. R. Gibbs

Los Alamos Scientific Laboratory

ABSTRACT

The basic theory of pion-nucleus interaction is reviewed. Connection is made with recent theories of nuclear matter and the relevance of pion condensation and precursor effects is discussed.

I. INTRODUCTION

I wish to discuss how the classical theories of the pion nucleus interaction may lead us to consider the nucleon-nucleon potential in the nuclear medium. We may well remember that in the original proposals for LAMPF many statements were made that it would be useful to use as a probe a particle which itself formed the basis of the interaction which binds the nucleus (the pion). Since that time little has been heard of this motivation. I am happy to report that recently (at last) some progress is being made in that direction.

This progress is slow and, in fact, is almost unnoticed in this context. In order to show how this has come about I shall go through the "classical" theory of pion nucleus reactions to let us arrive at a logical scheme.

This classical method takes the form of attempting to express all reactions as collisions among billiard balls, a concept we can all understand. In spite of this strong bias, we shall be led to the point of view that a pion field in the nucleus can be described by these same equations.

I shall talk briefly about the fixed-nucleon solution of the multiple scattering equations and the delta-hole Isobar model of the pion-nucleus interaction but I shall express these in terms of the optical model framework. Thus I will spend most of the time on the multiple scattering equations and the optical model expansion.

II. MULTIPLE SCATTERING EQUATIONS AND THE PION-NUCLEUS OPTICAL MODEL

Let us start with the Schrödinger equation with the assumption that the pion interacts with each nucleon separately by means of a two-body potential.

$$(K + \sum_{i=1}^{A} V_i (\vec{r}_i - \vec{r}) + H_N - E)\, \psi = 0$$

Here K is the pion kinetic energy and H_N is the nuclear Hamiltonian. We assume that the solution to the nuclear problem is known, i.e.

$$H_N \phi_n = E_n \phi_n \quad .$$

We further define

$$G_o = (E - K - H_N)^{-1} \quad ; \quad g = (E - K)^{-1} \quad .$$

Formally we express the solution to our problem as

$$\psi = \phi_o e^{i\vec{q}\cdot\vec{r}} + G_o \sum_{i=1}^{A} V_i \psi \quad .$$

Defining

$$T_i (\vec{q},\vec{q}') = \frac{1}{(2\pi)^3} \int d\vec{r}\, V_i (\vec{r},\vec{r}_i)\, \psi_{\vec{q}}\, e^{i\vec{q}'\cdot\vec{r}}$$

and

$$T(\vec{q},\vec{q}') = \sum_{i=1}^{A} T_i (\vec{q},\vec{q}') \quad ,$$

we can write

$$T_i = V_i + V_i G_o \sum_{j=1}^{A} T_j \quad .$$

To get to the form of multiple scattering equations, we define the operator τ_i to be the solution of

$$\tau_i = V_i + V_i G_o \tau_i$$

so that

$$V_i = (1 + \tau_i G_o)^{-1} \tau_i \quad .$$

Substituting for V_i we now have

$$T_i = \tau_i + \tau_i G_o \sum_{j \neq i} T_j \quad ,$$

or iterating

$$T = \sum \tau_i + \sum_{j \neq i} \tau_i G_o \tau_j + \sum_{\substack{i \neq j \\ j \neq k}} \tau_i G_o \tau_j G_o \tau_k + \quad \ldots .$$

The pion-nucleus elastic scattering amplitude is given by the ground state expectation value of T:

$$f(\vec{q},\vec{q}') = \langle 0|T|0\rangle \quad .$$

Note that

$$\langle 0|T|0\rangle = \sum \langle 0|\tau_i|0\rangle + \sum_{\substack{j \neq i \\ n}} \frac{\langle 0|\tau_i|n\rangle\langle n|\tau_j|0\rangle}{E - K - E_n}$$

$$+ \sum_{\substack{j \neq i \\ j \neq k}} \sum_{n\ m} \frac{\langle 0|\tau_i|n\rangle\langle n|\tau_j|m\rangle\langle m|\tau_k|0\rangle}{(E-K-E_n)(E-K-E_m)} + \quad \ldots .$$

$$= \sum \langle 0|\tau_i|0\rangle + \sum \langle 0|\tau_i|0\rangle (E-K)^{-1} \langle 0|\tau_j|0\rangle$$

$$+ \sum \langle 0|\tau_i|0\rangle (E-K)^{-1} \langle 0|\tau_j|0\rangle (E-K)^{-1} \langle 0|\tau_k|0\rangle$$

$$+ \quad \cdots$$

$$+ \text{terms with intermediate nuclear excited states.}$$

Keeping only the ground states terms and using anti-symmetrized wave functions to give

$$\langle 0|\tau_i|0\rangle = \bar{\tau} \quad ,$$

we have

$$\begin{aligned}\bar{T} &= \langle 0|T|0\rangle \\ &= A\,\bar{\tau} + A\,(A-1)\bar{\tau}\, g\, \bar{\tau} + A(A-1)^2\, \bar{\tau}\, g\, \bar{\tau}\, g\bar{\tau} + \cdots \\ &= A\,\bar{\tau}\,[1-(A-1)\, g\bar{\tau}]^{-1} \quad .\end{aligned}$$

If

$$\tilde{T} = \frac{A}{A-1}\,\bar{T}$$

then

$$\tilde{T} = (A-1)\bar{\tau} + (A-1)\bar{\tau}\, g\tilde{T}$$

and we can solve this equation since it is the Schrödinger equation with a potential given by

$$V = (A-1)\bar{\tau} \quad = \text{1st order optical potential}$$

Our problems are of two types

1) Calculate $\bar{\tau}$ so that we have the first order potential.

2) Correct for the excited state terms which have been left out.

First problem: Note that

$$\tau_i = V_i + V_i\, G_o\, \tau_i$$

is still a many-body equation since G_o contains the nuclear Hamiltonian. If we neglect H_N completely then, we have

$$\tau_i = V_i + V_i\, g\, \tau_i \quad ,$$

which has as a solution the free pion-nucleon t-matrix,

$$\tau(\vec{q},\vec{q}',\vec{r}_i) = t(\vec{q},\vec{q}')\; e^{\,i(\vec{q}-\vec{q}')\cdot\vec{r}_i}$$

$$\bar{\tau}\,(\vec{q},\vec{q}') = t\,(\vec{q},\vec{q}')\; S\,(\vec{q}-\vec{q}') \quad .$$

Note: $\bar{\tau}$ is complex because t is complex. This means "optical model" absorption due to nucleon knock out. This knock out is free,i.e., there is no restriction on the phase space for the final nucleon.

We can improve things by using nuclear intermediate states,

$$\tau_i = V_i + \Sigma V_i |n\rangle (E\cdot K - E_n) \langle n|\tau_i \ .$$

If $E_n = \bar{E}$ (some average energy)

$$\bar{\tau} = t(\vec{q},\vec{q}', E-\bar{E})\ S(\vec{q}-\vec{q}') \ .$$

Now we may use the free pion-nucleon t-matrix, but at a lower energy to take account of the binding of the nucleons. This is still crude. The subtraction energy should depend on the angle of the pion-nucleon scattering.

One can get a better calculation of τ by noting that there is no interaction between the pion and the $j\neq i$ nucleons. By using a single-particle shell model the solution becomes a three-body problem. The three bodies are: the pion, the struck nucleon, and the central potential.

Note also that we will get a dependence on the motion of the struck nucleon (and the "core") in these three body models which means that $\bar{\tau}_i$ is not factorable into an effective pion-nucleon t-matrix and a nucleon form factor.

Landau and Thomas[1] extract the t-matrix at the peak of the integral while Liu and Shakin[2] do the complete integral. Both groups obtain three body "energy shifts" using plane waves for the intermediate nucleon states.

In reality one should use waves interacting with the same potential in which they are bound initially. Recently Garcilazo and I[3] have made a study of such effects. Note that bound-state to bound-state transitions in such a calculation are also included.

Figure 1 shows the effect of a well in the intermediate state. As we see there is a great deal of difference between a well and plane waves.

Figure 2 shows an interesting isospin effect. The curves correspond to the difference between proton and neutron knock out. The result is a charge dependent effect, above the Coulomb potential, even on an isospin zero nucleus.

Since the intermediate pion-nucleon states are mostly in a 3/2 - 3/2 state the intermediate bound states are of a delta. Of course, we have to make a hole in the nucleon space so the dominant part of this piece will be Δ-hole.

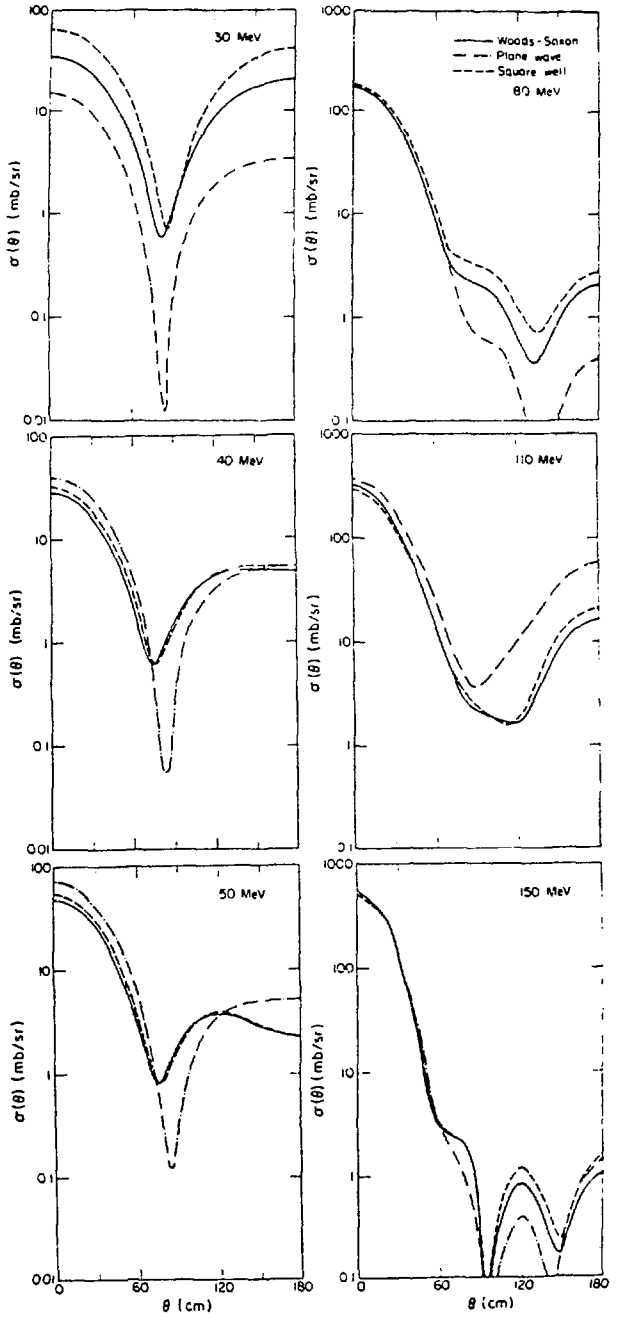

FIG. 1.

Demonstration of the importance of including interaction in the intermediate propagation. The case treated here is pion elastic scattering by ^{12}C. Note that in some cases there is a noticeable difference due to the shape of the well with which the intermediate (struck) nucleon is interacting.

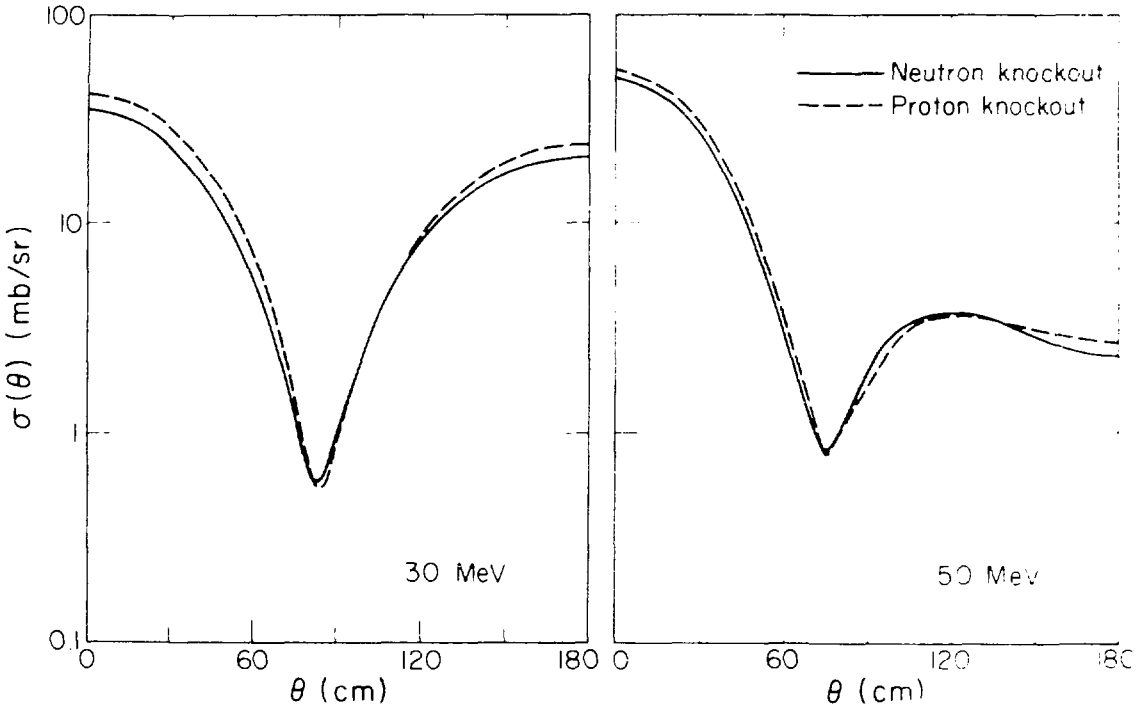

Fig. 2.

The effect of the presence or absence of a Coulomb potential in the intermediate state. Note that, because of 3-3 dominance, this leads to a difference between π^+ and π^- scattering beyond the direct Coulomb field acting on the incident pion.

There is one more thing which can be done with the "τ" equation and that is to model true absorption. I will address this question later.

Let us now return to the problem of the nuclear excited states. To investigate this "correction" I will use the simplest form for τ_i, i.e.,

$$\tau_i(\vec{q},\vec{q}') = t_i(\vec{q},\vec{q}')\, e^{i(\vec{q}-\vec{q}')\cdot\vec{r}_i}$$

and consider the full expansion with independent particle shell model wave functions.

Remember

$$T = \sum_i \tau_i + \sum_{j\neq i} \tau_i G_o \tau_j + \sum_{\substack{i\neq j\\ j\neq k}} \tau_i G_o \tau_j G_o \tau_k + \cdots$$

$$(o|T|o) = \sum_i (o|\tau_i|o) + \sum_{j\neq i} (o|\tau_i|n)(E-K-E_n)(n|\tau_j|o)$$

$$+ \sum_{\substack{i\neq j\\ j\neq k}} (o|\tau_i|n)(E-K-E_n)^{-1}(n|\tau_j|m)(E-K-E_m)^{-1}(m|\tau_k|o) \quad ,$$

where $|n)$ denotes independent particle wave functions (products) and H_N is the independent particle Hamiltonian. Since the τ_i we are using is a function only of $\vec{r}_i$ (not $\vec{r}_j$, $j\neq i$) orthogonality gives

$$\bar{T} = A\bar{\tau} + A(A-1)\bar{\tau}\, g\, \bar{\tau} + A(A-1)^2\, \bar{\tau}\, g\, \bar{\tau}\, g\, \bar{\tau} + \cdots$$

$$+ A(A-1) \sum \frac{(o|\tau|n)(n|\tau|n)(n|\tau|o)}{(E-K-E_n)^2} + \cdots$$

or the same result as before except for the correction terms on the second line. Thus correction terms to the first order optical potential can be expressed as correlations among nucleons where the correction terms above are treated as self correlations. Eisenberg, Hüfner, and Moniz[4] (EHM) showed that, with some reasonable approximations, at zero energy, the entire series can be summed, assuming a short-range correlation function leading to a modified form for the optical potential

$$\rho \to \rho/(1 + \xi\, \tfrac{4\pi}{3}(A-1)b\,\rho) \quad ,$$

where b is the pion-nucleon scattering volume and ρ is the nuclear density. Note that the effect is to weaken the optical potential, both real and imaginary parts.

It is clear that the absorption is too strong in the first order potential since it is assumed that there are no transitions into an excited state and back.

The quantity ξ depends on the range of the correlation and the range of the pion-nucleon interaction. For a zero-range interaction, $\xi = 1$. In this form this correction was introduced long ago by the Ericsons[5] as the Lorentz-Lorenz effect analogous to a similar effect in electro-magnetism.

EHM[4] found, for values of the ranges consistent with their calculation, that ξ was very small, $\sim$0.1-0.2. Since ξ depends on the holding apart of pairs of nucleons it might be expected that the Pauli principle may play a role. Indeed predictions of the order $\sim$0.5 were made[6].

Using the reasonable assumption that the Lorentz-Lorenz formula should be valid for pion energies of the order of 50 MeV and relying on the geometric consequences of this correction, we[7] fit pion-nucleus elastic scattering data to find general agreement with $\xi \sim 0.5$ for light nuclei.

There are two more points to be considered with respect to the theory outlined so far. The first is the form of the pion-nucleon t-matrix. By far the commonest assumption is separability in each partial wave. The most popular type of analysis uses the known (and guessed) pion-nucleon phase shifts as a function of energy to get the momentum dependence of the form factors. These form factors are defined differently in potential models and relativistic calculations and the difference in range has been the source of some confusion. A number of determinations have been made of these functions[8]. The most commonly used are those by Londergan, McVoy, and Moniz[8]. It is possible that there are problems with the separability assumption itself, but it is clearly reasonable and is only a parametrization of the off-shell dependence, the on-shell functions being given by the phase shifts.

The second point is that of true pion absorption. This is a very difficult effect to handle. One might well ask why it is so difficult since reasonable interaction operators are available (psuedo-scalar or pseudo-vector).

A large part of the problem is due to relativity. The assumed operators are in Dirac space and the usual nuclear wave functions are in Pauli space. Thus to make connection with ordinary nuclear physics a non-relativistic reduction of the operator must be made. It would seem that there is an ambiguity of the form of this operator, possibly involving intrinsically relativistic information.[9]

Another problem centers around the large momenta needed for the reaction to occur. Absorption on a single nucleon is possible but contributes only a small fraction of the reaction cross section. Two nucleon absorption is more important

and the role of 3, 4 ··· n nucleon absorption is not clear. It would seem likely that some is present however.

An interesting way of including this effect is to recognize that the τ equation can have a bound-state solution in the $T = 1/2$, $J = 1/2$ channel. Including this state in the intermediate sum leads to an additional term in τ which corresponds to

$$\pi + N \rightarrow N \quad .$$

Inserting this τ in the multiple scattering series leads to terms corresponding to one-nucleon absorption, uncorrelated two-nucleon absorption, correlated two-nucleon absorption, and various types of multinucleon absorption. This technique has the advantage of giving a prescribed series of corrections without double counting problems. Unfortunately, there is not a direct relationship between this expansion which is appropriate for the optical model and the observed high energy nucleons except in some special limits.

In order to know the importance of these terms it is necessary to know the degree of (optical) absorption from other sources (quasi-elastic) and the momenta available in the nucleus, both to the pion and the nucleons.

For these reasons many groups have resorted to assuming that the result of true absorption is a term in the optical potential proportional to ρ^2 and the coefficient of this term is fit to data. Of course, the value of this coefficient is very dependent on the rest of the optical model used. We have found that by adjusting the other parameters of the theory slightly, we can get excellent fits with zero for this coefficient.

III. OTHER FORMS OF THE THEORY

A. Fixed Nucleons

If one assumes that the nuclear Hamiltonian is only active in producing the nuclear wave function and that the pion scatters rapidly enough that the nucleon interactions play no role during the pion scattering, one obtains the fixed-nucleon approximation.[10]

At first glance this seems a severe approximation, and some important corrections, such as nucleon motion, must be put in by hand in an approximate way. Another disadvantage is that the exact solution of the problem at this point requires considerable computer time since an exact quantum mechanical scattering problem from a fixed nucleon is solved many times.

The further approximation of dominant forward scattering may be made to simplify the calculation but is not well justified for pions at or below the resonance energy.

In spite of these disadvantages these calculations can be very useful however. There is no optical model truncation so that short range and Pauli correlations can be included to arbitrary accuracy (in principle). The most useful area of application of this method may well be the calculation of coherent (nearly elastic) reactions such as charge exchange or inelastic scattering to low lying levels since multistep transitions may be included up to high order.

By dropping the requirement of the quantum mechanical solution of the problem (so losing phase information) but allowing energy loss between scatterings, one arrives at the intranuclear cascade. While this model is cruder yet, it treats certain aspects of reactions that are not easily predictable with other methods, such as the probability of leaving a given residual nucleus or the probability of knocking out a certain number of protons.

B. Isobar Doorway Models

As was remarked while looking at the τ equation, the dominant intermediate state involves the 3-3 channel or Δ-resonance. If one considers these intermediate Δ-hole states one can ask if they can be rediagonalized into a few "doorways." This has been done in a general formalism by Moniz[11] and collaborators and developed as a general technique for solving any scattering problem. The doorway technique was first used by Kisslinger and Wang[12] and has been used more recently by Saharia and Woloshyn[13] to predict simple reactions (i.e. γ,π°) from parameters fit to pion elastic scattering. This type of theory focuses on quantities such as Δ-nucleon or Δ-nucleus interaction and the reduction of phase space for decay of the delta due to the occupied nucleon orbitals. Thus we learn about how a delta behaves in the nuclear medium.

IV. CONNECTION WITH THE PION FIELD IN THE NUCLEUS

One of the original motivations for meson factories was to use pions as nuclear probes because it is (at least the Boson exchange picture) one of the particles most important in providing the nucleon-nucleon potential. Very little I have said until now bears on the fact that the scattered particle is the same as that providing the nuclear binding.

A very exciting development over the last few years is a definite movement in the direction of providing a unified theory of the binding of nuclear matter and

pion-nucleus scattering. This attempt is in a somewhat crude state at the moment but some interesting and provocative results are already emerging.

A number of groups have participated in the effort including the Ericsons[5], Ericson and Delorme and the Lyon group[14], Weise, Bäckman, Oset, Toki, Mukophadoyay, Rho, Brown, and Bayme.[15] The work is connected with attempts to understand pion condensates and a large number of other groups have contributed to that effort.[15]

The present discussion will be in regard to a local density approximation to nuclear matter One notes that the spin-isospin operator appropriate to pion exchange is $\vec{\tau}_1 \cdot \vec{\tau}_2 \; \vec{\sigma}_1 \cdot \vec{\sigma}_2$ and that this form has a long-range attractive contribution from the pion exchange and a short-range repulsive contribution from vector-meson exchange. If we consider the short-range part to be zero range, then it can be represented as a constant (g') in momentum space

$$V \sim (g' - \frac{q^2}{\mu^2+q^2-\omega^2}) \quad .$$

This interaction is to be used in an RPA calculation and has contributions from both nucleon-hole states and delta-hole states, e.g.,

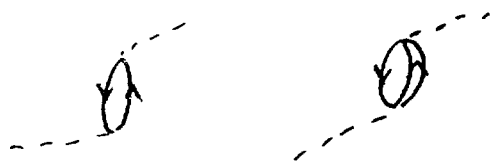

The effect of the averaging of the propagations, including the Pauli effect in the case of the nucleons, is to provide a pion self-energy given by

$$\pi = (g' - \frac{q^2}{\mu^2+q^2-\omega^2}) \; (\mu^2+q^2-\omega^2) \; U$$

where U has a contribution from the delta-hole graphs ($\sim\rho$) and a contribution from the nucleon-hole graphs ($\sim \rho^{1/3}$). For ω=0 the nucleon-hole graphs dominate and it is at this point that pion condensates are sought or precursor effects are looked for. For $\omega \gtrsim \mu$, the nucleon-hole graphs become negligible and if one identifies the pion self-energy with the pion potential the pion wave function satisfies

$$[(\mu^2 + q^2 - \omega^2)(1 + q'U) - q^2U] \; \phi = 0 \quad .$$

or

$$[q^2 - k^2 - \frac{q^2U}{1 + q'U}] \; \phi = 0 \quad .$$

This is identical to the Lorentz-Lorenz effect, as was pointed out by Bayme and Brown, if we identify

$$g' = \xi/3 \quad .$$

Estimates of g' vary widely but current values are in the range .75-.375. Even the smallest of these are seemingly not allowed by low energy pion nucleus elastic scattering on light nuclei. The resolution of this question is not clear. It may be that the light nuclei studied so far are too small for the nuclear matter concepts to be valid or it may be that the g' (representing an effective potential) may be rather different for the nucleon-hole states and the delta-hole states. Perhaps low energy pion nucleus scattering should be regarded as a technique for measuring the delta-hole g'.

For the static field, the equation becomes

$$[q^2 + \mu^2 - \frac{q^2 U}{1+g'U}] \phi = 0 \quad .$$

This equation has no solutions for g' larger than some critical amount which is known as g' critical or more generally the equation

$$[q^2 + \mu^2 - \omega^2 - \frac{q^2 U}{1 + g'U}] \phi = 0$$

has only solutions of $\omega^2<0$ for $g'>g'_c$. Of course, we may always solve for the complete set of functions which are the solutions of the eigenvalue problem,

$$[q^2 + \mu^2 - \frac{q^2 U}{1 + g'U}] \phi_n = \omega_n^2 \phi_n \quad .$$

If there exists a solution with $\omega_n^2 \geq 0$, it is said that a condensate exists. Note that each nucleon can act as a source of pions so that the equation is driven. Of course, the pion field dies out as we get further from the nucleon but if g' is not too large, we may have a correlation of fairly long range. Of course, for $g'=g'_c$ the range is infinite.

The driven equation is

$$[q^2 + \mu^2 - \frac{q^2 U}{1 + g'U}] \phi = (q^2 + \mu^2)\phi_0 \quad ,$$

so that

$$\phi = [q^2 + \mu^2 - \frac{q^2 U}{1 + q' U}]^{-1} (q^2 + \mu^2)\, \phi_0$$

$$= \Sigma \frac{\phi_n}{\omega_n^2} \langle \phi_n | q^2 + \mu^2 | \phi_0 \rangle \quad .$$

And if $g' = g'_c$, then $\phi = \phi_0$ and the pion field in the nucleus is given by the condensate solution.

A number of ways have been suggested to investigate this static field. Some of them are inelastic electron scattering[14], pion production by pions[17], one-nucleon absorption of stopped pions[18], and threshold pion production by polarized protons.[19]

If this field is as strong as the Lyon group suggests (and maybe even if it isn't) we should be able to see effects of this enhancement, perhaps even in inclusive reactions. I will close with some examples of the kind of things I mean.

First looking at pion production in reactions in which the nucleus is completely demolished, one might hope to see remnants of the "spectator" pions in the nucleus, in other words, knocking the nucleons out of the nucleus leaving the pion field behind as in any spectator model. Of course, one must also consider production from the nuclear field.

Another possibility is the interaction of pions directly with this pionic field in single or double charge exchange. Germond and Wilkin[20] proposed this mechanism for double charge exchange on ^{4}He some time ago, but simply from the unenhanced field. Here double charge exchange is assumed to go via charge exchange in the π-π interaction. As an example, take ^{18}O. We would consider

$$^{18}O \longleftrightarrow {}^{18}F^* + \pi^-$$

$$^{18}Ne \longleftrightarrow {}^{18}F^* + \pi^+ \quad .$$

Then

$$\pi^+ + {}^{18}O \rightarrow \pi^+ + ({}^{18}F^* + \pi^-) \rightarrow \pi^- + ({}^{18}F^* + \pi^+) \rightarrow \pi^- + {}^{18}Ne \quad .$$

Note that, while the parentage for the breakdown of these states is small, only one step is needed for the reaction to take place. Note also that there will be no resonance effect from this part of the reaction and the angular distribution will be determined largely by the shape of the pion field. Thus there may be sufficient signatures to separate the effects of the pion field from other "background" terms.

REFERENCES

1. R. H. Landau and A. W. Thomas, Nucl. Phys. A302, 461 (1978).

2. L. C. Liu and C. M. Shakin, Phys. Rev. C16, 333 (1977).

3. H. Garcilazo and W. R. Gibbs, Los Alamos Report LA-UR-80-6036 submitted to Nuclear Physics.

4. J. M. Eisenberg, J. Hüfner, and E. J. Moniz, Phys. Lett. 47B 381 (1973).

5. M. Ericson and T.E.O. Ericson, Ann. Phys. (N.Y.) 36, 323 (1966).

6. J. Delorme and M. Ericson, Phys. Lett. B60, 451 (1976).

7. W. R. Gibbs, B. F. Gibson, and G. J. Stephenson, Jr., Phys. Rev. Lett. 39, 1316 (1977).

8. R. Landau and F. Tabakin, Phys. Rev. D5, 2746 (1972); J. T. Londergan, K. W. McVoy, and E. J. Moniz, Ann. Phys. 85, 147 (1974); M. Reiner, Phys. Rev. Lett. 38, 1467 (1977).

9. M. Bolsterli, W. R. Gibbs, B. F. Gibson, and G. J. Stephenson, Jr., Phys. Rev. C10, 1125 (1974).

10. W. R. Gibbs, A. T. Hess, and W. B. Kaufmann, Phys. Rev. C13, 1982 (1976).

11. E. J. Moniz in NATO Advanced Study Institute on Theoretical Methods in Intermediate Energy and Heavy-Ion Physics, Madison, Wisconsin, June 1978.

12. L. S. Kisslinger and W. L. Wang, Ann. Phys. 99, 374 (1976).

13. A. N. Saharia and R. M. Woloshyn, Proceedings on Nuclear Structure with Intermediate-Energy Probes (Los Alamos) January 1980, LA-8303-C, page 423.

14. J. Delorme and M. Ericson, Phys. Lett. B60, 451 (1976).

15. W. Weise, Nucl, Phys. A278, 402 (1977); E. Oset and W. Weise, Nucl. Phys. A319, 477 (1979); J. Delorme, M. Ericson, A. Figuleau, and C. Thevent, Ann. of Phys. 102, 273 (1976); Mannque Rho, Nucl. Phys. A231, 493 (1974); J. Delorme, A. Figureau, and P. Guichon, Preprint Lyon, March 1980; S. Barshay, G. E. Brown, and M. Rho, Phys. Rev. Lett. 32, 787 (1974); H. Toki and W. Weise, Zeitschrift für Physik A292, 389 (1979); H. Toki and W. Weise, Phys. Rev. Lett. 42, 1034 (1979); M. Ericson and J. Delorme, Phys. Lett. 76B, 182 (1978). M. C. Mukophadoyay, H. Toki, and W. Weise, Phys. Lett. 48B, 38 (1979); G. Bayme and G. E. Brown, A 302, 1493 (1978); G. E. Brown, S. O. Bäckman, E. Oset, and W. Weise, Nucl. Phys. A286, 191 (1977).

16. R. F. Sawyer, Phys. Rev. Lett 29, 382 (1972); A. B. Migdal, Phys. Rev. Lett. 31, 257 (1973); G. Bertsch and M. B. Johnson, Phys. Rev. D12, 2230 (1975); B. H. Wilde, S. A. Coon and M. D. Scadron, Phys. Rev. D18, 4489 (1978); D. K. Campbell, Session XXX; Les Houches 1977, Nuclear Physics with Heavy Ions and Mesons, North-Holland Publishing Company, 1978; J. Meyer-ter-Vehn, Z. Physik, A287, 241 (1978).

17. J. M. Eisenberg, preprint Tel Aviv (1980).

18. M. A. Trotskii, M. V. Koldaev, and N. I. Chekunaev, JETP 46 (4), 662 (1977).

19. W. R. Gibbs, Proceedings of Workshop on Nuclear Structure with Intermediate-Energy Probes, Los Alamos, NM, Janury 14-16, 1980, LA-8303-C.

20. J. F. Germond and C. Wilkin, Lett Nuovo Cimento 13, 605 (1975).

THEORY OF PRECOMPOUND REACTIONS AND NUCLEON SPECTRA AFTER PION ABSORPTION[+]

by

J. Hüfner

with the collaboration of H. C. Chiang[++]

Institut für Theoretische Physik der Universität Heidelberg

and

Max-Plank-Institut für Kernphysik. Heidelberg

Federal Republic of Germany

ABSTRACT

A pragmatic approach to nuclear precompound reactions and to the intranuclear cascade after pion absorption is presented. We propose a multiple scattering expansion. Single collision dominates nuclear precompound reactions. The absorption of the negative pion on two nucleons plus a few nucleon-nucleon collisions can explain the available experimental nucleon spectra in magnitude and shape.

I. Introduction

By how many nucleons is the pion absorbed? Despite thirty years of study, this question has not yet been answered satisfactorily.[1-5] To our opinion the reason for this situation does not lie in a lack of good experimental data but in a transparent analysis of the complicated process. On the other hand, the future of pion-nucleus physics is closely linked to a thorough understanding of the absorption process.[6] Therefore, a transparent method to analyze the phenomena after pion absorption is desirable.

[+]Supported in part by a grant from the Federal Ministry of Research and Technology (BMFT).

[++]On leave from the Institute of High Energy Physics, Academia Sinica, Peking, China.

It is customary, not necessarily right, to divide the absorption process into two steps: Pion is absorbed by a "cluster" of nucleons, i.e. the kinetic energy and the rest mass of the pion are converted into kinetic energy of nucleons; the original nucleons, which have taken part in the absorption of the pion may leave the nucleus without colliding with the other nucleons (then they are called primary) or only after several collisions with other nucleons in the nucleus (the striking and the struck ones are labelled secondary). The observed spectrum is the sum of primary and secondary nucleons. Clearly the difficulty in understanding pion absorption itself, is to separate the influence of the final state collisions from the primary event.

The final state nucleon-nucleus interaction after pion absorption is very similar to the nucleon-induced precompound reactions in the energy domain of several tens of MeV. Instead of the nucleons originating from π^- absorption, in the precompound reactions, one nucleon with definite momentum P_0 collides with nucleus ^{A}Z from outside of the nucleus. The momentum of the outgoing nucleon is measured, while the rest of the system remains unobserved. One can sum up π-absorption and nuclear preequilibrium reactions as follows:

$$h + {}^{A}Z \longrightarrow N' (P) + X \qquad (1)$$

$$h + {}^{A}Z \longrightarrow N_1 (P_1) + N_2 (P_2) + X' \qquad (2)$$

Here h (hadron) stands for a pion or a nucleon. In type (1) only one nucleon is measured. Correlated nucleons are observed in reactions of type (2).

The basic idea of a sequence of nucleon-nucleon (NN) collisions, which generates a hierarchy of nuclear excitation underlines every calculation for precompound reactions so far. The intranuclear cascade,[7] the exciton model,[8] and the multi-step direct reaction (MSDR)[9,10] approaches are the main methods to describe precompound reactions. All these approaches are successful when they are compared to the data. Since the three approaches differ considerably, some basic ingredients common to all approaches must be responsible for the success. We think that the simplicity of precompound processes lies in the fact that only very few collisions of the projectile determine quantitatively the inclusive cross section.

We propose a pragmatic approach which is based on a multiple scattering expansion of the inclusive cross section. It has been derived rigorously for

high energies by Glauber et al.[11] Its basic structure coincides with Feshbach's statistical theory of multi-step processes.[12] Apart from a few physically reasonable modifications, we keep the basic structure of the formulae when going from high energies to the preequilibrium domain.

For simplicity, we only discuss here the reactions of type (1). The formulae for nucleons after pion absorption and for nucleons from a precompound reaction are nearly identical. More complicated formulae for correlated spectra are given in a paper by Hüfner et al.[13]

One-nucleon inclusive momentum distribution after π^- absorption:

We formulate the momentum distribution of outgoing nucleon N (proton or neutron) as an expansion,

$$\frac{dW\ (N,\underset{\sim}{P})}{d^3P} = \sum_{\mu=0}^{\infty} G_\mu\ C_\mu(N)\ \frac{d\ D_\mu(\underset{\sim}{P})}{d^3P} \quad . \tag{3}$$

Here we define $dW(N,P)/d^3P$ as the probability to observe, per stopped pion, a nucleon of type N which has a momentum in the interval d^3P around P. μ refers to the number of NN collisions in the intranuclear cascade. $\mu = 0$ corresponds to the distribution of primary nucleons after π^- absorption. $\mu = 1$ term is the secondary nucleon distribution with one NN collision after π^- absorption. Each term is factorized into three factors. In the following, we describe each factor in detail.

The factor G_μ gives the integrated probability for one event in which the original nucleon undergoes μ collisions. It is calculated from geometry considerations.

$$G_\mu = \int d^3r\ S(r)\ \frac{T^\mu(r,e)}{\mu!}\ e^{-T(r,e)}\ \frac{d\ \Omega_e}{4\ \pi} \quad . \tag{4}$$

Here S(r) gives the location where the pion is absorbed. At the same time it is the source function of the original nucleons from which they start cascading. S(r) is calculated from the pionic wave function and π-nucleus optical potential, and is normalized to 1.

$$S(r) = -g\ (\mathrm{Im}\ U_{op}^{Local}\ |\ \psi_\pi(r)|^2 + \mathrm{Im}\ C_0\ \rho^2(r)|\ \nabla\psi_\pi(r)|^2)$$

and

$$\int d^3r\ \ S(r) = 1 \quad . \tag{5}$$

In eq. (4), $T(\underset{\sim}{r},\underset{\sim}{e})$ is the thickness of the target looking along the e direction starting from r. $T(\underset{\sim}{r},\underset{\sim}{e})$ is measured in units of nucleon mean free path λ.

$$T(\underset{\sim}{r},\underset{\sim}{e}) = \int_{Z}^{\infty} \frac{dZ'}{\lambda} \cdot \frac{\rho(b,Z',\underset{\sim}{e})}{\rho(o)} \quad , \tag{6}$$

where $\rho(r)$ is the nuclear density function.

The factor $dD_\mu(\underset{\sim}{P})/d^3P$ describes the momentum distribution of the outgoing particle, which is normalized to 1. For pion absorption, the initial momentum distribution dD_o/d^3P is calculated from the two-nucleon mechanism using a short-range interaction, $V_{\pi NN}$. For $\mu \neq o$ the dD_μ/d^3P are obtained by folding,

$$\frac{dD_\mu(\underset{\sim}{P})}{d^3P} = \int d^3P' \; \frac{d\sigma}{d^3P}(\underset{\sim}{P}' \rightarrow \underset{\sim}{P}) \; \frac{dD_{\mu-1}(\underset{\sim}{P}')}{d^3P'} \quad , \tag{7}$$

where

$$\frac{d\sigma}{d^3P}(P' \rightarrow P) = C \int_{k'<P_F} d^3k' \int_{k<P_F} d^3k \; \frac{d\sigma}{d^3P'}(\underset{\sim}{P}',\underset{\sim}{k}' \rightarrow \underset{\sim}{P},\underset{\sim}{k})$$

$$\times \; \delta(\underset{\sim}{P}' + \underset{\sim}{k}' - \underset{\sim}{P} - \underset{\sim}{k}) \quad \delta(P'^2 + k'^2 - P^2 - k^2) \tag{8}$$

and

$$\int d^3P \; \frac{d\sigma}{d^3P} = 1 \quad . \tag{9}$$

Here the energy and momentum conservation for each collision and the Pauli principle are taken into account.

The counting factor $C_\mu(N)$ gives the number of nucleons of type N after μ collisions, which is calculated by the recursion relation according to the initial number and type of nucleons. For instance, for π^- absorption by an n-p pair $C_o(n) = 2$ and $C_o(p) = 0$. If one approximates $Z = N$ and $\sigma_{pp} \simeq \sigma_{pn}$ one finds

$$\begin{aligned} C_1(n) &= 3 \\ C_1(p) &= 1 \end{aligned} \tag{10}$$

and so on. Of course, the initial number and type of nucleons depend on the absorption mechanism; in turn the initial $C_o(N)$ affects the shape and the magnitude of the final distribution. Within the two-nucleon mechanism we define

$$R_{np} = \frac{2\ (A - Z)}{(Z-1)} \quad . \quad R$$

and

$$R = \frac{r\ (\pi^- + n + p \rightarrow n + n)}{r\ (\pi^- + p + p \rightarrow n + p)} \quad . \tag{11}$$

One finds

$$C_o(n) = \frac{2}{1 + R_{np}^{-1}} + \frac{1}{1 + R_{np}}$$

and

$$C_o(p) = \frac{1}{1 + R_{np}} \quad . \tag{12}$$

We can extract R from the comparison with experiments.

Inclusive cross section for precompound reactions:

In going from pion absorption to nuclear precompound reactions, instead of the probability of the momentum distribution dW/d^3P, now we have a cross section,

$$\frac{d\sigma}{d^3P} = \sum_{\mu=1}^{\infty} \sigma_\mu \ C_\mu(N) \ \frac{dD_\mu(\underset{\sim}{P})}{d^3P} \tag{3a}$$

One only needs to replace eqs. (4), (5), and (10) by the following expressions, respectively.

$$\sigma_\mu = \int d^3r \ S'(r) \ \frac{T^\mu(\underset{\sim}{r},\underset{\sim}{e})}{\mu!} \ e^{-T(\underset{\sim}{r},\underset{\sim}{e})} \tag{4a}$$

$$S'(r) = \delta(Z + \infty) \tag{5a}$$

$\underset{\sim}{e}$ = beam direction

$$\frac{dD_o}{d^3P}(\underset{\sim}{P}) = \delta(\underset{\sim}{P} - \underset{\sim}{P}_o) \tag{13}$$

and

$$C_0(p) = 1$$

$$C_0(n) = 0$$

$$C_1(p) = 1.5 \qquad \text{(for proton induced reactions)}$$

$$C_1(n) = 0.5 \qquad (10a)$$

The summation in eq. (3a) only goes from 1 to infinity because one only considers the inclusive inelastic reaction. In this case, σ_μ however has the meaning of integrated cross section for μ collisions.

In practice, the summation eq. (3a) converges rapidly for two reasons: (i) the rather long mean free path and (ii) fairly large energy loss after one NN collision. This is discussed extensively in a paper by Chiang et al.[14] Only a few terms are needed except for compound nucleus formation in the 15-100 MeV domain. Because of the above two reasons, we count as compound nucleus formation all multiple scattering with $\mu>2$ and those fractions of single and double collisions where the laboratory energy of the outgoing particle is below the Coulomb barrier for protons or below zero for neutrons.

Comparison with data:

The theory described above has no adjustable parameter for precompound reactions, and the ratio R, which is an important quantity for π^--absorption, is fit to the data. The nuclear densities $\rho(r)$ are taken from the results of elastic electron scattering. Values of Fermi momentum P_F are tabulated by Moniz et al.[15] The mean free path of a nucleon inside the nucleus is a quantity which is still debated.[5] We choose λ between 3 to 5 fm according to the discussion in Ref. 14.

Figure 1 shows the cross section for a proton-nucleus reaction at 62 MeV. The solid curve is our calculation in which one, two collisions and the compound nucleus contribution are included. It fits well in shape and in magnitude. The agreement with the cascade calculation is nearly perfect. Deviations are significant only for the small energy losses. Double scattering turns out to be unimportant except for the small final energies. The double differential cross sections $d\gamma/dEd\Omega$ for proton induced reactions at 90 MeV are calculated and compared with experiments done by Wu et al.[17] Two examples are shown in Fig. 2. Again the trends and absolute magnitudes are reproduced. Discrepancies appear also here, at small energy loss and for forward angles.

Figures 3 and 4 show the energy spectra of neutrons and protons after π^- absorption on ^{12}C. Both the absolute magnitude and the shape are well reproduced by the calculation truncated after $\mu = 1$. The primary neutrons dominate the spectrum above 50 MeV (Fig. 3) and the primary protons dominate only above 90 MeV (Fig. 4). These parts of the spectra are sensitive to the ratio R. We find $R = 6 \pm 3$.

In Fig. 5, we compare our calculation with the measured energy distribution for correlated nucleons. The largest intensity is seen at 180°, the back-to-back emission of the two nucleons, which is expected from a two-nucleon mechanism. The intensity falls down rapidly with increasing angles. This occurs at least at neutron energies above 20 MeV. The calculation reproduces the shape and the absolute value of the data fairly well for ^{12}C, but the calculation is significantly below the data at small energies. We attribute the discrepancy to our truncation at an early stage.

Summary:

We have presented a multiple scattering expansion to describe precompound reactions and the energy and angular distributions for nucleons after the absorption of stopped negative pions. We observe the following characteristics:

1) The multiple scattering expansion series converges rapidly. Single scattering dominates nucleon-nucleus inclusive cross section for energies between 15-100 MeV. Double collision contributes only at the low energy end of the spectra. There is no need for higher order multiple scattering, except compound nucleus formation and its decay. Therefore, we characterize our precompound approach by "one, two, infinity, meaning single and double collisions plus compound nucleus formation."

2) Two-nucleon mechanism plus one or two final state nucleon-nucleon collisions give the observed nucleon data after π^- absorption. But we were not able to give a quantitative upper limit for processes where the pion is absorbed by a larger cluster.

3) A significant portion of the observed energy spectra and also of the angular distribution is dominated by the primary nucleons. The discrepancy between primary distributions and the experimental data can be accounted for by another collision except at the very low energy end where the compound nucleus decay dominates.

4) Our approach calculates both the shape and the magnitude for all available experimental data essentially without adjustable parameters, except the ratio R for π^- absorption which is not quite well known. We subtract R = 6 ± 3 from the experiments.

ACKNOWLEDGMENTS

We have profited from discussions with friends at SIN and our colleagues in Heidelberg, in particular with F. Hachenberg, A. Klar, H. J. Pirner. Mrs. Seitz drew the figures. One of us, H. C. Chiang, acknowledges a fellowship from the Max-Planck-Gesellschaft and the hospitality from the theory group in Heidelberg.

REFERENCES

1. D. S. Koltun, Advances in Nucl. Phys. 3, 71 (1969).
2. T. I. Kapaleishvili, Particles and Nuclei, 22, 87 (1973).
3. J. Hüfner, Phys. Reports, 21C, 1 (1975).
4. H. K. Walter, Proceed. 7th. International Conference on High Energy Physics and Nuclear Structure, Zürich, 1977; M. Locher et al., eds. (Birkhäuse Verlag Basel, 1977) p. 225.
5. J. P. Schiffer, Proceed. 8th. International Conference on High Energy Physics and Nuclear Structure, 1979, Nucl. Phys. A335, 33(1980).
6. M. Thies, Invited Talk at International Symposium on Few Particle Problem in Nuclear Physics, Dubna, June 5-8, 1979.
7. J. Ginocchio and M. Blann, Phys. Lett. 68B, 405 (1977).
8. M. Blann. Ann. Rev. Nucl. Sci. 25, 123 (1975); D. Agassi, H. A. Weidenmüller and G. Mantzouranis, Phys. Lett. 22C, 220 (1975).
9. H. Feshbach, Rev. Mod. Phys. 46, 1 (1974).
10. T. Tamura, T. Udagawa, D. H. Feng, and K. K. Kan, Phys. Lett. 66B, 109 (1977).
11. R. J. Glauber and G. Matthiae, Nucl. Phys. 21B, 135 (1970).
12. H. Feshbach, A. Kerman, and S. Koonin, Ann. Phys. 125, 429 (1980).
13. J. Hüfner and H. C. Chiang, To be submitted
14. H. C. Chiang and J. Hüfner, to be published in Nucl. Phys. A.

15. E. J. Moniz, I. Sick, R. R. Whitney, J. K. Ficenae, R. D. Kephart, and W. P. Trower, Phys. Rev. Lett. 26, 445 (1971).

16. F. E. Bertrand and R. W. Peelle, Phys. Rev. C8, 1045 (1973).

17. J. R. Wu, C. C. Chang, and H. D. Holmgren, Phys. Rev. C19, 698 (1979).

18. H. L. Anderson, E. P. Hincks, C. S. Johnson, C. Rey, and A. M. Segar, Phys. Rev. B133, 392 (1964).

19. B. Bassalleck, H. D. Engelhardt, W. D. Klotz, F. Takeutchi, and H. Ullrich, Nucl. Phys. A319, 397 (1979).

20. R. Hartmann, H. P. Isaak, R. Engfer, E. A. Hermes, H. S. Pruys, W. Dey, H. J. Pfeiffer, U. Sennhauser, H. K. Walter, and J. Morgenstern, Nucl. Phys. A300, 345 (1978).

21. U. Klein, G. Büche, W. Kluge, H. Matthäy, G. Mechtersheimer, and A. Moline, Nucl. Phys. A329, 339 (1979).

22. F. W. Schlepütz, J. C. Comisco, T. C. Meyer, and K. O. H. Ziock, Phys. Rev. C19, 135 (1979).

23. H. S. Pruys, R. Engfer, R. Hartmann, E. A. Hermes, H. P. Isaak, F. W. Schlepütz, U. Sennhauser, W. Dey, K. Hess, H. J. Pfeiffer, and W. Hesselink, SIN Report PR-80-009 (Feb. 1980).

24. G. Mechterscheimer, G. Büche, U. Klein, W. Kluge, H. Matthäy, D. Münchmeyer, and A. Moline, Phys. Lett. 73B, 115 (1978).

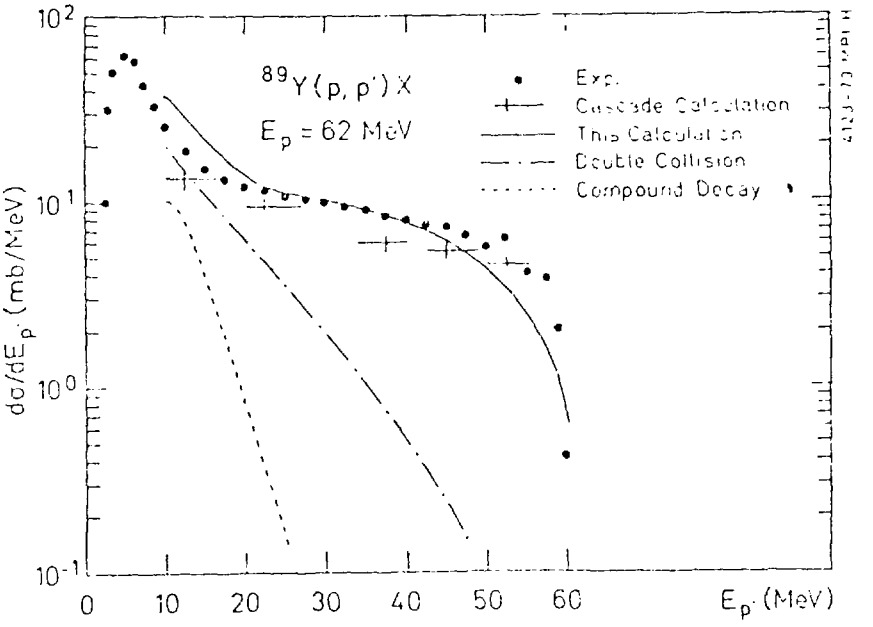

Fig. 1.

The inclusive cross section $d\sigma/dE_{p'}$ for the (p,p') reaction on Y at an energy of 62 MeV plotted as a function of the energy $E_{p'}$ of the final proton. The experimental values are taken from Bertrand et al.;[16] the solid curve represents our calculation (λ = 4.2 fm). For Y, the contribution of double scattering and compound nucleus decay and the results of a cascade calculation by Ginocchio et al.[7] are given.

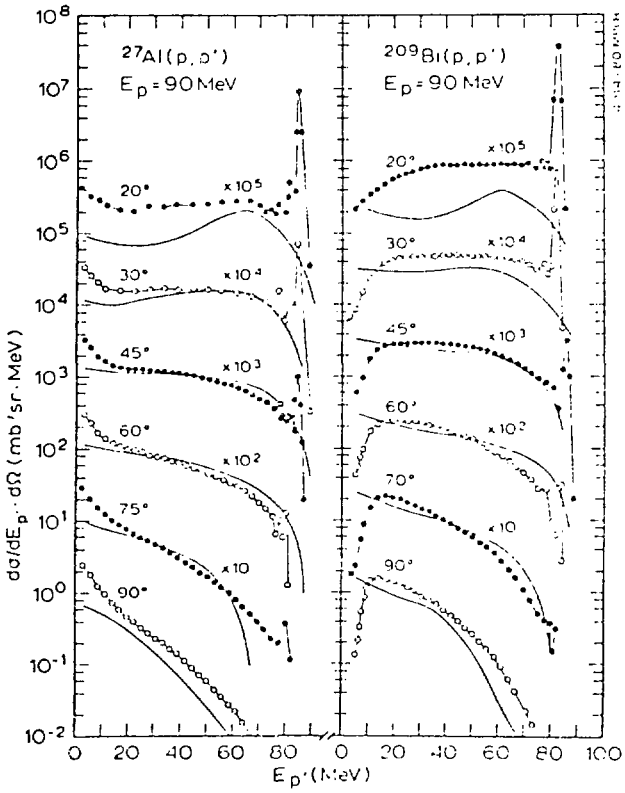

Fig. 2.

Double differential cross sections $d\sigma/d\Omega dE_{p'}$ for the (p,p') reaction on Al and Bi for different angles and as a function of $E_{p'}$. The experimental points (connected by a thin line) are from Wu et al.[17] The solid line represents the results of our calculation (λ = 3 fm).

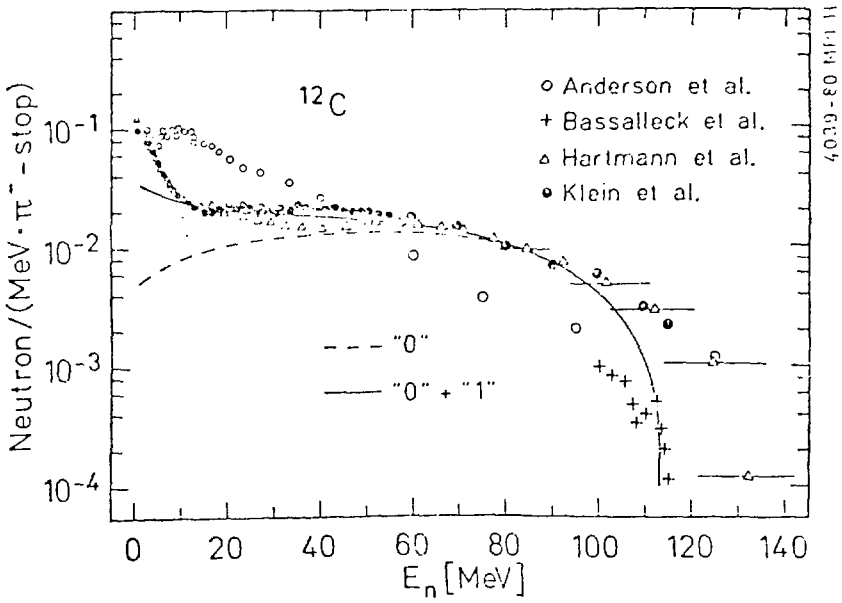

Fig. 3.

Experimental and calculated energy spectra of neutrons after a stopped π^- is absorbed by ^{12}C. The data are from Anderson et al.,[18] Bassalleck et al.,[19] Hartmann et al.,[20] and Klein et al.[21] The dashed curve represents the contribution from the primary neutrons. The solid line includes in addition those events with one inelastic collision in the intranuclear cascade.

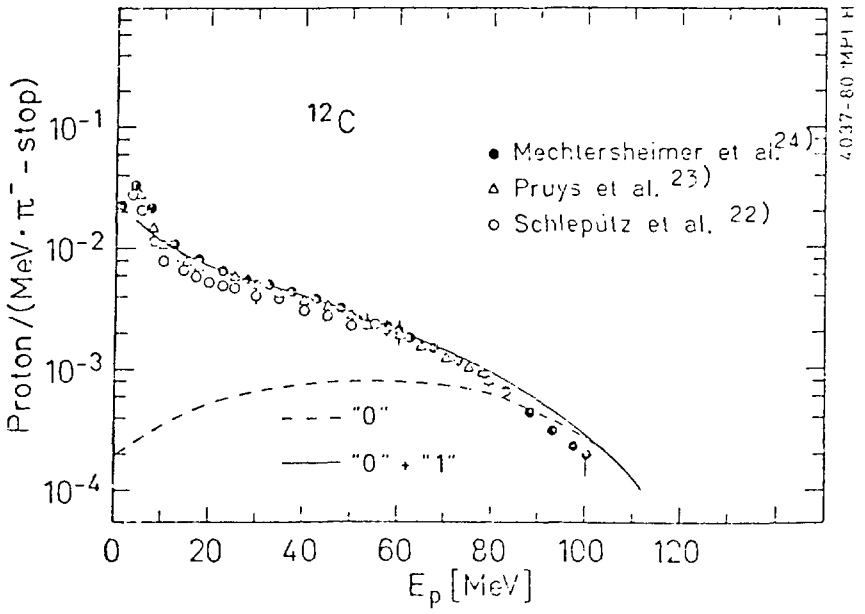

Fig. 4.

Experimental and calculated energy spectra for protons after the stopped π^- absorption by ^{12}C. The contribution from primary protons is shown by the dashed line. The solid one includes primary ones plus secondary ones. The curve is calculated for $R_{np} = 9.6$.

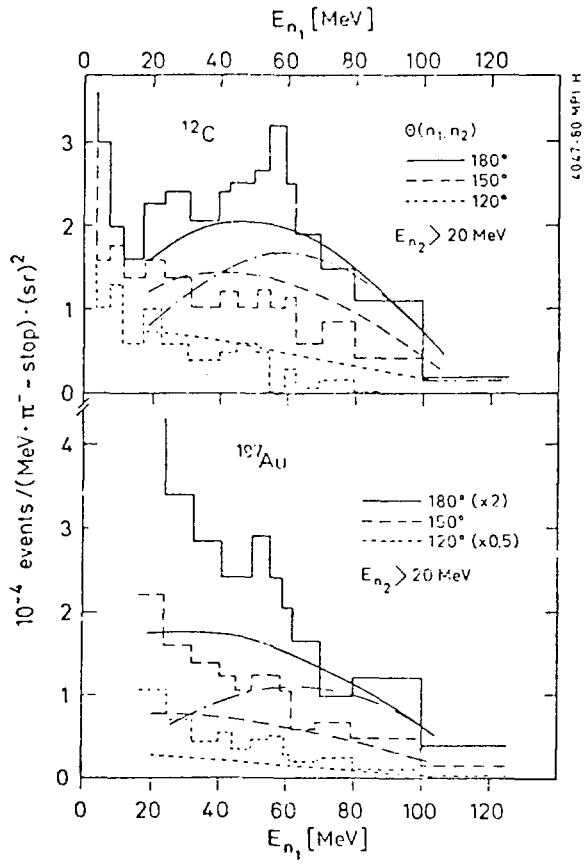

Fig. 5.

Energy and angular distributions of a neutron which is measured in coincidence with a second neutron for π^- absorption in ^{12}C and ^{197}Au. The reference counter for neutron n_2 has a lower threshold of 20 MeV. The counter which measures the energy of neutron n_1 is located at angles of 180°, 150°, and 120° with respect to the reference counter. The experimental values by Hartmann et al.[20] are given in the form of the histogram. The curves represent our calculation. Solid lines in the curve correspond to 180°, dashed lines to 150°, and short dashed ones to 120°. The contribution of the primary neutrons is shown by the dash-dot line for 180° only.

CURRENT NUCLEAR REACTION STUDIES IN JAPAN

by

T. Nishi
Kyoto University, Japan

Several studies of the interaction between pions and complex nuclei which have been performed at the National Institute for High Energy Physics (KEK) in Japan by several nuclear physicists and chemists groups are presented very briefly in this article.

1. The first subject is the study of the inclusive neutron production from complex nuclei bombarded by π^-. This work[1,2] was done by Prof. T. Yanabu of Kyoto University and his collaborators at the T1 beam channel. Thick targets of Be, Al, Fe, Cd, and Pb were bombarded by π^- with momenta ranging from 0.5 to 1.5 GeV/c with an intensity of about 10^4/s and with purity of higher than 80%.

Neutrons emitted from the targets with energies from 3 to 100 MeV were measured by a liquid scintillation counter, 14 cm in diameter and 19 cm in depth, at three laboratory angles, 50°, 90°, and 130° with respect to the incident pion beam. The neutron energy was measured by a time-of-flight method with a resolution of 3.6 ns. The amounts of the secondary neutrons were estimated by a Monte Carlo method to be from 10 to 30% of the total neutrons depending on the neutron energies and the target used, and were corrected.

Figure 1 shows the inclusive cross sections obtained. As shown in the figure, the INC-evaporation calculation (MECC-7 and EVA)[21] reproduces quite well the low energy neutron yields of heavy mass targets, but still fails to reproduce those of light mass targets, and completely fails to reproduce the yields of higher energy neutrons (E_n > 10 MeV) over the entire target mass region. The predicted yields of higher energy neutrons are much less (factor of 3 to 7) than the experimental results.

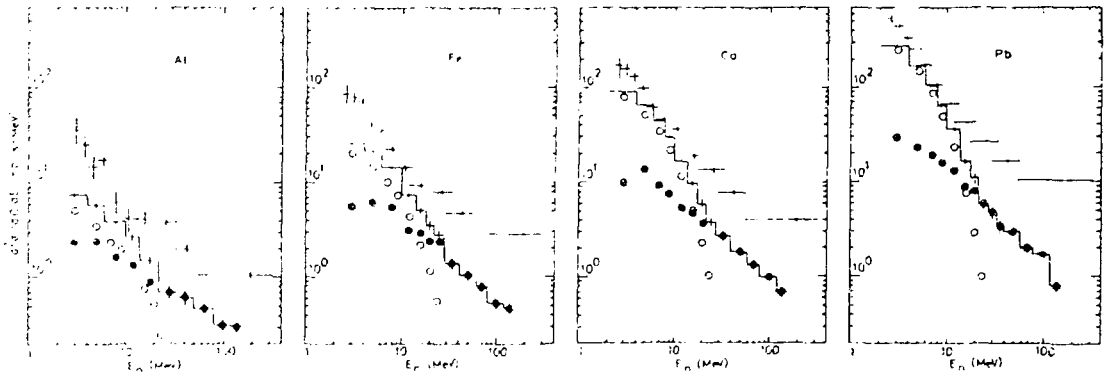

Figure 1.
Energy spectra of neutrons induced by 0.75 GeV/c negative pions on Al, Fe, Cd, and Pb. Crosses are experimental with error bars. Solid circles indicate INC calculations. Open circles, the evaporation calculations. Stepwise line, summed values of INC and evaporation. Detection angle is 50° (lab).

The low energy neutrons are found to be emitted equally at all angles, but higher energy neutrons show forward peaking.

Differential cross sections of high energy neutrons (40 ~ 60 MeV) show mass number dependence of $A^{1.0}$, in comparison with the theoretical expectation of mass dependence $A^{2/3}$.

"Quasi-Two-Body-Scaling" (QTBS) was examined with the inclusive neutron spectra emitted at backward angles. As shown in Fig. 2, QTBS holds at the intranuclear nucleon momenta (k_{min}) higher than 0.25 GeV/c at 90° (lab) and holds at all k_{min} at 130° (lab). This study is the first observation that the scaling holds not only in proton-induced nucleon emission, but also in pion-induced reactions.

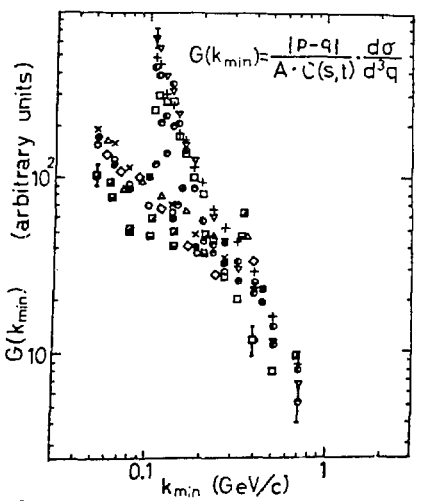

Target	p_π (GeV/c)	θ
Al	0.75	90°
Fe	0.75	"
Cd	0.75	"
Cd	1.5	"
Pb	0.75	"
Pb	1.0	"
Pb	1.5	"

Target	p_π (GeV/c)	θ
Be	1.0	130
Al	0.75	"
Fe	0.75	"
Cd	0.75	"
Pb	0.75	"

Figure 2.
$G(k_{min})$ vs k_{min}: $\pi + A \rightarrow n + X$ (90° and 130°).

2. The second subject is the inclusive pion production reaction by positive pions and protons. This work[5] was done by Prof. A. Kusumegi and his collaborators at the π2 beam channel. The beam at 4.3 GeV/c is ~10^5/s in intensity and contains 82% protons and 15% positive pions. The beam intensity was monitored by three scintillation counters and a threshold Čerenkov counter which identify pions. The beam struck targets of Be, Al, Cu, and W with 0.2 - 1.0 nuclear collision mean-free paths. The produced positive pions were measured by a single-arm magnetic spectrometer, which consisted of three arrays of scintillator hodoscopes, a threshold Čerenkov counter, a bending magnet and eight planes of wire spark chambers, and was set to $\theta_{lab} = 28.8°$ with respect to the incident beam.

The inclusive production cross sections of π^+ having transverse momentum p_T between 0.4 and 1.0 GeV/c were measured both in pion- and proton-induced reactions on the above-mentioned four targets. The exponent of α in the invariant cross section,

$$E\, d^3\sigma(p_T, A)/d^3p = E\, d^3\sigma(p_T, A=1)/d^3p \cdot A^{\alpha(p_T)},$$

was deduced by taking the ratio of the cross sections for Al, Cu, and W to that of Be.

As shown in Fig. 3, the exponent α shows a minimum value at about p_T ~600 MeV/c and increases with increasing p_T both for proton-induced and π^+-induced reactions, and exhibits a similar behavior to the other proton-induced reactions.[7,8,9]

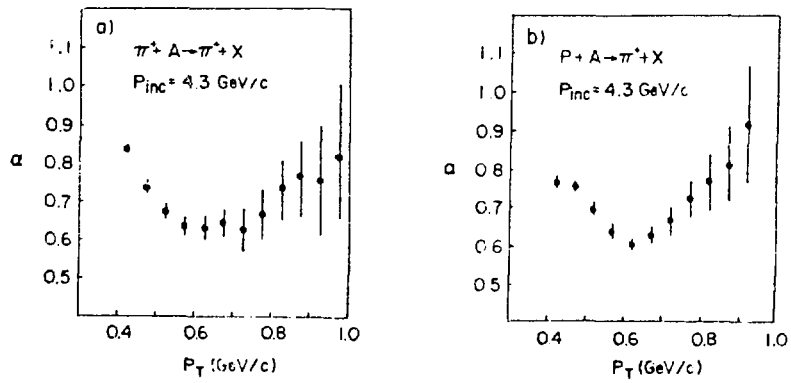

Figure 3.
The exponent α of the A-dependence of the invariant cross section of π^+ production at 4.3 GeV/c, versus p_T, for incident (a) pions and (b) protons.

The beam ratio $\sigma(pA \to \pi^+A)/\sigma(\pi^+A \to \pi^+X)$, as shown in Fig. 4, is fairly consistent with the quark-parton prediction for elementary processes at $p_T > 600$ MeV/c, where the exponent α starts to increase. The decreasing tendency of the beam ratio with increasing p_T can be naturally understood from the expected different quark distributions within the protons and the pions of the beam. The increase of α to unity may imply that nucleons inside the nucleus begin to act independently.

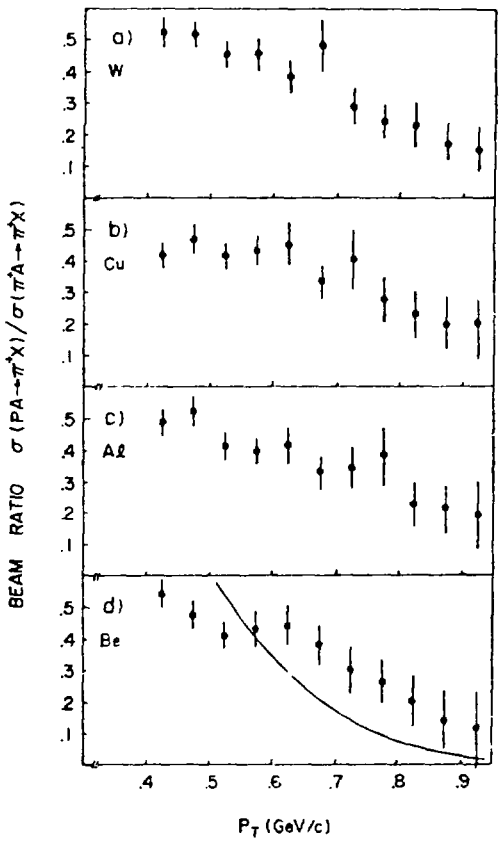

Figure 4.
The beam ratio $\sigma(pA \to \pi^+X)/\sigma(\pi^+A \to \pi^+X)$ versus p_T for targets, (a)W, (b) Cu, (c) Al, and (d) Be. The solid curve represents the prediction of Field and Feynman for a single-nucleon target.

3. The third topic is the real exclusive absorption cross sections of π^+ and π^-, and the angular momentum of the entry state. This study was done by Prof. K. Nakai of Tokyo University and his collaborators.[10] This work was done at the low momentum meson course, π-μ channel.

The method is based on the single- and multiple-coincidence measurements of gamma-rays following the pion absorption. The nuclear gamma-rays were detected with eight 3"ϕ x 3" thick NaI(Tl) detectors set around the target. The gamma signals were triggered by the signal from the counter telescope, which identified

pions in the beam by the time-of-flight method. In order to detect gamma-rays following inelastic scattering, seven liquid scintillation counters were set in coincidence with the NaI(Tl) detectors. From the ratio of the difference of the two sets of single and coincidence measurements, corrected for the contributions of the single charge exchange processes, the true pion absorption cross section and the gamma multiplicity were deduced.

The pion absorption cross sections obtained are shown in Fig. 5 with the experimental results of Navon et al.[11] and with the theoretical values calculated by the Michigan State University group.[12] The two sets of experimental results were in good agreement in spite of the different methods used. The low energy part of the cross section shows the influence of the Coulomb effect clearly.

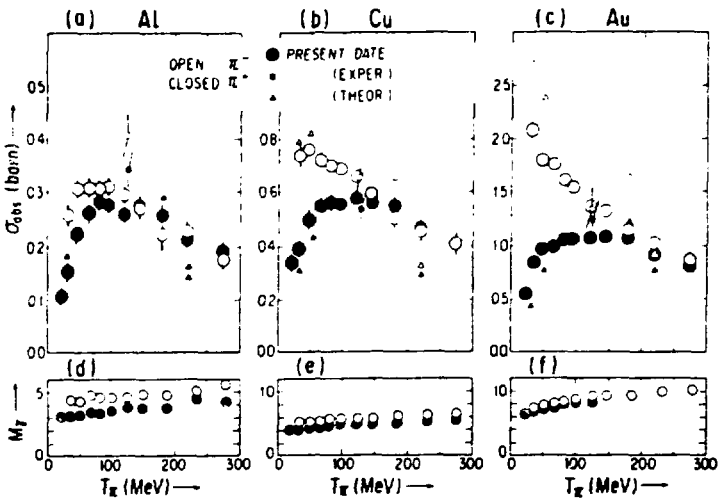

Figure 5.
Cross sections for pion absorption by (a) Al, (b) Cu, and (c) Au; (d) - (f) multiplicities of γ rays. Closed and open circles are for positive and negative pions, respectively. Squares are experimental data for Al, Fe, and Bi by Navon et al. (Ref. 11) and triangles are theoretical values by Stricker, McManus, and Carr (Ref. 12).

Theoretical calculations have reproduced the cross sections in the low energy region fairly well, but failed to reproduce the observed behavior across the (3,3) resonance.

The mean angular momenta of the entry state are deduced from the multiplicity of γ rays observed and are shown in Fig. 6.[13] $\langle L \rangle_\gamma$ are the mean angular

momenta of the entry state after nucleon evaporation, calculated from the relation which holds quite well in low energy nuclear reactions,

$\langle M_\gamma \rangle = \langle L \rangle_\gamma / 2 + K$ and K = 2.5−4, assuming K statistical transitions with $\sum_{i=1}^{\nu} \vec{L}_i = 0$ and $\langle L \rangle_{\gamma/2}$ stretched E2 transitions. $\langle L \rangle_\pi$ stretched E2 transitions. L_π is the mean angular momentum which the incident pion may bring into tne nucleus assuming simple geometrical considerations and is $\langle L \rangle_\pi = 2/3\ (p \cdot R/hc)$. $\langle L \rangle_\pi$ is much less than the $\langle L \rangle_\gamma$ value, and is contrary to those for usual low energy nuclear reactions. $\langle L \rangle_c$ is the calculated mean angular momentum with the assumption that the pion is absorbed by a pair of nucleons and that one of the constituents is emitted with one-half of the total energy. $\langle L \rangle_c$ is much higher than $\langle L \rangle_\pi$ and is nearly equal to the $\langle L \rangle_\gamma$ value. This fact may suggest the mechanism of the pion absorption.

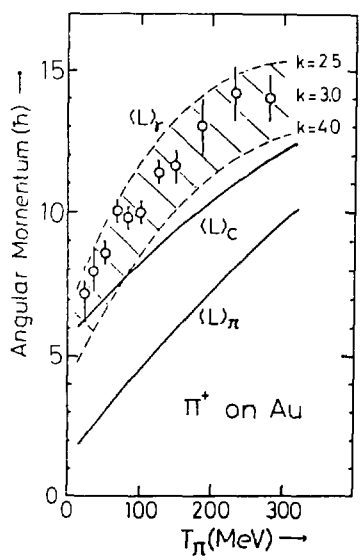

Figure 6.
Mean angular momenta of entry state, π^+ + Au.

The true absorption cross section and gamma multiplicity of pion absorption leading to a specific residual nucleus was also measured by a similar method using Ge(Li) and NaI(Tl) detectors.[14] The results are shown in Fig. 7. The gamma multiplicity seems to be independent of the number of nucleons emitted in the case of Al and Au targets. This fact implies that the average momenta left after nucleon emission are the same in each reaction channel, and supports the mechanism that the angular momentum change is determined by the fast nucleons emitted in the first stage of pion absorption.

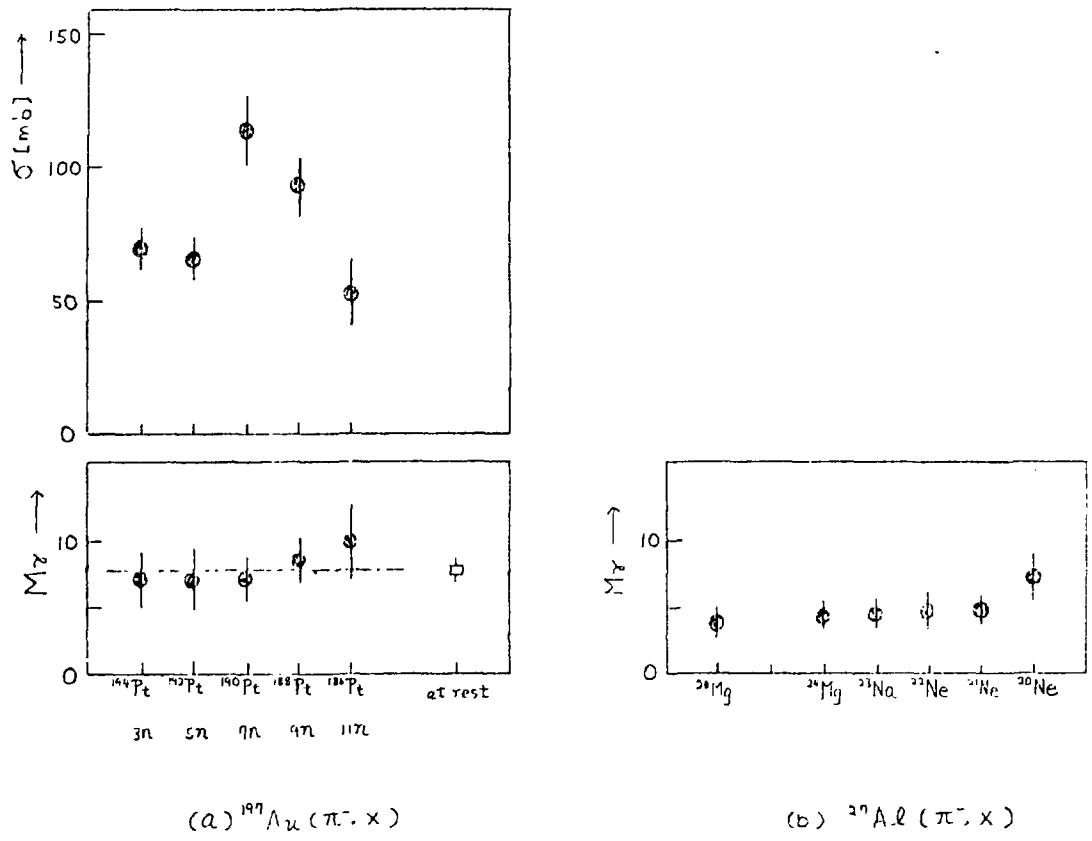

(a) ^{197}Au (π^-, x) (b) ^{27}Al (π^-, x)

Figure 7.
Pion absorption cross sections and gamma multiplicities leading to the specific residual nucleus, (a) π^- + Au and (b) π^- + Al.

4. The fourth topic is the cross section of π^--induced reactions on ^{9}Be, ^{12}C, and ^{19}F between 0.4 and 1.9 GeV. This work was performed by our nuclear chemistry group.

The absolute formation cross sections of ^{8}Li and ^{6}He from ^{9}Be bombarded by negative pions, those of ^{11}C, ^{8}Li + ^{8}B and ^{6}He from C, and the relative cross sections of ^{18}F from ^{19}F were measured. All the cross sections determined are in good agreement with the available data.[15-19] The excitation functions of the ^{9}Be(π^-, πN)^{8}Li, ^{12}C(π^-,π^-n)^{11}C, and ^{19}F(π^-,π^-)^{18}F reactions show striking differences in the shape between (π^-,πN) and (π^-,π^-n) reactions. The former one exhibits the resonance structure (T = 1/2, Eπ = 0.6 and 0.9 GeV) of the (π^-p) free-particle collision and the latter shows that (T = 3/2, E_π = 1.3 GeV) of the (π^-n) collision. Broadening of resonance peaks is attributed to the Fermi motion of the struck nucleon. The excitation of function of the ^{12}C(π^-,π^-n) ^{11}C

reaction multiplied by a scaling factor of 0.75, which is obtained for the $^{19}F(\pi^-,\pi^-n)^{18}F$ reaction around the (3,3) resonance, reproduces quite well the cross section of the $^{19}F(\pi^-,\pi^-n)^{18}F$ reaction above the resonance energy. Those facts suggest that the quasi-elastic knockout is the predominant process both in the $(\pi,\pi N)$ and (N,2N) reactions.

Figure 8 shows the ratio of the cross sections of the one-nucleon-out reaction and that of the πN collision for three pion-induced reactions and two proton-induced reactions. The ratios for the proton-induced reactions decrease monotonically with increasing incident energy. In contrast to the proton reaction, the ratio of the pion-induced reaction shows broad peaks at 0.58 GeV for $^{12}C(\pi^-,\pi^-n)^{11}C$ $^{12}C(\pi^-,\pi^-n)^{11}C/N\bar{\sigma}_{\pi N}$ and $^{19}F(\pi^-,\pi^-n)^{18}F/N\bar{\sigma}_{\pi n}$, and is partly attributed to the enhancement due to the nucleon charge exchange through the T = 1/2 isobar.

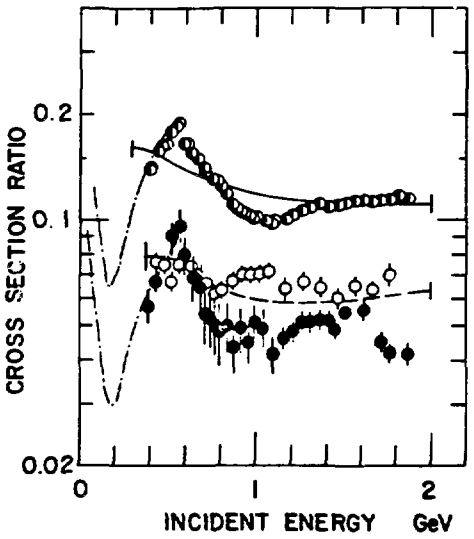

Figure 8.
The ratios of the specific reaction cross sections to the pion plus free-nucleon collision cross section, averaged over the Fermi momentum of a nucleon. The open circles are for $\sigma(^9Be(\pi^-,\pi N)^8Li)/Z\ \bar{\sigma}_{\pi p}$, the semi-open circles for $\sigma(^{12}C(\pi^-,\pi^-n)^{11}C)/N\ \bar{\sigma}_{\pi n}$, the closed circles for $\sigma(^{19}F\ (\pi^-,\pi^-n)\ ^{18}F)/N\ \bar{\sigma}_{\pi n}$. The solid and dashed lines are for $^{12}C(p,pn)^{11}C/N\ \bar{\sigma}_{pn}$ and $^{19}F(p,pn)^{18}F/N\ \bar{\sigma}_{pn}$, respectively. The dash-dot lines represent the corresponding ratios extended across the (3,3) resonance.

The ratios of $^9Be\ \pi^-\ ^6He$ and $^{12}C\ \pi^-\ (^8Li + ^8B)$ reaction cross sections to the averaged free-nucleon interactions $Z\bar{\sigma}_\pi$ and $1/2(Z\sigma^-_{\pi p} + N\bar{\sigma}_{\pi n})$ are rather constant within experimental errors over the whole energy region as shown in Fig. 9.

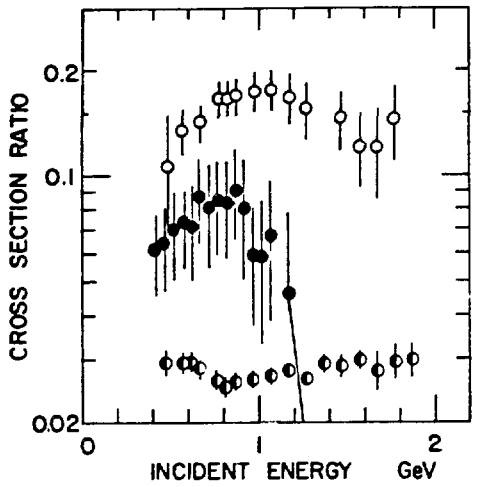

Figure 9.
The ratios of cross sections of specific pion-induced reactions to the pion plus free-nucleon collision cross section averaged over the Fermi momentum of a nucleon. Open circles are for $\sigma(^{9}Be \xrightarrow{\pi^-} {}^{6}He)/Z\ \bar{\sigma}_{\pi p}$, semi-closed circles for $\sigma(^{12}C \xrightarrow{\pi^-} (^{8}B, {}^{8}Li))/(Z\ \bar{\sigma}_{\pi p} + N\ \bar{\sigma}_{\pi n})$ and closed circles for $\sigma(^{12}C \xrightarrow{\pi^-} {}^{6}He)/Z\ \sigma_{\pi^- p \to \pi^0 n}$.

5. The fifth topic is the measurement of the angular distribution of recoiled ^{8}Li in the $^{9}Be(\pi^-,\pi N)^{8}Li$ reaction, done by Mr. S. Hayashi and Prof. S. Iwata.

A stack of a Be foil and ten sheets of nitrocellulose solid state track detector (SSTD) film on each side of the Be foil was irradiated by negative pions with a momentum of 1 BeV/c.

The angular distribution of hammer tracks corrected for the contribution of those produced in the SSTD itself, which is mostly due to ^{8}Li and minor contributions from ^{8}B and ^{8}He, shows a characteristic forward peak, as shown in Fig. 10. The calculated results on the basis of quasi-free knockout mode in two cases are also shown in the same figure. Contrary to common expectation, the calculation based on the heavy-fragment knockout process can reproduce the experimental results quite well.

6. The last subject is the π^- induced spallation reaction on V at 0.87 and 3.36 GeV performed by the same nuclear chemistry group referred to in topic 4.

Spallation yields of more than 26 products were measured radiochemically. From the cross sections obtained, charge-dispersion curves were derived for three mass regions, A=27~29, 42~44, and 46~48, where more than four independent and/or

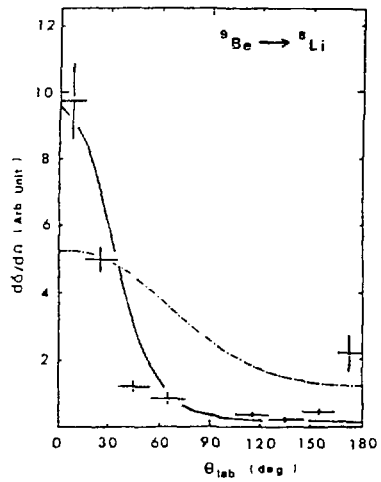

Figure 10.
The angular distribution of the recoil ^{8}Li nuclei induced by the $^{9}Be(\pi^{-},\pi N)^{8}Li$ reaction *in the laboratory system, summed over all* energies. The tracks around $\theta_{lab} = 90°$ cannot be detected by the solid state track detectors. The incident pion momentum was 1.0 GeV/c. Experimental results: crosses. Theory: dot-dashed curve -- proton knockout; solid curve -- heavy-fragment knockout.

mostly independent cross sections were measured. The mass yields were estimated following the procedure of Husain and Katcoff.[20]

The INC-evaporation calculations[21] were performed for incident pion energies of 0.87 and 2.5 GeV, because of lack of available information in pion-nucleon interactions of high energy π^{-} at 3.36 GeV, in the latter case. Both sets of calculated results reproduce fairly well the general trends of the observations. The calculation, however, fails to reproduce the yields of the near-target mass spallation products and underestimates those of neutron-rich isotopes from deep spallation (A<30). In Fig. 11, the mass yields for 3.36 GeV π^{-} spallation of V are plotted with those of 3 GeV protons on the same targets.[22] Mass yields of deep spallation products agree with each other for π^{-}-induced and proton-induced reactions. Mass yields of near-target products for π^{-}-induced reactions are much higher than those for proton-induced reactions and the calculated results.

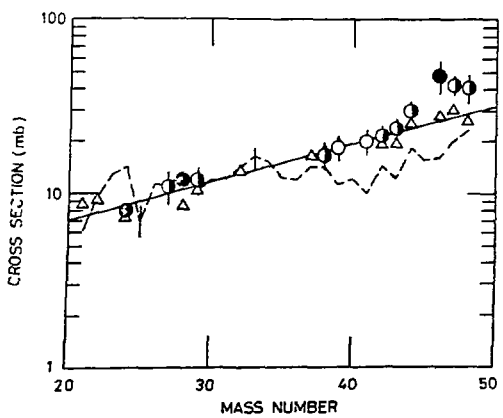

Figure 11.
Mass yield curve for 3.36 GeV π^{-} spallation of V. Filled circles show those for more than 50% of total yield are observed, half filled circles for 25~50% and open circles for less than 25%, and triangles are for 3-GeV protons on V. The dashed curve goes through calculated values. The solid curve is drawn to aid the eye.

The relative slopes of the linear part of the mass yield curve at both energies fit quite well the general tendency of the reported results,[22,23] shown in Fig. 12.

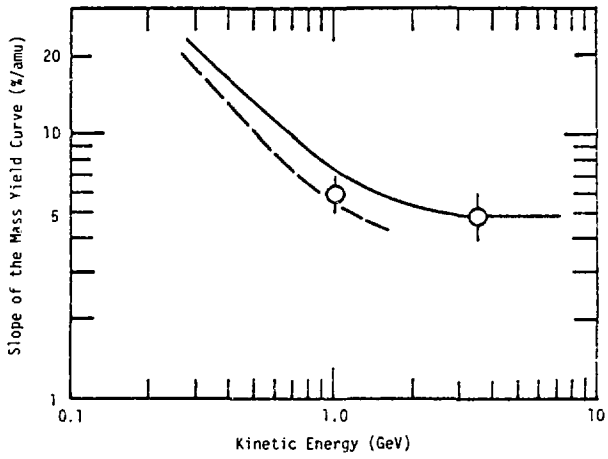

Figure 12.

Slope of the mass yield curve for spallation of V and Cu. Open circles show the values for V + π^-, and solid and dashed curves are for Cu + p and for Cu + π^- (Ref. 22 and 23), respectively.

REFERENCES

1. S. Matsuki et al., Phys. Lett. 84B, 67 (1979).

2. T. Higo et al., private communication and to be submitted to Nucl. Phys.

3. S. Frankel, Phys. Rev. Lett. 38, 1338 (1977).

4. S. Frankel, Phys. Rev. C 17 694 (1978).

5. M. Ono et al., Phys. Lett. 84B, 515 (1979).

6. C. R. Symons, CERN Program Library, X501, X502, and X503.

7. J. W. Cronin et al., Phys. Rev. D11, 3105 (1975) and
L. Kluberg et al., Phys. Rev. Lett. 38, 670 (1977).

8. V. Becker et al., Phys. Rev. Lett. 37, 1731 (1976).

9. D. A. Garbutt et al., Phys. Lett. 67B, 335 (1977),

10. K. Nakai et al., Phys. Rev. Lett. 44, 1466 (1980).

11. I. Navon et al., Phys. Rev. Lett. 42, 1465 (1979).

12. K. Stricker, H. McManus, and J. A. Carr, Phys. Rev. C19, 929 (1979).

13. K. Nakai, private communication.

14. K. Nakai, private communication.

15. D. T. Chivers et al., Nucl. Phys. A126, 129 (1969).

16. B. J. Dropesky et al., Phys. Rev. C20, 1844 (1979).

17. N. P. Jacob, Jr. and S. S. Markowitz, Phys. Rev. C13, 754 (1976).

18. C. L. Morris et al., Phys. Rev. Lett. 39, 1455 (1977).

19. A. M. Poskanzer and L. P. Remsberg, Phys. Rev. 134, B779 (1964).

20. L. Husain and S. Katcoff, Phys. Rev. C7, 2452 (1973).

21. H. W. Bertini and M. P. Guthrie, Nucl. Phys. A169, 670 (1971);
H. W. Bertini, Phys. Rev. C6, 631 (1972); R. L. Hahn and H. W.
Bertini, ibid C6, 660 (1972); H. W. Bertini, M. P. Guthrie, and
O. W. Hermann, ORNL-4564 (1973).

22. P. E. Haustein and T. J. Ruth, Phys. Rev. C18, 2241 (1978).

23. C. J. Orth et al., Phys. Rev. C18, 1426 (1978).

CLUSTERS, NUCLEONS, AND QUARKS IN INTERMEDIATE-ENERGY REACTIONS

by

David H. Boal

Theoretical Science Institute
Department of Chemistry
Simon Fraser University
Burnaby, B.C., V5A 1S6

I. INTRODUCTION

Inclusive production of many different hadronic systems, from pions to nuclear fragments with more than forty nucleons, has been intensively studied for several years. The targets have also covered a wide range, from ^{4}He to U, as have the projectile themselves. Although I will concentrate here on proton induced reactions, mention will also be made of muon, electron, photon, and heavy ion induced reactions.

As a function of the bombarding energy, many of the experimentally observed quantities, such as differential cross sections, undergo significant changes. The largest changes in the "intermediate energy" regime occur between 100 MeV and 30 GeV, and so I will expand the usual definition of intermediate energy to include this entire transition region. I feel that to narrow this definition down to a smaller energy range would eliminate a good deal of experimental information which is important to unravelling what is happening in these reactions. For our purposes, then, low energy will be less than 100 MeV in the lab, while high energy will be greater than 30 GeV.

The remarkable thing about the inclusive differential cross sections observed in all of these projectile-target-produced particle combinations is that (as a function of the energy of the produced particle) they look very similar as shown in Fig. 1: Region III on this diagram corresponds to reactions involving the low-lying energy levels of the nuclei involved, and falls outside the domain of this talk. Region I, which may or may not have a distinguishable peak, is

generally described as the evaporation region, where the excitation energy of the nucleus is not carried by a limited fraction of the nucleons, but is distributed in some statistical fashion among all of the constituents of the nucleus. Because of its ready experimental availability, this region has been studied for several decades and there seems to be general agreement that it is well described by a model[1] in which the particles or fragments "evaporate" in a statistical fashion from an excited residual nucleus left over from an earlier, fast reaction. Because there is agreement about the interpretation of this region, we will not discuss it further here.

Instead, we will concentrate on Region II. Now, a cynic might say that one does indeed expect the cross sections for all of these reactions to look similar because their Feynman diagrams look the same as in Fig. 2, where the wavy lines represent gluons and the other lines represent quarks. While every theorist would agree that Fig. 2 is, in fact, what is happening in these reactions, few if any would have any enthusiasm for calculating the 10^n diagrams required for even as simple a process as $p + {}^4He \rightarrow X$. Hence, the question becomes what is the best approximation to these diagrams that is theoretically tractable. My purpose in this talk, then, is to look at several of the popular approximations and see whether current data can limit their applicability or disprove their validity. I will try to do this by discussing the trends of the data as a function of the energies, angles and hadronic systems involved. Because the differential cross sections in Region II (on which we will concentrate exclusively) are generally simple exponentials as a function of the lab kinetic energy of the emitted particle, most models fit the data reasonably well if their parameters are allowed to vary with angle, target etc. Hence, it is this variation which deserves our attention. Models in which the angle, energy, and projectile dependence of the parameters cannot be predicted will not receive detailed analysis here.

II. THE INTERACTION OF THE PROJECTILE

The first question we can try to address is how many significant interactions does the incident projectile have when it enters the nucleus? (Significant in the sense that each successive collision results in a change in the cross section of more than, say, 10%. While this may be a coarse definition of significant, to a theoretician fitting data over 10 orders of magnitude, which is the case here, factors of 10% are insignificant.) To answer this question, we can first look at

electron vs proton induced fragmentation. In Fig. 3, the ratio of $d^2\sigma/d\Omega dE$ of the (e,α) reaction[2-4] (electron kinetic energy = 120 MeV) to that of the (p,α) reaction[5] (proton kinetic energy = 100 MeV) is plotted vs lab angle for α's emitted with 30 MeV kinetic energy from a nickel target. The cross sections are both forward peaked, although clearly the (e,α) results are less so than the (p,α). The square of the electromagnetic fine structure constant is also shown. If the excited system (whatever it is) which emits the α particle required several interactions of the projectile for its production, then one would expect this ratio to be a higher power of α_{em} than α_{em}^2. Hence, it is likely that there is only one "significant" scattering of the incident projectile to produce the state from which the α is emitted if the (e,α) and (p,α) reactions have a common mechanism such as shown in Fig. 4. While the plot in Fig. 3 has been made for 30 MeV α's, roughly the same ratio is found for the evaporation region and 50 MeV α's.

Similar behavior appears to be true for the (γ,p) reactions,[6-17] where the cross sections are down by roughly α_{em} compared to (p,p'). Comparison here is a little more difficult in that the photons are from a bremsstrahlung source and so there is some question about the relevant energy at which to compare cross sections. I will have more to say about this reaction in the following section.

Lastly, the spectrum of fast neutrons emitted in μ^- capture[18-20] is also similar in form, and is appropriate to a single weak interaction.[21,22]

Further evidence for a single "significant" scattering of the projectile can be found from the target dependence of the cross section. For both (p,α) and (e,α), the cross section increases[5,2] with increasing target mass number, A_T, (Actually, faster than A_T) at roughly the same rate. Again, if multiple collisions of the incident projectile were required to produce the excited state, one would expect the (p,α) cross sections to increase faster with A_T than (e,α) due to the shorter mean free path.

So, the evidence quoted above seems to point to only one significant scattering of the incident particle, and this assumption will be made in the remainder of this talk. It would, of course, be useful to know what the cross sections for electron induced reactions look like at electron energies higher than 100 MeV, to see if the ratio of electromagnetic to strong interaction cross sections remains at about α_{em}^2 throughout.

III. INCLUSIVE PROTON PRODUCTION

Once the nucleon in the nucleus has been struck, there are several possible scenarios for its subsequent interaction:

1) it can be emitted with little further change;
2) it can lose some of its energy and momentum in further collisions, perhaps emerging as a jet or bound cluster of nucleons;
3) it can lose most of its energy and momentum to the nucleus as a whole.

To introduce some nomenclature, we will describe the emission of particles by steps 1, 2, or 3 as direct (DE), preequilibrium (PE), or statistical (SE) emission, respectively. There are certainly many refinements allowed under each of these categories, which will be delineated as necessary, but for our present purpose, the categories will be kept quite broad. First, we will ask whether there is any evidence for DE processes.

Looking for DE processes in fragment emission is probably not a good starting point, since it is clear that energy and momentum have been transferred to a multiparticle object. Hence, we will first look at proton emission so as to avoid at least one source of multiple collision effects.

In the forward hemisphere, the inclusive proton spectra show a clear peak at the energy and angle corresponding to quasi-free scattering of the projectile. Are the events that one observes as one moves away from the quasi-free peak in Region II predominantly due to the Fermi motion of the nucleons, multiple scattering of the struck nucleons, or both?

To measure the effects of multiple scattering, one can contrast results from very light targets to those from very heavy. Data from light targets, such as ^{4}He, ^{7}Li, and ^{9}Be, are available,[24-31] and it is highly unlikely that PE and SE processes should be important for as light a target as ^{4}He. If one further restricts the particles to be emitted with high energy (say, 1/3 or more of the energy of the incident projectile) then the observed proton is probably not the incident proton (the transition amplitude for pp scattering goes like e^{bt} where b is in the 7 GeV^{-2} range at 800 MeV lab bombarding energy and t is the four momentum transfer squared. This will greatly suppress backward emission.)

A rather large number of models[32-49] have been proposed to explain these and similar data, most of which cluster around either the direct[33-39] or statistical[40-48] extremes, with few attempts[49] being made to bridge the extremes. Some of these models have already been ruled out through the measurement of angular

distributions[50] (not available at the time the models were proposed). Because many of the statistical models are either not absolutely normalized, or yield only information on energy- or angle-integrated spectra, the discussion will begin with DE models.

If the energetic nucleon observed in the backward hemisphere is indeed not the incident nucleon, then its momentum in the nucleus before being struck must be substantial: one is sampling the high momentum components of the nuclear wave function, as shown in Fig. 5

Let us look at a simple model in which the recoil momentum is carried off by a sum[36-39] over particles B (which can arise from multiple scattering or the longer range correlations).[36-38] We assign the labels of energy, momentum and mass number as per Fig. 6.

The expression for the differential cross section would look like

$$\frac{d^2\sigma}{d\Omega dE} \sim \sum_n \left(\begin{matrix}\text{Normalization} \\ \text{factors}\end{matrix}\right) \int \frac{|T|^2 \; f(k) \; F(E_n^*) dE_n^*}{(\text{phase space factors})} \; d\Omega_f \qquad (1)$$

where:

1. $|T|^2$ is the transition matrix element for p-AB interaction (often approximated by pp scattering) squared.
2. $f(k)$ is the probability of finding a nucleon with momentum k.
3. $F(E_n^*)$ is the distribution of excitation energies in the n + residual nucleus system.
4. Ω_f is the solid angle of the projectile after collision.
5. A sum is carried out over particles n ($1 \leq n \leq A_T - 1$).

Several different functional forms for $f(k)$ have been tried, all of which have a part which falls like e^{-k/k_o} for large k. The parameter k_o is found by fitting the data to have a value in the 100 MeV range (Quoted values vary from model to model. We will return to the theoretical estimation of this function later.) Results of a recent calculation[51] are shown in Fig. 7 to demonstrate the quality of fit. For this calculation, k_o was chosen to be 120 MeV/c, and the contribution of each term was weighted by g^{n-1}, with $g \simeq 0.9$. The jet of nucleons was assumed to behave as a single body (for phase space simplification).

At any given angle and bombarding energy, an equally good fit to the one shown can be had by assuming coherent recoil of the residual nucleus ($n = A_T - 1$), for which $k_o = 90 \pm 5$ MeV/c. In the calculation shown on Fig. 7, n is summed from 1 to $A_T - 1$, the relative contribution for each term being shown as well. The

n = 1 term is forbidden kinematically for large angles and emission energies which are substantial compared to the incident energy. As the incident energy is raised (holding $\vec{q}$ fixed), lower values of n give a greater contribution, leading to a cross section which rises faster with incident energy than the elementary p-p, p-D (or whatever) cross section. This is, in fact, observed experimentally. Above about 5 GeV or so incident energy, most of the light objects in the sum over n contribute, and the predicted cross section then largely follows the elementary one in energy dependence. The calculation described above has been carried out to as far as 400 GeV, (see Fig. 8) and the agreement with experiment[31] is reasonably good, considering the lack of detailed inclusion of pion production. (The amplitude $|T|^2$ in Eq. (1), is assumed to follow the pp total cross section rather than the elastic).

Further evidence for a direct emission of protons comes from the target dependence of the cross section. At T_p = 800 MeV, θ_q = 160°, and T_q = 100 MeV, the differential cross section rises[25] linearly with A. This is what one would expect from a model in which the excited state is formed by a scattering from any of the available nucleons in the nucleus. At T_q = 300 MeV, the increase is faster than A, but certainly not as fast as even A^2. If we assume 3-body kinematics for the final state then conservation of energy and momentum require that the value of n must be greater than 3 in this range. (The n-particle system must carry a fair amount of momentum forward, but not too much energy). These larger values of n are more likely to be found in a heavy target regardless of whether the model assumes that B is the result of a cascade from the initial NN short range interaction, or is the result of a many body correlation, and so one would expect a faster-than-A increase in the cross section for high energy ejectiles.

However, evidence that there is some additional process contributing to the heavy targets can be found by looking at the analyzing power results from TRIUMF[30] and LAMPF.[26] For ^{4}He, the analyzing power at 500 MeV is generally small and negative (shown on Fig. 9), but for nickel it is small and frequently positive (Fig. 10). The nickel results are similar to the Be and Ta data obtained at 800 MeV. While it is difficult to know exactly what ingredients to put into a calculation of the analyzing power (whether to use p-p or p-d analyzing powers is one ambiguity), and certainly the integral in Eq. (1) will tend to average out the results, nevertheless one can conclude that multiple scattering is playing some role for the heavier targets.

Many of the PE models[5] can give as good a fit to the 100-MeV data as this DE model gives to the 500 MeV-400 GeV data. Unfortunately, several of the PE models are arbitrarily normalized (from angle to angle) and one cannot test them as strenuously as one might like. Rather than go through the details of these models, I will try, instead, to test the normalization of the DE model outlined above.

Although the momentum distribution used in the (p,p') analysis has necessitated the introduction of two parameters, k_o and g, the expression is otherwise normalized. One can then test the model by using this momentum distribution to make absolute predictions for other projectiles for which the projectile-nucleon vertex is known. We choose to examine the (γ,p) reaction[52] at energies for which the same range of internal momenta, k, as in (p,p') are required to produce the ejected proton. [We choose to look at the same range of k in both (p,p') and (γ,p) since the (p,p') calculations have not been carried out at small k, the quasi-free region.] The cross section for the (γ,p) reaction reads:

$$\frac{d^2\sigma}{d\Omega_q dE_q} = \frac{1}{Q}\frac{C\,\alpha_{em}}{2^4\pi}\,q\sum_{n=1}^{A_T-1}\frac{a_n n(n+1)}{M_n}\iint\frac{\delta(\text{Energy})}{E_k}\,f(k)\,\frac{N(E_\gamma)}{E_\gamma}\,\overline{\sum}\,|\varepsilon\cdot J|^2 \;dE_\gamma\;\frac{e^{-\left(\frac{\delta\mu_n}{\eta}\right)^2}}{\sqrt{\pi}\,\eta}\;d\mu_n \qquad (2)$$

where

1. $Q = 1/E_o \int N(E)EdE$
2. $N(E_\gamma)$ is the distribution of photons of energy E_γ (see Ref. 53)
3. $\overline{\Sigma}\,|\varepsilon\cdot J|^2 = 4q^2\sin^2\theta_q + 2E_\gamma{}^2(1+\kappa)^2 + O(q^2/4m_p^2)$
4. $C = Z\,\dfrac{2^4\pi^3 M_p}{I\Sigma a_n}$
5. $I = \int f(k)d^3k.$

The quantities f(k) and $a_n(\equiv g^{n-1})$ are taken from the (p,p') analysis. A comparison of these predictions is made with the proton spectrum from 1050-MeV bremsstrahlung on ^{12}C in Figs. 11 and 12. The agreement is suprisingly good. Shown for comparison is a quasi-deuteron model[54] calculation done by Matthews and Turchinetz,[55] in a survey of quasi-deuteron predictions. A PE model[56] and an intranuclear cascade model,[57] both based on the quasi-deuteron model, have also

been used to fit (γ,p) data. The fits are quite acceptable, although the lack of a prediction for the quasi-deuteron constant makes the calculations arbitrarily normalized.

As the bremsstrahlung end-point energy is lowered to about 300 MeV, the DE calculations overpredict experiment by at least a factor of 2. Because the photons contributing to these data have an energy in the 200-250 MeV range, the calculations are very sensitive to excitation energies of the residual system etc., which are poorly determined from the 800-MeV (p,p') data. Hence, the disagreement is not surprising. (Taking into account the excitation energy of the residual nucleus will move the predictions toward the data.)

Lastly, the normalization and k dependence of the DE models were also checked by looking at the fast neutron spectrum in μ^- capture. Again, the agreement was surprisingly good.[21,22]

While heavy ion reactions are not really part of the topical core of this talk, mention should be made of work on proton emission in relativistic heavy ion collisions. There are many models[58-64] of a statistical nature which have been made to describe the inclusive cross sections in heavy ions. These models are what one might expect if the mean free path of a nucleon is short, as there are certainly a good many nucleons available for collision. However, Hatch and Koonin have shown[65,66] that a model using the same high momentum component of the nuclear wave function as we have used in (p,p') and (γ,p) fits the data well. Preliminary results from a 2p coincidence experiment[67] support the idea that a significant portion of the inclusive proton spectrum is due to single scattering. An intranuclear cascade model with a sharp cutoff momentum distribution was also used by Hatch[65] to estimate the (p,p') cross sections for targets in the Li to Ta range. The predictions are low by roughly an order of magnitude for all targets.

IV. LIGHT FRAGMENT EMISSION

As the number of nucleons in the emitted object increases, the mechanism should become more statistical in nature. In this section, we will discuss ^{4}He and other light cluster emission[68-72] in an effort to see what evidence there is for DE, PE, and SE processes. First, we will look at DE.

Models in which the cluster is "preformed" in the nucleus have been successful[73,74] in describing low energy proton induced emission of α's. To see whether they should be applicable to intermediate energy reactions, let us first consider the target dependence of the cross section. Figure 13 shows a plot of log

$d^2\sigma/d\Omega dE$ vs log A_T for both (p,α)[5] and (e,α)[2]. One might expect that only those clusters near the surface of the nucleus stand a reasonable chance of getting out. If we define the effective number of α's as n_{eff}, and fit the (p,^{4}He) backward hemisphere differential cross section with some α momentum distribution (and, of course, the p-^{4}He scattering amplitude), then one finds[75] for a silver target that $n_{eff} \simeq \frac{1}{5}(A/4)$. This factor of 1/5 presumably would be a function of at least two variables: that the nucleus spends a certain amount of its time as a subgroup of α's and that those α's are near enough to the nuclear surface so as to be able to escape when struck. One might expect that when one goes to light targets such as ^{9}Be or ^{12}C, whose surface to volume ratio is greater and whose ground state wave function contains a greater fraction of α particles than Ag or Al, then $n_{eff}(4/A)$ should increase. In fact, it decreases.[60,75] Plotted in Fig. 14 is the ratio of $1/A_T(d^2\sigma/d\Omega dE)$ at fixed θ_α and T_α for a series of targets compared to ^{90}Zr (in the (p,α) reaction[5] at 90 MeV) or ^{94}Mo [in the (e,α) reaction[2] at 100 MeV]. (The ^{12}C point[60] was omitted from the figure as the published paper only allows comparison with a gold target. Compared to Au, $(1/A_T)(d^2\sigma/d\Omega dE)$ for ^{12}C is down by more than a factor of two.)

One can at least qualitatively understand this behavior if the alpha is formed in some multi-step process. The multi-step process is suggested by the analyzing power measurements for (p,α) taken at TRIUMF.[76] Unlike the (p,p') reaction at the quasi-free angle and energy, the (p,α) shows an analyzing power which is consistent with zero (see Fig. 15). Although the p + ^{4}He analyzing power[77] which is put into Eq. (1) in DE models does change sign over the range of Ω_f in the integral, it would be rather suprising if it cancelled exactly everywhere. There is also very little evidence for a quasi-free peak.

If the process is multi-step, then presumably the initially struck nucleon must travel some distance r, on the average, in order to have enough interactions to "coalesce" into an alpha. Coarsely, one could argue that any nucleon closer than r to a given point on the nuclear surface is not available for α production at that point. The fraction of nucleons so available, f_α, is then approximately given by (where we have used 1.07 $A^{1/3}$ for the nuclear radius).

$$f_\alpha \approx 1 - \frac{r^3}{2 \times 1.07^3 A} \quad (r \text{ in F}) \quad . \tag{3}$$

A fit to the points in Fig. 14 gives $r \sim 3.3$ F, which compares to the ^{4}He diameter[78] of ≈ 2 F. One finds that this "excluded volume radius" increases with A_f (fragment mass number) as one would expect. Thus, the mechanism is probably PE and/or SE in origin.

A test of the appropriateness of SE models can be found in analyzing the invariant cross section $E\, d^3\sigma/d^3q$ of the (p,α) reactions.[79] If a particle is emitted isotropically from a non-relativistic source, then a plot of $p_\perp/m$ vs rapidity, y, ($y \equiv 1/2 \ln(E+P_\parallel/E-P_\parallel)$ where $p_\perp$ and $p_\parallel$ are the perpendicular and parallel components of the particle's momentum with respect to some axis at constant invariant cross section will be a circle centered at the rapidity of the source. Such plots made by Green and Korteling[80] for incident proton kinetic energies in the 200-500 MeV range incident on Ag are approximately circular [Fig. 16a].

The source rapidities from the analysis of a series of fragments are shown in Fig. 16b as a function of y_R. Without dwelling on the nature of the functional form, it is significant that the source rapidities (which go over to the source velocities in the non-relativistic limit) are quite substantial. This translates into a very large momentum if the source is very heavy. Taking 100 MeV α's for example, conservation of energy and momentum demands that the source have no more than $\sim$60 nucleons. For sources near this upper limit, the remaining 50 or so nucleons must recoil in the opposite direction. It is difficult to imagine a model which can produce such sources, particularly if we demand that the model connect in some smooth way to what we believe is happening in proton emission.

Hence, we will proceed on the assumption that the struck nucleon rescatters from a few nucleons on its way out, losing momentum and energy in so doing. These secondary nucleons may or may not coalesce with the primary one to form a cluster. We do not mean to imply that these are "billard ball" collisions, in that the mean free path may be several times the internuclear separation.[49]

There are several calculations one can do to see the effects of the multiple scattering. In the exciton model approach,[81-83] a fair amount of information may be put in about the energy level densities etc., but little on the spatial correlations of the nucleons (i.e., a four particle wave function is not used to determine when the emerging nucleons are close enough to form an alpha). This approach is then largely used to describe angle integrated data. An example of the quality of the fit[83] is shown on Fig. 17 for the (p,α) reaction with incident proton energy of 90 MeV. To get angular information, which is certainly available from experiment, one needs to work in considerably more detail.

The picture for which I will do a simple calculation is shown in Fig. 18. The struck nucleon 1 will be presumed to have a momentum $-\vec{k}$ before the collision and $\vec{q}$ after, while the n recoiling nucleons will carry momentum $\vec{k}$ [with the same weightings as in (p,p')]. At each of the j-1 collisions (for a cluster of j nucleons) after the primary interaction, nucleon 1 will be assumed to lose q/j of its momentum to a nucleon at rest. (This assumption is made to simplify kinematics.) The 4-momentum transfer, t, in each of these j-1 reactions is then approximately $-(q/j)^2$, assuming that q/j is sufficiently small that it does not introduce relativistic corrections. Now, of course one should integrate over the momenta of each of the nucleons 2...j, and then put some cut on what ranges of momenta are allowed for the nucleons in the cluster. The approximation here is to just take averages.

With this model, Eq (1) is simply multiplied by

$$\left[g_c \, e^{-b\left(\frac{q}{j}\right)^2} \right]^{j-1} f_j \qquad (4)$$

for the n - 1 collisions, where g_c is a normalization factor for the probability of collision, and f_j is the fraction of nucleons available for cluster formation. Another normalization factor ought to be included to reflect the fact the not all jets will form a fragment. This formulation of the model has been used to fit[84] the ^{4}He data at 500 MeV and g_c is found to have a value around 0.7. The fit is shown (at 90°) in Fig. 10. This calculation was also carried out at 5.5 GeV, and the result is shown in the same figure. One can see that the predicted cross section rises faster than the pp cross section (which increases by roughly a factor of 2 over the same energy range) but still not quite as fast as the observed cross section.

Omitted from this calculation is the constraint that the emitted particles ought to occupy some localized volume of phase space in order to be called a "cluster." At present, this remains a difficult problem to solve in any exact sense. Some progress[85-87] in this area has been made in heavy ion reactions and fragments emitted at forward angles. The effect will become more significant as one increases the fragment mass, or goes away from the minimum of the valley of β-stability, and so fragments in this intermediate mass regime should provide some constraints on this phase space volume. The only thing which I will mention

about this fragment mass regime is that, neglecting the thorny point just outlined, the parameter g_c in Eq. (4) must be near unity, i.e. the decrease in cross section with increasing fragment mass (for Ag) seems to be entirely accounted for by the changes in f(k) of Eq. (1).

V. HEAVY FRAGMENT EMISSION

For non-relativistic fragments of j nucleons (each with mass M), the momentum per nucleon, q/j, is related to the kinetic energy T by

$$\frac{q}{j} = \sqrt{\frac{2MT}{j}} \tag{5}$$

so that q/j decreases for j increasing at fixed T. For fragments in the 100-200 MeV kinetic energy range, q/j will drop down into the same momentum range as the internal momenta once j is in the 10 to 20 range. For these combinations of j and T, SE models (by which we simply mean systems with many degrees of freedom available,not necessarily an evaporation model) must be playing a more important role.

Further evidence for a non-DE mechanism (DE in the sense of proton emission) can be found in the energy dependence of the differential cross section. As was indicated in the section on energetic proton emission, the differential cross section is highly non-isotropic over the range from 200-MeV to 400-GeV bombarding energy (at 400 GeV, only protons in the 70°-160° range have been measured, but the decrease in $d^3\sigma/d^3q$ with increasing angle is more than an order of magnitude at large emission energies). This is not the case with heavy fragments.[89-94] In the energy integrated cross section for Sc nuclei emitted from a U target, it is observed[93] that the data are forward peaked for energies of ∿1 GeV, gradually becoming sideways peaked at 10 GeV, and remaining sideways peaked at least up to 300 GeV (Fig. 20). Now, the excess of forward or sideways events compared to the average (∿20% in the energy integrated cross section) is certainly much less than that observed for proton emission, or α emission at TRIUMF energies. However, the amount of forward or sideways peaking in $d^2\sigma/d\Omega dE$ will probably be a strong function of T_q. As shown in Fig. 21 for the double differential cross section measured by Fortney and Porile,[93] there is significant cross section below the Coulomb barrier associated with Sc nuclei emitted from a system near U in mass. The Sc nuclei with kinetic energy around 100 MeV are probably going to have a

more isotropic distribution as a function of angle than those emitted with higher energy. This is what has been found by Remsberg and Perry (unpublished) for lighter fragments.

We can learn something about the nature of the process merely by looking at the kinematics. Taking the same 3-body kinematic labels which we introduced before, we can calculate the minimum values of the recoil momentum, k_{min}, for a given $\vec{q}$ of the Sc nuclei. For illustrative purposes, we choose $A_q = 40$, and $T_q = 100$ MeV. Then, if a proton were recoiling against the fragment, we would find k_{min} as a function of θ_q as shown in Fig. 22. As one might expect, the values of k_{min} are small only in the forward hemisphere, and indeed $\theta_q > 90°$ is largely kinematically forbidden. These results are also true for other very small values of A_k.

Most models which one might want to apply to these reactions have a functional dependence on k_{min}, or a kinematical variable closely related to k_{min}, which decreases rapidly with increasing k_{min}. For example, in the DE or PE model described above, the momentum distribution goes like e^{-k/k_o}, and it is clear that the larger k_{min} is (the lower limit on the k integration) the smaller the predicted cross section will be. Similarly, in a model[95-99] in which some equilibrated slowly moving source is produced, which then decays isotropically in its rest frame with fragment and recoil object carrying momenta $-\vec{k}'$ and $\vec{k}'$, one finds that $\vec{k}'$ and $\vec{k}$ will be closely related. Hence, a model in which the emission probability for a given fragment falls with $\vec{k}'$, will also decrease (by and large) with $\vec{k}$.

It is clear, then, that light recoils will produce forward peaking in the cross section at energies where no such peaking is observed experimentally. At the other extreme, if we demand that the entire residual nucleus carry off the recoil momentum, then the range of k_{min}'s is shown in Fig. 23. Here, we see that θ_q is allowed to run from 0 to 180° for all of the bombarding energies chosen. Further, the 1-GeV kinematics are significantly different than the 10-100 GeV numbers, with 3 GeV somewhat in between. One sees that there will be forward peaking at 1 GeV, shifting to sideways peaking by 10 GeV.

If the k_{min} dependence was all there was to the story, then one would predict that the sideways peaking would be very strong. However, one must also include the 4-momentum transfer[100] $[\equiv t \equiv (E_i - E_f)^2 - (\vec{p}_i - \vec{p}_f)^2]$ dependence of the interaction of the bombarding proton. The Mandelstam variable t falls rapidly (from $t = 0$ at $\theta_f = 0$) as θ_f increases. Since the elementary p-p, p-D, p-^{4}He...

amplitudes also fall with more negative t, then large θ_f values will be suppressed. Fixing θ_q at 70°, we show in Fig. 24 how k varies with t. Clearly, the very small values of k_{min} at 10 GeV occur at large momentum transfer, and will thus be suppressed.

Just to show what happens when these factors are folded in together, the results of a crude calculation are shown in Fig. 25 for emission of Na. We have simply taken a pp amplitude, integrated over a $\cosh^{-2}$ momentum distribution, and added the appropriate phase space factors (and an arbitrary normalization constant). One can see the trend away from forward peaking toward sideways peaking, for T_q = 54 MeV. (I've fiddled with the binning of the experimental data to allow a better comparison of the TRIUMF and Brookhaven[94] experiments, so the data will not coincide with the published data).

There are a number of reasons why this calculation should not be taken too seriously. In the α emission case to which the model was applied, the lab momentum per nucleon (for 100 MeV α's) is about 200 MeV/c, whereas for the Na nuclei it is about 60 MeV/c. Since this is down in the range of the average internal nucleon momentum, the n-1 collisions which were averaged in the PE discussion will be of much more significance now. Thus, the "true" model will be much more statistical than the coarse calculation which has been presented here. At the other extreme, there are many calculations which are completely statistical in nature, and do not pay enough attention to the details of the first steps in the formation of the excited nucleus. The solution will be found in a proper marriage of these extremes.

VI. QUARKS

Of the ingredients to the calculations done above, the most critical one, and at the same time the least known, is the momentum distribution f(k) which has been introduced. In particular, because of the fact that these reactions require knowledge of the high momentum component of the wave function, we are far away from the regime where conventional single particle nuclear potential models are of use; we are presumably looking at the effects of few body correlations. Even here, we must be aware that final state interactions etc., have really all been folded into the f(k) measured with this phenomenology,[101] so we may have to work a littler harder to extract the true momentum distribution.

Calculations on momentum distributions which include few body correlations are not common, but a recent calculation done by Zabolitzky and Ey[102] has given

some indication that we are on the right track. Shown in Fig. 26 is their calculation of the ^{16}O ground state momentum distribution, with and without two nucleon correlations. Also shown is f(k) introduced above with compatible normalization. Although the absolute normalization of the high energy tails is somewhat different, the overall fall-off with increasing momentum is definitely very similar.

The calculation of Zabolitzky and Ey is certainly not the last word on the subject for, in spite of the short distances, the quark degrees of freedom are not taken into account. The first question we must ask in an effort to understand the role of quarks in the nucleus, is to what extent is the nucleus A nucleons or 3A quarks.[103]

It was proposed by Brown, Rho, and Ventc[104,105] that the 3 quarks in a nucleon were actually confined to a "little bag" (to use MIT bag model[106] terminology) of radius $\sim$0.28 F, so that one need not worry about quark degrees of freedom at all. This certainly flies in the face of an enormous amount of evidence to the contrary from elementary particle physics. Because of the highly model dependent nature of their result, we will not pursue it further.

Instead, we will assume the bag model[106] and potential model[107,108] results that the quarks occupy a volume roughly 1 F in radius. It is clear from the internucleon separation distance of $\sim$1.8 F that there is some overlap between quark wave functions on adjacent nucleons even at normal densities. Is the nucleus, then, just a quark gas at normal densities?

A variety of simple calculations[109,110] say no. In a calculation done several years ago,[109] Chapline and Nauenberg used several estimates of the MIT bag model parameters to calculate the density required for a phase transition to quark matter. The densities they obtained were in the range of 10-60 times normal nuclear matter.

To do a more rigourous calculation of the energy levels of 3A quark states, is, of course, very difficult.[111-119] Most work has concentrated on 6 quark states, to keep the calculations as simple as possible. Since we already know that the deuteron ground state is not tightly bound ($\sim$4 to 5 F), we do not expect to see a significant 6-quark (as opposed to 2-nucleon) component to the ground state. Nevertheless, the calculations should give some measure of the energies at which more collapsed states might be expected.

Although the estimates vary, most are in the 300-MeV range for the 6 quark collapsed state, with a radius for the state of about 1.5 F. While this energy is large it is still not as great as the $\Delta\Delta$ state ($\sim$600 MeV). However, before

continuing this discussion, let us look at the Feynman diagrams involved in producing these states.

Without looking at quarks, we are content to say that the NN potential is mediated by the exchange of mesons (see Fig. 27). In the quark-gluon picture of quantum chromodynamics, this would look something like the diagram in Fig. 28.

If the gluon and quark exchange is such that the 3-quark states are each color singlets, then Fig. 28 is just the usual NN interaction that we would expect to find in the deuteron. If, however, the right hand side of Fig. 28 has the 6 quarks in a color singlet, but the 3-quark substates in color octets, then the rhs represents a color excitation of the two-nucleon system.[112-120]

It is clear that the greater the number of quarks around, the richer is the color spectroscopy. Shown in Fig. 29 is one calculation of excited states for a 6-quark system with S = 0, -1 or -2. As yet, there is no clear evidence for these states.

Probably the most unambiguous evidence for the quark structure of the nucleus comes from scattering[121] experiments. To probe down into the tenths of a Fermi region of space, one needs four-momentum transfer squared, t, in the GeV^2 region. One can show[122,123] from the quark parton model that at high t, the electromagnetic form factor should behave like t^{-3A} as diagramed in Fig. 30. Shown in Fig. 31 are data taken at SLAC for large momentum transfer. One can certainly see the correct asymptotic behaviour for π, p, and n, with the d results approaching $1/t^5$. These quark parton model arguments have also been made for hadronic collisions,[126-128] and the predicted behaviour has been observed. Time limitations prevent me from dealing with this subject in any more detail, (Ref. 123 makes an excellent starting point for those wanting to pursue the matter further) but it is an area to which nuclear chemistry techniques may find application: the detection of the recoil nucleus at high momentum transfer.

VII. ODDS AND ENDS

While I feel that the verification, modification, or wholesale revision of our understanding of these inclusive reactions will require coincidence and multiplicity experiments, nevertheless, there are some experimental and theoretical holes in the inclusive domain that might be worthwhile filling in. Without specifying energies, angles etc., (this will be done in the panel discussions) some of the holes that come to mind are:

1. Proton induced reactions:
   a) (p,p'): $d^2\sigma/d\Omega dE$ to higher proton energies for $1 < T_p < 20$ GeV.
   b) (p,d): polarization and $d^2\sigma/d\Omega dE$ in quasi-free region.
   c) (p,α): more detailed target dependence (Be...U) at several energies (0.5...10 GeV); polarization in quasi-free region at 500-800 MeV.
   d) (p, light fragment): differential cross sections for one or two light targets to compare with TRIUMF and Berkeley data.
   e) (p, heavy fragment): $d^2\sigma/d\Omega dE$ at more energies and angles with absolute normalizations.
   f) $^2H(p,p')$ and $^2H(p,2p)$ cross sections and polarization measurements.
2. Electron induced reactions:
   a) (e,p): at energies so as to be comparable to (p,p')
   b) (e,α): ditto for (p,α)
   c) (γ,α): measurements out to greater α energies.
3. Theoretical holes:
   a) (p,p') and (e,e'): inclusion of quasi-free region in fit.
   b) (p,p'): explanation of polarization.
   c) more work on heavy fragment emission.

APOLOGIES AND ACKNOWLEDGMENTS

In any review lecture of this sort one necessarily selects material that fits best into the main topic to be covered. Where possible, I have included references to other work not included in the lecture. However, because the field is so broad, a non-trivial number of papers have not been referenced, sometimes through my own ignorance, sometimes because their subject area is too far removed.

Those who have collaborated on various parts of the calculations presented here, or provided data for their comparison, or gave this manuscript a critical reading include R. Woloshyn and K. P. Jackson at TRIUMF, R. E. L. Green and R. G. Korteling and M. Soroushian at Simon Fraser University and G. Roy, G. Moss, and their collaborators at the University of Alberta. Lastly, thanks are due to L. Remsberg (Brookhaven) and S. Frankel (Pennsylvania) for providing unpublished compilations of data.

REFERENCES

1. For a review, see J. M. Blatt and V. F. Weisskopf, Theoretical Nuclear Physics (Wiley and Sons, New York, 1952); I. Dostrovsky, Z. Fraenkel, and P. Rabinowitz, Phys. Rev. 118, 791 (1960) and references therein.

2. A. G. Flowers et al., Phys. Rev. Lett. 40, 709 (1978); 43, 323 (1979).

3. J. J. Murphy et al., Nucl. Phys. A277, 69 (1977).

4. L. Meneghetti and S. Vitale, Nucl. Phys. 61, 316 (1965).

5. J. R. Wu, C. C. Chang, and H. D. Holmgren, Phys. Rev. C19, 698 (1979).

6. C. Whitehead et al., Phys. Rev. 110, 941 (1958).

7. M. Q. Barton and J. H. Smith, Phys. Rev. 110, 1143 (1958).

8. Y. S. Kim et al., Phys. Rev. 129, 1362 (1963).

9. B. T. Feld et al., Phys. Rev. 94, 1000 (1954).

10. R. J. Cence and B. J. Moyer, Phys. Rev. 122, 1634 (1961).

11. D. N. Olson, Ph.D. Thesis, Cornell University, 1960 (unpublished).

12. I. Endo et al., University of Tokyo Preprint, 1979.

13. J. Arends et al., Bonn University preprint, Bonn-HE-78-19.

14. P. Dougan and W. Stiefler, Z. Phys. 265, 1 (1973).

15. Yu. P. Antuf'ev et al., Sov. J. Nucl. Phys. 13, 265 (1971).

16. H. J. von Eyss and G. Lührs, Z. Phys. 262, 393 (1973).

17. M. Gary and H. Hebach, Phys. Rev. C10, 1629 (1974).

18. M. H. Kreiger, Thesis, Columbia University Report NEVIS-172, 1969 (unpublished).

19. R. M. Sundelin and R. M. Edelstein, Phys. Rev. C7, 1037 (1973).

20. W. O. Schröder et al., Z. Phys. 268, 57 (1974).

21. P. Singer, N. C. Mukhopadhyay, and R. D. Amado, Phys. Rev. Lett. 42, 162 (1979).

22. M. Lifshitz and P. Singer, Phys. Rev. C22, 2135 (1980).

23. D. M. Corley et al., Nucl. Phys. A184, 437 (1972).

24. S. Frankel et al., Phys. Rev. Lett. 36, 642 (1976).

25. S. Frankel et al., Phys. Rev. C18, 1375 (1978).

26. S. Frankel et al., Phys. Lett. 41, 148 (1978).

27. V. I. Komarov et al., Nucl. Phys. A326, 297 (1979).

28. V. I. Komarov et al., Phys. Lett. 69B, 37 (1977); 80B, 30 (1978).

29. R. C. Allen, A. S. Kanofsky, and M. A. Hasen, Lehigh University preprint LEH-HEP-79-8-3.

30. G. Roy et al., TRIUMF preprint (1980).

31. Y. D. Bayukov et al., Phys. Rev. C20, 764 (1979).

32. For a review of DWIA work on specific final states, see N. S. Chant and P. G. Roos, Phys. Rev. C15, 57 (1977).

33. S. Frankel, Phys. Rev. Lett. 38, 1338 (1977).

34. R. D. Amado and R. M. Woloshyn, Phys. Rev. Lett. 36, 1435 (1976).

35. H. J. Weber and L. D. Miller, Phys. Rev. C16, 726 (1977).

36. T. Fujita, Phys. Rev. Lett. 39, 174 (1977).

37. T. Fujita and J. Hüfner, Nucl. Phys. A314, 317 (1979).

38. T. Fujita, Nucl. Phys. A324, 409 (1979).

39. R. M. Woloshyn, Nucl. Phys. A306, 333 (1978).

40. C. C. Chang, N. S. Wall, and Z. Fraenkel, Phys. Rev. Lett. 33, 1493 (1974).

41. J. R. Wu and C. C. Chang, Phys. Lett. 60B, 423 (1976).

42. M. Blann, Ann. Rev. Nucl. Sci. 25, 123 (1975).

43. R. Weiner and M. Weström, Phys. Rev. Lett. 34, 1523 (1975); Nucl. Phys. A286, 282 (1977).

44. T. Nomura et al., Phys. Rev. Lett. 40, 694 (1978).

45. V. I. Bogatin, O. V. Lozhkin, and Yu. P. Yakovlev, Nucl. Phys. A326, 508 (1979).

46. G. Mantzouranis, D. Agassi, and H. A. Weidenmüller, Phys. Lett. 57B, 220 (1975); Z. Phys. A278, 145 (1976).

47. J. M. Akkermans, Phys. Lett. 82B, 20 (1979).

48. J. Knoll, Phys. Rev. C20, 773 (1979).

49. H. C. Chiang and J. Hüfner, University of Heidelberg preprint 80-493 (unpublished).

50. D. H. Boal, Phys. Rev. C21, 1913 (1980).

51. D. H. Boal and R. M. Woloshyn, Phys. Rev. C23, (in press).

52. G. L. Vysotskii and A. V. Vysotskaya, Sov. J. Nucl. Phys. 9, 689 (1969).

53. L. I. Schiff, Phys. Rev. 83, 252 (1951).

54. J. S. Levinger, Phys. Rev. 84, 43 (1951).

55. J. L. Matthews and W. Turchinetz, LNS Internal Report 110, 1966 (unpublished).

56. J. R. Wu and C. C. Chang, Phys. Rev. C16, 1812 (1977).

57. T. A. Gabriel, Phys. Rev. C13, 240 (1976).

58. H. W. Bertini, T. A. Gabriel, and R. T. Santoro, Phys. Rev. C9, 522 (1974).

59. A. A. Amsden, G. F. Bertsch, F. H. Harlow, and J. R. Nix, Phys. Rev. Lett. 35, 905 (1975).

60. J. P. Alard et al., Nuovo Cimento A30, 320 (1975).

61. G. D. Westfall et al., Phys. Rev. Lett. 37, 1202 (1976).

62. S. T. Thornton et al., Phys. Rev. C19, 913 (1979), for model comparisons.

63. H. G. Baumgardt et al., Z. Phys. A273, 360 (1975).

64. A. M. Poskanzer et al., Phys. Rev. Lett. 35, 1701 (1975).

65. R. L. Hatch, Ph.D. Thesis, California Institute of Technology, 1979 (unpublished).

66. R. L. Hatch and S. E. Koonin, Phys. Lett. 81B, 1 (1979).

67. S. Nagamiya, Nucl. Phys. A335, 517 (1980) and references therein.

68. A. M. Poskanzer, G. W. Butler, and E. K. Hyde, Phys. Rev. C3, 882 (1971).

69. E. K. Hyde, G. W. Butler, and A. M. Poskanzer, Phys. Rev. C4, 1759 (1971).

70. R. G. Korteling, C. R. Toren, and E. K. Hyde, Phys. Rev. C7, 1611 (1973).

71. G. D. Westfall et al., Phys. Rev. C17, 1368 (1978).

72. R. E. L. Green and R. G. Korteling, Phys. Rev. C22, 1594 (1980).

73. L. Milazzo-Colli and G. M. Braga-Marcazzan, Nucl. Phys. A210, 297 (1973).

74. L. Milazzo-Colli et al., Nucl. Phys. A218, 274 (1974).

75. D. H. Boal and R. M. Woloshyn, Phys. Rev. C20, 1878 (1979).

76. R. E. L. Green, K. P. Jackson, and R. G. Korteling, unpublished.

77. G. A. Moss et al., Phys. Rev. C21, 1932 (1980).

78. L. R. B. Elton, Nuclear Sizes (Oxford University Press, 1961).

79. See, for example, J. Gosset et al., Phys. Rev. C16, 629 (1977).

80. R. E. L. Green and R. G. Korteling, Phys. Rev. C18, 311 (1978).

81. A. Mignerey, M. Blann, and W. Scobel, Nucl. Phys. A273, 125 (1976).

82. W. Scobel, M. Blann, and A. Mignerey, Nucl. Phys. A287, 301 (1977).

83. J. R. Wu and C. C. Chang, Phys. Rev. C17, 1540 (1978).

84. D. H. Boal and M. Soroushian, unpublished.

85. S. T. Butler and C. A. Pearson, Phys. Rev. Lett. 7, 69 (1961); Phys. Lett. 1, 77 (1962); Phys. Rev. 129, 836 (1963).

86. A. Schwarzschild and C. Zupancic, Phys. Rev. 129, 854 (1963).

87. H. H. Gutbrod et al., Phys. Rev. Lett. 37, 667 (1976).

88. For an introduction to the high energy data, see I. Otterlund, Nucl. Phys. A335, 507 (1980).

89. Ø. Scheidemann and N. T. Porile, Phys. Rev. C14, 1534 (1976).

90. K. Beg and N. T. Porile, Phys. Rev. C3, 1631 (1971).

91. S. B. Kaufman and M. W. Weisfield, Phys. Rev. C11, 1258 (1975).

92. S. B. Kaufman, E. P. Steinberg, and M. W. Weisfield, Phys. Rev. C18, 1349 (1978) and references therein.

93. D. R. Fortney and N. T. Porile, Phys. Lett. 76B, 553 (1978); Phys. Rev. C21, 664 (1980).

94. L. P. Remsberg and D. G. Perry, Phys. Rev. Lett. 35, 361 (1975); and private communication.

95. For a review, see J. M. Alexander, in Nuclear Chemistry, L. Yaffe ed., (Academic, New York (1968)) Vol. 1, p. 273.

96. N. Sugarman, M. Campos, and K. Wielgoz, Phys. Rev. 101, 388 (1956).

97. N. T. Porile and N. Sugarman, Phys. Rev. 107, 1410 (1957).

98. N. Sugarman et al., Phys. Rev. 143, 952 (1966).

99. J. R. Nix and W. J. Swiatecki, Nucl. Phys. 71,1 (1965).

100. For a review of Mandelstam variables and the functional dependence of cross sections on them, see M. L. Perl, High Energy Hadron Physics (Wiley and Sons, New York, 1974).

101. R. D. Amado and R. M. Woloshyn, Phys. Lett. 69B, 400 (1977).

102. J. G. Zabolitzky and W. Ey, Phys. Lett. 76B, 527 (1978).

103. For a review, see C. de Tar, Nucl. Phys. A335, 203 (1980).

104. G. E. Brown, M. Rho, Phys. Lett. 82B, 177 (1979).

105. G. E. Brown, M. Rho, and V. Vento, Phys. Lett. 84B, 383 (1979).

106. A. Chodos, R. L. Jaffe, K. Johnson, and C. B. Thorn, Phys. Rev. D10, 2599 (1974).

107. R. P. Feynman, M. Kislinger, and F. Revndal, Phys. Rev. D3, 2706 (1971).

108. For a review, see N. Isgur, lectures in the Proceedings of the XVI International School of Subnuclear Physics, Erice (1978).

109. G. Chapline and M. Nauenberg, Nature 264, 235 (1976).

110. G. Beym, Physica 96A, 131 (1979); G. Baym and S. Chin, Phys. Lett 62B, 241 (1976).

111. C. S. Warke and R. Shanker, Phys. Rev. C21, 2643 (1980).

112. A. N. Mitra, Phys. Rev. D17, 729 (1978).

113. A. Th. M. Aerts, P. J. G. Mulders, and J. J. de Swart, Phys. Rev. D17, 260 (1978).

114. D. A. Liberman, Phys. Rev. D16, 1542 (1977).

115. G. W. Barry, Phys. Rev. D16, 2886 (1977).

116. H. Høgaasen, lecture in the Proceedings of the 3rd Nordic Meeting on High Energy Reactions in Nuclei, Geilo (1979) and references therein.

117. D. Robson, Nucl. Phys. A308, 381 (1978) for a possible extension to more complex nuclei.

118. M. Kislinger, Phys. Lett. 79B, 474 (1978).

119. P. J. G. Mulders, A. Th. M. Aerts, and J. J. de Swart, Phys. Rev. Lett 40, 1543 (1978).

120. W. J. Romo and P. J. S. Watson, Phys. Lett. 88B, 354 (1979).

121. For a review, see S. J. Brodsky, invited lecture at the First Workshop on Ultra-Relativistic Nuclear Collisions, Berkeley (1979) [also issued as SLAC-PUB-2395].

122. S. J. Brodsky and B. T. Chertok, Phys. Rev. Lett. 37, 269 (1976); Phys. Rev. D14, 3003 (1976).

123. S. J. Brodsky in Proceedings of the International Conference on Few Body Problems in Nuclear and Particle Physics, Quebec (1974).

124. R. G. Arnold et al., Phys. Rev. Lett. 40, 1429 (1978).

125. B. T. Chertok, Phys. Rev. Lett. 41, 1155 (1978).

126. D. Sivers, S. J. Brodsky, and R. Blankenbecler, Phys. Reports 23C, 1 (1976).

127. R. Blankenbecler and I. Schmidt, Phys. Rev. D15, 3321 (1977); D16, 1318 (1977).

128. R.H. Landau and M. Gyulassy, Phys. Rev. C19, 149 (1979).

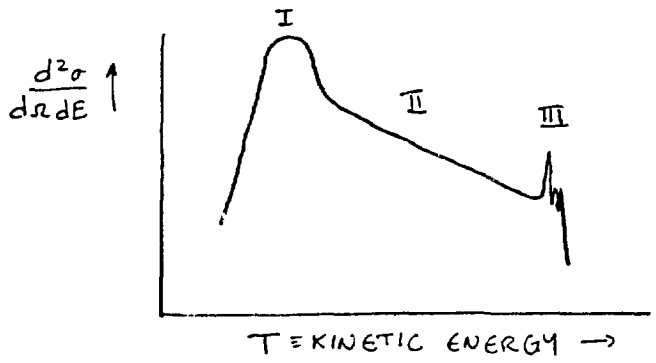

Fig. 1.

Inclusive differential cross section as a function of the kinetic energy of the ejectile at fixed angle.

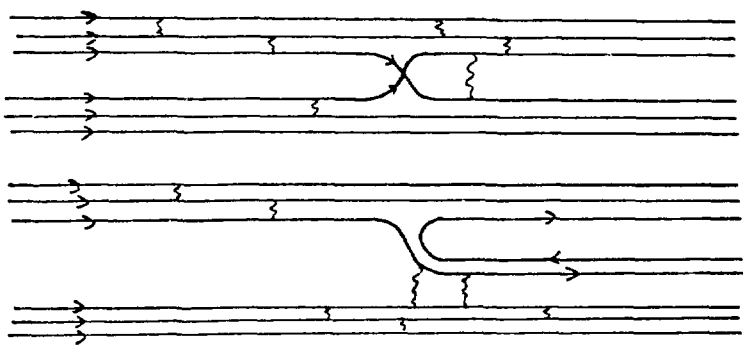

Fig. 2.

Possible quark-gluon diagram for a process like $P + {}^3He \rightarrow P + X$.

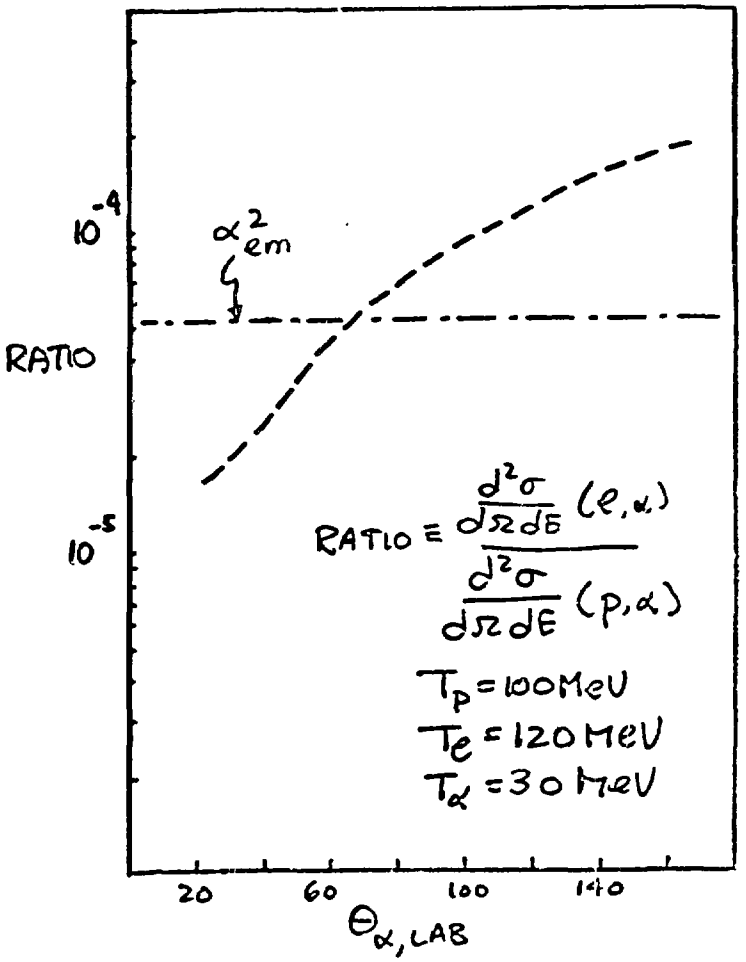

Fig. 3.

Ratio of the differential cross sections for the (e,α) and (p,α) reactions as a function of angle. The α energy is fixed at 30 MeV, while the bombarding energies are 100 and 120 MeV for the p and e induced reactions, respectively. Data are from refs. 2 to 5.

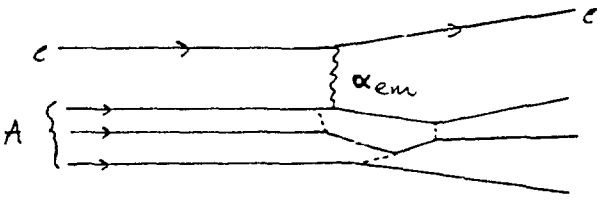

Fig. 4.

Direct knockout mechanism for electron induced reactions.

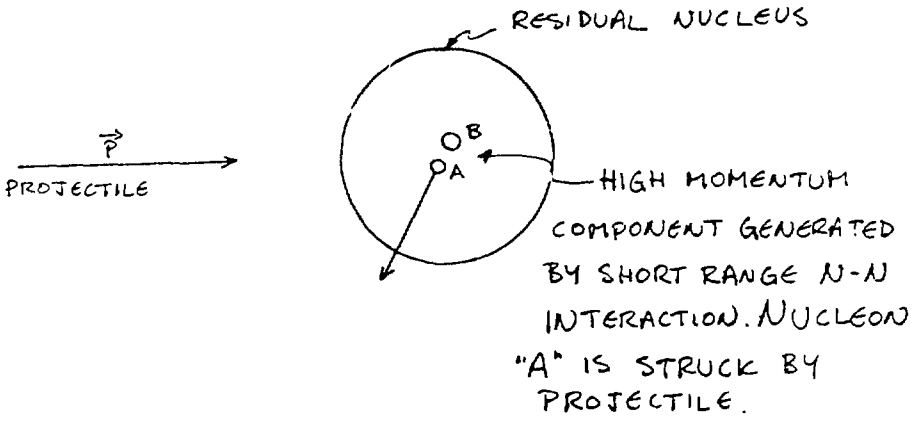

Fig. 5.

Direct knockout mechanism for emission of ejectiles with large momentum.

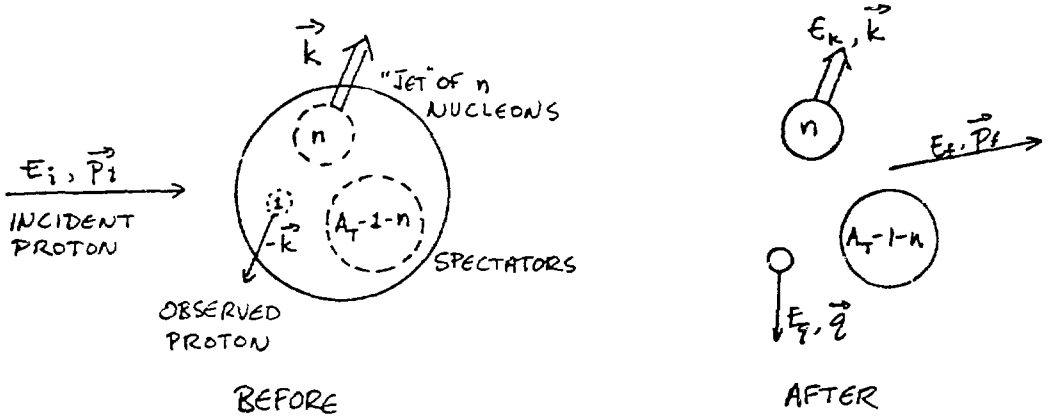

Fig. 6.

Kinematic labels used in the direct knockout model.

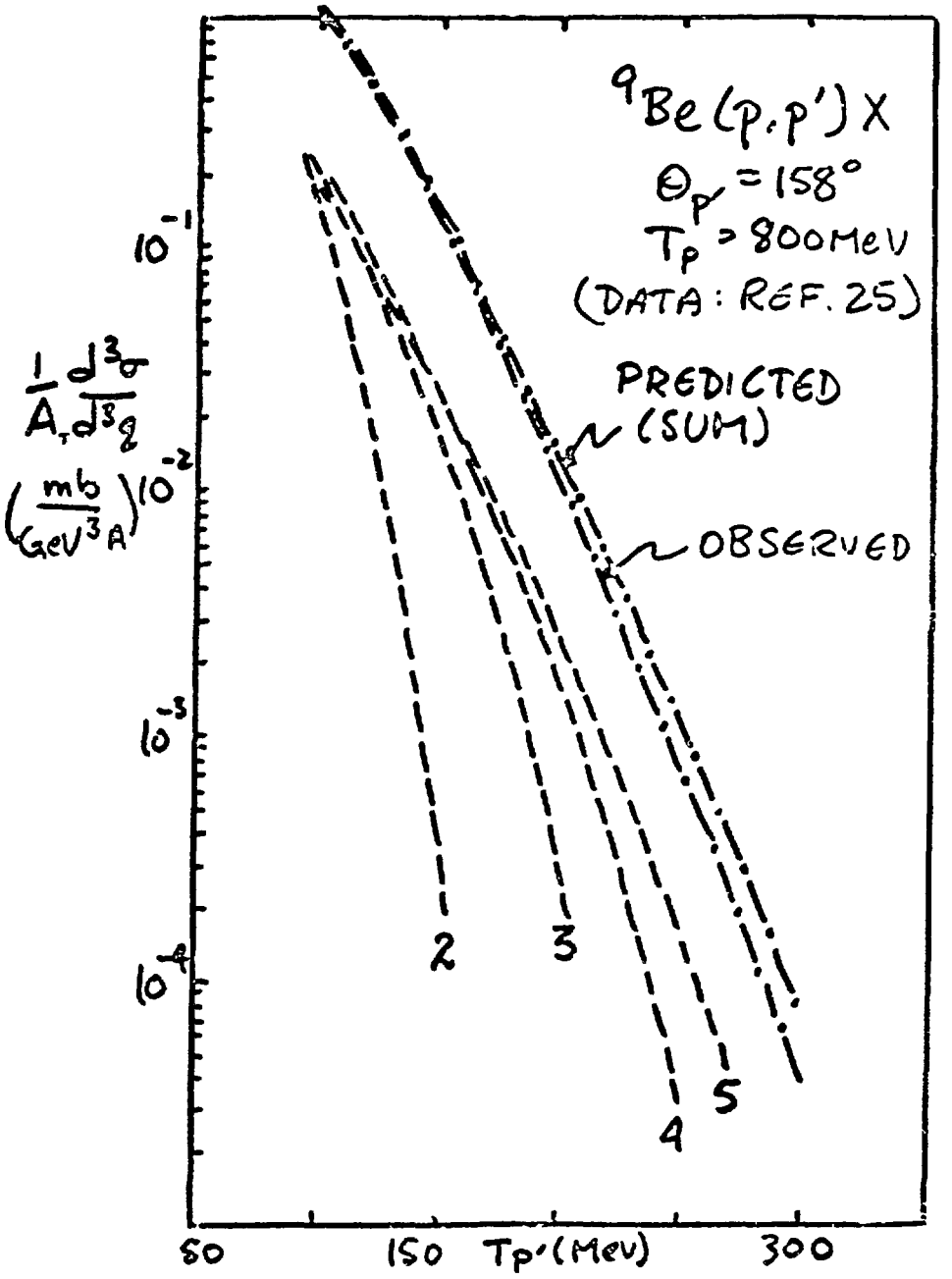

Fig. 7.

Plot of differential cross section per target nucleon as a function of ejectile energy for the $^9Be(p,p')X$ reaction. The prediction is broken down into a sum of terms involving 2,3,4 ... nucleons. Data are from ref. 25.

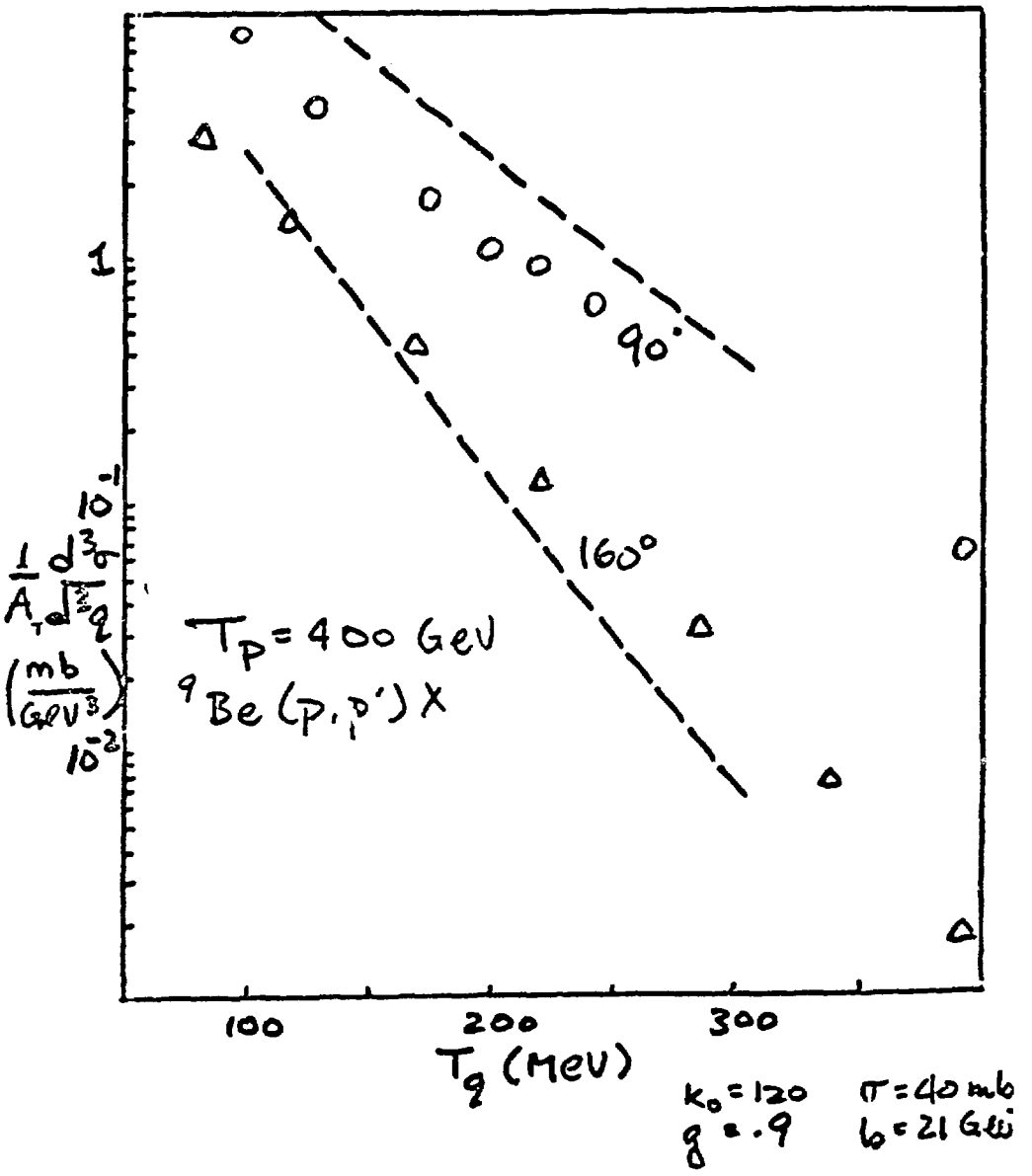

Fig. 8.

Differential cross section per target nucleon for the $^9Be(p,p')X$ reaction with bombarding proton energy equal to 400 GeV. Direct knockout model predictions are the dashed lines. Data from ref. 31.

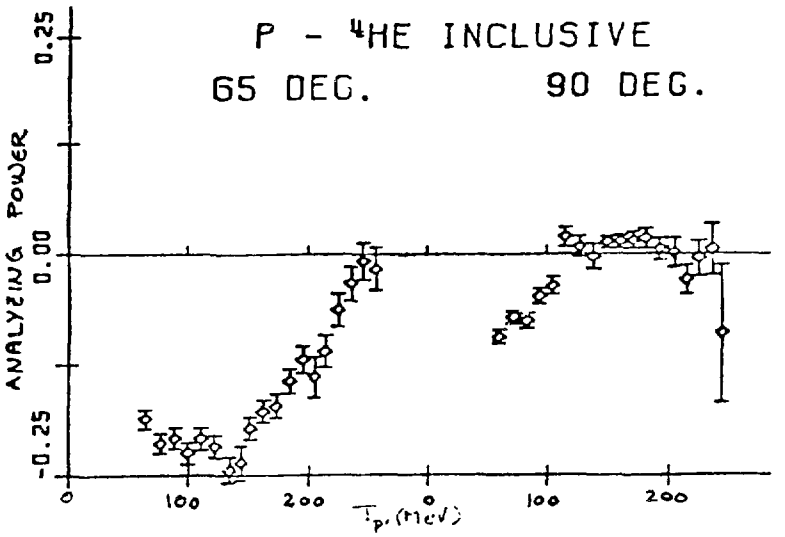

Fig. 9.

Analyzing power as a function of ejectile energy for the ^{4}He(p,p')X reaction at 400 MeV bombarding energy. Data from ref. 30.

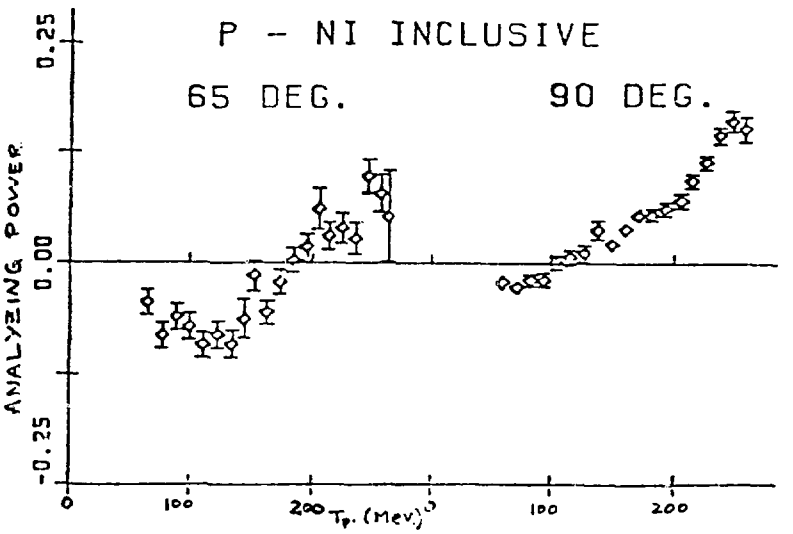

Fig. 10.

Same as Fig. 9, but for the Ni(p,p') X reaction.

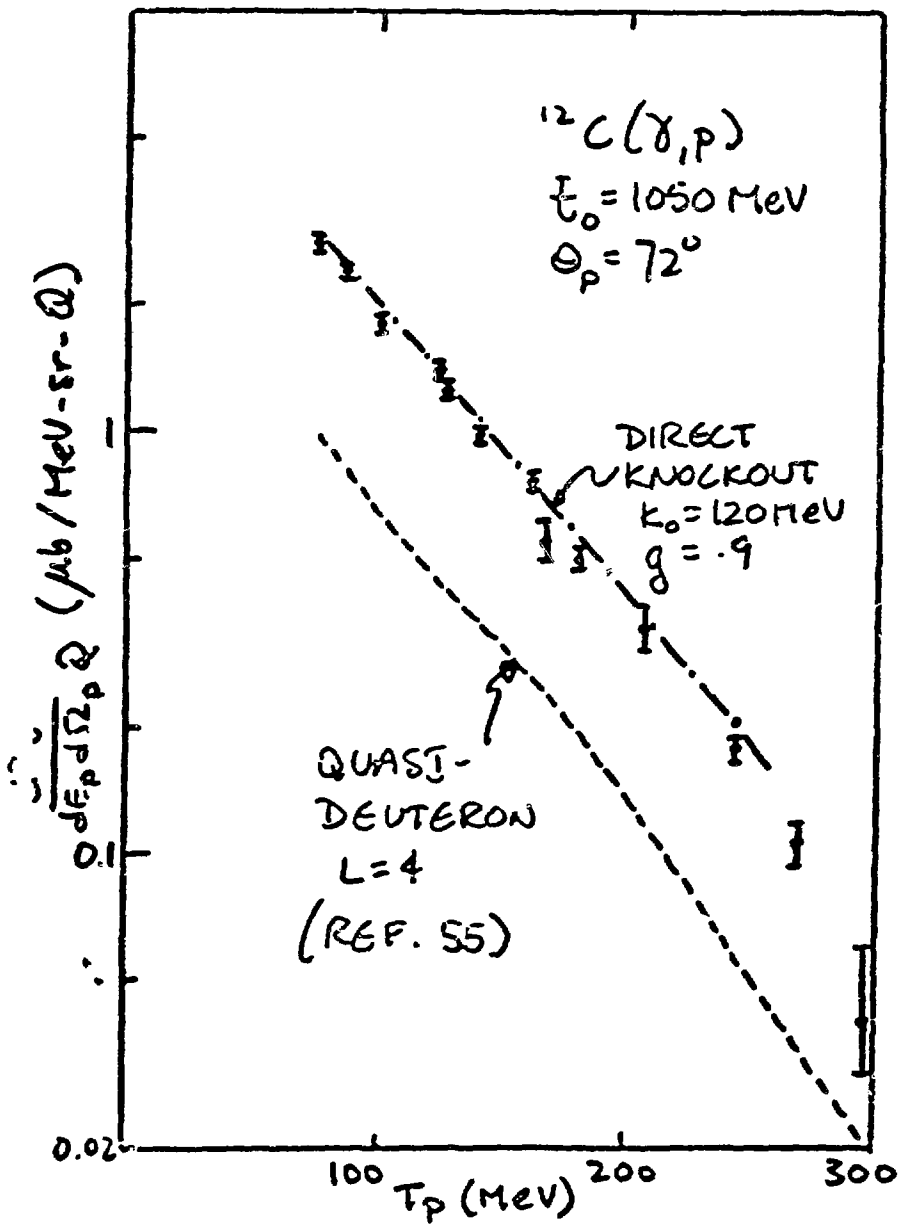

Fig. 11.

Differential cross section for the $^{12}C(\gamma,p)X$ reaction with the proton observed at 72°, shown as a function of proton energy. The bremsstrahling end point energy is 1050 MeV. The direct knockout model predictions are shown as a dot-dash curve, and a quasi-deuteron model prediction from ref. 55 is shown as a dashed curve. Data are from ref. 11.

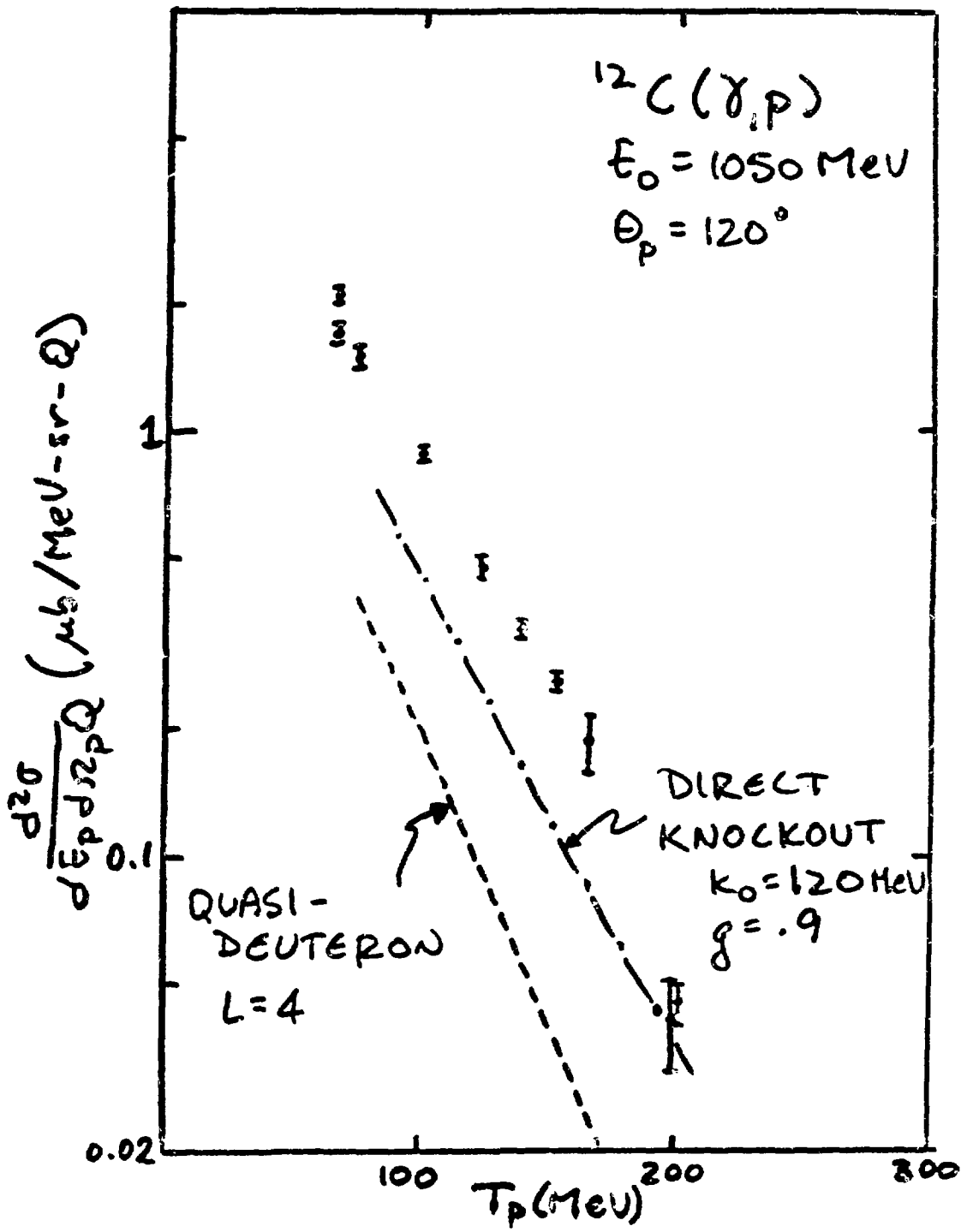

Fig. 12.

Same as Fig. 11, but for an observed proton angle of 120°.

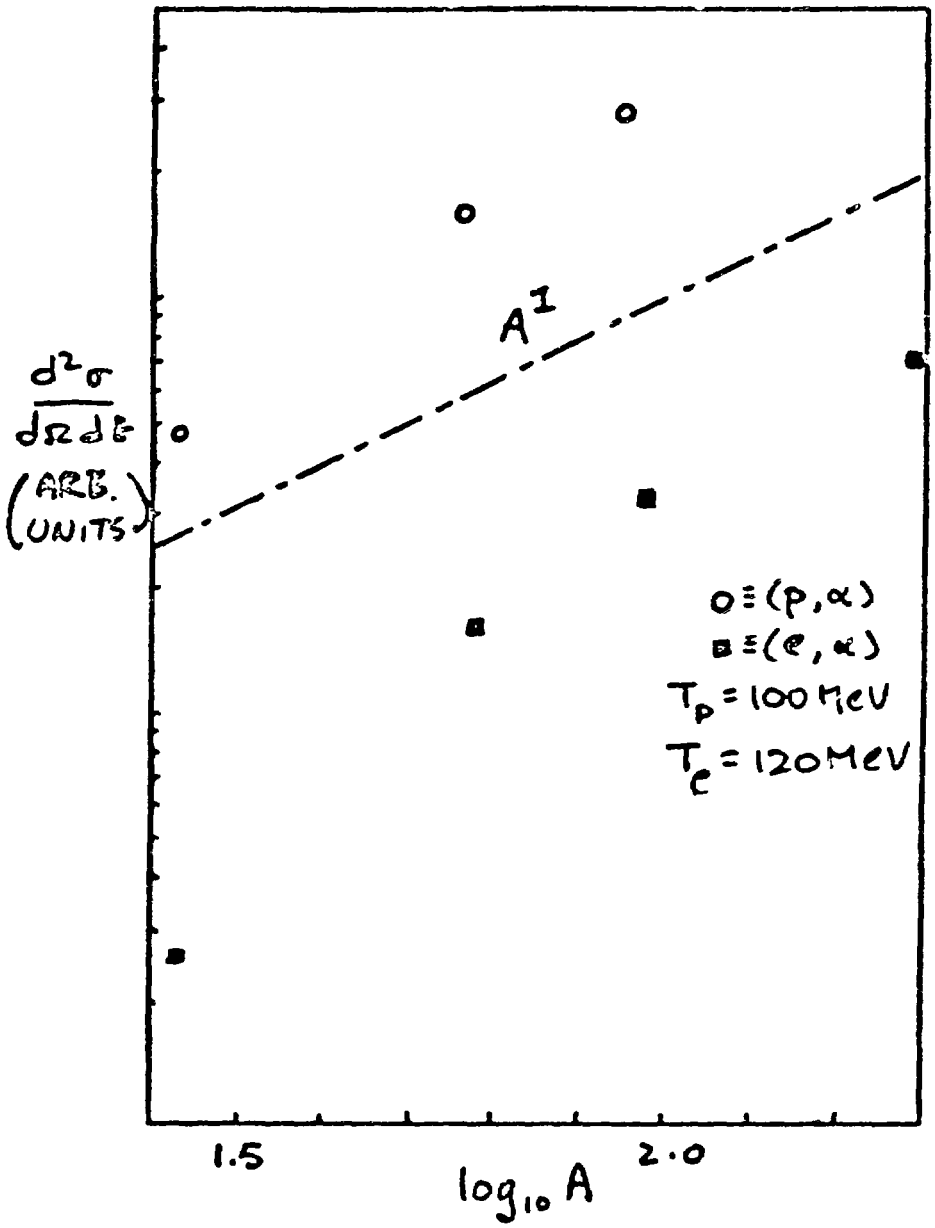

Fig. 13.

Differential cross section at fixed energy and angle as a function of target nucleon number for the (e,α) and (p,α) reactions.

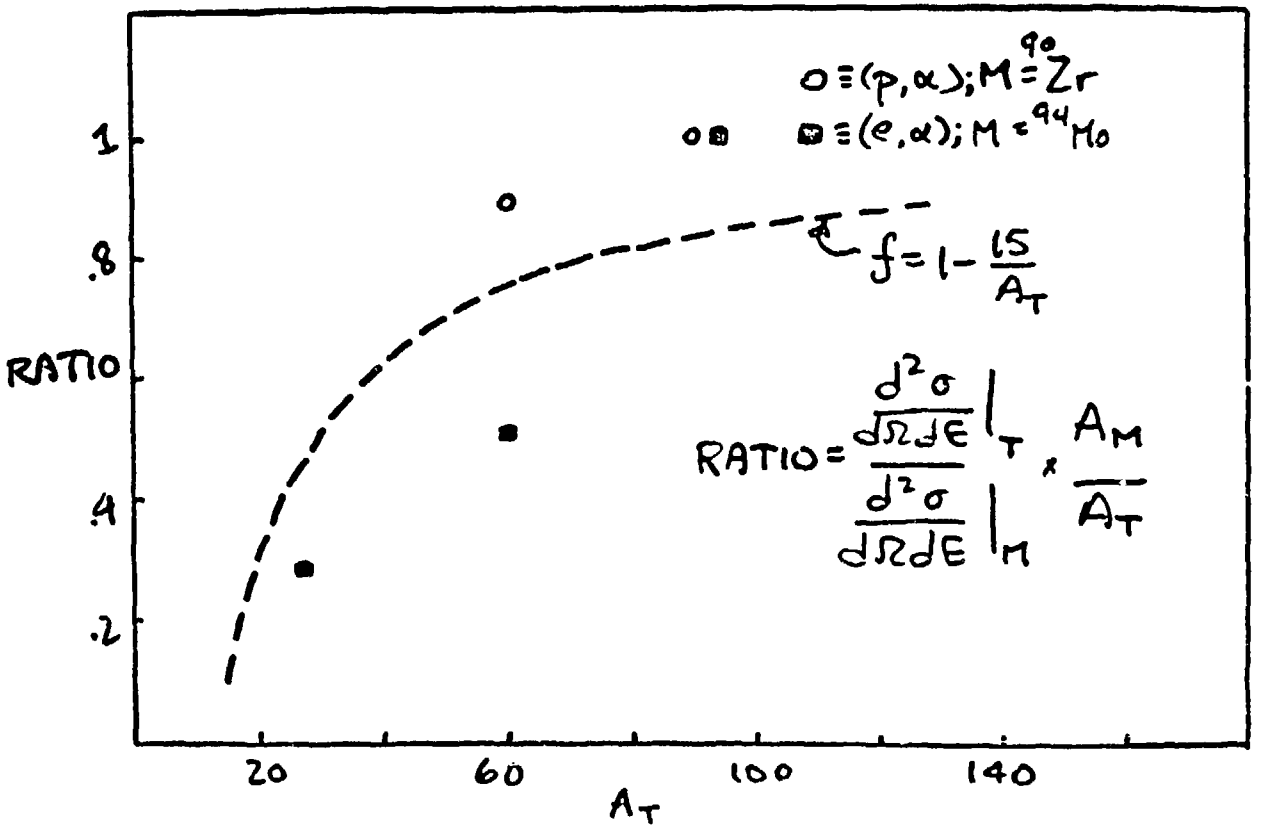

Fig. 14.

Ratio of differential cross section per nucleon at a given A to that for a target with about 90 nucleons [90 for the (p,α) reaction and 94 for the Mo reaction].

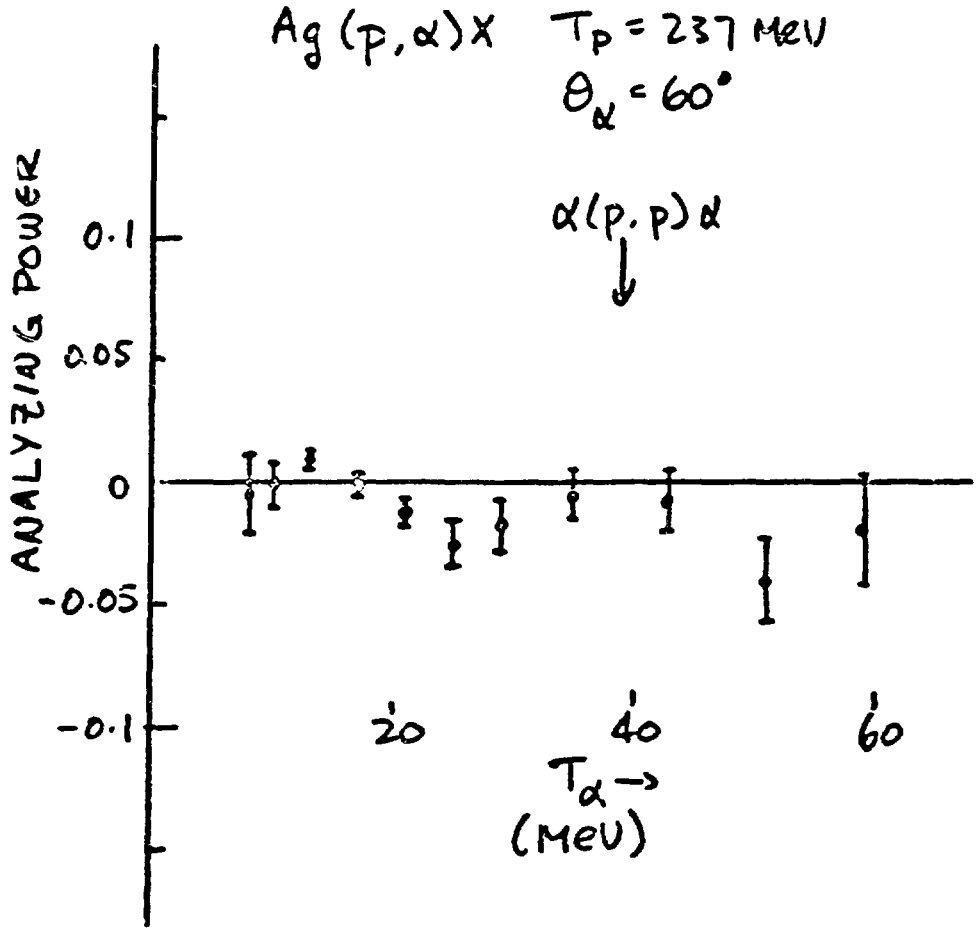

Fig. 15 (from Ref. 76).

Analyzing power as a function of fragment energy for the Ag(p,α)X reaction with T_p = 237 MeV and θ_α = 60°. The energy corresponding to quasi-free p + α scattering is indicated by the arrow. Data from ref. 76.

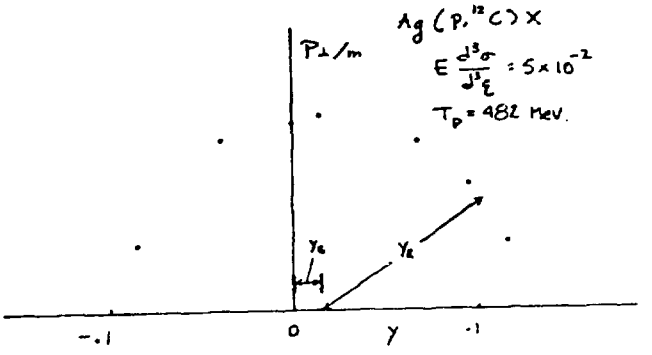

Fig. 16a.

Plot of $P_\perp/m$ vs y at constant cross section for the reaction $Ag(p,{}^{12}C)X$ at a bombarding energy of 482 MeV. The variables y_R and y_S are shown.

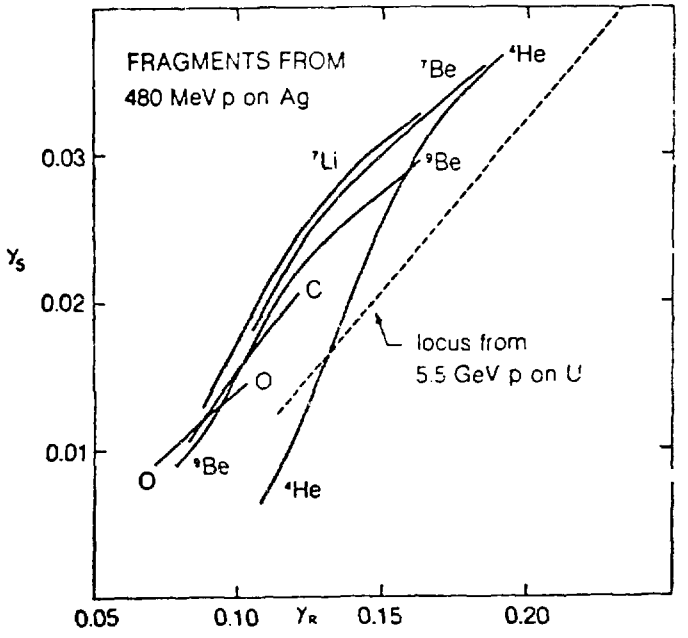

Fig. 16b.

Plots of y_S vs. y_R for different fragments in the p + Ag reaction at 482 MeV incident proton energy. Shown for comparison is an average determined from the p + U reaction at 5.5 GeV. From ref. 79.

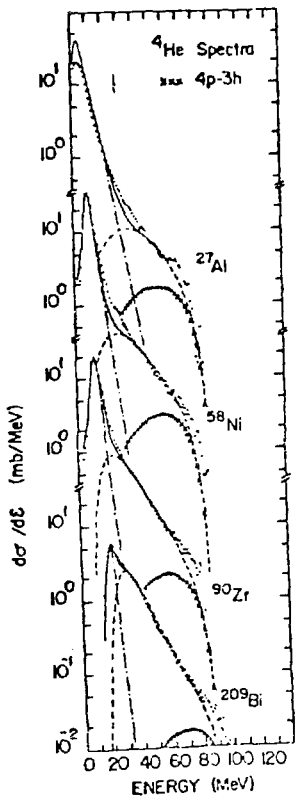

Fig. 17.

Comparison of **preequilibrium** model calculation with experiment for proton induced α emission. The cross sections are angle integrated. From ref. 83.

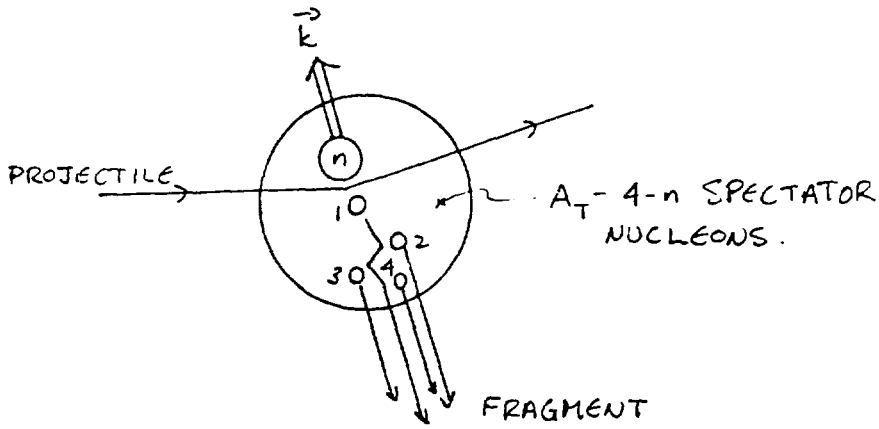

Fig. 18.

Possible multiple scattering mechanism for fragment emission.

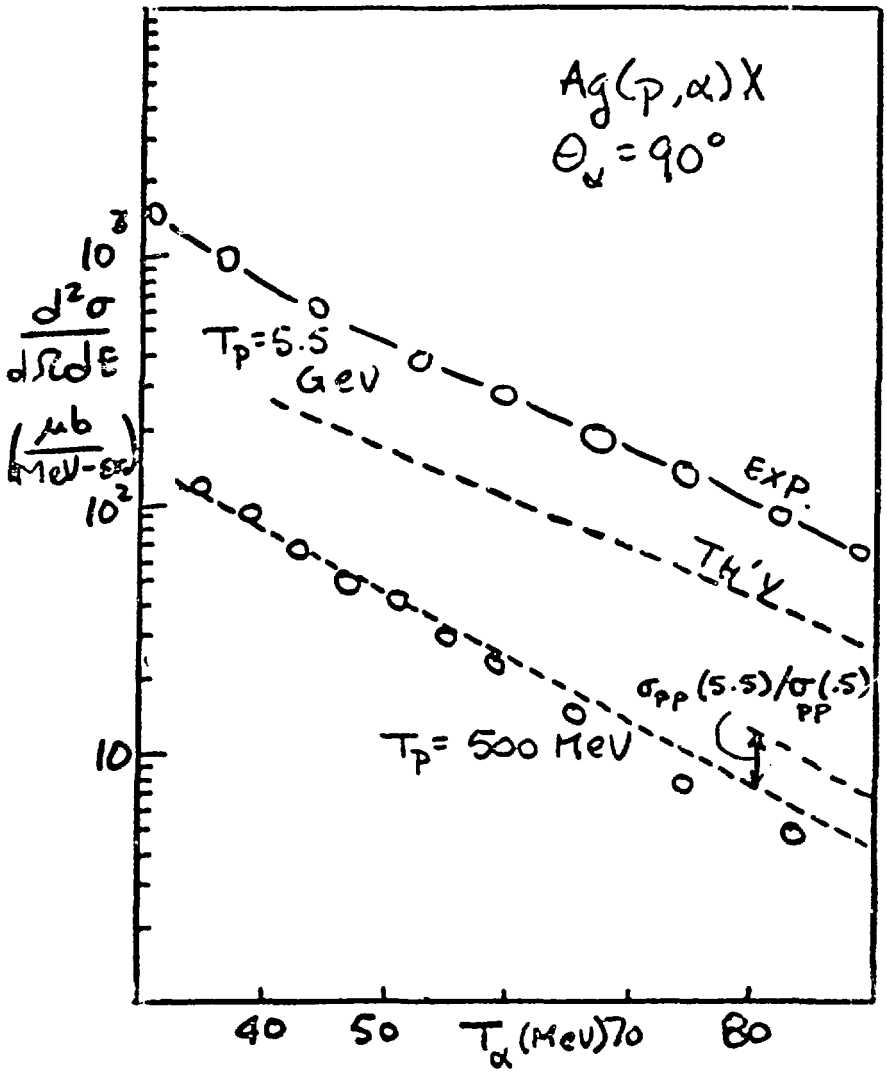

Fig. 19.

Simple multiple scattering calculation for the Ag(p,α)X reaction. The normalization is fixed by the 500 MeV data, and predictions are made for the 5.5 GeV data. The increase in cross section expected by considering the total pp cross section only is also shown.

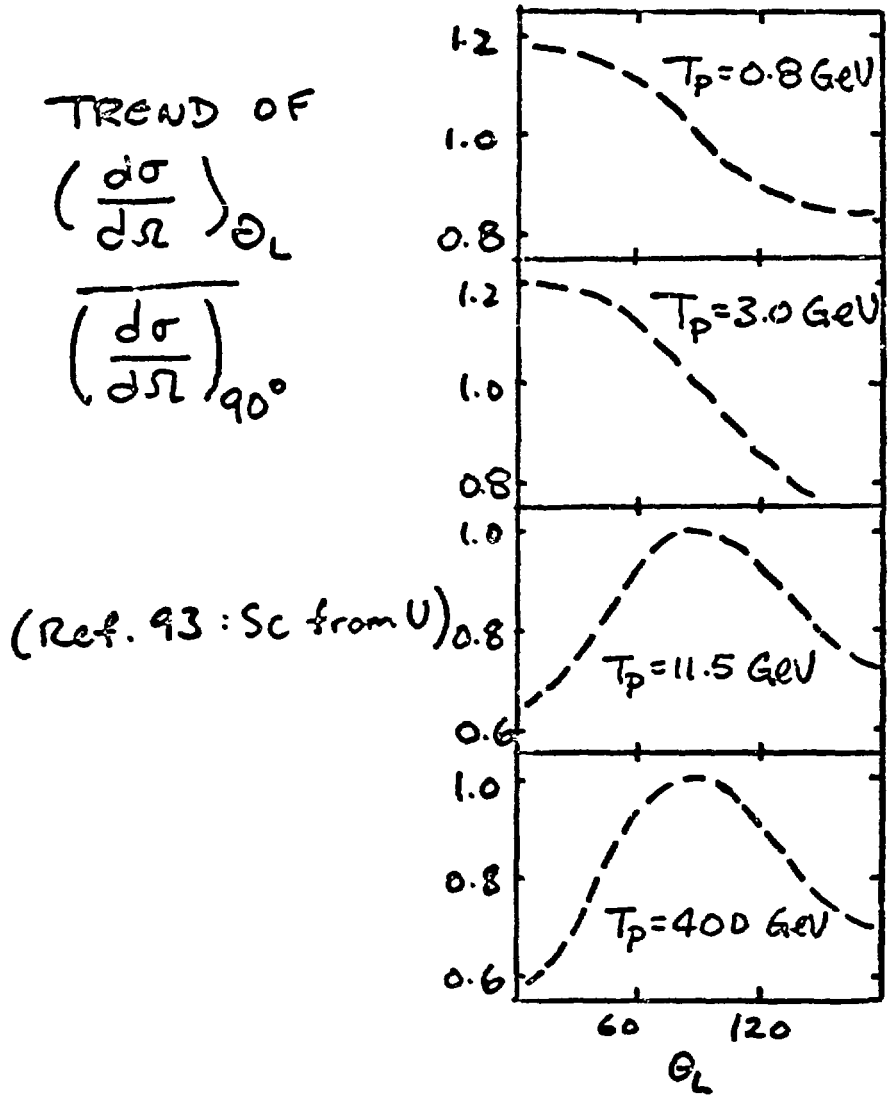

Fig. 20.

Trend of ratio of energy integrated differential cross section to value at 90°, shown for the U(p,Sc)X reaction at T_p - 0.8, 3.0, 11.5, and 400 GeV. From ref. 93.

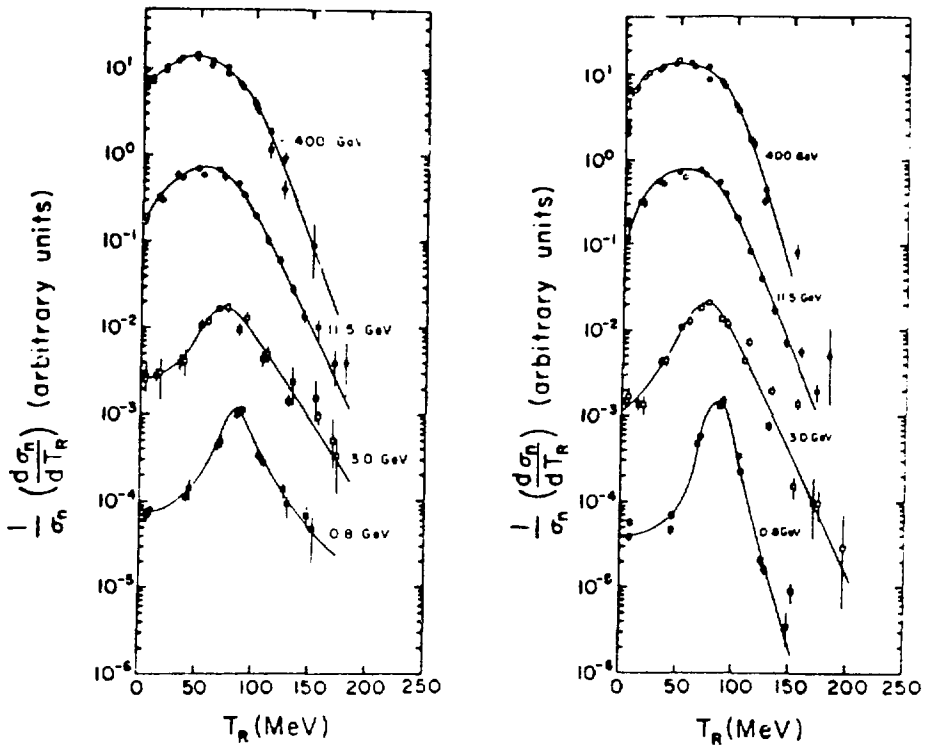

Scandium fragments from ^{238}U at 90°.

Fig. 21.

Differential cross sections for the U(p,Sc)X reaction at the same energies as in Fig. 20. The fragment is observed at 90°. From ref. 93.

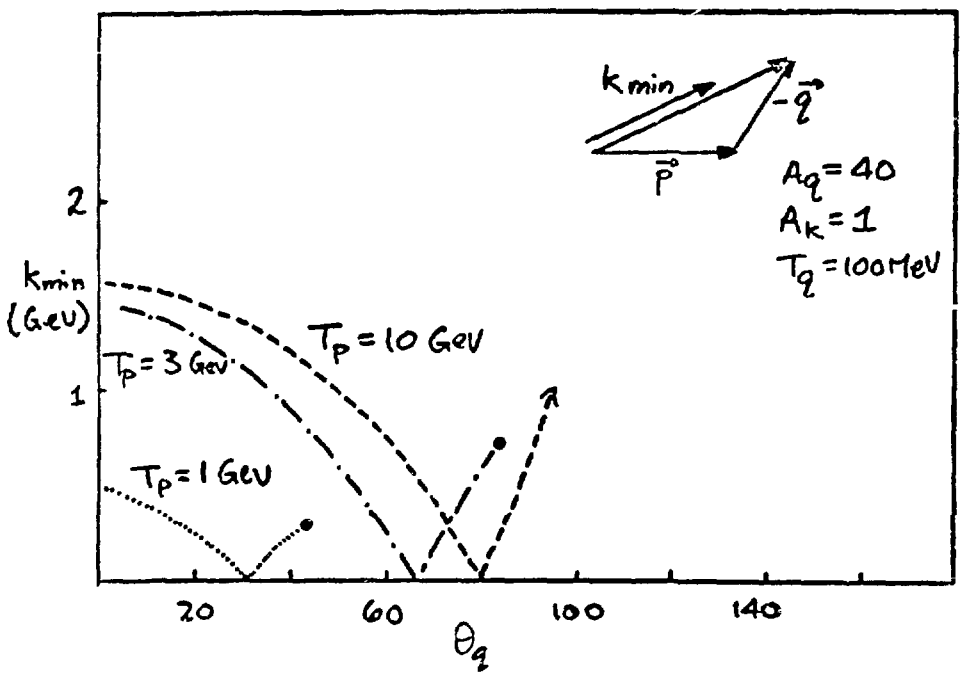

Fig. 22.

Plot of k_{min} as a function of observed fragment angle for a variety of energies. The recoil momentum is carried off by a single nucleon. See text for definition of symbols.

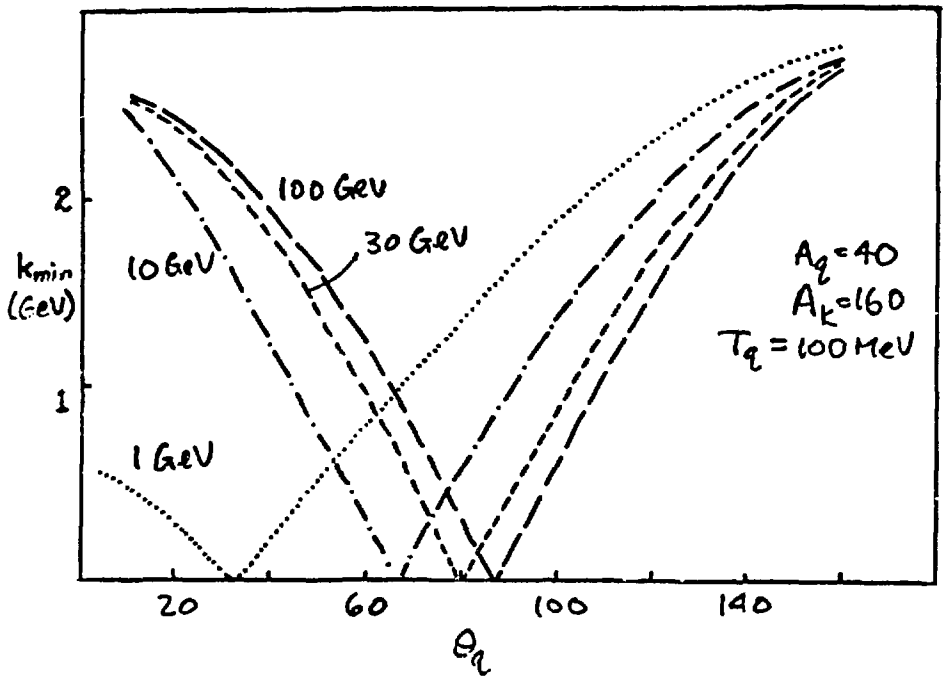

Fig. 23.

Same as Fig. 22, but for a 160 nucleon recoiling object.

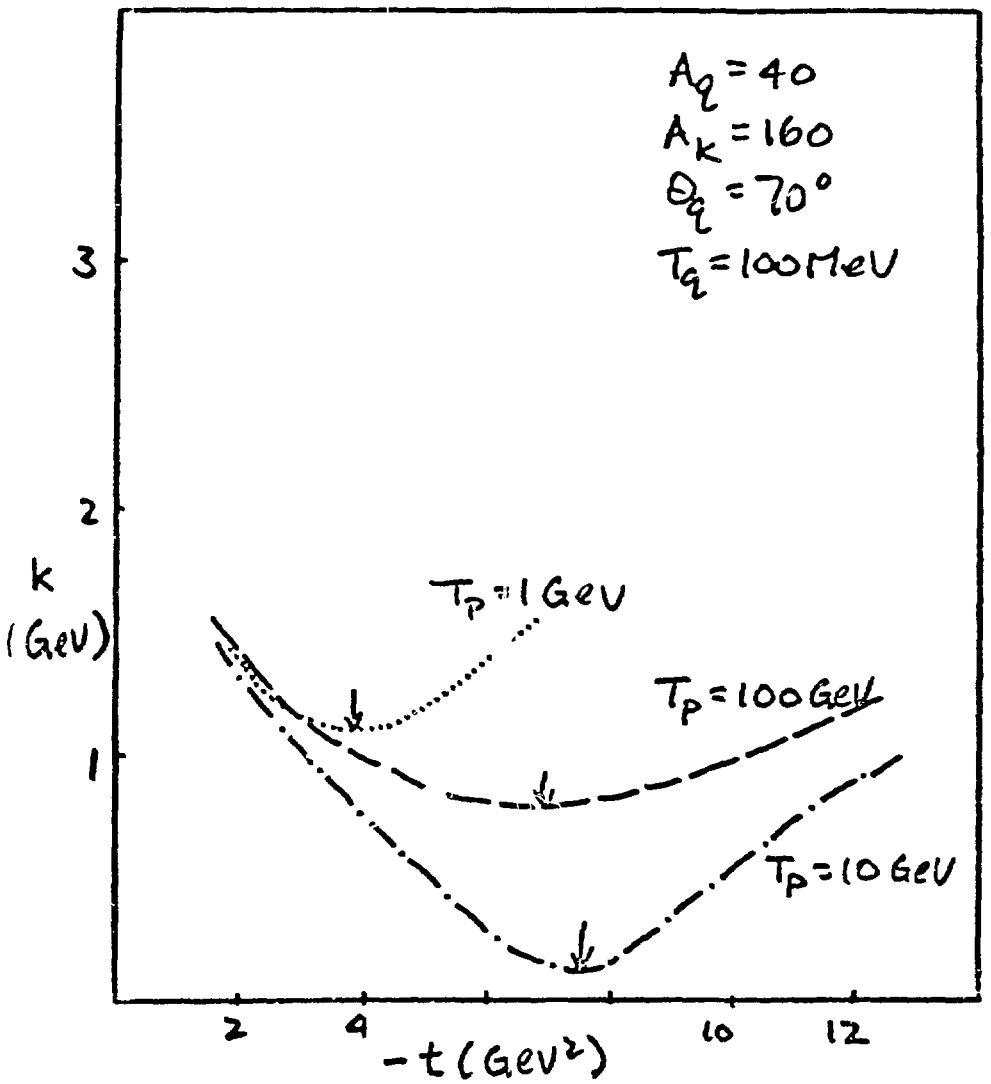

Fig. 24.

Recoil momentum k as a function of four-momentum transfer squared for various bombarding energies.

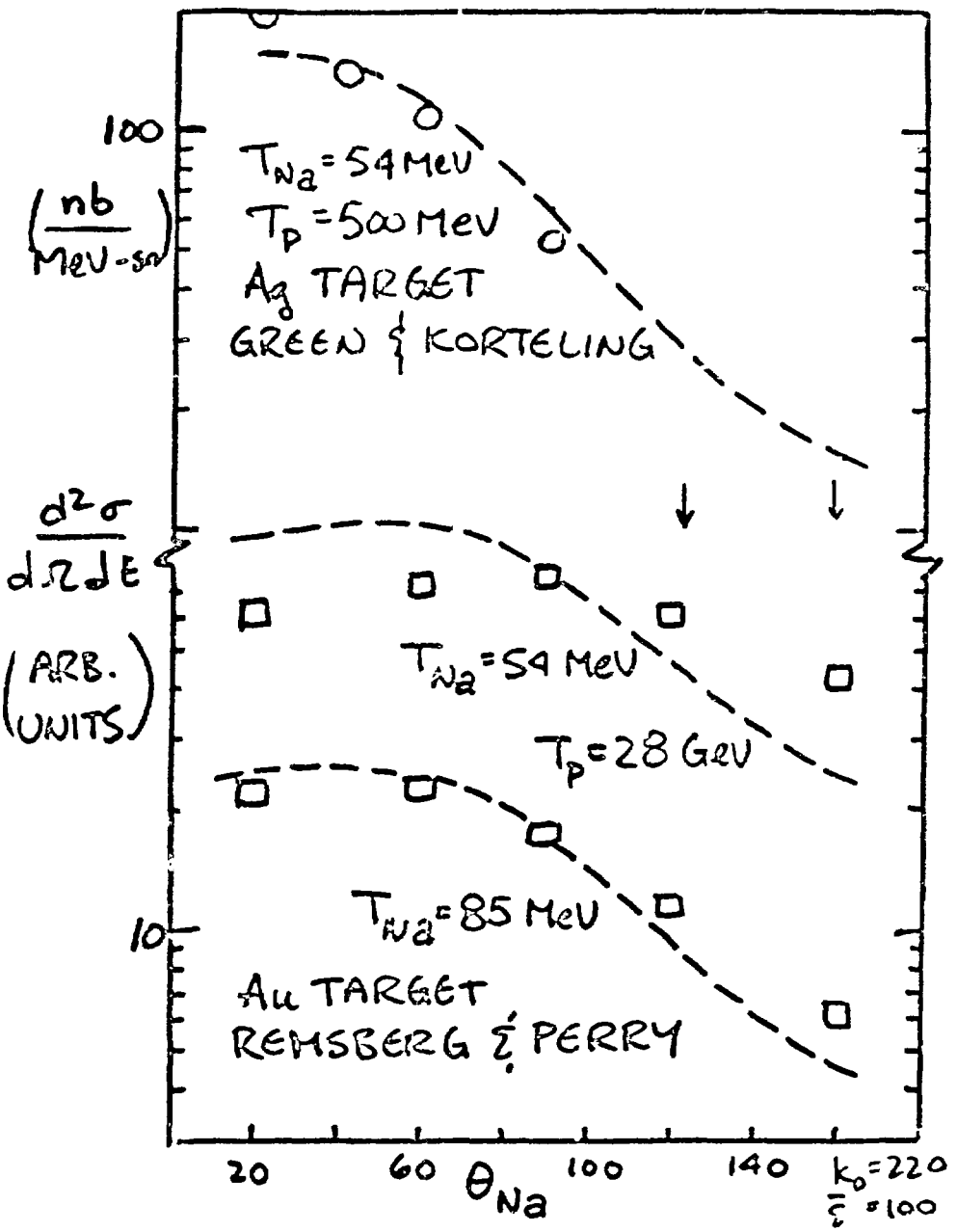

Fig. 25.

Differential cross section for (p,Na) reaction showing trend away from forward peaking with increasing bombarding energies. Calculation (dashed curve) is described in text. Data from refs. 80 and 94.

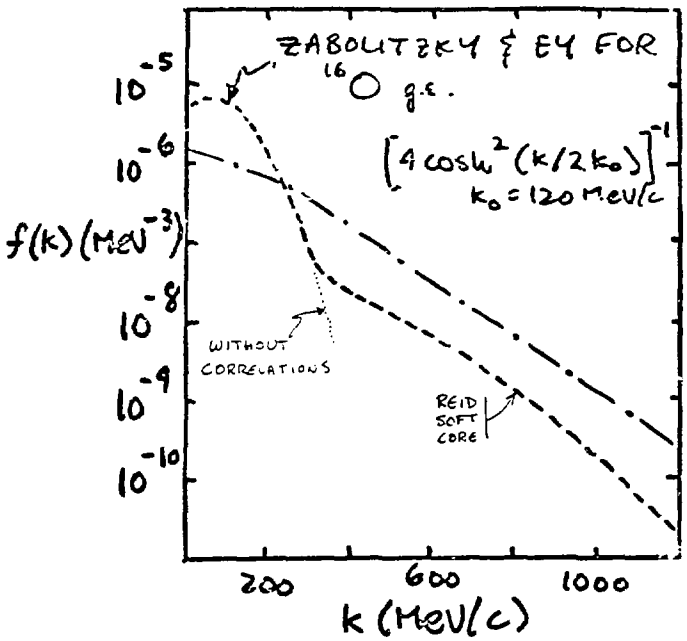

Fig. 26.

Comparison of phenomenological momentum distribution of direct knockout model with many-body calculation of ref. 102.

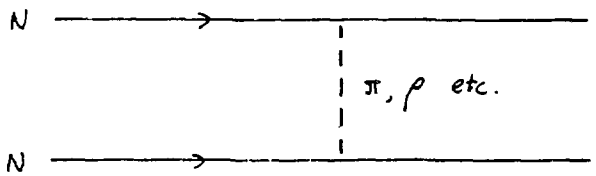

Fig. 27.

Meson exchange picture of NN force.

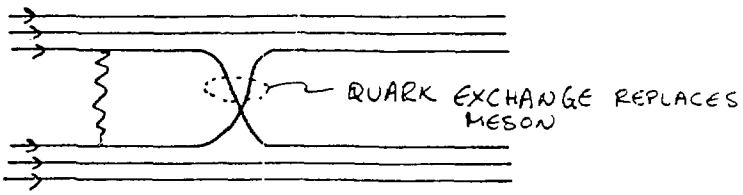

Fig. 28.

Quark exchange picture of NN force.

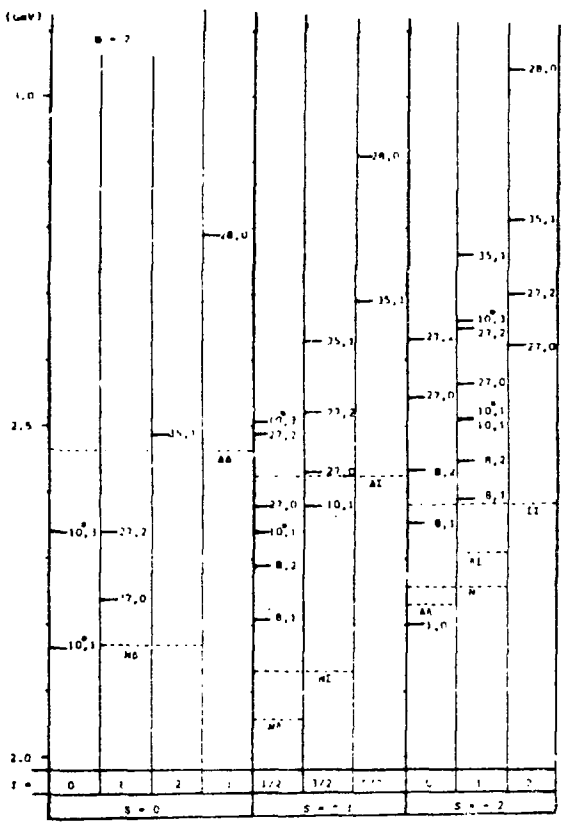

Fig. 29.

Masses of 6-quark baryons with S = o, -1, -2,
Labeled by: SU(3) representation and spin.
From ref. 113.

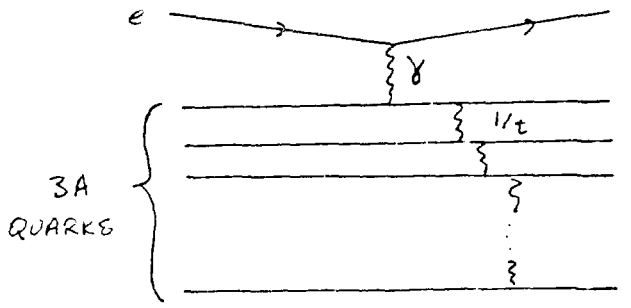

Fig. 30.

Mechanism for electron scattering on 3A quarks.

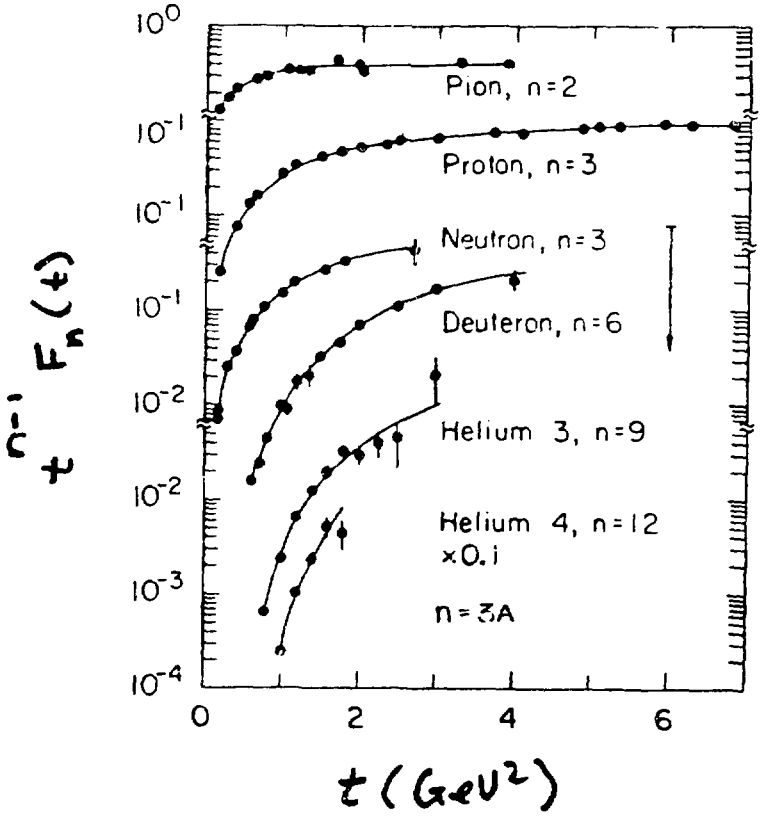

Fig. 31.

Electromagnetic form factor multiplied by t raised to the 3A-1 power, shown as a function of t for various nuclei. From ref. 121.

NUCLEI FAR FROM β-STABILITY

SOME METHODS AND RESULTS

by

Marcelle Epherre
Laboratoire Rene Bernas du CSNSM
91406 Orsay - France

I. Where do we stand? - The extensive study of the alkaline elements

The time of the "Why and how should we investigate nuclides far off the stability line," subject of the Lysekil Conference in 1966[1], is far behind us. All the results obtained, particularly in the last ten years - new isotopes, new modes of radioactive decay, new magic numbers, new regions of deformation - are now many proofs of the validity of these studies. The field has grown rapidly and widely: many powerful experimental methods of investigation have been developed for the production of these very unstable nuclei as well as for their subsequent identification and study. They have been described in particular in the proceedings of the two conferences[2] held on this field since its beginning. Nevertheless, all we know about nuclear structure is still based on the systematic experimental study of some hundreds of nuclei, the near-stable ones, out of the 8000 which could exist, being bound to nucleon emission. Do the established laws hold for all of them? The search for new isotopes reaching toward the limits of stability and the study of the structure and properties of the thousand unstable nuclei now known are being pursued in parallel. The region of the light nuclei, though rather favored, can be considered as an example of the present status of the study of nuclei far from stability. Figure 1 shows the well-known segment of the chart[3] updated with the 23 new isotopes mostly between Z = 11 and Z = 19 produced in heavy-ion induced reactions both at Orsay (6-8 MeV/amu ^{40}Ar on ^{238}U)[4] and at Berkeley (205 MeV/amu ^{40}Ar on ^{12}C and 212 MeV/amu ^{48}Ca on ^{9}Be).[5]

We first observed that the study of the properties of these exotic nuclei is at its very beginning. Most of those known have only been identified (half-filled squares) and even their decay has not yet been observed. The identification of a nucleus gives just qualitative information: It is bound, but how far is it from

the drip line? Much remains to be done in that sense. The second observation is that for now the more systematically studied unstable isotopes are those of the alkali elements, Li, Na, K, shown on Fig. 1, but also Rb, Cs, and, to a less degree, Fr. I mean that many nuclear properties have been measured on each series of isotopes: half-lives, binding energies[6,7], spins[8,9], quadrupole and magnetic moments[8,9], isotope shifts[9,10], energies of the first excited states, gamma decay schemes[11], and delayed neutron branches[12]... Interesting results have come out of these measurements which have been done mostly in the last few years, and I have selected from among them several examples to illustrate the physics aspect of such studies. Before entering this subject, a third remark has to be made dealing with the production of these exotic nuclei.

II. Protons or heavy ions, what is the best tool?

I think that despite all the work done at Berkeley, Darmstadt, and Orsay, intermediate- and high-energy protons are still the most universal way to produce nuclei far from stability. Indeed, it is interesting to note that the neutron drip line, which is accessible in the region of the lightest nuclei, has only been reached with ^{11}Li and ^{14}Be, both produced in the interaction of high energy protons with a U target.[13,14] In the same "universal" targets were produced the most neutron-rich isotopes known: ^{34}Na with 20-GeV protons[6] and ^{52}K, ^{102}Rb, ^{152}Cs with 600-MeV protons.[15] Also with 600-MeV protons the limit of proton instability was very likely reached for a nucleus as heavy as ^{74}Rb.[16] Figure 2 illustrates two other major advantages of the protons for the production of nuclei far from stability: the large yields and the very wide isotopic distribution of the reaction products in almost all regions of the nuclidic chart. This allows, in particular, systematic studies of the nuclear properties of series of isotopes which are very fruitful, as will be discussed later. Here, with the same target, more than 20 isotopes of the same element can be produced in sizeable amounts, and more than 30 isotopes can be covered with two targets. Also shown are the production yields of the same isotopes with thermal neutrons and heavy ions. Note that cross sections are not compared, but the number of atoms available are plotted, which is for our purpose, a more significant parameter. It takes into account the beam intensity available and also the useful thickness of the target, which is much lower in the case of the heavy ion reactions owing to the short ranges of these particles. The product, ϕN_t, of the incident flux times the number of atoms of the target, corresponding to the four curves presented, are

Table I.

	PROJECTILE	TARGET	ϕN_t ($s^{-1} \times cm^{-2}$)
UNILAC *(Darmstadt)*	^{58}Ni 5MeV/amu $\sim 8\times10^{11}\ s^{-1}$	^{58}Ni $4mg\times cm^{-2}$	3×10^{31}
TRIGA *(Mainz)*	Thermal neutrons $\sim 1.7\times10^{11} s^{-1}\times cm^{-2}$	^{238}U 200mg	8×10^{31}
SC *(CERN)*	protons 600MeV $\sim 6\times10^{12}\ s^{-1}$	^{238}U $13g\times cm^{-2}$	2×10^{35}
BEVALAC *(Berkeley)*	^{48}Ca 212MeV/amu $\sim 10^{7}\ s^{-1}$	^{9}Be $890mg\times cm^{-2}$	6×10^{29}
PS *(CERN)*	protons 20GeV $\sim 4\times10^{12}\ s^{-1}$	^{238}U $30g\times cm^{-2}$	3×10^{35}

compared in Table 1 as a crude estimation, neglecting other factors which depend on the detection methods considered. It shows how, despite the high cross sections of thermal neutron induced fission, more neutron rich radioactivity is obtained from fission with high energy protons than with reactor neutrons. The comparison of the corresponding parameters calculated for the Bevalac and the proton synchrotron of CERN, in the case of targets and projectiles used to produce the exotic Na isotopes, also shows the greater efficiency of protons. In this case the cross sections are surprisingly identical as shown in Fig. 3. One can also observe (as in Fig. 2) that the isotopic distribution obtained with heavy ions never extends for more than ten isotopes, and is usually around 6-8. Nevertheless, for some experimental techniques, the kinematic orientation of the products in the beam direction is a real advantage of the HI reactions. Another advantage also compared to the proton reactions is that the distribution can be centered, with a discerning choice of projectile and target, far from stability. This means, in particular, that highly selective methods are not so much needed to separate the products,

and that on the neutron deficient side of the valley, where the production yields of the proton induced reactions drop rapidly, heavy ion reactions are able to give better yields. This is shown, in particular, in Fig. 2 and has been observed also around Z = 40.[18] The production yields shown in Fig. 2 have been obtained with only a 1 μA proton beam. For the most extreme isotopes the half-life could be measured through p- or n-delayed emission. A few mass numbers away fairly detailed spectroscopy can be done; 10^4 atoms are enough for precise mass measurements, and 10^5 atoms are adequate for atomic hyperfine structure measurements. We can readily conclude that the high proton beam intensities now attained at meson factories would provide, a gain in nuclide production in addition to the possibility of studying other elements for which our detection methods have lower efficiency.

III. The on-line mass separation technique for fast A and Z selection

A great mixture of nuclei is produced in high-energy proton-induced nuclear reactions, with amounts which can vary by several orders of magnitude. Thus, to study a nucleus of particular interest, which usually has very short half-life, the detection technique has to be selective, fast, and sensitive. On-line mass separation not only has high selection in A, but also in Z. Figure 4 is an example of such an installation, the largest of its kind, CERN's ISOLDE installed on-line to the 600-MeV proton beam of the synchrocyclotron and providing intense ion beams of short-lived nuclei for experimental investigations. The fast release of the radioactive ions, which is required in order to minimize the decay losses of short-lived nuclei, depends strongly on the target-ion source unit, which in addition, has to withstand the heating and radiation damage induced by the proton beam. The fastest systems developed are based on fine-grained mixtures (target element + graphite) at high temperature.[17,20] The experiments which are presented in Fig. 4 were on the floor in 1978 and give a good sampling of the work currently done at ISOLDE. They concern mainly nuclear spectroscopy (α,β,γ) and β-delayed particles[11]; the optical pumping and laser spectroscopy of the Mainz group which observed shape coexistence in the light mercury isotopes[8]; the atomic beam magnetic resonance apparatus[9] which is still on-line measuring spins and magnetic moments; and finally the double focusing mass spectrometer[7] with which we measured about 30 new masses of short-lived isotopes of Rb, Cs, and Fr. This experiment, together with the hyperfine optical spectrometry experiment performed afterwards[10,21] on the same elements, brought particularly interesting results not only because they measured some fundamental properties of nuclei adding new

data to those existing, but especially because their joint analysis revealed unexpected behavior of some of those nuclei. Some more details are therefore given on these experiments.

IV. Direct mass measurements on long series of isotopes

Measuring masses with a mass spectrometer has been done for a long time for stable isotopes, and precision of the order of 2×10^{-8} is currently achieved. However, the number of stable atoms available is not limited, and a high resolution apparatus which has low transmission can be used. With unstable isotopes, only 10^5 to 10^{10} atoms are available (10^{-17}g to 10^{-12}g for Rb) for very short times (half-lives from several minutes to several tens of ms), and a compromise has to be found between transmission and resolution. The mass spectrometer we used, and which can be seen in Fig. 4, normally operated at a resolving power of 5000 with a corresponding transmission of 10^{-3}. The accuracy reached when not limited by statistics was better than 10^{-6}.[7]

The scheme of the experiment is shown in Fig. 5. The double focusing apparatus is of the Mattauch-Herzog type consisting of a spherical electrostatic deflector followed by a homogeneous magnetic sector and is equipped with high stability power supplies (10^{-6}). The monoisotopic ISOLDE beam of 60 kV is stopped, reionized, and accelerated to 9 kV in the ion source of the mass spectrometer; the transmitted ions are counted with a movable dynode electron multiplier. This last device plays an essential part in the mass measurements of the francium and of the rare isotopes; it takes off the radioactivity which normally accumulates at this point giving a background able to completely hide the signal.[22] For the measurements, the magnetic field is kept constant and the electric potentials, while keeping constant ratios, vary in absolute value so that ions of different masses follow the same trajectory. From the precise measurement of the potentials and from two previously known masses, a third mass is determined: $M_A(V_A+\delta) = M_B(V_B+\delta) = M_C(V_C+\delta)$. The jumps which are necessary between the different isotopes are performed by modifying synchronously the magnetic field of ISOLDE and all the voltages of the mass spectrometer. Two reference masses are needed to start, and then the measurements proceed through a step by step mode: the masses of isotopes near stability are directly measured from masses previously known and are subsequently used for the mass determination of more and more exotic nuclei. The accuracy finally obtained is shown in Fig. 6 together with the span of masses measured on both side of the valley of stability. One can notice that

the accuracy is in many cases better than 100 keV which corresponds to a precision of a few 10^{-7}, and that there is an increase at the end in going away from stability, which is essentially due to the propagation of errors through the reference masses. The precision is limited by statistics only for the extreme isotopes; those for which the production yield is $\lesssim 10^4$/s. As an example it took less than 1h to reach 100-keV experimental accuracy on ^{75}Rb (production yield of $\sim 2 \times 10^4$/s) whereas we spent 10h measuring the mass of ^{74}Rb, a case of particular interest as the heaviest odd-odd N = Z nucleus known, to reach 300-keV accuracy. This graph does not take into account the error due to possible isomer contamination, which our method is not able to discriminate. But considering the known isomers, the error thus introduced could not be greater than a few hundred keV, which does not disturb the main points of the physics interpretation of these results.

In addition to these masses of the Rb, Cs, and Fr isotopes which we directly measured, 28 new masses also could be determined in the region (N < 126,Z > 82) owing to long chains of α decay energies known prior to our work, but which had no connection with the known masses[7b] (Fig. 7).

What do we learn from these new data which represent three cross sections through the hills and valleys of the nuclear energy surface?

V. A test for the predicting power of mass formulae

First, they provide severe tests for the validity of mass predictions[23] and hence to nuclear stability. How do the mass formulae adjusted in the valley of stability extrapolate far from it? There is not one best formula working equally well for the three elements Rb, Cs, and Fr, but rather systematic trends of disagreement away from stability. In the Rb isotopes the local formulae of the Garvey-Kelson type give the best predictions (Fig. 8) even for the n-rich isotopes, where the macroscopic calculations deviate by 3 to 5 MeV. This general disagreement can be related to the irregular behavior of the binding energies in this region which these formulae are unable to predict. I'll come back to it later. For the heavier elements Cs and Fr, the semi-empirical shell model of Liran and Zeldes give the best predictions; the other mass formulae deviate by up to 2-3 MeV for the extreme isotopes we measured. This is shown in Fig. 9 for Cs, and it is even clearer for the isotopes of Fr and its neighbors as shown in Fig. 10. One can compare with the results of the Darmstadt calculations which give the best fit among the macroscopic calculations.

VI. The possibility of revealing unexpected nuclear structure

Secondly, masses depend on nuclear structure, and an interesting way of emphasizing what these measurements reveal about nuclear structure is to plot the differential representation of the mass surface such as presented in Fig. 11. One can then observe in the rubidium data the well-known rapid drop at the major neutron shell N = 50, the smaller drop at N = 56, presumably representing the closure of the d5/2 subshell; towards the light masses and especially towards A = 74 which corresponds to N = Z = 37 where the isospin projection is zero, the increased binding can be accounted for in part by the so-called Wigner symmetry energy term; and finally a bump at N > 60 which, if compared to the situation in the rare earth region, could be an indication of deformed nuclei. It is worth noting that a pure liquid drop model would expect a monotonic decrease of S_{2n} and that the discontinuities here observed are ascribed to single particle effects. In particular, a region of deformation had been predicted (around Z = 40, N = 60) by microscopic calculations[25] but without details on the way it translates to experimental facts. The first experimental indication was given in the pioneering work of Cheifetz et al.[26] Then spectroscopy on ^{99}Sr (Ref. 27) and later on ^{100}Sr (Ref. 28) have shown that ^{98}Sr and ^{100}Sr were nearly perfect rotors and among the most deformed nuclei outside the fission isomers (Fig. 12).

VII. Laser spectroscopy, a powerful probe for nuclear structure study far off stability

Then another experiment performed by the collaboration of two groups from Orsay - one of Laboratoire Rene Bernas and one of Laboratoire Aime Cotton -[21] on the same series of isotopes brought complementary information by the use of atomic beam laser spectroscopy. It is perhaps worthwhile to remember that hyperfine structure (hfs) and isotope shift (IS) of atomic spectra were among the earlier sources of information on nuclear structure, yielding spins, moments, and isotopic changes of charge distribution of nuclear ground states of the stable isotopes. With the advent of modern on-line mass separation, as well as new techniques in atomic physics (tunable dye lasers), the study of hfs of radioactive atoms of a large variety of elements has become possible. The methods used by the Orsay group are outlined in Fig. 13: the 60-keV ionic beam from ISOLDE is stopped and neutralized to form a thermal atomic beam which interacts at a right angle (to minimize Doppler effects) with the light of a tunable dye laser. When tuned at the resonance with one of the hyperfine components of the D^1 line ($^2S\ 1/2 \rightarrow {}^2P\ 1/2$)

the laser light may induce an optical pumping which changes the relative population of the 2 hfs levels of the atomic ground state. Then the beam enters a strong magnetic sextupole field where the hfs is decoupled in two groups of Zeeman levels with $m_j = + 1/2$ and $- 1/2$. Only the group $m_j = + 1/2$ is focused by the Stern-Gerlach force of the field gradient to impact on an ionizer which converts alkali atoms into ions of 10 kV, which are then mass separated and detected by an electron multiplier. The mass spectrometer assures a selective and efficient detection, eliminating in particular the high background of stable impurity ions coming from the hot ionizer. Pumping via a and b decreases the ionic current and via c and d increases it, giving rise to the pattern sketch on the screen. The transmission of the whole system from the target down to the multiplier is of the order of 10^{-5}, and the experiment ran with a minimum production yield of 10^5 ions of ^{98}Rb. It should be mentioned here that the tunable laser controlled by an interferometric device developed at Laboratoire Aime Cotton was stable for days to the fantastic precision of 2×10^{-9} (MHz). From the position of the observable transitions, nuclear magnetic moments and electric quadrupole moments (with D^2 line) can be deduced, and from the shift of the center of gravity of the D^1 line between two isotopes the change of the nuclear charge distribution between these two isotopes can be deduced. In addition, spins can be measured by magnetic resonance in a weak static magnetic field.

Spins and magnetic moments give useful information in the determination of the single particle properties of nuclei, but of particular interest is the more quantitative information obtained from the quadrupole moments and isotope shift (IS): The electric quadrupole moment is a measure of the extent to which the nuclear charge distribution deviates from spherical symmetry and the IS provides a very sensitive measure of the small changes in the nuclear charge radius that occur when neutrons are added to the nucleus. This is the only method of nuclear radii determination that is applicable to radioactive nuclei (others require weighable amounts of material) and the IS can indicate nuclear deformation even in those cases ($I = 0$ or $I = 1/2$) where there is no spectroscopic quadrupole moment. Figure 14 shows as an example the results of the IS measurements performed on the Rb isotopes. The most striking features of these new data are the decrease of the radius with increasing neutron number for $N < 50$ and the sudden increase at $N = 60$. This last observation checks very nicely with the deformation observed in the mass measurements and γ spectroscopy. It is interesting to note that the

first evidence for the famous deformation in the Sm isotopes was also observed through isotope shifts by Brix and Kopfermann[29] some 30 years ago.

VIII. Quantitative interpretation of anomalous binding energies and radii, a test of the validity of the self-consistent mean field theories

With all these independent and convergent available data, it was tempting to extract more quantitative information, and this has been done through a self-consistent mean field calculation[30] identical to the one performed some years ago on the Na isotopes[31] and which had succeeded in interpreting the anomaly observed in the S_{2n} of the n-rich isotopes. In this Hartree-Fock calculation the intrinsic quadrupole moments and the single-particle energy levels determined show effectively that a deformation starts at N = 58 and is completely developed at N = 60; the experimental observations on both S_{2n} and $\delta\langle r^2\rangle$ are nicely reproduced without introducing any new ad hoc phenomenology. But even more, some new ideas have come out from the comparison between theory and experiment. In Fig. 15, where calculated and measured S_{2n} values are plotted, an unusual good agreement can be observed above the magic shell N = 50, but some disagreement occurs for the n-deficient isotopes. These nuclei are experimentally known to have a pronounced vibrational spectra and the experimental deformation parameter β_2 deduced from B(E2) transition probabilities are in fact much larger than those given by the permanent deformation in the static DDHF density-dependent calculation. This suggests the existence of large zero-point quadrupole vibrations in the ground state of these nuclei. Now going to the comparison of the calculated and measured $\delta\langle r^2\rangle$ values, Fig. 16 shows that the variations of the isotope shift are well reproduced by the DDHF calculation above N = 50 and, in particular, the marked increase for N = 60 is a consequence of the onset of deformation. But for N < 50 the calculated values are far from the experimental ones, and, as in the case of S_{2n}, the same explanation can hold the existence of large zero-point quadrupole vibrations. When taking into account these vibrations, using the β_2 experimental values deduced from the measured B(E2) transition probabilities, the calculated values thus corrected are in better agreement with the experiment. Of course, a more refined treatment is needed to conclude a quantitative interpretation of this anomalous isotope shift for N < 50 (i.e., the decrease of the nuclear charge radius with increasing neutron number).

IX. β-delayed neutron emission, dominant aspect of the β decay of very neutron-rich isotopes

Going on in this short review of some of the latest results obtained in the study of the far unstable isotopes of alkali elements, I come to another on-line mass separation experiment which has studied and is still studying the n-rich Na isotopes. The mass spectrometer, after several movings and improvements, is now back on-line to the 20-GeV proton beam of the Proton Synchrotron at CERN. The first experiments started in 1969 with the measurements of the half-lives of ^{27}Na. (Ref. 32). In 1971 the masses of $^{27-30}$Na (Ref. 33) were measured and two new isotopes identified, ^{32,33}Na (Ref. 34). In 1973, the measurement of their masses showed that contrary to what was expected, N = 20 was no longer a magic number far from stability, and this gave the first evidence of a new region of deformation.[35] In 1977, βγ and βγγ coincidence experiments[11] performed on these isotopes yielded a particularly low energy for a transition very likely $2^+ \rightarrow 0^+$ in the ^{32}Mg decay product of ^{32}Na, an improved precision of the masses of ^{31,32}Na, as well as the new measurement of the mass of ^{33}Na (Ref. 6), and these constituted many corroborations of this deformation. In this 1977 campaign, ^{34}Na was also shown to be bound, and the hfs of these Na isotopes were studied, using the same technique as the one described previously for the heavier alkali elements. Spin and magnetic moments of $^{26-31}$Na were measured.[8] All of these strides in the study of the Na exotic nuclei obtained through the years reflect the increased sensitivity of the experiment. A gain of 500 was realized between 1971 and 1977 owing to the increase of target thickness, mass spectrometer yield, proton intensity, and to important improvements in the shielding. These improvements are particularly beneficial to the study of the decay modes of these isotopes; high quality solid-state detectors can be used now without any damage, and the background is very low. The γ spectra of the last known isotopes have just been measured and are still being processed, but interesting results have yet been obtained on the delayed particle emission of these nuclei and particularly on the multiple n-delayed emission. If a nucleus can β decay to energy levels that are unbound to nucleon emission, its radioactivity will be characterized by the presence of energetic nucleons with the same half-life as the initial β decay. This mode of decay is one feature characteristic of nuclei far from stability and has been reviewed in detail.[36] If delayed proton radioactivity has been much studied experimentally, as well as theoretically in light nuclei, the delayed neutron process has been studied only more recently and has the prospect of being

the dominant aspect of β decay of very neutron-rich isotopes. Figure 17 shows the results obtained for the measurements of the probability of β-delayed neutron emission P_n in the Na isotopes plotted against the energy window of β branches to neutron unstable levels. For the odd A Na isotopes from ^{33}Na up, P_n should tend to 100% (it has just been measured and its value will be known soon). For the even isotopes, the P_n should depend on the possibility of the Gamow-Teller β transitions to the first states (0^+ and 2^+) of the even Mg. For very n-rich Na isotopes, several modes of β-delayed emission can be expected, as can be seen in Fig. 18. The E_n-delayed emission has been observed recently, and, the P_{2n} value measured for ^{30}Na as well as for ^{31}Na and ^{32}Na in two different experiments; one at ISOLDE is based on a n-n time correlation method[37] and the other at the PS detects daughter products following the neutron emission by γ spectroscopy.[38] In the case of the example of Fig. 19, ^{28}Mg was measured through the γ lines in ^{28}Al and ^{28}Si, and it could be measured off-line owing to its exceptionally long half-life of 21h. It is worth mentioning that half of the neutrons observed in the decay of ^{32}Na originate in the 2n process. We also looked for the emission of three delayed neutrons in ^{31}Na (energetically possible), but only a preliminary upper limit of $P_{3n} \sim 10^{-4}$ was obtained.

This multiple neutron emission was in fact first observed at ISOLDE in ^{11}Li (Ref. 37), which is an extreme case due to the low energy thresholds of many particle emission channels (Fig. 19). It is currently being studied by the two groups mentioned above, the 1n, 2n, 3n, and light charged particle channels have been observed. The data are still being processed, but already confirm that the high probability of β-delayed neutron emission is clearly the dominant aspect of β decay of very neutron-rich isotopes. For Na the 1n branch is highly predominant in odd A isotopes, and the 2n branch has a noticeable contribution in the even A isotopes. When fully determined in all the known exotic Na isotopes, i.e., up to ^{34}Na, these n-branching ratios will provide sensitive tests for β strength functions and other nuclear parameters.

X. Concluding remarks.

These are only a few examples taken from among the studies which are presently being carried out on nuclei far from stability. A more complete overview of the field, which has grown very rapidly in the last few years, can be found in recent review papers.[17,19] These examples show how valuable systematic studies

of the principal properties of the nuclear ground states of long series of isotopes can be for the nuclear structure knowledge, with the additional possibility of revealing unexpected features. We feel encouraged to pursue these experiments on other elements - laser spectroscopy and nuclear spectroscopy on the unstable K isotopes have now started at ISOLDE and at the PS - and to search for technical innovations - new optical methods for studies of the atomic hyperfine structure and a new type of mass spectrometer for mapping the nuclear mass surface with high precision.

And finally upstream of these experiments are the mass spectrometer or mass separator and the proton beam. On-line mass separation is not the only technique to study nuclei away from stability, but it has so far been the best, and intermediate- and high-energy protons have produced higher yields of those nuclei over a wide mass range than any other technique. In particular, high intensity proton beams such as those at meson factories have great promise for this kind of research (provided elaborate radiation precautions are taken!). The possibility of moving the ISOLDE facility to SIN is presently being actively studied.

REFERENCES

1. Proceedings International Symposium on Why and How Should We Investigate Nuclides Far Off the Stability Line, Lysekil, Sweden, 1966, eds. W. Forsling, C. J. Herrlander, and H.Ryde, Ark. Fys. 36 (1967).

2. Proceedings International Conference on the Properties of Nuclei Far from the Region of Beta Stability, Leysin, 1970, CERN 70-30 (1970) 2 vols.

   - Proceedings 3rd International Conference on Nuclei Far from Stability, Cargese, 1976, CERN 76-13 (1976).

3. J. Cerny and A. M. Poskanzer, Scientific American, 238, 60 (1978).

4. P. Auger, T. H. Chiang, J. Galin, B. Gatty, D. Guerreau, E. Nolte, J. Pouthas, and X. Tarrago, Z. Physik A289, 255 (1979).

   - D. Guerreau, J. Galin, B. Gatty, X. Tarrago, J. Girard, R. Lucas, and C. NGô, Z. Physik (March 1980).

5. T. J. M. Symons, Y. P. Viyogi, G. D. Westfall, P. Doll, G. E. Greiner, H. Faraggi, P. J. Lindstrom, D. K. Scott, H. J. Crawford, and C. McFarland, Phys. Rev. Letters 62, 60 (1979).

   - G. D. Westfall, T. J. M. Symons, D. E. Greiner, H. H. Heckman, P. J. Lindstrom, J. Mahoney, A. C. Shotter, D. K. Scott, H. J. Crawford, C. McFarland, T. C. Awes, C. K. Gelbke, and J. M. Kidd, Phys. Rev. Letters 43, 1859 (1979).

6. C. Thibault, M. Epherre, G. Audi, R. Klapisch, G. Huber, F. Touchard, D. Guillemaud, and F. Naulin, Atomic Masses and Fundamental Constants 6 (Plenum Press) p. 291, (1980).

7. M. Epherre, G. Audi, C. Thibault, R. Klapisch, G. Huber, F. Touchard, and H. Wollnik, Phys. Rev. C 19, 1506 (1979).

- M. Epherre, G. Audi, C. Thibault, R. Klapisch, G. Huber, F. Touchard, and H. Wollnik, Nucl. Phys. A 340, 1 (1980).

8. G. Huber, F. Touchard, S. Büttgenbach, C. Thibault, R. Klapisch, H. T. Duong, S. Liberman, J. Pinard, J. L. Vialle, P. Juncar, and P. Jacquinot, Phys. Rev. C, 18, 2362 (1978).

9. C. Ekström, L. Robertsson, G. Wannberg, and J. Heinemeier, Phys. Scripta 19, 514 (1979).

10. G. Huber, F. Touchard, S. Büttgenbach, C. Thibault, R. Klapisch, S. Liberman, J. Pinard, H. T. Duong, P. Juncar, J. L. Vialle, and P. Jacquinot, Phys. Rev. Lett. 61, 659 (1979).

11. C. Detraz, D. Guillemaud, G. Huber, R. Klapisch, M. Langevin, F. Naulin, C. Thibault, L. C. Carraz, and F. Touchard, Phys. Rev. C 19, 164 (1979).

12. C. Detraz, M. Epherre, D. Guillemaud, P. G. Hansen, B. Jonson, R. Klapisch, M. Langevin, S. Mattsson, F. Naulin, G. Nyman, H. L. Ravn, A. M. Poskanzer, M. de St. Simon, K. Takahashi, C. Thibault, and F. Touchard, submitted to Phys. Lett. B.

13. A. M. Poskanzer, S. W. Cosper, E. K. Hyde, and J. Cerny, Phys. Rev. Lett. 17, 1271 (1966).

14. J. D. Bowman, A. M. Poskanzer, R. G. Korteling, and G. W. Butler, Phys. Rev. Lett. 31, 614 (1973).

15. ISOLDE internal report, June 1978.

16. J. M. D'Auria, L. C. Carraz, P. G. Hansen, B. Jonson, S. Mattsson, H. L. Ravn M. Skarestad, and L. Westgaard, Phys. Lett. 66B, 233 (1977).

17. H. L. Ravn, Phys. Reports 54, 201 (1979).

18. Y. Lebeyec, Colloque Franco Japonais Gif 1979, Report IPNO, R.C. 79-10.

19. P. G. Hansen, Ann. Rev. Nucl. Part. Sci. 29, 69 (1979).

20. F. Touchard, J. Biderman, M. de Saint Simon, G. Huber, C. Thibault, M. Epherre, R. Klapisch, Proceedings of the 10th International Conference EMIS to be published in Nucl. Instr. Methods.

21. C. Thibault, et al. To be published in Phys. Rev. C.

22. F. Touchard, G. Huber, R. Fergeau, C. Thibault, and R. Klapisch, Nucl. Instr. Methods 155, 669 (1978).

23. 1975 Mass Predictions, Ed S. Maripuu, At. Dat. and Nucl. Dat. Tables 17 (1976).

24. P. Möller and J. R. Nix, Preprint LA-UR-80-813, Los Alamos (1980).

25. D. A. Arseniev, A. Sobiczewski, and V. G. Soloviev, Nucl. Phys. A 139, 269 (1969).

- J. Ragnarsson, A. Sobiczewski, R. K. Sheline, S. E. Larsson, and B. Nerlo-Pomorska, Nucl. Phys. A 233, 329 (1976).

26. E. Cheifetz, R. C. Jared, S. G. Thompson, J. B. Wilhelmy, Phys. Rev. Lett. 25, 38 (1970).

27. H. Wollnik, F. K. Wohn, K. D. Wünsch, and G. Jung, Nucl Phys. A 291, 355 (1977).

28. R. E. Azuma, G. L. Borchert, L. C. Carraz, P. G. Hansen, B. Jonson, S. Mattsson, O. B. Nielsen, G. Nyman, I. Ragnarsson, and H. L. Ravn, Phys. Lett. 86, 5 (1979).

29. P. Brix and H. Kopfermann, Festschrift Göttinger Akad, p. 17(1951) Springer Verlag and Phys. Rev. 85, 1050 (1952).

30. X. Campi and M. Epherre, submitted for publication in Phys. Rev. C.

31. X. Campi, H. Flocard, A. K. Kerman, and S.Koonin, Nucl. Phys. A251, 193 (1975).

32. R. Klapisch, C. Thibault. C. Detraz, J. Chaumont, R. Bernas, and E. Beck, Phys. Rev. Lett. 23, 652 (1969).

33. R. Klapisch, R. Prieels, C. Thibault, A. M. Poskanzer, C. Rigaud, and E. Roeckl, Phys. Rev. Lett. 31, 118 (1973).

34. R. Klapisch, C. Thibault, A. M. Poskanzer, R. Prieels, C. Rigaud, and E. Roeckl, Phys. Rev. Lett. 29, 1256 (1972).

35. C. Thibault, R. Klapisch, C. Rigaud, A. M. Poskanzer, R. Prieels, L. Lessard, and W. Reisdorf, Phys. Rev. C 12, 697 (1975).

36. J. Hardy in Nuclear Spectroscopy and Reactions, Part C, Ed. J. Cerny, (Academic Press) p. 617 (1976).

- J. Cerny and J. Hardy, Ann. Rev. Nucl. Sci. 27, 333 (1977).

37. R. E. Azuma, L. C. Carraz, P. G. Hansen, B. Jonson, K. L. Kratz, S. Mattsson, G. Nyman, H. Ohm, H. L. Ravn, A. Schröder, and W. Ziegert, Phys. Rev. Lett. 63, 1652 (1979).

38. C. Detraz et al., to be published.

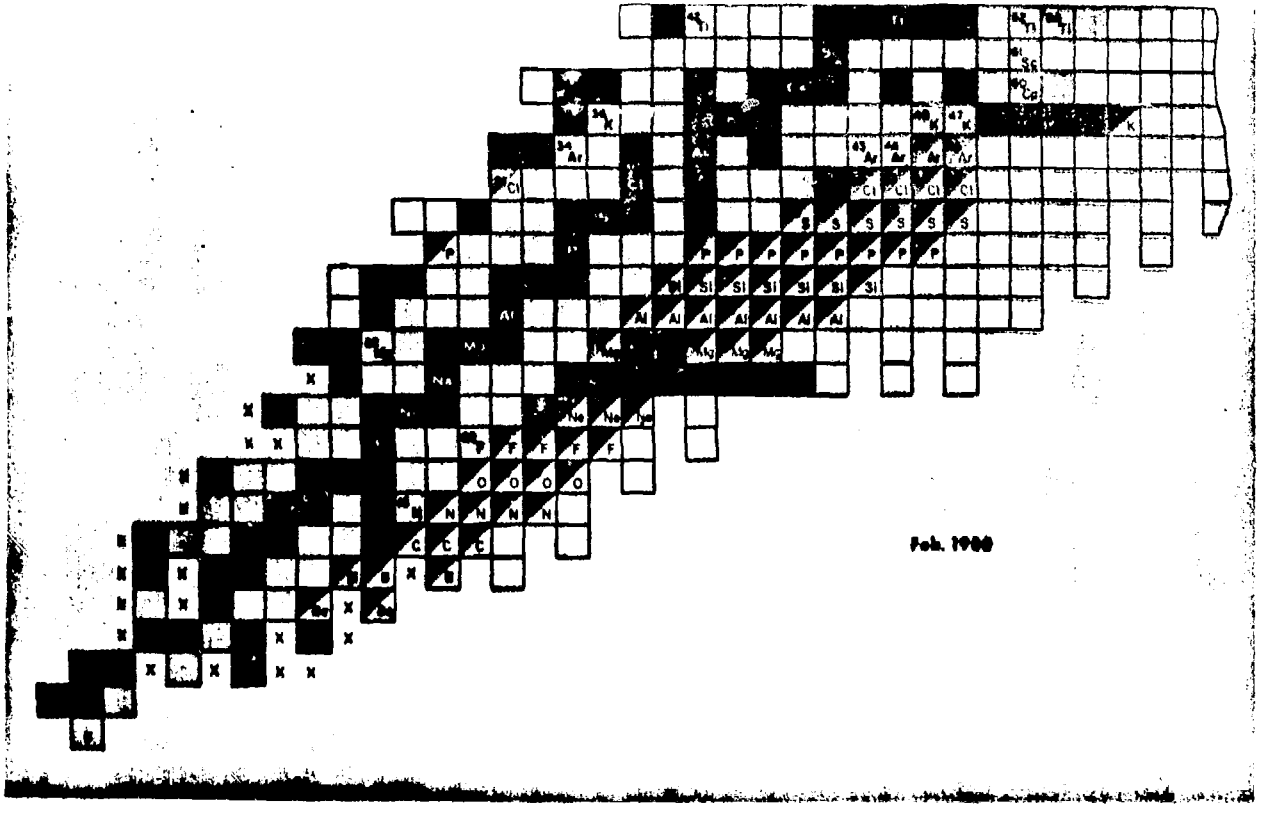

Fig. 1.

Chart of the nuclides. the light elements taken from Ref. 3 (A. M. Poskanzer courtesy).

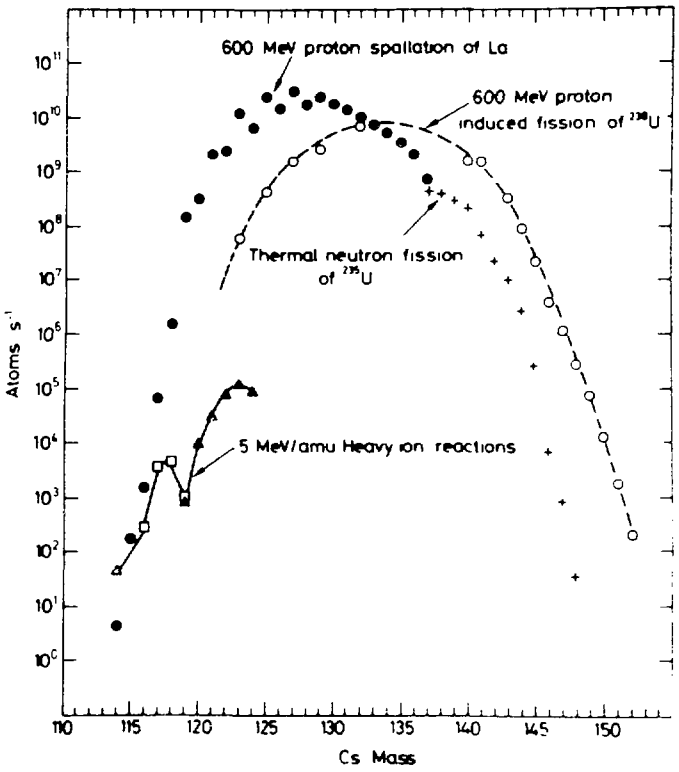

Fig. 2.

1979 Status of the Cs isotopic yields as obtained with different bombarding particles and targets and measured at the On-Line Isotope Separators (from Ref. 7).

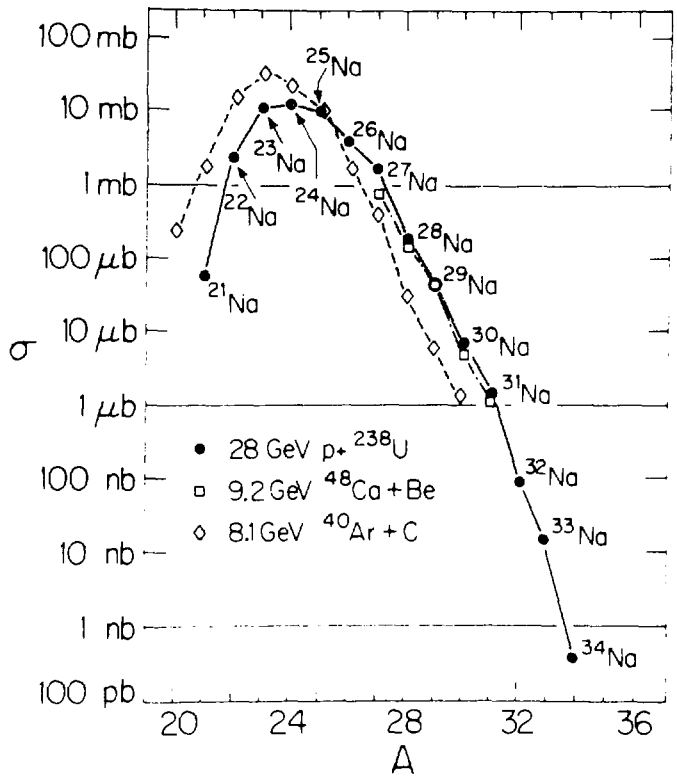

Fig. 3.

Comparison of sodium production cross sections (from Ref. 5b).

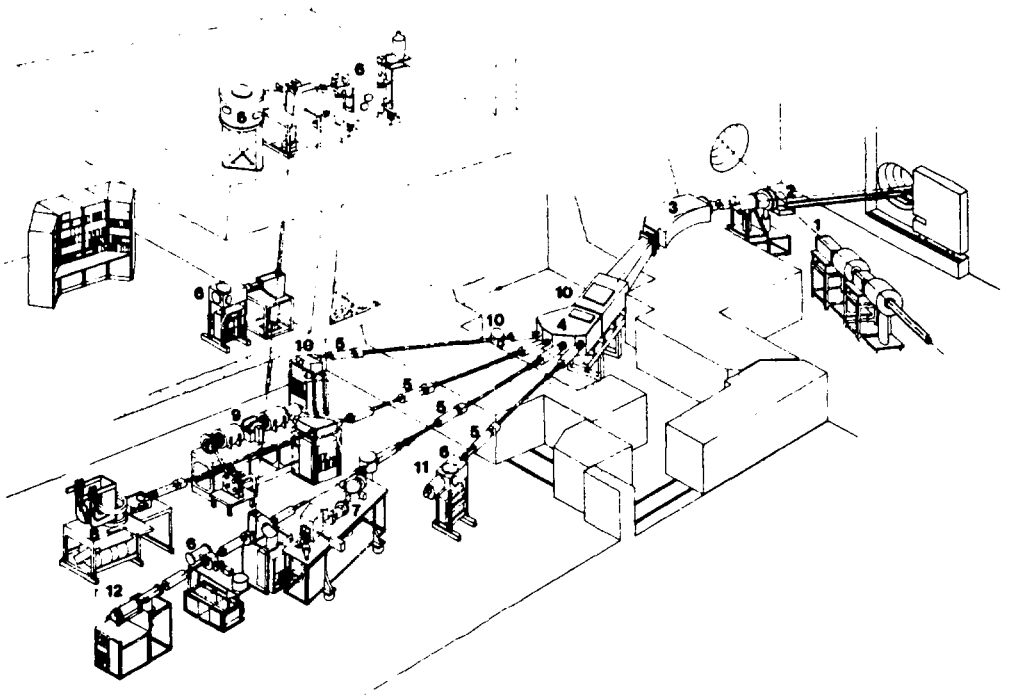

Fig. 4.

The On-Line Isotope Separator ISOLDE II: The 600-MeV proton beam (1) is focused on the target-ion source (2). The 60-kV ions produced are mass analyzed in the magnet (3) and the individual masses selected in the electrostatic switchyard (4) are distributed through the external beam lines (5) to the experiment (from Ref. 19).

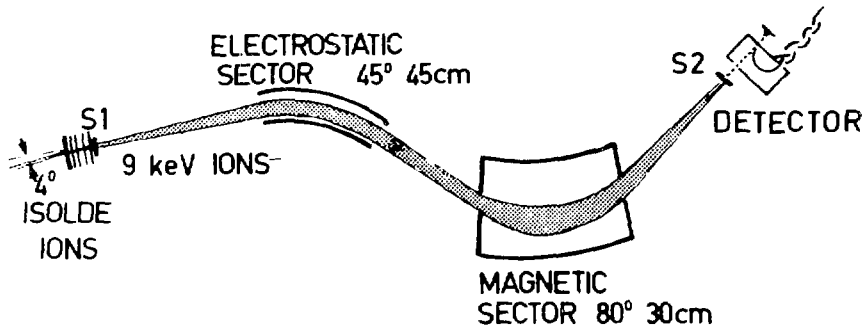

H cst V deflecting potential
U accelerating potential

$$U = kV$$

$$M \times V = \text{cst}$$

Fig. 5.

Schematic view of the mass spectrometer - on-line with ISOLDE - Used for the mass measurements of unstable isotopes.

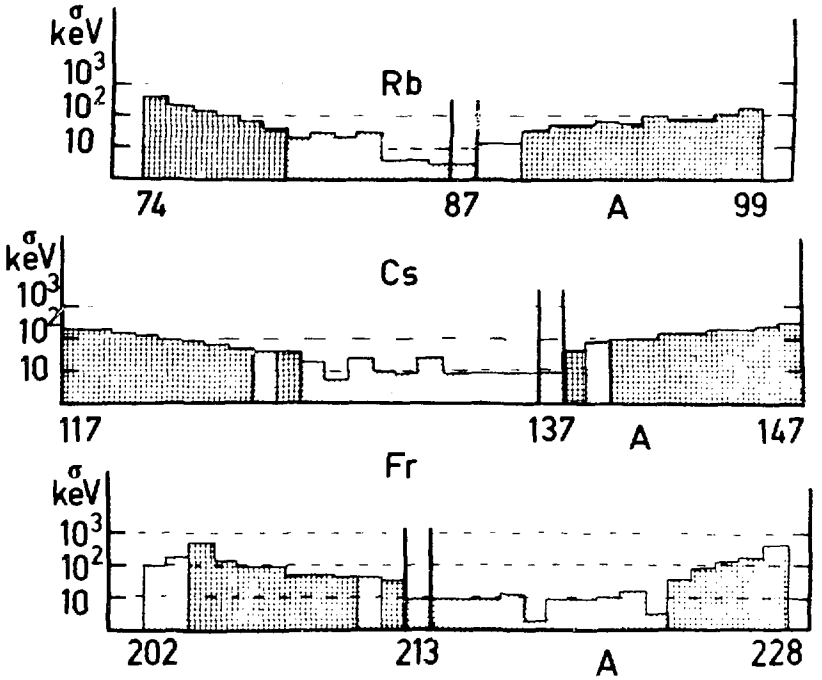

Fig. 6.

Precision of the mass measurements. Dotted: previously known masses used as primary references, doubly hatched: measured masses at ISOLDE with the on-line mass spectrometer.

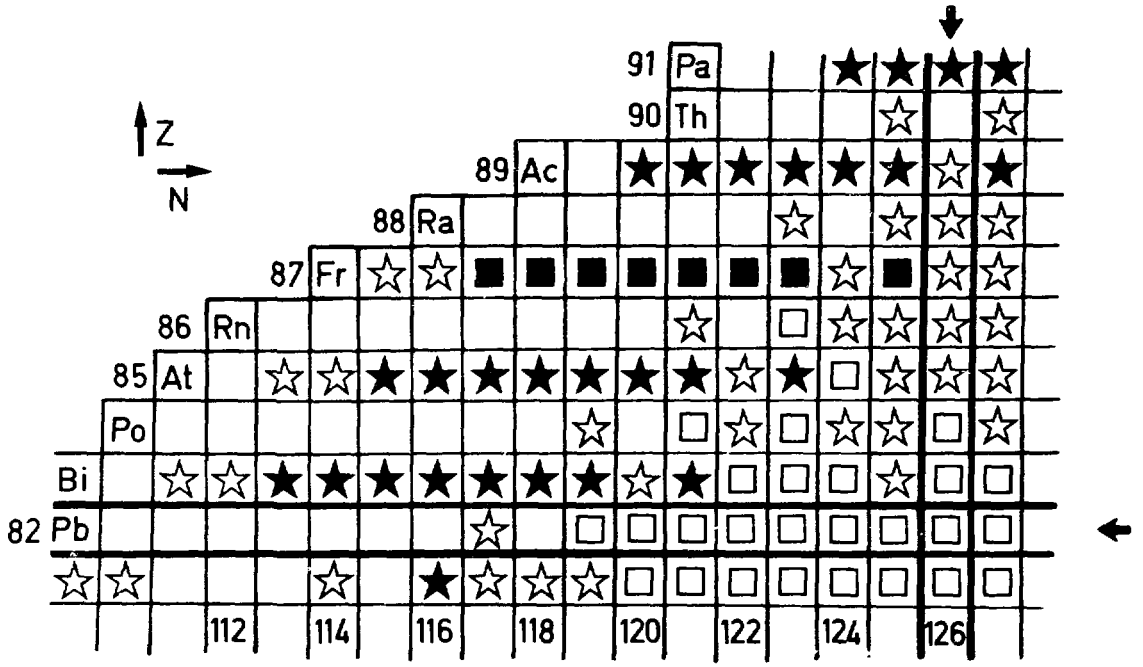

Fig. 7.

Isotopes in the region (Z>82, N<126) which masses have been determined (solid stars) from the masses directly measured (solid squares) and from previous measured E_α values. The open symbols represent the isotopes which masses were known prior to our experiments (from Ref. 7b).

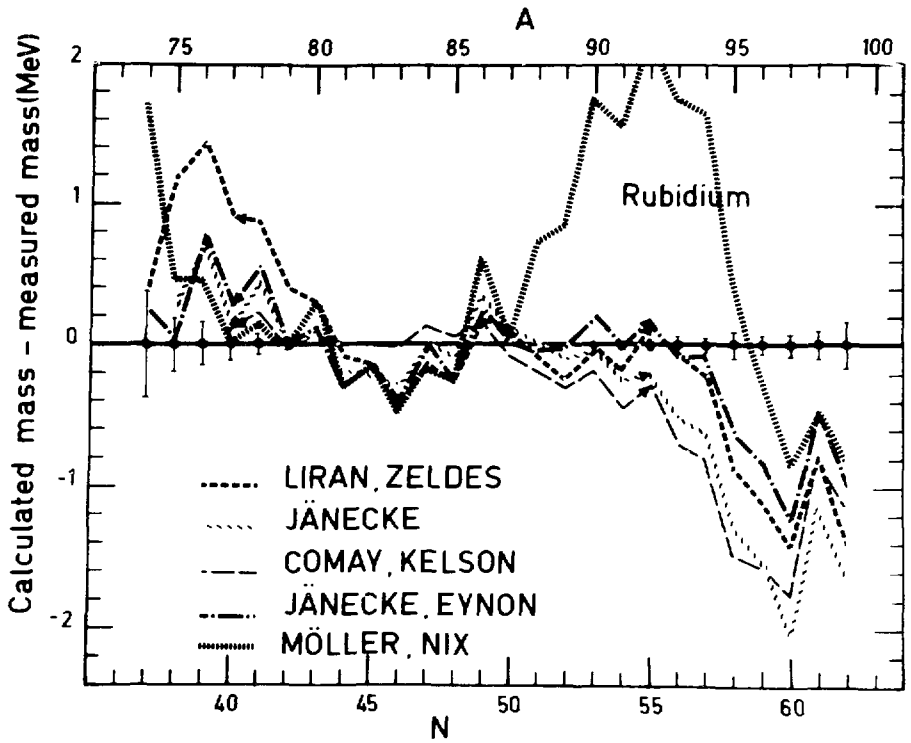

Fig. 8.

Comparison between calculated masses and measured masses of Rb isotope. The recent calculations of Möller and Nix (Ref. 24) have been added.

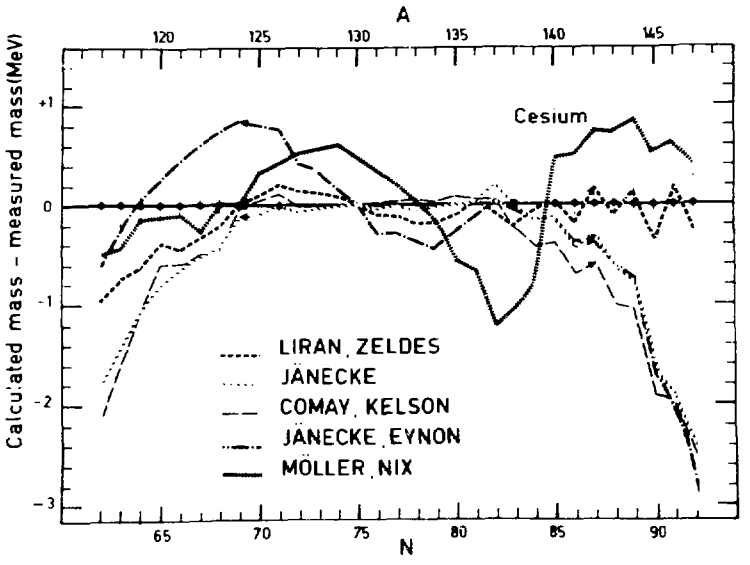

Fig. 9.

Comparison between calculated masses and measured masses of Cs isotopes. The recent calculations of Möller and Nix (Ref. 24) have been added.

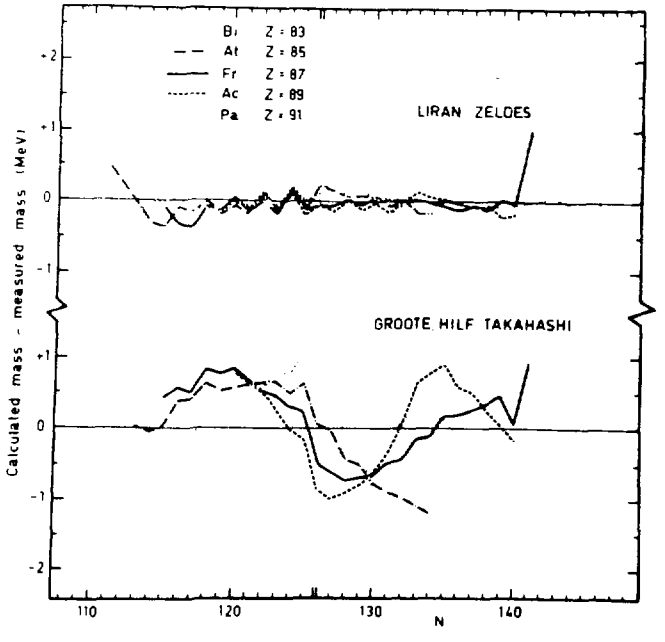

Fig. 10.

Comparison between calculated masses and measured masses of isotopes with $83 \leq Z \leq 91$ (from Ref. 7b).

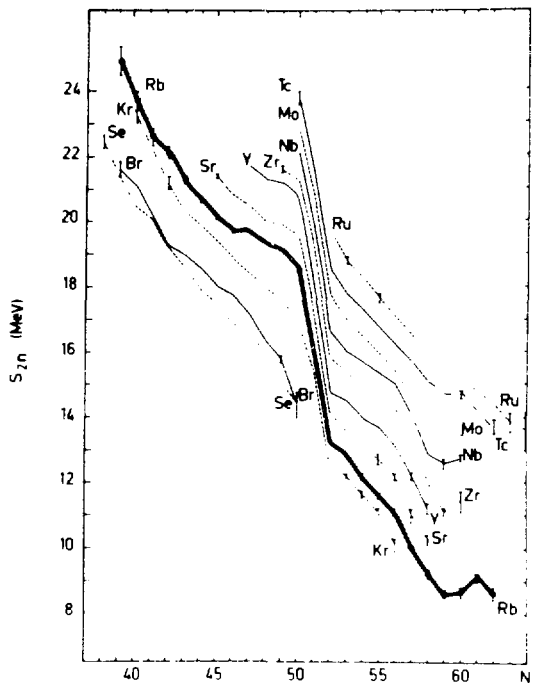

Fig. 11.

Experimental two-neutron separation energies, S_{2n} (from Ref. 7a).

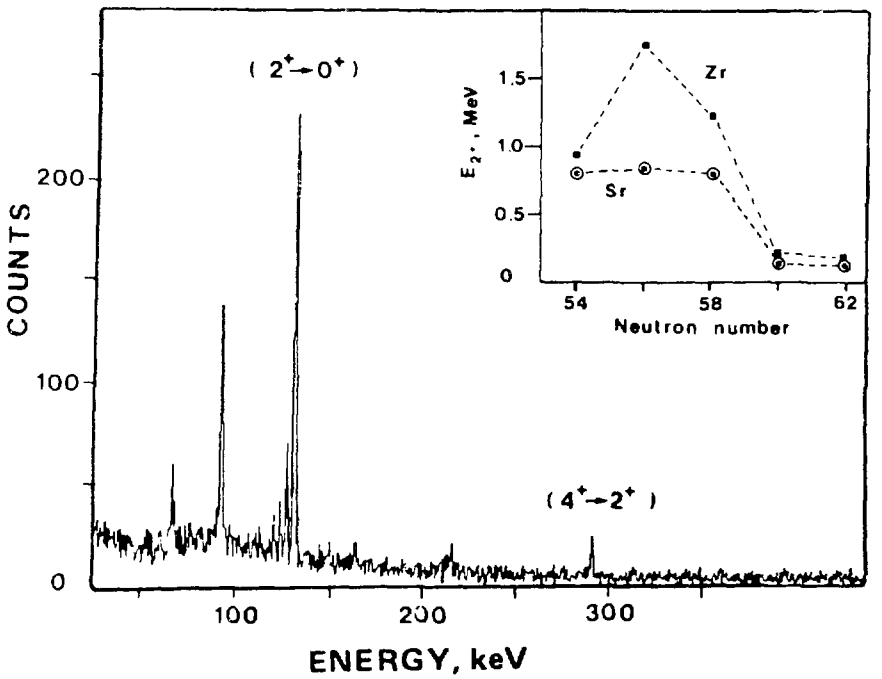

Fig. 12.

E-coincident γ spectrum of ^{100}Rb. The inset shows the systematics of 2^+ energies for heavy Sr and Zr isotopes (from Ref. 28).

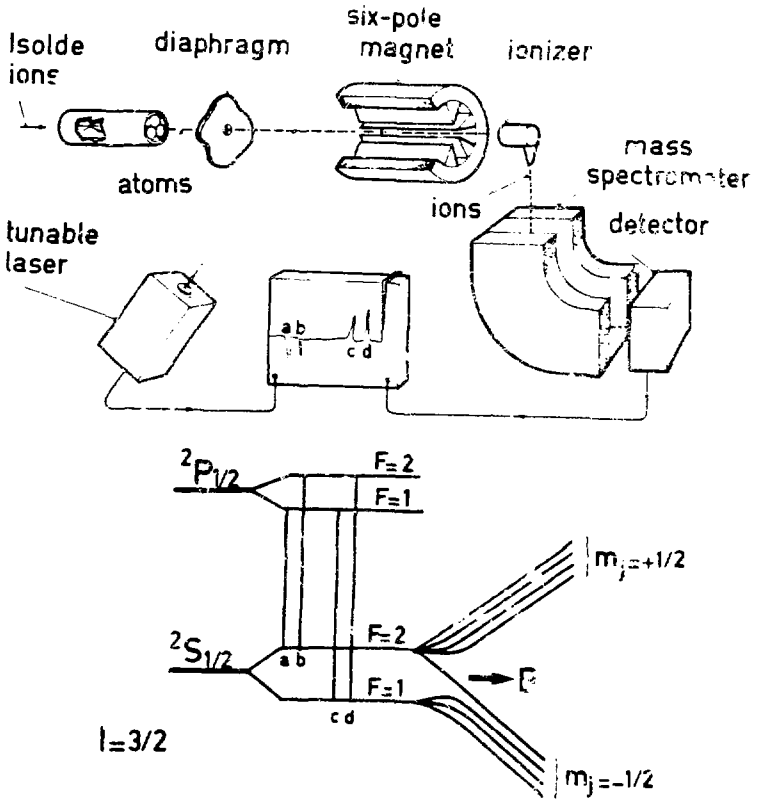

Fig. 13.

Schematic view of the laser optical spectroscopy experiment performed by the Orsay Group (Refs. 10, 21). The lower part shows the hfs level diagram of the D1 resonance line of an alkaline isotope with I = 3/2.

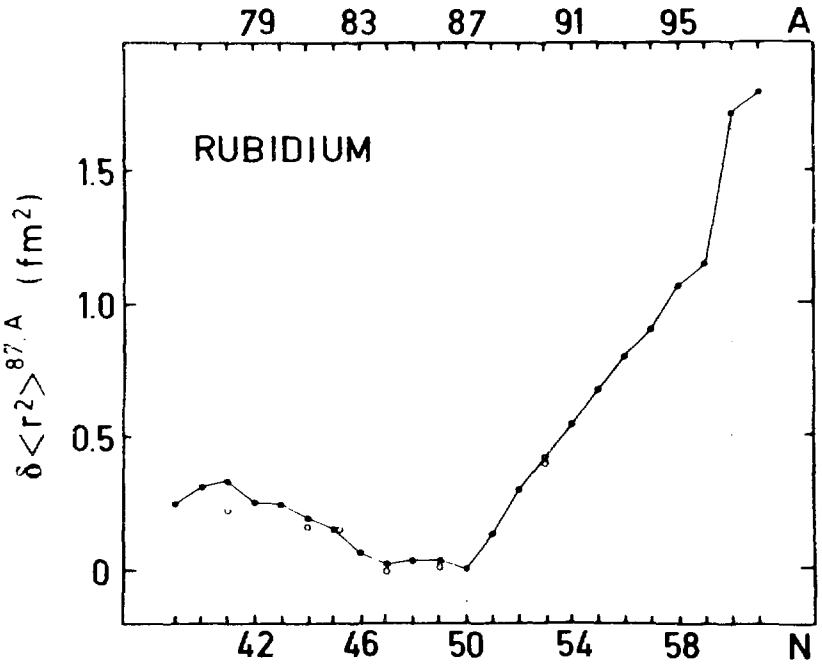

Fig. 14.

Experimental runs charge radii difference $\delta\langle r^2\rangle_{N,50} = \langle r^2\rangle_N - \langle r^2\rangle_{50}$ of the Rb Isotopes (from Ref. 21).

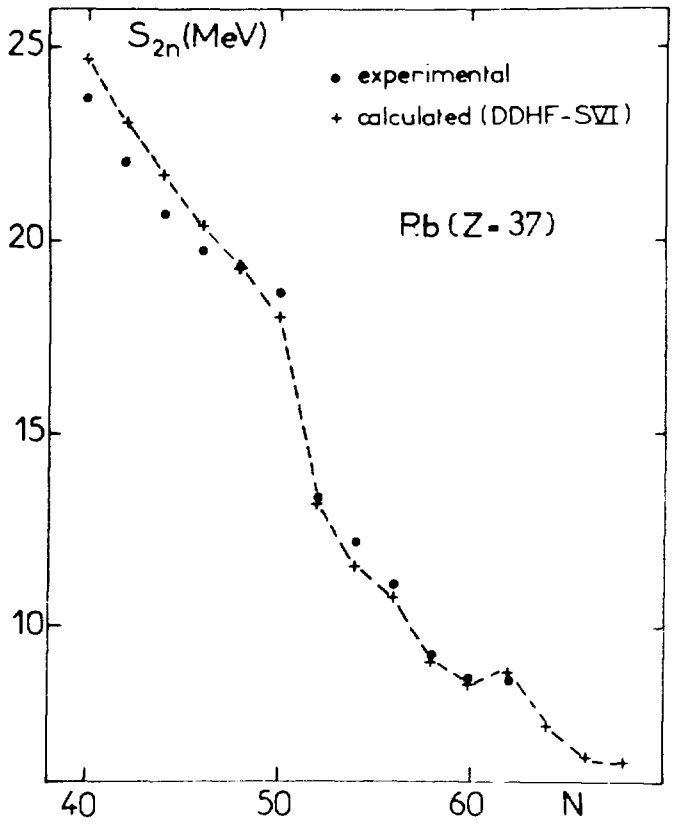

Fig. 15.

Comparison between measured and calculated (DDHF) values for S_{2n} separation energies in Rb isotopes.

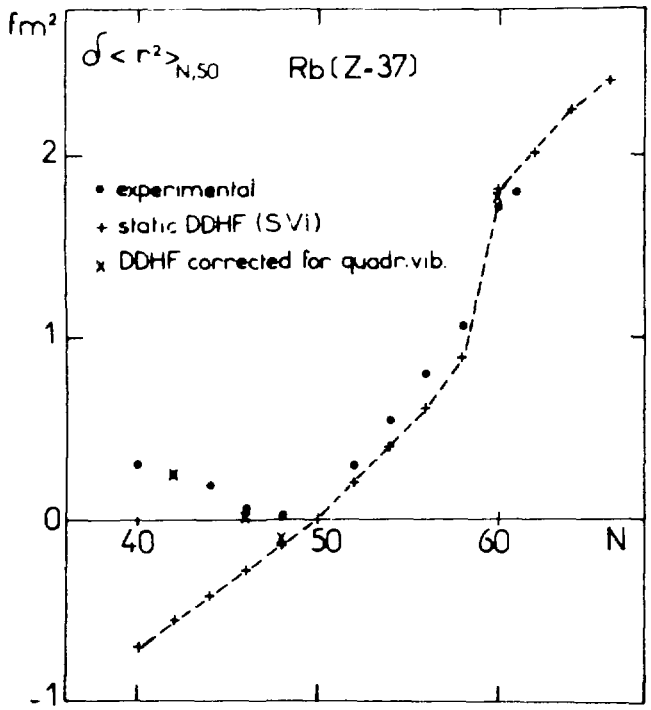

Fig. 16.

Comparison between measured and calculated (DDHF) values for $\left(\delta \langle r^2 \rangle_{N,50} = \langle r^2 \rangle_{Z,N} - \langle r^2 \rangle_{2,50}\right)$.

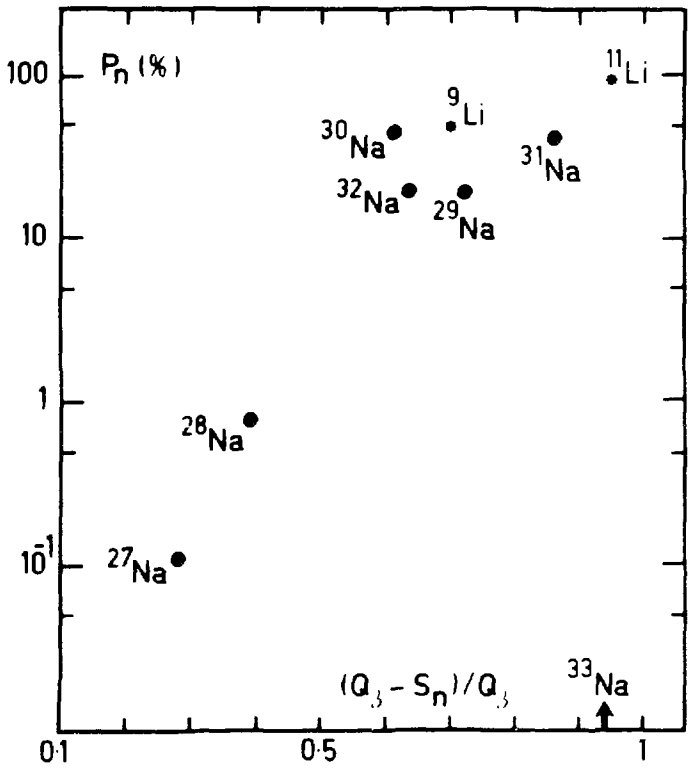

Fig. 17.

P_n values of the Na isotopes plotted as a function of the energy window $(Q_\beta - S_n)/Q_\beta$.

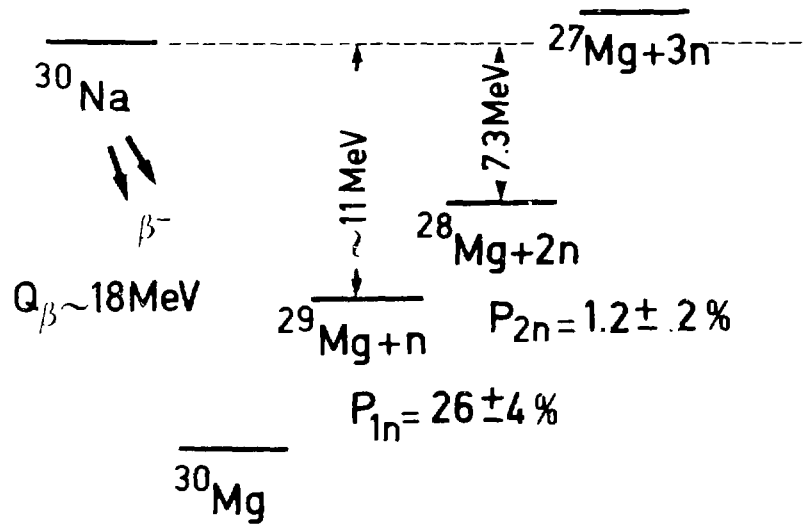

Fig. 18.

Open channels for n-delayed emission in ^{30}Na.

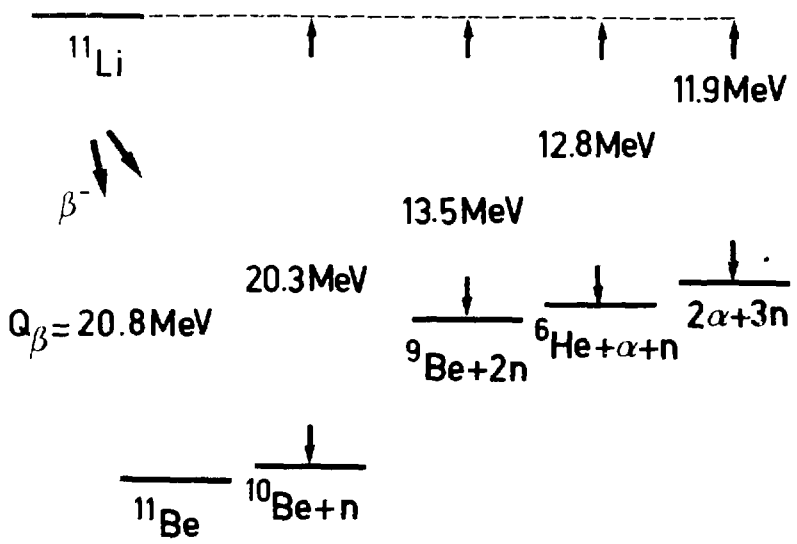

Fig. 19.

Open channels for n-delayed emission in ^{11}Li.

INTRANUCLEAR CASCADE THEORY AS A QUANTUM MECHANICAL APPROXIMATION

by

E. A. Remler

College of William & Mary, Virginia

I. INTRODUCTION

Nuclear theorists have usually maintained an indifferent attitude towards intranuclear cascade theory (INC). Since it was 'classical' it was said to be of no interest to a quantum mechanician. As a result it has had virtually no theoretical development since its inception.

But INC as well as other closely related 'quasi-classical' theories do give a reasonable account of the gross features of a large variety of complex nuclear reactions. Therefore there must be a series of approximations leading from the full QM theory to INC. By retracing these, one should be able to develop INC (much the same as WKB) into a systematic QM approximation procedure.

In this talk, I wish to sketch some progress which has been made towards this end. In particular, the following questions will be discussed:

1) What QM object does INC provide an approximation of?
2) What is the relation between INC and other quasi-classical theories?
3) How can its accuracy be increased?
4) What is its scope and how can that be increased?

II. A CLASSIFICATION OF THEORIES

The task of linking QM to quasi-cassical theories is part of the domain of nonequilibrium statistical mechanics. Entering this field, one is struck by the overabundance of different approaches being used (Pauli Master, Generalized Master, Langevin, Fokker-Planck, Landau, Boltzmann, TDHF, Fluid Dynamic, ... etc. equations). There is a need to establish one's bearings by relating these to each other and to QM. Hence one finds in this literature many charts and tables proposing to do this. Table I is my own contribution.

CLASSIFICATION OF STATISTICAL MECHANICAL THEORIES USED FOR NUCLEAR REACTIONS

Relevant Statistical Variables	Name of Class of Equations	Members of this class	References to Derivations (Nuclear Theory)
$Tr(\|a'\rangle\langle a\|\rho)$	Transport	Boltzmann Fokker-Planck	1,2,3
$Tr(\psi^{\dagger}_{a'}\psi_a\rho)$	Kinetic	Landau, Vlasov, Boltzmann, TDHF	4,5,6,7
$\sum_{a'a} M_{a'a}\, Tr(\psi^{\dagger}_{a'}\psi_a \times \rho)$	Moment	Hydrodynamic	8
$Tr(E_{\Delta}\rho)$	Master	Pauli, Generalized, Pre-equilibrium	9,10,13
$Tr(\|a'\rangle\langle a\| \otimes E_{\Delta}\rho)$	Transport ⊗ Master	Generalized Excitation	11,
$Tr(\|a'b'\rangle\langle ba\| \otimes E_{\Delta}\rho)$	Transport ⊗ Master	Generalized Master	12
$Tr(\|1'..A'\rangle \times \langle A..1\|\rho)$	INC	Monte-Carlo	13,14,15,16

Table I

It organizes some of the approaches used in Nuclear theory on the basis of their choice of dynamical variables. Such a choice is a first step of a statistical theory. It selects from the large number of degrees of freedom of a few- or many-body system, a smaller 'relevant' set. These are supposed to carry the information relevant to the measurements of interest and to satisfy closed dynamical equations. In the second column a name has been assigned to all equations having the same relevant variables. Usage is not uniform in the literature, so I have merely picked one typical name. Different subsequent approximations lead to different equations for the same variables. Some of these are given in column three. In the last column are references to some derivations, neglecting the many papers devoted primarily to applications.

A brief outline of the notation and contents of Table I goes as follows. The entire system's density operator is ρ. Complete sets of single particle quantum numbers are abbreviated by integers, e.g.

$$1 = \{ \underset{\sim}{p}_1, \tau_1, \ldots \} \qquad (1)$$

or by letters a, a', b, b', etc., which range over the integers.

A transport theory (as the word is used here) describes the evolution of the reduced density $T_r(|a'\rangle\langle a|\rho)$ of a selected particle traveling through a nuclear medium. It is useful when the dynamical evolution of the medium is irrelevant. For example, to predict an inclusive cross section for pions which can be assumed to be moving fast enough to escape the effect of their disturbance of the nuclear ground state, the pion's reduced density in a transport theory could serve as a relevant variable.

A kinetic theory on the other hand treats all particles equally. Their single particle distribution function (singlet) is a relevant variable. ψ_a is the annihilation operator for the nucleon field.

A kinetic theory leads to an equation for a function of six variables plus time. To reduce this number, a moment expansion of the singlet can be made. This leads to a linked series of equations which can be truncated by some further assumption. Most commonly, moments of momentum are taken, e.g.

$$M_{a'a} = \{ \delta_{a'a}, \underset{\sim}{p}_a \delta_{a'a}, \underset{\sim}{p}_{a'} \underset{\sim}{p}_a \delta_{\tau_{a'}\tau_a}, \ldots \} \quad (\tau \sim \text{isospin}) \qquad (2)$$

This leads to equations of Hydrodynamic form.

Master equations (Refs. 17-19) use variables very different from any of the preceding. These are expectation values of projections E_Δ onto subspace spanned by eigenstates of some mutually commuting set of operators $\mathcal{O}$. The subset of eigenvalues $\mathcal{O}'$ defining these subspaces is Δ. Therefore

$$E_\Delta = \sum_{\mathcal{O}' \in \Delta} |\mathcal{O}'\rangle\langle\mathcal{O}'| \quad . \tag{3}$$

The relevant dynamical variables in this case are also the probabilities for finding the system in Δ. As an example, in the simple exciton model,

$$\mathcal{O} = \{ \#\ \text{particles}, \#\ \text{holes} \} \quad , \tag{4}$$

and each Δ is the set of particle and hole numbers which add up to the same exciton number.

The next two entries are examples of mixtures of the preceding two types of variables. The first has been introduced for pre-equilibrium decay in particle nucleus collisions. $|a'\rangle\langle a|$ operates on the bombarding particle's coordinates while E_Δ operates on those of the nucleus. Thus correlations between them are included in the set of relevant dynamical variables. The second entry is essentially the same concept applied to heavy ion collisions. $|a'b'\rangle\langle b\,a|$ operates on the ions centers of mass while E_Δ operates on their internal degrees of freedom.

The last entry in Table I is that of INC. The simultaneous eigenket for all A single-particle operators in the system is $|1 \cdots A\rangle$. This means that INC attempts to provide nothing less than an approximation to the complete density of the system. It is not, as is often erroneously stated, merely an approximation to the Boltzmann equation since that is an equation for only the singlet component of the full density. An INC solution provides information about all correlations among participating particles and therefore about multi-particle and bound state production cross sections. In contrast a Boltzmann equation's solution by itself without further hypotheses, can predict only single particle inclusive cross sections.

A Monte Carlo (MC) INC program is a computer simulation of the INC approximation of nuclear reactions. This is the original and still primary way to calculate this approximation. The results to be discussed in this talk will therefore be phrased in this context. However, one should bear in mind that analytic treatments of INC are possible for which these results should also apply.

III. RECONSTRUCTION OF THE DENSITY

What exactly is the approximation to the density provided by an MC-INC program? The answer is the minimum information needed to link it up with QM. It (as well as further results) will be given neglecting spin and isospin. These require simply an elaboration of notation to be included. Thus, in Table I, we replace

$$Tr\left(|1\cdots A\rangle\langle A'\cdots 1'|\rho\right) \rightarrow$$

$$Tr\left(|\underset{\sim}{k}_1\cdots\underset{\sim}{k}_A\rangle\langle\underset{\sim}{k}'_A\cdots\underset{\sim}{k}'_1|\rho\right) = \langle\underset{\sim}{k}'_A\cdots\underset{\sim}{k}'_1|\rho|\underset{\sim}{k}_1\cdots\underset{\sim}{k}_A\rangle . \quad (5)$$

Now MC-INC does not provide an approximation to these momentum components of the density directly. Rather one obtains an approximation to the unitarily equivalent Wigner representation[15] of ρ which can be written as

$$\langle\langle\varphi_A\cdots\varphi_1|\rho\rangle\rangle = \int d\underset{\sim}{q}_1\, e^{i\underset{\sim}{q}_1\cdot\underset{\sim}{x}_1}\cdots d\underset{\sim}{q}_A\, e^{i\underset{\sim}{q}_A\cdot\underset{\sim}{x}_A}$$

$$\times\langle\underset{\sim}{p}_A+\tfrac{1}{2}\underset{\sim}{q}_A,\cdots\underset{\sim}{p}_1+\tfrac{1}{2}\underset{\sim}{q}_1|\rho|\underset{\sim}{p}_1-\tfrac{1}{2}\underset{\sim}{q}_1,\cdots,\underset{\sim}{p}_A-\tfrac{1}{2}\underset{\sim}{q}_A\rangle , \quad (6)$$

where $\hbar = 1$, and

$$\varphi_a = \underset{\sim}{x}_a, \underset{\sim}{p}_a \; ; \; a = 1\cdots A \quad (7)$$

denotes a point in the six-dimensional classical phase space of the a^{th} particle. Knowing ρ in the Wigner representation one can by suitable Fourier transformation find it in any other representation.

Let the MC-INC estimate of ρ be called ρ_{MC},

$$\langle\langle\varphi_A\cdots\varphi_1|\rho\rangle\rangle \approx \langle\langle\varphi_A\cdots\varphi_1|\rho_{MC}\rangle\rangle . \quad (8)$$

This is given by a sum of products of δ-functions constructed by the following algorithm[14]:

i) Let γ, I index respectively cascades and interactions during cascade γ. At each interaction (not Pauli suppressed) a new particle is 'created' out of the medium. At I = 1 the bombarding particle is created at the accelerator exit port. The number of cascading particles after interaction I at $t_{\gamma,I}$, and before interaction I + 1 at $t_{\gamma,I+1}$ is I. Particles are labelled according to their order of creation; the bombarding particle is particle #1; at interaction 2 (the first occurring in the nuclear medium) label the two emerging particles 1 and 2. The label assignment is arbitrary in the case of identical particles. The trajectory of particle i≤I during interval $t_{\gamma,I} < t \leq t_{\gamma,I+1}$ is

$$\varphi^{(i)}_{\gamma,I}(t) = \underset{\sim}{x}^{(i)}_{\gamma,I} + (\underset{\sim}{p}^{(i)}_{\gamma,I}/m)(t - t_{\gamma,I}) \,,\; \underset{\sim}{p}^{(i)}_{\gamma,I} \,. \qquad (9)$$

These indexing rules are illustrated in Fig. 1.

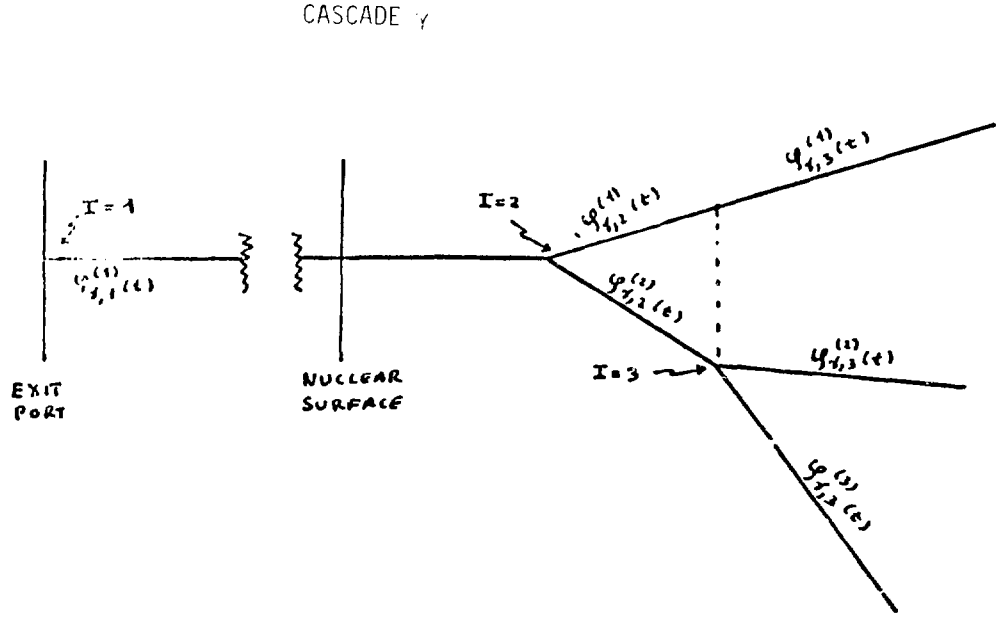

Fig. 1.

ii) Each interval I of γ contributes $|\rho_{\gamma,I}\rangle\rangle$ to $|\rho_{MC}\rangle\rangle$:

$$|\rho_{MC}\rangle\rangle = \sum_{\gamma} \sum_{I} |\rho_{\gamma,I}\rangle\rangle \tag{10}$$

where

$$\langle\langle \varphi_A \cdots \varphi_1 | \rho_{\gamma,I}\rangle\rangle = \sigma_0 \int_{t_{\gamma,I}}^{t_{\gamma,I+1}} dt\, v \times \prod_{i=1}^{I} \langle\langle \varphi_i | \varphi_{\gamma,I}^{(i)}(t)\rangle\rangle \langle\langle \varphi_{I+1} \cdots \varphi_A | \rho\rangle\rangle , \tag{11}$$

$$\langle\langle \varphi' | \varphi\rangle\rangle = h^3 \delta(\underset{\sim}{p}' - \underset{\sim}{p}) \delta(\underset{\sim}{x}' - \underset{\sim}{x}) , \tag{12}$$

$$\langle\langle \varphi_{I+1} \cdots \varphi_A | \rho\rangle\rangle = \int d\varphi_1 \cdots d\varphi_I \langle\langle \varphi_1 \cdots \varphi_A | \rho\rangle\rangle , \tag{13}$$

$$d\varphi = d\underset{\sim}{x}\, d\underset{\sim}{p} / h^3 , \tag{14}$$

σ_0 = unit area/number of cascades, (15)

v = beam particle velocity, (16)

and $\langle\langle \varphi_2 \cdots \varphi_A | \rho\rangle\rangle$ is the Wigner distribution of the nucleus localized at the origin.

The remainder of this talk illustrates the advantages of having this information.

IV. IMPROVING THE ACCURACY OF INC

Let $|i^{(+)}\rangle$ denote the outgoing wave solution corresponding to an initial state $|i\rangle$ in ordinary time independent scattering theory. Assume one has an approximation to it, $|\tilde{i}^{(+)}\rangle$, it can be used to calculate the transition matrix to a final state $|f\rangle$ in either of two ways. Its asymptotic outgoing waves give directly a formula equivalent to

$$\langle f | T | i \rangle \cong \langle f | E_i - H_0 | \tilde{\psi}^{(+)} \rangle \quad (17)$$

Alternatively, it may be cast in a perturbation formula,

$$\langle f | T | i \rangle \cong \langle f | H - H_0 | \tilde{\psi}^{(+)} \rangle \quad (18)$$

The latter will generally be more accurate for a variety of reasons. For example, the potential may neglect parts which may have been neglected in the approximations leading to $|\tilde{\psi}^{(+)}\rangle$ and these may have large matrix elements leading to the particular final state of interest. Also, the latter formula uses possibly important off-shell or near wave zone information contained in $|\tilde{\psi}^{(+)}\rangle$ whereas the former does not.

Now scattering theory can be rewritten equivalently in terms of densities[15] instead of waves. The density describing the outgoing wave solutions is

$$\rho = |\psi^{(+)}\rangle\langle\psi^{(+)}| \quad (19)$$

Equations equivalent to Eqs. (17) and (18) may be written down. If ρ_{MC} is used in place of ρ in the equation equivalent to Eq. (17), the usual expression for the cross section from a MC-INC calculation is obtained. If, however, it is used in the equivalent to Eq. (18) a more accurate expression is obtained.[16]

A simplified version of this for the single particle inclusive cross section is

$$\sigma(\underset{\sim}{p}'; \underset{\sim}{p}; A) = \sigma_0 \sum_{\gamma,i} \int_0^\infty dt\, \mathcal{P}_\gamma^{(i)}(t)\, \mathcal{L}(\underset{\sim}{x}_\gamma^{(i)}(t), \underset{\sim}{p}') \times \sigma(\underset{\sim}{p}'; \underset{\sim}{p}_\gamma^{(i)}(t), \underset{\sim}{x}_\gamma^{(i)}(t)) \quad (20)$$

where σ_0, γ, i are as before while $\varphi_\gamma^{(i)}(t)$ is the complete phase space trajectory of particle i during cascade γ and, $\mathcal{L}(\varphi)$ is the probability that a particle can escape from the nucleus starting at $\underset{\sim}{x}$ with momentum $\underset{\sim}{p}$ having no further collisions and, $\sigma(\underset{\sim}{p}'; \varphi)$ is the scattering cross section into $d\underset{\sim}{p}'$ by the medium, of a particle at $\underset{\sim}{x}$ with initial momentum $\underset{\sim}{p}$.

Thus the cross section for any p' can be calculated by a line integral over all the M-IN generated trajectories which now serve as an integration grid. The formula [illegible] all the information obtained by the cascade calculation - the trajectories of the nucleons, positions and correlated momenta - rather than just the final values of momenta. This is near wave zone and off-shell information. The fact that it uses more pieces of information can be shown to imply that its statistical accuracy is better.

There are a number of ways in which this formula can be used to significant advantage. For example, although in a standard MC-INC calculation low probability events are determined with low statistical accuracy, here all events are determined with basically the same accuracy. Thus one needs only a moderate number of MC-INC computations to achieve good uniform accuracy. The formula also provides a self consistency check in the program since the two ways of calculating cross sections must agree. Other examples are given in Ref. 16.

V. COMPOSITE PARTICLE PRODUCTION

The QM scattering theory cross section for reactions leading to composite particle productions can also be rewritten in terms of densities. Again, if ρ_{MC} is substituted for ρ of Eq. 19, one discovers a way to increase the scope of MC-INC by using it to calculate composite particle production cross sections.[14,15]

The result will be illustrated using a simplified model of inclusive Deuteron production neglecting again spin and isospin. The algorithm goes as follows.
1) Pick a pair of nucleons produced in the same cascade. Think of this pair as a single entity moving in 12-dimensional phase space. The pair is considered first created when the final member joins the cascade. The pair is considered to interact with the nuclear medium whenever either member interacts. Label each interaction of a pair by the index K. Thus, referring to Fig. 1, in cascade γ, the pair 1-2 is created at I = 2 and has a subsequent interaction at I = 3. These are labeled K = 1 and K = 2, respectively, when considering this pair. The 1 - 3 pair on the other hand is created at I = 3 so that its interaction is labeled K = 1 for this pair. The phase space coordinates of a pair immediately after the K^{th} interaction is written as

$$\underset{\sim}{\chi}_K' \; \underset{\sim}{p}_K' \; \underset{\sim}{\chi}_K'' \; \underset{\sim}{p}_K'' \quad .$$

The K^{th} interaction causes the pair to jump in phase space:

$$\underset{\sim}{\chi}'_K \underset{\sim}{\rho}'_{K-1} \underset{\sim}{\chi}''_K \underset{\sim}{\rho}''_{K-1} \longrightarrow \underset{\sim}{\chi}'_K \underset{\sim}{\rho}'_K \underset{\sim}{\chi}''_K \underset{\sim}{\rho}''_K \quad . \tag{21}$$

One can say the pair is "created" at $\underset{\sim}{\chi}'_1 \underset{\sim}{\rho}'_1 \underset{\sim}{\chi}''_1 \underset{\sim}{\rho}''_1$ by the K = 1 interaction it is "destroyed" at $\underset{\sim}{\chi}'_2 \underset{\sim}{\rho}'_1 \underset{\sim}{\chi}''_2 \underset{\sim}{\rho}''_1$ and then recreated at $\underset{\sim}{\chi}'_2 \underset{\sim}{\rho}'_2 \underset{\sim}{\chi}''_2 \underset{\sim}{\rho}''_2$ by the K = 2 interaction, etc.

2) To every creation at K associate a positive contribution $+\sigma_0 \delta(\underset{\sim}{D} - \underset{\sim}{\rho}'_K - \underset{\sim}{\rho}''_K) \times \langle\langle \underset{\sim}{\chi}_K \underset{\sim}{\rho}_K | D \rangle\rangle$ and to every destruction a negative contribution $-\sigma_0 \delta(\underset{\sim}{D} - \underset{\sim}{\rho}'_{K-1} - \underset{\sim}{\rho}''_{K-1}) \langle\langle \underset{\sim}{\chi}_K \underset{\sim}{\rho}_{K-1} | D \rangle\rangle$ to the inclusive Deuteron cross section with respect to momentum $\underset{\sim}{D}$, $d^3\sigma/d\underset{\sim}{D}$ where

$$\langle\langle \underset{\sim}{\chi} \underset{\sim}{\rho} | D \rangle\rangle = \int d\underset{\sim}{q}\, e^{i\underset{\sim}{q}\cdot\underset{\sim}{\chi}} \langle \underset{\sim}{\rho} + \tfrac{1}{2}\underset{\sim}{q} | D \rangle \langle D | \underset{\sim}{\rho} - \tfrac{1}{2}\underset{\sim}{q} \rangle \tag{22}$$

is the Wigner transform of the density associated with the Deuteron center of mass wave function $|D\rangle\langle D|$ and

$$\underset{\sim}{\chi} = \underset{\sim}{\chi}' - \underset{\sim}{\chi}'', \quad \underset{\sim}{\rho} = (\underset{\sim}{\rho}' - \underset{\sim}{\rho}'')/2 \quad . \tag{23}$$

3) Sum over all pairs in all cascades.

4) An exception to the above occurs when the pair is created with zero initial separation as is the 1 - 2 pair in Fig. 1. In such cases the initial creation at K = 1 and the initial destruction at K = 2 are not to be counted. This exception arises from the fact that the two-nucleon scattering wave function is orthogonal to the ground-state wave function.

5) Note that one can have interactions in which the pair is destroyed and not recreated when either member falls back into the Fermi sea due to an energy loss which cannot lift another particle out in its place. This is properly accounted for by the rules as a simple negative contribution.

Note that there is another mechanism for producing Deuterons and other composites, that due to pickup, which is not included in the model given here. This requires an extension of the MC-INC program to include scattering by correlated clusters to be properly implemented.[2,20]

This result has a number of intuitively reasonable properties. For example, the coalescence probability of a pair is proportional to the Wigner function of

the Deuteron at their relative phase coordinates. Thus even if they were closely matched in momenta, they could not coalesce if at the same instant they were not spatially on the scale set by the Deuteron wave function. This obvious requirement was missing from the original coalescence model.

Another feature relates to the fact that positive contributions due to pair creation at interaction K tend to be cancelled by negative contributions at K + 1. The matching is closer as the distance between successive interactions is smaller. Thus the stronger the interaction between nucleons and nucleus the more frequent and closely spaced are the interactions and the stronger the cancellation from regions inside the nucleus. The next contribution from a pair therefore tends to come from the last uncompensated production. Similarly the less bound the composite, the more difficult it is to both escape the nuclear medium and coalesce and the more rapidly it will be created and destroyed in the process.

A test of this formula[21] has shown agreement with data with however, very poor statistical accuracy. This is simply because we have here an example of trying to use MC-INC to predict a relatively low cross section. In order to become practical, this approach would therefore have to be combined with the method introduced to improve the accuracy of MC-INC. This had not yet been done.

An alternative is to use the INC model but not to rely in the MC simulation. This was done with some success in a simple case in which a reasonable analytic model for the scattering state density was assumed.[14]

VI. QM CORRECTIONS

Transport theory indicates how to systematically take into account effects of refraction and diffraction of particles moving through the nuclear medium. Recall the semi-classical theory of the propagation (or transport) of light through matter. The refractive potential seen by light corpuscules, as manifested in the index of refraction, is caused, from the wave point of view, by multiple scattering of light waves. Diffraction, on the other hand, cannot be described by a classical corpuscular theory. Those same ideas apply to the present problem.

It can be shown that[2,22] the equation describing transport of a particle through the nucleus between collisions can be written as

$$\left[\partial_t + \underset{\sim}{v}\cdot\underset{\sim}{\partial}_x + i\,U(\underset{\sim}{x},\underset{\sim}{p})\exp\left[(\overleftarrow{\underset{\sim}{\partial}}_p\cdot\overrightarrow{\underset{\sim}{\partial}}_x - \overleftarrow{\underset{\sim}{\partial}}_x\cdot\overrightarrow{\underset{\sim}{\partial}}_p)/2i\right] + c.c.\right] \langle\langle \underset{\sim}{x}\,\underset{\sim}{p}\,|\rho\rangle\rangle = 0, \tag{24}$$

where $\langle\langle \varphi|\rho\rangle\rangle$ is the reduced density in the Wigner representation of the particle in question.

$$U(\varphi) = \int d\varphi'\; T_W(\underset{\sim}{x}-\underset{\sim}{x}';\ \tfrac{1}{2}(\underset{\sim}{p}-\underset{\sim}{p}'))\; n_A(\varphi') \tag{25}$$

is an effective potential seen by this particle which is equal to the Wigner tranform of the optical potential and also equal, as shown in Eq. 25, to the convolution over the nuclear singlet $n_A(\varphi')$ of the Wigner transform T_W of two-body transition matrix. Thus, e.g. for a shell model nucleus.

$$n_A(\varphi') = \sum_{a=1}^{A}\int d\underset{\sim}{q}\; e^{i\underset{\sim}{q}\cdot\underset{\sim}{x}'}\langle \underset{\sim}{p}'+\tfrac{1}{2}\underset{\sim}{q}\,|a\rangle\langle a|\,\underset{\sim}{p}'-\tfrac{1}{2}\underset{\sim}{q}\rangle \tag{26}$$

where $|a\rangle$ are the shell model states and

$$U(\varphi) = \sum_{a=1}^{A}\int d\underset{\sim}{q}\; e^{i\underset{\sim}{q}\cdot\underset{\sim}{x}}\, d\underset{\sim}{k}\, d\underset{\sim}{k}' \times \langle \underset{\sim}{k}'|a\rangle\langle a|\underset{\sim}{k}\rangle\langle \underset{\sim}{p}+\tfrac{1}{2}\underset{\sim}{q},\ \underset{\sim}{k}\,|\,T\,|\,\underset{\sim}{k}',\ \underset{\sim}{p}-\tfrac{1}{2}\underset{\sim}{q}\rangle. \tag{27}$$

The zeroth order term in the expansion of the exponential in powers of the Poisson bracket operator gives one straight line propagation. The first-order term gives one classical motion of the particles,

$$\partial_t\,\underset{\sim}{p} = -\underset{\sim}{\partial}_x\,\mathrm{Re}\,U(\underset{\sim}{x},\underset{\sim}{p}), \tag{28}$$

$$\partial_t\,\underset{\sim}{x} = +\underset{\sim}{\partial}_p\,(\underset{\sim}{p}^2/2m + \mathrm{Re}\,U(\underset{\sim}{x},\underset{\sim}{p})). \tag{29}$$

This result agrees with that obtained in the Landau Theory of Fermi liquids by rather different considerations. It does not agree with current MC-INC practice which is rerived from purely intuitive considerations.

Higher order terms result in non-classical (stochastic) propagation via possibly a Fokker-Planck equation[22]

VII. A HEISENBERG RELATION CRITERION FOR APPLICABILITY OF INC

An equation similar to Eq. 24 has been investigated in a simplified model to determine the criteria for convergence of the exponential series. It was found[22] that convergence is rapid when

$$(\Delta P)_{Detector}\,(\Delta X)_{System} >> 1\,, \tag{30}$$

where $(\Delta P)_{Detector}$ is the momentum width of the detector and (ΔX) is an appropriate length parameter describing the nucleus. Thus for scattering from the nuclear interior

$$(\Delta X) \sim A^{1/3} F\,, \tag{31}$$

$$(\Delta P) >> A^{-1/3} F^{-1}\,,$$

while to also accurately describe scattering by the skin of thickness $\sim 1F$ we should have uniformly

$$(\Delta P) >> 1 F^{-1}\,. \tag{32}$$

This result casts an interesting light on the reason why INC describes only reaction cross sections. Elastic and almost elastic scattered particles are forwardly peaked. Hence a detector with the requisite momentum width cannot separate them from unscattered particles- they are counted as unscattered.

VIII. OFF-SHELL SCATTERING

In almost all INC calculations to date two-body scattering and two-body energy-momentum conservation is used. Particles can however scatter from clusters

for which 3-body kinematics holds. A precise definition of this can be given.[2] Such mechanisms must be eventually included in INC calculations in order to properly describe high-momentum transfer reactions.

IX. NUCLEAR DENSITY

Current practice in INC and similar theories is to use a position dependent Fermi sea for the nuclear singlet. For consistency with all the preceding discussion, however, the Wigner distribution of the nucleus should be used. (See e.g., Eq. 26.) This may be especially significant for reactions taking place primarily on the nuclear surface such as pion absorption.

X. CONCLUSION

I have gathered together here bits and pieces of a comprehensive theory of complex nuclear reactions which reduce in lowest order to INC. These are scattered in published and unpublished papers in which this theory has slowly been developed over the past six years. Most of these results are relatively rigorously proved but some are only close to educated guesses. Much work remains to be done but it is clear that this general approach can be developed into an important QM approximation procedure with much the same stature and power as for example, that of WKB.

REFERENCES

1. J. Hüfner, Ann. Phys. 115, 43 (1978).
2. E. A. Remler, Ann. Phys. 119, 326 (1979).
3. M. Theiss, Ann. Phys. 123, 411 (1979).
4. G. F. Bertsch, in Proc. Summer School on Heavy Ions and Masons in Nuclear Physics. Les Houches France, 1977 to be published.
5. C. Y. Wong and H. H. K. Tang, Phys. Rev. C 10, (1979).
6. F. Villars, Hartree-Fock Theory and Collective Motion in Dyanamic Structure of Nuclear States, D. Rowe, S. Wang, L. Trainor, T. Donnelly, eds. (U.of Toronto Press, 1972).
7. E. A. Remler, Nuclear Kinetic Theory, to be published.
8. J. R. Nix, in Progress in Nuclear and Particle Physics, D. Wilkinson ed. Vol. 2 (Pergammon 1979).
9. C. K. Cline and M. Blann, Nucl. Phys. A172, 225 (1971).
10. D. Agassi, H. A. Weidemuller, G. Mantzouranis, Physics Reports 22C, 147 (1975).
11. G. Mantzouranis, H. A. Weidenmuller, D. Agassi, Z. Phys. A276, 145 (1976).
12. S. Avik and W. Norenberg, Z. Phys A288, 401 (1978).
13. V. E. Bunakov, Foundations and Models of Pre-Equilibrium Decay, Winter Course on Nuclear Physics and Reactors, ICTP 1978.
14. E. A. Remler, A. P. Sathe, Ann. Phys. 91, 295 (1975).
15. E. A. Remler, Ann. Phys. 95, 455 (1975).
16. E. A. Remler, Phys. Rev. C18, 1786 (1978).
17. G. L. Sewell, in Lectures in Theoretical Physics, ed. A. O. Borut and W. E. Brittin (Colorado Associated Univ. Press, Boulder, 1968) Vol. 10A.
18. N. G. van Kampen, in Fundamental Problems in Statistical Mechanics, ed. E. G. D. Cohen (North Holland, Amsterdam 1962), p. 173.
19. F. Haake, in Springer Tracts in Modern Physics (Springer, New York 1973) V. 66.

20. E. A. Remler, Phys. Rev. C18, 2293 (1978).

21. E. A. Remler, unpublished.

22. E. A. Remler, Particle Transport in Nuclei, unpublished.

SOME STRANGE K, π, AND γ REACTIONS WITH NUCLEI

by

H. A. Thiessen
Los Alamos Scientific Laboratory

This is a short talk intended to be an introduction to the subject of nuclear physics with strange particles. We start with Table I,[1] which indicates some of the properties of mesons which can be considered for nuclear probes, and baryons, which might be observable as excited states in nuclear matter. The puzzle of thirty years ago, namely, strong production cross section and weak decay, was solved by the postulate of a new quantum number, called strangeness, which is conserved in the strong interaction but not in the weak interaction. Strong production is possible if particles are produced in pairs with total strangeness 0. The fact that only negative strangeness baryons exist limits the possible reactions for producing strange nuclei. In particular, the (K^-,π^-) or (π^+,K^+) reactions are the only strong reactions which will produce a Λ in a two-body reaction on a neutron.

It is interesting to plot the mean free path in nuclear matter of the various probes versus projectile momentum. Figure 1 shows the dramatic differences which occur.[2] Near 400 MeV/c, the K^+ has a mean free path of 6 Fermis, while the $\bar{p}$ has a mean free path more than a factor of 10 shorter. The long mean free path of the K^+ means that it will be a particularly good probe of nuclear structure since initial and final state interactions are relatively weak. The long mean free path is a result of the lack of strangeness +1 baryons, which would allow K^+ N resonances if they existed. We note that the K^- has a short mean free path since many resonances exist in the K^- N channel. Note also that in the 500-700 MeV/c region, the pion has a substantially longer mean free path than at 300 MeV/c. The pion's usefulness as a probe of nuclear structure would be enhanced if higher energy pion facilities existed.

In the past five years, there has been a significant increase in the number of experiments performed in the area of strange nuclear physics. Groups at Brookhaven National Laboratory and CERN are actively pursuing this field. Both use accelerator technology which is 20 years old, and the Brookhaven beam line is more than 10 years old and was not designed for this purpose. Beam intensities are low, on the order of 10^4 to 10^5 K^- per second, and the beams are contaminated with 10-20 pions per kaon. The energy resolution is poor, on the order of 2-4 MeV, and the low counting rate has led both groups to use thick targets which further compromise the resolution. Nevertheless, experiments can be done and the low rate has not reduced the enthusiasm of the several groups working in this field.

The simplest experiment, K^+ and K^- scattering, has rarely been done. The most recent such experiment is that of the CMU/BNL collaboration.[3] A typical spectrum is shown in Figure 2. In Figure 3 we show the angular distribution for elastic scattering on ^{12}C. Inelastic scattering is shown in Figure 4. The conclusions from this experiment are that K^+ data are more readily explained, most likely resulting from the long mean free path of the K^+. It is also clear that additional K-nucleon scattering data of high quality are needed as input to the kaon nucleus calculations.

The subject of hypernuclei, or nuclei with non-zero strangeness, has been the subject of most of the recent work in this field. There are several reasons why such experiments are interesting, i.e.

1. A new kind of insight into nuclear matter is possible by using a (strangeness) tagged neutron (tagged quark?) which does not obey the Pauli Principle.
2. Hypernuclei are a testing ground for theories of baryon-baryon interactions. In particular, the lifetimes of Λ and Σ are modified in nuclear matter; a study of the lifetime, which is likely to be state dependent, can provide new information.
3. Triply magic nuclei, e.g. $^{6}He_{\Lambda\Lambda}$, can be seen.
4. Finally, we have the aspect of general curiosity, namely, will we find something strange and unexpected?

For all of these reasons two groups, at CERN and at BNL, have been active in the field recently.

The (K^-,π^-) reaction has been used in most experiments to date. The main reason is that near 0° and 550 MeV/c, this reaction can convert a neutron to a Λ with negligible momentum transfer. Thus the largest cross section should be observed under these conditions and in particular, if strangeness analog states exist, they should be best seen with small momentum transfer. The experimental difficulties of such experiments are severe, namely, pions from reactions in the target must be distinguished from pions resulting from kaon decay, which occurs much more often and can result in pions of the same momentum as reaction pions. Very good angle measurements are required in the vicinity of the target in order to test the projection of the beam kaon and reaction pion to a single point in the target. The CERN group uses liquid hydrogen Cherenkov counters before and after the target in order to be very sure of the particle identification. In addition, the latest CERN setup uses a very short kaon channel in which the second half of the beam line also serves as a kaon spectrometer. The latest CERN setup is shown in Figure 5.

Some typical 0° spectra[4] are shown in Figure 6. The most prominent peak in the spectra occurs when mass of the hypernucleus is ~195 MeV, or 20 MeV heavier than the Λ-neutron mass difference. These states have been identified as particle hole states, with the neutron hole and the Λ particle in the outer shell. The 20 MeV mass difference indicates that the Λ is approximately 20 MeV less tightly bound than the neutron it replaces.

The most striking observation of hypernuclei occurred when the Heidelberg-Saclay-Strasbourg collaboration compared the spectra for carbon and oxygen.[5] The data are presented in Figure 7. The carbon spectrum shows two prominent peaks. The larger peak has an angular dependence consistent with a 0^+ transition, whereas the smaller peak is consistent with a 1^-. It is reasonable to assume that both result from a $p_{3/2}$ neutron hole, then the larger has a $p_{3/2}$ Λ and the smaller peak a $s_{1/2}$ Λ. In oxygen, four peaks are observed. We may assume that the two larger peaks are the $(p_{3/2\Lambda}, p_{3/2n}^{-1})$ and $(p_{1/2\Lambda}, p_{1/2n}^{-1})$ states respectively. Both states have angular dependence consistent with 0^+ transitions. Similarly, the two smaller peaks can be identified as $(s_{1/2\Lambda}, p_{3/2n}^{-1})$ and $(s_{1/2\Lambda}, p_{1/2n}^{-1})$, respectively. The interesting observation is that the splitting of these pairs of states is ~6 MeV, which is just the splitting of the neutron hole states observed in traditional nuclear physics experiments. The CERN

collaboration concludes that the L•S splitting for the Λ is 0, or that the Λ acts like a spinless neutron.

The collaboration at BNL has studied ^{12}C also.[6] Their data include an angular distribution obtained at much larger q^2 than the CERN data. The angular distribution for the ($p_{3/2\ \Lambda}$, $p_{3/2\ n}^{-1}$) state requires both a 0^+ and 2^+ contribution. From the spectra, they conclude that the splitting of the 0^+ and 2^+ is less than 400 keV if one 2^+ state is assumed, or less than 800 keV if there are two 2^+ states. These data are consistent with the conclusions of the Heidelberg-Saclay-Strasbourg collaboration.

That the spin orbit potential for the Λ is zero is a surprise. Various theoretical efforts have been made to explain this phenomenon.[7-11] At this moment, the weight of evidence seems to be in favor of this interpretation. I would like to insert a note of caution. There are very few data points with poor resolution and only a very few angular distributions. The arguments used are consistency checks, not compelling arguments that can prove every point on their own merits. We should wait for data on more targets, higher L states, and more angular distributions before dropping this issue.

One possible explanation of the observation that $V_{L\cdot S}$ is zero has been discussed by Pirner.[11] Starting with the assumption that the Λ consists of an up quark, a down quark, and a strange quark with the u and d quarks in a state of relative $I = J = 0$, he finds that the ratio of L•S potentials for n, Σ, and Λ should be in the ratio of 3:4:0 respectively. If true, this is a striking success for the quark model. The next experimental step involves finding the L•S potential for Σ hypernuclei, which we shall discuss later.

It is possible to detect gamma rays from hypernuclear transitions, at least for light nuclei which do not emit nuclear gammas when the nucleus breaks up after the lambda decay. The CERN/Lyon/Warsaw collaboration has observed the γ's from $^4H_\Lambda$ and $^4He_\Lambda$.[12,13] A spectrum is shown in Figure 8, and the energy level diagram in Figure 9. The major benefit of detecting γ's is the ability to make energy measurements on the low energy γ, rather than perform a difference measurement on the much higher energy π and K. In addition, selection rules make J^π determination on a sounder basis than has usually been used. The MIT/BNL collaboration has been working with γ

detectors in coincidence with their (K^-,π^-) setup and feel that they will be able to make hypernuclear γ measurements on a few light targets.[14]

The lifetime of the Λ in nuclear matter has been the subject of some experimentation and of considerable theoretical interest. Experiments indicate that the lifetime becomes shorter as the mass of the hypernucleus increases, as expected from the availability reactions involving a nucleon and a Λ. The lifetime of the Σ in nuclear matter is an especially interesting subject. The reaction $\Sigma^o + N \rightarrow \Lambda^o + N$ is expected to go strongly and result in widths of Σ hypernuclear states on the order of 50 MeV, which would make them unobservable. However, the Heidelberg-Saclay-Strasbourg collaboration has seen structure in the (K^-,π^-) spectrum on ^{9}Be at the mass region where Σ hypernuclear states should be seen,[15] as shown in Fig. 10. The widths are comparable to the experimental resolution of $\leq$10 MeV. Since only one experiment has seen these states, it is necessary to confirm this observation. Both the CERN and BNL groups will study Σ hypernuclei in the next year. Considerable theoretical interest has been shown in this problem. More experiments on the widths (lifetimes) of both Λ and Σ hypernuclei are needed to distinguish among the theoretical explanations.

The (K^-,π^-) reaction was initially chosen because of the low momentum transfer to the Λ. This reaction, at 0^o, populates preferentially 0^+ and 1^- states. To get to higher spin, it is necessary to get higher momentum transfer, which can be obtained by going to larger angles. The cross section is very small and counting rates are very low at large angles. The (π^+,K^+) reaction should be advantageous in this situation since a 1000 times higher beam intensity is possible for π^+ than for K^-. Ludeking, Walker, and Dover[16] have studied this problem theoretically, and Thiessen et al. have studied the experimental aspects.[17] Near 1050 MeV/c, the two-body reaction $\pi^+ + n \rightarrow K^+ + \Lambda$ shows a maximum cross section (see Figure 10) which is on the order of 5 times smaller than for $K^- + n \rightarrow \pi^- + \Lambda$. The momentum transfer is ~300 MeV/c, which matches to a 4^+ state in ^{28}Si, which is the highest J available within the s-d shell. In fact, the momentum transfer matches reasonably well to the stretched states throughout the periodic table, as is shown in Figure 11.

Results of calculations for (π^+,K^+) and (K^-,π^-) on ^{16}O and ^{48}Ca are shown in Figures 12 through 15. These calculations use the eikonal approximation of Ludeking and Walker, which agree within 5% with the more complete calculations of Dover et al. The (K^-,π^-) results are identical to those of Dover et al.[5] for the 2^+ states in ^{12}C, which have been checked by experiment. We conclude from these results that if the beam intensity can really be increased by 1000 fold, then the (π^+,K^+) rate will be a factor of 10 higher than (K^-,π^-) for the 2^+ in ^{16}O, and 100 times for the 6^+ in ^{48}Ca. The LASL/Houston... proposal for (π^+,K^+) has been approved to run at BNL, but because of the long queue for experiments , it cannot be run before early 1982. If (π^+,K^+) experiments are feasible, then they offer the possiblities of reaching high spin states and of studying heavier hypernuclei than have been seen with (K^-,π^-). Included in these are the ground states of the heavier hypernuclei which have not yet been observed. Collective effects which have been predicted but have not yet been observed may also be seen.

The two-body interactions, $\pi^+ + n \rightarrow \Lambda + K^+$ and $K^- + n \rightarrow \Lambda + \pi^-$, are not expected to flip the spin of the neutron for the small scattering angles presently used. This is a benefit in that the spectrum is easier to interpret than if all possibilities were included, and is unfortunate in that states involving spin flip are only weakly observed. Recently, Donnelly[18] has considered the (γ,K^+) reaction. The kinematics of this reaction are nearly identical to that of (π^+,K^+) which we have already discussed. The (γ,K^+) reaction should be driven largely by the $\vec{\sigma} \cdot \vec{k}$ term and should emphasize the spin flip states. With a 100% duty factor accelerator, both (γ,K^+) and $(e,e'K^+)$ may be observable. This is an interesting possibility for the 2 GeV 100% duty factor electron machine which is being discussed by several groups.

In conclusion, we have seen the results from a new field, that of nuclear physics with strangeness, which is in its infancy. Many exciting experiments are under way and more results can be expected within the next few years. With the advent of the high current, high duty factor electron and proton accelerators which are now being designed, this field will produce a wealth of new results comparable to those obtained in the first decade of conventional nuclear physics.

REFERENCES

1. N. Barash Schmidt, A. Barbaro-Galtieri, C. Bricman, R. L. Crawford, C. Dionisi, R. J. Hemingway, C. P. Horne, R. L. Kelly, M. J. Losty, M. Mazzucato, L. Montanet, A. Rittenberg, M. Roos, T. G. Trippe, G. .P Yost, and F. E. Armstrong, Phys. Lett/ 75B, 1 (1978).

2. C. B. Dover and G. E. Walker, Phys. Rev. C 19, 1393 (1979).

3. R. A. Eisenstein in Proceedings of Kaon Factory Workshop, Vancouver, August 13-14, 1979, TRIUMF TRI-79-1 unpublished.

4. B. Povh, "Progress in Particle and Nuclear Physics," D. Wilkinson Editor, to be published.

5. W. Bruckner, M. A. Faessler, T. J. Ketel, K. Kilian, J. Niewisch, B. Pietrzyk, B. Povh, H. G. Ritter, M. Uhrmacher, P. Birien, H. Catz, A. Chaumeaux, J. M. Durand, B. Mayer, J. Thirion, R. Bertini, and O. Bing, Physics Letters 79B, 157 (1978).

6. R. E. Chrien, M. May, H. Palevsky, R. Sutter, P. Barnes, S. Dytman, D. Marlow, F. Takeutchi, M. Deutsch, R. Cester, S. Bart, E. Hungeford, T. M Williams, L. S. Pinsky, B. W. Mayes, and R. L. Stearns, Physics Letters 89B, 31 (1979); and C. B. Dover, A. Gal, G. E. Walker, and R. H. Dalitz, Phy. Lett. 89B, 26 (1979).

7. A. Bouyssy, Phys. Lett. 84B, 41 (1979).

8. A. Gal, J. M. Soper, R. H. Dalitz, Ann. Phys. (N.Y.) 63, 53 (1971).

9. A. Gal, J. M. Soper, R. H. Dalitz, Ann. Phys. (N.Y.) 72, 445 (1972).

10. R. Brockman and W. Weise, Phys. Lett. 69B, 167 (1977).

11. H. J. Pirner, Phys. Lett. 85B, 190 (1979).

12. M. Bedjidian, A. Filipkowski, J. Y. Grossiord, A. Guichard, M. Gusakow, S. Majewski, H. Piekarz, J. Piekarz, and J. R. Pizzi, Phys. Lett. 62B, 467 (1976).

13. M. Bedjidian, A. Filipkowski, J. Y. Grossiord, A. Guichard, M. Gusakow, S. Majewski, H. Piekarz, J. Piekarz, and J. R. Pizzi, Phys. Lett., to be published.

14. M. Deutsch, private communication.

15. R. Bertini, O. Bing, P. Birien, W. Bruckner, H. Catz, A. Chaumeaux, J. M. Durand, M. A. Faessler, T. J. Ketel, K. Kilian, B. Mayer, J. Niewisch, B. Pietrzyk, B. Povh, H. G. Ritter, and M. Uhrmacher, Phys. Lett. 90B, 375 (1980).

16. C. B. Dover, L. Ludeking, and G. E. Walker, to be published; and L. Ludeking and G. E. Walker in Proceedings of Workshop on Nuclear Structure with Intermediate Energy Probes, Los Alamos Scientific Laboratory, LA-8303-C, (April 1980), unpublished.

17. H. A. Thiessen, BNL Experiment 758 proposal, private communication.

18. T. W. Donnelly, private communication.

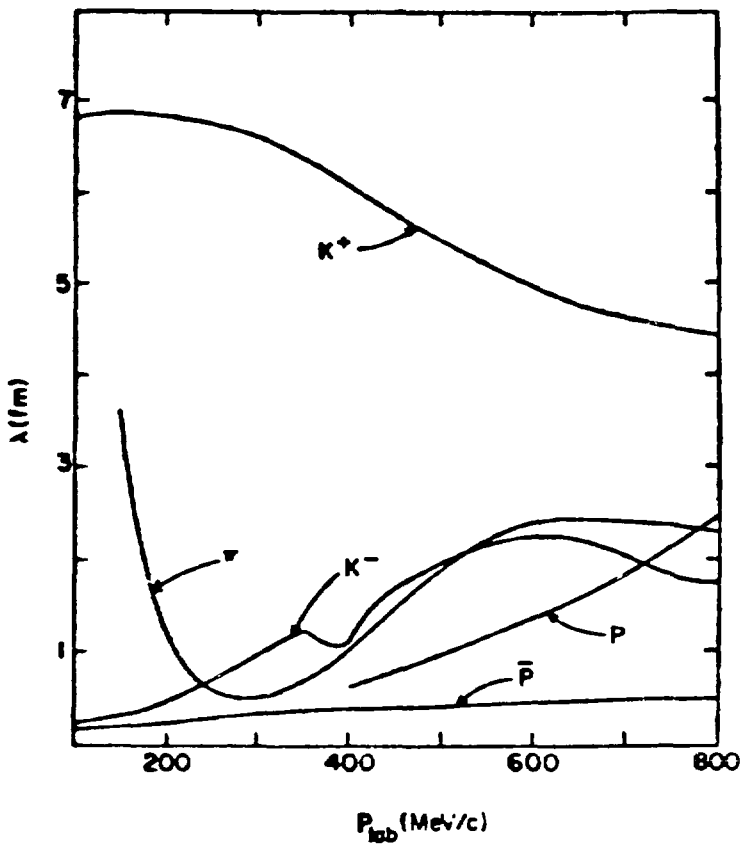

Fig. 1.

The mean free path in nuclear matter of various strongly interacting probes vs probe momentum, figure from reference 2.

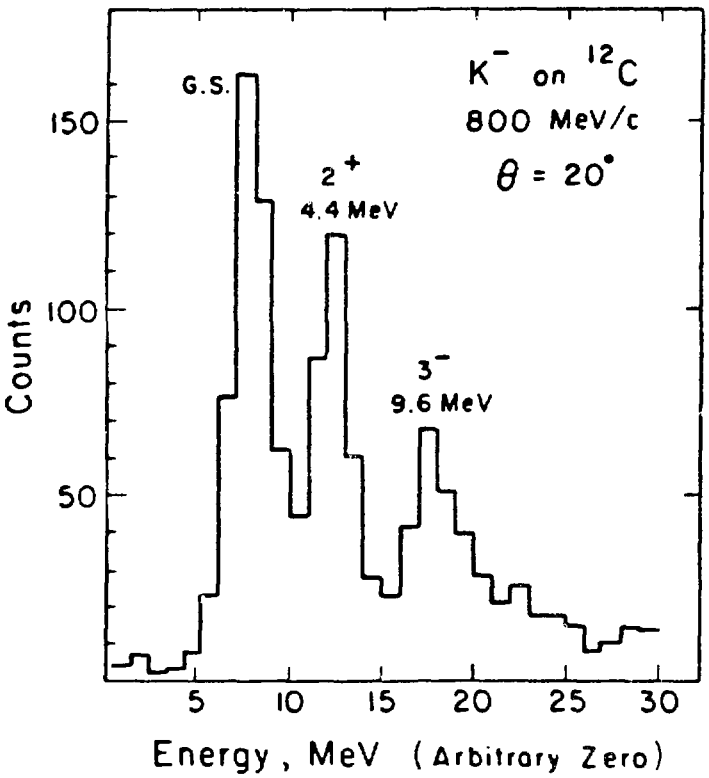

Fig. 2.

Spectrum for K^+ scattering on carbon, data from reference 3.

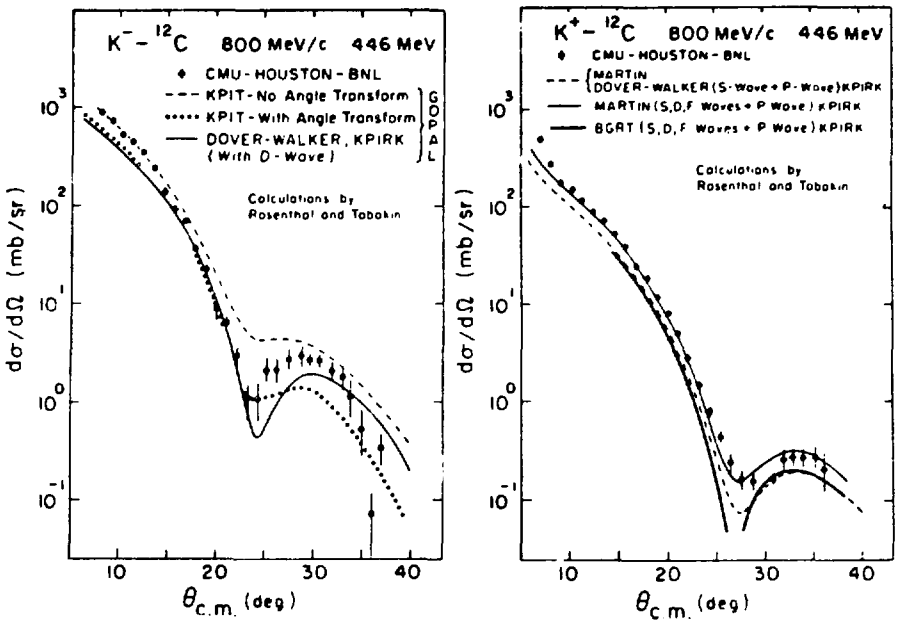

Fig. 3.

Angular distribution for K^+ and K^- elastic scattering on ^{12}C, figure from reference 3.

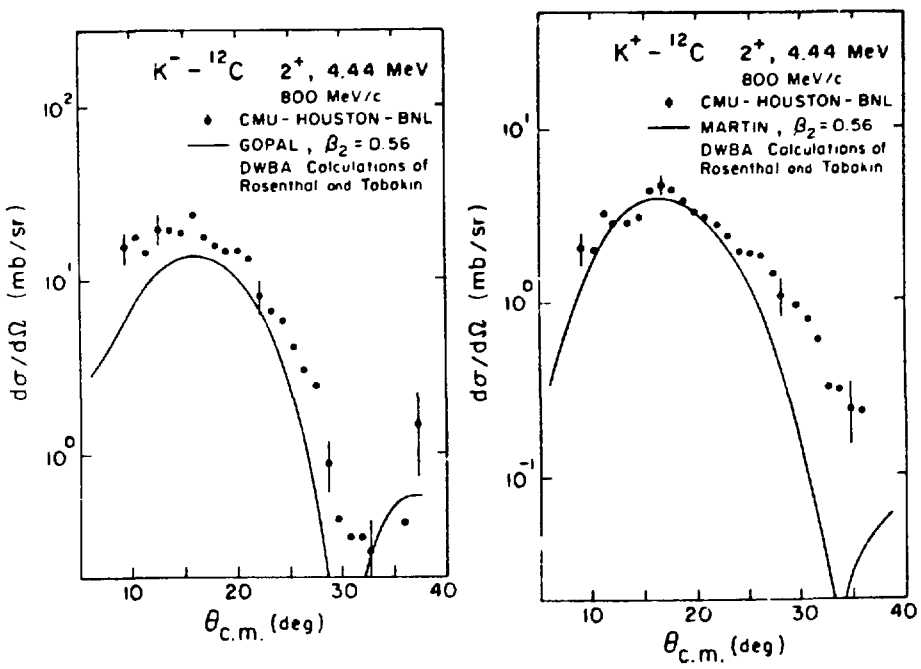

Fig. 4.

Angular distribution for K^+ and K^- inelastic scattering on ^{12}C, figure from reference 3.

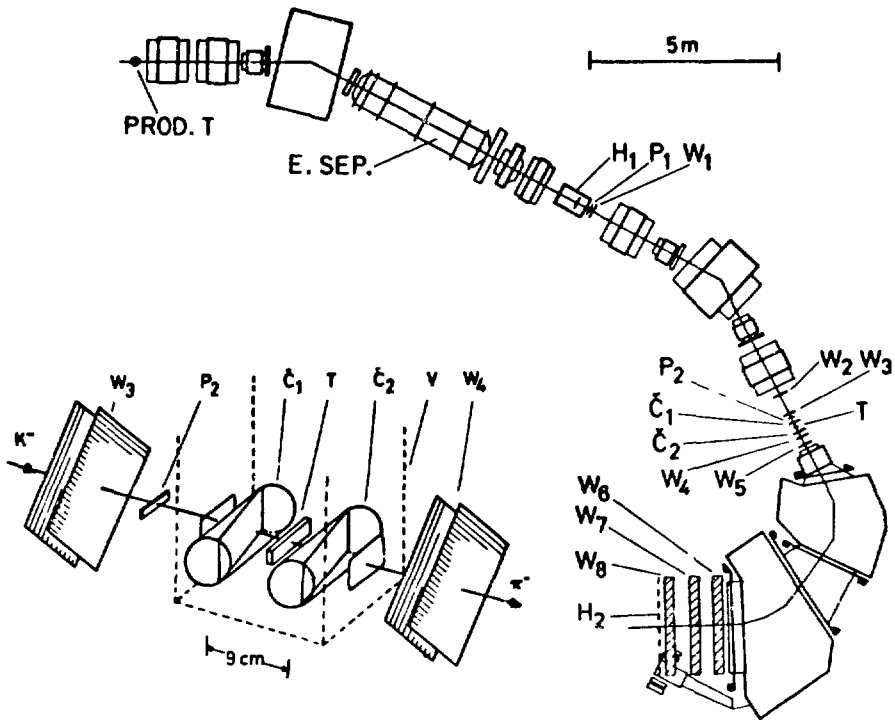

Fig. 5.

Setup for (K^-,π^-) at CERN from reference 4.

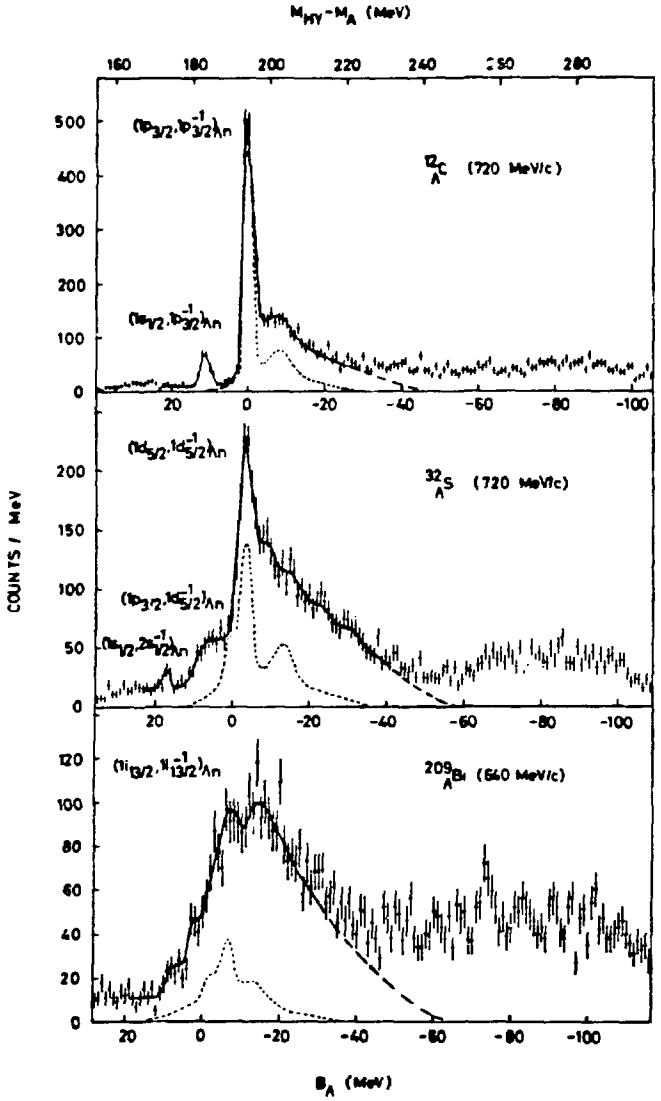

Fig. 6.

Typical spectra for (K^-,π^-) at 0°, data from reference 4.

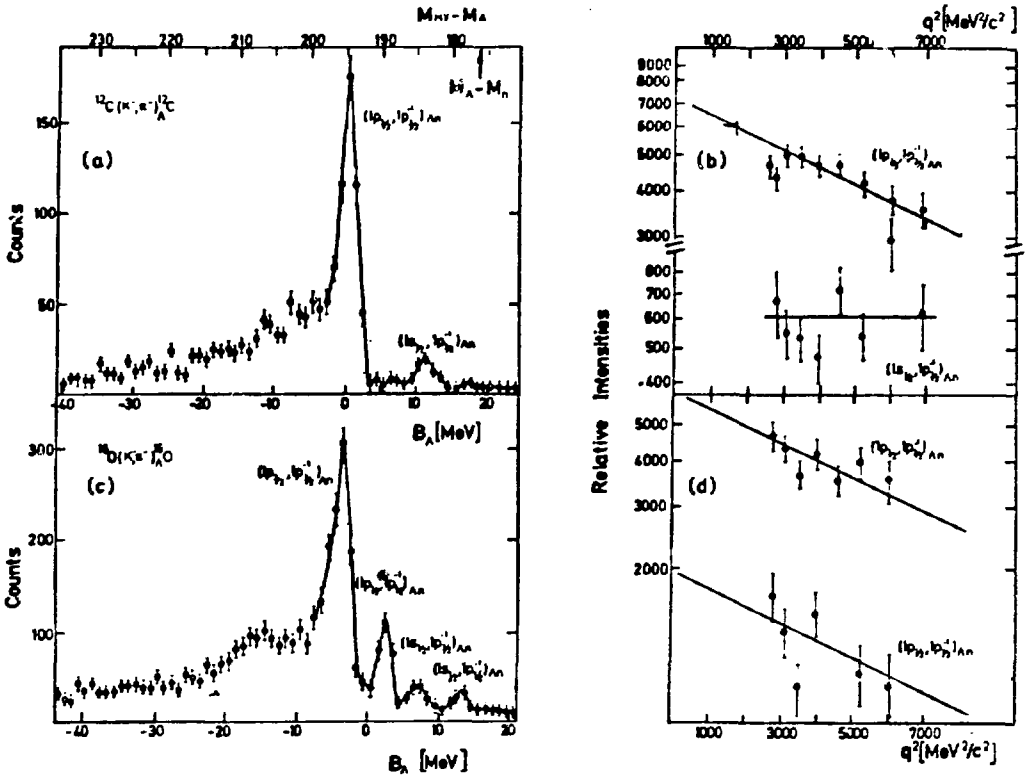

Fig. 7.

Spectrum for (K^-,π^-) on ^{12}C and ^{16}O from reference 5.

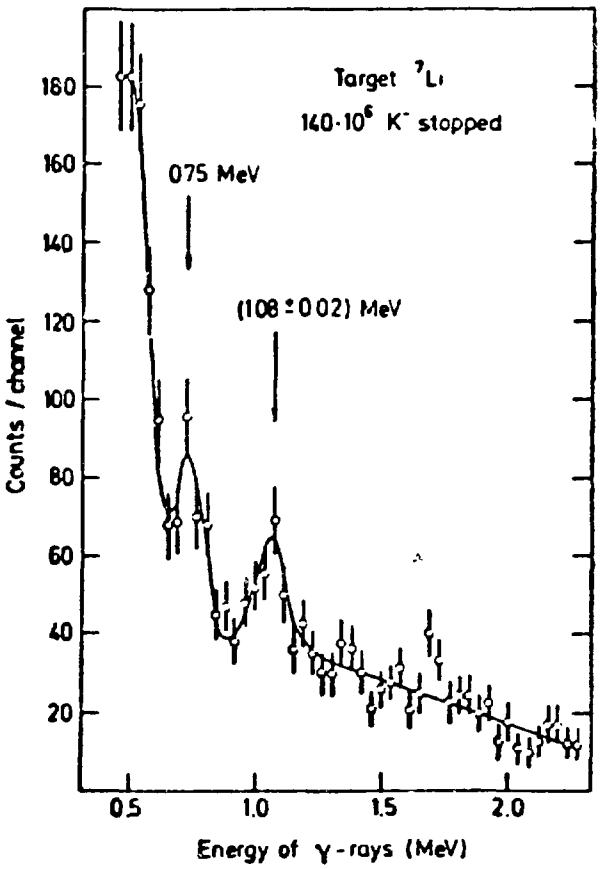

Fig. 8.

Spectrum of γ obtained in a stopping K^{-} beam, the line at 1.08 ± 0.02 MeV is identified as a $^{4}H_{\Lambda}$ transition (reference 12).

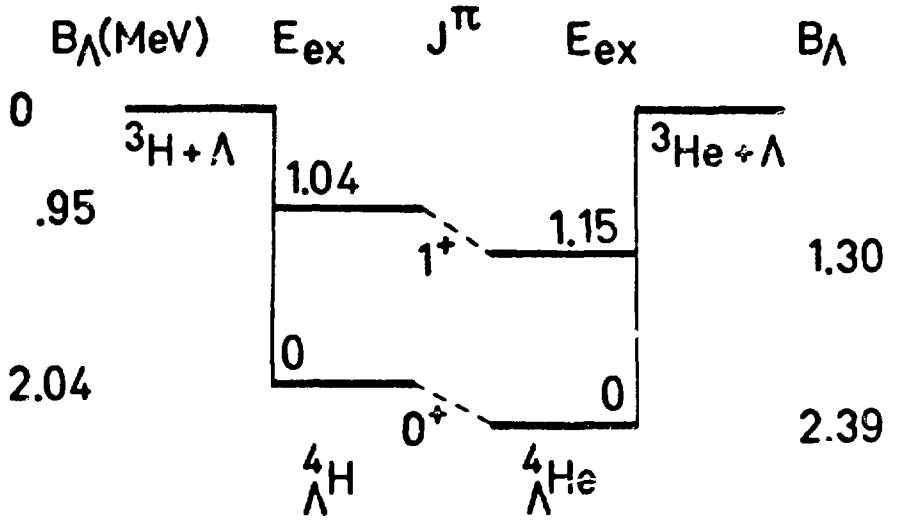

Fig. 9.

Energy level diagram of $^4H_\Lambda$ and $^4He_\Lambda$ reference 4.

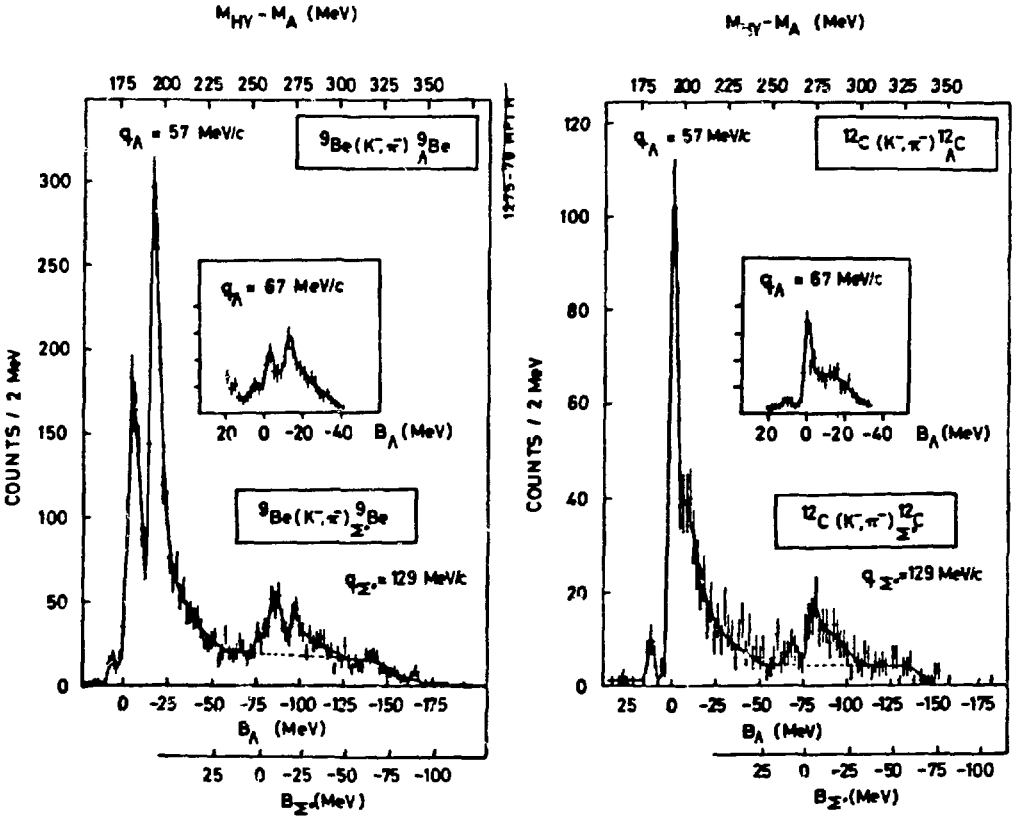

Fig. 10.

Spectrum of (K^-,π^-) on ^{9}Be showing states observed in $^9Be_\Sigma$ region.

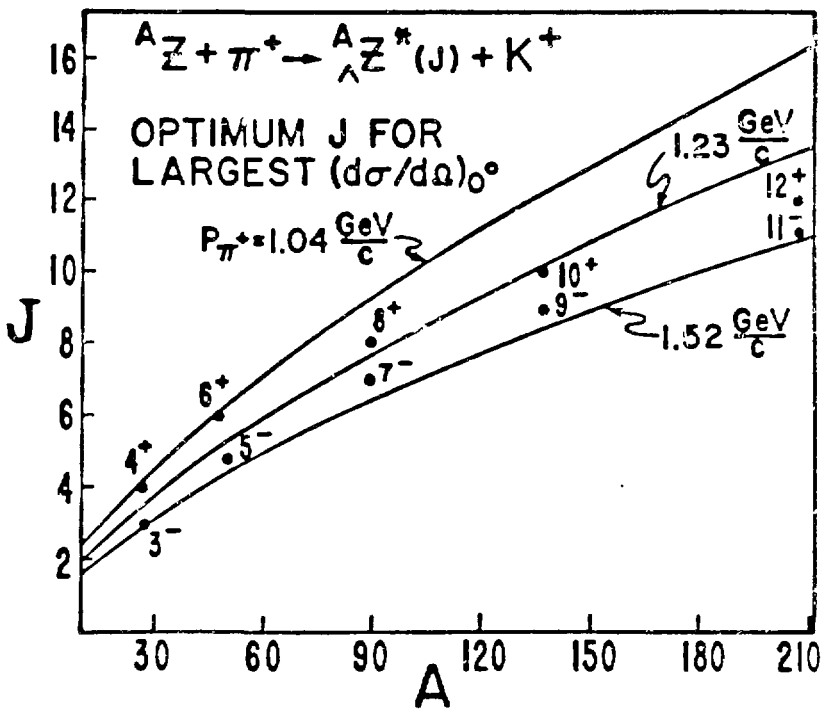

Fig. 11.

Momentum matching for (π^+, K^+) reactions from reference 16.

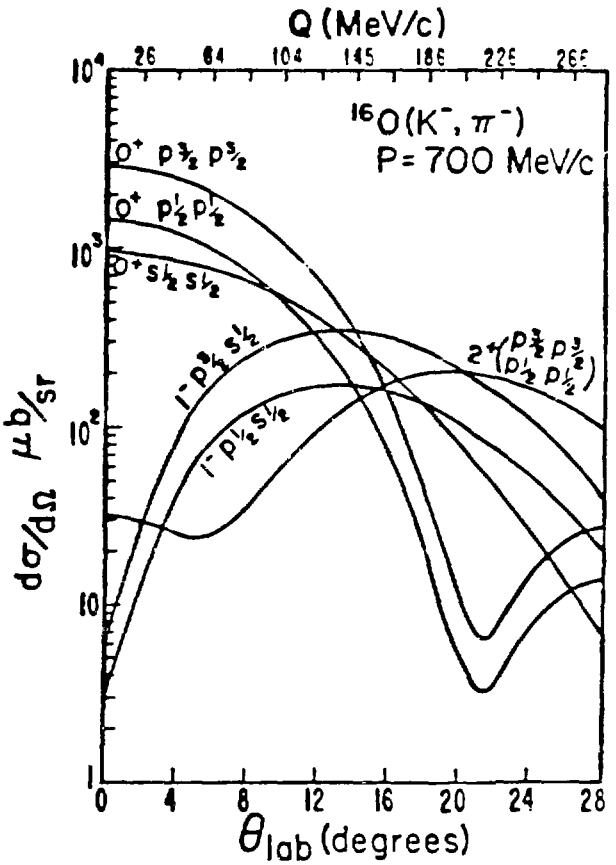

Fig. 12.

Cross section for (π^+,K^+) on ^{16}O at 1100 MeV/C, calculations from reference 16.

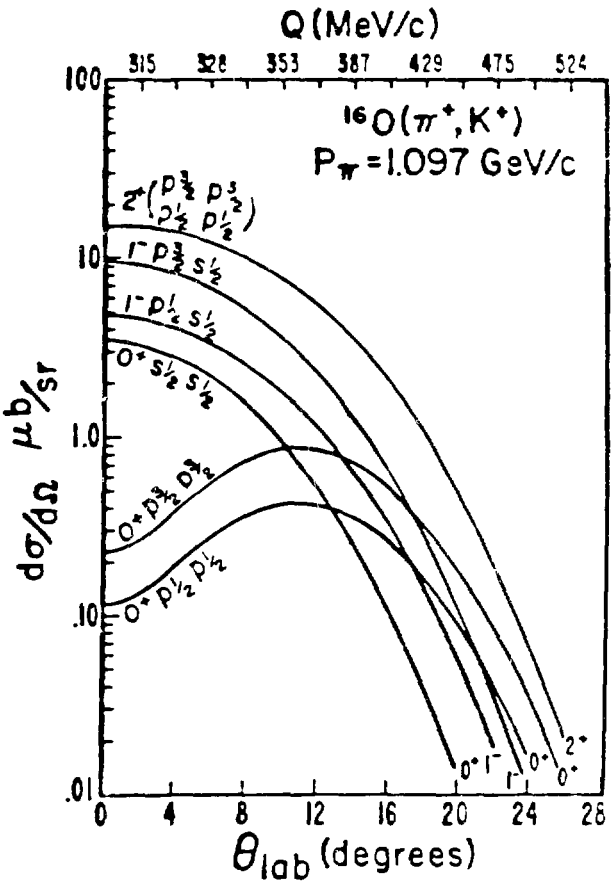

Fig. 13.

Cross section for (K^-,π^-) on ^{16}O at 700 MeV/c, calculations from reference 16.

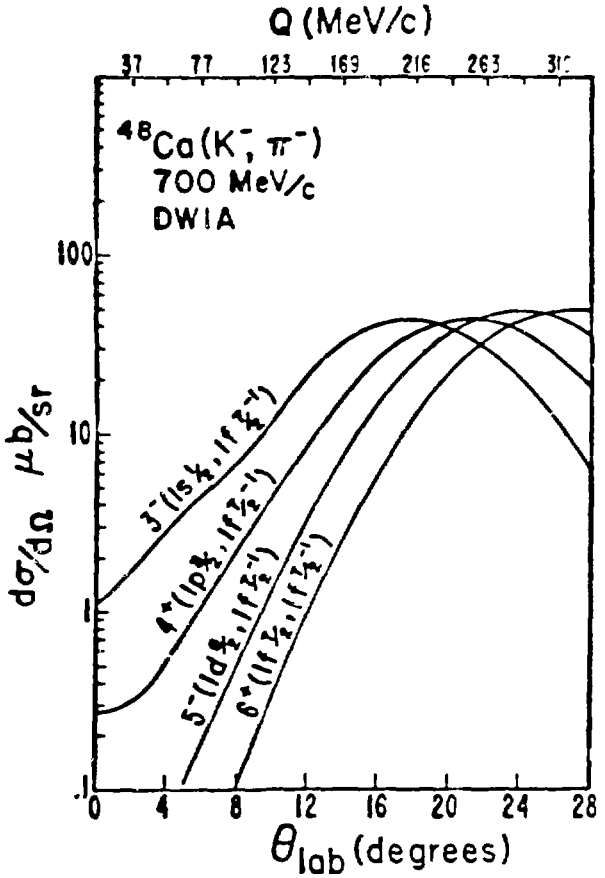

Fig. 14.

Cross section for (π^+,K^+) on ^{48}Ca at 1100 MeV/c, calculations from reference 16.

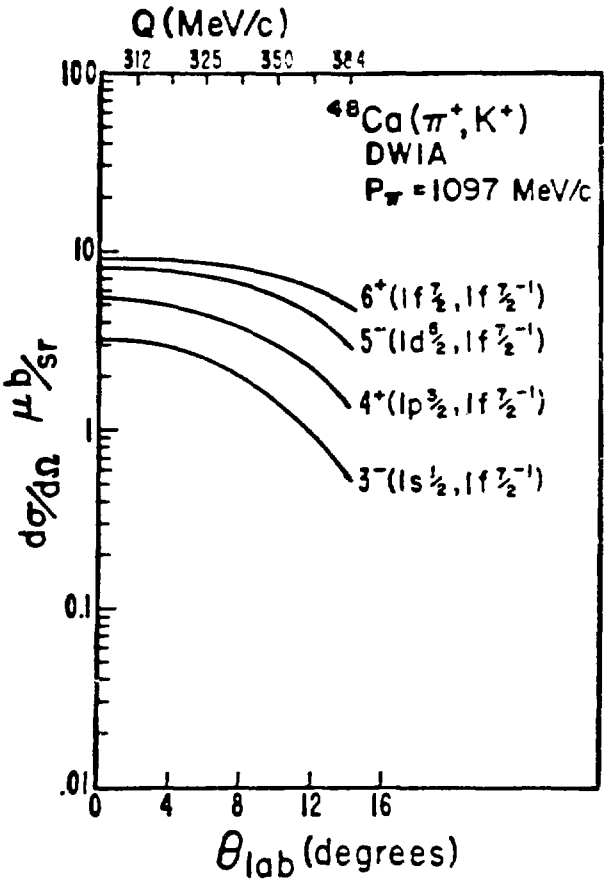

Fig. 15.

Cross section for (K^-,π^-) on ^{48}Ca at 700 MeV/c, calculations from reference 16.

Summary Report and Recommendations from Panel

NC-1 PION-NUCLEUS REACTIONS

by

E. P. Steinberg, Argonne National Laboratory, Chairman

C. J. Orth, LASL, Co-Chairman

I. INTRODUCTION

The program of the NC-1 Panel Sessions is given in Appendix A. Survey talks were presented in the various areas and served as a basis for further discussions. The session on Spallation, Fragmentation and Fission was held jointly with Panel NC-2 (Nucleon-Nucleus Reactions and Nuclei Far From Stability). The sessions were well-attended and the discussions were lively and stimulating. It is not possible to transmit the spirited atmosphere that prevailed or give appropriate credit to the many individuals who took part in the discussions, but the chairman and co-chairman wish to express their appreciation to all the participants. In the following, an attempt is made to present the highlights of the sessions, with particular emphasis on the directions indicated as most fruitful and important for future investigations. Two review papers are presented in their entirety as Appendices B and C.

II. STOPPED-PION REACTIONS

The extensive studies of residual product yields and particle spectra from stopped-π^- reactions carried out at SIN[1-3] were reviewed by H. S. Pruys (see Appendix B). These studies are directed toward an understanding of the pion absorption mechanism, in particular, the ratio (R) for the probability of π^- absorption on np versus pp pairs, and the extent of absorption on α clusters in the nucleus.

An example of residual product yield data for a Au target, using both activation and on-line γ-ray measurements at SIN, is shown in Fig. 1. Neutron and charged particle energy spectra are shown in Fig. 2.

An upper limit of about 30% for pion absorption on an α-cluster has been derived from a comparison of measured yield distributions with calculations and from the triton spectra such as shown in Fig. 2. However, in both cases absorption on an α cluster is not needed to explain the data.

Based upon the experimental yields of high energy neutrons and protons, from eight different target nuclei, the ratios for absorption on np versus pp pairs (R) range from 0.7 to 2.3. Due to charge exchange scattering of the primary nucleons these values may be too low. More reliable values for R could be obtained by an accurate measurement of the neutron and proton spectra at the highest energies, and by measuring nn and np coincidences.

J. Hüfner discussed the calculated[4] neutron and proton energy spectra for ^{12}C that he showed in his invited talk (See Op. Cit. Fig. 3 and 4). He emphasized that the absorption of the negative pion on two nucleons plus a few nucleon-nucleon collisions can explain the available experimental nucleon spectra in magnitude and shape. The discrepancy between primary distributions and the experimental spectra can be accounted for by another collision except at very low energy where the compound nucleus decay dominates. Their multiple scattering expansion calculations duplicate all available experimental data, except R, essentially without adjustable parameters. For ^{12}C Hüfner and Chiang calculated $R = 6 \pm 0.6$ which is considerably larger than the experimental values of 2.5 ± 1.0 from Ref. 4 and 2.3 ± 0.6 from Ref. 1.

C. J. Orth reported that yields of two-nucleon-out products following stopped-π^- absorption have been measured at LAMPF[5] for six neutron-rich nuclei ranging from A = 26 to 174. Ratios of the yields of the nn-out to the np-out products versus N/Z of the target nuclei are plotted in Fig. 3. The ratios are seen to increase from 6.8 at ^{26}Mg to 18.2 at ^{174}Yb. The observed ratios should correlate rather well with the initial probability for absorption on np and pp pairs because the yields of the observed two-nucleon-out residual products are very sensitive to excitation energy. If more than the binding energy of a valence nucleon is deposited in the nucleus by the recoiling pair a $\Delta A \geq 3$ product results. However, due to the sensitivity to excitation energy this method of determining R may selectively sample π^- absorption at the very surface of the nucleus rather than over a distribution centered at the half-density radius. The results are compatible with an increase in the neutron-to-proton ratio at the nuclear surface as a function of A, and L-C. Liu[6] is currently incorporating separate neutron and

proton densities into the ISOBAR code in order to model these $\Delta A = 2$ product yield ratios.

At Saclay, J. Julien and his collaborators[7] have performed coincidence measurements with stopped π^- and 70-MeV π^+ on Si targets. They have determined multiplicities for neutrons and protons in coincidence with incident pions plus deexcitation γ-rays of residual products. Neutron spectra in coincidence with A-2 and A-4 residues from stopped-π^- interactions should provide information about the mechanism of π^- absorption on nucleon pairs and α clusters. Although the experiment was performed with thick targets of natural Si (2.5 g/cm^2) and low pion fluxes ($\leq$ 6000 π^-/sec) the data indicate a neutron multiplicity of two for ^{26}Al as expected in a quasi-deuteron model. For E_n > 20 MeV lower multiplicities were observed for the other residual nuclei, as expected due to final state interactions. The exception was ^{24}Mg (A-4) where a multiplicity of about two was measured, suggesting some direct formation by a primary interaction of the pion with an α cluster. Neutron and proton spectra are shown in Fig. 4.

Future Directions for Stopped Pion-Nucleus Studies

1. The primary interaction of Coulomb-captured negative pions with the nucleus remains poorly understood. The determination of the ratio R for absorption on np and pp nucleon pairs, and absorption on α clusters is complicated by final state interactions. The following types of experiments should improve our understanding of the interaction.

   a. Measure proton energy spectra to the endpoint and obtain better statistics for high-energy neutrons so that n to p ratios can be obtained for T_N > 60 MeV.

   b. Perform more n-n and n-p 180° coincidence measurements over a large range of nuclei, similar to those reported in Ref. 4.

   c. More exclusive experiments requiring a triple coincidence among a pion stop, a recoil nucleon, and a deexcitation γ-ray of a residual nucleus should provide more meaningful data, especially with the higher beam intensities now available that permit the use of thin targets.

   d. Measurements of low-probability (π^-,n) and (π^-,p) yields should provide information about parallel momentum components of the absorbing nucleon pair.

2. Currently there are at least four different models[2,4,8,9] for the stopped-π^- interaction. The calculations reported by Hüfner and Chiang (Ref. 4) at this workshop indicate a larger value of R than required by other calculated fits to the particle and residual product data. Increased communications, or better, a meeting of the four theory groups, could lead to improved theoretical understanding of the interaction.

III. FAST PIONS - SINGLE NUCLEON REMOVAL REACTIONS

Theoretical aspects of pion-induced, single-nucleon removal reactions were discussed by M. M. Sternheim. Quasi-elastic pion-nucleon scattering at energies near the (3,3) resonance make up about half the reaction cross section, or about a quarter of the total pion-nucleus cross section. Accordingly, studying this process is an important part of the overall program of understanding the pion-nucleus interaction in general, and provides an opportunity to examine various aspects of the propagation of pions and nucleons in the nucleus. Specifically, it will probe Pauli and off-shell effects on the pion-nucleon amplitude, and will test our ideas concerning nucleon charge exchange.

Quantum mechanical (DWIA) calculations are necessary when an experiment detects a unique final state. In the Plane Wave Impulse Approximation (PWIA), the quasi-elastic amplitude is a free amplitude times $g^{PW}(q)$, the momentum distribution of the struck nucleon.[10] In the factorized DWIA, one includes distortion effects but assumes that the two-body amplitude for πN scattering varies only slightly over the ranges of momenta contained in the distorted pion and nucleon waves. This replaces g^{PW} by g^{DW}, the distorted momentum distribution of the struck nucleon. Note that in both models the g's cancel leaving only the free πN amplitudes when ratios are taken for π^+ to π^- or for p to n, assuming that the possibility of charge exchange is ignored.

Semiclassical models are likely to be valid when inclusive processes are considered, so that coherent effects of quantum mechanical wave calculations tend to cancel. Full semiclassical Monte Carlo codes, which include both cascade and evaporation processes, are available, but for some purposes it is easier and more revealing to use a simpler transport model in which straight-line propagation of the incident and outgoing particles is assumed, although they may charge exchange or be absorbed.[11]

Until recently, quasi-elastic pion experiments were limited to activation measurements which determined the total cross section to particle-stable final

states. The most extensive data[12] is available for $^{12}C(\pi,\pi n)^{11}C$, where the ratio R_n of the neutron removal cross sections for π^- and π^+ varies from less than one at threshold to 1.6 at 180 MeV and to 1.8 at 300 MeV. Using the free πn cross sections, one expects a ratio of close to 3 over this energy region. Since pn charge exchange is large at low energy and steadily decreases as the energy rises, it is possible to account for the data with a simple transport model which allows the outgoing nucleons to charge exchange. The model contains a single parameter representing the Pauli reduction of the pn charge exchange cross section.[13]

Experiments which detect the outgoing particles offer a much greater challenge to the theorist. Because of the background from pion absorption events in single-arm experiments, it is necessary to do coincidence experiments to study quasi-elastic scattering. In planning these experiments, it is important to insure that the kinematics are appropriate. The outgoing nucleons should have an energy well above the removal energy, because slow nucleons will multiple scatter due to the large NN cross sections at low energies, and the detectors must be able to see the full spread of energies and angles around the nominal quasi-elastic peak due to Fermi motion. The angular variations of the π^+ and π^- cross sections are such that their ratio can be very different at some angles from the total cross section ratio. Since the nucleon charge-exchange cross section varies as $T_N^{-1.9}$, this must also be taken into account when comparing two experiments at different energies. Finally, absorption of nucleons, corresponding to deflections out of the detectors by NN collisions, must be taken into account. When these factors are all included, we find[11] general agreement with the limited experimental data which exist. Results are expected soon from an experiment which will more fully define the angular and energy spread of the quasi-elastic peak.[14]

Several questions were raised in connection with the simple transport model. P. Karol[15] claims that the probability of charge exchange in the Sternheim-Silbar model is incorrectly calculated and that, in fact, it plays a minor role, not a major one, in the reaction mechanism for $^{12}C(\pi,\pi n)^{11}C$. The transport model is a simplification of the INC-Monte Carlo codes, and it is not clear why the results of the two should differ. This is being investigated by Sternheim and Long. Contributions from inelastic scattering followed by nucleon evaporation (ISE mechanism) are included in the INC calculations, but not the transport model. The mechanism has not been verified experimentally for $(\pi,\pi N)$ reactions. Recent results at SIN on $^{12}C(\pi^{\pm},\pi^{\pm}p)^{11}B$ at 245 MeV (reported by H. K. Walter) are consistent with the impulse approximation, and there appears to be no need to introduce NN charge exchange.

A review of current experimental work on $(\pi,\pi N)$ reactions was presented by H. S. Plendl. This covered primarily unpublished work, supplementing the coverage in the invited paper of H. K. Walter at this workshop. Preliminary results of experiments at SIN[16] and LAMPF[17] on π^+ scattering at discrete angles using magnetic spectrometers indicate that backward scattering is quasi-elastic at π^+ energies near the (3,3) resonance. Several LAMPF experiments[18] are measuring coincidences between an outgoing pion or proton and a prompt γ from the residual nucleus in $(\pi^{\pm},\pi N)$ reactions near the (3,3) resonance. Preliminary results confirm a quasi-elastic interaction mechanism and further work will examine the dependence on the pion energy and target mass in more detail. Other studies[19] are examining coincidences between the outgoing pion and nucleon at discrete angles and identifying specific excited states. The ratios of π^+- to π^--induced reaction cross sections are in agreement with PWIA calculations. The importance of the geometry and kinematics in coincidence experiments was noted, and the work of Jackson, Ioannides, and Thomas[10] on a fixed condition geometry was pointed out.

E. P. Steinberg reported on the present state of activation data on $(\pi,\pi N)$ reactions. The cross-section ratios for π^-- and π^+-induced reactions over a broad range of target mass numbers are nearly constant for 180-MeV pions and considerably lower than the value of R=3 expected from free pion-nucleon scattering (see Fig. 5). The R_n values for the neutron-excess targets ^{142}Ce and ^{197}Au are somewhat higher than the R_p values, possibly indicating the importance of other reaction mechanisms, such as ISE or collective (giant resonance) excitations followed by nucleon evaporation. The results are in fair agreement with the Sternheim-Silbar calculations only for low mass targets and with INC calculations only for high mass targets.

N. Imanishi reported on work on $(\pi,\pi N)$ reactions at higher pion energies at KEK. The excitation functions of the $^{12}C(\pi^-,\pi^-n)^{11}C$ and $^{19}F(\pi^-,\pi^-n)^{18}F$ reactions show evidence of the T=3/2 resonance at 1.3 GeV, and that for the $^{9}Be(\pi^-,\pi N)^{8}Li$ reaction shows the influence of the T=1/2 resonance at E_π = 0.6 and 0.9 GeV. The resonance peaks are broadened, apparently by the Fermi motion of the struck nucleon in the nucleus. The cross-section ratio $\sigma(^{9}Be(\pi^-,\pi N)^{8}Li)/\sigma_{\pi^-p}$, where σ_{π^-p} is the free-particle cross section averaged over the Fermi momentum, decreases monotonically (like that for the (p,pn) reaction) with increasing incident energy, while the ratios of $\sigma(\pi^-,\pi^-n)/\sigma_{\pi^-n}$ for the ^{12}C and ^{18}F reactions are enhanced around E_π = 0.6 GeV.

Future Directions for Single Nucleon Removal Studies

The present understanding of one-nucleon removal reactions is not satisfactory, and additional theoretical and experimental investigations are certainly in order. The following are suggested as important directions for future work:

1) Additional coincidence studies:
   a. π-N at carefully selected incident energies and detector angles.
   b. π-γ for neutron-excess nuclei.
2) Measure residual-nucleus recoil properties to establish extent of the ISE mechanism.
3) Extend systematics of $\sigma_{\pi^-}/\sigma_{\pi^+}$ ratio to other targets, in particular, heavy ones.
4) Reconcile transport and INC model differences.
5) Improve theoretical understanding of the reaction.
6) Extend studies to higher πN resonances.

IV. PION SINGLE CHARGE EXCHANGE

In activation studies performed at LAMPF[20], R. S. Rundberg reported that cross sections have been measured for the pion single charge exchange reactions $^{27}Al(\pi^-,\pi^0)^{27}Mg$, $^{45}Sc(\pi^+,\pi^0)^{45}Ti$, and $^{65}Cu(\pi^-,\pi^0)^{65}Ni$, integrated over all the particle-bound states and over all angles. These excitation functions, between 80- and 400-MeV pion kinetic energy, show no structure near the (3,3) resonance, but all exhibit a monotonic decrease in cross section roughly proportional to E^{-1} or k^{-2}. The cross section per nucleon is inversely proprotional to A and proportional to E_0^2, the energy above which the nucleus is particle unstable. The excitation functions for these three reactions are shown in Fig. 6. Measurements are underway to determine excitation functions for the $^{88}Sr(\pi^+,\pi^0)^{88}Y$, $^{88}Sr(\pi^-,\pi^0)^{88}Rb$, and the $^{139}La(\pi^+,\pi^0)^{139}Ce$ reactions,[25] and cross sections have been determined between 110 and 300 MeV for the $^{14}N(\pi^+,\pi^0)^{14}O$ g.s. reaction.[21] This reaction is of interest because it involves a spin-flip, isospin-flip transition from $^{14}N(T=0)$ to $^{14}O(T=1)$. Again, the results show smoothly decreasing cross sections with increasing pion kinetic energy, much like the results described above, except lower by one- to two-orders of magnitude.

The apparent disagreement between various theoretical treatments and the experimental measurements by Shamai, et al.[22] has provided the incentive for

nuclear chemists[23] at LAMPF to redetermine the $^{13}C(\pi^-,\pi^\circ)^{13}N$ excitation function. To date, measurements have been made at 50, 70, 100, and 164 MeV and the cross sections were determined at three target thickness (50, 80, and 130 mg/cm^2), since secondary (p,n) reactions were suspected of being the cause for the larger measured[22] cross sections than calculated. The present measurements give cross sections about one-half as large as previously measured,[22] and in agreement with a recent π° spectrometer measurement[24] at 150 MeV.

In another experiment at LAMPF, to study single charge exchange to a single final state, nuclear chemists[25] will use a rotating-wheel target assembly in order to measure ^{12}N g.s. ($T_{1/2}$ = 8 msec) produced in the $^{12}C(\pi^+,\pi^\circ)^{12}N$ reaction.

V. PION DOUBLE CHARGE EXCHANGE

A review of the present status of pion double charge exchange was presented by K. K. Seth. This is included in its entirety in Appendix C of this report.

A recent activation experiment to measure cross sections for the $^{209}Bi(\pi^+,\pi^-xn)^{209-x}At$ reactions was discussed by J. Clark. Astatine isotopes were radiochemically separated from Bi targets irradiated with π^+ and π^-, the latter to study secondary α and ^3He production of the At products. In Fig. 7 the absolute cross section for π^+ and π^- production of At isotopes show that there is a considerable excess yield with π^+, indicating a DCX cross section for ^{207}At of 103 ± 31 μb, in good agreement with the value of 120 ± 30 μb reported at 90 MeV by Batusov, et al.[26]

The early results indicate that the DCX cross sections for $^{205-207}At$ at the resonance (180 MeV) and above are very small.

VI. PION CHARGE EXCHANGE THEORY

W. R. Gibbs discussed the theory of pion charge exchange and noted that none of the single charge exchange (SCX) calculations using single scattering,[27] optical potential,[28] DWIA,[27] fixed nucleon,[29] or doorway models[30] can obtain as much as 1 mb for the $^{13}C(\pi^+,\pi^\circ)^{13}N$ (g.s.) reaction without extreme physical assumptions. Most calculations are in the range 0.2-0.5 mb.

The A dependence for SCX cross sections at 0° has been derived by M. Johnson[31] on the basis of strong absorption and an eikonal expression for the SCX cross section as follows:

$$\sigma(0^\circ) \sim (N-Z)\, A^{-4/3}$$

Gibbs noted that it is interesting to consider alternate mechanisms for the double charge exchange reaction, and a variation of one proposed by Germond and Wilkin[32] may have validity. This mechanism involves a charge exchange on a virtual pion in the pion field of the nucleus. To find this pion one must decompose the initial and final states.

$$^{18}O \leftrightarrow {}^{18}F^* + \pi^-$$
$$^{18}Ne \leftrightarrow {}^{18}F^* + \pi^+$$

Then:

$$\pi^+ + {}^{18}O \rightarrow \pi^+ + ({}^{18}F^* + \pi^-)$$
$$\rightarrow \pi^- + ({}^{18}F^* + \pi^+)$$
$$\rightarrow \pi^- + {}^{18}Ne, \text{ DCX}$$

There is no resonance effect in the basic reaction, although there will be in the distortion of the initial and final pion waves. The angular distribution looks like elastic scattering from the "bound" pion. To see how different this is from the usual ideas of DCX, consider the case of an S-wave pion in the nucleus. The following considerations lead to a "first guess" at the pion wave function:

i) $\langle\phi\rangle = r^2\, dr\, \phi\,(r) = 0$, since ϕ is an overlap of two orthogonal states, and

ii) it will be bilinear in the nucleon field at its first derivative (from, say, the Dirac matrix γ_5) so it has terms in ρ and $d\rho/dr$.

If no other scale factors are introduced,

$$\phi \sim \rho + 1/3\, r\rho' \sim \frac{1}{3r^2}\frac{d(r^3\rho)}{dr}$$

On the basis of isospin conservation, for a T = 1/2 target there are only two independent amplitudes, $f^{1/2}$ and $f^{3/2}$, and therefore the relationship between charge exchange and π^+ and π^- elastic scattering (ES) is given by:

$$f_{SCX} = 1/2\,(f_{ES}^{\pi^+} - f_{ES}^{\pi^-})\ .$$

The Fourier transform of ϕ gives the form factor for the calculation of pion scattering. The position of the first minimum in the DCX angular distribution, as calculated using this pion field concept, is closer to 0° than in calculations using the conventional two-step mechanism and is in better agreement with observations. A more quantitative treatment may yield even further improvement. The extensive new data on DCX has provided the incentive for current efforts to improve the theoretical treatments.

Future Directions for Charge Exchange Studies

Activation studies of single charge exchange reactions that have been completed and that are still in progress should be adequate for theorists to test their models. Perhaps some experimental work on a very heavy nucleus (A > 170) is desirable since the heaviest nucleus studied to date is ^{139}La.

In double charge exchange on-line measurements at EPICS do not have the sensitivity necessary to study DCX in heavy nuclei and here the nuclear chemist can make an important contribution. The current work on $^{88}Sr(\pi^-,\pi^+)^{88}Kr$ and $^{209}Bi(\pi^+,\pi^-)^{209-x}At$ should be continued and a few other targets such as ^{127}I with π^- might also be examined.

VII. SPALLATION, FRAGMENTATION, AND FISSION WITH INTERMEDIATE ENERGY PROJECTILES

Spallation

Studies of spallation reactions were reviewed by R. Segel. Both off-line measurements of residual-product cross sections and prompt (on-line) γ-ray measurements are utilized. The latter are well-suited to even-even nuclide identification, but have limited usefulness for odd mass nuclides. In addition, proton, deuteron, triton, ^3He, and ^4He particle spectra have been measured from proton bombardment[33,34] and proton spectra from pion bombardment[35,36] of various targets.

Higher cross sections are observed for pion spallation than for protons of about the same kinetic energy. The pion-induced yields of Ni isotopes show a concentration of cross section for the removal of 3-7 nucleons (Fig. 8) which is not seen with protons. This is interpreted as indicating that about four nucleons participate in the pion absorption. This effect is not seen in the pion spallation of ^{197}Au.[37] Data for the proton spallation of Ni are in good agreement with cascade-evaporation calculations, but the data for pion spallation are not.

For all but the lightest nuclei, the shapes of the proton spectra from pion interactions are similar for π^+ and π^- absorption, with the former yielding about 3 times as many protons. For two-step absorption through the Δ this ratio should be about 12. Again, participation of more than two nucleons in absorption may be indicated. A rapidity analysis indicates that the number of nucleons that share the incident pion's energy and momentum varies from about 3 to 6.

Measurements of p, d, T, ^{3}He, and α spectra from 100-MeV proton bombardment of various targets show only a weak, degraded peak attributable to quasi-free scattering at forward angles. This contrasts with the work of Wall and Roos,[38] who report a quasi-free peak dominating the proton spectra. However, the results are in good agreement with recent data from the University of Maryland.[39] At 800 MeV, a clear quasi-free peak is seen at 20° for all targets, but it becomes smeared out by 30° for all but the lightest targets.[40]

The relatively large cross section for producing ^{3}He from ^{58}Ni suggests that complex particle production may show a strong sensitivity to the composition of the nuclear surface.

Spallation is generally interpreted in terms of the two-step, intranuclear cascade-evaporation (INC) model.[41] Z. Fraenkel presented a comparison of the calculations of his group with a broad range of inelastic scattering data for protons[40] and pions,[42,43] pion single-charge exchange,[44] the number of protons emitted in π^+ and π^- absorption,[45] and proton and pion-induced spallation.[37] Calculated spallation cross sections show generally good agreement with proton bombardment data below $\sim$1 GeV, but poor agreement with pion bombardment data, particularly for energies below the (3,3) resonance. The INC calculations underestimate pion inelastic scattering and absorption at the lowest energies and overestimate them at energies above the (3,3) resonance. The discrepancy increases with increasing mass number of the target.

The INC calculations are in relatively good agreement with the data for inclusive particle emission in proton-nucleus interactions, but there is some disagreement as to how well the calculations fit the pion-nucleus data. Fraenkel's results show good agreement, but Segel's do not. This difficulty may be the result of the use of different calculation codes.

If, indeed, there is good agreement between the inclusive particle emission data for both proton-nucleus and pion-nucleus interactions and the INC calculations, this would indicate good understanding of the fast, cascade step in the mechanism which gives rise to the particle spectra observed. The systematic discrepancies

between data and calculation for the spallation cross sections may then be ascribed to an incomplete understanding of the slow (evaporation) step in the reaction mechanism or to additional mechanisms not included in the INC-evaporation models. At the present time, however, there remains a controversy over the agreement of the INC calculations with the pion-induced, inclusive particle data.

In general, the spallation product properties (e.g., yields, recoil and angular momenta) represent fully integrated information on the contributions from the cascade and evaporation steps in the assumed reaction mechanism. Hence, they would not appear to be very useful indicators of the characteristics of the individual steps. However, P. Karol pointed out that some selectivity may be obtained if one examines the properties of low-yield products on the wings of the mass and charge distributions as a function of the bombarding projectile (p,π^+, π^-,α). He also suggested that improvements in the evaporation calculation may be obtained by considering more realistic parameters for the cascade residue nuclei. Higher powers of the energy (rather than simply $E^{1/2}$) may have large effects on the level density calculated for nuclei at high temperature. The expansion of a hot nucleus may also affect the level density parameter as well as binding energies, Coulomb energies, and surface energies.

Systematics of the recoil properties of spallation and fragmentation products were reviewed by L. Winsberg. These suggest a clear distinction in these mechanisms for GeV proton-induced reactions. Similar studies of pion-induced reactions were suggested to provide a useful guide to the identification of reaction mechanisms and for comparison with proton data.

Fragmentation

N. T. Porile presented a review of proton- and pion-induced fragmentation reactions. Fragmentation only occurs to a significant extent at high bombarding energies. Excitation functions rise steeply up to 5-10 GeV before leveling off. At these high energies fragmentation accounts for a sizable fraction of σ_R over a broad range of target A. Individual fragment yields display a characteristic variation with target A which depends on fragment composition. The yields of neutron-excess fragments generally increase with target A while those of neutron-deficient fragments display the opposite trend. Fragmentation leads to a broad isotopic distribution of products of nuclides far from stability.

Because of the similar behavior of the excitation functions for fragment pion production, it was postulated long ago that fragmentation results from pion

production and subsequent reabsorption. While recent studies of fragment emission in reactions induced by pions (Fig. 9) indicate that the yields are higher than for protons of the same energy (yields are comparable to those for protons having $T_p \sim T_\pi + 140$ MeV) this cannot be the sole explanation of the process. It is well known that fragment emission also occurs in good yield for complex projectiles whose energy is such that the energy per nucleon is actually less than the pion production threshold. At higher energies, the fragmentation yields obtained in reactions induced by heavy ions are substantially larger than those obtained for protons of comparable energy. In fact, fragmentation appears to be the one process that does not obey the factorization hypothesis, according to which the yields should scale with σ_R.

The kinematics of fragmentation products undergo a remarkable change at a proton energy of ~3 GeV. The ratio of forward-to-backward emission (F/B) peaks rather sharply at this energy, a result that appears to be associated with a change in angular distribution from forward- to sideward-peaked. At the same time, the ranges of fragments, and hence their kinetic energies, decrease and the spectra broaden, as if increasing mass dissipation occurs prior to fragment emission. These results appear to be inconsistent with a two-step model involving a prompt intranuclear cascade followed by a slower breakup step. It has been postulated that at highly relativistic energies a near central collision of a proton instead involves a coherent interaction with a portion of the nucleus, with the fragments coming from the breakup of the spectator remnant. Such a process can qualitatively account for many of the kinematic changes.

Although considerable information about fragmentation has been obtained in recent years, the reaction mechanism is not, as yet, well understood. Experiments that are likely to increase our understanding of this process are outlined below.

Fast Pion-Induced Fission

Yields of fission and spallation products from 100-, 190-, and 350- MeV π^+ reactions with ^{238}U have been measured by radiochemical techniques at LAMPF.[46] The results show that:

1. The fission cross section is higher at 190 MeV, near the (3,3) resonance, than at 100 MeV (10-30%) and at 350 MeV (30-40%).
2. The reactions result in predominantly symmetric fission, centered around mass A = 110.

3. Neutron-deficient isotopes of elements from Sb to Ba are produced in fair yield, especially at 350 MeV, whereas such isotopes were not observed for elements between Mo and Cd, probably due to insufficient sensitivity. At Ga and As, yields of neutron-deficient isotopes were again detected.
4. The single-nucleon removal cross sections (^{237}U and ^{237}Pa yields) are very large (57-97 mb) despite the competition from fission.
5. Neutron-deficient Pb isotopes appear to be α- and EC-decay daughters of highly neutron-deficient Ra, Ac, and Th spallation products.

Comparison with proton-induced reactions in ^{238}U indicates that pions of equal total energy ($T\pi$ + 140 MeV) produce ratios of neutron-deficient isotopes to neutron-rich (fission) products comparable to those due to protons. However, due to the (3,3) resonance effect, pion fission cross sections between 100 and 190 MeV are somewhat larger than for protons in the 200 to 400-MeV kinetic energy range.

Future Directions for Spallation, Fragmentation, and Fission Studies

Spallation

1) More exclusive measurements, including
   a) Angular distributions of emitted particles
   b) π-particle, π-γ, particle-γ coincidence measurements
   c) Recoil properties of residual nuclei
2) Measurements of low-yield products on wings of Z,A distributions as a function of target N/Z and projectile to try to distinguish cascade and evaporation contributions.
3) Reconcile various INC codes and establish best treatment.

Fragmentation

1) Extend data for pion-induced fragmentation.
2) Systematic studies of the dependence of fragmentation properties on projectile and target A.
4) Determination of the multiplicity and energy and angular distribution of particles accompanying fragment emission.

Fission

The mechanism for the production of neutron-deficient isotopes in the A = 60 to 140 mass region is not well understood. Since protons of kinetic energy equal to that of the pion plus 140 MeV seem to produce comparable residual product yield ratios, the protons, due to higher available fluxes should be utilized for

further studies of this process. A careful survey of yields of neutron-deficient isotopes in elements from Cu to Ce plus recoil measurements on isotopes of elements from Cu to Sn, should provide valuable information for the understanding of the mechanism.

REFERENCES

1. H. S. Pruys, R. Engfer, H. P. Isaak, T. Kozlowski, U. Sennhauser, H. K. Walter, and A. Zglinski, pp. of these proceedings.

2. H. S. Pruys, R. Engfer, R. Hartmann, U. Sennhauser, H.-J. Pfeiffer, H. K. Walter, J. Morgenstern, A. Wyttenbach, E. Gadioli, and E. Gadioli-Erba, Nucl. Phys. A316, 365 (1979).

3. H. S. Pruys, R. Engfer, R. Hartmann, E. A. Hermes, H. P. Isaak, F. W. Schlepütz, U. Sennhauser, W. Dey, K. Hess, H.-J. Pfeiffer, H. K. Walter, and W. Hesselink, SIN-Preprint PR-80-009 (1980), to be published.

4. J. Hüfner and H. C. Chiang, "Theory of Precompound Reactions and Nucleon Spectra after Pion Absorption", pp. of these Proceedings.

5. B. J. Dropesky, G. C. Giesler, C. J. Orth (Spokesman), and R. S. Rundberg, LAMPF Exp. 415.

6. Lon-chang Liu is currently responsible for the improvements to and utilization of the VEGAS(ISOBAR) intranuclear cascade and DFF evaporation codes at LASL and is particularly concerned with comparisons of the ISOBAR model with experimental studies of fast- and stopped-pion reactions.

7. J. Julien, R. Letourneau, L. Rousell, R. Legrain, Y. Cassagnou, R. Fonte, and A. Palmeri, Phys. Rev. C (in press).

8. E. Gadioli and E. Gadioli-Erba, Nucl. Phys. A255, 414 (1976); E. Gadioli, private communication; E. Gadioli and E. Gadioli-Erba, Nucl. Phys. A256, 414 (1976), and private communication.

9. A. S. Iljinov, V. I. Nazaruk, and S. E. Chigrinov, Nucl. Phys. A268, 513 (1976).

10. D. F. Jackson, A. A. Ioannides, and A. W. Thomas, Nucl. Phys. A322, 493 (1979).

11. M. M. Sternheim and R. R. Silbar, Phys. Rev. C21, 1974 (1980).

12. B. J. Dropesky et al., Phys. Rev. Lett. 34, 821 (1975); Phys. Rev. C20, 1844 (1979); L. H. Batist et al., Nucl. Phys. A254, 480 (1975).

13. M. M. Sternheim and R. R. Silbar, Phys. Rev. Lett. 34, 824 (1975).

14. Marianne Hamm et al., to be published.

15. P. Karol, "Relevance of Final State Nucleon-Nucleon Charge Exchange in Inclusive (π,πN) Reactions," Phys. Rev. C (in press).

16. J. Bolger et al., to be published; D. Asheri et al., Phys. Rev. C, to be published.

17. H. E. Jackson and R. E. Segel, private communication.

18. V. G. Lind et al., Phys. Rev. Lett. 41, 1023 (1978); R. E. McAdams et al., to be published; V. G. Lind et al., LAMPF Exp. 439, in progress; C. Orth, D. Vieira, (Cospokesmen) et al., LAMPF Exp. 595.

19. L. W. Swenson et al., Phys. Rev. Lett. 40, 10 (1978); H. J. Ziock et al., Phys. Rev. Lett. 43, 1919 (1979) and preprint (1980); C. H. Q. Ingram et al., SIN Newsletter No. 12, p. 48 (Dec. 1979) and P. Gram, private communication; H. K.Walker, contribution to this Workshop; M. Hamm, et al. LAMPF Exp., in progress.

20. R. S. Rundberg, B. J. Dropesky, G. C. Giesler, G. W. Butler, S. B. Kaufman, E. P. Steinberg, and A. A. Caretto, to be published.

21. G. W. Butler, C. J. Orth, R. S. Rundberg, and D. J. Vieira (Spokesman), LAMPF Exp. 459.

22. Y. Shamai, J. Alster, D. Ashery, S. Cochavi, M. A. Moinester, A. I. Yavin, E. D. Arthur, and D. M. Drake, Phys. Rev. Lett. 36, 82 (1976).

23. G. W. Butler, B. J. Dropesky, W. Faubel, G. C. Giesler, N. Imanishi, R. S. Rundberg (Spokesman), and D. J. Vieira, LAMPF Exp. 553.

24. J. D. Bowman, Nucl. Phys. A335, 375 (1980).

25. G. W. Butler, B. J. Dropesky, N. Imanishi (Spokesman), R. S. Rundberg, and D. J. Vieira (Co-Spokesman), LAMPF Exp. 555.

26. Y. A. Batusov et al., Sov. J. Phys. 18, 250 (1974).

27. J. Warszawski and N. Averbach, Nucl. Phys. A276, 402 (1977).

28. L.-C. Liu, Bull. Am. Phys. Soc. 25, 606 (1980).

29. W. R. Gibbs, B. F. Gibson, A. T. Hess, G. J. Stephenson, and W. B. Kaufman, Phys. Rev. Lett. 36, 85 (1976).

30. N. Auerbach, Phys. Rev. Lett. 38, 840 (1977).

31. M. Johnson, "LAMPF Workshop on Pion Single Charge Exchange, " Los Alamos, Scientific Laboratory report LA-7892-C (January 1979) pp. 343.

32. J. F. Germond and C. Wilkin, Lett. Nuovo Cimento 13, 605 (1975).

33. M. Sadler et al., Phys. Rev. Lett. 38, 950 (1977).

34. M. Sadler et al., Phys. Rev. C21, 2303 (1980).

35. H. E. Jackson et al., Phys. Rev. Lett. 35, 641 (1975).

36. H. E. Jackson et al., Phys. Rev. C18, 2656 (1978).

37. S. B. Kaufman, E. P. Steinberg, and G. W. Butler, Phys. Rev. C20, 2293 (1979).

38. N. S. Wall and P. R. Roos, Phys. Rev. 150, 811 (1966).

39. J. R. Wu, C. C. Chang, and H. D. Holmgren, Phys. Rev. C19, 698 (1979).

40. R. E. Chrien et al., Phys. Rev. C21, 1014 (1980).

41. G. D. Harp, Phys. Rev. C10, 2387 (1974) and references therein.

42. I. Navon et al., Phys. Rev. Lett. 42, 1465 (1979).

43. D. Ashery et al., Tel Aviv University preprint (to be published).

44. R. E. Mischke et al., Phys. Rev. Lett. 44, 1197 (1980).

45. R. D. McKeown et al., Phys. Rev. Lett. 44, 1033 (1980).

46. B. P. Bayhurst, B. J. Dropesky (Spokesman), C. J. Orth, R. J. Prestwood, R. S. Rundberg, and K. Wolfsberg, LAMPF Exp. 416.

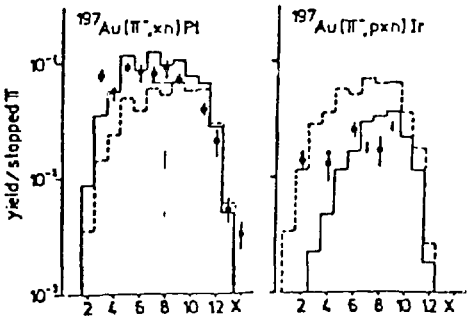

Fig. 1.

Yields of Pt and Ir isotopes produced from π^- absorption in ^{197}Au. The experimental points are compared with calculations starting with π^- absorption either on a np pair (full histogram) or a pp pair (dashed histogram).

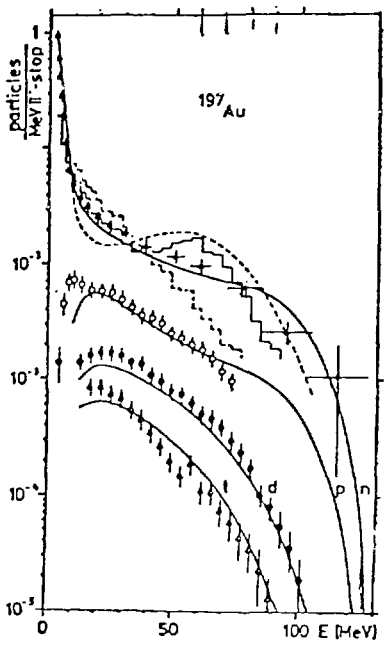

Fig. 2.

Energy spectra of neutrons, protons, deuterons, and tritons emitted from π^- absorption in ^{197}Au. The experimental points are compared with the present calculation (quasi-deuteron absorption, R = 2.0, full curves), the calculation of Gadioli and Gadioli-Erba[8] (quasi-deuteron absorption, R = 4.0, dashed curved) and the calculations of Ilijinov et al.[9] using either quasi-deuteron absorption (R = 3.03, full histogram) for α-cluster absorption (dashed histogram).

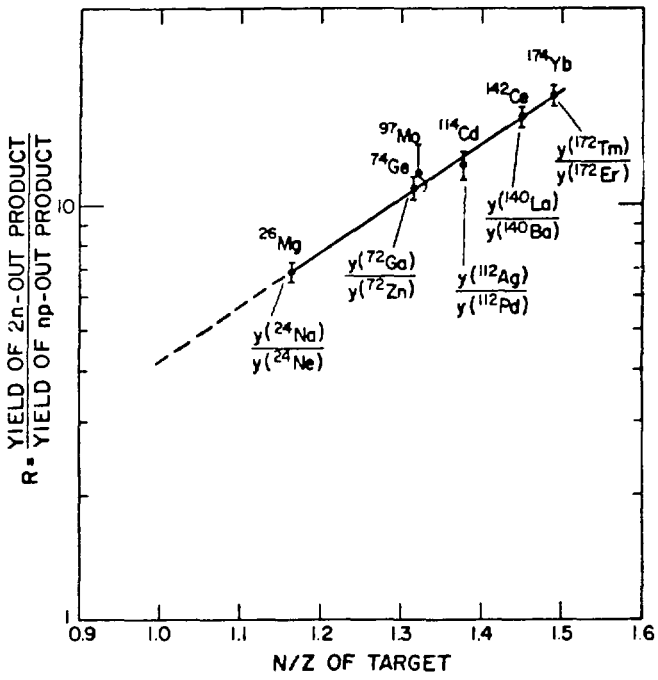

Fig. 3.

Ratios of 2n- to np-out-product yields versus N/Z of the target nucleus for stopped π^- reactions. The results for ^{97}Mo are preliminary. Extrapolation of the line to N/Z = 1 gives R = 4.2 compared with 3 ± 1 given in Ref. 6.

Fig. 4.

Left: Neutron energy spectra taken in coincidence with pionic X-rays and with ^{26}Al, ^{24}Mg, ^{23}Na, and ^{21}Ne γ-rays following the absorption of stopped π^- in ^{28}Si. Only statistical errors are indicated. The dashed curve, in the case of ^{26}Al, is a Gaussian distribution peaked at 55 MeV, i.e., half the total available energy (pion mass minus the proton and neutron binding energies in ^{28}Si). Full curves for ^{24}Mg and ^{21}Ne are from a preliminary calculation including preequilibrium and evaporation and starting from the above ^{26}Al dashed distribution to describe the first interaction of the π^- with a nucleon pair.[7]
Right: Proton energy spectra following the absorption of 70 MeV π^- by ^{28}Si for ^{26}Al, ^{24}Mg, and ^{21}Ne channels and for all channels.

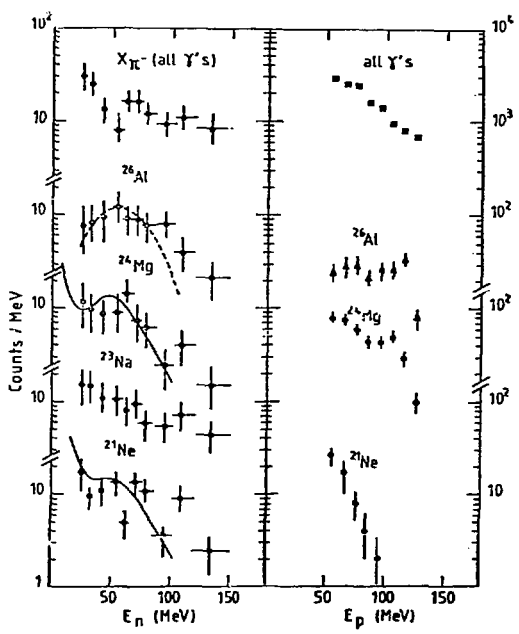

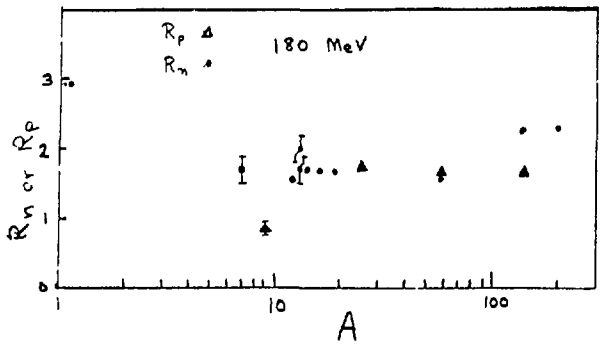

Fig. 5.

R_p and R_n ratios with 180-MeV pions as a function of the mass number of the target. (E.P. Steinberg, S.B. Kaufman, and G.W. Butler, reported at Intl. Conf. on Nuclear Reaction Mech., Varenna, Italy, June 18-21, 1979).

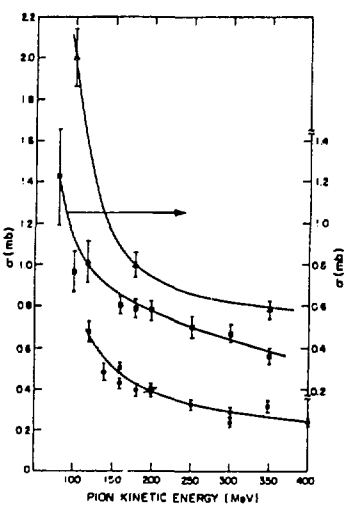

Fig. 6.

Excitation functions for single charge exchange reactions using activation techniques.
■= $^{27}Al(\pi^-,\pi^0)^{27}Mg$,
●= $^{65}Cu(\pi^-,\pi^0)^{65}Ni$,
▲= $^{45}Sc(\pi^+,\pi^0)^{45}Ti$.

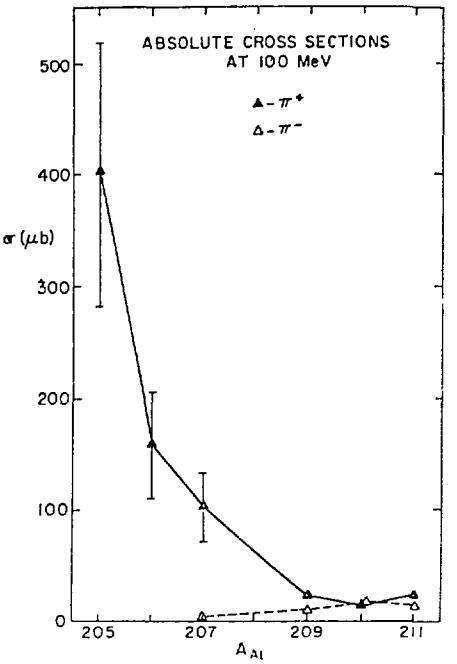

Fig. 7.

Astatine formation cross sections for 100 MeV π^+, π^- irraditions of Bismuth.

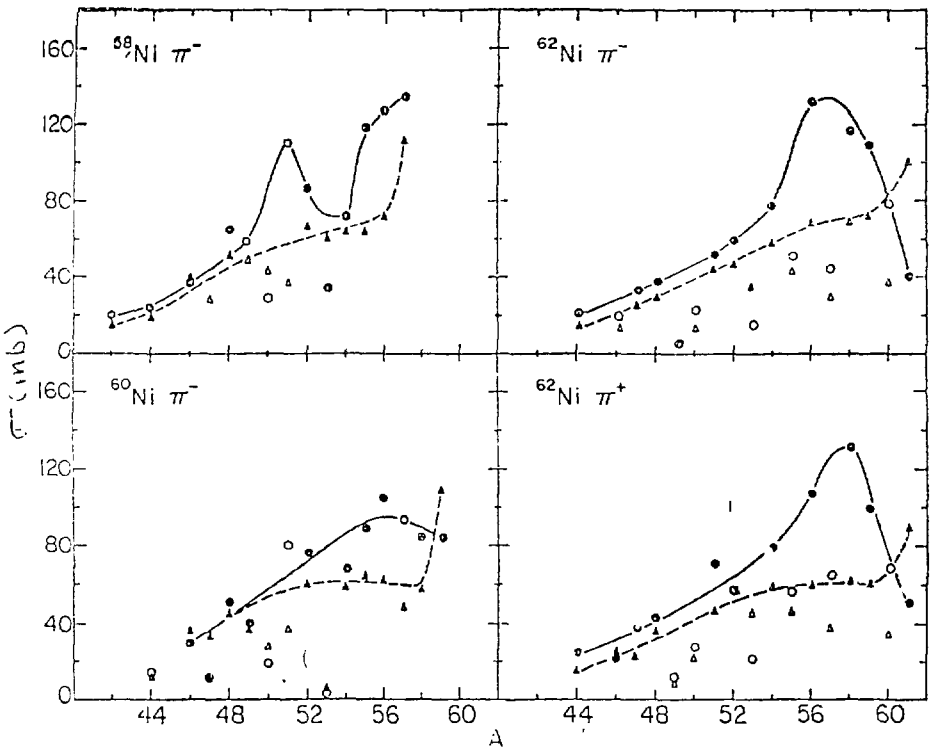

Fig. 8.

Nuclide production cross sections for (a) 220-MeV π^- in ^{58}Ni,$_+$(b) 220-MeV π^- on ^{60}Ni, (c) 220-MeV π^- on ^{62}Ni, and (d) 220-Mev π^- on ^{62}Ni as a function of A. The cross sections for all isobars observed in the prompt and delayed γ spectra have been summed to give each solid or open circle; the latter symbol is used for those A values for which a significant amount of cross section is likely to have been missed. The triangles show the results of the cascade calculation including only the observed nuclides, with open triangles used for those A values where a substantial portion of the yield is believed to be in nuclides not observed. The solid lines indicate the trends in the data, the dashed lines in the calculations.

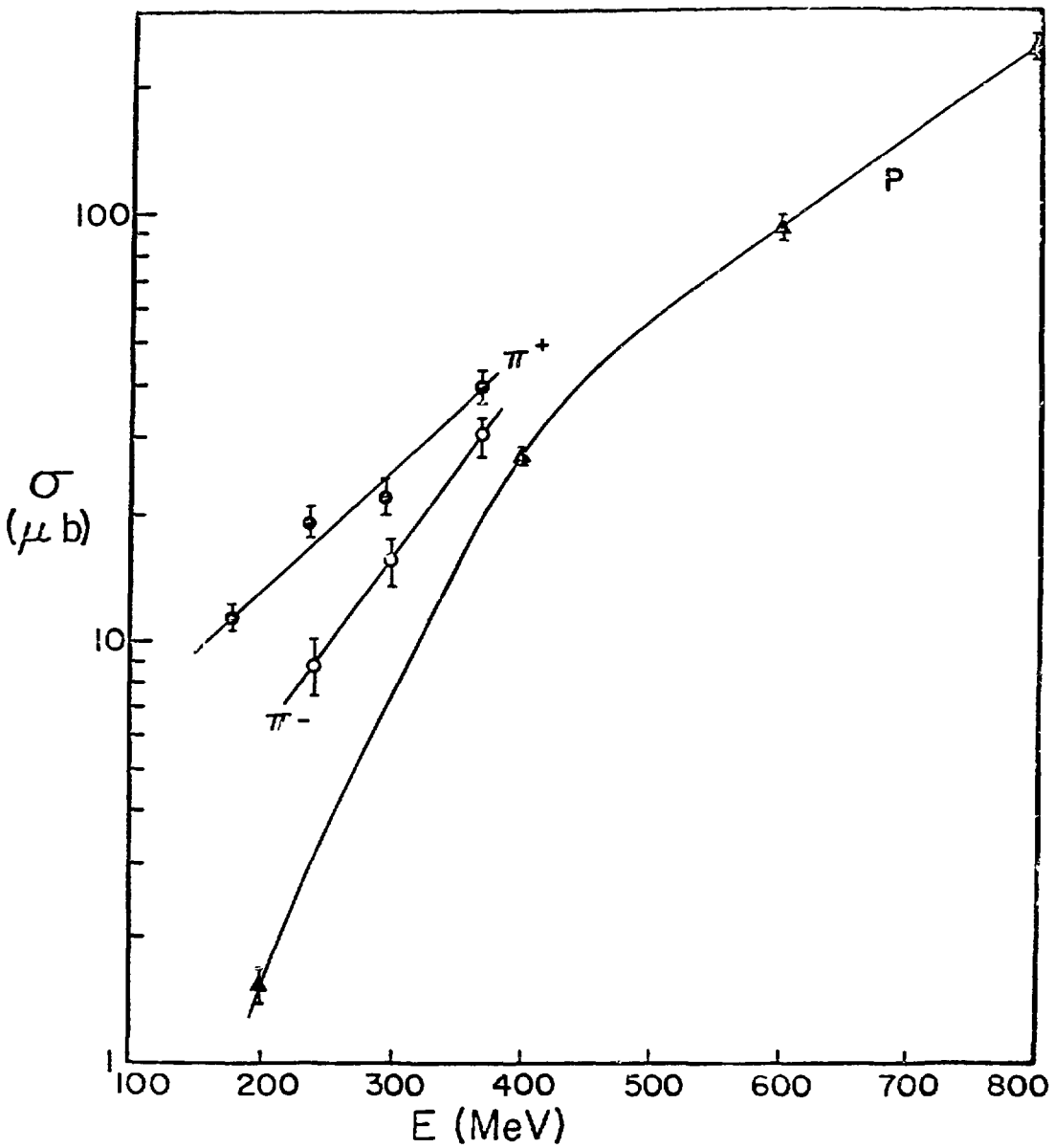

Fig. 9.

Excitation functions for the formation of ^{24}Na from gold by protons, π^+, and π^-.

APPENDIX A

PION-NUCLEUS REACTIONS

Final Program

Chairman - E. P. Steinberg

Co-chairman - C. J. Orth

Wednesday, June 25

8:30-10:00 - Stopped Pion Reactions

H. Pruys - Particles and Residual Products from the Interaction of Stopped Pions with Nuclei

J. Hüfner - Model for Calculating Nucleon Spectra

C. Orth - Yield of 2-Nucleon-Out Products

J. Julien - N-γ Coincidence Reactions in Si

Discussion

10:00-10:30 - Coffee

10:30-12:00 - Fast Pions, Single Nucleon Removal (SNR)

M. Sternheim - Theory

H. Plendl - Experiments

E. Steinberg - SNR Reactions in ^{25}Mg, ^{58}Ni, ^{142}Ce, and ^{196}Au

N. Imanishi - Light Target Studies at KEK

Discussion

12:00-13:30 - Lunch

13:30-15:00 - Charge Exchange (Single (SCX) and Double (DCX))

R. Rundberg - SCX Reactions in ^{13}C, ^{27}Al, ^{45}Sc, and ^{65}Cu

K. Seth - Review DCX Reaction Studies

J. Clark - DCX in ^{209}Bi

Discussion

15:00-15:30 - Coffee

15:30-17:00 - Charge Exchange (Cont.)

W. Gibbs - Theory

Thursday, June 26

Morning: NC-5 and NC-6 Sessions only

13:30-15:00 - NC-1 and NC-2 Joint Session on Pion and Proton Spallation, Fragmentation and Fission

R. Segel - Spallation

P. Karol - Spallation

L. Winsberg - Systematics of Recoil Properties

Discussion

15:00-15:30 - Coffee

15:30-17:00 - Spallation, Fragmentation, and Fission (Cont.)

N. Porile - Fragmentation

Z. Fraenkel - Theoretical Comments

Discussion

Friday, June 27

08:30-10:00 - Plenary Panel Reports

08:30 - E. Steinberg, Chairman - NC-1

APPENDIX B

PARTICLES AND RESIDUAL PRODUCTS FROM THE INTERACTION OF STOPPED PIONS WITH NUCLEI

by

H.S. Pruys, R. Engfer, H.P. Isaak, T. Kozlowski,

U. Sennhauser, H.K. Walter, and A. Zglinski

University of Zürich, c/o SIN

ABSTRACT

Recently measured yield distributions of residual products and neutron and charged particle spectra from π^- absorption in nuclei are compared with statistical calculations. Upper limits of about 30% can be given for the amount of α-cluster absorpsion. Model dependent values for the ratio R of np to pp pairs that can absorb the pion are 2.3 ± 0.6 for ^{12}C, 1.1 ± 0.3 for ^{59}Co, and 2.0 ± 0.5 for ^{197}Au.

I. INTRODUCTION

Due to energy and momentum conservation a π^- at rest is absorbed by correlated nucleons in a nucleus.[1] Sharing the pion rest mass, these nucleons can either be directly emitted or undergo final state interactions. A large amount of the available energy is thus carried away by a few energetic particles. The remaining highly excited nucleus de-excites by particle evaporation and γ-ray emission. Finally, the unstable nucleus decays by β-emission or electron capture.

To get the complete information on each step of the absorption process, we used different experimental techniques. In a series of experiments, neutron, charged particle, and γ-ray spectroscopy were applied to investigate π^- absorption in light, medium, and heavy nuclei.[2-4] In the present paper the results of these experiments are discussed and compared with statistical calculations.[3,5-7]

In our discussion we will concentrate on two important questions:

1. The importance of pion absorption on α-clusters in nuclei. Experimental and theoretical investigations support the quasi-deuteron model of pion absorption, whereas pion absorption on an α-cluster seems to be of minor importance.[1,8] A recent calculation of pion absorption rates in light nuclei shows that at most 10 to 20% of the absorption could be explained by mechanisms involving more than two nucleons.[9] By measuring neutron-triton coincidences after pion absorption in ^{12}C an estimate of $\geq 4.6\%$ per stopped pion of the amount of α-cluster absorption was obtained by Lee et al.[10]

The branching ratios for π^- absorption in ^4He have been measured to be:

$\pi^- + {}^4He \rightarrow$	t + n	(19.4 ± 1.8) %	{ref. 11}
	d + 2n	(58 ± 7) %	{ref. 12}
	p + 3n	(26 ± 6) %	{ref. 12}

By assuming the same ratios for π^- absorption on α-clusters in nuclei, we can derive some upper limits from our data.

2. The ratio R of np to pp pairs that can absorb the pion in the case of quasi-deuteron absorption. This ratio is not known, but neglecting spin effects, one expects for statistically distributed protons and neutrons in a nucleus absorption probabilities $w_{np} \simeq NZ + ZN$ and $w_{pp} \sim Z(Z-1)$ yielding

$$R = \frac{2N}{Z-1}$$

with N and Z the number of neutrons and protons in the target nucleus. Model dependent values for R can be derived by fitting the experimental data to calculations using R as a free parameter.

The interpretation of the experimental data in connection with these two questions will be given in detail for ^{197}Au since most calculations are performed for this nucleus or a similar heavy nucleus. In sections 2 and 3 the yield distribution of residual nuclei and the energy spectra of neutrons, protons, deuterons,and tritons are analyzed. In section 4 a summary of the results and the conclusions are given.

II. YIELDS OF RESIDUAL PRODUCTS FROM π^- ABSORPTION IN NUCLEI

In Fig. 1 experimental yields of Pt isotopes produced in the $^{197}Au(\pi^-,xn)Pt$ reactions are given. Calculations of Iljinov et al.[6] using π^- absorption either

on a quasi-deuteron or on an α-cluster are also shown. Clearly the experimental data can be explained by the quasi-deuteron absorption alone. To get a quantitative estimate of the amount of α-cluster absorption, a least squares fit has been plotted as a function of the percentage of α-cluster absorption (see insert in Fig. 1). From this fit an upper limit of about 8% can be derived. Since in the calculation only the complete break-up of the α-cluster into four nucleons has been considered we have to divide this 8% by 0.26 the probability for this channel giving 31% for the probability of α-cluster absorption. From a similar analysis for ^{75}As and ^{209}Bi the same upper limit of about 30% has been obtained.

In Fig. 2 the measured yields of Pt and Ir, isotopes produced in the ^{197}Au (π^-,xn)Pt and ^{197}Au(π^-,pxn)Ir reactions are compared with our calculations starting with π^- absorption either on a np pair or on a pp pair. The measured total yield extrapolated for the unmeasured isotopes is (74 ± 8)% per stopped pion for the xn reactions. The calculations give 79% for np absorption and 49% for pp absorption. For the pxn reactions the total measured yield is (20 ± 7)%, the calculated one is 17% for np absorption and 45% for pp absorption. In Fig. 3 the calculated values for the total yields of xn and pxn reactions are given as a function of R, the ratio of np to pp pair absorption. From a comparison with the experimental values a lower limit for R of 1.5 can be obtained. A similar analysis for ^{59}Co (Fig. 4) and ^{75}As gives lower limits of 1.2 and 1.5, respectively. Calculations of Gadioli and Gadioli-Erba[3,5] give the same result for ^{75}As and ^{197}Au (Fig. 3), whereas in the case of ^{59}Co (Fig. 4) the results are quite different. The reason for this disagreement is not clear.

III. ENERGY SPECTRA OF NEUTRONS AND CHARGED PARTICLES FROM π^- ABSORPTION IN NUCLEI

In Fig. 5 the experimental energy spectra of neutrons, protons, deuterons, and tritons emitted from π^- absorption in ^{197}Au are shown. The neutron energy was obtained by time-of-flight and thus the energy resolution worsens with increasing energy. The endpoint of the proton spectrum was given by the thickness of the Ge-detector used for the charged particle measurements.

Comparison of the measured neutron spectrum with the calculations of Iljinov et al.[6] (see Fig. 5) again favours quasi-deuteron adsorption, but the bump predicted at ~55 MeV is missing in the experimental spectrum. This bump is even more pronounced in the calculation of Gadioli and Gadioli-Erba,[5] whereas the present calculation does not show any enhancement (see Fig. 5). These differences can be explained by the different assumptions regarding the distribution of the

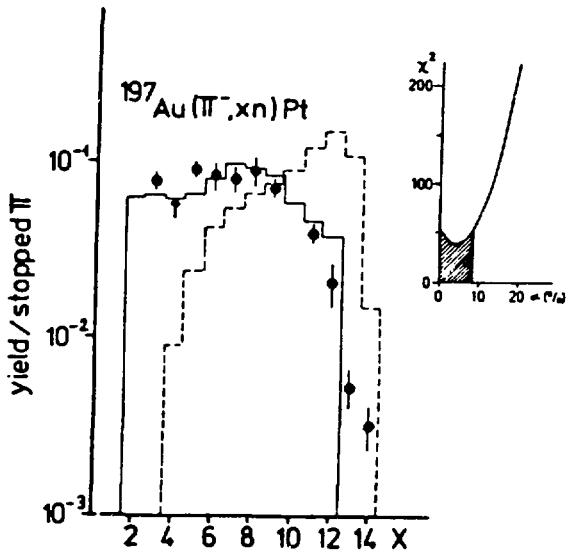

Fig. 1.

Yields of Pt isotopes produced from π^- absorption in ^{197}Au. The experimental points are compared with calculations of Iljinov et al.[6] using either quasi-deuteron absorption (R = 3.03, full histogram) or α-cluster absorption (dashed histogram). The insert shows a chi-square analysis indicating an amount of α-cluster absorption less than 8%.

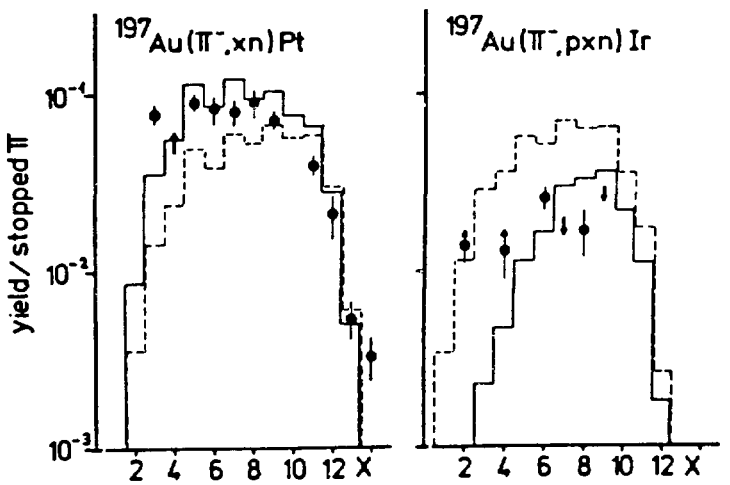

Fig. 2.

Yields of Pt and Ir isotopes produced from π^- absorption in ^{197}Au. The experimental points are compared with calculations starting with π^- absorption either on a np pair (full histogram) or a pp pair (dashed histogram).

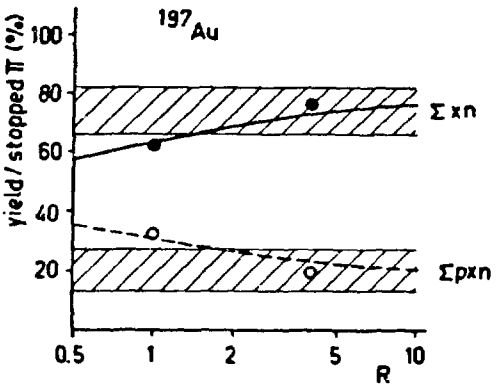

Fig. 3.

Calculated total yields of the $^{197}Au(\pi^-,xn)Pt$ and $^{197}Au(\pi^-,pxn)Ir$ reactions (full and dashed curves from the present calculation, full and open circles from the calculation of Gadioli and Gadioli-Erba[3,5]) are compared with experimental yields (hatched bands) for different ratios R of np to pp pair absorption.

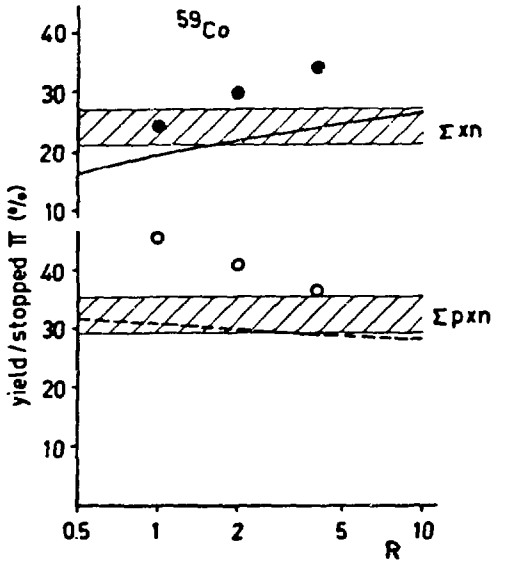

Fig. 4.

As Fig. 3 for π^- absorption in ^{59}Co.

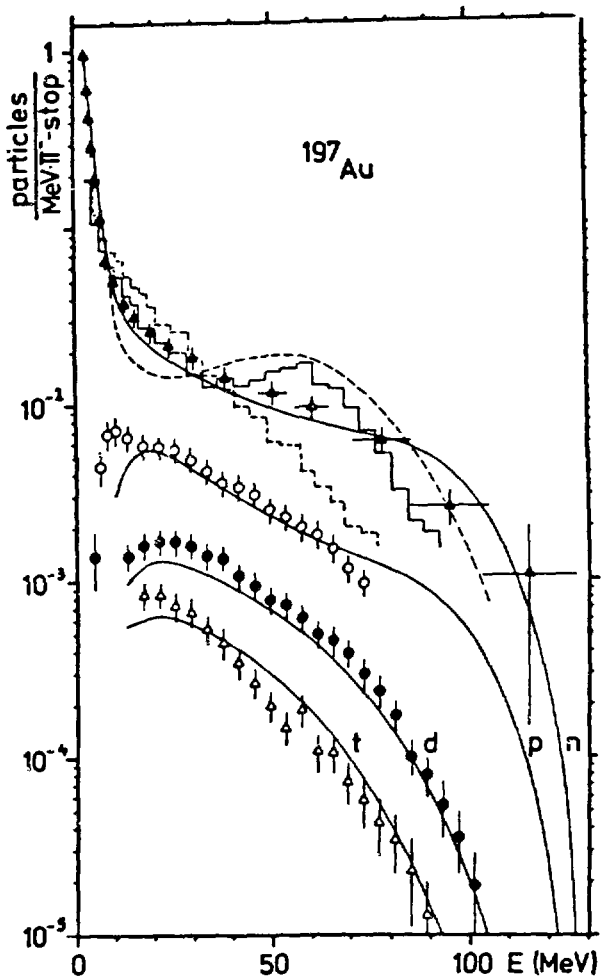

Fig. 5.

Energy spectra of neutrons, protons, deuterons, and tritons emitted from π^- absorption in ^{197}Au. The experimental points are compared with the present calculation (quasi-deuteron absorption, R = 2.0, full curves), the calculation of Gadioli and Gadioli-Erba[5] (quasi-deuteron absorption, R = 4.0, dashed curve) and the calculation of Iljinov et al.[6] using either quasi-deuteron absorption (R = 3.03, full histogram) or α-cluster absorption (dashed histogram).

initial energy among the two particles and two holes. In contrast to our calculation this energy is not statistically distributed in the two other calculations[5,6] due to the assumption that the two nucleons are emitted preferentially back to back. Therefore, any statement about the amount of α-cluster absorption would be model dependent. Our calculation agrees well with the experiment without any α-cluster absorption, whereas the calculation of Gadioli and Gadioli-Erba[5] would agree much better with the experiment if a considerable amount of α-cluster absorption were assumed. Because of this model dependence no conclusion can be obtained from the neutron spectrum. However, a rough estimate on the amount of α-cluster absorption can be obtained from the measured total yield of 2.5% of tritons. Since the pion is absorbed on the nuclear surface, about 50% of the tritons will escape from the nucleus. Thus, using the measured branching ratio for the t+n channel, a value of 25% is obtained. This value is an upper limit since triton emission can be explained also by secondary interactions of the primary nucleons formed in a quasi-deuteron absorption. Indeed, the calculated spectra for deuterons and tritons are in good agreement with the experimental spectra (Fig. 5). For ^{12}C and ^{59}Co an upper limit of 40% and 28% α-cluster absorption was estimated from the yield of high energy (E > 20 MeV) tritons.

The ratio R of np to pp pair absorption can be estimated from the yields of high energy (E > 20 MeV) neutrons and protons. Assuming that they come directly from π^- absorption on a np or a pp pair we obtain R = 2.0 ± 0.5 for ^{197}Au. However, due to charge-exchange scattering of the primary nucleons this estimate gives a lower limit only. Therefore, a comparison of the neutron and proton yields at the high energy end of the spectra would give a better estimate. Unfortunately the proton spectrum has not been measured above 77 MeV and the neutron spectrum has a low accuracy in the interesting energy region. The estimates for ^{12}C and ^{59}Co are 2.3 ± 0.6 and 1.1 ± 0.3. For the Ni isotopes the estimates for R vary from 0.7 to 1.7. In Fig. 6 the calculated yields of high energy neutrons and protons are given as a function of R. A comparison with the experimental yields gives the limits 1.2 < R < 3, in agreement with the estimate above. For ^{59}Co the calculated spectra of neutrons and protons are in fair agreement with the experimental spectra for R = 1. This value is somewhat lower than the value of 1.5 obtained from the xn total reaction yield.

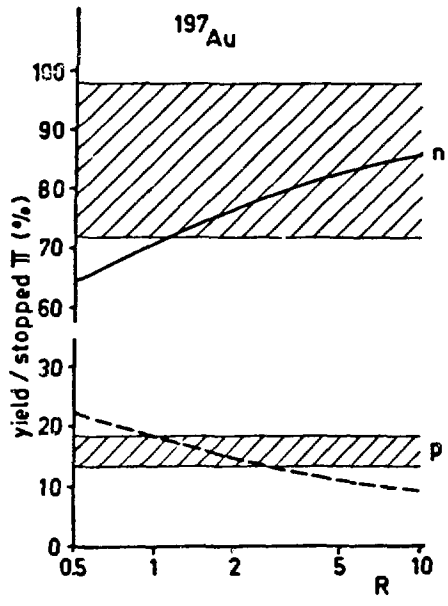

Fig. 6.

Calculated yields of high energy neutrons (E > 20 MeV) and protons (20 to 70 MeV) emitted from π^- absorption in ^{197}Au are compared with experimental yields (hatched bands) for different ratios R of np to pp pair absorption.

IV. SUMMARY AND CONCLUSION

In Fig. 7 the upper limits for pion absorption on an α-cluster are given as a function of A. These limits are derived from a comparison of measured yield distributions with calculations[6] and from the triton spectra. In both cases absorption on an α cluster is not needed to explain the data but a contribution up to about 30% cannot be excluded.

In Fig. 8 values for R, the ratio of np to pp pairs that can absorb the pion, are given as function of N/Z-1. These values are derived from the experimental yields of high energy neutrons and protons. Due to charge-exchange scattering of the primary nucleons these values could be too low. Our calculation shows that this effect is of minor importance and can be neglected for a rough estimate. The values for ^{12}C and ^{197}Au agree with the mean value of 3 ± 1 obtained by Nordberg et al.[13] for many light nuclei and with the expected value of 2N/Z-1. For ^{59}Co and the Ni isotopes the estimates for R are significantly lower. In addition the dependence on N/Z-1 is stronger than one expects from binding energy differences and a 2N/Z-1 dependence. Further experimental and theoretical

investigations are necessary to understand this behaviour. More reliable values for R could be obtained by an accurate measurement of the neutron and proton spectra at the highest energies and by measuring nn and np coincidences.

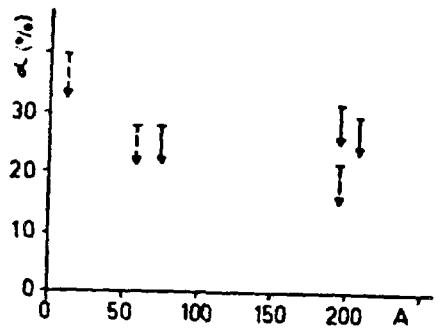

Fig. 7.

Upper limits for the amount of π^- absorption on an α-cluster in ^{12}C, ^{59}Co, ^{75}As, ^{197}Au, and ^{209}Bi obtained from a comparison of calculated[6] and measured yields of residual nuclei (full arrows) and from the yield of high energy tritons (E > 20 MeV, dashed arrors).

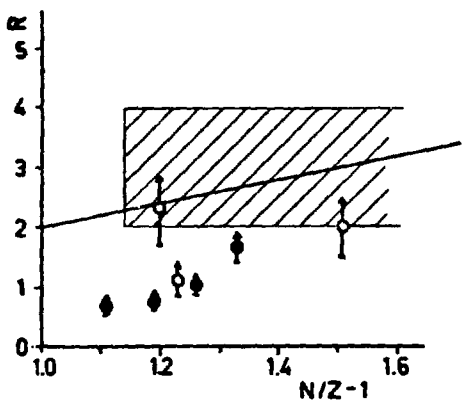

Fig. 8.

Estimates for the ratio R of np to pp pairs that can absorb the pion as a function of N/Z-1. Open circles are for ^{12}C, ^{59}Co, and ^{197}Au (with absolute errors). Full circles are for the nickel isotopes (relative errors only, the common error in the absolute normalization is 15%; the values are not corrected for binding energy differences). The mean value of 3 ± 1 obtained by Nordberg et al.[13] for many light nuclei with large N/Z-1 variation is indicated by the hatched band. The straight line shows the expected value 2N/Z-1.

REFERENCES

1. J. Hüfner, Phys. Report 21C, 1 (1975).

2. R. Hartmann, H. P. Isaak, R. Engfer, E. A. Hermes, H. S. Pruys, W. Dey, H.-J. Pfeiffer, U. Sennhauser, H. K. Walter, and J. Morgenstern, Nucl. Phys. A308, 345 (1978).

3. H. S. Pruys, R. Engfer, R. Hartmann, U. Sennhauser, H.-J. Pfeiffer, H. K. Walter, J. Morgenstern, A. Syttenbach, E. Gadioli, and E. Gadioli-Erba, Nucl. Phys. A316, 365 (1979).

4. H. S. Pruys, R. Engfer, R. Hartmann, E. A. Hermes, H. P. Isaak, F. W. Schlepütz, U. Sennhauser, W. Dey, K. Hess, H.-J. Pfeiffer, H. K. Walter, and W. Hesselink, SIN-Preprint PR-80-009 (1980), to be published.

5. E. Gadioli and E. Gadioli-Erba, Nucl. Phys. A256, 414 (1976); E. Gadioli, Private communications.

6. A. S. Iljinov, V. I. Nazaruk, and S. E. Chigrinov, Nucl. Phys. A268, 513 (1976).

7. T. Kozlowski and A. Zglinski, Nucl. Phys. A305, 368 (1978), to be published.

8. H. K. Walter, Proc. 7th Int. Conf. on High Energy Physics and Nuclear Structure, Zürich (Birkhaüser Verlag, Basel, 1977, Exp. Suppl. 31) p. 225.

9. G. F. Bertsch and D. O. Riska, Phys. Rev. C18, 317 (1978).

10. D. M. Lee, R. C. Minehart, S. E. Wobottka, and K. O. H. Ziock, Nucl. Phys. A197, 106 (1972).

11. M. M. Block, T. Kikuchi, D. Koetke, J. Kopelman, C. R. Sun, R. Walker, G. Culligan, V. L. Telegdi, and R. Winston, Phys. Rev. Lett. 11, 301 (1963).

12. F. Calligaris, C. Cernigoi, I. Gabrielli, and F. Pellegrini, Proc. 3rd Int. Conf. on High Energy Physics and Nuclear Structure, Columbia University (Plenum Press, N.Y., 1970) p. 367.

13. M. E. Nordberg.Jr., K. F. Kinsey, and R. L. Burman, Phys. Rev. 165, 1096 (1968).

APPENDIX C

PION DOUBLE CHARGE EXCHANGE

by

Kamal K. Seth

Northwestern University, Evanston, Il 60201*

A charge exchange (CX) reaction is naturally one which changes the charge of a nucleus without changing its atomic mass. Since the charge in the nucleus is carried by protons (we ignore quarks and quark bags in this discussion), it means that in a charge exchange reaction one or more neutrons change into protons or vice versa, i.e.,

$$X(A,Z) \rightarrow Y(A,Z'), \text{ with } |Z' - Z| = 1,2.... \tag{1}$$

The most common and familiar example of charge exchange is provided by nuclear β-decay

$$X(A,Z) \rightarrow Y(A,Z\pm 1) + \overset{+}{e} + \nu \tag{2}$$

with a neutron changing into a proton or vice versa. The β-decay process involves the weak interaction. Charge exchange can take place via hadronic interactions as well, and the most familiar example is provided by the well known (p,n) reaction,

$$X(A,Z) + p \rightarrow Y(A,Z+1) + n. \tag{3}$$

The same can be done by other reactions (^{3}He,t), (π^+,π^0), etc. Notice that both "reactions" (2)and (3) are <u>single charge exchange</u>, (SCX) reactions in which

---

* Supported in part by the U. S. Department of Energy.

nuclear charge changes by one unit only. To change charge by two units we would have to think of such improbable processes as double β-decay. Double charge exchange (DCX) reactions, in which

$$X(A,Z) \rightarrow Y(A,Z\pm2) \tag{4}$$

can in principle be performed with heavy ions and a few of them have been recently attempted. It is, however, fair to say that DCX reactions can be far more conveniently done with pions.[1] Since pions have isospin T = 1 and three charge states +1, 0, and -1, the reactions (π^+,π^-) and (π^-,π^+) are extremely clean DCX reactions, in contrast to heavy-ion DCX reactions which have to be identified in the presence of a large variety of reactions with many particle species and charge states.

Since too many medium energy physics experiments tend to be familiar experiments of low energy physics done with different particles or at different energies, it might appear that the uniqueness of pion DCX is reason enough to make it interesting to study. However, it can hardly be sufficient reason to launch into a program of what are obviously difficult experiments. What then is the lure of DCX? Superficially, DCX appears to just consist of two successive steps of SCX. However, the physics content of the DCX reaction is all its own. Let me illustrate this by three points.

Consider first the richness of the isospin spectra accessible to DCX. In Fig. 1(a) we see the isospin states which can be reached by inelastic or charge exchange scattering of isospin, T = 1/2 projectiles (common nuclear projectiles). In Fig. 1(b) we see the much greater wealth of isospin with a T = 1 projectile, the pion. In principle, one can study states ranging from $T = T_z$ to $T = T_z + 5$ in (π^+,π^-) DCX reactions!

The next point concerns one of the most fascinating and most elusive problems in nuclear structure, i.e. short-range correlations. It is, of course, quite clear that whatever correlations exist, at some level or another they affect all the observables of nuclear physics. It doesn't follow, however, that all these observables are equally good probes for studying correlations - even though at one time or another, somebody has made claims for every one of them. DCX, because it changes nuclear charge by two units and therefore must involve two nucleons, can lay a much more direct claim. It may be expected that in DCX, correlations produce effects at the first-order level, in contrast to other reactions for which such effects are of second or higher order.

The last point concerns isovector aspects of nuclear structure. In the simplest picture, the (π^+,π^-) reaction takes place on the (N-Z) extra-core neutrons. As such, it is expected to be extremely sensitive to their distribution. Once other things are well understood, one can, at least in principle, think of the (π^+,π^-) DCX reaction as providing particularly detailed information about neutron distributions in the ground state of the target nuclei and proton distributions in the excited states of the residual nuclei.

It is worth noticing that in addition to all the serious reasons given above for the pursuit of DCX reactions, there is one more - the lure of the exotic. The popular criteria for "exoticity" are: (a) the reaction should not be easily accessible (a little Mt. Everest, at least); (b) the cross sections should be very, very small (though non-zero); and (c) the reaction should confound the theorists (hopefully, not forever). As we shall see subsequently, DCX may not yet have satisfied the grand expectations I enumerated before, but it has already met all the above criteria of "exoticity". It has even reached exotic nuclei!

In order to put things in perspective let me present a short account of the history of DCX reactions. The history can be conveniently divided into three epochs: the pre-industrial revolution era (i.e. before the advent of meson factories); the pre-Zurich conference era (i.e. the era closed by Spencer's[2] talk at the Zurich conference); and the pre-sent era.

The Pre-Industrial Revolution Era (pre-1976)

In 1961 analog states in heavy nuclei were discovered in the SCX (p,n) reaction by Anderson and Wong.[3] It was demonstrated that corresponding to the low lying $T = T_z$ states in the parent nucleus $X(A,Z,N,T_z = (N-Z)/2)$, there exist relatively pure (i.e. unmixed) analog states of $T = T_z = T_{z'} + 1$ in the adjoining nucleus $Y(A,Z' = Z + 1, N' = N - 1, T_{z'} = (N'-Z')/2 = T_z - 1)$. It was natural to ask if the double-analog states, i.e. states for which $T = T_z + 2$, exist and how they could be best populated. Drell, Lipkin and deShalit[4] suggested that they should be looked for in the charge exchange of two neutrons in the pion DCX reactions (π^+,π^-). Garvey, Cerny and Pehl[5] (1964) looked for, and found these $\Delta T = 2$ states in the transfer of two neutrons, in the (p,t) reactions. The same year the existence of (π^+,π^-) DCX was demonstrated by Batusov et al.[6] in the USSR and Gilly et al, at CERN,[7] but no transitions to individual states could be identified.

The experimental progress between 1965 and 1970 was meager. As summarized in Table I, a number of emulsion experiments were reported by Batusov and his collaborators,[10-12,16] mostly σ_T on emulsion nuclei, and all attempts to observe DCX to discrete nuclear states were unsuccessful.[14,15]

In absence of experiments, theory had a good time. There were more theoretical papers (see Table II) than certified DCX counts to discrete nuclear states. In all these papers DCX was considered to proceed primarily in two successive steps of SCX, as in Fig. 2(a) or 2(b). Most calculations were done in some form of multiple scattering theory in the impulse approximation.[19-23] In this approximation the transition amplitude for the DCX reaction $X(A,Z) + \pi^+ \rightarrow Y(A,Z+2) + \pi^-$ at the incident π^+ energy E (with momenta $\vec{k}_+$ and $\vec{k}_-$ for π^+ and π^- respectively) is written as[41]

$$T_{fi}(\vec{k}_-,\vec{k}_+,E) = \langle \phi_f^{(z+2)} \chi(\vec{k}_-) \, |T(E)| \, \phi_i^z \, \chi(\vec{k}_+) \rangle \qquad (5)$$

where ϕ_i^z and $\phi_f^{(z+2)}$ are initial, (A,Z), and final, (A,Z+2), state wave functions, $\chi(\vec{k}_+)$ and $\chi(\vec{k}_-)$ are properly distorted π^+ and π^- waves, and the transition matrix

$$T(E) = \sum_\lambda \sum_{i \neq j} t_i(\omega)(\vec{\tau}_N.\vec{\tau}_\pi) \frac{|\phi_\lambda^{(z+1)}\rangle\langle\phi_\lambda^{(z+1)}|}{E-E_\lambda - K_\pi - U_\lambda(E)} t_j(\omega)(\vec{\tau}_N.\vec{\tau}_\pi). \qquad (6)$$

Here $t(\omega)$ is the πN scattering matrix for the elementary single charge exchange process at an effective energy ω within the nucleus, and τ_N and τ_π are isospin operators for the nucleon and pion, respectively. Subscript λ labels the intermediate states with excitation energy E_λ in the intermediate nucleus (A,Z+1), and the optical potential operator $U_\lambda(E)$ describes pion propagation within the intermediate state. The generally used approximations in the early calculations were to replace $\chi(\vec{k}_+)$ and $\chi(\vec{k}_-)$ by plane waves and replace the sum over intermediate states λ by a single term corresponding to just the single analog state in the intermediate nucleus. Further, in all but the optical model calculations of Kerman and Logan,[18] $U_\lambda(E)$ was effectively assumed to be real, i.e. no absorption (or removal) from the charge exchange channels was permitted. The result was that quite large cross sections were predicted. For example, it was predicted that

$$^{18}O(\pi^+,\pi^-)^{18}Ne(g.s.), \; \sigma(0°) = 42 - 305 \; \mu b/sr \text{ at } 137 \text{ MeV}[19] \qquad (7)$$

$$^{48}Ca(\pi^+,\pi^-)^{48}Ti(\text{analog}),\ \sigma(0°) = 250\ \mu b/sr \text{ at } 210\ MeV^{20} \quad (8)$$

The first significant improvement in these kinds of calculations was made by Bjornenak et al.,[28] who included rescattering on all nucleons and predicted rather low cross sections, $\sigma(8.5°) = 2\ \mu b/sr$ for the reaction $^{51}V(\pi^+,\pi^-)^{51}Mn$ at 200 MeV. This development brought multiple scattering calculations in line with optical model calculations by Kerman and collaborators in which very low cross sections were predicted quite early, e.g., $\sigma_T = 0.8\ \mu b$ for $^{56}Fe(\pi^+,\pi^-)\ ^{56}Ni$ at 60 MeV,[18] and $\sigma(0°) = 0.01$ to $0.4\ \mu b/sr$ for $^{63}Cu(\pi^+,\pi^-)^{63}Ga$ at 80 MeV.[25]

Between 1971 and 1976, there were no experimental papers on DCX. The reason was not that the experimentalists became lazy or forgot DCX. On the contrary, they were busy building meson factories so that they could attack DCX with renewed vigor. They submitted their grand proposals[29-33] and patiently worked for the day when they could translate proposals into experiments. The theorists, of course, had no such constraints, and they kept on producing. Rost and Edwards[34] revived optical model calculations, Kaufmann, Jackson and Gibbs[35] refined multiple scattering calculations in the fixed scatterer approximation, Miller and Spencer made exhaustive calculations in the coupled channel optical model,[36] and Liu and Franco[37] studied the problem in the Glauber approximation.

The Pre-Zurich Conference Era (1975-77)

The experimentalists entered this era in a rather confused state. The reasons are quite clear from the expectations and recommendations summarized below

a. $\sigma(DCX, 0°) \simeq 0.05$ to $250\ \mu b/sr$. Famine or feast?

b. $\sigma(DCX)$ should increase with (N-Z). Should one concentrate on neutron rich heavy nuclei?

c. $\sigma(DCX)$ should peak at the (3,3) resonance. $\sigma(DCX)$ should be a minimum at the (3,3) resonance. Furtunately, these two expectations cancel!

d. $\sigma(DCX)$ should be maximum for analog transitions between states of the same (J^π,T). Therefore, one should concentrate on (π^+,π^-) ground state analog transitions from $T_z = 1$ targets such as ^{18}O, ^{26}Mg, and ^{42}Ca, to the ground states of the $T_z = -1$ residual nuclei. One should not waste time on (π^-,π^+) reactions, for example, because they necessarily involve non-analog transitions.

What followed is rather well known. Burman and collaborators[38-41] did the first successful DCX experiment of the post-industrial revolution era on the LEP channel at LAMPF and measured $^{18}O(\pi^+,\pi^-)^{18}Ne$(g.s.) DCX transition at 0°. They went on to measure ground state transitions for several other nuclei. Their results are summarized in Table III.

Table III is very distressing if one tries to look for a pattern. These 0° cross sections seem to be scattered about at random. There is no pattern with A or (N-Z). The only trend one can see is that $\sigma(0°)$ for ^{18}O does not change appreciably with energy. There are two particularly surprising things in this table. We note that

$$\frac{\sigma[^{18}O(0^+_1,\ T = 1) \rightarrow {}^{18}Ne(0^+_1,\ T = 1)]}{\sigma[^{16}O(0^+_1,\ T = 0) \rightarrow {}^{16}Ne(0^+_1,\ T = 2)]} = 2.3 \cdot 0.7 \qquad (9)$$

i.e. the non-analog transition in ^{16}O is only a factor of two weaker compared to the analog transition in ^{18}O. [A similar discrepancy appears in Table III relating to $\sigma(^{26}Mg)/\sigma(^{24}Mg)$ but it turns out that since these g.s. transitions were not well resolved from their respective continua, the listed results are in error.]

There was one more experiment between the 0° LAMPF measurements described above and the new LAMPF measurements which I am about to describe. This was the measurement of the DCX reaction $^{18}O(\pi^+,\pi^-)^{18}Ne$ at 18° at the SUSI spectrometer at SIN by Perrin et al.[42] These authors reported $\sigma(18°) = 0.21 \cdot 0.08$ mb/sr at $T(\pi^+)$ = 145 MeV based on about 10 counts at each energy in the region of the expected ground state. Due to poor statistics clear evidence for the excitation of states other than the ground state could not be obtained.

These data,[38-42] though still scanty, catalyzed some revisions of theoretical predictions. The fixed scatterer calculations of Kaufmann, Jackson and Gibbs[35] were revised by Gibbs, Gibson, Hess and Stephenson[43] to obtain better agreement with data. Similarly, the optical model calculations of Miller and Spencer[36] were revised with some resultant improvement in the fit to the data.

The Present Era (1977 -)

It is against the above background of a rather poor agreement between experimental results and pre-experiment theory, that we started the new series

of DCX experiments[50] at the EPICS facility at LAMPF. The collaboration consisted of J. Hird, S. Iversen, M. Kaletka, H. Nann, D. Barlow, D. Smith and K. K. Seth all from Northwestern University and (in some earlier work) H. A. Thiessen from LAMPF. Recently another group,[51] which is a collaboration of New Mexico State University, University of Texas and Los Alamos Scientific Laboratory has also contributed to the results from EPICS.

The Double Charge Exchange Spectrometer

Let me first briefly describe the "Double Charge Exchange Spectrometer" (sometimes also called EPICS!). This is illustrated in Fig. 3. D_{1-4} are channel dipoles which bend the beam in a vertical plane and provide a vertically dispersed beam at the target in a vacuum scattering chamber. Between D_1 and D_2 is an E.F. particle separator (PS). The beam size at the target is about 3" x 2". The beam intensity is monitored by an ion-chamber and the beam target interactions are monitored by a scattered beam monitor telescope MT. Q_{1-3} is the quadrupole triplet which produces a one-to-one image of the target at the front drift chambers F_{1-4}. D_5 and D_6 are spectrometer dipoles which produce the final image at the rear chambers R_{1-4} located in the focal plane. Scintillators S_1 and S_2S_3 permit measurement of the time of flight of all the particles which go through the ~9 meter flight path through the spectrometer. $\bar{C}$ is a freon filled threshold Cerenkov counter. Time of flight measurement and $\bar{C}$ veto allows an excellent level of rejection of the electron background. Figure 4 illustrates this. Recently an improvement in this facility has been made. A circular magnet (indicated by C in Fig. 5 has been put between the target and the quadrupole triplet. This magnet sweeps the primary pions away from the direction of the charge exchanged pions as they head towards the spectrometer. The net effect is that the front chambers F_{1-4} are not flooded by the primary beam and the elastically scattered pions at the forward angles. This magnet has made measurements of DCX possible at angles as small as 5° whereas with it data at angles ~18° could only be taken with great difficulty. With thin targets and no S_1 in the beam, the system regularly provides energy resolution of the order of 250 keV.

As an illustration of the quality of the data which is being currently obtained at EPICS we show two examples of the energy loss spectra.[50b] Figure 6 shows the spectrum at $\theta = 18°$ for the reaction $^{18}O(\pi^+,\pi^-)^{18}Ne$ obtained by us with the set-up of Fig. 3 and with a thick target of ^{18}O ice. Notice the almost

complete absence of background on the left of the ^{18}Ne(g.s.) transition. The energy resolution, FWHM, is about 600 keV. The transition to the g.s. and the 2^+ state are clearly resolved and it appears that even some higher lying states are also being excited. For comparison we also show in Fig. 6 the spectra for the same reaction obtained by Burman et al.[40] at θ = 0° and Perrin et al.[42] at θ = 18°. The order of magnitude improvement in resolution and background in our work is obvious. It was with spectra such as this that we obtained the first angular distributions ever for discrete DCX transitions. Figure 7, shows a spectrum[50f] for the reaction ^{26}Mg(π^-,π^+)^{26}Ne obtained at θ = 5° with the setup of Fig. 5. The further improvement in resolution (FWHM ~200 keV) is once again obvious.

With the set-ups of Figs. 3 and 5, DCX data have been taken on several nuclei. These data are listed in Table IV.

THE UNDERSTANDING OF THE DCX REACTION

At this point I want to depart from the almost historical narrative that I have presented so far, and discuss instead, our emerging understanding of the DCX reaction. One of the best ways of presenting this, I find, is to focus on the problems posed by the data, as listed in Tables III and IV. For this purpose I will divide the following into four parts.

1. The Problem of the Analog versus the Non-Analog Transition

As mentioned earlier, the interest in DCX originated with the interest in exciting the $T = T_z + 2$ (or $\Delta T = 2$) double analog states in nuclei. Since an almost perfect overlap may be expected between the wave functions of the analog triplet of isospin T in the three nuclei [the target nucleus ($T_z = T$), the intermediate nucleus ($T_z = T-1$), and the final nucleus ($T_z = T - 2$)], the early conjecture was that this would be the most favoured transition.

This presumed primacy of the analog transitions, not only among the final states accessible to DCX, but also among the intermediate states (in the $T_z = T-1$ intermediate nucleus) through which DCX proceeds, has been challenged by three experimental observations. These are:

a. The observation by Holt et al.[39,40] that at $T(\pi)$ = 140 MeV the ^{16}O (g.s., T = 0) → ^{16}Ne (g.s., T = 2) non-analog transition which should be non-existent, is only a factor of two weaker than the ^{18}O(g.s., T = 1) → ^{18}Ne(g.s., T = 1) double analog transition. [See Table III.]

b. The observation by Seth et al.[50b] that in the reaction $^{18}O(\pi^+,\pi^-)^{18}Ne$ at $T(\pi) = 162$ MeV, the non-analog transition to the 2^+_1 state at 1.89 MeV has an integrated cross section, $\Sigma\sigma(\theta)\sin\theta$ which is almost as large (actually ~70%) as that for the double analog transition to the 0^+_1 ground state.

c. The observation by Seth et al.[50a] that the cross sections for the inverse DCX reaction, (π^-,π^+), which must necessarily proceed through non-analog channels, are almost as large as those for the direct DCX reaction (π^+,π^-) which may proceed through analog channels.

As a more recent example of this last observation, we note that for the reaction $^{26}Mg(\pi^+,\pi^-)^{26}Si(g.s.)$, Greene et al.[51] have measured $\sigma(5°) \simeq 300$ nb/sr, while for the reaction $^{26}Mg(\pi^-,\pi^+)^{26}Ne(g.s.)$, Nann et al.[50f] have measured $\sigma(5°) = 260 \cdot 70$ nb/sr.

There are several important points which these observations make. The first is that evidently the simplistic expectations based on pure single particle model wave functions for initial and final states are not met. According to these expectations the ratio $^{18}O/^{16}O$ should have been infinitely large. Lee, Kurath, and Zeidman[44] showed that the experimental ratio ($\simeq 2$) could be explained if one considered the ground state correlations in A = 16 and A = 18 nuclei. They pointed out that, for example, it has been known for a long time[45] that $^{16}O(g.s.)$ is far from being pure (op-oh). Actually

$$|^{16}O(g.s.)\rangle = \alpha|\ op\text{-}oh\rangle + \beta|2p\text{-}2h\rangle + \gamma|4p\text{-}4h\rangle + \ldots. \qquad (10)$$

and the (2p-2h) part of the wave function is in large measure

$|(2p)_{J=0,T=1}(2h)_{J=0,T=1}\rangle_{0,0}$, i.e., it looks like $\langle^{18}O\rangle \otimes \langle^{14}O\rangle$. They assumed that the DCX reaction mechanism is the same for ^{16}O and ^{18}O, and therefore concluded that the part of $^{16}O(g.s.)$ which looks like $^{18}O \otimes ^{14}O$ leads to DCX just as $^{18}O(g.s.)$ does. In other words, they showed that the finite DCX cross section for ^{16}O is a direct consequence of the nuclear structure of ^{16}O. This was a very satisfying explanation when first proposed. Unfortunately, it appears now that it is most likely not correct. The reason is that, since the above explanation is entirely based on the nuclear structure properties of ^{18}O, ^{16}O and ^{18}Ne and ^{16}Ne, it is entirely independent of any aspects of the DCX reaction mechanism. It is in particular independent of the energy of the incident pion.

This means that we should get $\sigma(^{18}O)/\sigma(^{16}O) \simeq 2$, at all energies. In a recent measurement, Greene et al.[51c] find that the ratio changes rapidly with pion energy and at $T(\pi^+) = 290$ MeV, $\sigma(^{18}O)/\sigma^{16}O) \simeq 20$ rather than 2. This means that the explanation given by Lee et al. cannot be but a small part of the complete story!

The observation of the relatively strong transition to the non-analog 2_1^+ state of ^{18}Ne is not too difficult to understand. The 2_1^+ state is largely $d^2_{5/2}$), as is the 0_1^+ g.s. Therefore, the direct overlap $^{18}O(0_1^+)$ $^{18}F(0_1^+)$ $^{18}Ne(2_1^+)$ is smaller than that for $^{18}Ne(0_1^+)$, but not too small. Further, if we consider other intermediate states in ^{18}F, both 0_1^+ and 2_1^+ become equally easy to reach. Let us examine this point in more detail.

Figure 8 illustrates the level structure of ^{18}O, ^{18}F, and ^{18}Ne. The assumption of the dominance of analog transitions dictates that only the transition ^{18}O(g.s., 0^+, T=1)$\rightarrow$$^{18}F$(1.04 MeV, 0^+, T=1)$\rightarrow$$^{18}Ne$(g.s.,$0^+$, T-1) need be considered. No other T=0 or T=1 states in ^{18}F play any part. This, of course, leads to great simplification. In equation (6) the sum over intermediate states λ can be replaced by just one term corresponding to the intermediate analog state, and the calculation can be very conveniently done within the optical model framework. This, no doubt, is the main reason for the great popularity of this assumption. We may recall that in the (p,n) reactions in which analog transitions were first discovered, the analog transitions were found to be stronger than those to any other individual states, but were still considerably smaller than the summed (p,n) strength to all other states. This is very clearly illustrated in Fig. 9 taken from the original paper on the discovery of the analog intermediate state. As a matter of fact, this point was recognized in the first published paper on DCX by Parsons et al.[19] They showed that the analog transition accounted for only ~15% of the total cross section obtained in the closure approximation*. Sparrow and Rosenthal[47] have re-examined this question recently. They find that

---

* In this approximation one assumes that the propagator in the DCX transition amplitude (Eq.6) can be replaced by an average, so that E_λ and U_λ are replaced by $\bar{E}$ and $\bar{U}$. The intermediate states $\phi^{(z+1)}$ are then eliminated by closure, and nuclear structure information for only the initial and final states, ϕ_i^z and $\phi_f^{(z+2)}$, is needed.

other T=1 intermediate states play an important part. They find, for example, that the channel

$$^{18}O(g.s.,0^+,\ T=1)\ \xrightarrow{L=2}\ ^{18}F(3.06\ MeV,\ 2^+,T=1)\ \xrightarrow{L=2}\ ^{18}Ne(g.s.,0^+,\ T=1)$$

makes a contribution which is almost equal to that made by the usual channel

$$^{18}O(g.s.,\ 0^+,T=1)\ \xrightarrow{L=0}\ ^{18}F(1.04\ MeV,\ 0^+,T=1)\ \xrightarrow{L=0}\ ^{18}Ne(g.s.,\ 0^+,T=1).$$

With this knowledge it is now easy to see how the non-analog DCX transition $^{18}O(g.s.,0^+,T=1)_{L=0}\ ^{18}F(1.04\ MeV,\ 0^+,T\text{-}1)_{L=2}\ ^{18}Ne(1.89\ MeV,\ 2^+,\ T=1)$ and $^{18}O(g.s.,0^+,T=1)_{L=2}\ ^{18}F(3.06\ MeV,\ 2^+,\ T=1)\ \xrightarrow[L=0+2+4]{}\ ^{18}Ne(1.89\ MeV,\ 2^+,\ T=1)$ can be nearly as strong as the analog DCX transition to $^{18}Ne(g.s.)$.

It is also easy to now see how (π^-,π^+) cross sections can be comparable to (π^+,π^-) cross sections. Since ground st[illegible] correlations in target nuclei can have pairs of proton particles and proton holes just as they have pairs of neutron particles and neutron holes, the (π^-,π^+) reaction can take place on these "valence" protons as conveniently as (π^+,π^-) takes place on the real valence neutrons.

We summarize this section with the following conclusions.

a. In order to understand, even qualitatively, the behavior of (π^+,π^-) and (π^-,π^+) reactions, details of nuclear structure must be carefully considered. Ground state correlations plan an important, and even dominant, part in many cases.

b. If the DCX reaction is considered in terms of two successive steps of SCX, it is generally quite inadequate to consider only one intermediate state. With all the physical intuition at one's command, an attempt should be made to identify and include the subset of "important" intermediate states. If this is not possible, closure approximation should be used.

c. The $\sigma(^{18}O)/\sigma(^{16}O)$ problem, which appeared to have been temporarily solved by realizations a) and b) above is really far from being solved. It is clear that energy dependent reaction mechanism aspects will have a large role to play in the eventual solution of this problem.

2. The Problem of the Angular Distributions

Angular distribution measurements for a reaction generally provide the most critical tests of reaction theories. The first DCX angular distributions were

reported by Seth et al.[50b,c,d] for the reaction $^{18}O(\pi^+,\pi^-)^{18}Ne$, and they immediately posed what has become the most difficult problem in the understanding of the DCX reaction. Let me,however, not shock you with the problem all at once. First let me attempt to create the impression, which will all too soon turn out to be illusory, that things are going well.

To show how well things work let me present the example of a DCX angular distribution from our unpublished work.[50j] We have studied the reaction $^{9}Be(\pi^+,\pi^-)^{9}C$ at 162 MeV. Figure 10 shows a typical spectrum. The g.s. is clearly resolved and some of the excited states can also be identified. Figure 11 shows the measured angular distribution. The new data, taken with the set-up of Fig. 5 (filled circles) is in excellent agreement with the older data (filled squares) taken earlier with the set-up of Fig. 3. The data shows a smooth, monotonically decreasing cross section with a trace of a dip at ~20°. How well does theory reproduce this data? Gibbs et al.[49] have made a calculation for this transition using their fixed-scatterer approximation. For this non-analog transition

$$^{9}Be(g.s.,\ J^{\pi} = 3/2^-,\ T = 1/2) \xrightarrow[L=0+2]{} {}^{9}C(g.s.,\ J^{\pi} = 3/2^-,\ T = 3/2)$$

both L = 0 and L = 2 transfers are allowed. Using Barker's[52] wave functions for A = 9 nuclei, these authors obtain the L = 0 and L = 2 components of the overlap. The incoherent sum of L = 0 and L = 2 cross sections is shown in Fig. 12. The absolute cross sections predicted are almost an order of magnitude too large, but the shape of $\sigma/8.3$ agrees quite well with the data. The theoretical curve does fall off a bit too fast at larger angles but this can be rather easily fixed by increasing the L = 2 component as indicated in Fig. 13. Things appear to be working quite well, and it almost appears that DCX angular distributions may be able to provide detailed insight into the structure of wave functions for individual states!

Unfortunately, the euphoria is short lived. Lee et al.[53] have done a DWBA calculation for the above DCX transition using Cohen-Kurath wave functions.[54] They predict cross sections which are too small by factors ranging from 35 to 3.5. As seen in Fig. 14, they predict almost no L = 0 component in their angular distribution and consequently have a shape which differs markedly from that measured by us. The drastic difference between the predictions of Lee et al.[53] and Gibbs et al.[49] is difficult to understand. Since the wave

functions of Barker[52] and Cohen-Kurath[54] are known to be very similar, it is very surprising that one calculation finds that the L = 0 component is essentially non-existent while the other finds it to be the dominant component. While differences are to be expected between fixed scatterer and optical model calculations, we believe that such large differences are most likely due to an error in one of the two calculations.

The $^{9}Be(\pi^+,\pi^-)^{9}C$ (g.s.) angular distribution was rather featureless. It showed no sharp minima or maxima against which sharp comparisons could be made. Further, since the transition was a non-analog one, the theoretical calculations were not as "clean" as one might wish. A "clean" example is provided by the angular distribution for the $^{18}O(\pi^+,\pi^-)^{18}Ne$ (g.s.) transition.

As mentioned earlier, angular distributions for the $^{18}O(\pi^+, \pi^-)^{18}Ne$ reaction were first measured by Seth et al.[50b] in the angular range θ_L = 11° to 45° using the experimental set-up of Fig. 3. Later the data was supplemented by measurements of Greene et al.[51a] who used the set-up of Fig. 5 to measure cross sections at more forward angles. The two data sets are in excellent agreement, as shown in Fig. 15 for the g.s. L = 0 transition. Figure 16 shows the angular distributions for the L = 2 transition to the 1.89-MeV 2^+ state in ^{18}Ne.

In Figs. 17 and 18 we show the predictions of Strottman, Oset and Brown[55] for the two transitions in ^{18}Ne. These Glauber model calculations predict cross sections which are a factor of ~5 too large for both the transitions. Otherwise their shape "appears" to be quite similar to that measured by us. A closer examination of the data, however, reveals very serious problems.

The most characteristic feature of the g.s. angular distribution shown in Fig. 15 is the location of the deep minimum at $\theta_{cm} \simeq 20°$. It is just this fact which is most problematic. As shown in Fig. 19, nearly all theoretical calculations for DCX give this minimum at θ = 35-40°, if a satisfactory fit to the elastic scattering data is simultaneously required, i.e., if the geometrical size of ^{18}O is kept realistic. Iversen et al.[56] have measured elastic scattering of 164-MeV π^+ and π^- from ^{18}O (with deep diffraction minima at 46.3 and 44.0° respectively) and have shown that the data is consistent with rms radii $r_n \simeq r_p$ and the charge radius r_p = 2.65 fm obtained in the model independent analysis of electron elastic scattering measured at Bates by Bertozzi et al.[57] (see Fig. 20). In Fig. 19 we see that the location of the DCX minimum is rather insensitive to the type of pion-nucleus potential used (Kisslinger, Laplacian or

LMM). It remains essentially unaffected whether the DCX calculation is made using only analog transitions, as was done by Miller,[58] or with the inclusion of non-analog intermediate states, as was done by Sparrow.[48] Sternheim[59] has shown that increasing r_n over r_p by plausible amounts, $\lesssim 0.3$ fm, also fails to bring the minimum below 30°. The reason for this relative insensitivity becomes very transparent if one looks at DCX in terms of semi-classical models, as has been done by Seth[50c,50d] and Johnson.[60]

Seth,[50c,50d] as well as Johnson[60] have used diffraction model arguments to show that if one uses a potential of the form

$$U(r) = U_0 f_0(r) + U_1 f_1(r)\ (\vec{t} \cdot \vec{T}/A) \tag{11}$$

where,

$$f_0(r) \equiv f_{\text{isoscal.}} \propto [N\rho_n(r) + Z\rho_p(r)]/(N + Z) \tag{12}$$

and

$$f_1(r) \equiv f_{\text{isovect.}} \propto [N\rho_n(r) - Z\rho_p)r)]/(N - Z), \tag{13}$$

one obtains the approximate results[61]

$$\sigma(\text{SCX}) \propto (N - Z)\, A^{-4/3}\, J_0^2\,(x) \qquad , x = qR \tag{14}$$

$$\sigma(\text{DCX}) \propto (N - Z)\,(N\text{-}Z\text{-}1)\, A^{-10/3}\, J_0^2\,(x)\left[1-\left(\frac{a}{R}\right)\{1-x\, J_1(x)/J_0(x)\}\right]^2 \tag{15}$$

where R is the 'strong absorption' radius which reproduces elastic scattering, and 'a' is the diffuseness.

Let us now see how the schematic result of Eq. 15 helps us get a better understanding of the angular distribution problem. Seth[50(c)] has shown that for ^{18}O the 164 MeV elastic and inelastic scattering data of Iversen et al.[56] can be fitted very well with a 'strong absorption' radius, $R \simeq 3.56$ fm. (At this 'radius', the proton density in Fig. 20 is ~10% of its central value. For this value of R, the complete expression for σ(DCX) in Eq. 15 gives the minimum at $\theta = 33.6°$ i.e., in the vicinity of the optical model minima in Fig. 19. In order to produce a minimum at the experimental position, i.e., $\theta = 20°$, one would require $R = 5.7$ fm. Clearly such a radius is completely unphysical since the density at this radius is much less than 0.5% of the central density. In other words, there is no physically plausible way in which the discrepancy between the

experimental data and the current theoretical predictions can be removed. One is therefore forced to the conslusion that the error must lie with assumptions about some basic aspect of the DCX reaction mechanism that is common to all the present calculations - the optical model calculations as well as the above diffraction model calculations. Indeed, the basic assumption made in all DCX calculations done to-date is that the operative potential is of the form of Eq. 11, i.e., it has only an isoscalar and an isovector part and that the two have only $\rho(r)$ type of radial dependence. This, of course forces the DCX form-factor to have the form

$$F_{DCX}(r) = [N\rho_n(r) - Z\rho_p(r)]/(N - Z) \qquad (16)$$

The inevitable consequence of this, given the physical size of ^{18}O, is that the minimum cannot be moved below 30°. Where do we go from here?

Seth[50(c)] has shown that in order to produce a minimum at small angles one requires at least two destructively interfering components of comparable magnitude in the DCX form-factor. Blair[62] has shown that if one does indeed take two amplitudes, each of the form implied in Eq.15, but of slightly different radii, one can fit the data in Fig. 15 almost perfectly. Following earlier arguments due to Miller and Spencer,[36] Blair[62] has suggested that the interfering component in the DCX form-factor might arise from additional $\rho^2(r)$ terms in the pion-nucleus optical potential. What is the origin of these terms? What is their isospin structure? We return to these questions later. For the present we summarize the conclusions of this section as we did in our paper:[50(b)] <u>The small angle minimum in the L = 0 angular distribution of Fig. 15 requires that there be other than a $\rho(r)$ component in the DCX form-factor and that such a component be of comparable magnitude</u>.

3. <u>The Problem of the Excitation Functions</u>

The first DCX excitation function was measured by Burman and collaborators[38-40] at the LEP. For the reaction $^{18}O(\pi^+,\pi^-)^{18}Ne$ (g.s.) they measured $\sigma(0°)$ at $T(\pi)$ 95, 126, and 139 MeV. In this rather limited energy region they found the cross section to be essentially constant (see Table III). Subsequently, for the same reaction, Greene et al.[51(a)] measured $\sigma(5°)$ at EPICS in an extended energy region, and found that for this analog transition $\sigma(5°)$ has a maximum at $T(\pi) \simeq 180$ MeV. and increases monotonically beyond that (Fig. 21). On the other hand, Seth et al.[50(j)] and Iversen et al.[50(i)] found that the excitation functions for the non-analog transitions $^9Be(\pi^+,\pi^-)^9C$(g.s.) and $^{12}C(\pi^+,\pi^-)^{12}O$(g.s.) have monotonically

decreasing cross sections from $T(\pi) = 140$ to 290 MeV, as shown in Fig. 22. Could it be that these measurements were indicating that the excitation functions for the analog and non-analog transitions were quite different? This question prompted Greene et al. to measure the excitation functions for the non-analog transitions $^{16}O(\pi^+,\pi^-)^{16}Ne(g.s.)$ and $^{24}Mg(\pi^+,\pi^-)^{24}Si(g.s.)$ and for the analog transition $^{26}Mg(\pi^+,\pi^-)^{26}Si(g.s.)$. The results of these measurements are also shown in Figs. 21 and 22. It turns out that indeed all non-analog transitions have cross sections which monotonically decrease with increasing energy, whereas the cross sections for the two analog transitions for ^{18}O and ^{26}Mg reach a minimum near the peak of the (3.3) resonance and then rise with increasing energy. This clear difference between the energy behavior of analog and non-analog transitions we really don't know. We can only speculate. If we take seriously our earlier suggestion that the angular distribution data requires two interfering components in the DCX form factor, then the above observation about the behavior of the excitation functions must imply that the energy variation of the two components is quite different. Further, at least one of the components is quite different. Further, at least one of the components must be sensitive to nuclear structure differences inherent between analog and non-analog transitions. The most obvious differences of course concern the degree of pairing correlations present in the initial and final state wave functions in the two cases.

Interesting as the above observations of excitation functions are, their explanation is bound to be more complicated than, for example, the explanation of the angular distribution problem. This is due to the fact that excitation functions add another dimension, i.e., energy variation of all parameters, to the overall problem.

Let me go on to add the last piece to the jigsaw puzzle that DCX appears to be.

4. The Problem of the (N - Z) Dependence of DCX

As mentioned earlier, all DCX reaction theories which have the DCX form factor proportional to $\rho(r)$ (Eq. 16) lead to cross sections which have the same basic proportionalities. The most intuitive of all these is that all SCX cross sections are proportional to the number of excess neutrons, (N - Z), and all DCX cross sections are proportional to the number of excess neutron pairs, (N - Z) (N-Z-1)/2. In one form or another this basic result exists in all theories listed in Table II. The increase in DCX cross sections with (N-Z) is to a certain extent offset by increased absorption with increasing A. In

optical model calculations this manifests itself in the form of the Lane term $(t \cdot T)/A$, so that a cross section proportionality of the type $(N-Z)(N-Z-1)/A^2$ is suggested.[36] In diffraction models, absorption also enters via the specification of a strong absorption radius, and as indicated in Eq. 15 the proportionality $(N-Z)(N-Z-1)/A^{10/3}$ is indicated.[60] In other words, as long as the DCX form factor is of the type of Eq. 16, we may expect that

$$\sigma(DCX) \propto (N-Z)(N-Z-1)/A^x \tag{17}$$

with $2 < x < 4$. This is borne out by actual calculations.

Let us consider the case of ^{42}Ca and ^{48}Ca. For the double analog transitions in both, according to Eq. 17, we get

$$R \equiv \frac{\sigma(^{48}Ca \rightarrow {}^{48}Ti(T=4))}{\sigma(^{42}Ca \rightarrow {}^{42}Ti(g.s.))} = 21.4 \text{ to } 16.4, \tag{18}$$

with Eq. 15 giving R = 17.95. In Fig. 23 we show the prediction of an eikonal model calculation due to Germond and Johnson[63] using realistic densities for ^{48}Ca and ^{42}Ca. The ratio R changes with angle, and is actually predicted to be about 32 at $\theta = 5°$. In Fig. 24 we show the prediction of a coupled channel optical model calculation due to Miller and Spencer.[58] The ratio for the total cross sections depends on the type of potential used, but above $T(\pi) = 150$ MeV it levels out to a remarkably stable value of ~18. In summary, we expect that the ratio R between forward angle DCX cross sections for ^{48}Ca and ^{42}Ca is $\gtrsim 18$.

Let us see what the experiments show. In Fig. 25 we show a spectrum for the $^{42}Ca(\pi^+,\pi^-)^{42}Ti$ reaction at $T(\pi) = 162.5$ MeV. [The spectrum is a composite of the 5° and 8° spectra. In the two spectra the g.s. was equally excited.] From this measurement we get $\sigma(5°) = 140 \pm 40$ nb/sr. We therefore expect that for the analog transition $^{48}Ca(\pi^+,\pi^-)^{48}Ti(T = 4)$, $\sigma(5°)$ should be $\gtrsim 18 \times 140$ i.e., $\sigma(5°) \gtrsim 2500 \pm 700$ nb/sr. What is experimentally found, however is really disasterous!

In a short run with what is essentially the world supply of ^{48}Ca we attempted to measure the huge (!) expected cross section. Since the T=4 state in ^{48}Ti is expected in the vicinity of $E^* \approx 17$ MeV, the 17 MeV excitation region was centered on the focal plane of the EPICS spectrometer. What was observed is shown in Fig. 26. The sensitivity of the measurement is ~60 nb/sr per count. Thus we expected to see a peak of FWHM $\lesssim$ 300 keV containing $\gtrsim 40 \pm 12$ counts. What we see is essentially a continuum with no clear peak sticking out anywhere. In order to

place an upper limit on the T = 4 cross section we may consider the 5 counts seen in the 1 MeV neighborhood of 17 MeV excitation. Thus for ^{48}Ca $\sigma(5°) \lesssim 290 \pm 130$ nb/sr and

$$R^{exp} \equiv \sigma(^{48}Ca)/\sigma(^{42}Ca) \lesssim 2 \pm 1 \qquad (19)$$

This is a most amazing result. It represents an order of magnitude supression of ^{48}Ca cross section as compared to that for ^{42}Ca. The increase expected from (N - Z) is being almost entirely eaten up by something else, something that increases even faster!

What is this mysterious effect? We cannot help but wonder if this 'something else' is the same, or is related to that which caused the drastic downward shift in θ_{min} for ^{18}O. We recall that we had to invoke destructive interference with a second component in the DCX form factor in that case. Could we try the same explanation in this case too?

Since we seem to repeatedly come back to the second component in the DCX form factor, we must look at it a little more seriously than we have so far. Corrections to first order optical potentials have been talked about for a long time. They have been talked about by many authors under many different names. One of the oldest such discussions is that due to Ericson and Ericson.[64] They showed that consideration of 'true pion absorption' leads to a pion-nucleus optical potential in which there is an additional isotensor part. Rather prophetically, they concluded that "the isospin tensor term may contribute significantly to 'elastic' double charge exchange to isobaric analog states" and went on to reiterate that, "It does not seem possible to show this term (isotensor) to be negligible compared to the contributions from the isospin vector term to second order." In spite of these very early prognostications, the isotensor components, which lead to $\rho^2(r)$ terms, were neglected in all DCX calculations till 1974. Miller and Spencer[36] considered them to some extent in terms of short range correlations, but it is safe to say that serious study of these terms has not yet been made.

Very recently Johnson[60] and Siciliano and Johnson[65] have considered the effect of a phenomenological introduction of $\rho^2(r)$ terms in their isomultiplet approach to the DCX reaction. Preliminary calculations show that introduction of such terms can provide the destructive interference which simultaneously produces a decrease in DCX cross sections, shift of the minima to small angles, and

a drastic reduction in the enhancement of DCX cross sections with increasing (N-Z). So far there is very little understanding of the full physics behind the $\rho^2(r)$ terms, but it is beginning to appear that they hold the answer to many of the problems posed by the experimental data on the DCX reactions. Elastic scattering and single charge exchange do not appear to possess the degree of sensitivity to isotensor terms found in DCX reactions and it appears that the DCX reactions provide a unique window looking into the isotensor aspects of the pion-nucleus interaction.

Before I turn to the final topic of my talk, i.e., the study of exotic nuclei by means of DCX reactions, let me, for the sake of completeness, present the miscellany of data about which I do not have the time to talk in any detail.

Double Charge Exchange in the Continuum

As listed in Table I, the early DCX experiments of Batusov could only measure total DCX cross sections. From these Batusov was able to infer that a large part of the total DCX cross section resides in the continuum. The new high resolution experiments confirm this. In Fig. 27 we show the 'angular distribution' for the integrated cross section in the 5-20 MeV excitation region as measured[50b] by us for the $^{18}O(\pi^+,\pi^-)^{18}Ne$ reaction. In Fig. 28 we show data for three angles for the reaction $^{16}O(\pi^+,\pi^-)^{16}Ne$ for $E^* > 25$ MeV from the experiment of Bolger et al.[66] at SIN.

At LAMPF, Davis et al.[67] have measured (π^+,π^-) and (π^-,π^+) DCX differential cross sections at $T(\pi) = 290$ MeV, $\theta_L = 60°$ for the targets ^{12}C, ^{40}Ca, ^{44}Ca and ^{48}Ca. In the continuum region, corresponding to excitations between ~35 MeV and 115 MeV in the residual 'nuclei', these authors measure double differential cross sections $d^2\sigma/d\Omega dT$ which range from ~4 to ~14 μb/sr-MeV. The results, presented in their entirety in Table V, are not easy to understand. The authors present some speculations about possible explanations for the irregularities observed.

Double Charge Exchange on Heavy Nuclei

When DCX reactions were first talked about, it was conjectured that the larger the neutron excess, the larger will be the (π^+,π^-) DCX cross sections. As mentioned earlier, this has proved to be a myth. No evidence for such increase was found either in the σ_T(DCX) measurements of Batusov et al. or in the

differential cross section measurements of Boyton et al. (Table I). In the latter work $\sigma(\pi^+,\pi^-)$ at 16° was found to be essentially the same for Li, V, and Zr targets. It was discovered that the enhancement due to greater neutron excess is 'eaten up' (may be even 'more than eaten up') by absorption due to the larger number of nucleons. As we have already seen, this fact appears to be borne out by the data on ^{48}Ca and ^{42}Ca.

No DCX experiments on nuclei heavier than ^{48}Ca have been reported so far using modern pion spectrometers. Part of the reason is, of course, that the going is already so tough with medium heavy nuclei like Ca and Ni. The other reason is that the favorite double analog, $\Delta T = 2$, transitions for heavy nuclei are expected to occur at excitations ranging from 20 to 30 MeV. At these excitations the continuum yield is expected to be large and one has very little hope of observing the resolved transitions in presence of the large continuum background. It is worthwhile to keep in mind, however, that all these are prognostications; the experiments have just not been done.

We do have an activation DCX experiment on ^{209}Bi. In 1974, Batusov et al.[68] studied the reaction $^{209}Bi(\pi^+,\pi^-xn)^{209-x}At$, and reported a total DCX cross section for ^{209}Bi of 120 μb and the integrated cross section of $\lesssim$ 10 μb for the analog transition. The value of the total cross section is a large one and it is very important that it should be verified. Clark et al.[69] have indeed repeated this experiment recently at Los Alamos with 300 MeV pions. Unfortunately, Clark et al. find that the total cross sections for the production of all At isotopes are $\lesssim$5 μb and all activities observed with π^+ beams are equally observed with π^- beams (see Fig. 29). These authors conclude that the observed activities arise from pion (π^+ or π^- - induced secondary reactions and only small residuals can probably be ascribed to DCX. They find these residual cross sections $[\sigma(\pi^+) - \sigma(\pi^-)]$ to be 0.17 ± 0.80 μb for ^{209}At, 0.20±1.00 μb for ^{208}At, and 1.5±0.4 μb for ^{207}At, and consider their net result to be that $\sigma_T(\pi^+,\pi^-) \lesssim 2$ μb for ^{209}Bi. In closing this subject let me add that the NMSU, Texas, LASL group at EPICS is currently trying to identify the double analog transition in the ^{209}Bi (π^+,π^-) ^{209}At reaction. Their very preliminary data has too poor statistics to make any definite statements yet.

DCX and the Study of Exotic Nuclei

Let us now move on to what is essentially a completely different subject. Quite apart from our understanding of the DCX reactions, and we have just seen that at present it is not too profound, we know one thing. The DCX reactions, both (π^+,π^-) and (π^-,π^+) can reach very exotic nuclei and we can use these reactions to produce and study these nuclei. The possibility was realized by Ericson very early[4] and Gilly et al.[7] did the first experiments along these lines at CERN.

Gilly et al.[7] looked for tetraneutron (^{4}n), hydrogen-7 (^{7}H), ^{9}He and ^{12}Be by means of the (π^-,π^+) reaction on the tragets ^{4}He, ^{7}Li, ^{9}Be, and ^{12}C. The experiment was done in a somewhat unusual fashion. The spectrometer was tuned to detect 180 MeV π^+ and the incident π^- energy was varied between 160 and 270 MeV. The experiment was essentially unsuccessful.

The next attempt was made by V. Perez-Mendez and his colleagues at Berkeley. In the reaction ^{4}He$(\pi^-,\pi^+)^4$n Kauffman et al.[70] found no evidence for the tretraneutron final state in the binding energy region 0 to 40 MeV. They put an upper limit of 0.7 nb/sr (corresponding to the detection of 1 event) for ^{4}n production.* on the other hand Sperinde et al.[73] found evidence for a resonant behavior of a ^{3}n state within a few MeV of the threshold in their study of the ^{3}He(π^-,π^+) reaction.

A recent search for the tetraneutron ^{4}Be was recently reported by Falomkin et al.,[74] using the reaction ^{4}He$(\pi^+,\pi^-)^4$Be at T(π^+) = 100 MeV. No tetraneutron was of course found. The total cross section for the four proton final state was found to be 0.30 ± 0.15 nb.

---

*Further attempts to study the tetraneutron have been made by Russian investigators. Batusov et al.[71] studied the reactions

production: $\pi^- + {}^{208}\text{Pb} \rightarrow {}^4\text{n} + \text{residuals}$

detection : $^4\text{n} + {}^{208}\text{Pb} + {}^{212}\text{Pb} + \gamma$

and established a limit $\sigma_{prod} \times \sigma_{detect} \leq 10^{-54}\text{cm}^4$. The experiment was repeated recently at SIN by Chultem et al.[72] and a limit of $\sigma_{prod} \times \sigma_{detect} \leq 2.5 \times 10^{-56}\text{cm}^4$ was set. The limit set by this complicated experiment is comparable to the direct limit set by the DCX experiment of Kaufman et al. described above.

Let us now move on to somewhat heavier light-nuclei. Here the DCX reaction can be used to study the stability, measure the g.s. masses and determine even the excited state spectra. In their study of the reaction $^{16}O(\pi^+,\pi^-)^{16}Ne$ Burman et al.[40] measured the mass excess of ^{16}Ne as 24. 4 ± 0.5 MeV. This value was later confirmed by Kekelis et al.[75] by means of the reaction (^4He,^8He) in which a value 23.92 · 0.08 MeV was obtained.

Proton rich nuclei are accessible to reactions in which a number of neutrons are removed. With the realization of reactions such as (^3He,^6He), (^3He,^8He), and (^3He,^8Li) many exotic proton-rich nuclei have been studied. In contrast the extremely neutron rich nuclei are not so readily accessible to the conventional nuclear reactions - sometimes even to the powerful heavy-ion induced reactions. Consider, for example, ^{48}Ar(Z = 18, N = 30, T_z = 6) which can be studied by the DCX reaction

$$^{48}Ca(\pi^-,\pi^+)^{48}Ar \quad .$$

It is essentially impossible to reach ^{48}Ar by any but the double charge exchange reaction from ^{48}Ca. Of course DCX can be accomplished not just by pions but by heavy ion reactions as well. However, in a heavy-ion induced DCX reaction, for example (^{18}O,^{18}Ne) one encounters severe particle identification problems. In the focal plane of the spectrometer analyzing reaction products one finds a great variety of masses and charge states. Even with the use of very sophisticated dE/dx - E telescopes and time-of-flight one has often great trouble in identifying species which have small yield. A typical example of this problem is illustrated by Fig. 30 taken from ref. 76.

In contrast, pion DCX is an extremely 'clean' reaction. The pions need to be distinguished only from electrons, and this is quite conveniently done by time-of-flight and threshold Cerenkov detectors as we have already illustrated in Fig. 4.

The first pion DCX experiment, expressely for the purpose of measuring the mass of an exotic nucleus, was done by our group two years ago.[50(a)] It had been shown earlier by Artukh et al.[77] that the T_z = 3 nucleus, ^{18}C, is particle stable. Unfortunately the GeV-proton induced fragmentation experiments were unsuitable for measuring masses.[78] Attempts to measure the mass by heavy-ion induced reactions were also unsuccessful.[79] The spectrum obtained by us for the reaction

$^{18}O(\pi^-,\pi^+)^{18}C$ is shown in Fig. 31. The g.s. transition is clearly identifiable. Fortunately we had available to us a very good calibration reaction, $^{12}C(\pi^-,\pi^+)^{12}Be$, whose Q_g-value is accurately known.[80] The spectrum for this reaction is also shown in Fig. 31. We are therefore able to obtain the mass of ^{18}C quite accurately. The mass excess was found to be 24.91 (15) MeV. This value is smaller than that predicted by many models based on mass systematics and indicates that ^{18}C is bound more strongly than anticipated. While we are on the subject of ^{18}C, let me indulge in some wishful thinking. Fig. 32 shows a rebinned plot of the ^{18}C spectrum. Since the spectrum is almost without any background, one wonders if the cluster of counts near 2 MeV excitation is statistically significant. If it is, could it be due to the 2_1^+ state of ^{18}C? Afterall, ^{18}C, which is like ^{24}Mg in its neutrons, is in all probability quite deformed. It is therefore quite likely that it has its 2_1^+ state at this low an energy. As a matter of fact Khadkikar and Kamle[81] have done a deformed Hartree-Fock calcualtion for ^{18}C and find that the 2_1^+ state is predicted at ~2 MeV (see Fig. 33).

Our next example of an exotic mass measurement is provided by ^{26}Ne. This $T_z = 3$ nucleus has the distinction of being one of the 'doubly magic deformed' nuclei. As illustrated in Fig. 34, taken from Bohr and Mottleson,[82] for 2:1 deformations the single particle spectrum develops gaps at nucleon numbers 2, 4, 10, 16, etc., instead of the familiar gaps at 2, 8, 20, ... etc. for the spherical case. One therefore expects 'magicity', or at least dramatic examples of co-existence of deformed and spherical states at relatively low excitations in nuclei such as ^{6}He, ^{14}B, ^{26}Ne,... etc.

Because of the above interest in ^{26}Ne, attempts were made earlier by Cerny and his collaborators[83] to measure the mass of ^{26}Ne by the heavy-ion DCX reaction (^{18}O, ^{18}Ne). However, background conditions were found to be quite bad and no definitive conclusions could be drawn from the data. We[50(f)] have however just completed the successful measurement of the ^{26}Ne mass by the $^{26}Mg(\pi^-,\pi^+)^{26}Ne$ reaction The spectrum is shown in Fig. 35. There are no counts, whatever, to the left of the transition identified as the g.s. transition. The mass excess is found to be +0.44 (7) MeV. An excited state, which is mostly likely 0_2^+ is clearly seen at ~3.75 MeV. The ground state mass is larger than the predictions of most model calculations (Table VI) but the 0_2^+ excitation energy is considerably smaller than that predicted by Wildenthal.[84] Both these observations may be manifestations of the coexistence of a spherical and deformed intrinsic state in ^{26}Ne, as anticipated.

We have attempted to measure the masses of ^{48}Ar and ^{58}Zn by the reactions $^{48}Ca(\pi^-,\pi^+)^{48}Ar$ and $^{58}Ni(\pi^+,\pi^-)^{58}Zn$, but are not yet in a position to report masses. The NMSU, Texas, LASL group has also measured masses of the T = 2 nuclei ^{24}Si, ^{32}Ar using (π^+,π^-) reactions.[51(b)]

I want to conclude this section and this talk by describing what I call the study of the super exotics. By super exotics I mean the lightest of the exotic nuclei, ^{5}H, ^{7}H, ^{9}He, etc.

In Fig. 36, we show the spectrum obtained by us for the $^{9}Be(\pi^-,\pi^+)^{9}He$ reaction.[50(j)] The spectrum shows a clear enhancement at the end of the phase space for the break-up $^{9}He \rightarrow {}^{8}He + n$. We obtain the mass excess of ^{9}He as 49.98 (20) MeV. Thus ^{9}He is 1 to 2 MeV more bound than predicted by the calculations listed in Table VII. What is even more exciting is that if we use our mass of ^{9}He in transerse Garvey-Kelson relations we find that the double magic ^{10}He is predicted to be bound by 0.93 MeV for single neutron emission, and predicted to be just unbound by 1.66 MeV for two neutron emission. Since these predictions are often in error by 1 MeV or so at the drip-lines, it is not inconceivable that ^{10}He is bound! That would be a most exciting situation indeed. Unfortunately to test this possibility by DCX reactions we need gram quantities of ^{10}Be.

In the same experiment in which ^{9}He was successfully identified, we also studied the reaction $^{7}Li(\pi^-,\pi^+)^{7}H$. The spectrum obtained is shown in Fig. 37. Obviously, no enhancement over phase space is seen and we can put an upper limit of <3 nb/sr for the production of ^{7}H. Fortunately this is not the end of the story. A most exciting conclusion emerges when an attempt is made to fit the observed phase space. Using an ingenious program for the calculation of relativistically invariant phase space for multi-particle break-up, written by M. Block[85], we find that the observed phase space has the very characteristic signature of the break up reaction $^{7}Li(\pi^-,\pi^+)^{5}H$ +n+n. The shape is completely different from that for break up channels ^{3}H+n+n+n+n or ^{4}H+n+n+n or ^{6}H+n.

I am quite aware of the fact that no serious claims can be made about the existence of a nucleus on the basis of phase space arguments. One can however state quite strongly that our data shows that the five nucleons, 1 proton and 4 neutrons have a very strong final state interaction. This is a very exciting conclusion in itself, in view of the fact that no such signature of a strong final state interaction has ever been found for the tetraneutron system. The final verdict of whether or not ^{5}H actually comes near being bound can only be provided

by an experiment in which ^{5}H appears in a two body final state. We propose to study the reaction $^{6}Li(\pi^{-},p)^{5}H$ for this purpose in the near future.

Let me end this review by returning to some of the hopes and aspirations which started the whole DCX story. It appears that after many years of waiting the DCX game has finally started in earnest. Excellent quality experimental data are beginning to come out. Already the experiments have posed several rather sharply defined questions about the nature of the DCX reaction mechanism. It appears that not only are we clearly on our way to understanding pion DCX, but that, in the process, we will have illuminated a hitherto inaccessible dark corner of pion physics -- the role of isotensor interactions in the pion-nucleus system. As anticipated long ago, short range correlations and other subtle aspects of nuclear structure are beginning to show up as first-order effects in DCX, and we are bound to reach a better understanding of these through DCX studies.

Pion double charge exchange is not meant to be the manufacturing arm of the exotic nucleus industry, but it has proved itself to be superb in catering to very special cases. Its most exciting contributions are likely to come from the study of the lightest of the exotic nuclei. The stability, or near stability of these nuclei may be expected to have the most fundamental impact on nuclear structure, since these are the nuclei in which many-body forces may be expected to have their simplest manifestations. These are also the nuclei which come closest to pure neutron matter!

REFERENCES

1. Kamal K. Seth, Proc. LAMPF Workshop on Single Charge Exchange LASL Report LA-7892C (1979), H. Baer, J. Bowman, and M. Johnson, editors, p. 205.

2. J. A. Spencer, Proc. VII Internat. Conf. on High Energy Physics and Nucl. Struct., Zurich (1977) p. 153.

3. J. D. Anderson and C. Wong, Phys. Rev. Lett. 7, 250 (1961).

4. T. E. O. Ericson, Proc. of CERN Conf. on High Energy Physics and Nuclear Science (Geneva, 1963), p. 68. The reference to Drell, Lipkin, and deShalit in published literature was first made in Ref. 19.

5. G. T. Garvey, J. Cerny, and R. H. Pehl, Phys. Rev. Lett. 12, 726 (1964).

6. Yu. A. Batusov et al., Sov. Phys. JETP 19, 597 (1964).

7. L. Gilly et al., Phys. Lett. 11, 244 (1964).

8. Yu. A. Batusov et al., Sov. J. Nucl. Phys. 1, 271 (1965).

9. L. Gilly et al., Phys. Lett. 19, 335 (1965).

10. Yu. A. Batusov et al., Sov. J. Nucl. Phys. 3, 223 (1966).

11. Yu. A. Batusov et al., Sov. J. Nucl. Phys. 5, 249 (1967).

12. Yu. A. Batusov et al., Sov. J. Nucl. Phys. 6, 727 (1968).

13. D. Chivers et al., Phys. Lett. 26B, 573 (1968).

14. P. E. Boynton et al., Phys. Rev. 174, 1083 (1968).

15. C. J. Cook, M. E. Nordberg, and R. L. Burman, Phys. Rev. 174, 1374 (1978).

16. Yu. A. Batusov et al., Sov. J. Nucl. Phys. 9, 91 (1969).

17. J. Massaue et al., as quoted in Ref. 27. Also thesis, University of Strasbourg (1970) unpublished.

18. A. K. Kerman and R. K. Logan, Argonne National Laboratory Report, No. ANL-6848 (1964) unpublished. Also, Bull. Amer. Phys. Soc. 9, 680 (1964).

19. R. G. Parson, J. S. Trefil, and S. D. Drell, Phys. Rev. 138B, 847 (1965).

20. S. Barshay and G. E. Brown, Phys. Lett. 16, 165 (1965).

21. T. Kohmura, Prog. Theor. Phys. (Japan) 33, 480 (1965).

22. D. S. Koltun and A. Reitan, Phys. Rev. 139B, 1372 (1965).

23. F. Becker and Z. Maric, Nuovo Cimento 36, 1395 (1965).

24. Yu. A. Batusov, Sov. J. Nucl. Phys. 6, 116 (1968).

25. A. K. Kerman and M. Koren (unpublished), M. Koren, Ph.D. thesis, MIT (1969) unpublished.

26. H. Bertini, Phys. Rev. C1, 423 (1970).

27. F. Becker and C. Schmit, Nucl. Phys. B18, 607 (1970).

28. K. Bjornenak et al., Nucl. Phys. B20, 327 (1970).

29. Kamal K. Seth et al., LAMPF Proposal #13 (1971).

30. R. L. Burman et al., LAMPF proposal #25 (1971).

31. V. Perez-Mendez et al., LAMPF Proposal #74 (1971).

32. G. C. Bonazzola et al., CERN Proposal #PH-III-74/22 (1974).

33. C. Perrin et al., SIN Proposal #R-71-04.10 (1976).

34. E. Rost and G. W. Edwards, Phys. Lett. 37B, 247 (1971).

35. W. B. Kaufmann, J. C. Jackson, and W. R. Gibbs, Phys. Rev. C9, 1340 (1974).

36. G. A. Miller and J. E. Spencer, Phys. Lett. 53B, 329 (1974), also Ann. Phys. 100, 562 (1976).

37. L. C. Liu and V. Franco, Phys. Rev. C11, 760 (1975).

38. T. Marks et al., Phys. Rev. Lett. 38, 149 (1977).

39. R. J. Holt et al., Phys. Lett. 69B, 55 (1977).

40. R. L. Burman et al., Phys. Rev. C17, 1774 (1978).

41. M. D. Cooper, contribution to the Banff Summer School (1978).

42. C. Perrin et al., Phys. Lett. 69B, 301 (1977).

43. W. R. Gibbs, B. F. Gibson, A. T. Hess, and G. J. Stephenson, Jr., Private communication.

44. T. S. H. Lee, D. Kurath, and B. Zeidman, Phys. Rev. Lett. 39, 1307 (1977).

45. A. P. Zuker, B. Buck, J. B. McGrory, Phys. Rev. Lett. 21, 39 (1968), also Phys. Rev. Lett. 23, 983 (1969).

46. D. Oset, D. Strottman, and G. E. Brown, Phys. Lett. 73B, 393 (1978).

47. D. A. Sparrow and A. S. Rosenthal, Phys. Rev. C18. 1753 (1978).

48. D. A. Sparrow, Private Communication 1979.

49. W. R. Gibbs, Private Communication 1978.

50. Kamal K. Seth et al., LAMPF Proposal #13, $413, #460, #463, $549, #550. Also:
    a. Kamal K. Seth, H. Nann, S. G. Iversen, M. Kaletka, J. Hird, and H. A. Thiessen, Phys. Rev. Lett. 41, 1589 (1978).

    b. Kamal K. Seth, S. G. Iversen, H. Nann, M. Kaletka, J. Hird, and H. A. Thiessen, Phys. Rev. Lett. 43, 1574 (1979), also 45, 147 (1980).

    c. Kamal K. Seth, invited paper on 'Pion Double Charge Exchange' at the LAMPF Workshop on Pion Single Charge Exchange Reactions, LASL Report LA-7892-C, 205 (1979).

    d. Kamal K. Seth, invited paper on "Pion Double Charge Exchange," Proc. II International Conference on Meson Nuclear Physics, Houston (1979); E. Hungerford, editor, AIP publishers.

e. H. Nann, invited paper, Proc. VI International Conference on Atomic Masses, East Lansing (1979) (in press).

f. H. Nann, K. K. Seth, S. G. Iversen, M. O. Kaletka, D. B. Barlow, and D. Smith, Phys. Lett. (accepted).

g. Kamal K. Seth et al., Bull. Amer. Phys. Soc., Washington (April 1980).

h. M. O. Kaletka et al., Bull. Amer. Phys. Soc., Washington (April 1980).

i. S. G. Iversen et al., to be published.

j. Kamal K. Seth et al., to be published.

51. W. J. Braithwaite et al., LAMPF Proposal #310.

G. R. Burleson et al., LAMPF Proposal #448. Also:

a. S. J. Greene et al., Phys. Lett. 88B, 62 (1979).

b. G. R. Burleson et al., Phys. Rev. C (in press).

c. S. J. Greene et al., Proc. Workshop on Nucl. Struct. with Intermediate-Energy Probes, Los Alamos (1980). LASL Report LA-8303-C, 430 (1980).

d. G. R. Burleson, invited paper, Proc. Workshop on Nucl. Struct. with Intermediate-Energy Probes, Los Alamos (1980). LASL Report LA-8303-C, 195 (1980).

52. Barker, Phil, Mag. 2, 5, 286, 780 (1957).

53. T. S-H. Lee et al., Private Communication (1980).

54. Cohen and D. Kurath, Nucl. Phys. A141, 145 (1970).

55. D. Strottman, D. Oset, and G. E. Brown, Private Communication (1979).

56. S. Iversen, H. Nann, A. Obst, K. K. Seth, N. Tanaka, C. L. Morris, H. A. Thiessen, K. Boyer, W. Cottingame, C. F. Moore, R. L. Boudrie, and D. Denhard, Phys. Lett. 82B, 51 (1979).

57. W. Bertozzi, Private Communication (1977).

58. G. A. Miller, Private Communication (1979).

59. M. Sternheim, Private Communication (1979).

60. M. Johnson, Proc. LMAPF Workshop on Pion Single Charge Exchange, H. Baer, D. Bowman, and M. Johnson, Editors, Los Alamos Report LA-7892-C, 343 (1979).

61. The result originally obtained by Seth in ref. 50(c) contained an error which was later corrected in ref. 50(d). The author wishes to thank Prof. J. Blair for pointing out the error.

62. J. S. Blair, Private Communication (1979), as reported in ref. 30(d).

63. Germond and M. Johnson, Private Communication (1980).

64. M. Ericson and T. E. O. Ericson, Ann. Phys. (N.Y.) 36, 323 (1966).

65. E. Siciliano and M. Johnson, Private Communication (1980).

66. J. Bolger, E. T. Boschitz, C. H. Q. Ingram, G. Probstle, R. Mischke, P. A. M. Gram, J. Jansen, and J. Zichy, Proc. II Internat. Conf. on Meson Nucl. Phys. Houston (1979); E. Hungerford, editor, AIP publisher, p. 268.

67. J. Davis, J. Kallne, J. S. McCarthy, R. C. Minehart, C. L. Morris, H. A. Thiessen, G. Blanpied, G. R. Burleson, K. Boyer, W. Cottingame, C. F. Moore, and C. A. Goulding, Phys. Rev. C20, 1946 (1979).

68. Yu. A. Batusov, G. G. Ganzerig, I. V. Dudova, B. P. Osipenko, V. M. Siderov, V. Khalkin, and D. Chultem, Sov. J. Nucl. Phys. 18, 250 (1974).

69. J. L. Clark, P. E. Haustein, J. Hudis, and A. A. Caretto, Bull. Amer. Phys. Soc. 24, 22 (1979).

70. L. Kaufman, V. Perez-Mendez, and J. Sperinde, Phys. Rev. 175, 185 (1968).

71. Yu. A. Batusov et al., Dubna report PI-7475 (1973).

72. D. Chultem, V. S. Evseev, V. M. Sidorov, V. A. Khalkin, R. Engfer, H. H. Muller, and H. K. Walter, Nucl. Phys. A316, 290.

73. J. Sperinde, D. Fredrickson, R. Hinkins, V. Perez-Mendez, and B. Smith, Phys. Lett. 32B, 185 (1970).

74. I. V. Falomkin, et al., Proc. Conf. on Meson Nucl. Phys. Pittsburgh (1976); P. D. Barnes, R. A. Eisenstein, and L. S. Kisslinger, editors. AIP Conference Report #33.

75. G. J. Kekelis, M. S. Zisman, D. K. Scott, R. Jahn, D. J. Vieira, J. Cerny, and F. Ajzenberg-Selove, Phys. Rev. C17, 1929 (1978).

76. J. A. Nolan, T. S. Bhatia, H. Hafner, P. Doll, C. A. Wiedner, and G. J. Wagner, Phys. Lett. 71B, 314 (1977).

77. A. A. Artukh et al., Nucl. Phys. A137, 348 (1969); A283, 350 (1977).

78. J. D. Bowman, A. M. Poskanzer, R. G. Korteling, and G. W. Butler, Phys. Rev. C9, 836 (1974).

79. J. A. Nolen, Private Communication (1979).

80. D. E. Alburger et al., Phys. Rev. C18, 2727 (1978).

81. Khadkikar and Kamle, Private Communication (1979).

82. A. Bohr and B. Mottelson, Nuclear Structure (Benjamin Publishers, Reading, 1975) Vol, II, p. 592.

83. J. Cerny, Proc. 3rd Internat. Conf. on Nuclei far from Stability, Cargese, 1976, CERN publication 76-13, 225 (1976).

84. B. H. Widenthal, Private Communication (1979).

85. M. M. Block, Private Communication (1980).

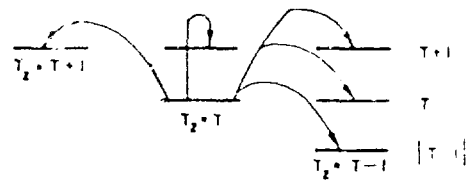

(a) Inelastic and charge exchange reaction with projectiles of I=½

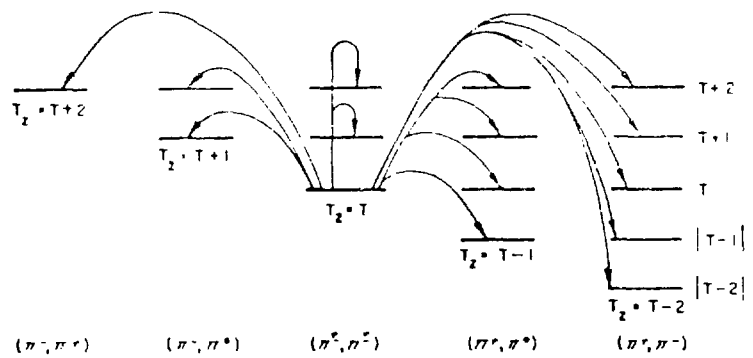

(b) Inelastic and charge exchange reaction with projectiles of I=1

Fig. 1.

(a) Isospin states reached by inelastic or charge exchange scattering of isospin, T = 1/2 projectiles (protons, neutrons, ^{3}He, etc.).

(b) Isospin states reached by inelastic or charge exchange scattering of isospin, T = 1 projectiles (e.g., pions).

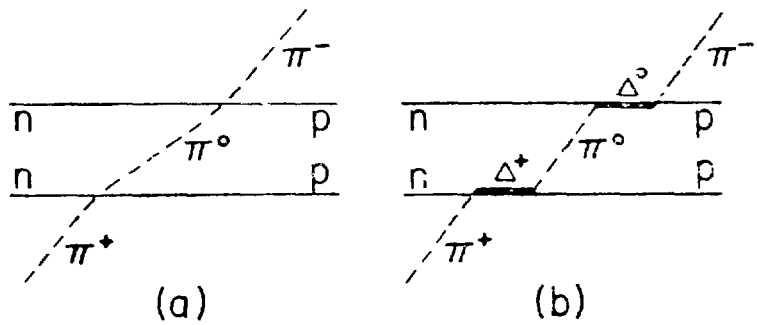

Fig. 2.

Pion double charge exchange visualized as two successive steps of single charge exchange; (a) without explicit Δ's in intermediate states, and (b) with Δ's in intermediate states.

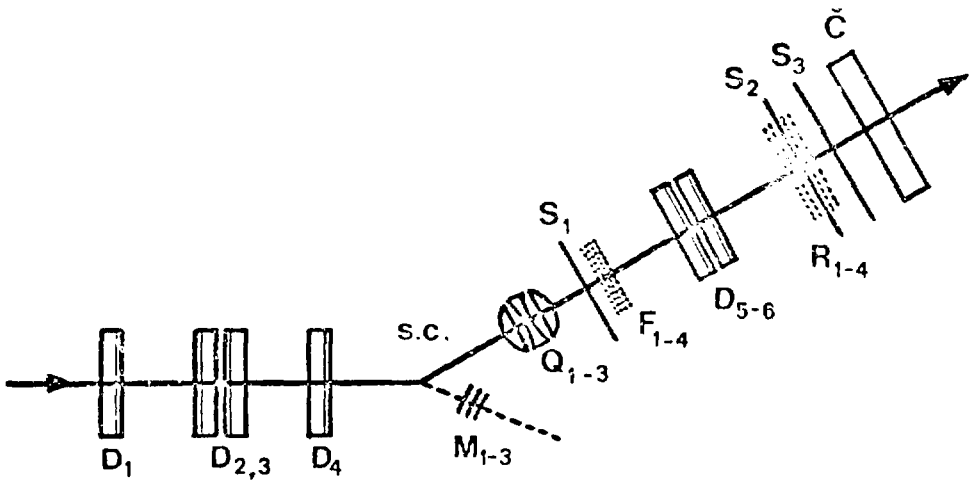

Fig. 3.

The EPIC spectrometer facility at LAMPF used in high resolution DCX measurements.

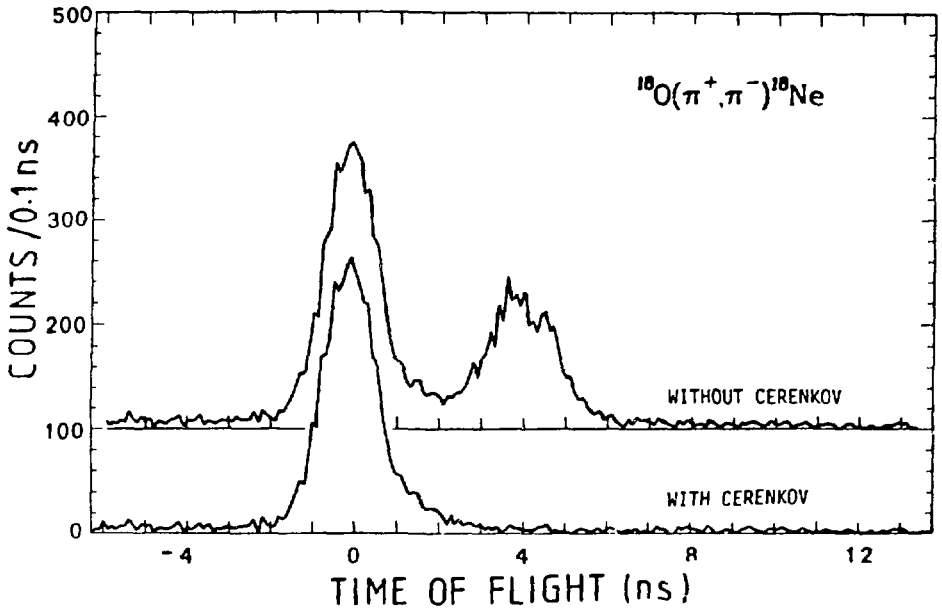

Fig. 4.

Particle identification at EPICS by the simultaneous use of time-of-flight and threshold Cerenkov counter.

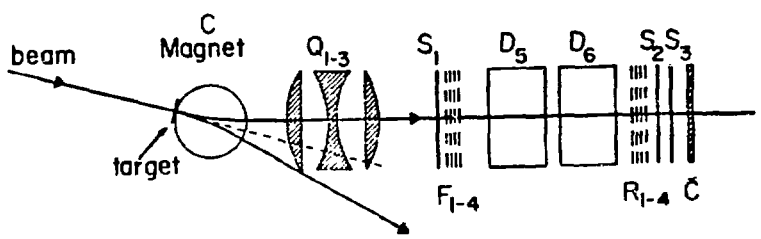

Fig. 5.

The small angle DCX setup at EPICS.

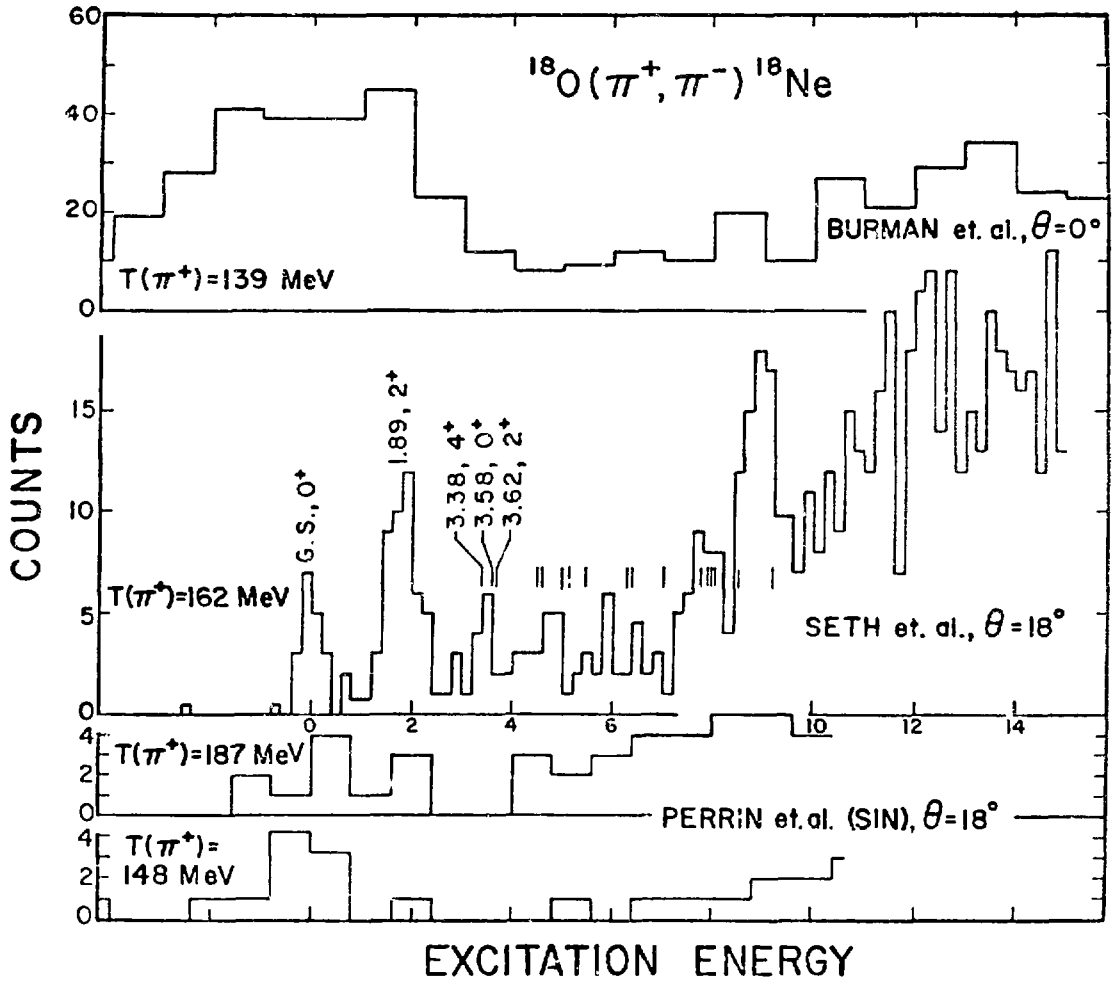

Fig. 6.

Spectra for the DCX reaction, $^{18}O(\pi^+,\pi^-)^{18}Ne$, (top)-0° spectrum taken by Burman et al.[41] at LEP at T(π) = 139 MeV; (middle) 18° spectrum taken by Seth et al.[50(b)] at EPICS at T(π) = 162 MeV; (bottom) - two 18° spectra taken by Perrin et al.[42] at SIN at T(π) = 148 and 187 MeV.

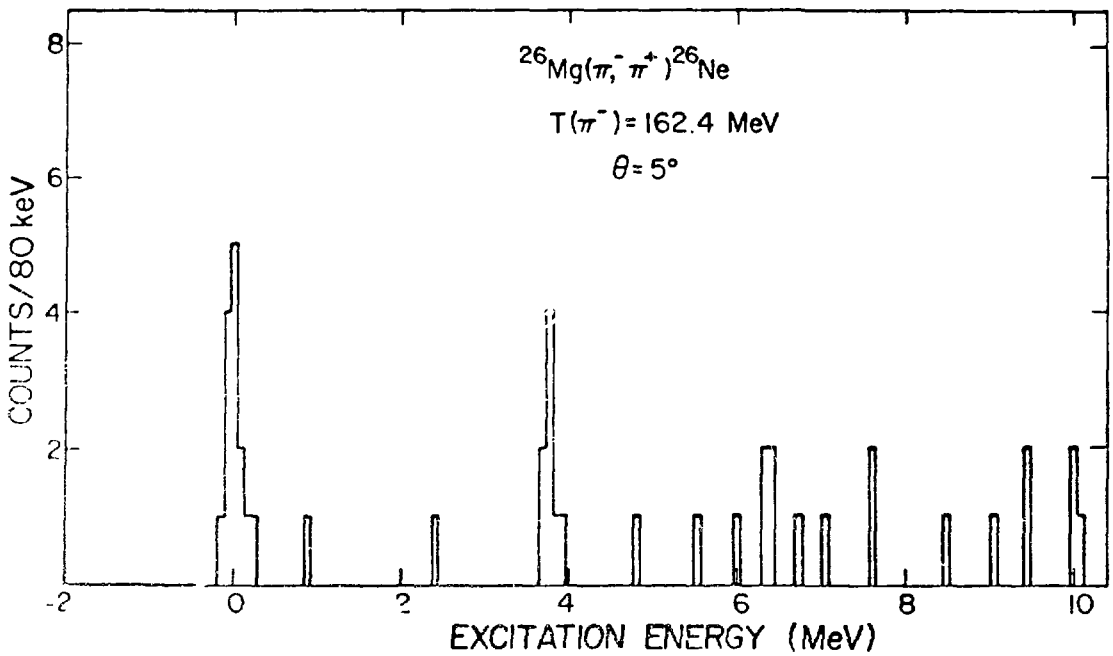

Fig. 7.

A typical spectrum taken with the small angle DCX setup at EPICS by Nann et al.[50(f)] Notice the almost background free nature of the spectrum and also that the energy resolution, FWHM ≈ 200 keV.

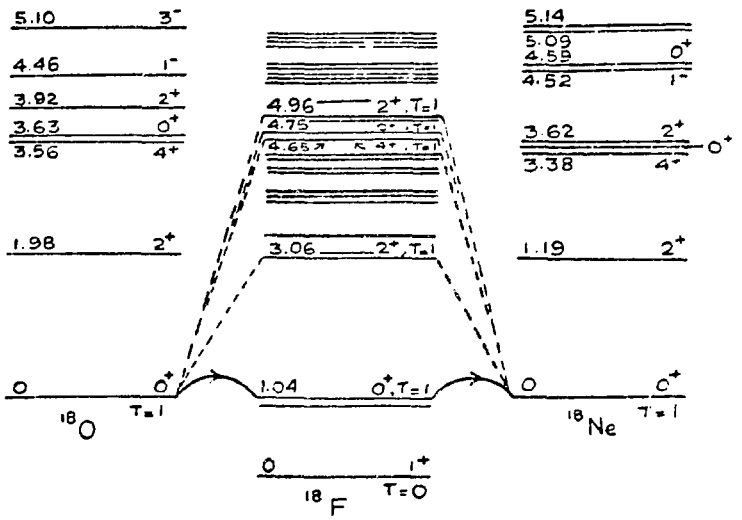

Fig. 8.

Level structure of ^{18}O, ^{18}F, and ^{18}Ne. The analog transitions are indicated by solid lines. Other, possibly important, T = 1 → T = 1 transitions are indicated by dashed lines.

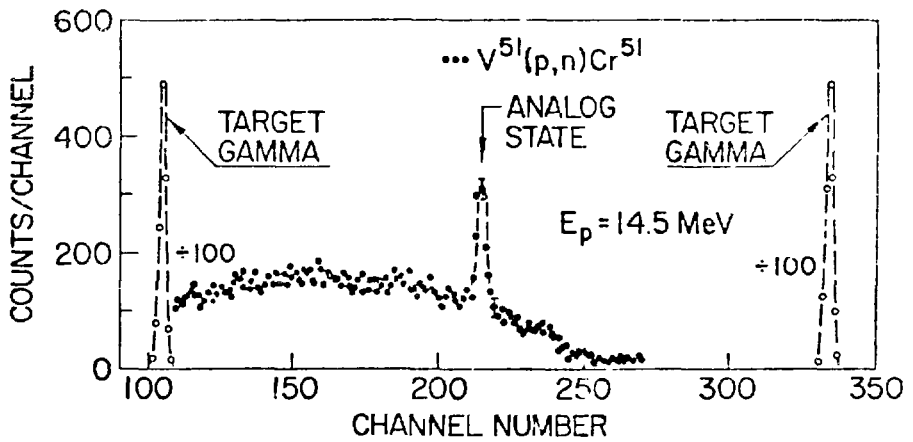

Fig. 9.

Spectrum for the single charge exchange reaction $^{51}V(p,n)^{51}Cr$ from Anderson et al. (ref. 3).

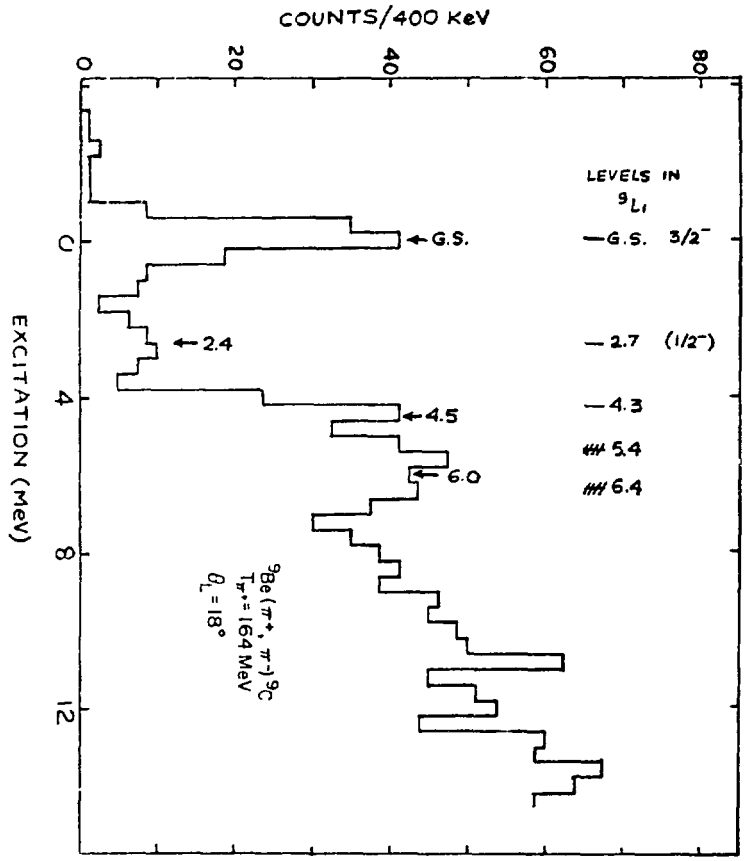

Fig. 10.

Spectrum for the DCX reaction $^{9}Be(\pi^{+},\pi^{-})^{9}C$ at $T(\pi)$ = 162 MeV, θ_{L} - 18° obtained in ref. 50(j). Note that the g.s. is clearly resolved. Several excited states are also indicated. They appear to correspond with known states in the mirror nucleus ^{9}Li.

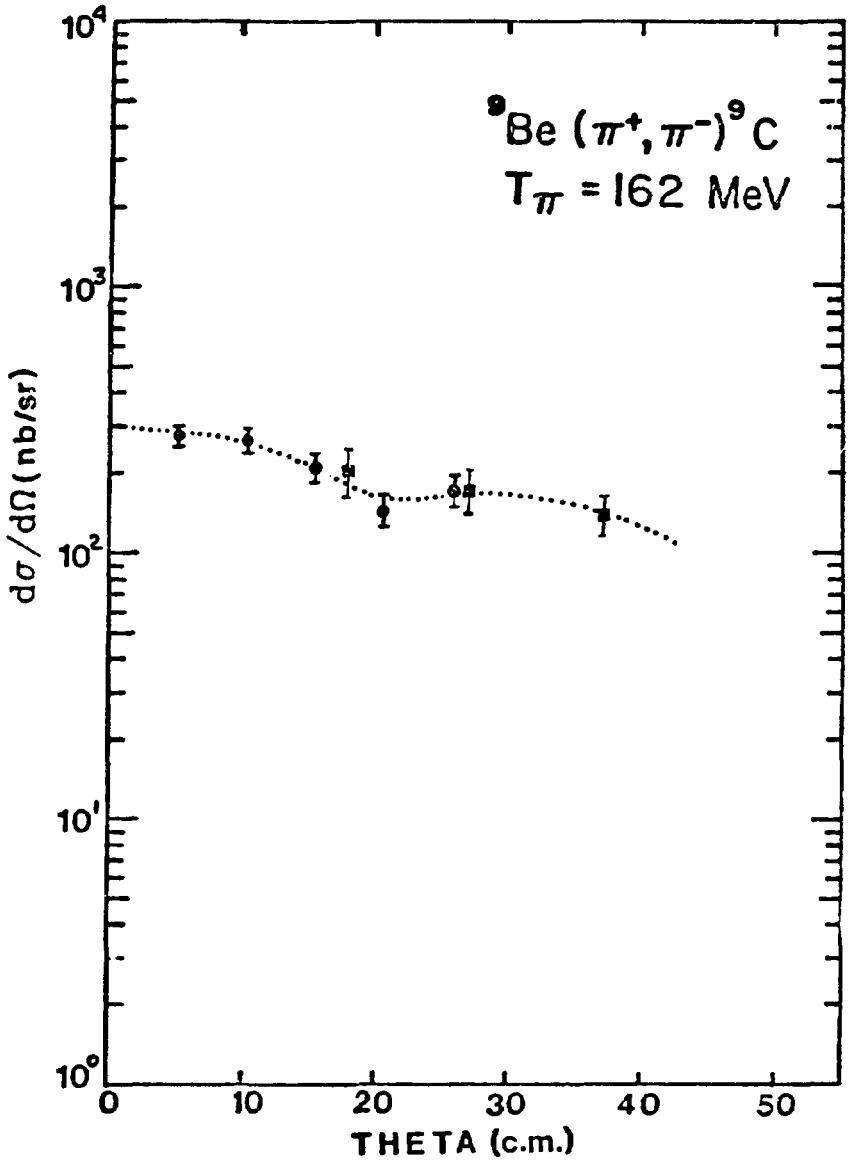

Fig. 11.

Angular distribution for the DCX reaction ^{9}Be(π^+,π^-)^{9}C (g.s.) as measured in ref. 50(j). The dotted curve is merely to indicate the trend of the data. The filled circles are data taken with the setup of Fig. 5. The filled squares are earlier data taken with the setup of Fig. 3.

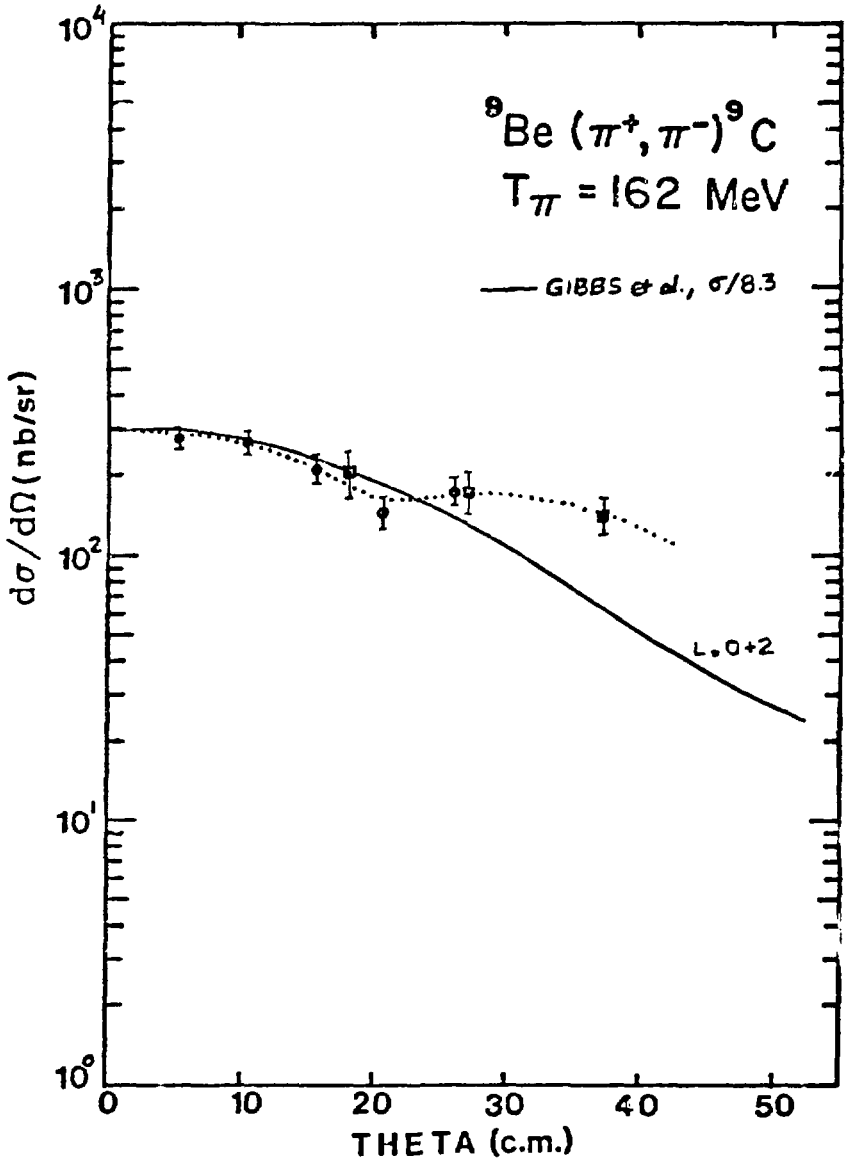

Fig. 12.

Illustrating the fit to the angular distribution shape for the ^{9}Be(π^+,π^-)^{9}C (g.s.) reaction obtained from the fixed scatterer calculations of ref. 49. Note that σ(theory)/8.3 is plotted. The dotted curve merely indicates the trend of the data.

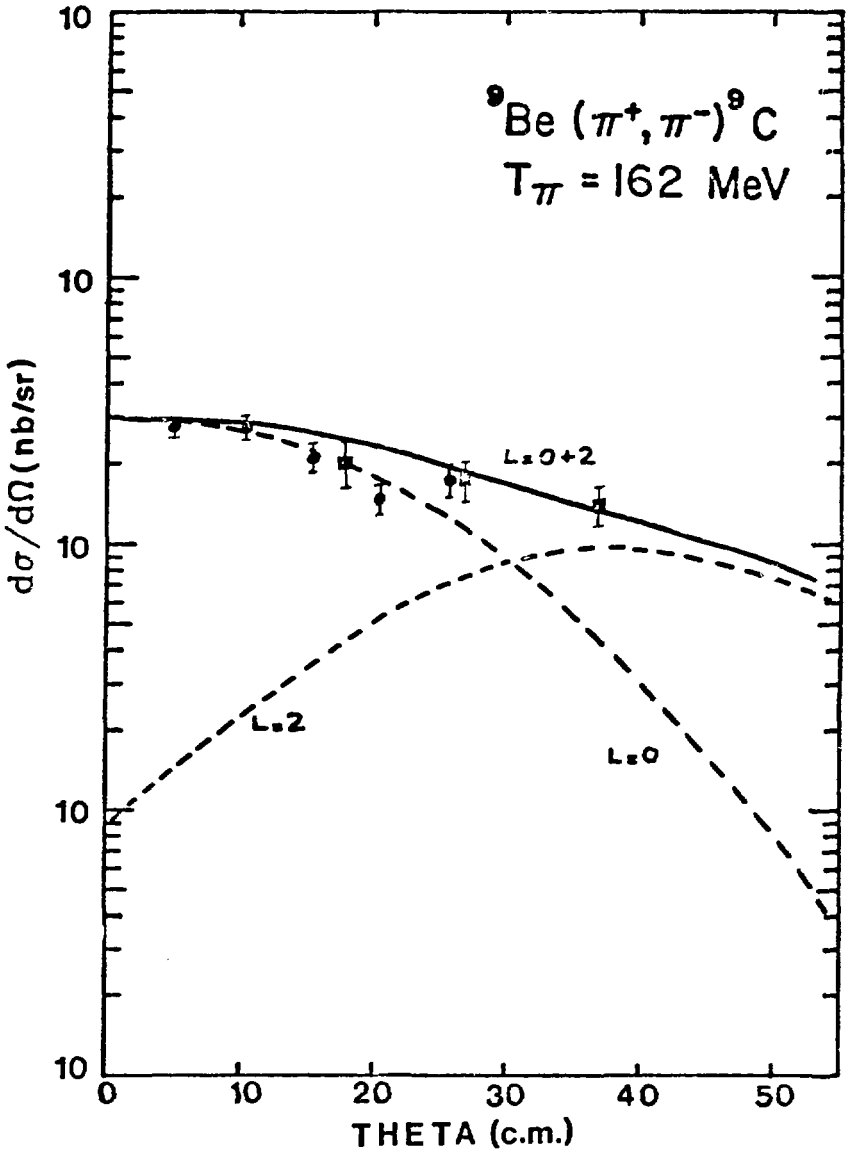

Fig. 13.

Illustrating the improvement in fit between σ(expt) and σ(theory) of ref. 49 if the L = 2 component is enhanced.

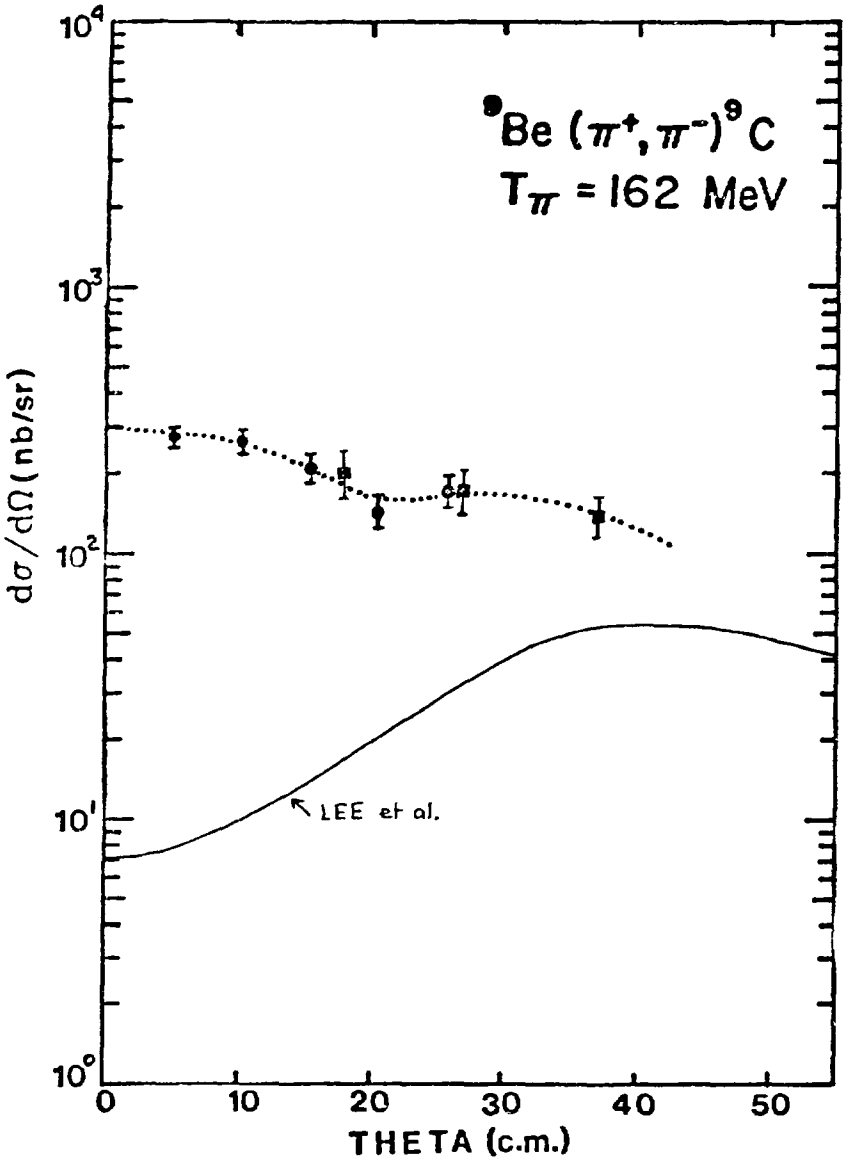

Fig. 14.

Illustrating the optical model prediction for ^{9}Be$(\pi^+,\pi^-)^9$C (g.s.) angular distribution due to Lee et al. (ref. 53).

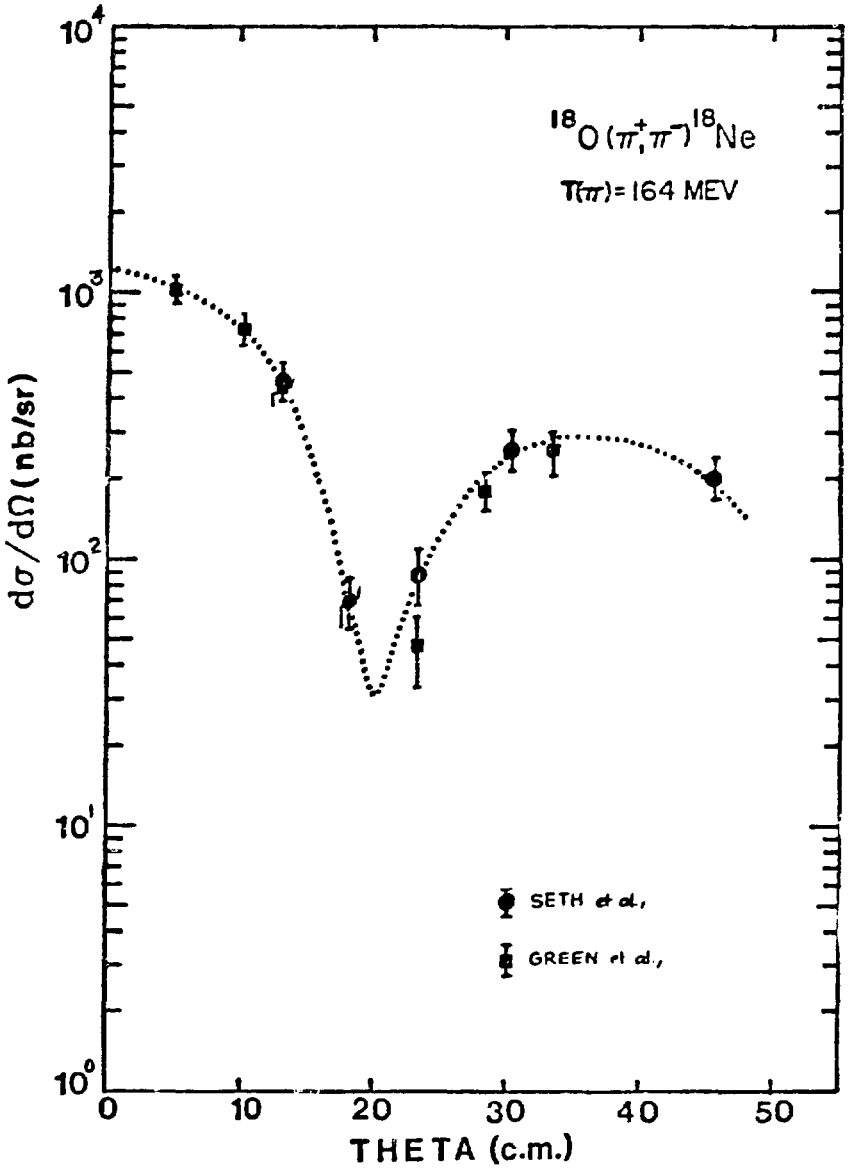

Fig. 15.

Angular distribution for the L = 0 ground state transition for the DCX reaction $^{18}O(\pi^+,\pi^-)^{18}Ne$. The data are from Refs. 50(b) and 51(a). The dotted curve is merely to indicate the trend of the data.

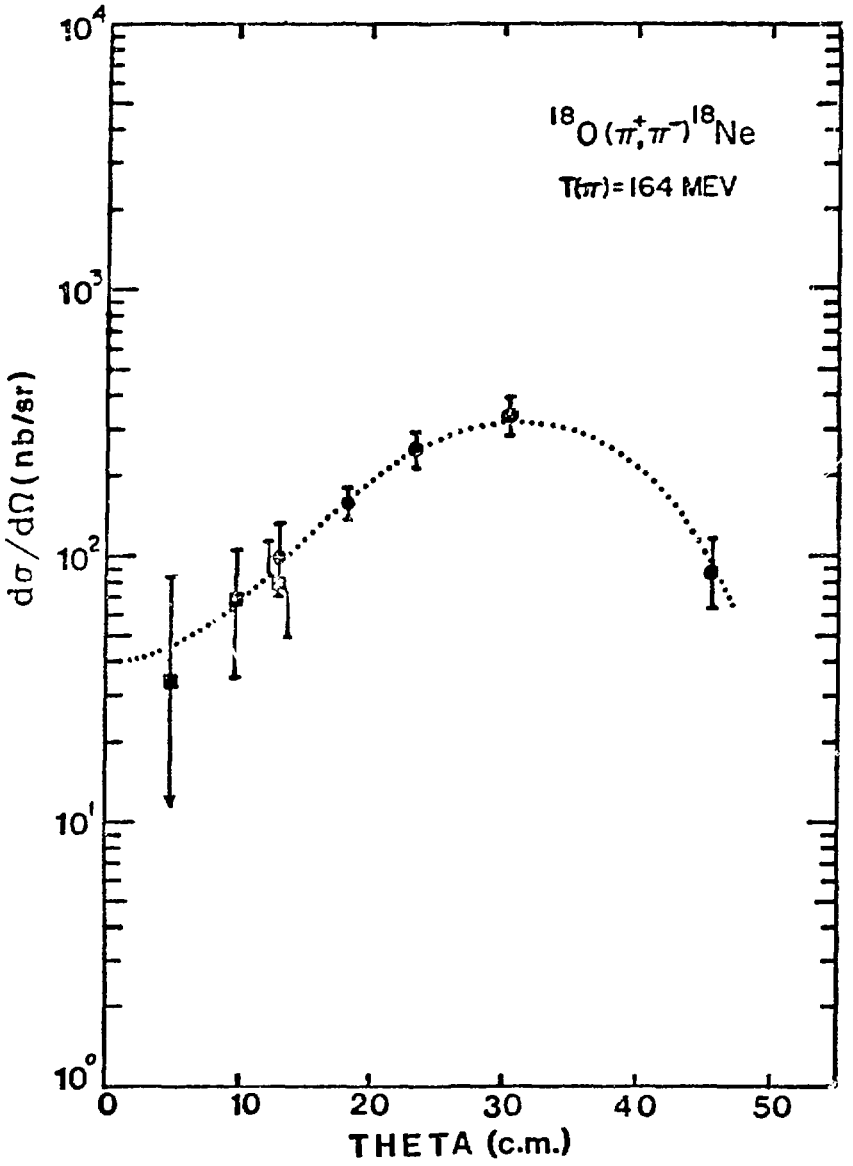

Fig. 16.

Angular distribution for the L = 2, E^* = 1.89 MeV transition for the DCX reaction $^{180}O(\pi^+,\pi^-)^{18}Ne$. The data are from Refs. 50(b) and 51(a). The dotted curve is merely to indicate the trend of the data.

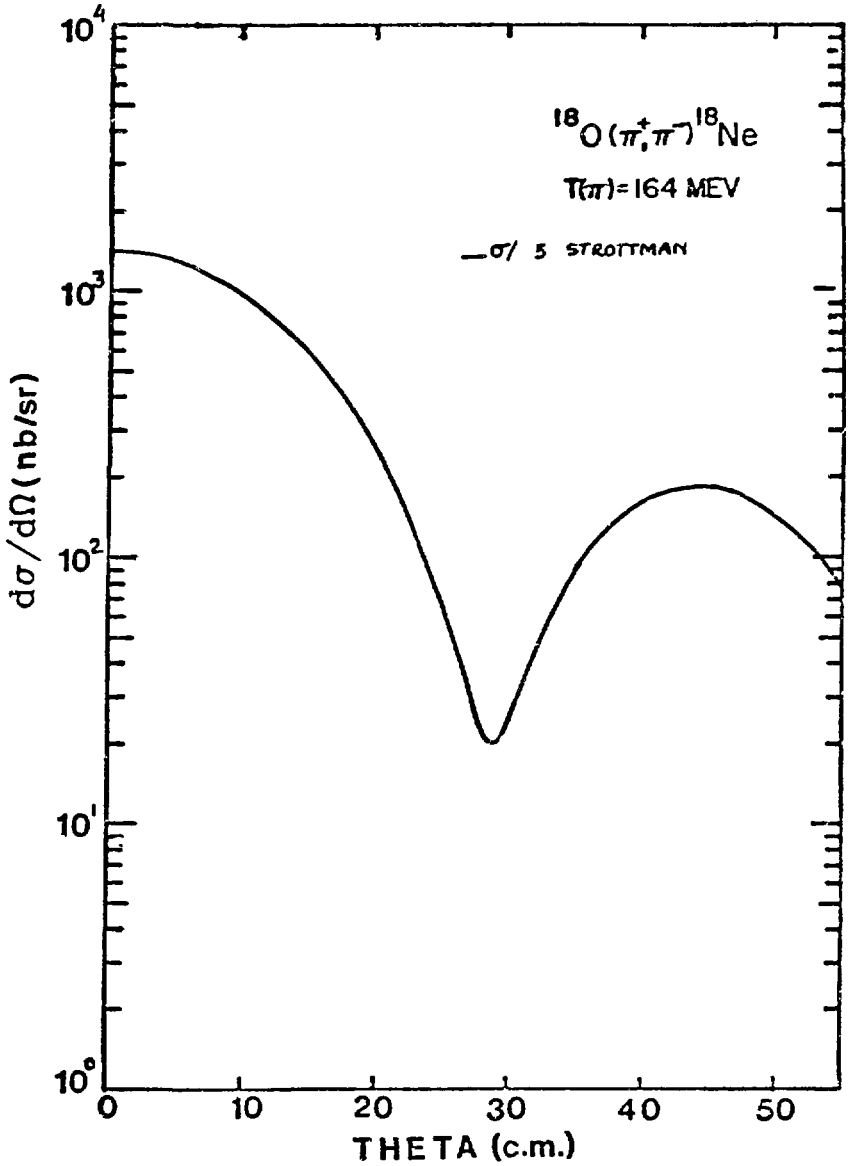

Fig. 17.

The angular distribution prediction for the transition $^{18}O(\pi^+,\pi^-)^{18}Ne$ (g.s.) from the Glauber model calculations of ref. 55.

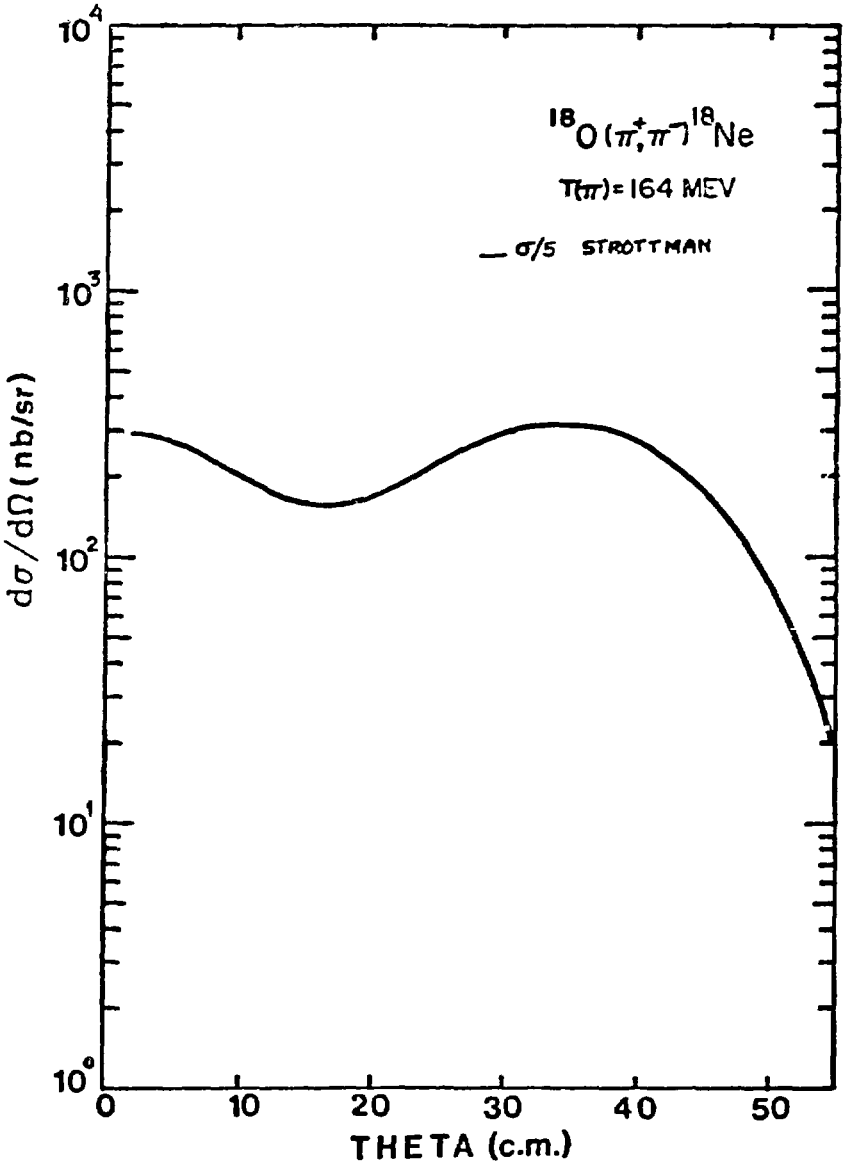

Fig. 18.

The angular distribution prediction for the transition $^{18}O(\pi^+,\pi^-)^{18}Ne$ (2^+, 1.98 MeV) from the Glauber model calculations of ref. 59.

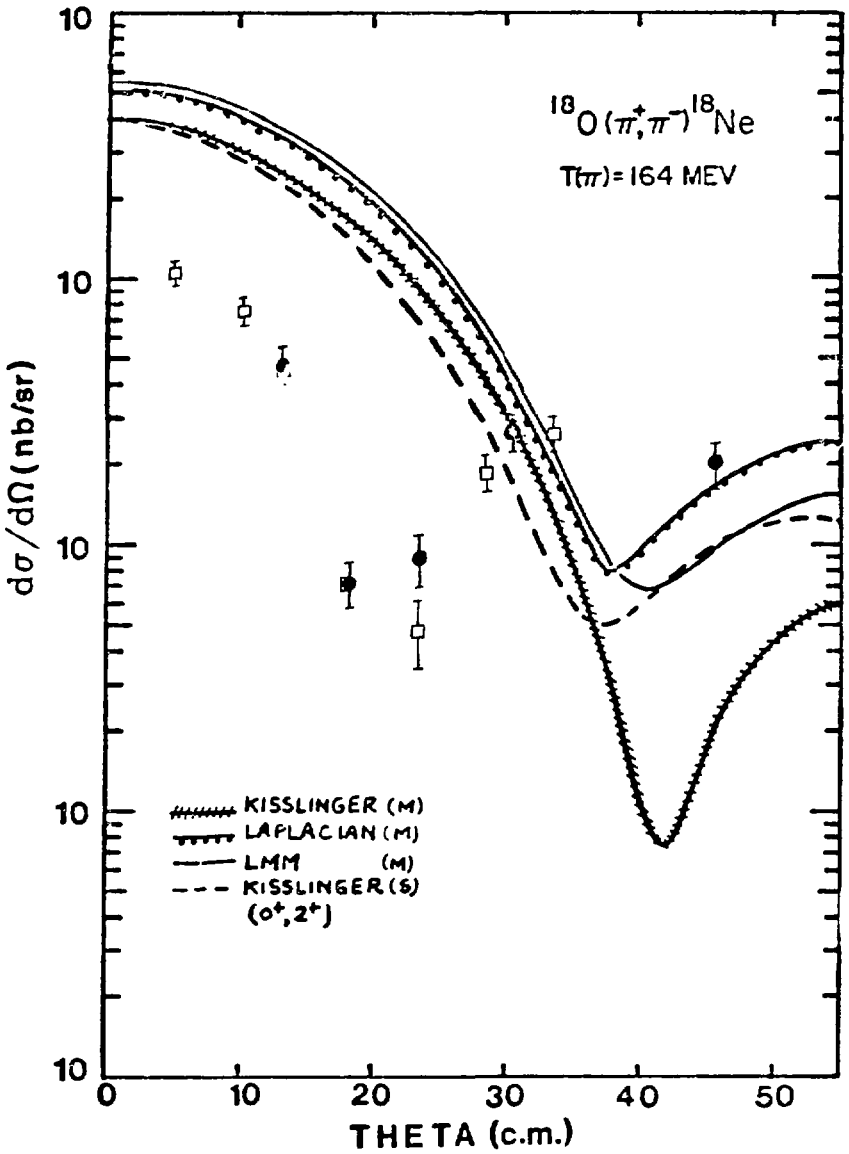

Fig. 19.

Results of several optical model calculations for the LL=00 DCX transition $^{18}O(\pi^+,\pi^-)^{18}Ne$ (g.s.) at T(π) = 164 MeV. The three curves due to Miller (ref. 58), identified as (M) use different forms for pion-nucleus optical potential but consider only $0^+ \rightarrow 0^+$ analog transitions. The dashed curve due to Sparrow (ref. 48), identified as (S) includes also the non-analog channel $0^+ \rightarrow 2^+ \rightarrow 0^+$.

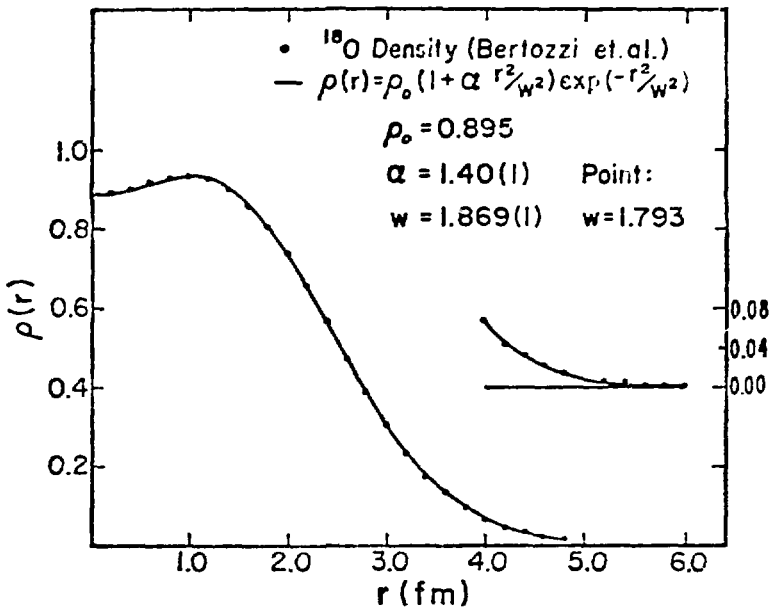

Fig. 20.

Parameterization of ^{18}O charge density as determined by Bertozzi et al. (ref. 57) in a model independent analysis of elastic electron scattering measured at Bates.

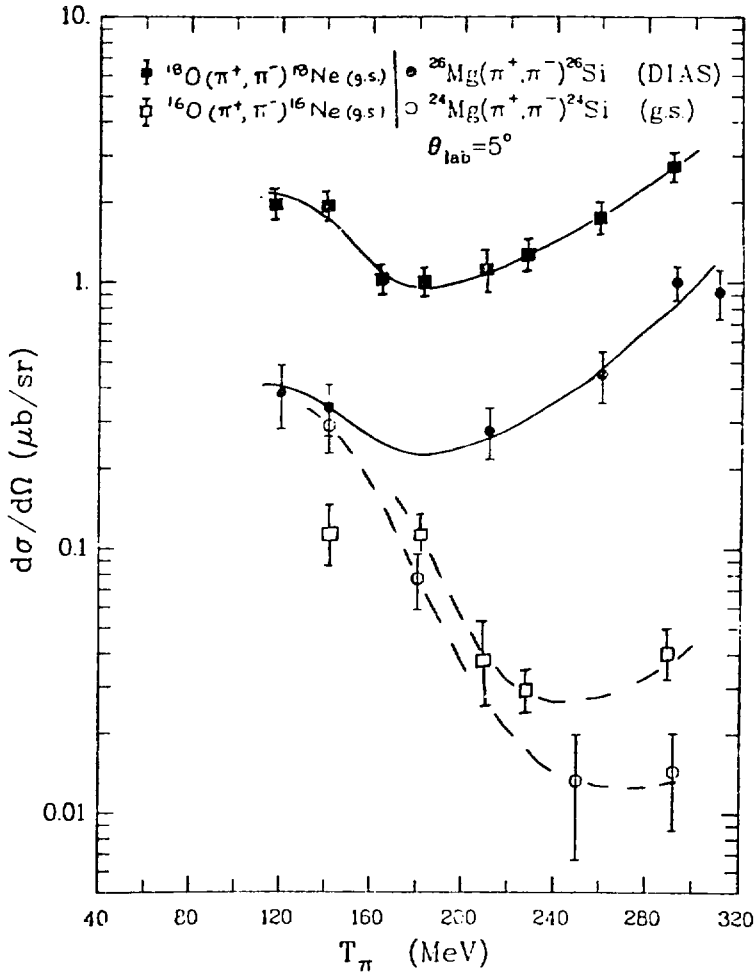

Fig. 21.

Excitation functions for analog transitions $^{18}O(\pi^+,\pi^-)^{18}Ne$ (g.s.) and $^{26}Mg(\pi^+,\pi^-)^{26}Si$ (g.s.) and non-analog transitions $^{16}O(\pi^+,\pi^-)^{16}Ne$ (g.s.) and $^{24}Mg(\pi^+,\pi^-)^{24}Si$ (g.s.) as measured in ref. 51. Notice the characteristic differences between excitation functions of the analog and the non-analog transitions.

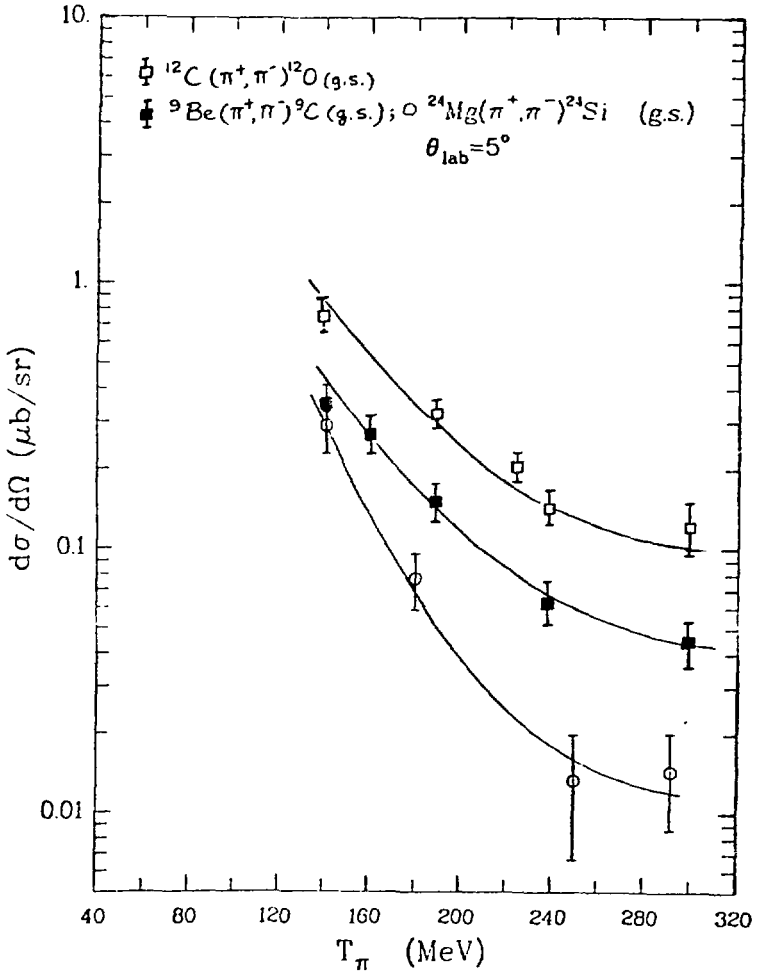

Fig. 22.

Excitation function for three non-analog transitions. The ^{12}C data are from Ref. 40(i), the ^{9}Be data are from Ref. 50(j) and the ^{24}Mg data are from Ref. 51. Notice the essential similarity of the three excitation functions.

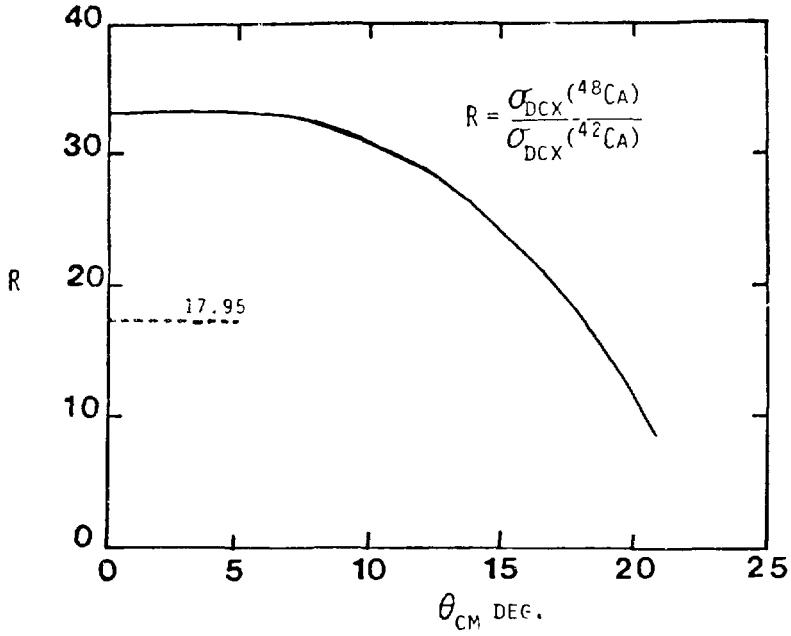

Fig. 23.

Prediction for the angular distribution of the ratio R based on the eikonal model calculation of Germond and Johnson (ref. 63) using realistic densities for ^{42}Ca and ^{48}Ca. The simple prediction of Eq. 15 is indicated by the dashed line.

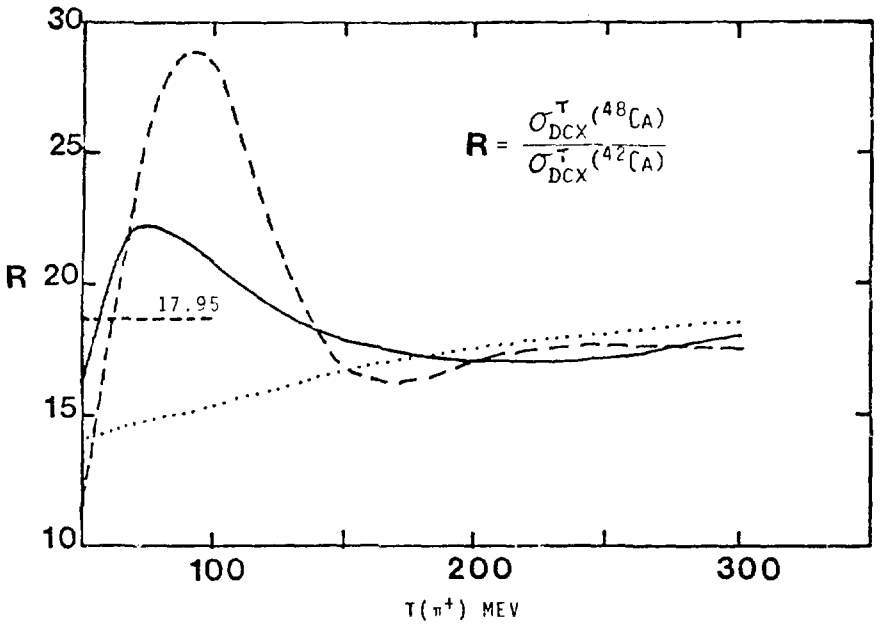

Fig. 24.

Predictions for the excitation functions of ratio R for total DCX cross sections based on optical model calculations of Miller and Spencer (ref. 58). The three different curves correspond to Kisslinger, Laplacian, and LMM potentials.

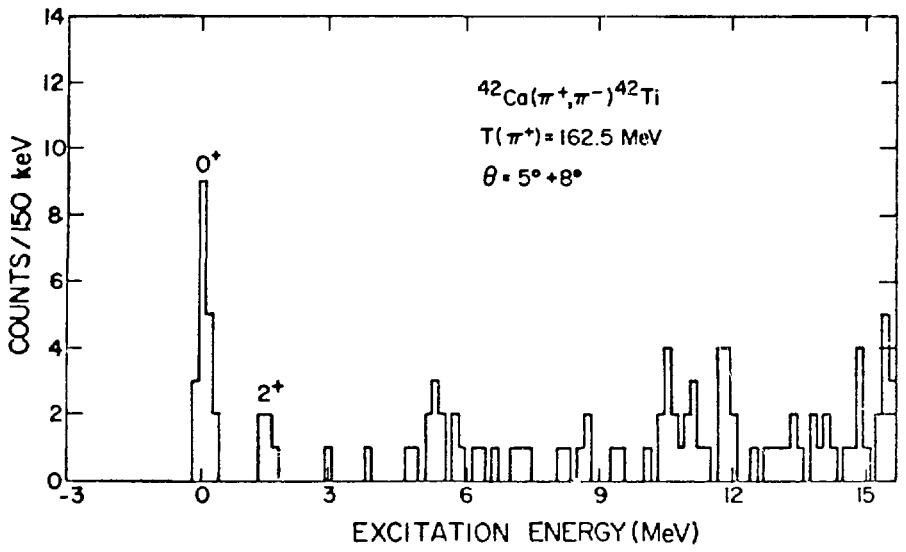

Fig. 25.

Spectrum for the reaction $^{24}Ca(\pi^+,\pi^-)^{42}Ti$. The spectrum is the composite of the 5° and 8° spectra which had essentially equal populations of the g.s. The data are from Ref. 50(j).

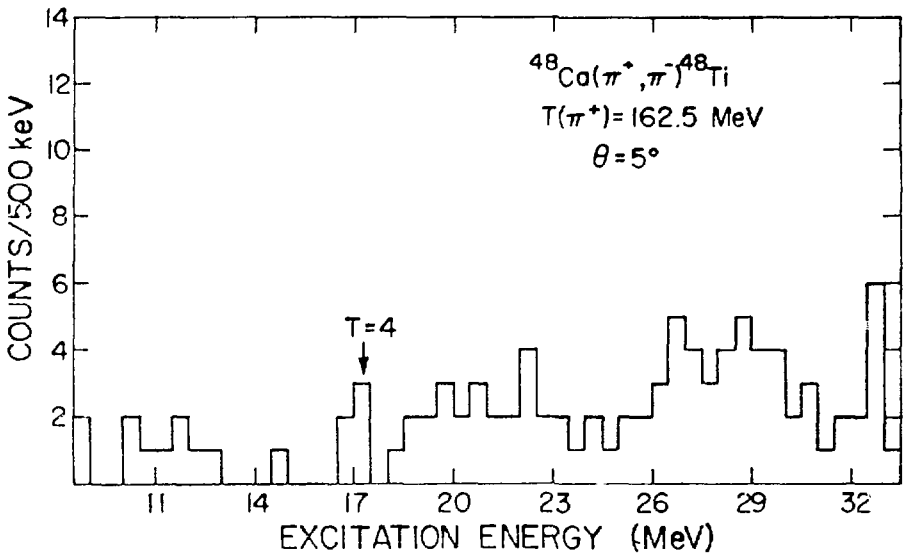

Fig. 26.

Spectrum for the reaction $^{48}Ca(\pi^+,\pi^-)^{48}Ti$ in the region of the expected T = 4 state ($E^* \simeq 17$ MeV). No clear peak is visible over the continuum background. The expectation was for a peak of 45 ± 12 counts in a ± 500 keV region around 17-MeV excitation.

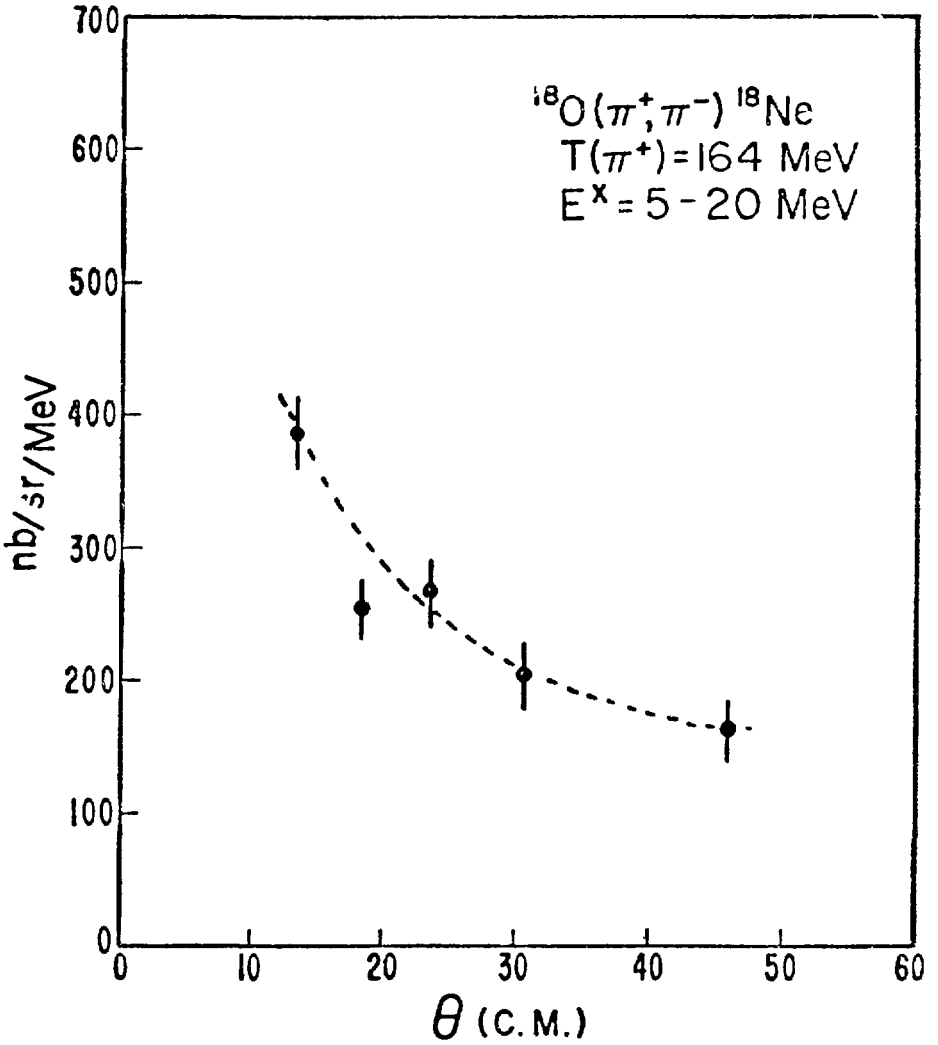

Fig. 27.

Angular distribution for the integrated cross section in the excitation region 5-20 MeV for the reaction $^{18}O(\pi^+,\pi^-)^{18}Ne$. (from Ref. 50(b).

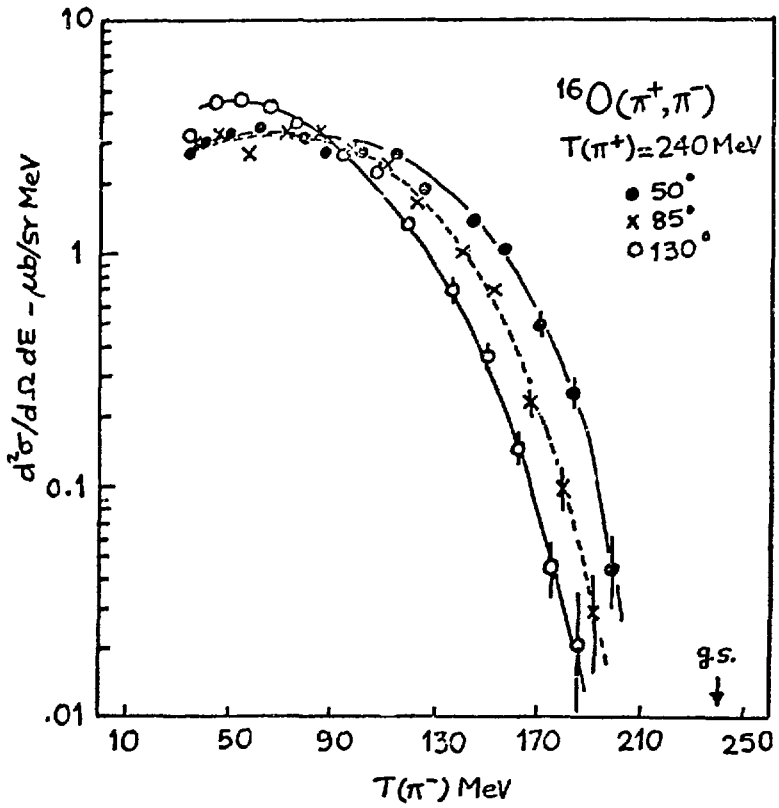

Fig. 28.

DCX double differential cross section $d^2\sigma/d\Omega E$ for the reaction $^{16}O(\pi^+,\pi^-)$ at $T(\pi^+)$ = 240 MeV (from Ref. 66).

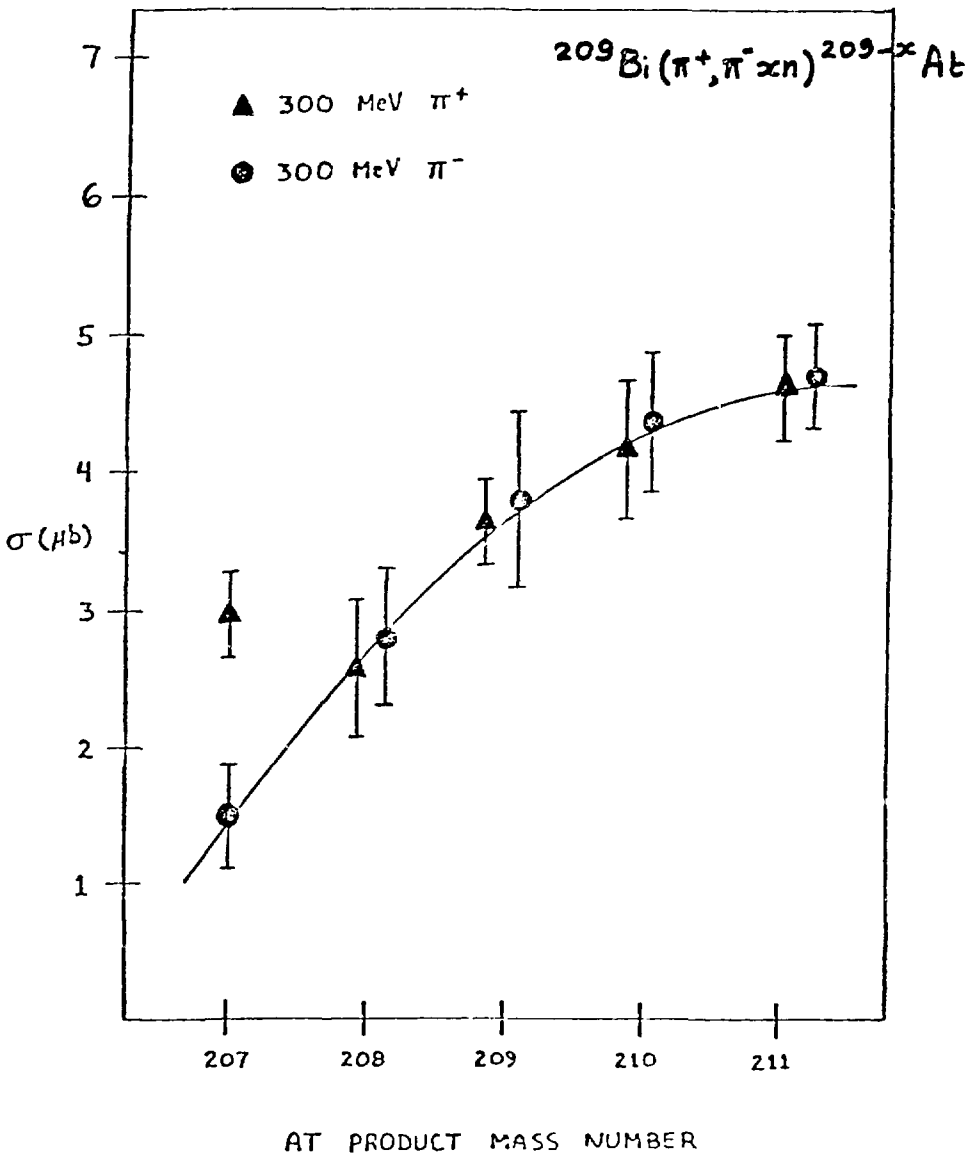

Fig. 29.

Activation cross sections for the reaction $^{209}Bi(\pi^+,\pi^-xn)^{209-x}At$. The filled circles indicate the measured cross sections. The filled triangles are 'background' measurements obtained by looking for the same activities when the incident particle was changed from π^+ to π^-.

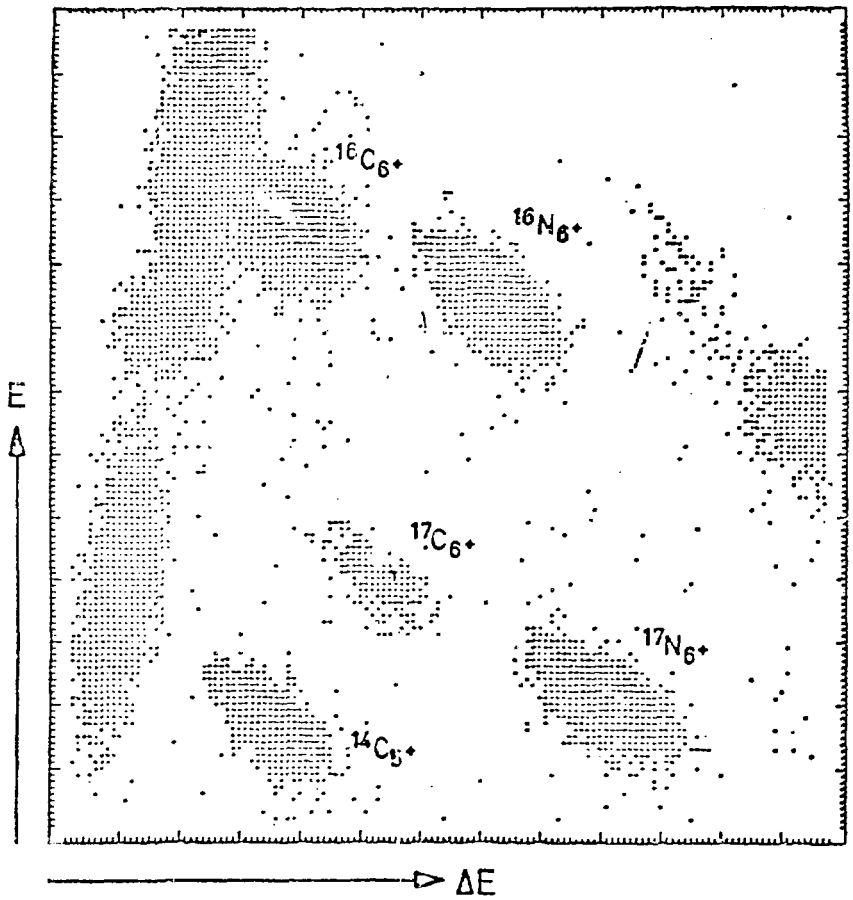

Fig. 30.

A typical particle identification spectrum in mass measurement by heavy ion reactions (from Ref. 76). Contrast this to the particle identification in pion DCX reactions as illustrated in Fig. 4.

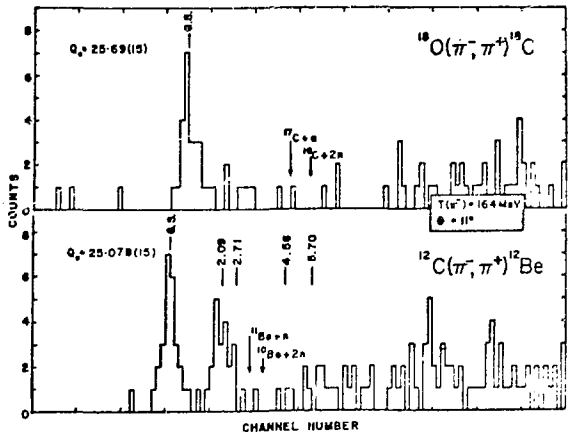

Fig. 31.

Spectra of (π^-,π^+) reaction on ^{18}O and ^{12}C at $T(\pi^-)$ = 165 MeV at Θ = 11°.

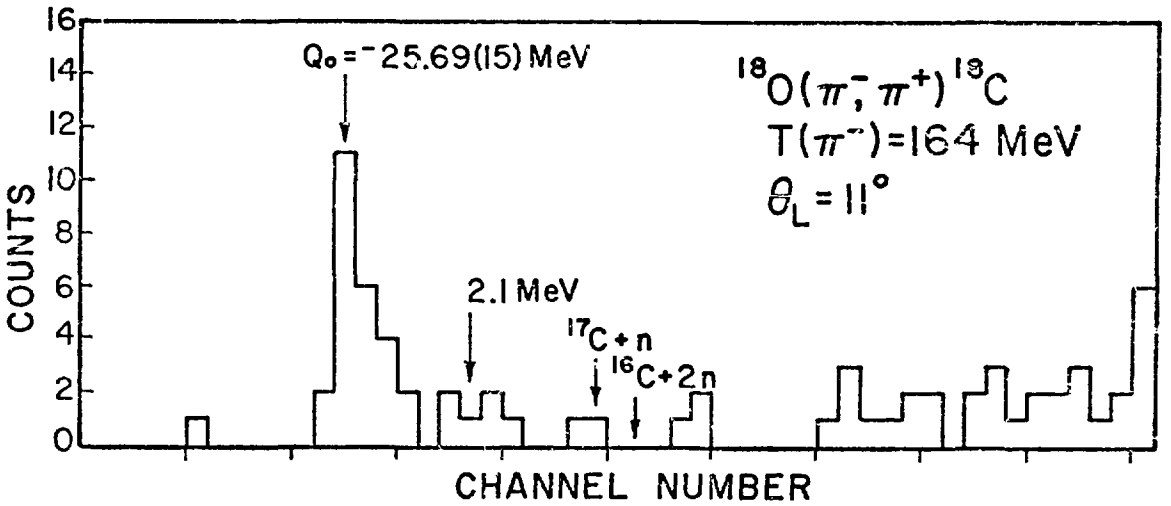

Fig. 32.

A rebinned spectrum for the reaction $^{18}O(\pi^-,\pi^+)^{18}C$. Notice the almost complete absence of background to the left of the g.s. transition. Is the concentration of counts at ∿2.1 MeV excitation statistically significant?

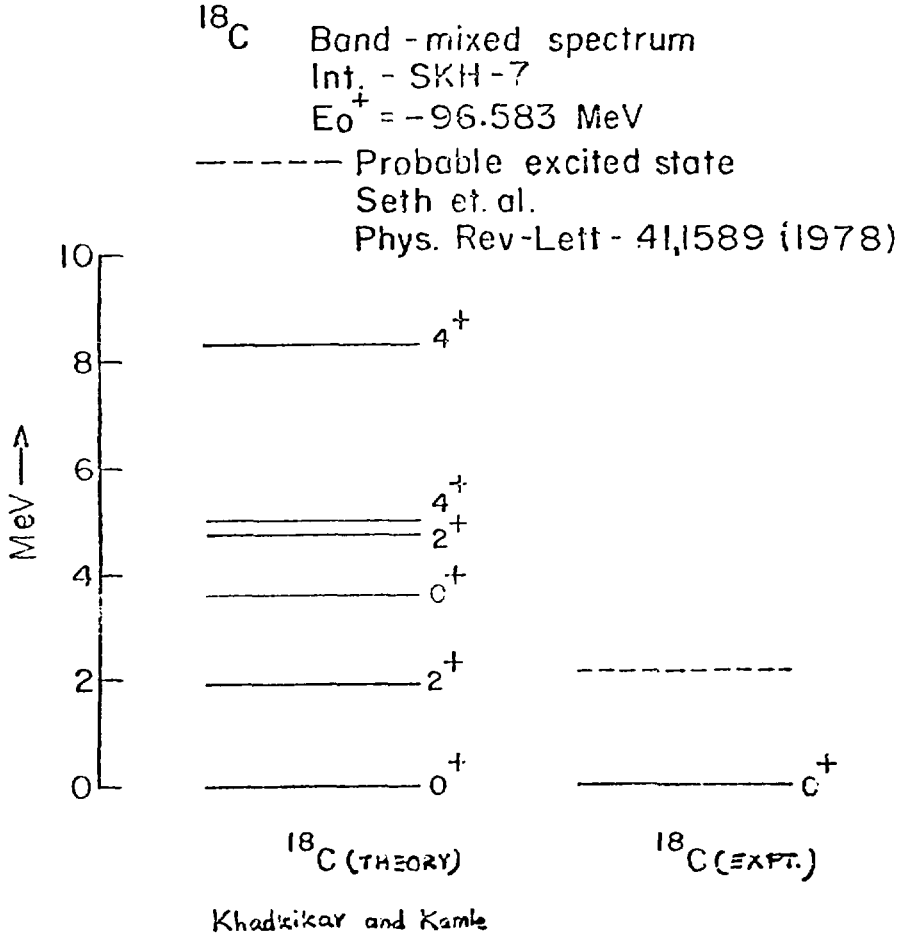

Fig. 33.

Prediction of the excited state spectrum of ^{18}C, based on deformed Hartree-Fock calculations of Khadkikar and Kamle (Ref. 71).

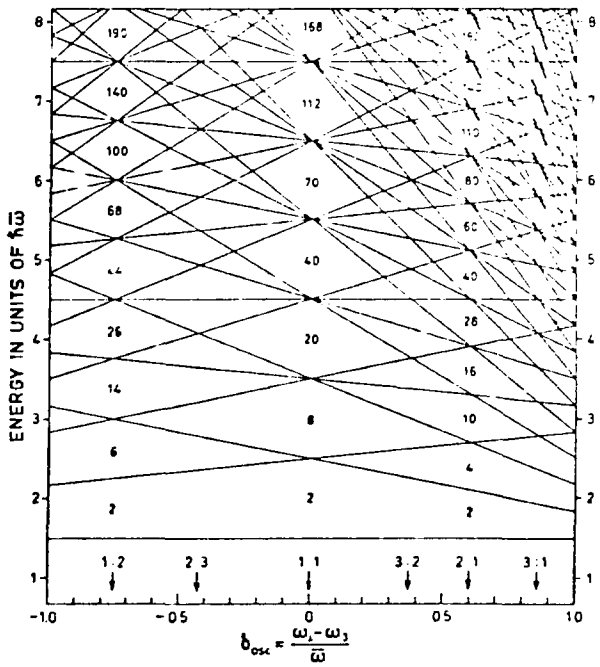

Fig. 34.

Single-particle spectrum for axially symmetric harmonic oscillator potentials (from Bohr and Mettleson, Ref. 82). Note the magic numbers at 2:1 deformation.

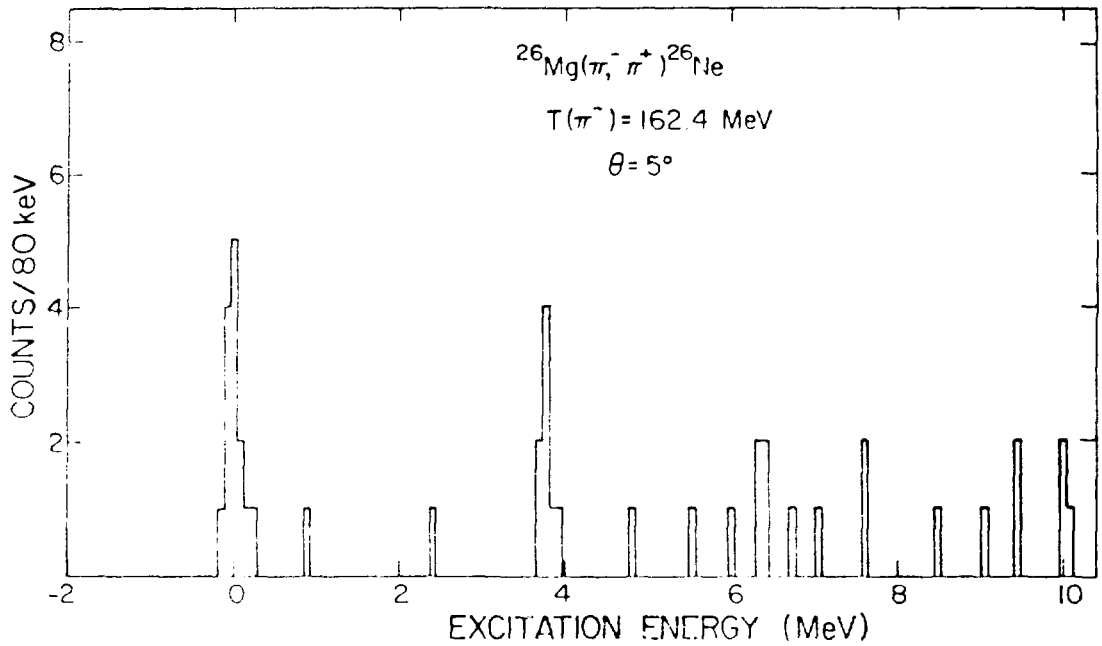

Fig. 35.

Spectrum for the reaction $^{26}Mg(\pi^-,\pi^+)^{26}Ne$.
The data are from Ref. 50(f).

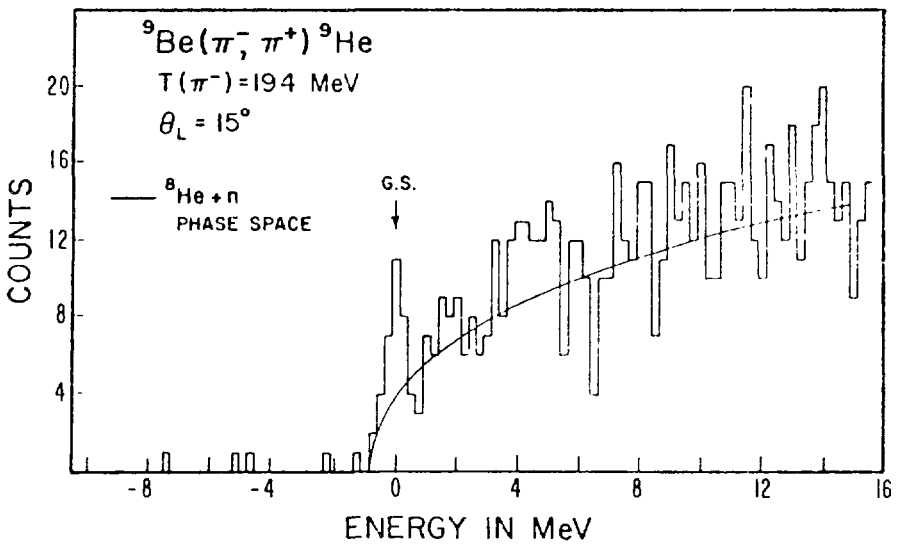

Fig. 36.

Spectrum for the reaction $^{9}Be(\pi^-,\pi^+)^{9}He$. Note the clear enhancement, identified as due to ^{9}He (g.s.), at the end of the phase space.

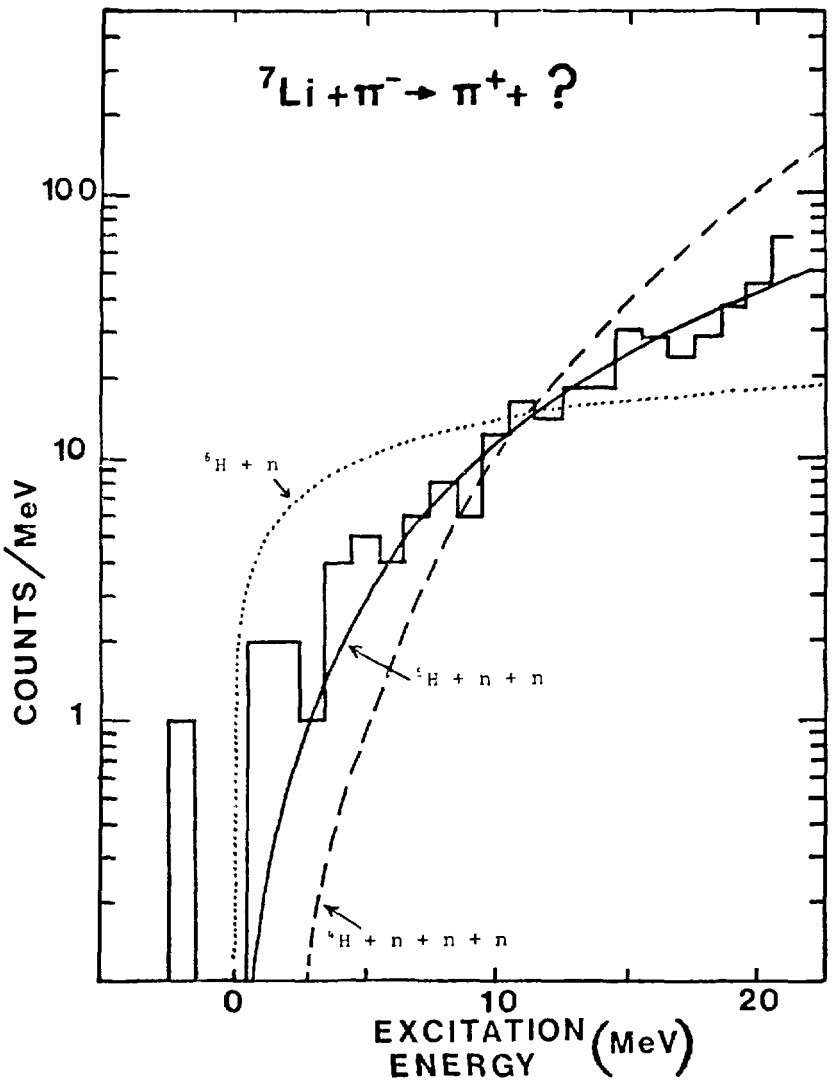

Fig. 37.

Spectrum for the reaction $^7Li + \pi^- \rightarrow \pi^+ +$ 'all'. The smooth trend of the data is only fit by 'all' = $^5H+n=n$.

Summary Report and Recommendations from Panel

NC-2 NUCLEON-NUCLEUS REACTIONS AND NUCLEI FAR FROM STABILITY

by

R. G. Korteling, Simon Fraser University, Chairman

G. W. Butler, LASL, Co-Chairman

I. INTRODUCTION

This panel covered two distinctively different topics, nucleon induced reactions and the production and study of nuclei far from stability. This report is therefore divided into these two topics. In addition, the panel joined panel NC-1 for a joint session on pion and proton spallation and fragmentation. As a result, some of the material of that session might appear in both of the reports.

II. NUCLEON-NUCLEUS REACTIONS

The subject was divided into three areas, fragment inclusive measurements, coincidence multiplicity measurements, and spallation studies. In addition, two distinctly different theoretical approaches to describe the initial interaction were presented. The following is a summary of the individual presentations and comments from the members of the panel divided into the three areas, followed by a consensus of the panel as to the direction the field should take in the future.

A) Fragment inclusive measurements

A general survey of the available data for light single particle inclusive spectra from p + A reactions of intermediate and higher energies was presented in tabular form as well as a presentation of some specific reactions (a copy of these tables are available from R. Green, Department of Chemistry, Simon Fraser University, Burnaby, B.C., Canada). In summary, the information available from the references cited in these tables provides a reasonable overview of inclusive spectra, excluding the study of the population of specific nuclear levels in two-

body final states. There are clearly some deficiencies, especially in reaction product energy ranges and in systematic target dependence studies (particularly for heavy fragments) with good relative normalization. However, the general features have been demonstrated and it is questionable whether additional inclusive measurements are needed except to answer specific theoretical questions.

These spectra seem to result from an evaporation component at the lower energy range and a high energy non-evaporative tail which dominates the spectra in most cases. The evaporative component needs little further theoretical treatment although it can be used to investigate the evaporating sources more critically than neutron, proton, or alpha emission. It is the non-evaporative tails which are not understood and need theoretical effort.

One approach involves a single scattering of the incident nucleon with the high momentum component of a nucleon within the nucleus with the emission of the struck nucleon or cluster generated by the struck nucleon. The recoil momentum is absorbed by a jet or cluster within the nucleus. With such a model good agreement has been obtained for backward emission of protons and alphas of various energies and angles. The intra-nuclear cascade (INC) calculation also has been able to fit a large range of nucleon and pion spectra. However, neither approach has directed much effort toward the heavier fragment data ($12 \lesssim A \lesssim 25$).

Very heavy fragment ($25 \lesssim A \lesssim 60$) emission has primarily been studied by radiochemical methods to date although some counter work is now underway. Although they too exhibit the same general characteristics as the lighter fragments, it has been noted that they undergo a remarkable kinematic change above bombarding energies of 3 GeV. Whereas the fragments are strongly forward peaked at the lower energies, when the incident energies are raised to $\sim$30 GeV, the angular distribution is shifted to sideways peaking and this shift is increased at 400 GeV. However, it should be mentioned that the higher energy fragments are not shifted as much as those with intermediate energies. An additional feature of the very high bombarding energies is the increase in cross section for the very low particle energies. Unfortunately little, if any, data exist for the light fragments to see if they also show these changes at the high bombarding energies.

Some sideways shifting of the angular distributions is expected by the single scattering model but very little work has been directed to this problem as yet.

B) Correlation and Multiplicity Measurements

Unfortunately there has been virtually no program in the field of nucleon-nucleus reactions to study the correlations and multiplicities of these processes. The field seems to be at the stage that relativistic heavy ion studies were a few years ago when a large amount of single particle inclusive data existed and established the basic characteristics of these reactions. However, these single particle data were insufficient to distinguish between the various models proposed and a new generation of experiments was begun employing more exclusive techniques. These included multiplicity-biased spectra, two-particle correlation measurements, and visual techniques such as streamer chambers. Several experiments have now been done and the added information has been useful in identifying and explaining specific processes. The future now lies in facilities which will make an effort to measure all particles generated in a reaction and therefore becoming a totally exclusive measurement. For the heavy ion program these are in the form of the plastic ball/plastic wall facility which will be capable of measuring up to 95% of the charged particles and the Heavy Ion Super-conducting Spectrometer (HISS) facility which will be able to make a totally exclusive measurement.

Both theoretical presentations urged the nucleon-nucleus field to follow the lead of the heavy ion program and start correlation and multiplicity studies. The single scattering model is able to predict the correlation between the emerging incident nucleon and the emitted fragment (proton and alpha). Furthermore, the multiplicity of the reaction seems to be dependent on the details of the recoiling jet form and so could be very useful in developing the model. Such measurements would also be of help in testing the INC calculation by giving a direct measure of the residual nuclide distributions and energies.

C) Spallation Studies

Some effort is being made to systematize the spallation yield as a function of target, bombarding projectile and energy, and cascade residues leading to the product. Some general trends are quite evident. It was pointed out that in most cases (all except for some heavy ion work) that the INC plus evaporation calculation underpredicted the products near the target and overpredicted the products further removed from the target although both the INC and the evaporation calculations independently seemed to be correct. It was also pointed out that the various codes for the INC calculation were slightly different and a strong plea

was made by the users of such calculations for the codes to be once again equated.

It was suggested that a more sensitive method of studying the cascade-evaporation model was to investigate the products on the wings of the isotopic yield distribution. However, there was some question whether the information could not be more directly obtained by direct measurement of the fast process through particle counter techniques. In any case, there was some hesitation on the part of the theorists to investigate the basics of the evaporation model further with an aim to improve the calculations for the highly-excited cascade residue systems.

D) Conclusions for future directions

There was a general consensus that future measurements should be more exclusive. There seemed to be little need to continue inclusive single particle measurements except for specific cases of theoretical interest. Some of these include further polarization studies, additional electron-induced studies, and a few specific cases to fill in the systematics as a function of target mass. In addition, some higher energy (many GeV) studies of the light fragments would be useful.

However, the strongest recommendation was to initiate programs involving correlation and/or multiplicity studies. It was felt by the theorists that these studies would probably be even more useful for nucleon-induced reactions than they have been for the heavy ion program and that without them the theoretical understanding of these processes will not proceed significantly. On the other hand, it was also clear that the experimental programs could be helped by greater theoretical interest in the problems and that they need some guidance as to what are the critical parameters to be measured.

III. NUCLEI FAR FROM STABILITY

The topic of "Nuclei Far From Stability" is a vast one and it has been the subject of several international conferences in recent years. The purpose of including this topic in Panel NC-2 was to demonstrate the strong interest among intermediate-energy nuclear chemists in studying the properties of nuclei far from the valley of β-stability. The following summary reviews the highlights of the individual presentations and the subsequent comments from the members of the panel, followed by the consensus of the panel concerning future directions for research in this area.

The study of nuclei far from stability has shown remarkable progress in the last ten years, resulting in the discovery of many new isotopes, new magic numbers, new regions of nuclear deformation and even new modes of radioactive decay. Several different experimental methods have been developed for the production, identification, and detailed study of nuclei far from stability. Nevertheless, only about a thousand radioactive nuclei are now known, whereas an additional ∿8000 nuclei far from stability have been predicted to be bound against nucleon emission, based on the currently known nuclear structure information. Only the search for new isotopes reaching towards the limits of nucleon stability will eventually determine how well the established theories of nuclear structure apply to nuclei even farther from the valley of β-stability.

The discoveries of many new neutron-rich nuclei far from the valley of β-stability in the last two years is indicative of the strong interest in studying such exotic nuclei. For a large number of these recently discovered nuclei, the only thing known about them is that they are stable with respect to direct neutron emission. However, even this information is important because particle stability is a sensitive check of the theoretical predictions of the masses of nuclei, especially in cases where the limits of nuclear stability can be established, as was the case recently for ^{14}Be and ^{17}B.

Several different methods have been used to produce and study nuclei far from stability, including fission, high-energy proton-induced spallation, deep inelastic heavy-ion reactions, direct transfer reactions, high energy heavy-ion fragmentation, and pion double charge exchange. Each of these methods has somewhat different applications, sensitivities, and limitations. An excellent example of the experimental efforts to determine the limits of particle stability is the recent discovery of the neutron stability of 14 new neutron-rich light nuclei by projectile fragmentation of a 200 MeV/amu ^{48}Ca beam at the Berkeley BEVALAC. In this experiment the heaviest N, F, and Ne isotopes observed were only 1 or 2 isotopes away from the predicted neutron drip line. There are currently several other active experimental programs to search for previously unknown nuclei very far from stability, including those at ORSAY, Berkeley, and LASL.

Clearly more detailed nuclear structure information is required for these exotic nuclei, beginning with the ground state mass, which is the most fundamental quantity of a nucleus. Three different methods have been used to measure masses of nuclei far from stability. Total beta decay energies have been determined by β-γ coincidence techniques for many nuclei, but this method has the restrictive

limitation that some knowledge about the decay scheme is necessary. The determination of nuclear reaction Q-values from complex transfer reactions has been used to measure the masses of many neutron-rich light nuclei. Q-value measurements have now been extended to include pion double charge exchange reactions, as illustrated by the recent determinations of the ^{18}C and ^{26}Ne masses. However, the reaction Q-value technique is not useful for measuring masses if the nuclei of interest cannot be produced in reactions with two-body final states. Another limiting factor in this technique is the uncertainty about whether the ground state of the residual nucleus will be significantly populated in exotic rearrangement reactions. The technique of direct atomic mass measurements overcomes most of the difficulties of the previously mentioned techniques. The ORSAY group, which pioneered the technique of on-line mass measurements, has successfully completed accurate mass measurements for nearly all of the known isotopes of the alkali elements by utilizing a mass spectrometer on-line with either the 28-GeV beam at the CERN proton synchrotron or the mass-separated ion beams of the ISOLDE facility at the CERN synchrocyclotron. Further developments of a negative ion source may enable them to do future mass measurements of the halide elements F, Cl, Br, I. In the near future the ORSAY group plans to make nuclear spectroscopic measurements on K and F isotopes in addition to accurate Q_β measurements on the decay products of the isotopes of the alkali and halide elements that are far from stability. A more remote future project is the development of an ultra-high resolution ($M/\Delta M \simeq 10^6$) RF mass spectrometer for the purpose of measuring the mass of the anti-proton to an accuracy of 1 eV (1 part in 10^9).

A group at Los Alamos is currently attempting to make direct mass measurements on neutron-rich light nuclei ($Z < 20$) produced by 800-MeV proton-induced fragmentation of uranium by a combined dE/dx, time-of-flight technique. These measurements are limited to a mass resolving power of $M/\Delta M \simeq 200$ by the accuracy with which the total kinetic energy of the fragments can be measured with conventional detectors, since the fragment mass depends linearly on the energy. Another limitation of this experiment is the extremely small solid angle ($\sim$ 5 μsr) subtended as a result of the long flight path utilized (4.3 m). This group has recently written a proposal to build a time-of-flight magnetic spectrometer at LAMPF to make accurate on-line mass measurements of neutron-rich light nuclei ($Z<30$) produced by proton-induced fragmentation of uranium. This spectrometer, which will be focussing in both energy and angle and be independent of flight time (isochronous), will have a mass resolving power of $M/\Delta M = 1000$ and the capability of

measuring the masses of many neutron-rich nuclei to accuracies of better than 200 keV. An important feature of this technique is that several isobars will be measured simultaneously and those near stability with known masses can be used as internal calibration points that differ in mass from the unknown isobar by only β-decay energies of ∿20 MeV. This new TOF magnetic spectrometer will represent an improvement in mass measurement capability of more than a factor of 200 over the current setup.

Detailed nuclear spectroscopic information about nuclei far from stability is essential for the further understanding of such phenomena as deformations, shell closures and binding energies. (This topic was recently covered rather extensively in the 1979 Nashville Conference on Future Directions in the Study of Nuclei Far From Stability). Radioactive decay spectroscopy provides a means for populating many high-lying states in exotic nuclei and a reasonably strong tool for determining the basic structures of many of these states, since β-decay is one of the few nuclear phenomena that retains some vestige of being a single-particle process. However the reactions for producing such exotic nuclei require heavy-ion or high-energy proton beams, and the production cross sections become increasingly smaller as the nuclide gets farther from β-stability. The half-lives of these nuclei are short, making a fast transfer system, such as a helium jet, essential. And the many competing reactions, especially when some form of spallation is used, make some sort of on-line isotope separation or rapid chemistry all but mandatory.

The ISOLDE facility at CERN is the outstanding example of an on-line isotope separator at a high-energy proton accelerator for research on nuclei far from stability. At ISOLDE there have been many successful research programs including mass measurements, nuclear spectroscopy, and optical spectroscopy. There is a possibility that the ISOLDE facility will be moved to SIN in a few years, at which time it would be upgraded to a more powerful and versatile facility.

The only isotope separator on-line with an accelerator for nuclear spectroscopy in the U.S. is the UNISOR facility at Oak Ridge National Laboratory. Research at UNISOR has been predominantly nuclear spectroscopic studies of neutron-deficient heavy mass nuclides produced by heavy ion reactions. There are at least two isotope separators on-line with nuclear reactors for nuclear spectroscopy studies in the U.S. The TRISTAN mass separator was recently moved from Ames Laboratory to the High Flux Beam Reactor (HFBR) at Brookhaven National Laboratory, where the experimental program is expected to begin during the summer of 1980.

It is anticipated that it will be possible to ionize and separate a number of non-gaseous fission product elements and to study the decay of isotopes with half-lives less than 1 second at the TRISTAN facility. The Battelle Northwest mass separator SOLAR is currently on-line with a reactor at Washington State University and it has been used for β-delayed neutron spectroscopy of alkali elements such as Rb.

A group at the Idaho National Engineering Laboratory is currently developing an on-line isotope separator facility that uses gas-jet transport of fission product activity from mg size ^{252}Cf sources into the ion source. They have evidence for formation of ion beams, with separation efficiencies in the percent range, for such fission product elements as Sr, Y, Mo, Tc, Ba, Pr, Nd, Pm, and Sm. They have also developed a rapid automated chemical separation technique that is based on solvent extraction by annular centrifugal contactors. This technique was recently applied to the separation of palladium from mixed fission products generated by a ^{252}Cf spontaneous fission source and transported to an on-line collection device by a helium jet system.

It is quite clear that there is a very strong interest among many nuclear chemists in studying nuclei far from stability. A strong recommendation was made by a consensus of several members of the NC-2 Panel that a program of study of nuclei far from stability should be instituted at LAMPF utilizing a gas-jet transport system coupled to a mass separator. Several papers presented at the workshop provided new scientific justification for such a program. For example, recent mass measurements at ISOLDE have shown that the current theoretical mass formulae are inadequate for nuclei very far from β-stability, with the result that theoretical predictions of the neutron drip line may be seriously in error. These measurements also provide evidence for new regions of nuclear deformation, the features of which require detailed nuclear spectroscopic study. Through 800-MeV proton-induced fission of ^{238}U at LAMPF, it should be possible to produce copious amounts of neutron-rich nuclei that have not been accessible through thermal-neutron-induced fission. Due to recent developments in the use of He-jet transport, most of the elements produced in the proton-induced reactions can be mass separated with relatively high efficiency. Such an approach promises to be simpler, more flexible and less expensive than those previously proposed for an on-line isotope separator facility at LAMPF. Several participants in the workshop, representing a number of institutions, were sufficiently encouraged by these new prospects to pursue collectively the development of such a facility.

Summary Report and Recommendations from Panel

NC-3 MESONIC ATOMS

by

R. A. Naumann, Princeton University, Chairman

J. D. Knight, LASL, Co-Chairman

I. INTRODUCTION

Mesonic atom research, the study of the formation and properties of atoms containing an exotic negative particle, has achieved noteworthy progress in the past few years. Experiments have progressed from the exploratory, broad survey type to those that seek exact answers to specific questions. The superior fluxes of stopping beams with well-defined energy provided by the meson factories now permit both the accumulation of data of higher accuracy and the mounting of more probing experiments. Theoretical studies, meanwhile, are treating the phenomena of mesonic atoms on a more realistic basis. These encouraging trends provide a foundation for significant future developments.

Our panel sessions dealt with theory and experiment related to (1) the initial meson capture process, and (2) the subsequent intraatomic (or molecular) cascade. Applications and some specific experimental techniques bearing on both chemical and nuclear reactions were presented and discussed.

II. THE COULOMB CAPTURE PROCESS

Melvin Leon introduced a session with an historical survey and evaluation of the Coulomb capture theories developed to date. Most of these have been semi-classical, involving concepts such as friction on a meson moving in some trajectory through a locally established Fermi electron gas. A quantum-mechanical treatment of meson capture in solids (1968) is thus far the only calculation explicitly including the effects of ionicity.

Willard Wadt and Richard Martin gave a status report on their new theoretical treatment -- more exact Hartree-Fock calculations of the muon capture process using modern techniques now employed to calculate atomic and molecular orbitals. This approach offers promise for the realistic analysis of the meson capture process. Their initial calculations have involved the stopping of muons on single atoms. In the near future, the transport problem for slowing down and capture will be solved. These results will then allow a prediction of relative muon capture probabilities in simple gas mixtures, such as Ne + Ar, for which experimental data already exist. The next goal will be the calculation of muon capture by bound atoms in simple molecules, that is, the explicit inclusion of the chemical bond.

Joachim Hartmann reported on the very extensive data the Munich group has obtained on the systematics of muon capture in oxides, fluorides, chlorides, and sulfides. Now that the experimental uncertainties have been significantly reduced, the correlation of muon capture ratios with elemental ordering in the periodic table, first reported for oxides by Zinov, has been extended also to the other simple binary compounds. Hartmann noted a strong correlation of capture ratio with bond ionicity and ionic radius. He also reported a change in the Ne/Kr capture ratio when excess Ar gas is added. This result contrasts with the observations for solid solutions. One concludes that the effective flux density in gas mixtures is varying with composition.

Mario Schillaci reported on experimental capture ratios for the group of alkali halides, archetypical cubic ionic solids. He made comparisons with the ratios calculated according to Daniel's model, the "fuzzy Fermi-Teller model" of Leon et al., and the prescription of Schneuwly et al. Experimental results for these solid-state analogs of rare gas mixtures should be more tractable for theoretical analysis.

One major goal in this work has been to relate the formation properties of mesonic atoms to the chemical properties of the compounds moderating and capturing the muons. Some results supporting this expectation were provided by Jere Knight; he described measurements of the N/O muon capture ratio for gaseous NO and for an equivalent $N_2 + O_2$ gas mixture, each target at a total pressure of 10 atmospheres. The experiment showed enhanced muon capture by the N atoms in the compound. Assuming that valence electron density correlates with muon capture, this result implies the molecular polarity $^-NO^+$. It is believed to be the first experimental determination of the orientation of the molecular dipole. Recent extended electronic structure calculations predict such a polarity.

Tak Suzuki reviewed his recent muon-decay measurements for a number of oxides. He showed how accurate timing data permit the determination of relative capture ratios for these compounds. The updating of this technique represents a valuable independent method for obtaining capture ratios in compounds.

III. THE MESONIC ATOM CASCADE PROCESS

Petr Vogel presented a review in which he first examined kinds of information provided by the best cascade calculations available, which now include monopole, quadrupole, and electron penetration effects. These calculations include the last stages of the de-excitation sequence, where the observable radiation processes predominate over the preceding Auger-dominated steps. An initial orbital quantum number distribution of mesonic states $P_n(\ell)$ at a single principal quantum number (e.g., n=20) is usually assumed, and the subsequent Auger and radiation steps are calculated. By comparison with the experimental intensities the form of $P_n(\ell)$ is deduced. Vogel concluded that: for heavier atoms the standard statistical shape $P_n(\ell) \propto (2\ell + 1)$ is appropriate; 2) the form of $P_n(\ell)$ correlates with the element's position in the periodic table; 3) for lighter atoms the electronic K shell refilling rate indicated by the cascade calculations is 3 to 4 times smaller than the K width already known from x-ray studies. This reduction probably arises from electron L shell depletion effects from the preceding Auger steps in the cascade. To better test the cascade programs, Vogel suggested measuring complete experimental muonic x-ray spectra for a few heavier elements, where the cascade assumptions should best apply.

Peter Ehrhart and Jere Knight reported measurements on the muonic x-ray intensity patterns observed for several target gases as a function of pressure. By adjusting gas densities and thereby changing the rate of collisions where Auger-produced electronic vacancies are refilled, one may intervene in the de-excitation cascade during its $\sim 10^{-13}$ -sec course. Successful modeling of this process will probably involve Monte Carlo techniques to treat the time evolutions of the gas collisions, electronic refillings, and the muonic cascade.

IV. OTHER PHENOMENA

James Reidy addressed the possibility of altering the per-atom muon capture ratio in composite targets involving granular mixtures of two elements, as opposed to true solutions involving dispersal at the atomic level. The effect

depends upon differing stopping powers and consequent differing spectral flux distributions for each phase of the granular mixture. Such effects would have consequences for quantitative analyses employing muons.

Donald Fleming reported μ^+ spin rotation studies (μSR) of consequence for chemical reaction kinetics. Specifically, these studies involve the muonium system, which here plays the role of a light (At. Wt. = 1/9) hydrogen isotope. Striking effects, such as muonium tunnelling through the molecular potential barriers involved in hydrogen transfer kinetics, evidence that muonium studies can uniquely illuminate basic areas of chemistry. Fleming encouraged the development of analogous ties, wherever possible, relating the studies of the μ^- atomic phenomena to molecular and atomic chemistry and physics.

William Johnson reviewed experiments on the formation of muonic atoms with heavy elements for the study of nuclear fission. In phenomena of this family, the normal muonic atom de-excitation channels -- Auger electron emission and x-radiation -- are supplemented by a third: radiationless excitation of the nucleus. When this process occurs in an atom of a fissionable element, the muon is still present after fission and will accompany one of the fragments. From measurement of the muon decay rate (as influenced by nuclear absorption) one infers to which of the two fragments the muon was bound; experiments conducted so far indicate that in $\geq$ 80% of the events, the muon accompanies the heavy fragment. A successful measurement of the light-fragment capture fraction would determine the non-adiabaticity of the scission process and thereby provide valuable information on the dynamics of fission. Prospects of success for this and similar important experiments will depend on development of considerably improved muon channels.

V. FUTURE PROSPECTS

Although the great majority of the presentations and subsequent discussions of mesonic atom phenomena at our workshop sessions developed important plans, recommendations, or hopes for future action, we have chosen to set aside this separate section to highlight some prospects that appeared especially interesting and promising.

A. Meson Capture in Small Molecules

A central question of mesonic atom research is the extent to which the character of the bonding electrons can affect the capture and cascade processes. As might be expected, simple molecules of the lightest elements appear to show

the largest effect of bonding electrons on meson capture. It is for such molecules that modern quantum mechanical calculations can best describe the electronic structures. Thus, the study of meson capture in these well-characterized systems appears theoretically promising and experimentally reasonable. Examples might be CO, CO_2, NO, and BF_3. In any case, it appears now that an optimal strategy should involve neither a long program of additional experimental measurements nor a similar program of theoretical analysis, but rather a series of smaller steps in which each side is closely coupled to and influenced by the results of the other.

B. Very Slow Muons and Other Negative Particles

For many years now the negative meson fraternity has felt the need for energy-controlled beams of very slow negative mesonic particles -- particles with velocities well below αc (i.e. <2 keV) -- to study atomic capture and scattering phenomena. The Munich team at SIN has now begun to make some significant strides in this direction. Herbert Daniel and Joachim Hartmann reported the successful development of a magnetic monochromator/time-of-flight spectrometer permitting the study of muons with energies below 2 keV. At 1 keV and below, beams of 9 muons per second are now available. With installation of slow muon electrostatic analysis and improved muon channels, an increase of two orders of magnitude appears reasonable. Clearly, this very important development makes possible the direct study of the interaction of energy-selected muon beams with individual atoms or molecules in the capture region ($\leq$ 1 keV). The use of ultra-thin targets (monolayers and possibly highly collimated gas streams) is required; however, the experimental scattering and capture data obtainable can be directly compared with the theoretical predictions now becoming available, justifying the emphasis in this challenging area. The range measurements and the determination of muonic spectral distribution functions stemming from this development are of central importance both to mesic atom research and to stopping power theory at low energies.

The availability of relatively intense very low energy antiproton beams in the near future also merits the attention of experimentalists in this area.

C. $p\mu^-$ Transfer Studies

Although it was not covered extensively in our workshop, we recognize that this area of muonic atom chemistry has considerable fundamental interest and practical importance. Since the transfer of a muon from a muonic hydrogen to a heavy atom involves the Coulomb stripping of the $p\,\mu^-$ system in its ground

state by a (point) nucleus, the theoretical studies of the transfer should be well-founded and tractable. Experimental measurements of relative transfer cross sections of muons to various gases appear possible using hydrogen gas targets containing traces of two or more gases of interest, at hydrogen pressures attainable without employment of special and costly target vessels. The potential of muon transfer as a probe of surfaces is important, and early steps in this direction have already been reported by the Bertin group in Italy. An alternative method for studies of this kind, in which cryogenics is substituted for hydrogen pressure engineering, is the use of liquid hydrogen; as yet there have been no reports of the successful employment of this variation of the hydrogen transfer technique.

D. Fission Studies Using Negative Muons

Further progress in this interesting area awaits the development of muon beams with lower energy combined with higher fluxes, favorable duty factor, and high beam purity.

E. Practical Applications of Muon Capture

1. Non-destructive Chemical Analysis. Herbert Daniel and Richard Hutson reported studies involving elemental analysis of ceramic, archeological, and biological specimens. A true element sensitivity of $1/10^4$ appears possible, and we note that the technique has a wide range of potential application. With muons of well-defined but variable energy, depth scanning analyses and imaging studies are possible. Although we recognize that muon beams and apparatus are expensive, one can foresee that in special circumstances, e.g., in-vivo analysis, or unusual rare samples for which the non-destructive aspect is critical, muonic x-ray analysis may be the most cost-effective or even unique.

2. Study of Surface and Critical Phenomena. The detection of muonic x-rays accompanying the capture of very slow muons in surface monolayers provides a unique method of elemental or structural analysis for surface studies.

One interesting possibility for studying cluster formation in gases near the critical point may be based on the difference in K muonic x-ray intensity patterns between substances in the gas state and the same substances in the condensed state. This is an aspect of the gas density effect noted in the section on the atomic cascade process, and the effect depends on the availability of electrons (from neighbors of the cascading muonic atom) to replace those lost by Auger decay steps. In the critical regime application, there may be a

minimum condensation cluster size, of the order of a few molecules or tens of molecules, for which condensed-state-like electron replacement can be sufficient to furnish a "normal" muonic x-ray intensity pattern. If the number of gas particles in this potential transition region is sufficiently high, the changes in x-ray intensity pattern may serve as a sensitive tool for a small-cluster regime in the approach to condensation.

3. μ^-SR Studies and μ^--Catalyzed Fusion. Although these topics were not discussed at length or represented by research teams at our workshop, we note that considerable interest has been expressed in them.

The first is a form of μSR and employs μSR experimental techniques, but the atomic scale phenomena are different from those for stopped μ^+: the Coulomb capture and atomic cascade place the μ^- eventually at a nuclear site in a molecule or a solid, but a major part of its initial polarization may be lost before it reaches the site. Thus, the depolarization can serve as a different kind of probe of the solid state.

The second topic, the catalysis of fusion of hydrogen nuclei by the μ^- bonding them together in a muonic hydrogen molecule ion, was an interesting and novel phenomenon when it was first turned up in 1957 at Berkeley, but the number of p-d or d-d reactions produced per muon was not sufficient to give the catalyzed reaction any utility. Recently, however, USSR workers have predicted and have verified experimentally a resonance in the reaction $t\,\mu + d \longrightarrow t\,\mu\,d$, as a result of which the effective nuclear fusion rate is enhanced several orders of magnitude and the question of fusion energy release is being revived. Thus, though time constraints in our workshop did not permit examination of this timely subject, we recognize that it should be treated in future workshops.

Summary Report and Recommendations from Panel

NC-4 EXOTIC INTERACTIONS

by

A. L. Turkevich, University of Chicago, Chairman

E. V. Hungerford, III, University of Houston, Co-Chairman

I. INTRODUCTION

To state the difficulties involved in summarizing and projecting the ideas of such a diverse panel into the future are to document the obvious. Still, the point must be made that our crystal ball is cloudy and that propagation of today's conclusions into the future have a rather short temporal mean-free path in the real world. More to the point, many topics are left unmentioned, more as a matter of time and personal taste, than as a judgement of their importance or expected importance to the field. We would encourage all to flavor their science as they perceive the beauty (or charm, or truth, or strangeness) of nature.

The usefulness of this report then is to remind Nuclear Chemists that they have made, and are making important contributions in nuclear and particle physics and that nuclear chemical techniques offer unique advantages for a certain class of problems. Of particular relevance to this panel is the sensitivity of these techniques in the measurement of processes with extremely low probabilities and the ability of these techniques to detect or sum over multiparticle final states. These advantages mean that nuclear chemists can attack problems at the forefront of science often before they can be addressed by others. In fact, such experiments can lay the foundation for the development of more specific and detailed experiments which will follow.

The panel addressed its charge by discussing the role nuclear chemistry might play in four representative areas. These were: A) Antiproton-nuclear interactions; B) Role of mesons in nuclei; C) Neutrino properties and nucleon decay; and D) Interaction of kaons with nuclei. Each subject was briefly reviewed, and there then followed contributions from panel members highlighting specific

questions that might be investigated. This summary is therefore divided into the major headings outlined above. Personal credit for contributions and ideas are not always given. The organization of the workshop and participants are listed in the Appendix to this summary report.

A. Antiproton-Nucleus Interactions

The available data on antiproton annihilation suggest that the factors that have the greatest significance for antiproton-nucleus interactions are:

a. The high multiplicity (5-7) of pions produced in the annihilation process. A few percent of annihilations lead to the production of strange particles (K,Λ).

b. The very short mean-free path in ordinary nuclear matter of antiprotons. This mean-free path increases slowly as the kinetic energy of the antiprotons increases.

Item b. suggests that most annihilations in complex nuclei will occur in the dilute outer surface of a nucleus (at $\rho/\rho_0 < 0.1$). Thus, although large and very local energy depositions are possible, many annihilations will lead to the less drastic consequences of having only a few pions traversing the complex nucleus.

At the same time, there will be significant probabilities of multi-meson interactions with the same nucleus, as well as somewhat rare occasions when the full >2 GeV of annihilation plus kinetic energy is deposited moderately deep inside a heavy nucleus. This raises the possibility of producing exotic final states such as those of baryonium, nuclei with abnormal n/p ratios, and hypernuclei.

The presently available data on the detailed nature of $\bar{p}$-complex nucleus interactions are sparse.[1] Total cross sections are larger than with protons of the same energy.[2] Katcoff (BNL) summarized for the panel the available nuclear chemical data using $\bar{p}$ of several GeV/c momenta. Emulsion stars with heavy fragments ($Z \geq 2$) are produced twice as frequently as by protons of the same energy.[3] Similarly, the fission cross sections of U, Bi, and Au are 2-3 times higher than when protons are incident.[4] These semiquantitative observations are in agreement with the expectation that large energy depositions are possible with antiprotons. They are confirmed by the occasional presence of very large stars ($n_h \sim 16$) seen in emulsions exposed to antiprotons.[1a] On the other hand, the cross section for producing ^{11}C from ^{12}C is about the same with $\bar{p}$ as with protons.[5]

The paucity of information about $\bar{p}$-nucleus interactions is related to the low intensity ($\sim$100 sec^{-1}) if pure, or relatively intense (10^4 sec^{-1}) if contaminated ($\pi/\bar{p} \simeq 20$) beams available up until recently.

This situation is changing. The KEK accelerator in Japan has a pure $\bar{p}$ beam of 10^4 sec^{-1}. Brookhaven has $\bar{p}$ beams of comparable intensity, but badly contaminated by pions. Finally, the CERN LEAP program, already underway, should produce very high purity beams of $\bar{p}$ in the 10^6 sec^{-1} range of intensity, probably in 1983.

There are special problems that have been identified in radiochemical studies of antiproton interactions. The beam purity is of special concern since the principle contaminants are negative pions, and the thrust of many investigations would be to compare the behavior of antiprotons with that of pions in nuclei. Another practical consideration is that the thick targets needed in many studies at low beam intensities are likely to be especially subject to secondary particle effects.

A more fundamental consideration is relative to the most desirable antiproton energy. This depends on the phenomena to be studied. To the extent that the special characteristics of the annihilation process in nuclear matter are to be investigated, an intermediate energy (500-2500 MeV) would appear desirable. The total cross section is smaller than at lower energies, thus allowing the $\bar{p}$ to penetrate into regions of higher nuclear density. Likewise the relativistic transformation would focus the annihilation pions into a more forward bundle. Too high an energy would mix in the effects of pions produced from the kinetic energy with those produced from annihilation.

The experiments that appear desirable and feasible with $10^4 sec^{-1}$ pure antiprotons are still of the survey type. They will not be easy because interesting radioactive products can be expected to have production rates of only a few per sec. This will require the use of low level measurement techniques that have usually not been utilized in such studies.

The first objective of such a survey might be to establish the main features of the spallation curve from the interaction of e.g. 1 GeV $\bar{p}$ with two or three heavy nuclear targets. A comparison could then be made with calculations based on the known yields of products of pion interactions with the same nuclei to check if the yields with antiprotons can be reproduced by a model that assumes completely additive effects from separate pions. Significant deviations might be due to correlation effects between the mesons (do the mesons interact, e.g., as ρ mesons?).

A similar examination of the probability, as well as of the characteristics, of nuclear fission induced in medium Z elements by antiprotons is worth investigating. The results of Katcoff[4] indicate an enhanced fission probability in Au, Bi,

and U. The probability of fission of lighter elements is a more sensitive measure of excitation energy and even more sensitive to the presence of collective effects.

The possible production of exotic species by antiproton interactions with complex nuclei has often been stressed. Among such species are long-lived baryonium states, nuclei with abnormal n/p ratios as well as hypernuclei or even double hypernuclei. The special suitability of $\bar{p}$ annihilation in complex nuclei for the formation of such states has recently been stressed by Rafelski.[6]

In conclusion, the lack of detailed data on antiproton-nucleus interactions suggests an important role for nuclear chemistry experiments of a survey type that can identify the main features of the phenomena and that can be open to the possibility of surprises not anticipated on standard models based on free particle interactions.

B. Role of Mesons in Nuclei

The realization in the last ten years or so that nuclei consist of more than just nucleons, but include mesonic degrees of freedom and probably various isobars, has been one of the most important developments in intermediate energy physics.[7] Of course the idea of mesons and mesonic currents has been invoked ever since the introduction of the meson exchange nature of the nucleon-nucleon force. In particular,the contribution of mesonic currents to the magnetic moments of nuclei has been known for some time.[8]

However, it has been only in recent years that nuclear probes have been able to provide sufficient momentum transfer to investigate explicity mesonic currents and to stimulate theoretical postulations as to the role that mesons play in nuclei. Present wisdom is that the mesonic degrees of freedom of a nucleus are important, and contribute significantly to the development of nuclear properties.[7]

Still, it is rather difficult to isolate unambiguously these mesonic degrees of freedom in a nucleus. One reason is because these processes are not completely orthogonal so that a given model of the nucleus, say one with isobar components in the nuclear wave function, may be at least partly contained in another model, perhaps one with mesonic exchange currents.

However, treatments of the pionic field within the nucleus are now beginning to elucidate the problem. These models are parameterized in terms of a factor, g', which describes the renormalization of the pion field in nuclear matter due to short-range correlations and Pauli blocking.[9] Thus, the strongly attractive

p-wave πN interaction is reduced by the NN and NΔ correlations (g' factor) and the repulsive s-wave πN coupling. If g' is small, then the p-wave coupling dominates and, in fact, one might expect a pion condensate at nuclear densities. Such a condensate would result in an alignment of the nucleon spins and isospins in a crystalline form in the nucleus.[10]

However, normal nuclei are not pion condensed. Although condensation may occur at abnormal densities such as may occur in heavy ion collisions,[11] these processes will not be discussed here. The results of any calculation for normal finite nuclei are very sensitive to g'. At nuclear densities, a value of g' = 0.4 would be sufficent to cause pion condensation, while a value of g' = 0.5 to 0.8 seems most favored. An experimental determination of g' would be extremely valuable.

The precritical behavior of the pion condensate has recently become a fashionable topic. There have been a number of experiments proposed to measure the pion field in a nucleus. Of course, the closer g' is to the critical condensate value the more observable such effects would become. Experiments should look for enhanced transitions to states of unnatural parity with unit change of isospin; for example: $^{208}\underset{T=0}{Pb}(0^+) \rightarrow {}^{208}\underset{T=1}{Pb^*}(1^+)$[12]. Since one is mainly interested in transition strengths, an integrated or even an inclusive reaction may be used in certain cases.[13] Measurement of an inclusive reaction reduces dependence on the nuclear physics and perhaps provides an experiment amenable to nuclear chemical techniques. In this respect, processes such as (n,π^+) are better than (p,π^-) for radiochemical analysis because competing background reactions are reduced.

Another example where the nuclear pion field might be observed is the renormalization of the axial vector current in nuclei.[14] The axial vector coupling constant of a bare nucleon is renormalized by the pion field surrounding a free nucleon. However, this coupling constant is renormalized again in a nuclear medium due to the alteration of the pion field in the nucleus. If the pion field is supressed due to short range correlations as expected, then the value of g_A will also be suppressed. The measurement of g_A then provides a measure of the strength of the mesonic field in a nucleus. An attempt to make such a measurement for several light nuclei was presented some time ago by Wilkinson,[15] but there may have been some ambiguities in the interpretation of the data. It would be useful to review theoretically these experiments again and to consider an

extension of the measurements to heavier nuclei. In this regard, it might be possible to use charge exchange reactions to measure the Gamow-Teller strength in nuclei.[16] This problem is also related to the renormalization of the pseudoscalar coupling constant in μ capture.[17]

One interesting suggestion is to investigate Δ knock-out reactions with a neutron beam. For example, the elastic collision of an incoming neutron with a Δ^{++} inside a $^{A}_{Z}$ nucleus might be measured using the sensitivity of radiochemical techniques to detect the residual $^{A}(Z-2)$ nucleus.[18] Although cross sections are expected to be small, the known backgrounds are predicted to be low enough to observe a signal even if the Δ^{++} component is less than 1% of the ground state wave function. To extract the Δ knock-out contribution, however, one must understand two-step processes such as $(n + p \rightarrow p + n)$ followed by $(p + p \rightarrow n + p + \pi^{+})$ inside the same nucleus, since these could lead to the identical final states.

A single definitive measurement of the pion field or of the isobar components of a nucleus probably cannot be made. Final resolution of this problem will require the comprehensive study of many experiments over a number of years. Hopefully, nuclear chemists can help supply some of the pieces to this puzzle.

C. Neutrino Properties and Nucleon Decay

Current popular theories consider the possibilities of a non-zero neutrino mass, neutrino oscillations between several forms, and baryon decay as connected natural consequences of grand unification theories. Such theories also make predictions about the rates of classically-"forbidden" processes, such as $\mu \rightarrow e\gamma$. These theoretical speculations have received recent stimulus by reports of experimental evidence for neutrino oscillations[19] and for a finite mass for the electron antineutrino.[20]

In this exciting area of science, radiochemical techniques have contributed in the past and have great potential for additional contributions. The present status of the radiochemical detection of solar neutrinos in the Brookhaven solar neutrino experiment, based on the neutrino capture reaction $^{37}Cl(\nu,e^{-})^{37}Ar$, gives a signal above known backgrounds that corresponds to a total solar neutrino capture rate of 2.2 ± 0.4 SNU (Solar Neutrino Units).[21] The most recent standard solar model calculations[22] give a capture rate of 7.8 SNU. In these calculations, a new set of opacities from Los Alamos and Livermore and a new solar composition advocated by Ross and Aller have been used. There still seems to be some doubt about the cross section of the $^{3}He(\alpha,\gamma)^{7}Be$ reaction, and new measurements are

urgently needed. However, the discrepancy between the observed neutrino flux from the sun and that calculated has now persisted for several years, and more fundamental causes are being explored. A possible explanation of this discrepancy is that the neutrinos from the sun oscillate during the trip from sun to earth and come to equilibrium with another form that cannot convert ^{37}Cl to ^{37}Ar.

Aside from the solar neutrino problem, the new interest in "non-classical" neutrino properties suggests a re-examination of radiochemical techniques to study these properties as well as to detect nucleon decay. Among the possibilities are:

1) Neutrino detection via the $^{71}Ga + \nu_e \rightarrow {}^{71}Ge + \bar{e}$ reaction. This has a much lower threshold than the $^{37}Cl(\nu_e,e^-)^{37}Ar$ reaction. The chemical processing has already been tested on the 1.3 ton scale. On a 10-60 ton scale it could be used to study both solar neutrinos and neutrinos from other sources (see below).

2) Neutrino detection via

a) $^{7}Li(\nu_e, e^-)^{7}Be$ (t 1/2 = 53 d) ref. 23
b) $^{81}Br(\nu_e, e^-)^{81}Kr$ (t 1/2 = 2.1 x 10^5y) ref. 24
c) $^{41}K(\nu_e, e^-)^{41}Ca$ (t 1/2 = 1.0 x 10^5y) ref. 25

reactions have been proposed. Aside from different energetic thresholds, reactions b) and c) have the possibility (if suitable samples from a sufficient depth in the earth are obtained) of providing a history, over a 10^5yr period, of the solar neutrino emission. None of these detectors has been developed to the stage of the ^{37}Cl or ^{71}Ga detectors. In particular, the detection capabilities for the small number of atoms produced have to be demonstrated. In this connection, techniques being developed by Hurst[26] and others for the detection of less than 10^6 atoms by LASER techniques are worth encouraging. They will have many applications when they are developed.

3) E. Fireman described a proposed[27] radiochemical experiment to detect nucleon decay via the production of ^{37}Ar from ^{39}K. This technique has the special virtue of detecting the disappearance of a nucleon independent of the mode of decay. In order to measure the nucleon decay rate in ^{39}K with 10-20% accuracy in the 10^{31} to 10^{32} years half-life range, 6000 tons of potassium are needed (about 10 X the weight of the Davis chlorine experiment) at 8000 meters water equivalent depth to shield from cosmic rays. It is proposed to evaluate the residual contribution from cosmic rays or other sources via the simultaneous measurement of the production of another nuclide (e.g. ^{39}Ar) which cannot be produced by nucleon

decay. Measurements have already been performed on a ∿2 ton scale at various depths in the earth. The techniques of measuring ^{37}Ar have been well estabished by Davis; that for measuring ^{39}Ar still have to be developed.

Such radiochemical detectors could be used to address both the important problem of solar constitution and energy production and the currently interesting problems of neutrino properties. Among the near term specific experiments that should be considered are:

1) Experiments at the LAMPF beam stop. This is an intense source of muon antineutrinos and electron neutrinos arising from the decay of positive muons:

$$\mu^+ \rightarrow \bar{\nu}_\mu + e^+ + \nu_e$$

The energy spectrum, intensity, and spatial distribution of this source are quite well defined. The radiochemical detectors could provide information on neutrino oscillations both by a check of the apparent absolute cross section for reversing beta decay, and by measuring the observed rate as a function of distance from the source. The uniqueness of the LAMPF beam stop neutrino source would argue for making it more available than it is now for the large scale experiments characteristic of all neutrino studies.

2) Experiments near a nuclear reactor. Although a nuclear reactor should primarily be a source of electron antineutrinos, if these oscillate between different forms (as indicated recently by Reines - ref. 19), a sensitive test should be made of whether one of these forms could induce beta decay. The older experiments of Davis suggest a limit to the apparent cross section of $\frac{1}{60}$ that expected if all the particles were neutrinos. A more sensitive test using a radiochemical detector is possible now as well as measurements at several distances from a reactor.

3) The nuclide ^{65}Zn decays by electron capture emitting monoenergetic neutrinos of 1.35 MeV, with a 265 day half-life. A megacurie source of ^{65}Zn could be prepared at Oak Ridge and then brought near various radiochemical neutrino detectors. Such an experiment would provide the cleanest test of absolute cross section calculations as well as a method of studying neutrino oscillations by changing distances between a compact source and detector.

As a final contribution, W. Haxton reviewed the status of experiment and theory of double beta decay.[28] Although originally focused on possible contributions of nonclassical neutrino properties, his detailed calculations on the

basis of classical V-A theory predict half-lives that are orders of magnitude (see Table I) shorter than those deduced from the observed accumulation of decay products during geological times. This raises questions about the correctness of these experiments. If the calculated half-lives are correct, new techniques such as those being developed by Hurst[26] could provide results on a time scale of a year.

TABLE I

DOUBLE BETA DECAY

COMPARISON BETWEEN OBSERVED AND CALCULATED MEAN-LIVES (REF. 27)

τ (years)

System	Theory	Expt.	Method
$^{82}Se \rightarrow {}^{82}Kr$	1.5×10^{19}	2.6×10^{20}	geology
		$(1.0 \pm 0.4) \times 10^{19}$	counter
$^{128}Te \rightarrow {}^{128}Xe$	1.1×10^{23}	3.5×10^{24}	geology
$^{130}Te \rightarrow {}^{130}Xe$	3.2×10^{19}	2.2×10^{21}	geology

D. Interaction of Kaons with Nuclei

Recently there have been several reviews of the prospects for Kaon physics.[29] Still, it is probably worthwhile to review briefly the properties of the K meson and why it is that there is so much interest in kaons as a probe of the nucleus.

The classification scheme SU(3) allows the lightest mesons and baryons to be grouped into an octet. These particles are composed of various combinations of three quarks (u,d,s) and their antiparticles, with the provision that the mesons are formed from quark-antiquark pairs and the baryons are formed from three quarks. Color and other restrictions in the formation of these observable quark composites are not really important for these discussions. The K mesons and the Λ and Σ baryons have one s (strange) quark while the Ξ particle is formed from two s quarks. In this scheme s and d quarks are coupled via the weak interaction so that the s quark can weak decay into a d quark. This explains, for example, the weak decay $\Lambda \rightarrow N + \pi$, with a mean-life of 2.6×10^{-10} sec. However, strangeness is a good quantum number under the strong interaction.[30,31]

Note that in the meson octet the K meson is an isospin 1/2 object and that the (K^+, K°) and $(K^-,\bar{K}^\circ)$ are isospin doublets. These doublets may, and indeed do, have completely different strong interactions. Thus the $(K^-,\bar{K}^\circ)$ exhibit many resonances, some in fact are quite narrow, while the (K^+,K°) are very weakly interacting with other hadrons. The K^+ has the longest mean free path in nuclear matter of any of the conventional hadrons.[32] Therefore the K has a volume dependent interaction in nuclei while that of the K^- is surface dependent.[33]

The major thrust of kaon-nuclear physics has been the formation and spectroscopy of hypernuclei formed via the $A(K^-,\pi^-)_\Lambda A$ reaction.[29] This reaction is similar to a conventional charge exchange reaction except an s quark is exchanged instead of a d quark, for example. The reaction is associated with a low momentum transfer for incident momenta of interest, so that the resulting Λ has a high probability of remaining bound to the nucleus. However, the binding energies of many of the lightest hypernuclei have been determined by emulsion and bubble chamber techniques rather than by counter experiments.[34]

The spectroscopy of hypernuclear levels is just beginning. Present experiments are designed to obtain $d\sigma/d\Omega$ for a variety of light hypernuclear levels[35] and to detect the γ transitions from excited levels[36] using the reaction $A(K^-,\pi^-\gamma)_\Lambda A$. Ground state binding energies can be determined, but because of the surface nature of the (K^-,π^-) reaction these determinations will be limited to hypernuclei with $A \lesssim 40$.

The hypernuclear lifetime and decay products have not been pursued with vigor. Only a few measurements have been made and all[37] for $A \leq 16$. In this area much remains to be done although the experiments would be quite difficult. Weak decay of the Λ occurs via $N\pi$ emission with the release of about 37 MeV. In a nucleus a bound Λ should make electromagnetic transitions to the 1s shell (note that it may be distinguished from protons and neutrons so that it can occupy this fully closed shell) and then decay. However, except for $A \lesssim 4$, Pauli blocking of the recoil nucleon inhibits this decay channel. One would then expect the Λ lifetime to increase in heavy nuclei, but the following additional decay channel begins to compete:

$$\Lambda + N \rightarrow N + N$$

This is a four fermion weak decay, and can only be observed in nuclei. This channel dominates hypernuclear decay for $A > 4$ and apparently[38] has a mean-life

similar to the free mean-life of the Λ. Thus, all hypernuclear lifetimes are expected to be similar, but there may be surprises. The four fermion weak decay should be sensitive to nuclear correlations and perhaps a lifetime variation might occur.[39] Certainly lifetimes of the heavier hypernuclei should be measured.

It would also be interesting to determine the decay products of a hypernucleus. In hypernuclear decay a hole is created in the nucleus, most probably in the 1s shell. The resulting nucleons are emitted with approximately 70 MeV, perhaps interacting with the nucleus before reaching the nuclear surface. The residual nucleus however is left with a hole in the 1s shell and nuclear rearrangements occur as the nucleus returns to equilibrium. A study of the mass yield curve would appear particularly amenable to nuclear chemical techniques. This can be done on existing hypernuclear targets after irradiation, but background from pion induced reactions would have to be subtracted.

A further example of where nuclear chemists might make a significant contribution in strange particle physics is the investigation of double hypernuclei. To date two candidates for the production of a nucleus with two bound Λ's have been reported.[40] Both events have been observed in emulsion and were formed after the fragmentation of the initial nucleus. Aside from nuclear physics interest, such nuclei give us the only hope of experimentally studying the ΛΛ potential. Although the (K^-,K^+) or (K^-,K°) reactions have been proposed to produce such nuclei,[41] the cross sections would be extremely small - probably too small to be measured directly with present kaon beams. However, nuclear chemical techniques or multitrack detectors might provide such measurements. Representative reactions are listed below:

$$K^- + {}^{7}Li \rightarrow K^+ + {}^{7}_{\Lambda\Lambda}H$$

$$K^- + {}^{6}Li \rightarrow K^\circ + {}^{6}_{\Lambda\Lambda}He$$

$$\Xi^- + {}^{12}C \rightarrow {}^{7}Li + {}^{6}_{\Lambda\Lambda}He$$

$$p + A \rightarrow K^+ + K^+ + \Lambda\Lambda + X'$$

The associated production reaction may be the most favorable.

Speculation[42] also exists on the formation of a dihyperon, H. Essentially this is a six quark system that might decay into a ΛΛ if not strongly bound. It is not a deuteron-like state, being instead six quarks in one bag with a radius

of a fermi or so. Speculation is that the H would be strongly bound, perhaps even stable in the sense of undergoing only double weak decay. Mass predictions are, however, unreliable and formation rates are not at all certain. Again, searches for neutral particles undergoing meson decay or with large energy release can be approached by nuclear chemical techniques.

The above examples are but a few processes in kaon physics that might be best addressed by nuclear chemists. Of course, the same type of studies that are now being done with pions could be done with kaons as well. It is not clear in this respect that kaon induced reactions would have major advantages over pion or other more conventional nuclear probes. However, many other possible investigations will occur as the field becomes less "strange" and more mature.[33]

REFERENCES

1. For early reviews on antiproton interactions with complex nuclei, see e.g.
   a) E. Segre, Ann. Rev. Nucl. Sci., 8, 127 (1958).
   b) A. G. Ekspong, A. Frisk, S. Nilsson, and B. E. Ronne, Nucl. Phys. 22, 353 (1961).

2. See e.g. J. C. Rushbrook, Phys. Rep. 44, 1-29 (1978).

3. S. Katcoff, Phys. Rev. 157, 1126-1130 (1967).

4. S. Katcoff and L. Husain, Phys. Rev. C 4, 263-267 (1971).

5. S. O. Thompson, L. Husain, and S. Katcoff, Phys. Rev. C 3, 1538-1540 (1971).

6. J. Rafelski, Phys. Lett. 91B, 281 (1980).

7. For recent reviews, see e.g. "Mesons in Nuclei," edited by M. Rho and D. H. Wilkinson, North Holland, 1979. Also, "Program Options at Intermediate Energies," Los Alamos Scientific Laboratory Report. LA-8335-C (1979).

8. F. Villars, Phys. Rev. 22, 256 (1948).

9. A. B. Migdal, Rev. Mod. Phys. 50, 107 (1978); G. E. Brown and W. Weise, Phys. Rev. 27C, 1 (1976); J. Delorme, A. Figureau, and N. Giraud, Phys. Lett. 91B, 328 (1980); R. B. Wiringa, Workshop on Nuclear Structure with Intermediate Energy Probes, Los Alamos Scientific Laboratory Report LA-8303-C(1980).

10. T. Takatsuka, et al, Prog. Theor. Phys. 59, 1933 (1978).

11. M. Gyulassy and W. Greiner, Ann. Phys. 109, 485 (1977).

12. J. Delorme, et al, Phys. Lett. 89B, 327 (1980); H. Toki and W. Weise, Phys. Rev. Lett. 42, 1034 (1979).

13. G. Stephenson and W. Gibbs, private communication, (July 1980).

14. J. Delorme, et al, Ann. Phys. 102, 273 (1976).

15. D. H. Wilkinson, Phys Rev. C 7, 930 (1973); Nucl. Phys. A209, 470 (1973); and Nucl. Phys. A225, 365 (1974).

16. V. A. Madsen, The Two-Body Force in Nuclei, edited by S. M. Austin and G. M. Crowley, Plenum, New York, p 315.

17. P. Guichon, et al, Phys. Rev. C 19, 987 (1979).

18. A. Turkevich, LAMPF proposal,#603, private communication, (July 1980).

19. F. Reines, H. W. Sobel, and E. Pasiero, U. of Calif. (Irvine) preprint: 10- p19-144, June (1980).

20. V. A. Lyubimov, G. E. Novikov, V. Z. Nozik, E. F. Tretyakov, and V. S. Kosk, Preprint, Inst. Theor. and Exptl. Physics, ITEP-62 Moscow, 1980.

21. J. K. Rowles, B. T. Clevelaun and R. Davis, Jr., BNL preprint 27190 (1980).

22. Bahcall, Huebner, Lubow, Magee, Merts, Parker, Rozgnyai, Ulrich, and Argo, submitted to Phys. Rev. Lett. May 1980.

23. J. M. Bahcall, Rev. Mod. Phys. 5, 881 (1978).

24. Originally proposed by R. D. Scott, Nature 264, 729 (1976).

25. W. C. Haxton and G. A. Cowan, "Solar Neutrino Production of Long Lived Isotopes and Secular Variations in the Sun", submitted to Science, June (1980).

26. C. H. Chen, G. S. Hurst, and M. G. Payne, "Direct Counting of Xenon Atoms", Preprint June 1980 (ORNL).

27. E. L. Fireman, a) Neutrino 77, BAKSAN, USSR, 1, 53 (1978); b) 16th International Cosmic Ray Conference, Kyoto, Japan, 13, 321 (1979).

28. W. C. Haxton, G. J. Stephenson, and D. Strottman, "Rates of Double Beta Decay and Lepton Number Conservation", High Energy Physics Conference, University of Wisconsin, July 17-23, 1980.

29. E. V. Hungerford, Workshop on Nuclear Structure with Intermediate Energy Probes; Los Alamos Scientific Laboratory Report, LA-8303-C; B. Povh, Nucl. Phys. A335, 233 (1980), and Ann. Rev. Nucl. Part. Sci. 28, 1 (1978); Meson Nuclear Physics - 1979 (Houston) LAIP Conference Proceedings, 54, E. V. Hundgerford, editor; TRIUMF Kaon Factory Workshop, internal report.

30. H. Harari, Phys. Rep. 42C, 235 (1978).

31. Review of Particle Properties, Rev. Mod. Phys. 48, 51 (1976).

32. C. B. Douce, Workshop on Pion Single Charge Exchange" Los Alamos Scientific Laboratory Report, LA-7892-C (1979).

33. Proceedings of the Summer Study meeting on Kaon Physics and Facilities, H. Palevsky, editor, BNL report 50579.

34. D. M. Rote, A. R. Bochmer, Nucl. Phys. A148, 97 (1970); M. Juric, et al, Nucl. Phys. B52, 1 (1973).

35. R. Chrien, et al, Phys. Lett. 89B, 31 (1979); W. Bruckner, et al, Phys. Lett. 79B, 157 (1978).

36. M. Deutsch, et al, AGS proposal (April 1980).

37. K. J. Nield, et al, Phys. Rev C 13, 1263 (1976).

38. R. H. Dalitz, Proceedings of the Conference on Nuclear and Hypernuclear Physics with Kaon Beams, BNL report 18335.

39. G. Coremans, et al, Nucl. Phys. B16, 210 (1970); R. H. Dalitz, R. C. Herndon, and Y. C. Tang, Nucl. Phys. B47, 109 (1972).

40. M. Danysz, et al, Nucl. Phys. 49, 212 (1963); D. J. Prowse, Phys. Rev. Lett. 17, 17 (1966).

41. C. B. Dover, Proceedings of the International Conference on Hypernuclear and Low Energy Kaon Physics, Sablonna, Poland, 1979.

42. R. Jaffe, Phys. Rev. Lett. 38, 195 (1977).

APPENDIX

ORGANIZATION AND PARTICIPANTS

Organization

1. Antiproton-Nucleus Interactions
   - Review: R. Eisenstein (Carnegie-Mellon)
   - Contribution: S. Katcoff (BNL) "Nuclear Chemical Studies with Antiprotons"

2. Role of Mesons in Nuclei
   - Review: R. B. Wiringa (LASL)
   - Contribution: G. J. Stephenson (LASL)
   - A. Turkevich (U. of Chicago/LASL)

3. Neutrino Properties and Nucleon Decay
   - Review: R. C. Slansky (LASL)
   - G. J. Stephenson (LASL)
   - Contribution: R. Davis (BNL)
   - E. Fireman (Smithsonian Astrophysics Obs.)
   - W. Haxton (LASL)

4. Interaction of Kaons with Nuclei
   - Review: E. V. Hungerford (U. of Houston)

Participants

D. A. Boal, Simon Fraser University
D. Bowman, LASL
D. Boyce, University of Chicago
A. A. Caretto, Carnegie-Mellon University
R. Davis, Brookhaven National Laboratory
B. Dropesky, LASL
R. Eisenstein, Carnegie-Mellon University
E. L. Fireman, Smithsonian Astrophysics Observatory
G. A. Cowan, LASL
W. Haxton, LASL
H. R. Heydegger, Purdue University (Calumet) & University of Chicago

E. V. Hungerford,III, University of Houston

N. Imanishi, Kyoto University/LASL

S. Katcoff, Brookhaven National Laboratory

L.-C. Liu, LASL

H. S. Plendl, Florida State University

R. E. Segal, Northwestern University

R. C. Slansky, LASL

G. J. Stephenson, LASL

A. Turkevich, University of Chicago/LASL

D. J. Vieira, LASL

L. Winsberg, University of Illinois (Circle)

R. B. Wiringa, LASL

Summary Report and Recommendations From Panel

NC-5 NEW THEORETICAL APPROACHES

by

M. M. Sternheim, University of Massachusetts, Chairman

L.-C.Liu, LASL, Co-Chairman

I. INTRODUCTION

The theory panel met only for one morning, rather than for the longer time allocated for most of the panels. This presumably reflected the idea that theory in this field is usually most productive when it is related to specific experiments. The panel accordingly dealt mainly with questions of a more general and fundamental character such as the applicability of specific theoretical methods and possible improvements to practical calculational schemes.

The six talks presented to the panel were of two complementary types, reflecting the status of the field. We heard talks aimed at exploring and extending the fundamental applicability of the intranuclear cascade and related methods. Other talks explored simpler, alternative descriptions of the complex hadron-nucleus interaction, or examined the validity of the currently used dynamical assumptions. The panel also discussed ways of improving the existing calculational methods.

II. SUMMARY OF SESSIONS

Remler discussed "recent approaches to nuclear kinetic theory". By kinetic theory he means a theory in which there exists a closed dynamical equation for the nuclear single-particle distribution function ("Singlet"). He has obtained such an equation by assuming that the true density matrix can be replaced by one which is a functional of the singlet alone. With this assumption, he has shown that the best approximate density matrix is the one that maximizes the entropy. He has recovered several commonly used many-body formalisms by this approach. He further

suggests a way to improve on the treatment of the hard-core interactions. (See Appendix A for further details.)

Hüfner presented a derivation of the Boltzmann Equation based on Glauber's multiple-scattering theory applied to inclusive nuclear reactions. The derivation neglects nuclear ground-state correlations and the second derivatives of the optical potential for the projectile. By treating the interaction perturbatively, Hüfner obtained a multiple-scattering expansion of the theory, which he applied with some success to pion-nucleus scattering. These ideas are the basis for the calculations he presented on the first day of the workshop. (This work was published in Ann. Phys., (N.Y.) 115, 43 (1978), and Phys. Rev. C20, 273 (1979)).

Hüfner next presented some preliminary results on a thermodynamic description of spallation and fragmentation. He showed that for a large class of experiments the shape of the isotopic distribution curve can be fitted very well by a two-parameter function. One parameter corresponds to the neutron-removal energy of the most abundant isotope. The other one seems to be proportional to the number of the particle stable states in the final fragment. Fraenkel noted that the idea presented here may be regarded as a "constant-temperature" approximation to the evaporation model. (See Appendix B for further details.)

Winsberg discussed nuclear reactions in the region above 1 GeV. Motivated by a collision-tube picture, he showed that a great deal of data exhibits simple functional dependences on the number of nucleons emitted and on the excitation energy of the struck nucleus. He suggested that such analyses will provide a way to study the primary projectile-target interaction. (This work is to appear in Phys. Rev. C, August 1980).

Long presented some preliminary results concerning a comparison between an intranuclear cascade calculation and a simpler transport model for pion production in nucleon-nucleus collisions below the two-pion production threshold. His study shows the critical importance of understanding the effects of the nuclear medium on the elementary processes. He found that the two models agree in the limit where the true absorption of pions is large enough so that the multiple-scattering series converges rapidly. (See Appendix C for details.)

Liu presented a review of the dynamics used in pion intranuclear cascade calculations at LAMPF. He suggested that the lack of nuclear structure information in the INC theory and an inadequate treatment of Coulomb effects on the

projectile inside the nucleus may explain some of the discrepancies between calculations and experimental data. He also commented on recent analysis by Ginocchio and Johnson who used a pion-nucleus optical potential to take into account the effects of the nuclear medium on the pion mean free path. He also showed that the inclusion of the optical potential does not significantly improve the fit to the spallation data. (See Appendix D for details.) Fraenkel pointed out that the cleanest test of cascade calculations is not spallation where evaporation is important, but rather fast reactions. Hüfner suggested double charge exchange as a suitable fast reaction.

III. CONCLUSIONS AND RECOMMENDATIONS

Our general recommendations are based on the discussions both in this panel and in the plenary sessions.

We feel that continued efforts are needed both to study the fundamentals of the field and to improve the existing models. Work on the fundamental aspects of nuclear many-body physics should provide us with a better understanding of the domain of applicability of practical calculational methods. It may possibly also offer an alternative computational scheme which can be realistically implemented.

Most of the recent intranuclear cascade calculations have been done by the use of cascade codes developed by people other than the current users. The developers often have had quite different physical descriptions in mind. The inherent limitations of these codes for the problems of contemporary interest are sometimes not readily apparent to the users. Therefore, we recommend that careful investigations be made of the validity and importance of the dynamical inputs. Also, in many situations, simpler models or approaches may be more convenient or instructive. This is true even though their domain of applicability may be more restricted than that of the general cascade theory.

Finally, some specific suggestions were made for improving on existing cascade or related models. It was emphasized in the panel that improvements should be done in an internally self-consistent manner. It was suggested that the conventional local density Fermi distribution should be replaced by the Wigner density in order to improve the Fermi motion corrections. Also, forces acting on the particles arising from the optical potentials for the particles have not so far been included and may well be important. Related to this is the need to relate the heuristic reflection and refraction models in present codes to more

basic concepts. Finally, in the plenary session Remler sketched a method for efficiently using Monte Carlo methods to calculate low probability events; efforts to implement these ideas would seem very worthwhile.

In conclusion, existing calculational methods are generally quite successful when the available energy and number of states are both large, but less satisfactory for processes not so close to the thermodynamic limit. The discussions in the panel were quite encouraging and have provided some useful ideas for improving our theoretical capabilities.

APPENDIX A

RECENT APPROACHES TO NUCLEAR KINETIC THEORY

E. A. Remler

Kinetic theory is used here to mean a closed dynamical equation for the nuclear single particle distribution function ('singlet') defined as

$$n(a';a) = \mathrm{tr}\,(\psi_a^\dagger, \psi_a \rho) \tag{A-1}$$

where the field operator for a nucleon is $\psi_a = \psi_{\vec{p}a, \sigma a, \tau a}$ (labels denoting momentum, spin, and isospin) and ρ is the total density operator of the system. Thus an equation of the form

$$\partial_t\, n = F[n], \tag{A-2}$$

F denoting some functional. Of course, it is not possible for Eq. (A-2) to be unconditionally true since Schroedinger's equation implies

$$\partial_t\, \mathrm{tr}\,(\psi_a^\dagger \psi_a^\dagger \rho) = \mathrm{tr}\,([iH, \psi_a^\dagger, \psi_a]\rho) \tag{A-3}$$

while the Hamiltonian H (and hence the commutator) is a function not only of the singlet operator $\psi_a^\dagger \psi_a^\dagger$ but also of the doublet $\psi_a^\dagger \psi_b^\dagger \psi_b \psi_a$ and possibly higher operators. But kinetic theory may be true under suitably restricted initial conditions at least for a period of time. If this is so, one can say the system

possesses a "Kinetic Regime". This will be of interest only if systems naturally enter upon Kinetic Regimes under a decent variety of experimental conditions. We know such is the case for macrosystems and a similar assumption for nuclear systems is necessary to derive either Time-Development Hartree-Fock (TDHF) the Landau Equation or nuclear 'hydrodynamics'. Since these approaches have had some success[2] and it is in any case necessary for more such simplifying assumption to be used to handle the nuclear physics (fission, heavy ions, etc.) for which they were developed, it is reasonable to at least begin with the same assumption.

One way a kinetic equation can follow from Eq. (A-3) is if the true density ρ can be replaced by some fixed functional of the singlet $\tilde{\rho}[n]$ for the purpose of calculating $\partial_t n$ (i.e. on the right hand side of Eq. (A-3)). This is a suggestion which essentially is due to Bogoliubov in classical gas kinetics. What functional could this be? The standard 'simplest possible' ansatz one can make for $\tilde{\rho}[n]$ is that it is the state of maximum entropy[3] consistent with n. That is, it is the state which maximizes

$$S = -\mathrm{tr}(\tilde{\rho} \ln \tilde{\rho}) \tag{A-4}$$

consistent with the constraints,

$$n(a';a) = \mathrm{tr}(\psi_a^\dagger, \psi_a \tilde{\rho}) \ . \tag{A-5}$$

It can then be shown[4] that such a $\tilde{\rho}$ implies the following relation between multiplets and the singlet:

$$\mathrm{tr}(\psi_A^\dagger, \psi^\dagger_{(A-1)}, \ldots . \psi_1', \psi_1 \ldots \psi_A) = A\, n(A';A) \ldots n(1';1) , \tag{A-6}$$

where A is the antisymmetrizer on 1 . . A.

This relation, which is trivially true for a Hartree-Fock state, is in fact also true for a much wider class of important states.

Now if $\tilde{\rho}$ is restricted to be of Hartree-Fock form (i.e. the density of the single determinant wave function) and if H is replaced by an effective (e.g. Skyrme) Hamiltonian, this leads, after changing $\rho \to \tilde{\rho}$ in Eq. (A-3), to TDHF[2]. When the number of nucleons become too large, these equations become unmangeable. Bertsch[2] has therefore proposed that these be further approximated by (1) making a semi-classical Wigner approximation, (2) adding an ad hoc collision term in

the manner of the Landau equation, (3) taking a moment expansion which leads to hydrodynamic equations. This program has been applied to good effect in explaining the giant resonances.

As a preliminary point, note that the mean field approximation which results from the use of Eq. (A-6) and had been thought[2] to require the Hartree-Fock assumption, in fact applies to the infinitely larger class of maximum entropy states. The only requirement on the Hermitian matrix of values n(a';a) is that its eigenvalues N_α be sumable and

$$0 \leq N_\alpha \leq 1 \quad . \tag{A-7}$$

Thus, in particular the derivation by Bertsch does not depend on TDHF.

In a recent paper[1], I have attempted to go beyond this framework by using a better approximation for $\tilde{\rho}$. The two-nucleon interaction is divided into a slowly varying part $\overline{V}$ and a hard core V_c. It is easy to see that transitions due to core collisions are not correctly given by using the $\tilde{\rho}$ previously defined. It is shown that a simple improvement is to write instead

$$\partial_r n = \mathrm{tr}([iH_0+\overline{V}),\psi_a,\psi_a]\tilde{\rho} + [i V_c,\psi_a,\psi_a]\Omega_c \tilde{\rho}\Omega_c^{+}) \tag{A-8}$$

where Ω_c is the wave operator describing scattering by the core alone. That is, the mean field approximation is retained for contributions due to the long-range part of the interaction, but dynamical core correlations, corresponding to free two-body scattering, are inserted in calculating transitions due to core collisions.

After making this assumption, the remainder of the problem is essentially algebra. The following results are obtained:

(1) A kinetic equation is obtained of the form

$$\partial_t \langle a'|n|a\rangle = \langle a'|[-i\, h,\, n]|a\rangle + I_c \tag{A-10}$$

(it is convenient to define $\langle a'|n|a\rangle = n(a;a')$

where h is, as in TDHF, a functional of n and, I_c denotes collision terms.

(2) This equation reduces to the Landau, Boltzmann, and Vlasov equation in their apopropriate limits.

(3) h is non linear in the singlet (i.e. density dependent) and, by itself, provides an approximation to the TDHF Hamiltonian which is derived from first principles

and not merely assumed from static Hartree-Fock Theory.

(4) The collision term is that due only to V_c and thus may substantially differ from the usual one which corresponds to using V. In addition it contains numerous quantum mechanical corrections.

Further details are to be found in Ref. 1.

REFERENCES

1. E. A. Remler, Nuclear Kinetic Theory, to be published.
2. G. Bertsch, Heavy Ion Dynamics at Intermediate Energy, M.S.U. preprint 1979.
3. J. R. Nix and A. J. Sierk, Phys. Rev. C21, 396 (1980).
4. A. Katz, Principles of Statistical Mechanics (Freeman, San Francisco 1967).
5. E. A. Remler, Maximum Entropy States, Hartree-Fock States and Nuclear Kinetic Theory, unpublished; an extended version is in preparation.

APPENDIX B

TOWARD A THERMODYNAMIC DESCRIPTION OF SPALLATION AND FRAGMENTATION CROSS SECTIONS INDUCED BY HIGH ENERGY PROTONS, HEAVY IONS, AND PIONS

J. Hüfner

We consider reactions of the type projectile + target → $^{A}_{N}Z$ + X, where the projectile may be a high energy proton (10-300 GeV)[1], the target a heavy (U, Th, Au) or medium mass (Fe) nucleus and $^{A}_{N}Z$ the isotopes of a much lighter element (Li, Na, Ar, . . .). The same fragments can be observed in relativistic heavy ions reactions (9.2-GeV ^{48}Ca + Be, 8.1-GeV ^{40}Ar + C)[2], or after a π^- is stopped by a nucleus that de-excites by particle evaporation[3]. We observe:

i) The shape of the experimental cross section $\sigma\,(^{A}_{N}Z)$ to produce the isotope $^{A}_{N}Z$ shows a parabolic shape peaked around the most stable one, if $\ln \sigma(^{A}_{N}Z)$ is plotted against N for fixed Z (cf. Fig. B-1).

ii) The shape depends very little on the particular reaction, on projectile, target, and incident energy.[2]

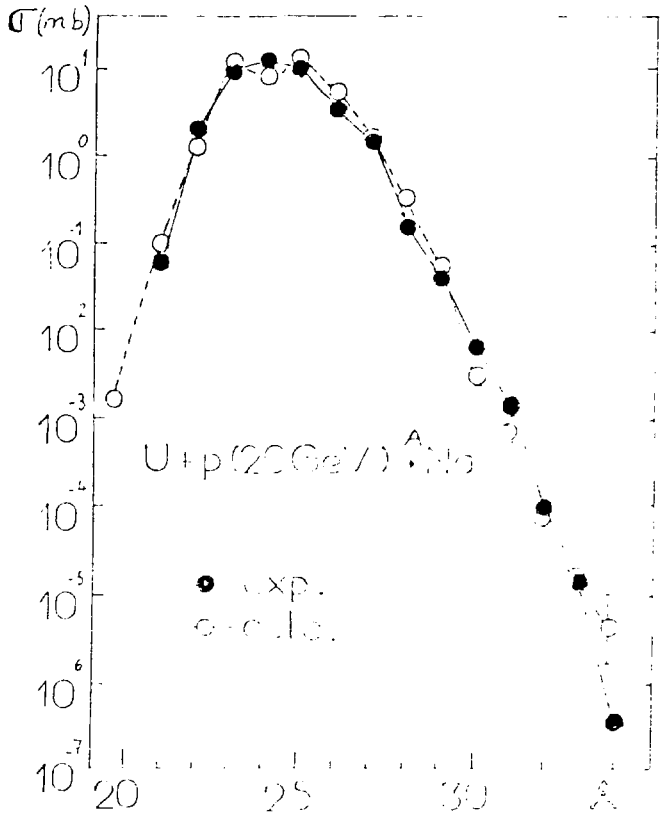

Fig. B-1.

The observation ii) can be a key to a tremendous simplification: Obviously one does not need to understand the whole reaction (as pretended in cascade type calculations) but the cross sections depend only on the properties of the final product (thermodynamic limit) where all memory of the initial and intermediate processes is lost. Among the properties of the final nucleus, we consider the ground state energy $E_{gs}(N,Z)$ and the number of neutrons N. In the spirit of the surprisal analysis[4], we try the ansatz

$$\sigma\left({}^{A}_{N}Z\right) \propto e^{-\beta\left(E_{gs}(N,Z)+\mu N\right)}$$

where the experimental ground state energies are negative numbers, β and μ are fit parameters. The fit to the data is usually very good (Fig. B-1) over several orders of magnitude.

What do the obtained parameters β and μ tell us? In analogy to thermodynamics, we call μ the chemical potential and $\beta = 1/T$ the inverse temperature. Indeed, we find from the fits that μ corresponds to the experimental separation energy of one neutron (5-10 MeV) of the most abundant isotope. And what about the inverse temperature β? For a Fermi gas, the mean excitation energy $\langle \Delta E^* \rangle$ is related to the temperature T by

$$\langle \Delta E^* \rangle = a T^2 \quad ,$$

where a is the level density parameter. We observe for many isotopic distribution the regularity

$$\langle \Delta E^* \rangle \simeq \mu \quad .$$

To demonstrate it, we plot

$$a_{fr} = \beta^2 \mu$$

as a function of A (represented by X in Fig. B-2) and compare with the level density parameters obtained from other methods (heavy dots). We observed the

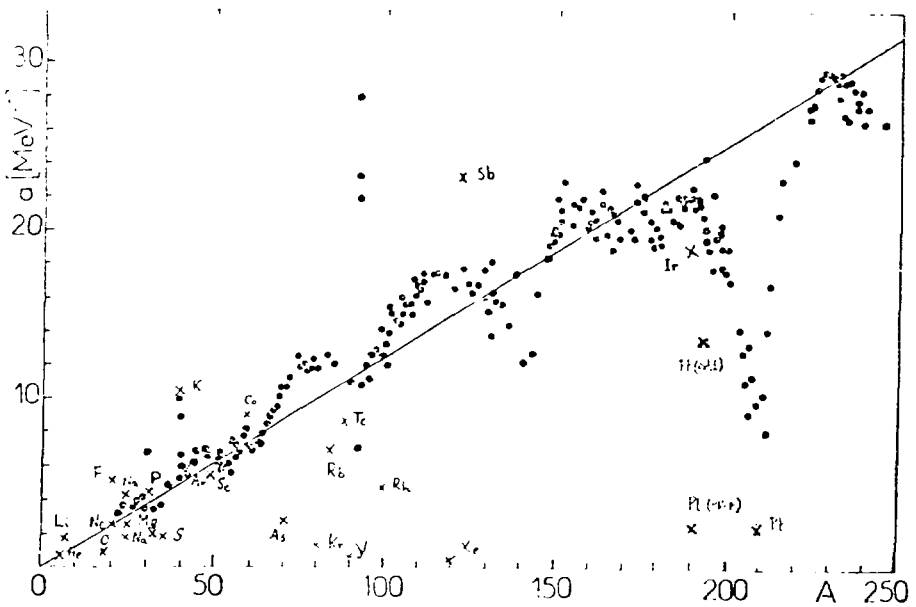

Fig. B-2 .

values of a_{fr} follow rather well (at least for light fragments) the general trend ($a \approx A/8$) of the level density parameters. Therefore, we suspect the spallation and fragmentation cross sections to be simply proportional to the number of available states (states below neutron emission threshold) in the final fragment and to be practically independent of the reaction. However, we have not yet understood it completely.

REFERENCES

1. J. D. Bowman et al., Phys. Rev. C9, 836 (1974); C. Thibault et al., Phys. Rev. C12, 644 (1975), and private communication; S. Regnier, Phys. Rev. C20, 1517 (1979); M. Lagarde-Simonoff and G. N. Somonoff, Phys. Rev. C20, 1498 (1979); N. T. Porile, et al., Phys. Rev. C19, 2288 (1979); J. B. Cumming, et al., Phys. Rev. C14, 1554 (1976).

2. T. J. M. Symons, et al., Phys. Rev. Lett. 42, 40 (1978); V. P. Viyogi, et al., Phys. Rev. Lett. 42, 33 (1978).

3. H. S. Pruys, et al., Nucl. Phys. A316, 365 (1979).

4. R. D. Levine, et al., Phys. Rev. Lett. 41, 1537 (1978), and ref. therein.

APPENDIX C

PION PRODUCTION IN NUCLEI

D. G. LONG

Pion production in nuclei is very different from pion scattering. For example, since the mean free path of a 700-MeV nucleon for pion production is about 5 fermis, the pions are produced all over the nucleus. Thus, a larger percentage of pion detected come from further inside the nucleus than is the case for pion scattering.

A simple transport model[1] has been successful in reproducing the data. It is equivalent to the intranuclear cascade[2] in the limit of forward nucleon and pion scattering, given the same inputs. However, the present versions of the cascade have become so long and passed through so many hands that no one is sure what is in them.

To check how well the transport model approximates the cascade when scattering is not forward, a small cascade program designed only for pion production was written . It was determined that the transport model should give a good approximation to the full cascade when the mean free path for pion scattering is less than or equal to the mean free path for pion absorbtion. This defines the limit where the pions scatter at most once or twice before getting out. In a comparison of the experimental data[3] with this simple cascade model surprising results were obtained. Fig. C-1 and Fig. C-2 show that reasonable agreement with the data can be obtained only by reducing the pion scattering to one fifth of its free -N value. Including Pauli corrections and fermi averaging does not help.

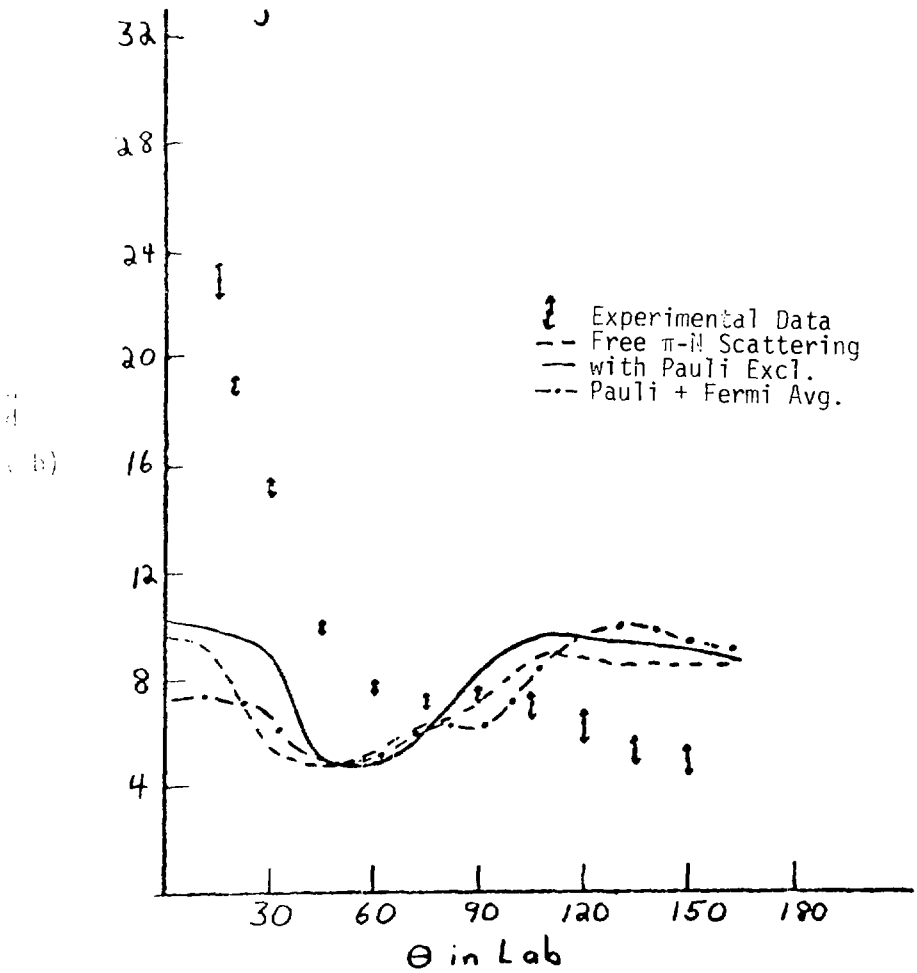

Fig. C-1.

$d\sigma/d\Omega$ for π^+ from Pb.

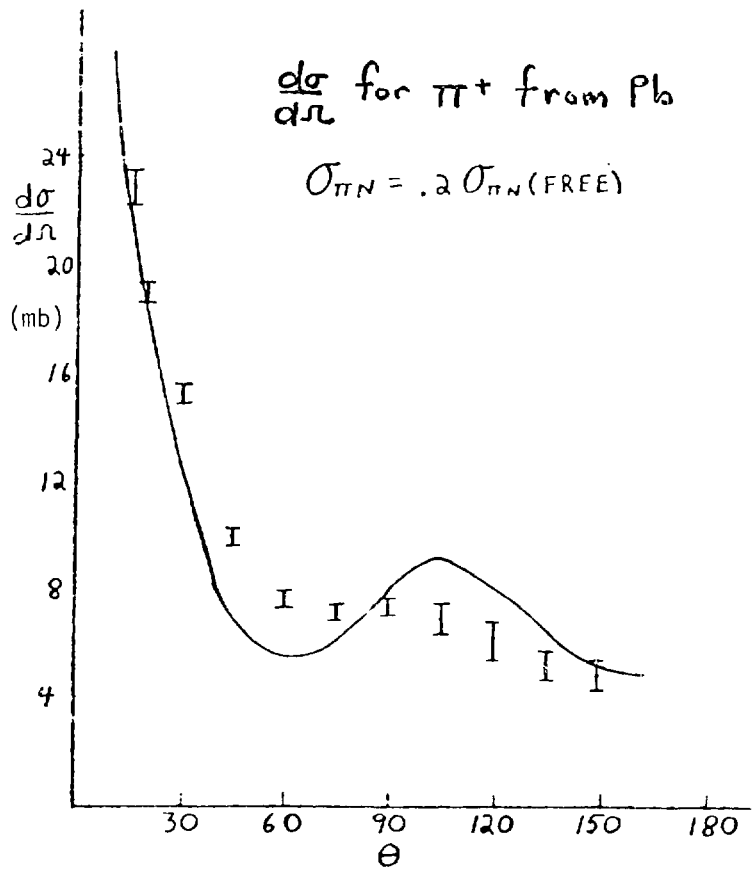

Fig. C-2.

This result is not suprising when one considers the large size of the (3,3) pion-scattering resonance. The problem is also confused by the energy dependence of pion absorption which is not well determined as an input since it occurs only in a nucleus and not on a single nucleon. However, it was found that to make the pion absorption large enough to inhibit the scattering, for any energy dependence, reduces the total number of pions to get out substantially below the experimental data.

It is my finding that deep in the nucleus pion scattering is drastically reduced from the free π-N scattering. This also raises the question of what is buried in these black box cascades in use today, especially as the LAMPF-ISOBAR model had no trouble[2] reproducing the data without including,to my knowledge, anything substantially different from the small cascade. Hopefully this confusion will soon be cleared up.

REFERENCES

1. M. M. Sternheim and R. R. Silbar, Phys. Rev C 8, 492 (1973).
2. G. D. Harp, Phys. Rev. C 10, 2387 (1974).
3. D. R. Cochran et al., Phys. Rev. D 6, 3085 (1972).

APPENDIX D

COMMENTS ON SOME ASPECTS OF INTRANUCLEAR CASCADE CALCULATIONS FOR PION INDUCED NUCLEAR REACTIONS

L-C. Liu

In recent years, intranuclear cascade (INC) theories have been extensively used to analyze nuclear chemistry experiments on pion-induced complex nuclear reactions.[1-5] While these theories are successful in providing qualitative descriptions of the experimental results, quantitative discrepancies between theoretical results and experimental data exist in almost all the cases studied. In this note, I shall discuss some basic dynamical inputs used in the INC theory and their possible relations to the observed disagreements between theory and experiment.

In most INC theories, the target nucleus is being treated as a Thomas-Fermi gas. While this approximation is quite convenient for computations, it precludes, however, any study of nuclear structure effect by the theory. Since nuclear structure effects are important in reaction processes involving a small number of target nucleons, we believe that the INC theory will be generally inaccurate in predicting results for these reaction processes. As an example, we present in Fig. D-1 the comparison between calculated and experimental pion-induced spallation cross sections as a function of the number of nucleons removed from the target nucleus, ΔA. As it may be expected, the discrepancies between the theory and experiment are most remarkable at low ΔA values. We suggest, therefore, that in the future, the inclusion of nuclear structure information in the INC theory should be emphasized.

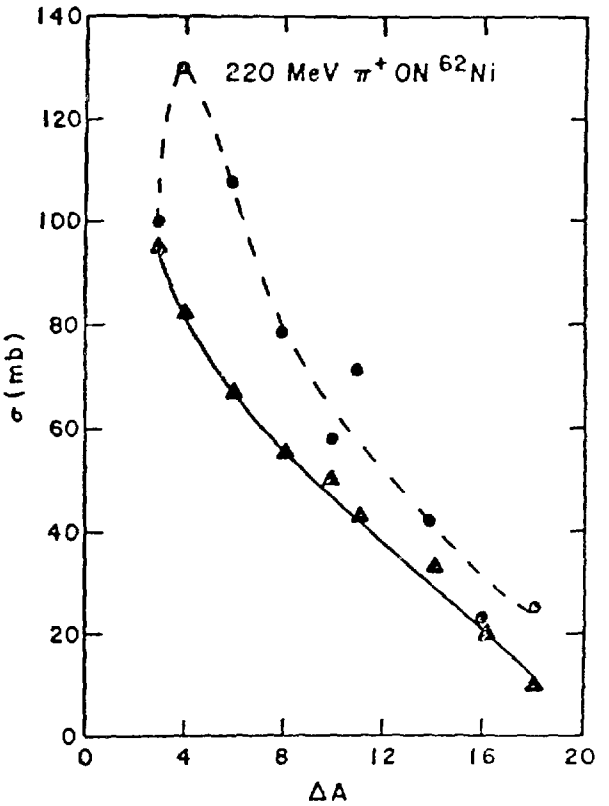

Fig. D-1.

Theoretical (——) and experimental (-----) spallation cross sections, σ, for 220 MeV π^+ incident on ^{62}Ni as a function of the number of nucleons removed from the target, ΔA, (Ref. 6)

In the LAMPF INC theory (ISOBAR) for pion-nucleus interactions, one assumes the formation of the (3,3) isobar by the interacting πN pair as an intermediate step in all reaction modes. Further, the propagation of all particles is treated semi-classically. For example, the probability of having an interaction between a pion and a particle of type i within a distance x is given by

$$p^i(x) = (1 - e^{-x/\lambda})q^i$$

Here, λ is the pion mean free path and q^i is related to the elementary pion-particle (i) cross section and represents the probability for the pion to interact at the position x with the particle i. In the original (Brookhaven) version

of the ISOBAR, the pion mean free path is calculated from the free πN cross sections, $\sigma_{\pi n}$ and $\sigma_{\pi p}$; i.e. $\lambda = (\bar{\sigma}\rho)^{-1}$, where ρ is the nuclear density and $\bar{\sigma} = (N\sigma_{\pi n} + Z\sigma_{\pi p})/A$. Ginocchio and Johnson[6] have evaluated a nuclear medium correction to the pion mean free path, λ, by making use of either a pion-nucleus optical potential (Model I in Ref. 6) or a spreading width of the (3,3) resonance (Model II in Ref. 6). Their investigation shows (Fig. D-2 and D-3) that inclusion of the nuclear medium correction of λ in the INC theory yields improved fits for both the total reaction cross section, σ_R, and the total pion absorption cross section, σ_A, for pions incident on ^{12}C.

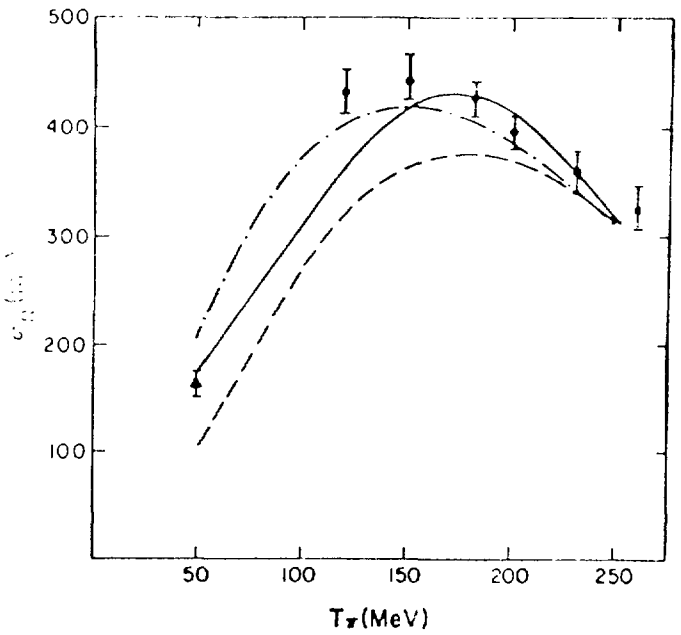

Fig. D-2.

The total reaction cross section σ_R for π^+ incident on ^{12}C as a function of pion kinetic energy, T_π. The dashed curve corresponds to theoretical results obtained without the medium correction to the pion mean free path. Other curves correspond to calculated results due to the inclusion of the optical potential (——) or the spreading width of the (3,3) resonance (—·——·—) in the INC theory (Ref. 6).

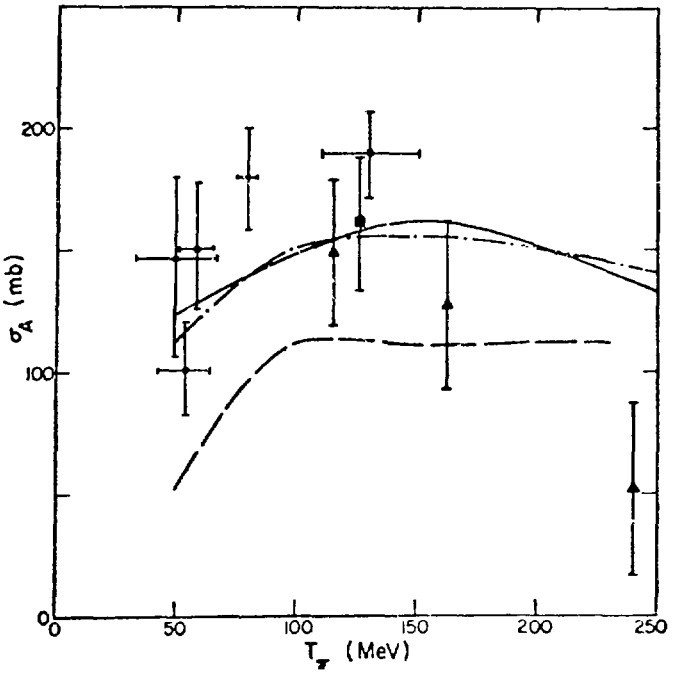

Fig. D-3.

The true pion absorption cross sections for π^+ incident on ^{12}C. Curves have same meanings as in Fig. D-2.

While the Ginocchio-Johnson model improves theoretical fits to the total reaction and absorption cross sections for the π^--^{12}C system, it does not significantly improve calculated spallation cross sections.[3-5] As an example, we present in Fig. D-4 the comparison between theoretical and experimental excitation functions[7] for the reaction $^{27}Al \xrightarrow{\pi^-} {}^{24}Na$. Inspection of Fig. D-4 indicates that the INC theory with the incident of the medium correction of pion mean free path does not provide a significantly improved fit to the data. Since spallation products yields involve also the evaporation part of the nuclear reaction, it is not possible to draw conclusions from these spallation studies as to the general quality of the Ginocchio-Johnson approach. To answer this latter question, calculations of σ_A and σ_R for nuclei other than ^{12}C are necessary.

However, the nuclear medium modifies not only the pion mean free path, λ, but also the elementary pion-nucleon scattering amplitude, which determines the probability p^i. A self-consistent treatment of the medium correction in the INC theory thus requires that both these modifications be included. In the (3,3) resonance region, the free πN amplitude can be parametrized by

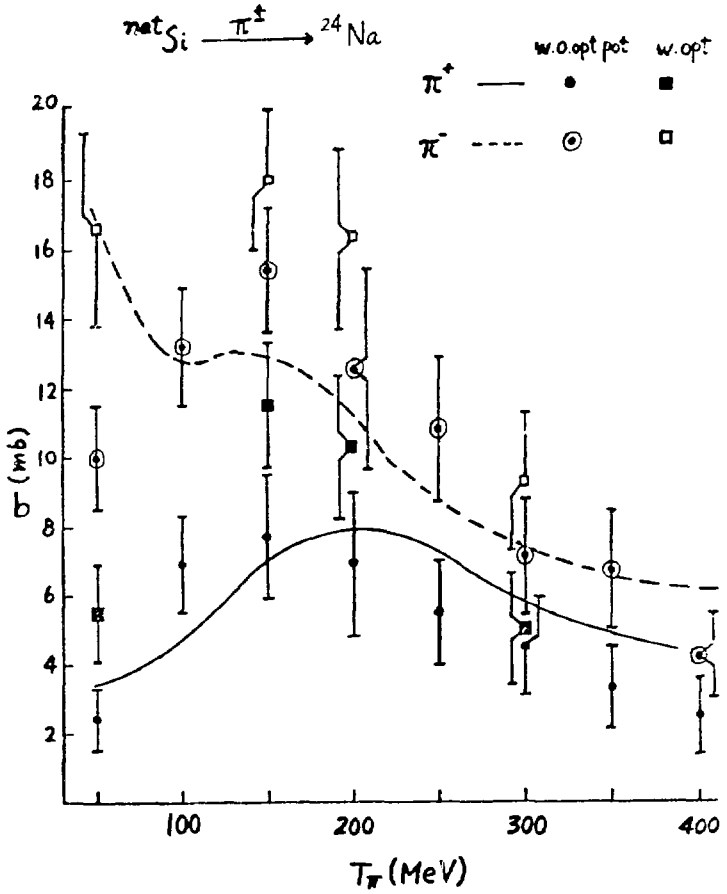

Fig. D-4.

Excitation functions for the production of ^{24}Na from ^{27}Al by fast pions. Experimental cross sections are presented by solid (π^+) and dashed (π^-) curves (Ref. 7). Theoretical results obtained without the medium correction are represented by • (π^+) and Θ (π^-). Cross sections calculated with the inclusion of the medium correction are given by ■ (π^+) and □ (π^-).

$$< k' | t_{\pi N}(E) | k > = \alpha(E)\, V(k')\, V(k)/D(E) \quad ,$$

where α represents the coupling constant and V the form factors. The quantities k, k', and E denote, respectively, the initial and final relative momentum, and the total energy in the center-of-mass frame of the πN system. Further, the demoninator function D(E) describes the energy-dependence of the pion-nucleon scattering. The πN amplitude in the nuclear medium is then given by[8]

$$< k'|t_{\pi N}^{med.}(E)|k > = \alpha(E)\ V(k')\ V(k)/\bar{D}(E) \quad ,$$

where the denominator function $\bar{D}(E)$ describes the effective πN scattering inside the nucleus. In general, we have $|1/\bar{D}(E)|^2 < |1/D(E)|^2$ in the (3,3) resonance region[8]. That is to say, the medium correction will weaken the q^i used in the calculation of $P^i(X)$. This latter effect is therefore opposite to the enhancement of $P^i(X)$ due to the medium correction of the pion mean free path, λ. It may well be possible that the overall effect of the medium correction is much weaker than those given by Ref. 6.

Finally, we mention that in the ISOBAR code the Coulomb distortion of the pion trajectory inside the nucleus has not been considered. At low energies these effects should be important. Inclusion of the Coulomb distortion of the pion trajectory inside the nucleus may well provide an answer to current difficulties in explaining the low-energy part of the negative-pion-induced excitation function (see Fig. D-4).

In summary, we suggest that both the nuclear structure and reaction dynamics of the ISOBAR code should be improved. Inclusion of nucleon clustering, self-consistent treatments of medium corrections, and other off-shell effects would make current INC theories a better description for pion-induced complex nuclear reactions. The Coulomb distortion of trajectories and other improvements within the framework of a semiclassical formalism should also have important effects on calculated results. For these latter improvements, it may be fruitful to consider employing the formalism presented by E. Remler at this Workshop. Finally, it will also be useful to perform some nuclear chemistry experiments which are of more exclusive character, so that the improvements of the INC theory can be more easily tested.

REFERENCES

1. J. N. Ginocchio, Phys. Rev. C17, 195 (1978).

2. B. J. Dropesky, G. W. Butler, C. J. Orth, R. A. Williams, and M. A. Yates-Williams, Phys. Rev. C20, 1844 (1979).

3. S. B. Kaufman and E. P. Steinberg, Phys. Rev. C20, 2293 (1979).

4. C. J. Orth, B. J. Dropesky, R. A. Williams, G. C. Giesler, and J. Hudis, Phys. Rev. C18, 1426 (1978).

5. C. J. Orth, W. R. Daniels, B. J. Dropesky, R. A. Williams, and G. C. Giesler, Phys. Rev. C 21, 2524 (1980).

6. J. N. Ginocchio and M. B. Johnson, Phys. Rev. C21, 1056 (1980).

7. B. J. Dropesky, G. W. Butler, G. C. Giesler, C. J. Orth, and R. A. Williams, "Excitation functions for the production of ^{18}F and ^{24}Na from Al and Si with fast pions," report in preparation.

8. L. Celenza, L. C. Liu, W. Nutt, and C. M. Shakin, Phys. Rev. C14, 1090 (1976).

Summary Report and Recommendations from Panel

NC-6 NEW EXPERIMENTAL TECHNIQUES AND NEW NUCLEAR CHEMISTRY FACILITIES

by

J. Hudis, Brookhaven National Laboratory, Chairman

D. J. Vieira, LASL, Co-Chairman

I. INTRODUCTION

Panel NC-6 was given the charge of reviewing presently available beams and experimental facilities and gathering into one place, to the extent possible, the planned and proposed future accelerator developments and facilities which are of interest to intermediate-energy nuclear chemists. It was also deemed advisable to assimilate the nuclear chemistry community's future experimental needs, many of which became only generally apparent during the course of this Workshop.

In this report we will attempt to summarize the highlights of this panel's discussions which, clearly, only briefly touch on the above points. The panel met on Thursday morning with about half of the Workshop in attendance. Individual contributions to this panel are not specifically identified in this report; however, we wish to acknowledge and thank all of the speakers who presented talks as outlined in the NC-6 agenda given in Appendix A, the other panel chairmen and co-chairmen who summarized and expressed many of the experimental needs of their respective panels, and the many attendees who participated in the discussions of this panel.

II. PRESENTLY AVAILABLE INTERMEDIATE-ENERGY FACILITIES

Reviews of the beams and experimental facilities available at TRIUMF, SIN, LAMPF, and KEK were presented during the panel session. The AGS kaon beam facility was also described at this time and the CERN SC - ISOLDE facility was described by M. Epherre in her featured talk entitled "Nuclei Far from Beta Stability" and in her contributed talk in Panel NC-2. Three intermediate energy accelerators not reviewed were the Indiana University Cyclotron Facility, the Bates Electron accelerator, and the SATURNE accelerator in France. Tables I-V represent much of

TABLE I

INTERMEDIATE-ENERGY PROTON BEAMS

Institution	Type of Accelerator	Energy Range	Meson Production Intensity	Proton Intensity for Nucleon-Induced Reaction Studies	Repetition Rate	Duty Factor	Microscopic Pulse Length	Unique Nuclear Chemistry Facilities
TRIUMF	Cyclotron	180-520 MeV 70-100 MeV	30-100 μA typ.	10 μA 300 nA $\vec{p}$	continuous	100%	~2.0 ns every 44 ns	• He-Jet System • 1-m-diam Scattering Chamber for TOF Experiments • Radioisotope Production Facilities
SIN	Cyclotron (Injector)	590 MeV (72 MeV)	100-150 μA typ.	~1 nA $\vec{p}$ (~1 μA $\vec{p}$)	continuous	100%	~0.5 ns every 20 ns	• Radioisotope Production Facilities
LAMPF	Linac	300-800 MeV	500 μA typ.	6 μA 15 nA $\vec{p}$	120 Hz	5-9%	<0.3 ns every 5 ns	• Thin Target Area for TOF Experiments • Pneumatic Rabbit System • Radioisotope Production Facilities
CERN	Synchro-cyclotron	600 MeV	3 μA	3 μA	360 Hz	1-50%	Slow extraction ~1.4 ms Fast extraction ~40 μs	• ISOLDE II
KEK	Synchrotron	12 Gev	~2 p/pulse	~2×10^{12} p/pulse	0.4 Hz		Slow extraction ~0.4 s Fast extraction ~2 μs	• Radioisotope Production Facilities
	(Booster)	(500 MeV)	(~6×10^{11} p/pulse)	(~6×10^{11} p/pulse)	(20 Hz)			
AGS	Synchrotron	28 GeV	~9×10^{12} p/pulse	~9×10^{12} p/pulse	0.4-0.7 Hz		Slow extraction ~ 0.4 s Fast extraction ~2 μs	• Chemistry Irradiation Facility and Radioisotope Production Facility at the Injector
	(Injector)	(200 MeV)		(100 μA)	(10 Hz)			

TABLE II

NEUTRON BEAMS

Institution	Energy Range	Average Flux (n/cm^2 sec)
TRIUMF		
Thermal Neutron Facility	Thermal (10-100 meV)	2×10^{12} Surface Flux
	Epithermal (0.1 eV-100 keV)	8×10^{11} Surface Flux
	(0.1 - 20 Mev)	2×10^{11}
Liquid D_2 Target	160-500 MeV	5×10^{4} $\vec{n}$ (8 cm x 8 cm)
SIN		
Thick Target E	100-590 MeV	2×10^{7} (3 cm x 5 cm)
LAMPF		
WNR	Thermal	2×10^{11} Surface Flux
	Epithermal	1×10^{12} Surface Flux
Beam Stop Rabbit	0.1-20 MeV	5×10^{11}
Liquid D_2 Target	300-800 MeV	1×10^{6}
KEK		
Neutron Facility at 500 MeV Booster	Cold (<5 meV)	1×10^{11} Surface Flux
	Thermal	2×10^{11} Surface Flux
	Epithermal	1×10^{12} Surface Flux
CERN SC		
Neutron Production Target	20-600 MeV	2×10^{8} (14 cm x 14 cm)
AGS		
Medium Energy Intense Neutron (MEIN) Facility at 200-MeV Injector	25-200 MeV	1×10^{11} (3 cm x 3 cm)

TABLE III

PION BEAMS

Institution	Energy Range	Momentum Range	$(\Delta p/p)_{max}$	Typical Spot Size X x Y (FWHM)	$\Phi_{\pi^+ max}$	Purity(%) $\pi^+:\mu^+:e^+$	$\Phi_{\pi^- max}$	Purity(%) $\pi^-:\mu^-:e^-$
TRIUMF (30 μA assumed)	20-110 MeV (110-350) MeV	75-210 MeV/c (210-470) MeV/c	±7%	2.5 cm x 1.5 cm	5×10^7 π^+/s @ 50 MeV	93:5:2	2×10^7 π^-/s @ 90 MeV	80:4:16
					(6×10^7 π^+/s @ 150 MeV)		(2×10^7 π^-/s @ 150 MeV)	
					(2×10^7 π^+/s @ 300 MeV)		(6×10^6 π^-/s @ 300 MeV)	
SIN (100 μA assumed)	20-310 MeV	75-430 Mev/c	±5%	2.0 cm x 3.0 cm	5×10^8 π^+/s @ 50 MeV	38:4:58	1×10^8 π^-/s @ 50 MeV	11:1:88
					2×10^9 π^+/s @ 150 MeV	85:9:6	4×10^8 π^-/s @ 150 MeV	63:6:31
					(9×10^9 π^+/s @ 250 MeV)	99:<1:<1	(7×10^8 π^-/s @ 250 MeV)	99:<:<1
LAMPF (500 μA assumed)	30-600 MeV	90-730 MeV/c	±6%	2.5 cm x 1.5 cm	7×10^7 π^+/s @ 50 MeV	58:13:29	2×10^7 π^-/s @ 50 MeV	41:6:53
					5×10^8 π^+/s @ 150 MeV	80:12:8	2×10^8 π^-/s @ 150 MeV	58:7:35
					2×10^9 π^+/s @ 300 MeV	99:<1:<1	3×10^8 π^-/s @ 300 MeV	99:<1:<1
CERN SC (3 μA assumed)	50-300 MeV	130-420 MeV/c	±5%	3.0 cm x 3.0 cm	3×10^6 π^+/s @ 150 MeV		2×10^6 π^-/s @ 150 MeV	
KEK (2×10^{12}p/pulse assumed)	0.1-8.0 GeV	0.2-8.0 GeV/c	±6%	1.0 cm x 1.0 cm	$4\text{-}40 \times 10^6$ π^+/pulse		$1\text{-}10 \times 10^6$ π^-/pulse	
AGS (3×10^{12}p/pulse assumed)	0.4-25.0 GeV	0.5-25.0 GeV/c	±4%	3.0 cm x 3.0 cm	$4\text{-}60 \times 10^6$ π^+/pulse		$1\text{-}15 \times 10^6$ π^-/pulse	

TABLE IV

MUON BEAMS

Institution	Momentum Range	$(\Delta p/p)_{max}$	Typical Spot Size X x Y(FWHM)	Φ_{μ^+} max	Purity(%) $\mu^+:\pi^+:e^+$	Φ_{μ^-} max	Purity(%) $\mu^-:\pi^-:e^-$
TRIUMF (30 μA assumed)	20-165 MeV/c	±5%	5 cm x 5 cm	6×10^5 μ^+/s @ 30 MeV/c	98:<1:2		
				3×10^5 μ^+/s @ 85 MeV/c	99:<1:<1	6×10^5 μ^-/s @ 85 MeV/c	99:<1:<1
				5×10^6 μ^+/s @ 130 MeV/c	99:<1:<1	9×10^5 μ^-/s @ 130 MeV/c	99:<1:<1
SIN (100 μA assumed)	25-125 MeV/c	±7%	6 cm x 5 cm	1×10^7 μ^+/s @ 30 MeV/c	95:<1:5		
				3×10^7 μ^+/s @ 85 MeV/c	99:<1:<1	8×10^6 μ^-/s @ 85 MeV/c	99:<1:<1
				2×10^8 μ^+/s @ 130 MeV/c	99:<1:<1	3×10^7 μ^-/s @ 130 MeV/c	99:<1:<1
LAMPF (500 μA assumed)	25-250 MeV/c	±6%	4 cm x 10 cm	3×10^6 μ^+/s @ 30 MeV/c	85:<1:15		
				3×10^7 μ^+/s @ 85 MeV/c	99:<1:<1	6×10^6 μ^-/s @ 85 MeV/c	99:<1:<1
				1×10^8 μ^+/s @ 130 MeV/c	99:<1:<1	2×10^7 μ^-/s @ 130 MeV/c	99:<1:<1
CERN SC (3 μA assumed)	100-250 MeV/c	±10%	5 cm x 5 cm	3×10^4 μ^+/s @ 130 MeV/c	83:<1:17	1×10^4 μ^-/s @ 130 MeV/c	83:<1:17

TABLE V

KAON/ANTIPROTON BEAMS

Institution	Momentum Range	$(\Delta p/p)_{max}$	Typical Spot Size X x Y(FHWM)	ϕ_{K^+} max	Purity(%) $K^+:\pi^+$	ϕ_{K^-}max	Purity(%) $K^-:\pi^-$	$\phi_{\bar{p}}$ max	Purity(%) $\bar{p}:K^-:\pi^-$
KEK (2×10^{12} p/ pulse assumed)	0.5-2.0 (GeV/c)	±3%	2.5 cm x 2.5 cm	3-100 x 10^4 K^+/pulse	9:91-33:67	1-50 x 10^4 K^-/pulse	similar to K^+	10^3-10^5 $\bar{p}$/pulse	95:<3:<3
AGS (4×10^{12} p/ pulsed assumed)	0.6-1.0 (GeV/c)	±2%	1.0 cm x 1.0 cm	6-30 x 10^4 K^+/pulse	8:92	2-10 x 10^4 K^-/pulse	similar to K^+	10^3-10^4 $\bar{p}$/pulse	poor

the pertinent data about beam characteristics presented at the Workshop. In general, these numbers represent the best beam characteristics available at these various accelerators to date. Also included in Table 1 are brief descriptions of experimental facilities of particular interest to nuclear chemists.

III. IMPROVEMENTS AND FUTURE PLANS

There was some discussion of future plans for new beams and experimental facilities at these accelerators. We describe some of these briefly and note that they range from projects under construction to desires not yet in the proposal state.

Future plans at TRIUMF include the possibility of two or three major additions. Design studies are underway to determine the cost and interest in converting the existing medium-resolution proton spectrometer into a high-resolution (<50 keV) device. Plans to extract a third proton beam from the cyclotron for a proposed new experimental area north of the machine are proceeding. As conceived to date, this area would consist of a new high-flux muon channel, a biomedical channel, as well as an additional area for further nucleon and pion studies. The largest project under discussion for the future involves using this new beam line to feed two additional synchrotrons, run in tandem, to accelerate protons to energies of 3 and 8.5 GeV, respectively, providing a high intensity kaon facility. Initial design studies have been started for this long range project; a Kaon Factory Workshop sponsored by TRIUMF was held at the University of British Columbia on August 13-14, 1979.

At SIN a host of new improvements and upgrades are planned. Recently completed and starting to produce data is the new pionic x-ray crystal spectrometer, πKS, which employs a variable Gatchina-type x-ray target. The first experimental results obtained for aluminum demonstrate the success of this new spectrometer which achieved an energy resolution of better than 150 eV and a true-to-background ratio of 1 to 1. A new high-intensity injector for SIN is presently under construction. This will consist of an 800-keV Cockcroft-Walton injector followed by a new 72-MeV four-magnetic-sector cyclotron. This new injector system is planned to be completed and coupled to the main-ring cyclotron sometime in 1981-82 and, after a six-month shutdown scheduled for 1983, full-energy proton beams of 1-2 mA in average intensity are anticipated. Extensive reconfiguration of the experimental hall is also planned for the 1983 shutdown. This includes the installation

of a new beam stop capable of withstanding 2 mA, a spallation neutron source for cold and thermal neutrons, and a new low-energy pion channel called "Yo-Yo" which is intended for the πE3 area. After 1984 a new experimental hall, located downstream of the new biomedical pion applicator, is being discussed. This new area would be limited in primary intensity to 100 μA, and, at this early time, is envisioned to contain two new μSR channels, a new low-energy pion/muon channel, the present polarized proton spectrometer, and possibly ISOLDE III, a proposed on-line isotope separator facility for low-energy nuclear physics studies and radioisotope production. The latter facility is of great interest to the nuclear chemistry community. However, the question of whether there will be an ISOLDE III project at SIN is far from being decided.

Facility developments at LAMPF have progressed steadily during the last year and an ambitious set of improvements are planned for the near, mid, and far future. Dual-energy beam operation has recently been implemented at LAMPF. This enables the energy of the H^- beam to be varied independently from 300 to 800 MeV, while simultaneously delivering a high-intensity 800-MeV H^+ beam for meson production to Area A. With this new feature, a variety of excitation function type experiments using polarized and unpolarized protons (and unpolarized neutrons from the liquid D_2 target) can be undertaken in Areas B and C. During the three-month shutdown scheduled for the fall of 1980, the A-6 beam stop will be replaced. The installation of a water degrader in this region is expected to improve the neutrino flux by at least 30%, thus increasing the sensitivity of a series of new neutrino experiments which have just recently been proposed. During 1982 the new staging area located north of Area A East is expected to be completed.

Proceeding towards completion in 1985 is the proton storage ring (PSR) for the weapons neutron research (WNR) area. Funding for this project has been approved and the final designed details are being completed at this time. The PSR is planned to operate in two different modes, the short-bunch mode for neutron time-of-flight experiments, and the long-bunch mode for condensed matter neutron scattering studies. In the short-bunch mode a 12-μA average current proton beam is extracted as 1-nsec wide pulses at a rate of 720 Hz. This mode affords an increase in the instantaneous neutron flux of two orders of magnitude. In the long-bunch mode a 100-μA average current proton beam is extracted from the ring with a pulse length of 270 nsec at a rate of 12 Hz. This is anticipated to provide some of the highest epithermal and thermal peak neutron fluxes in the world, with the feature of low repetition rate for improved background discrimination. As a

result of the PSR project, two additional undertakings are required: the development of a high intensity (100 μA) H^- source and the modification of the switchyard area to provide H^- beam to the PSR. The latter is anticipated to preclude H^- beams going to Areas B and C for a period of six months or more in 1984.

Among these improvements and others too numerous to mention here, the intermediate-energy nuclear physics and chemistry community is exploring the idea of developing a high intensity kaon facility at LAMPF. At present such a facility is conceived to consist of a fast cycling (30 Hz) synchrotron using LAMPF as an injector. 15-GeV protons at an average current of 100 μA would be used to produce kaons, antiprotons, and other particles with expected intensities at least two orders of magnitude larger than presently available at other machines. A conference entitled "Nuclear and Particle Physics at Energies Up to 31 GeV: New and Future Aspects" is scheduled to be held in Los Alamos in January 1981, to investigate some of the interesting scientific questions which such a facility would address.

KEK is planning to start using the 500-MeV booster cyclotron as a source of slow pions, muons, neutrons, and protons. New μSR and neutron diffraction (thermal and epithermal) facilities have just recently been completed. Experiments utilizing these new facilities will be commencing before the end of 1980. Other facilities using the 500-MeV booster include a facility for nuclear medicine applications, a thin-target proton irradiation facility for activation studies (Φ_p = 1-2 μA), and a low-energy pion channel ($E_\pi \lesssim 65$ MeV) with fluxes up to 3×10^6 π^-/s and 1×10^7 π^+/s for on-line and activation experiments.

At the Brookhaven AGS, an improved kaon channel is under design incorporating superconducting magnets to shorten the overall length of the channel. The primary goal of this new channel would be to improve the π to K ratio from 12/1 to ∿1/1, while simultaneously increasing the kaon flux by a factor of three or more. A working group, chaired by E. V. Hungerford, has been established for those interested in using such a facility and a funding proposal is expected to be submitted to DOE some time in early 1981. Final completion of this new beam line, if approved, would be in 1984 or 1985. E. V. Hungerford pointed out that the present design does not take into consideration the needs of the nuclear chemistry community in providing high-purity kaon and antiproton beams, and he encouraged an active expression of our experimental requirements to the AGS kaon channel working group.

IV. NEW EXPERIMENTAL TECHNIQUES

During the second session of the NC-6 panel, we heard of three newly developed or proposed experimental techniques (see the agenda given in Appendix A). In this section we will attempt to briefly summarize these presentations and try to convey the potential scientific impact which these techniques afford.

The first presentation, given by R. G. Greenwood, deals with helium gas transport (He-jet) systems employing fast chemical separations and on-line mass separators. At the Idaho National Engineering Laboratory (INEL) in Idaho Falls, Greenwood and his associates have developed a He-jet system to investigate the decay properties of short-lived fission products as generated by a 100-μg ^{252}Cf spontaneous fission source. Fission products are transported via the He-jet system to either a fast chemistry laboratory or a mass separator. Fast chemical separation techniques employing high performance liquid chromatography or continuous flow solvent extraction have been applied to rare-earth and palladium activities. These radiochemical separations have been automated via the use of a microprocessor controller such that species with half-lives as short as three minutes can now be studied. Further developments are under way to increase the speed of these chemical separations so that shorter-lived activities can also be investigated.

Work on developing a He-jet coupled mass separator at INEL is proceeding. To date, the development of an effective coupling scheme between the He-jet and the ion source has been investigated. An operational test stand has been fabricated which consists of a gas skimmer arrangement (to prevent a high pressure He buildup in the ion source region), a modified Sidenius-type hollow cathode ion source, and an extractor electrode. After extraction the ions are collected in a Faraday cup and the efficiencies measured with a Ge(Li) detector. Overall He-jet/ion source efficiencies on the order of 0.1 to 1.0% have been obtained for the following fission-product elements: Sr, Y, Mo, Tc, Te, I, Cs, Ba, La, Ce, Pr, Nd, Pm, and Sm. Future plans at INEL involve coupling the He-jet system to an existing mass separator, which is being fitted with a similar hollow cathode ion source, so that nuclear spectroscopy of mass-separated fission products can be undertaken.

Sufficient interest was aroused by this presentation that a working group which consisted of several Workshop participants, representing a number of different institutions, was established to investigate the possibility of developing such a He-jet coupled mass separator facility at LAMPF. They pointed to the

copious amounts of neutron-rich nuclei which could be produced at LAMPF via 800-MeV proton-induced fission of ^{238}U. Many of these fission products of interest are not effectively produced via thermal neutron-induced fission. Moreover, proton-induced fragmentation and spallation of both heavy and medium mass targets provide a rich spectrum of neutron-rich and neutron-deficient nuclei. Nuclear structure studies of these exotic nuclei involving measurements of their masses, decay properties, magnetic moments, and spins remain one of the most fruitful areas of research in nuclear chemistry and physics today. Since the Workshop, a LAMPF proposal (sponsored by several people from the above mentioned working group) to explore the technical feasibility of establishing a He-jet system in the A-6 beam stop area has been approved.

In the second presentation one of us, D. J. Vieira, discussed a proposal submitted (to DOE for funding) by a group of scientists from Los Alamos Scientific Laboratory, Brookhaven National Laboratory, Lawrence Berkeley Laboratory, and the University of Giessen, West Germany, to construct a time-of-flight magnetic spectrometer for precision mass measurements. This spectrometer, which would be installed in the Thin Target Area at LAMPF, consists of three magnetic dipoles and three magnetic quadrupole doublets arranged in such a fashion as to make the transport of an ion through the system isochronous, or in other words, independent of the velocity of the ion. Thus, the transport time of different reaction products through such a spectrometer depends only on their mass-to-charge ratio. Further, by performing measurements of the total kinetic energy and time-of-flight of the ion after the focal plane of the spectrometer to an accuracy of one percent and from knowledge of the approximate magnetic rigidity of the ion as limited by the acceptance of the spectrometer ($\delta B\rho/B\rho \simeq 2\%$), the charge state of the ion can be uniquely defined. This enables the mass of the reaction product to be obtained from one fundamentally precise measurement, the time-of-flight through the spectrometer. Mass resolving powers of 1000 are expected with such a system.

In addition to this good mass resolution, the proposed spectrometer has a solid angle acceptance of 1 msr, some 200 times larger than the present time-of-flight system. This increase in solid angle more than offsets losses due to the limited momentum acceptance of the spectrometer and the charge state distribution of the reaction products emitted from the target. Overall, the proposed spectrometer represents a 25-fold improvement in mass measuring accuracy over

that presently available and the added capability of performing mass measurements on even more neutron-rich or neutron-deficient nuclei which could not be attempted otherwise. An estimated number of new or improved mass measurements, which the proposed spectrometer is capable of determining with accuracies ranging from 100 keV to 1 MeV depending on the production statistics, is expected to be on the order of 60 for nuclei with A < 70!

This proposed time-of-flight spectrometer, which represents a natural extension of experiments performed in the Thin Target Area, affords a unique opportunity to undertake a systematic investigation of the entire nuclear mass surface up to A ≈ 70. Mass measurements are an important first step in our progress toward understanding the nuclear properties of very neutron-rich or neutron-deficient nuclei. We feel that this project is an important future research direction at LAMPF and Vieira encourages and welcomes those interested in collaborating on such mass measurement experiments or those interested in using the proposed spectrometer for their own experimental purposes to contact him.

In the third presentation, H. Daniel discussed an experimental technique which they have developed at the University of Munich and at SIN to produce slow (< 1 MeV) and very slow (< 2.8 keV) muons. Their system consists of a magnet followed by a wedge degrader whose thickness is matched to the momentum dispersion of the magnet. Thus the degrader, which is positioned along the focal plane of the system, is thicker on the high momentum side of the focal plane and thinner on the low momentum side in such a fashion that the resulting muon beam emerging from the degrader after transit has the same uniform energy. This enables them to produce reasonably monochromatic low energy muon beams without sacrificing large losses in intensity. To date, these low-energy muons have been applied to measurements of the Z_1^3 term in the Bethe stopping-power formula and to investigations of the elemental composition of thin films or surfaces. For a more detailed discussion of this technique, we refer you to H. Daniel's contribution which has been reproduced in Appendix B.

V. EXPERIMENTAL NEEDS AND RECOMMENDATIONS

The future directions discussed by Panels 1-4 are in large part shaped by present or already proposed accelerator projects. Historically this has been the approach taken by nuclear chemists. The community has always been a relatively small one, content to shape experimental programs around existing facilities, and having very little input into the design of new accelerators or beam

lines. The strength of the group has come from their willingness, indeed eagerness, to attack problems in nuclear reactions and nuclear spectroscopy which defy simple analytical explanation. The techniques employed have varied over the years but the overriding interest in complex systems and phenomena has remained constant. It is interesting to note, however, that in many areas, notably in pion and heavy-ion induced reactions, the interests of physicists and chemists are coming closer together although their experimental techniques are often very different.

Although no demands for specific new accelerators or beams were voiced at this Workshop there were mentioned a number of needed improvements to presently available beam lines.

1. Protons - One worry here is that with the ever decreasing number of proton synchrotrons and the trend toward higher energies, it may soon be extremely difficult, if not impossible, to carry out experiments over the complete intermediate energy range. Many of the most interesting phenomena associated with reactions in complex nuclei have thresholds and rapidly changing cross sections in this energy region and new experimental techniques and new theoretical models will certainly call for continued work here. The push for beams of new particles and higher energies must not eliminate this possibility.

2. Pions - Researchers in this field are blessed with a number of first-rate sources of these projectiles. As usual, the need of those nuclear chemists who are applying their special techniques to the study of exotic nuclear species or rare reaction processes is for the highest possible beam intensities, even at the cost of energy resolution. For most on-line experiments, the highest possible duty factor is of prime concern.

3. Neutrinos - Although there are only a few nuclear chemists working on neutrino-induced reactions, the present high level of interest in neutrino oscillations coupled with the proven capabilities of radiochemists to perform isolations of very rare reaction products that represent the detection of neutrinos made this subject worthy of inclusion in the Workshop. A strong plea was issued by Panel NC-4 for increased availability of the LAMPF beam stop area for the massive targets required for such experiments.

4. Antiprotons - Panel NC-4 reviewed past experiments with antiprotons and the availability of such beams today. At present, only KEK has relatively pure beams of antiprotons at an intensity of 10^4 $\bar{p}$/sec. The AGS has similar intensities but these beams are badly contaminated, whereas CERN expects to have very pure beams

of 10^6 $\bar{p}$/sec by 1983. At this level, a number of interesting experiments could be performed which would provide new insight into the $\bar{p}$-nucleus interaction. What are really needed for the investigation of $\bar{p}$-nucleus phenomena and for the production of exotic species, such as double hypernuclei, are high intensity antiproton beams of good purity at energies between 500 and 2500 MeV.

5. Kaons - There is active interest among nuclear and high-energy physicists in kaon-induced reactions, especially as a means of producing and studying hypernuclei. Spectroscopic studies of hypernuclei promises to shed new light on Λ-nucleon forces, while the investigation of double hypernuclei would provide valuable information about the $\Lambda\Lambda$ potential and how it is modified by the nuclear environment. Radiochemical-type experiments with kaons will always be difficult, not only because beam intensities are low, but beam purity is generally poor. However, the skills of nuclear chemists in reaction and spectroscopic studies of samples containing only a few decaying nuclei may lead some of our adventuresome colleagues into contributing to this field. Here, as with the case of antiprotons, the need will be for higher beam intensity, but more importantly, much higher beam purity. We encourage the improvement of present kaon/antiproton beam lines and the development of new facilities which will provide these needed beams.

Probably the most notable and laudable future technological directions expressed by the community assembled were the design and/or development of a number of sophisticated experimental systems, each of which would open up a new and exciting area of nuclear chemistry research. These included the time-of-flight magnetic spectrometer for precision mass measurements proposed for LAMPF, the He-jet on-line mass separator also being considered at LAMPF, the possibility of an ISOLDE III at SIN, and the development of plastic ball/plastic wall detector arrays for the study of exclusive reactions, all of which are examples of experimental systems already in the planning stage and should have the full support of all scientists interested in intermediate-energy phenomena. Perhaps more importantly, there is associated with each of these instruments a group of scientists willing to devote the time and effort necessary to get large projects funded and built. We believe that this mode of research is one of the best ways in which a relatively small community of researchers can continue to perform first-rate work and we encourage expanded efforts along these lines.

APPENDIX A

NEW EXPERIMENTAL TECHNIQUES AND

NEW NUCLEAR CHEMISTRY FACILITIES

Final Agenda

Chairman - J. Hudis, BNL

Co-Chairman - D. J. Vieira, LASL

Thursday, June 26

8:30 - 10:00 - Overview of Current Intermediate Energy Facilities and Future Improvements

R. Kortelinq, TRIUMF

N. Imanishi, KEK

H. K. Walter, SIN

D. Cochran, LAMPF

E. Hungerford, AGS Kaon Facility

10:00 - 10:30 - Coffee

10:30 - 12:00 - Experimental Techniques

R. G. Greenwood - "He-Jet Fast Chemistry and He-Jet Fed On-Line Mass Separators"

D. J. Vieira - "A TOF Magnetic Spectrometer for Precision Mass Measurements"

H. Daniel - "Production and Application of Slow and Very Slow Muons"

Open Discussion of Experimental Needs

Friday, June 27

10:30 - 12:00 - Plenary Panel Reports

11:30 - 12:00 - J. Hudis, Chairman- NC-6

APPENDIX B

PRODUCTION AND APPLICATION OF SLOW AND VERY SLOW MUONS

by

H. Daniel

Physics Department, Technical University of Munich,
Garching, Fed. Rep. of Germany

Production and application of slow muons ($1\ \text{MeV} > E_\mu > m_\mu(\alpha c)^2/2$) and very slow muons ($E_\mu < m_\mu(\alpha c)^2/2$) are discussed. A set-up to increase the flux, consisting basically of a magnet and a wedge, is presented. Typical results are given.

I. INTRODUCTION

The muon has a number of properties which make it an ideal probe for many phenomena determined by electromagnetic interactions. The most important properties are: the absence of strong interactions, the occurrence of two species with singly positive and negative charges, respectively, the intermediate mass, the "long" lifetime, the easy availability, the easy detection even as stopped particles, the easy determination of the trajectory during flight and of the position in space at rest by tracing the decay electron and, in the case of μ^-, the easy identification of the element into which the particle has been Coulomb captured. I shall exclude from the present consideration applications due to the spin of the muon because this area, μSR, is a field of its own.

With present techniques muons are usually produced at energies on the order of 100 MeV in muon channels, preferably of the superconducting type. A rather new way of production is in the form of "surface" and "cloud" beams, particularly suitable for μ^+, where the particles emerge from a solid target or its immediate environment at much lower energies. Nevertheless, if we define slow muons as having kinetic energies between 1 MeV and $m_\mu(\alpha c)^2/2$ (i.e. 2.8 keV), and very slow muons as having energies below $m_\mu(\alpha c)^2/2$, where m_μ is the muon rest mass,

α the fine structure constant and c the velocity of light, we still have to moderate the muons coming from surface or cloud beam channels. Moderation is usually done by energy loss due to the stopping power of matter. In this case we have the following formula for the spectral flux density n(W), leaving the moderator compared to the same quantity entering it, where n(W)dW is the number of particles entering a small sphere of radius r per unit time with energies between W and W + dW, divided by πr^2:

$$n(W)\, S(W) = n(W_0)\, S(W_0) \qquad (B1)$$

where S(W) is the stopping power at energy W. No deflection devices, either by electric or magnetic forces, can change the relation Eq. (B1) as long as the energy change is done via the stopping power technique. Except at very low energies the phase space density is reduced. Nevertheless, we may transform a beam of particles in phase space (cf. Section II.2).

Low-energy muons are well suited for measuring correction terms to the ordinary Bethe stopping-power formula, particularly for measuring the Z_1^3 term. This term depends on the sign of the charge and with ordinary heavy particles, namely atomic nuclei, can only be measured in combination with the Z_1^4 term. In the case of muons, however, Z_1^4 is the same for μ^+ and μ^- and hence its effect cancels when comparing μ^+ and μ^- data. Emulsion experiments of this kind have been performed by Barkas et al.,[1] while the first counter experiment has recently been carried out at SIN.[2]

In the case of very slow muons one can, of course, perform the same kind of experiment as for low-energy muons. However, the experimental determination of energy loss for very slow particles is in such a poor state, particularly for negatively charged particles, that the first goal is to obtain any experimental data at all. Experiments of this type were recently performed at SIN and will be continued.[3]

Slow and very slow muons can also be used for the investigation of thin films or surfaces where the elemental composition, either at the surface or just below the surface is to be determined. Such practical applications of muon capture were discussed in the NC-3 panel and a brief summary of this work can be found in their report.

II. SET-UP FOR PRODUCTION OF SLOW AND VERY SLOW MUONS FOR AN EXPERIMENT AT SIN

II.1 Production of slow muons

Slow muons were obtained by degrading muons of either 16 MeV or 30 MeV with a polyethylene degrader down to the desired energy. Muons of 3.8-MeV/c momentum, or more, were magnetically selected. Figure 1 shows the set-up. Target 1, the scintillation counter Sc4, and the Ge(Li)-detector were used by a simultaneous experiment for measuring muonic x rays and are of no concern to the discussion of the stopping power experiment described herein. The scintillation counter Sc5 is the "source" for muons in a magnetic spectrometer which is of a slice of an "orange" ($1/r$ field where r is the distance from a symmetry axis of the field). The scintillation counter Sc6 is the detector of the spectrometer. Scintillation counter Sc8 is in anti-coincidence and serves only to decrease the background due to fast muons. The counter Sc2 is in coincidence with Sc5 and in delayed coincidence with Sc6, thus defining a telescope which takes into account the time-of-flight of the slow muons through the spectrometer.

The stopping power is measured with the help of Eq. (B1). In order to measure the Z_1^3 term, the rate $2 * \overline{3} * 5 * 6 * \overline{8}$ for μ^+ is compared with its corresponding rate for μ^-.

II.2. Production of very slow muons

The set-up used for the production of very slow muons is very similar to that described in Section II.1. However, instead of the detector Sc6 which is the final destination for the muons in the slow muon experiment, we use a wedge in front of a very thin scintillation counter, thin enough to let very slow muons emerge into a time-of-flight chamber. Figure 2 shows the set-up. The very slow muons are finally stopped in target 2, which consists of either a thin metal film on a thick sheet of another element or a rather thick sheet of a pure element such as silicon. The detection of these very slow muons is via muonic x rays registered in the germanium detector "Ge," which is shielded against decay electrons by the veto-counter Sc7. The first target arrangement (thin film on top of a thick layer of another material) is for range measurements and the second one (a pure element target) for spectral flux density measurements. The time-of-flight of each slow muon is measured electronically.

The wedge, and in particular scintillation counter Sc6, are rather delicate. The purpose of the wedge is to transform a narrow beam with large energy spread,

whose dimension is defined by Sc5, into a broad beam of minimum energy spread after the wedge degrader. The beam immediately behind Sc5 is narrow in order to reduce the total number of muons entering the time-of-flight set-up and thus reducing background without a loss of slow muon flux. The wedge is at the focus of the magnet. The thickness of the scintillation counters involved and the wedge degrader are such that the range curve maximum is at the downstream surface of Sc6. Presumably the very slow muons will show a cosine angular distribution around the axis (Lambert's Law).

A new version of the time-of-flight chamber, now under construction makes use of an ellipsoidal electrostatic mirror which focuses slow muons from the center of Sc6 onto the center of target 2 with the direct beam blocked by an absorber. It is hoped that this will increase the intensity and further reduce background. This set-up is scheduled for its first experiment in July 1980.

Bound negative muons can easily be produced in gas. Of practical importance are muons captured by hydrogen because the pμ (in addition to dμ and tμ) atoms are electrically neutral and can transfer the muon to heavier Z atoms upon atomic collisions. Figure 3 shows a high pressure gas target for up to 1000 atm which was used at CERN for such studies.

III. SOME RESULTS WITH SLOW AND VERY SLOW MUONS

III.1 Results with slow muons

As a typical example, results on the Z_1^3 term in Al are summarized in Table 1. Our experimental values are compared with values from a semi-empirical formula by Andersen et al.,[4] the new theoretical values by Ritchie and Brandt,[5] and earlier values by Jackson and McCarthy[6] which, however, according to Lindhard[7] are too low by about a factor of two.

III.2 Results with very slow muons

Results with very slow muons were obtained using both range and stopping power techniques (cf. Section II.2). Typical data are summarized in Table II. A typical time-of-flight spectrum accumulated in only nine hours is shown in Figs. 4 and 5.

REFERENCES

1. W. H. Barkas, N. J. Dyer, and H. H. Heckman, Phys. Rev. Lett. 11, 26 (1963).

2. R. Bergmann, H. Daniel, T. von Egidy, P. Ehrhart, G. Fottner, H. Hagn, F. J. Hartmann, E. Köhler, and W. Wilhelm, SIN Newsletter No. 12, 63 (1979).

3. Munich group (unpublished).

4. H. H. Andersen, J. F. Bak, H. Knudsen, and B. R. Nielsen, Phys. Rev. A 16, 1929 (1977).

5. R. H. Ritchie and W. Brandt, Phys. Rev. A 17, 2102 (1978).

6. J. D. Jackson and R. L. McCarthy, Phys. Rev. B 6, 4131 (1972).

7. J. Lindhard, Nucl. Instr. Meth. 132, 1 (1976).

TABLE I

BARKAS EFFECT IN Al; VALUES OF THE Z_1^3 TERM (IN PER CENT OF Z_1^2 TERM)

Energy[a] (keV)	v/c	This Work	Andersen[b]	Ritchie[c]	Jackson[d]
812 (80)	0.213	1.4 ± 0.7	1.4	0.8	0.5
510 (50)	0.098	1.9 ± 0.9	2.5	1.6	0.9
350 (40)	0.081	6.0 ± 1.3	4	2.7	1.5
217 (20)	0.064	7 ± 2	7	5	2.6
108 (10)	0.045	19 ± 5	16	12	6
69 (8)	0.036	23 ± 12	27	20	9

a. In parentheses, FWHM of distribution

b. Semi-empirical formula based on positive atomic ion data (Ref. 4)

c. Theory with adapted parameter (Ref. 5)

d. Theory (Ref. 6)

TABLE II

EXPERIMENTAL RANGE-ENERGY RELATIONS

Target	Thickness ($\mu g/cm^2$)	Exp. Energy (keV)	Energy from proton data (keV)	
			Path Length[a]	Proj. Range[b]
Al	40 ± 4	16.8 ± 2.5	15.3	18.0
Cu	40 ± 4	4.2 ± 0.5	4.4	10.1
Au	120 ± 10	19.5 ± 6.0	6.6	20.0
Au	192 ± 8	22 ± 4	14.6	31.5
Au	9200 ± 300	450 ± 20	450	450

[a] True path length

[b] Projected along surface normal (beam axis)

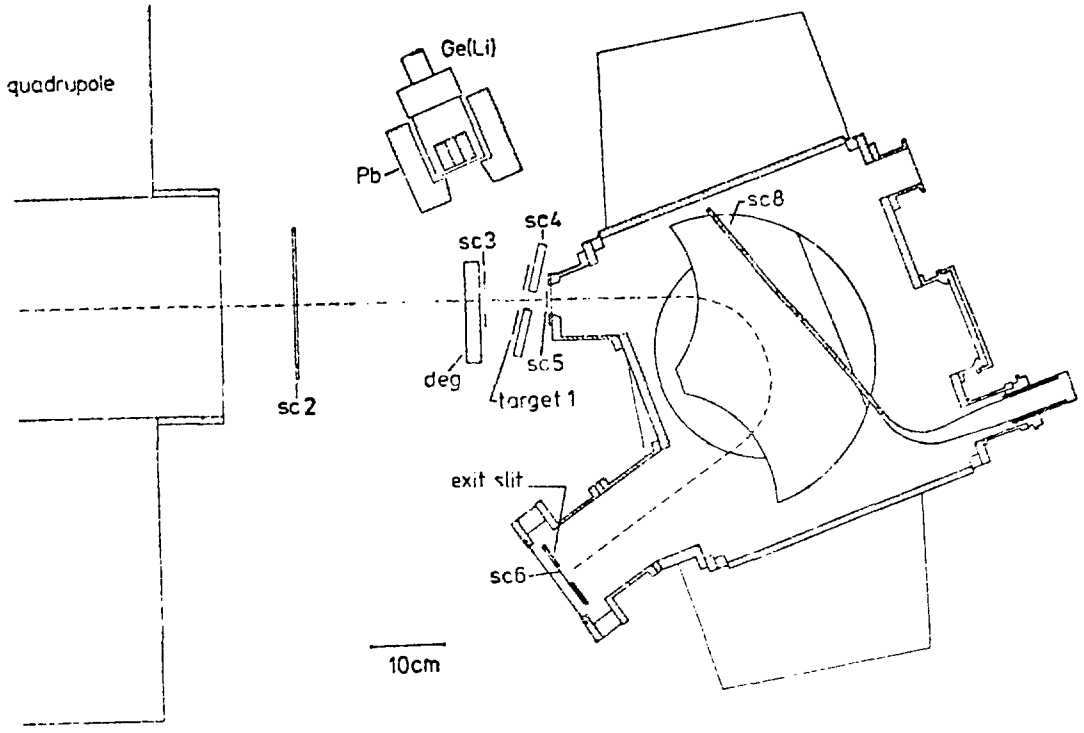

Fig. 1.

Set-up for slow muons. Sc2, Sc3, Sc4, Sc5, Sc6, and Sc8 are scintillation counters; Ge(Li), germanium detector; Deg, degrader. Events (Sc2 * $\overline{Sc3}$ * $\overline{Sc4}$ * Sc5 * Sc6 * $\overline{Sc8}$) are registered for the spectral flux density experiment. Events (Sc2 * Sc3 * $\overline{Sc4}$ * Ge(Li)) are registered for muonic x-ray experiments running simultaneously.

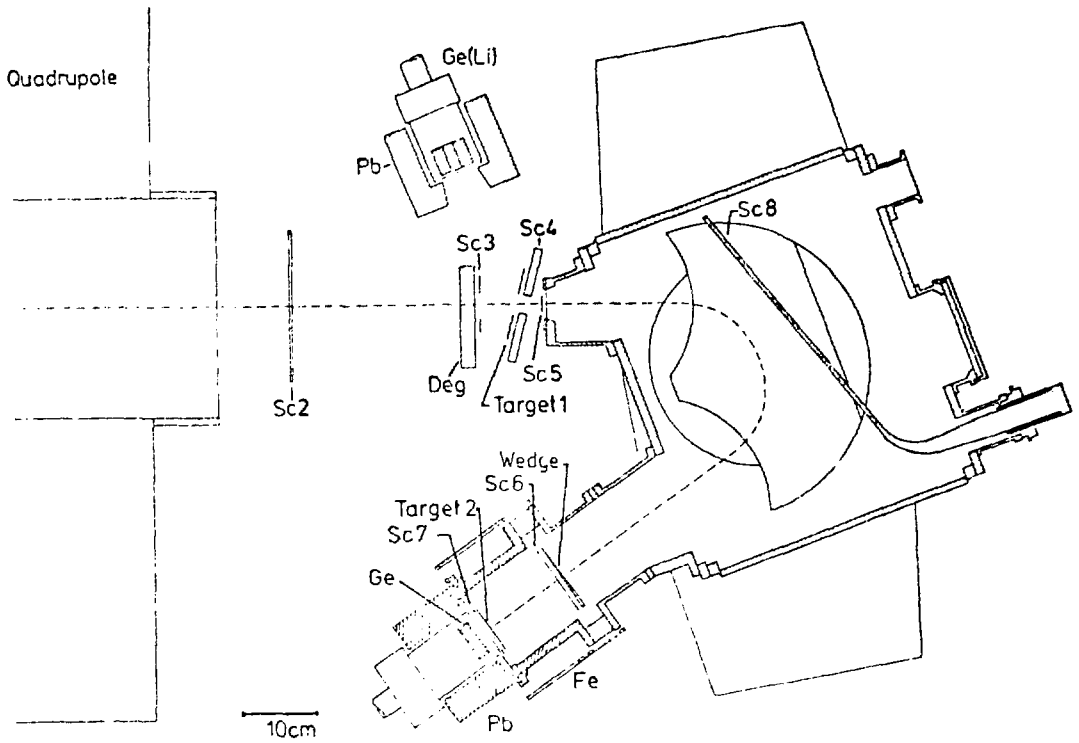

Fig. 2.

Set-up for very slow muons. Sc2, Sc3, Sc4, Sc5, Sc6, Sc7, and Sc8 are scintillation counters (Sc6: 3 mg/cm^2); Ge(Li) and Ge, germanium detectors; Deg, degrader. Events (Sc2 * $\overline{Sc3}$ * $\overline{Sc4}$ * Sc5 * Sc6 * $\overline{Sc7}$ * $\overline{Sc8}$ * Ge) are registered for the spectral flux density experiment. The μ time of flight between Sc6 and target 2 (for example, 40 μg/cm^2 Cu on Si) is measured for each event individually. Deflecting magnet and wedge transform a thin beam of large energy spread into a broad beam of small energy spread. The degrader thickness is such that the maximum of the μ stopping distribution is on the downstream surface of Sc6.

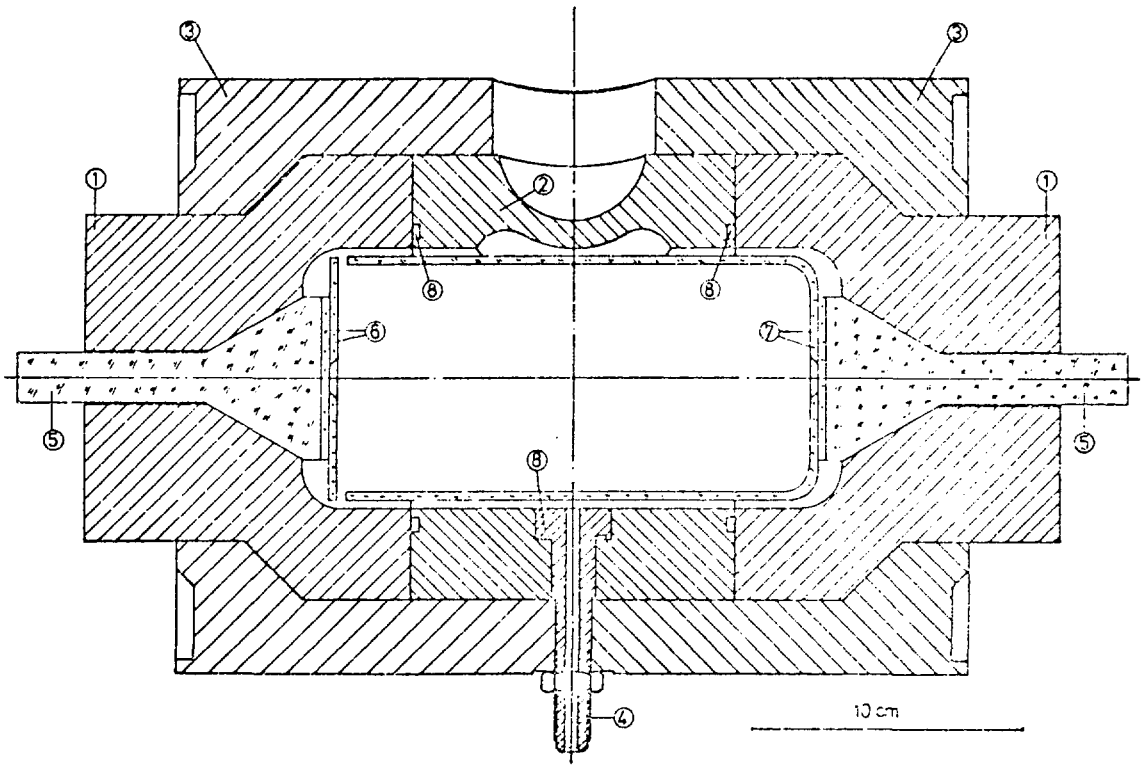

Fig. 3.

Cross section of high pressure gas target (up to 1000 atm). 1: side pieces (Al). 2: middle piece with semi-spherical window, 1 cm Al. 3: steel caps. 4: gas inlet. 5: lucite light pipes. 6: plastic scintillation counter, in coincidence with Ge detector (not shown). 7: plastic scintillation counter, in anticoincidence with Ge detector. 8: O rings. The steel caps are fixed by 8 steel clamps (not shown).

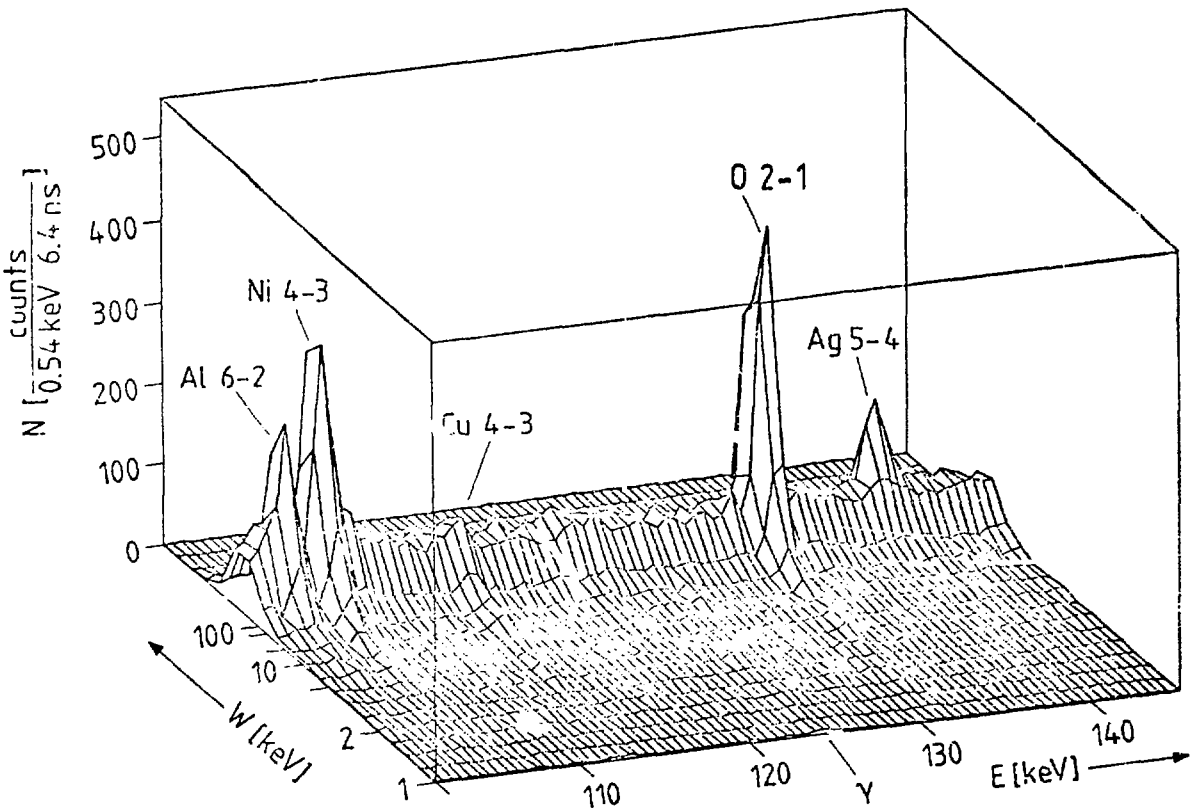

Fig. 4.

Two-dimensional spectrum. Target 2 consisted of 60 μg/cm² Cu on Si. A Ag foil (0.16 mg/cm²) covered the downstream surface of Sc6 in this run. It is that material whose spectral μ flux density n(W) was measured, and also gave a zero marker for the time-of-flight electronics. N is the number of counts per energy channel (0.54 keV) and time-of-flight channel (6.4 ns). E is the x-ray energy, W the muon energy as measured by the time of flight. Accumulation time: 14 hours.

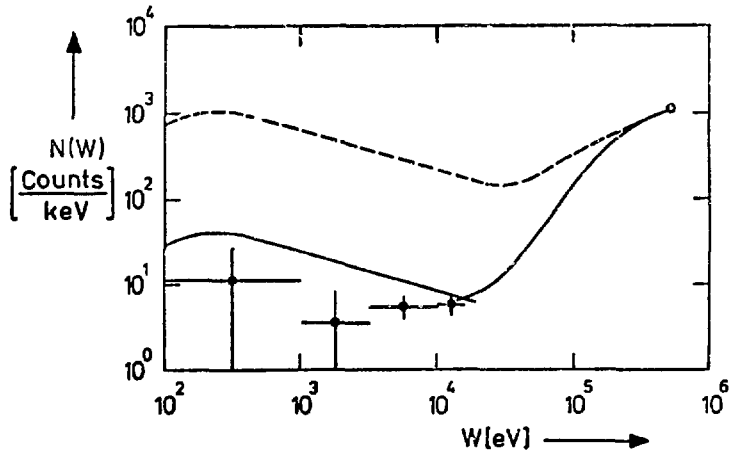

Fig. 5 (a).

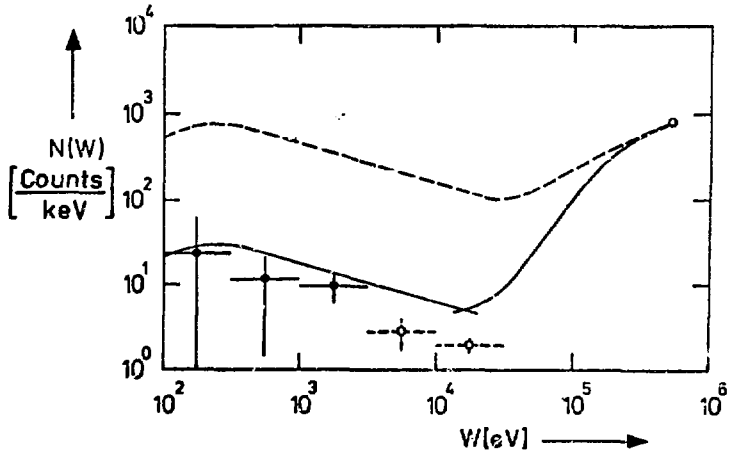

Fig. 5 (b).

Spectral flux density n(W) versus muon energy W. Open circle: Normalization point. At this energy "ordinary" energy loss calculations are still reliable and the multiple scattering is negligible under run condition. Dashed line: Calculation of n(W) performed by our group neglecting multiple scattering. Solid curve: Calculation of n(W) taking multiple scattering into account; right part: Gaussian approximation; left part: validity of Lambert's Law assumed. Part a: same run as in Fig. 4. Part b: 40 $\mu g/cm^2$ Cu on Si. Accumulation time: 16 hours. The two high-energy points are somewhat too low because the Cu layer was not thick enough to reliably stop all muons.

CLOSING COMMENTS

by

D. E. Nagle
Alternate MP-Division Leader
Los Alamos Scientific Laboratory

I know that Louis Rosen would wish me to express his regret at not being able to assist at this conference which I, myself, have found extremely stimulating, at least the portions which I have been able to attend. Nobody regrets at this moment Rosen's absence more than I do.

I briefly considered and dismissed the notion that I would present to you at this time the quintessence of the quintessence of all the wisdom herein expressed for the last week. It's a job which I feel incapable of, and so I am not going to try it.

I wondered during the last week what is a radiochemist and what is a nuclear physicist. I found it very hard to set down a series of criteria which would infallibly enable you to distinguish a nuclear chemist from a nuclear physicist. The two types of scientists exhibit extreme lability and, from time to time, they appear in one state or the other, apparently depending on some phase of oscillation in some abstract space. The experimental methods used are similar; you will find either group using nuclear emulsions, chambers, Lexan plates, scintillation counters, etc., so you can't tell from their methods either. I think it comes down partly to a question of background and of self image. If you think you are a nuclear chemist, you are one; and if you think you are a nuclear physicist, you are! Well, what is it that I'm going to talk to you about? I decided that I would review with you some outstanding problems and challenges which I, as an outsider and one who was not able to hear more than a small fraction of the sessions here, consider particularly interesting and topical. Some of them you have discussed at this meeting. Let's enumerate some of them.

One is to observe the neutrino oscillations terrestrially. After revealing myself again as something of an outsider, upon reviewing the evidence for the existence of neutrino oscillations today, I consider that the only indication

which carries any conviction whatsoever is the Davis experiment on solar neutrinos and, as you know, that is open to a number of possible interpretations as to why the observed flux of solar neutrinos is lower than the calculations made by Bahcall and others. Davis submitted to LAMPF a proposal to look at electron neutrino reactions in his detector, and I think that is an idea we should reexamine, and I think it should be reexamined in the context of looking specifically for neutrino oscillations while doing other things. I think that if you have one tank, perhaps one should have two tanks--using the same processing equipment to look at the products at two distances from the reactor, and maybe that is a viable thing. As you may well know, we are in receipt of proposals and letters of intent to look at neutrino oscillations by other means, also using big tanks of materials but looked at with light detectors basically. Nobody has come up with a neutrino detector that hasn't used tons and tons of material. It seems that you can't get away from using big tanks of materials; it seems to be a "tankless" task. But I can tell you of one possibility that Bill Visscher and I discussed many years ago. If you think of K-capture, in that process a nucleus can emit a monoenergetic neutrino. It can be done if you cool the emitting nucleus to a low temperature; you can get a recoil-free emission of neutrinos, so it is the perfect source of recoilless, ultra monoenergetic neutrinos. Now all you have to do is to prepare a suitable target to cause the inverse process and your cross section is no longer $10^{-34}cm^2$; instead, it is $10^{-16}cm^2$. And preparing a suitable target is certainly a task for which you gentlemen are eminently equipped, so I invite you to think about that for a little bit. There is a paper by Visscher some years ago about the process of recoilless emission of neutrinos. All we have to do is the other half--recoilless absorption of neutrinos, and we'll have huge cross sections. That is, perhaps, one way to do it without huge tanks.

Now another proposal which came out very recently, which is extremely intriguing to me, is that of Cowan and Haxton to look at paleosolar neutrinos, that is, to see whether the flux of neutrinos from the sun varied over eons, and that, of course, ties into the problem of the too-few "snus" and that is a charming proposal.

Now going on to some other topics of interest to nuclear chemists, you should find the free quark. George Zweig came here and gave a lecture on the chemistry of free quarks. It's an outstanding task for the chemical fraternity to find quarks. I will say no more about that now.

Other heavy objects which are believed to be present in unified field theories might be looked for by cnemists. Glashow, in his talk at the Washington Physical Society meeting last spring, speculated on the presence of other very heavy neutral objects required by some versions of unified field theories. This might be found some by chemical methods. The case for wanting there to exist magnetic monopoles is still reasonably interesting from theoretical grounds, having to do with quantization of the electron charge, having to do with the origin of gauge theories. Our great theorists, such as Dirac and Yang and others, over the years have speculated on the presence of these objects. Perhaps one of you may find one of these an interesting object.

Other things coming in from outer space, having to do with nuclear matter being present in neutron stars, might be looked for: what happens when two neutron stars hit? do they eject neutronium in big chunks? does that come to the earth from time to time? I don't know.

Coming back to the earth a little bit more, it is a job for nuclear chemists, I believe, to push the conditions of nuclear matter to be observed in our laboratories--LAMPF, SIN, the BEVALAC, etc.--to the extremes; we wish to push to nuclei as far as possible from the valley of stability. We wish to look at pion double-charge-exchange reactions. What was an extremely exotic phenomenon many years ago, and fell exclusively to the chemist to observe, is now routine; we do it on the EPICS spectrometer all the time, and we explore the angular distribution--the energy space possible. So, let's go on and we'll have you gentlemen look at double-charge exchange in very heavy nuclei where the cross section is very small. Possibly the triple-charge exchange, would you believe? How about π^+ on U-238 to give $\pi^- + \pi^- +$ Am-238? Or, single-charge exchange on U-234, giving rise to, what is it? If you go down one from U-234, what do you get? Yes, you might be able to detect that.

Another reaction which has been studied on hydrogen, which I think is very interesting, is

$\pi^- + p \rightarrow \pi^+ + \pi^- + N$, or in a diagram,

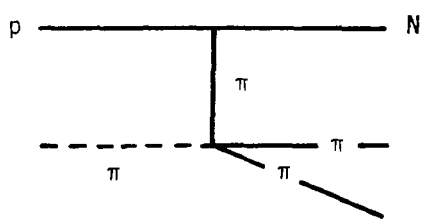

i.e., pion-pion scattering, and the thing of importance there is the scattering lengths a_0 and a_2, if you do this at very low energy near the threshold of this reaction. So, the two possibilities are a singlet state for the two pions or a quintuplet state, and this experiment was done at LAMPF recently with about 500 MeV pions, but it could be done also in nuclei. Perhaps one could begin to study this in nuclei and look at two-pion production in heavier nuclei, and I think this would be an interesting process to examine.

Exotic nuclei are a fashionable topic and their importance cannot be too heavily stressed. They are one of the reasons why we are interested in kaon factories. It's a new kind of matter with different quantum numbers; a new nuclear physics is possible with these new quantum numbers, and so exotic nuclei are, of course, of interest to people who are interested in nuclear structure under extreme conditions.

In chatting with Walecka, he mentioned to me that one should be alert to see if there are other signals for transitions to a transitory, or evanescent, form of nuclear matter which occurs, let us say, when a heavy ion plows into uranium. Would you see a meson or some other transient particle come out, or is there some residue that you could identify by nuclear chemical techniques? What new signals might one be looking for?

There are a few more mundane requests I have of you. Perhaps, before you embark on all of these above, it would be nice if we could have even more accurate and convenient and available monitors for the pion fluxes at all energies, perhaps to 5% or 2%. The carbon $(\pi,\pi N)$ reaction is in standard use around here, and we would like to be able to use this in 15-MeV pion or 10-MeV pion beams and monitor very precisely the integrated flux of pions. Other beam monitors might possibly be developed.

The chemists, I must say, have been derelict in their duty in not devising monitors of polarized beams! Now, if you take a polarized proton and shine it into a polarized target, then the reaction is spin-dependent on that target and chemists ought to be able to monitor this! I would not presume to tell them how, but it would be a very interesting thing to do.

Finally, I think that one should be alert to the possibility that we could have, perhaps not a kaon factory, but a super-pion factory. Would there be a case for increasing the intensity of pion beams a hundred-fold over what we have, or would there not? I believe that this is possible. I also think that we could build a pion factory in a quarter of this room, and I think that we

could probably get a kaon factory into a space not much larger than this room. So accelerator physicists could do a lot more if they were requested to do so and if there were resources to do it with, but on that note, I think I will end my remarks and express my great pleasure in at least being able to attend some of your sessions. Thank you.

ROUNDUP OF WORKSHOP

by

P. J. Karol
Carnegie-Mellon University

I want to bring the Workshop around full cycle. One of the problems I have back at my home base, which is a University, is explaining, as Dr. Nagle did, "What is a nuclear chemist?" I talk to my colleague chemists and they say, "What are you interested in in your research?" I tell them, "I am interested in irradiating target material and analyzing the radioactive products, looking at their yields trying to learn something about the reaction mechanisms, and studying nuclear transformations". They say, "But that is not chemistry, that is physics!" When I talk to my physics colleagues they say, "What do you do at Los Alamos?" I tell them "I am looking at spallation reactions, trying to learn about the structure of the nuclear skin and also about the equation of state of nuclear matter." They say "Why is a chemist doing this?" The problem seems to be one of language. I decided, therefore, to windup here with a little throw-back to language. The question seems to be "What is chemistry and what is physics?" The difficulty in defining those terms is that one is stuck with the English language, so I have gone to some symbolism. I would like to have the first slide. This illustration (see Fig. 1) really resolves the problem for those of you keen enough to recognize these symbols. The upper symbol is both the Chinese and Japanese character for "chemistry"; the lower one is for "physics". If you delve into Chinese/Japanese etymology, (which I had done for me), the actual translation of this disyllable for chemistry is "the study of changes or transformations". Putting syllables together gives "chemistry". It is a much better description of what is meant by chemistry. The lower symbol, which in English translates as physics, breaks up etymologically into meaning "the theory or science of matter or nature". It is really not so much a difference, but it is expressed much, much better using the Chinese and Japanese characters, hence the problem seems to be one of language more than anything else.

I began the Workshop pointing out that we are now about fifty years after the invention of the cyclotron. You could go so far as to say that nuclear physics, in fact, is not quite a hundred years old. But, having pointed out that the word "chemistry" has to do with transformations, the very next slide (Fig. 2) deals with the origin of the English word "chemistry" and shows, in fact, that "nuclear chemistry" goes back 2000 years! The word "chemistry," in English, is a spin-off of the word "alchemy," which became outmoded about a hundred years ago. But if you look into the etymology of the word "alchemy," it comes from the Middle English, "alkamie," which in turn came from the Old French, (and I won't try to pronounce that, but it is similar), which in turn came from Medieval Latin, which I will not say either, and that from Arabic. The Arabic "al" just means "the" and the "kimiya" (or however that is pronounced), comes from Late Greek "Khemeia" which translates as meaning "the art of transmutation practiced by the Egyptians," and traces all the way back to before the Christian Era from ancient Greek "Khemia," the word for Egypt. The conclusion of my little wind-up here is that, although nuclear physicists have been in the business for less than a hundred years, the chemists, whoever they are, have been in the business for 2000 years.

With that, I would sincerely like to acknowledge the people associated with the Workshop who have really put in the work; I have just been the frontispiece for this operation. I have listed here, my co-chairman, Bruce Dropesky, and Workshop Administrator, Dave Vieira, who have done much of the work; the steering committee members and the panel chairmen and co-chairmen, who have put in a tremendous effort, and the two women out in the front office, who, although you don't see how much they are working for the conference, really ought to be commended for their efforts. With that, I would like to thank, and I think you should too, all the people on this list and also yourselves for what I feel has proven to be a very successful workshop.

Fig. 1.

al·che·my (ăl 'kə-mē)

[Middle English *alkamie*, from Old French *alquemie*, from Medieval Latin *alchymia*, from Arabic *al-kīmiyā*: *al* "the" + *kīmiyā*, from Late Greek *khēm(e)ia*, "the art of transmutation practiced by the Egyptians", from Greek *khēmia*, "Egypt"]

Fig. 2.

ACKNOWLEDGMENTS

The organizing committee expresses its gratitude to the many people who contributed to making this Workshop a success. First of all, we thank Louis Rosen for his encouragement to proceed with the planning of a nuclear chemistry workshop and for the support he provided from MP Division for executing these plans. John Allred provided much helpful guidance in the early stages of planning for this meeting. We are particularly grateful for the abundant advice and assistance we received from Alice Horpedahl, whose experience from previous workshops was invaluable.

We also express our appreciation to George Cowan, Darleane Hoffman, and James Sattizahn for their encouragement and support.

The members of the PUB Department of LASL, particularly Floyd Archuleta and his associates contributed importantly to the smooth operation of the meeting by providing many services at the Study Center. Sue Wooten's assistance in making lodging and travel arrangements for our visitors was much appreciated. The secretarial aid we received from Alice Staritzky of CNC-11 during the meeting was very helpful.

We join all the participants in thanking LASL's Director Donald Kerr for his support and for the first evening's welcoming reception. Likewise, CANBERRA Industries is to be thanked for providing Wednesday's predinner refreshments, through the efforts of their Regional Systems Engineer, Ed Chunglo.

Finally, we express our gratitude to Fabiola Lucero for the prodigious amount of secretarial work she did on the correspondence needed in the planning for the Workshop, for the on-the-spot work during the meeting, and for her versatile contributions in the preparation of these Proceedings.

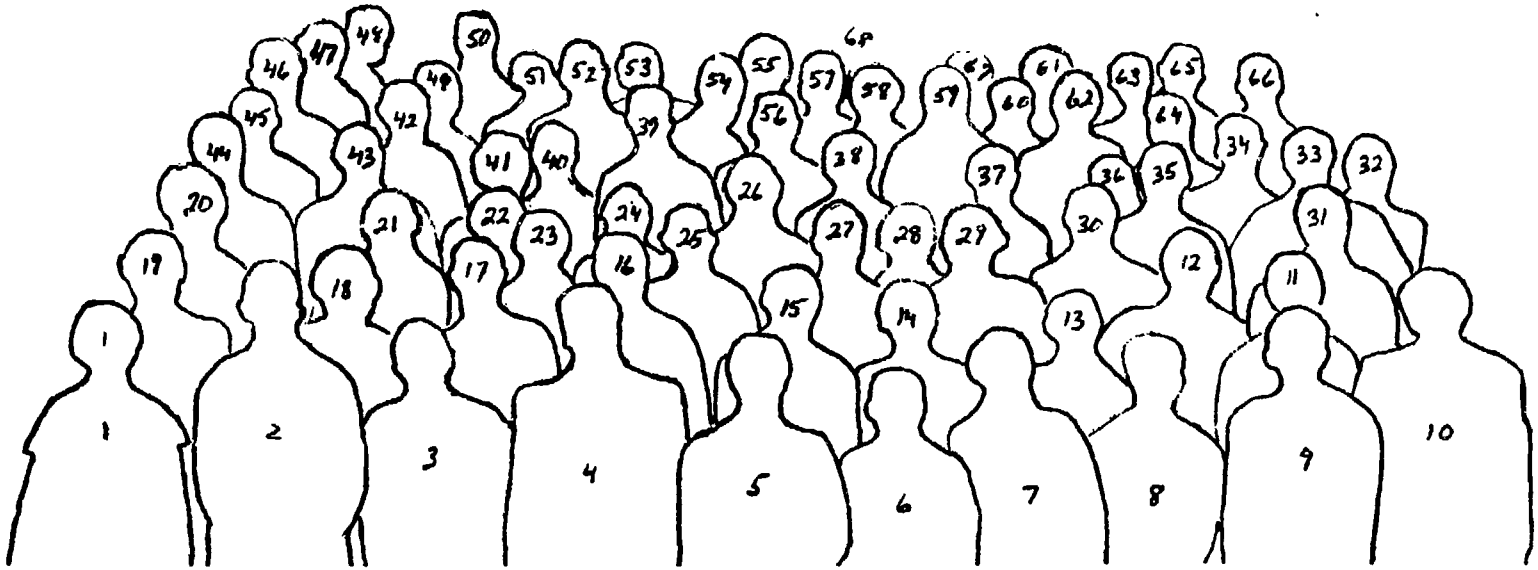

1. D. Hoffman
2. B. Dropesky
3. J. Hogan
4. M. Sternheim
5. P. Karol
6. L-C. Liu
7. N. Porile
8. N. Imanishi
9. T. Nishi
10. R. Greenwood
11. S. Shibata
12. F. Hartmann
13. J. D. Knight
14. T. Suzuki
15. H. Daniel
16. W. L. Talbert
17. D. Long
18. E. Remler
19. H. Kaji
20. D. Joyce
21. E. Fireman
22. W. Gibbs
23. D. Boyce
24. K. K. Seth
25. A. Turkevich
26. R. Nix
27. R. Naumann
28. B. Gnade
29. P. Ehrhart
30. B. Srinivasan
31. H. C. Walter
32. W. Dharmvanij
33. D. H. Boal
34. L. Winsberg
35. R. Rundberg
36. G. Rundberg
37. E. Hungerford
38. R. Korteling
39. S. Katcoff
40. J. Hill
41. J. Norton
42. G. Butler
43. A. Caretto
44. D. Vieira
45. W. Faubel
46. C. W. Reich
47. H. Plendl
48. E. Hermes
49. M. Epherre
50. G. Giesler
51. E. Steinberg
52. C. Orth
53. H. Funsten
54. M. W. Johnson
55. G. Westfall
56. R. Green
57. W. McHarris
58. J. Hüfner
59. M. Tobin
60. R. Segel
61. M. A. Yates
62. J. Clark
63. R. Petry
64. P. Vogel
65. J. Lieb
66. H. Oddeson
67. K. Anderson
68. ?

LIST OF PARTICIPANTS AND ADDRESSES

John C. Allred
LASL
MP-DO, MS-850

David Harold Boal
Simon Fraser University
Department of Chemistry
Burnaby, B.C.
V5A 1S6 Canada

Dale E. Boyce
University of Chicago
5630 S. Ellis Avenue
Chicago, IL 60637

James Bradbury
LASL
MP-3, MS-844

H. C. Britt
LASL
P-7, MS-456

David J. Brenner
LASL
MP-3, MS-809

Merle E. Bunker
LASL
P-2, MS-776

Gilbert W. Butler
LASL
CNC-11, MS-514

Albert A. Caretto, Jr.
Carnegie-Mellon University
4400 Fifth Avenue
Pittsburgh, PA 15213

James L. Clark
Carnegie-Mellon University
4400 Fifth Avenue
Pittsburgh, PA 15213

Huan-ching Chiang
Max-Planck Inst.
Heidelberg, W. Germany

Herbert Daniel
Technische Universität München
D-8046-Garching,
Federal Republic of Germany

Wanchai Dharmvanij
University of Oklahoma
720 W. Boyd #21
Norman, OK 73069

Raymond Davis
Brookhaven National Laboratory
Upton, NY 11973

Dick DiGiacomo
LASL
P-7, MS-456

Bruce J. Dropesky
LASL
CNC-11, MS-824

Peter Ehrhart
Technical University of Munich
James-Franck-Strasse
D-8046 Garching,
Federal Republic of Germany

Marcelle Epherre
Laboratoire Rene Bernas
C.S.N.S.M. B.P. N°1 - Bat. 108
91406 Orsay, France

Werner Faubel
LASL
CNC-11, MS-824

Edward L. Fireman
Smithsonian Ast. Obs.
60 Garden St.
Cambridge, MA 02138

Donald G. Fleming
TRIUMF/U.B.C.
Department of Chemistry
University of British Columbia
Vancouver, B.C. V6T 1Y6, Canada

Zeev Fraenkel
Weizmann Institute
Rehovot, Israel

H. O. Funsten
College of William & Mary
Williamsburg, VA

William R. Gibbs
LASL
T-5, MS-454

Gregg Giesler
LASL
CNC-11, MS-824

Bruce Gnade
Chemistry Department
Georgia Institute of Technology
Atlanta, GA 30332

Robert J. Gehrke
EG&G Idaho, Inc.
Idaho National Eng. Lab.
P.O. Box 1625
Idaho Falls, ID 83415

Ray E. L. Green
Simon Fraser University
Burnaby, B. C.
V5A 1S6, Canada

Steven J. Greene
LASL
MP-10, MS-841

Reginald C. Greenwood
EG&G Idaho, Inc.
Idaho National Eng. Lab.
P.O. Box 1625
Idaho Falls, ID 83415

F. Joachim Hartmann
Techn. Univ. Munich, E 18
James-Franck-Strasse
D-8046 Garching,
Federal Republic of Germany

Erwin A. Hermes
University of Zurich/SIN
5234 Villigen, Switzerland

H. R. Heydegger
Purdue University
Calumet
Hammond, IN 46323

Robert A. Hilko
LASL
MS-809

John C. Hill
Department of Physics
Iowa State University
Ames, Iowa 50011

Darleane C. Hoffman
LASL
CNC-DO, MS-760

James J. Hogan
McGill University
Deparment of Chemistry
801 Sherbrooke St. W.
Montreal, Quebec H9W 2Y7 Can.

Jerome Hudis
Department of Chemistry
Brookhaven National Laboratory
Upton, NY 11973

Jörg Hüfner
University of Heidelberg
D-6900 Heidelberg,
W. Germany

Edward V. Hungerford, III
Physics Department
University of Houston
Houston, TX 77004

Richard Hutson
LASL
MP-3, MS-844

Nobutsugu Imanishi
Institute of Atomic Energy
Kyoto University
Gokanosho, Uji
Kyoto 611 Japan

M. William Johnson
Department of Chemistry
University of Maryland
College Park, MD 20742

Donald Joyce
Department of Physics
College of William & Mary
Williamsburg, VA 23185

Harumi Kaji
Tohoku University
Aramaki-aza-aoba
Sendia, 980 Japan

Paul J. Karol
Chemistry Department
Carnegie-Mellon University
4400 Fifth Avenue
Pittsburgh, PA 15213

Seymour Katcoff
Brookhaven National Laboratory
Upton, NY 11973

J. D. Knight
LASL, CNC-11, MS-824

H. B. Knowles
Physics Department
Washington State University
Pullman, WA 99163

Ralph Korteling
Chemistry Department
Simon Fraser University
Burnaby, B.C.
U5A 1S6 Canada

Mel. Leon
LASL, MP-3, MS-844

B. Joseph Lieb
Physics Department
George Mason University
Fairfax, VA 22039

Lon-chang Liu
LASL, CNC-11, MS-824

David G. Long
Nuclear Physics
University of Mass.
Amherst, MA 01003

William C. McHarris
Michigan State University
East Lansing, MI 48824

Richard L. Martin
LASL, T-12, MS-569

N. A. Matwiyoff
LASL, CNC-DO, MS-760

Leonard F. Mausner
RER Division
Argonne National Laboratory
Argonne, IL 60439

D. E. Nagle
LASL, MP-DO, MS-846

Robert A. Naumann
Princeton University
Princeton, NJ 08545

Ray Nix
LASL, T-9, MS-452

Tomota Nishi
Institute of Atomic Energy
Kyoto University
Gokanosho, Uji,
Kyoto 611 Japan

Joseph M. Norton
Florida State University
Tallahassee, Florida 32304

Yoshi Ohkubo
Purdue University
West Lafayette, IN 47907

Charles J. Orth
LASL, CNC-11, MS-514

Michael Paciotti
LASL, MP-3, MS-844

Robert F. Petry
Department of Physics
University of Oklahoma
Norman, OK 73019

Chandraseghara Pillai
Physics Department
OSU
Corvallis, OR 97331

Hans S. Plendl
Florida State University
Tallahassee, FL 32304

Norbert T. Porile
Department of Chemistry
Purdue University
West Lafayette, IN 47907

Henk S. Pruys
Universität Zürich/SIN
CH-5234 Villigen, Switzerland

Charles W. Reich
EG&G
Idaho National Eng. Lab.
P.O. Box 1625
Idaho Falls, ID 83415

James J. Reidy
Physics Department
University of Mississippi
University, MS 38677

E. A. Remler
College of William & Mary
Williamsberg, VA 23185

Robert Rundberg
LASL, CNC-11, MS-514

Virginia L. Rundberg
LASL, CNC-11 MS-514

Scott A. Sandford
LASL, MP-3, MS-844

M. E. Schillaci
LASL, MP-3, MS-844

Ralph E. Segel
Physics Department
Northwestern University
Evanston, IL 60201

K. K. Seth
Northwestern University
Evanston, IL 60201

Seiichi Shibata
Carnegie-Mellon University
4400 Fifth Avenue
Pittsburgh, PA 15213

R. R. Silbar
LASL, T-5, MS-454

B. Srinivasan
Department of Chemistry
Washington State University
Pullman, WA 99164

Ellis P. Steinberg
Argonne National Laboratory
9700 S. Cass Avenue
Argonne, IL 60439

Morton M. Sternheim
Nuclear Physics
University of Mass.
Amherst, MA 01003

D. Strottman
LASL, T-9, MS-452

Takenori Susuki
Department of Physics
University of British Columbia
Vancouver, B.C.
V6T 1W5 Canada

Willard L. Talbert
LASL, AT-DO, MS-811

Henry A. Thiessen
LASL, MP-10, MS-841

Michael J. Tobin
Chemistry Department
Carnegie-Mellon University
4400 Fifth Avenue
Pittsburgh, PA 15213

Anthony Turkevich
University of Chicago
5630 S. Ellis Avenue
Chicago, IL 60637

David J. Vieira
LASL, CNC-11, MS-824

Petr Vogel
Cal Tech
Pasadena, CA 91125

Willard R. Wadt
LASL, T-12, MS-569

H. Christian Walter
Lab. of High Energy Phys. ETH LHE/SIN
CH-5234 Villigen, Switzerland

Gary D. Westfall
Accelerator Research
LBL
Berkeley, Ca 94720

Les Winsberg
U of Southern Cal.
Los Angeles, CA 90007

Mary Ann Yates
LASL, L-4, MS-554

INDEX TO PAPERS CONTRIBUTED TO PANELS

☆U.S. GOVERNMENT PRINTING OFFICE: 1981-0-777-022/82